LONG-TERM CONSEQUENCES OF ROMAN EXTREMITY FRACTURES

RESILIENT ROMANS: CROSS-SECTIONAL EVIDENCE FOR LONG-TERM FUNCTIONAL CONSEQUENCES OF EXTREMITY TRAUMA

By REBECCA JEANNE GILMOUR, B.A. (Hons), M.Sc.

A Thesis Submitted to the School of Graduate Studies in Partial Fulfilment of the Requirements for the Degree Doctor of Philosophy

McMaster University DOCTOR OF PHILSOPHY (2017)

Hamilton, Ontario (Anthropology)

TITLE:	Resilient Romans: Cross-Sectional Evidence for Long-Term Functional Consequences of Extremity Trauma
AUTHOR:	Rebecca Jeanne Gilmour, B.A. (Hons) (Simon Fraser University), M.Sc. (Durham University)
SUPERVISORS:	Professors Megan Brickley and Tracy Prowse

NUMBER OF PAGES: xxxvi, 462

LAY ABSTRACT

Immobility and disuse of a fractured arm or leg can result in bone loss. Using radiographs, this research evaluated physical activity and long-term fracture complications in adult skeletons from ancient Roman communities at Ancaster, UK and Vagnari, Italy (1st-4th century AD). Compared to Ancaster, Vagnari individuals had thicker bones that indicated they were more physically active. Evidence for physical consequences were not associated with the type or location of a fracture; only two individuals from Ancaster (and none from Vagnari) had evidence of disuse.

This study of fracture consequences contributes to our understanding of injury risk and recovery in the past. Although fractures can cause lasting physical consequences, these results show that fractures that appeared 'severe' did not necessarily result in long-term impairment. Most residents at Ancaster and Vagnari were physically active and recovered from their injuries, a finding that emphasizes the importance of continued physical activity after injury.

ABSTRACT

Long-term repercussions of extremity trauma can include fracture mal- and non-union, osteoarthritis, pain, and impairment of physical movement, which can result in disuse of the limb and eventual bone loss. Although trauma is commonly investigated in palaeopathology, the functional repercussions of injuries are not typically considered. By integrating palaeopathological fracture analyses and biomechanical investigations of cross-sectional properties, this thesis explores individual and group experiences of extremity fracture risks, responses, and consequences at two Roman sites.

Adults from 1^{st}-4^{th} century AD Roman cemeteries at Ancaster, UK (n=181), and Vagnari, Italy (n=66), were examined for limb fractures. Data on fracture type, location, malunion, and associated infection and osteoarthritis were collected. Bone areas and asymmetries were calculated using biplanar radiographs for individuals without fractures, and compared to those of individuals with fractures. Patterns in bone amounts and asymmetries associated with fracture attributes were identified.

Extremity fractures were observed in 39 individuals from Ancaster and 12 individuals from Vagnari, but the prevalence rates did not differ between the sites. Cross-sectional properties suggested that compared to Ancaster, individuals living at Vagnari experienced greater mechanical loading (i.e., larger bone areas). Disuse of a fractured limb was only identified in two old adult individuals from Ancaster; no Vagnari individuals had evidence for post-traumatic dysfunction. Functional consequences of injuries were not associated with observable fracture attributes (e.g., fracture type, malunion), meaning that physical impairment cannot be recognized based only on an injury's appearance.

By incorporating biomechanical methods in palaeopathological analyses of trauma, this thesis reveals the physical experiences of injury acquisition and recovery among residents of Ancaster and Vagnari over the life course. The relative absence of post-traumatic disuse speaks to the resilience of Romans at these sites, and contributes to the growing literature on the human experience of trauma and impairment in the past.

ACKNOWLEDGEMENTS

I would like to thank my co-supervisors, Dr. Megan Brickley and Dr. Tracy Prowse, for their valuable guidance throughout my doctoral program. I am so grateful for your support in everything from helping to organize and transport 'Zappy', the portable digital X-ray, around Europe, to providing tireless advice and edits to the development of this thesis. Many thanks also go to Dr. Erik Jurriaans, my third committee member, for sharing his radiographic expertise with me. I have learned so much from my Ph.D. committee, and I cannot express enough how much I appreciate what you have done for me over the past years.

While away on fieldwork, I was fortunate to visit collections in the UK, Italy, Austria, and Hungary. I am grateful to all the people who hosted Zappy and I on our journey. Special thanks to Dr. Simon Mays and Historic England for access to the Ancaster skeleton collection, and the Fondazione Ettore Pomarici Santomasi and the Centro Operativo, Gravina, Soprintendenza per i Beni Culturali e Archeologici della Puglia for access to the Vagnari skeletal collection. I am particularly grateful to the staff at the Centro Operativo Gravina for our daily espresso and Italian lessons!

Although they were not included in this thesis, I also collected data on skeletal collections in Austria and Budapest and would like to acknowledge the support I received as a Ph.D. researcher using these collections. I am very grateful to Dr. Ildiko Pap, Sandor Evinger, and all the staff of the Anthropology Department at the Hungarian Natural History Museum in Budapest for access to the Graphisoft, Aquincum skeletal collection. Thank you also to Dr. Pollhammer, Mag. Müller, Mag. Blesl, Mr. Braunecker and the staff at the Archaeologie Service, Bundesdenkmalamt, and Kulturhaus Hainburg an der Donau for access to the Carnuntum skeletal collections. A very special thanks to Mag. Roman Igl, my friend and former archaeological site supervisor in Austria, for his unending support in facilitating access to skeletal collections excavated around Vienna.

My acknowledgements would not be complete without thanking the people who assisted me abroad while I was undertaking fieldwork. I am forever grateful to Mike Burchett and the staff of the Jolly Roger in Gosport, UK; Anna-Lena, Marie-Lisa, and Traudl Lock in Vienna, Austria; and Aniko Nanasi in Budapest, Hungary. These lovely people took me in, gave me a place to live, and helped me haul Zappy around their respective countries. The kindness you showed me was unparalleled, and made a long field year a very happy one.

During my PhD, I have been very lucky to have had the support of an excellent network of friends, peers, and colleagues. To Lori D'Ortenzio, Creighton Avery, Heather Battles, Kathy Kondor, and so many others who have commented on my writing, shared a coffee, and kept me sane over the last few years, thank you for always being there to listen to my crazy ideas!

Last but not least, my two greatest supporters: my mom, Cathie Smart, and my partner, Greg Meila-Heuse. Mom, thank you for always supporting my doctoral dreams. I'm so glad you joined me in Italy and Hungary as my research assistant; it would not have been the same without you! Greg, your support throughout my Ph.D. has been unfaltering and endless. Your calming influence has helped me to push through and excel in even the most challenging moments of this process. Thank you both.

TABLE OF CONTENTS

LIST OF FIGURES

LIST OF TABLES

TABLE OF EQUATIONS

LIST OF ABBREVIATIONS AND SYMBOLS

< – Smaller than normal
> – Larger than normal
σ – Standard deviation
2σ – Two standard deviations
χ^2 – Kruskal-Wallis statistic
A – Ambiguous
AA – Absolute asymmetry
ADO – Adolescent (15-19 years old)
ANG – Angulation
AP – Antero-posterior; also used to refer to measurements of subperiosteal width in the antero-posterior view
ap – Measurements of medullary width in the antero-posterior plane
APP – Amount of poor apposition
BM – Body mass
C – Clavicle
C_A – Cortical area
C_A%DA – Cortical area directional asymmetry
CI – Cortical index
CI_x – Confidence interval
CPR – Crude prevalence rate
DA – Directional asymmetry
DD – Distal diaphysis segment
DDA – Digital Detector Array
DE – Distal epiphysis segment
df – Degrees of freedom associated with the statistical test
EMM – Ellipse model method
F – Female
Fem – Femur
F? – Possible Female
FA – Fluctuating asymmetry
FH – Femoral head
Fib – Fibula
H – Humerus
INF – Inflammation
IQR – Interquartile range
IQRx1.5 – 1.5 times the interquartile range, a value used to identify the ‘normal’ spread of data and outliers.

kV – Kilovolt
L – Distance from the distal point to a feature along the longitudinal axis of a bone
L – Left
LCM – Latex Cast Method
LL – Lower limb
LP/mm – Line pairs per millimeter (a measure of spatial resolution)
M – Male
M? – Possible Male
M_A – Medullary area
MA – Middle Adult (35-49 years old)
mA – Milliamps
M_A%DA – Medullary area directional asymmetry
MC2 – Second metacarpal
MC2 50% - Second metacarpal midshaft
MD – Middle diaphysis segment
MD% – Mean percent difference
ML – Medio-lateral; also used to refer to measurements of subperiosteal width in the medio-lateral view
ml – Measurements of medullary width in the medio-lateral plane
MT2 – Second metatarsal
MW – Medullary width measurement
OA – Old Adult (50+ years old)
OA_x – Osteoarthritis
OR – Odds ratio
OV – Overlap
p – Significant at ≤ 0.05
PD – Proximal diaphysis segment
PE – Proximal epiphysis segment
p_{FET} – Fisher's exact tests
R – Right
r – Spearman's rank correlation coefficient
Rad – Radius
RO – Rotation
ROI – Region of interest
ROI%DA – Region of interest area directional asymmetry
s – Seconds (x-ray exposure time)
T – Tibia
t – t-test value
T_A – Total area

T_A%DA – Total area directional asymmetry
TL – Total length of a long bone
TL% – Percent location relative to the total length of a long bone
TPR – True prevalence rate
TW – Total width measurement
U – Mann-Whitney U value
U – Unknown
UD – Undetermined
Ul – Ulna
UL – Upper limb
χ^2_{Yates} – Chi-square test with Yate's correction
Y – 'Yes'
YA – Young Adult (20-34 years old)

DECLARATION OF ACADEMIC ACHIEVEMENT

I declare that the content of the research in this document has been completed by myself, Rebecca J. Gilmour, with recognition of the contributions of Dr. Megan Brickley, Dr. Tracy Prowse, and Dr. Erik Jurriaans in both the research process and the completion of the thesis.

Chapter I – INTRODUCTION

1.1 Introduction

Fractures are one of the most often recorded pathological lesions in skeletal material and can be used to understand the forces behind the injury, the possible causes, and infer the absence or unsuccessful application of treatment. What is currently missing from our understanding of fractures in the past is the study of the impact these injuries had on an individual's physical function in the long term. Some biological anthropological case studies of adapted or impaired function after fracture have been published (e.g., Holt et al. 2002; Lovell 2016; Trinkaus et al. 1994), and the functional consequences of other pathological conditions, such as tuberculosis, have been reported by Sparacello et al. (2016). To date, no larger scale studies of the biomechanical consequences of fractures in archaeological contexts have been published.

This thesis addresses the long-term consequences of extremity fractures using palaeopathological and biomechanical analyses of limb bones from 1st to 4th century AD Roman period cemeteries at Ancaster, UK, and Vagnari, Italy. It is hypothesized that fractures to the extremities can be debilitating in the long term and may impact an individual's ability to physically participate in tasks and activities. This research explores the associations between healed fractures and physical consequences to function, contributing to the understanding of the functional repercussions of injuries in the past. Interactions between habitual physical activity, fracture attributes, and long-term injury consequences are also investigated, and provide insight into the influence that extremity fractures had on the lives and lived physical experiences of the residents at Ancaster and Vagnari.

1.2 Research Aims

This investigation of the functional repercussions of extremity fractures contributes to the growing literature concerning human experiences in the past. By considering the long-term consequences of injuries, impediments to physical activity can be deduced. Additionally, inferences can be made about individual and social attitudes toward injury and injury recovery. Through the understanding of the relationship between fractures and function, this research outlines how fractures can be appropriately used by palaeopathologists to discuss physical consequences in the past. Specifically, the impact that a fracture has on an individual's ability to physically function will be considered, and used to advise palaeopathological analyses of extremity trauma, adding to the understanding of trauma longevity.

In addition to contributing to palaeopathological studies and discourse surrounding the human experience, the outcomes of this research provide insight into what it was like to be injured in a small, Roman community, in diverse regions of the Roman Empire. Comparison of extremity trauma and biomechanical evidence for mechanical loading and physical activity between Ancaster and Vagnari permit interpretations of fracture hazards, activity levels, fracture repercussions, and injury responses between the sexes and throughout the life course.

1.3 Research Questions

The central aim of this research is to identify relationships between fractured bones and cross-sectional areas and asymmetries in order to reveal an individual's functional experiences before and after injury. To address this, this thesis investigates three main questions using palaeopathological analyses of fractures and biomechanical assessments of cross-sectional properties:

1) Are there differences in how fracture types, locations, and/or complications are distributed within or between Ancaster and Vagnari?
2) What are the normal ranges of bone areas and asymmetries for individuals without fractures? How do these ranges differ between groups and/or sites?
3) Do the cross-sectional properties of individuals with fractures differ from the normal ranges? If so, are there patterns in how anomalous cross-sectional properties are distributed (e.g., sex, age, site, fracture type)?

The first question helps to identify the different injury risks, causes, and complications experienced by residents at Ancaster and Vagnari. The second question elucidates the levels of mechanical loading, and therefore the habitual physical activity, endured by different groups at these sites. Together, the results from these first two questions provide the foundation necessary to understand the physically active environments of, and hazards encountered by, individuals at Ancaster and Vagnari. The final question builds on these previous questions to assess if, and how, the cross-sectional properties of individuals with fractures differ from those of individuals without fractures. With this, long-term functional consequences of fractures are identified, facilitating a discussion of injury recovery at Ancaster and Vagnari.

By investigating fractures and cross-sectional properties, relationships between habitual physical activities, fracture hazards, fracture repercussions, and injury responses are recognized at, and between, Ancaster and Vagnari. Results from these lines of inquiry work together to illuminate the active lives of Ancaster and Vagnari residents. Consideration of these variables provides insight into the link between more, or less, physically active habits and one's predisposition for, or protection against, fractures and impairment.

1.4 Structure of the Thesis

This thesis is divided into ten chapters. Following this introductory chapter, Chapter II provides the necessary background in bone biomechanics, fracture healing and complications, disability and impairment, and Greco-Roman fracture treatments. The skeletal assemblages used in this research, and their archaeological and historical contexts, are introduced in Chapter III. The methods used to record skeletal sex, age, preservation, as well as fracture types, healing, and complications are outlined in Chapter IV, along with an explanation of the radiographic methods and techniques used in cross-sectional analysis. The placement of measurement locations used in cross-sectional analyses, and a new method for analysing the amount of bone present within a diaphyseal area are described in Chapter V.

The results are divided into Chapters VI, VII, and VIII; Chapter VI presents the results of the analyses at Ancaster, Chapter VII presents the results from Vagnari, and Chapter VIII compares the results from both sites. The results are integrated, interpreted, and discussed in Chapter IX. Chapter X summarizes the key findings and contributions of this research to palaeopathological and biological anthropological studies.

Chapter II – BACKGROUND

Fractures are defined as the partial or complete interruption of cortical bone continuity (Hamblen et al. 2007). Skeletal biomechanics are often used in fracture studies to investigate the susceptibility of bone to fracture, as well as to understand the mechanisms and possible causes of fractures (McGee et al. 2004). The long-term consequences of injuries can be assessed in skeletal materials with a thorough understanding of bone and fracture biomechanics, fracture complications, the acquisition of trauma, and the habitual activities of individuals. In addition to providing a biomechanics background, this chapter introduces the concept of impairment, and reviews recent archaeological insights into impairment and disability in the past. Information on Greco-Roman fracture treatment is also outlined in order to help contextualize the Roman experience of injury.

2.1 Bone Biomechanics

Throughout life, the shape, thickness, and area of bone are influenced by various genetic, developmental, age-related, environmental, nutritional, and mechanical stimuli (Martin et al. 2015; Ruff et al. 2006; Seeman 2008). Bone responds and adapts to mechanical stimuli in predictable ways. This response is understood and interpreted by applying mechanical engineering principles to biological tissues (biomechanics). Biomechanics have been used in palaeoanthropological and bioanthropological studies to better understand activity and mechanical environments in the past.

2.1.1 Mechanical Loading Forces and Bone Response

Bone is a dynamic and adaptive tissue that adjusts to changes in the loading environment (i.e., stresses and strains) through processes of modelling and remodelling (Athanasiou et al. 2000; Frost 1990; Turner and Burr 1993). In biomechanics, stress is defined as the amount of force that is applied per unit area and strain represents the relative shape deformation (length relative to width) exhibited by a bone under stress (Knudson 2007; Turner and Burr 1993). Knudson (2007) describe loads as comprised of forces and moments; force is applied in a single, linear direction, whereas a moment of force (often called torque) involves the rotational or turning effects of a force around an axis. Stresses on bone include tension, compression, and shear forces, as well as torsion moments, all of which can act alone or in combination (Figure 2.1) (McGee et al. 2004; Wescott 2013). Tension and compression forces deform both the length and width of a bone; in tension, the bone elongates and the width contracts, and while under compression, the length shortens and the width expands (bulges) (Turner and Burr 1993). Shear planes are oriented at 45° angles relative to compression and tension forces (Wescott 2013). According to Einhorn (1992), bones are more resistant to loads applied in the same direction as normal loading. Similarly, Turner and Burr (1993) suggest that bone is weaker under shear and tension forces than compression forces.

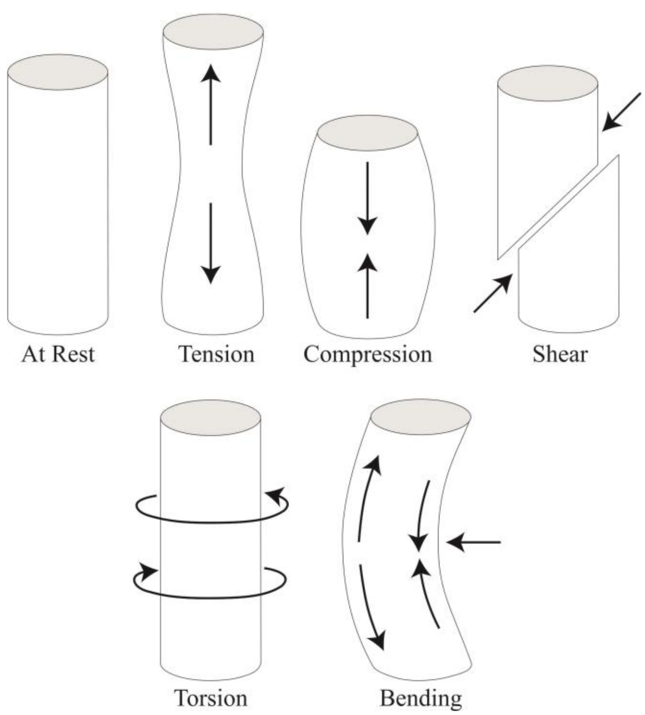

Figure 2.1 – Mechanical forces applied to bone. Arrows used to depict the direction of the applied force (or moment of force in the case of torsion). Figure developed based on images and text descriptions from McGee et al. (2004) and Turner and Burr (1993).

Modelling is the process of bone formation, usually during growth; remodelling involves both bone formation and resorption primarily for the purposes of bone maintenance and repair (Frost 1990; Hazelwood et al. 2001; Martin et al. 2015). When a bone is strained, such as through muscle contraction, gravity, and ground forces, remodelling is activated via a process called mechanotransduction (Goodman et al. 2015; Pearson and Lieberman 2004). In mechanotransduction, the physical signal (i.e., strain) is sensed by the bone cells (osteocytes), which in turn signal to the osteoblasts and osteoclasts to repair and/or adapt the bone to resist failure (Goodman et al. 2015; Huang and Ogawa 2010; Martin et al. 2015). According to Turner (1998), mechanical stimuli of even short durations can initiate adaptive responses that lead to changes in bone thickness, geometry, and density. For example, experimental research on loading cycles applied to rats by Umemura et al. (1997) found that over a period of eight weeks, five loading cycles per day, five times a week, were sufficient to produce significant changes in cross-sectional parameters.

Differences in the pattern and rate of modelling/remodelling exist throughout the life course. During growth and development, the rate of periosteal bone apposition exceeds endosteal resorption in order to allow wider and thicker cortices to develop (Frost 1990; Seeman 2008). Peak bone mass is typically achieved by early young adulthood and is a determinant of the amount of bone mass present in later adulthood (Khosla 2012; Weaver et al. 2016). Ruff et al. (2006) note that remodelling continues through life, but that juvenile and mature bone adapts to strain in different ways. As juveniles are still growing, they model more bone on the periosteal surface and also adapt to mechanical loading at a faster rate than adults. Mature bone still responds and adapts to mechanical loading, but changes at the endosteal surface are more common in adult individuals (Ruff et al. 2006).

The response of human bone to high levels of activity and great amounts of mechanical loading results in documented differences in its geometry and thickness (Bass et al. 2002; Dowthwaite and Scerpella 2009). Studies, such as those by Dowthwaite and Scerpella (2009) and Ducher et al. (2005), demonstrate that individuals engaged in higher levels of activity involving greater mechanical loads tend to exhibit more robust bones. Additionally, Dowthwaite and Scerpella (2009) observed that shape and thickness changes differ within a bone depending on the location and type of stimuli involved. For example, articular surfaces are not as reactive to mechanical stimuli as long bone diaphyses, meaning that a comparatively greater amount of adaptive change is evident in the diaphyses (Ruff et al. 2006; Ruff 2005). Within the diaphysis, the shape and distribution of cortical bone about the bone's centroid (centre of mass) reflects the bone's resistance to bending, and can be used as evidence for different activity requirements (Shaw and Stock 2009). For example, Shaw and Stock (2009) and Warden et al. (2009) explain the round humeral cross-sectional shapes identified in baseball and cricket players by torsional forces that act in a circular manner around the bone during throwing activities. In contrast, Holt (2003) and Ruff (2005) report that circular cross-sections in weight bearing bones are usually more indicative of reduced bending forces (i.e., relatively lower activity); increased terrestrial activity is therefore better associated with angular cross-sectional shapes due to adaptive buttressing in areas of higher strain.

With advancing age, the rate of endosteal cortical bone resorption begins to exceed the rate that new bone is laid down (Martin et al. 2015; Seeman 2008). Post-menopausal women are particularly at risk for bone loss due to estrogen deficiency that increases remodelling of the endosteal cortex (Seeman 2008). However, Lazenby (1990) and Russo et al. (2006) report that adults also exhibit varying degrees of subperiosteal bone apposition in order to functionally counterbalance the effect of resorption on the endosteal bone surfaces. Despite the continued subperiosteal apposition of bone, bone is usually lost faster on the endosteal surface than it can be replaced. As such, the cortex thins and, even with the limited mechanical compensation provided by periosteal apposition, the biomechanical properties of the bone deteriorate (Ahlborg et al. 2003; Athanasiou et al. 2000; Russo et al. 2006). This stage can pose a serious risk for fracture as the thickness and geometry of the bone can be depleted to a level that the bone can no longer withstand normal mechanical loads (see Section 2.2.2 for a discussion of such fractures) (Ahlborg et al. 2003; Wescott 2013).

2.1.2 Mechanical Unloading

Mechanical unloading due to disuse can result in bone atrophy, osteopenia, and/or osteoporosis (Alexandre and Vico 2011; Schlecht et al. 2012). An individual may experience diminished loading forces and disuse hypotrophy of bone as a result of pathology, such as paralysis or trauma or due to changes in the mechanical environment (e.g., space flight, bed rest) (e.g., Giangregorio and McCartney 2006; Kulkarni et al. 1998; Lang et al. 2004; Leblanc et al. 1990; Morbeck et al. 1991).

Just as bone can be deposited in response to mechanical loading stimuli, it can also resorbed in the absence of, or due to decreased strain (i.e., mechanical unloading). Disuse associated with mechanical unloading results in weakened and atrophied muscle tissues. Consequently, muscular contractions and gravitational and ground forces acting on the bone are diminished, which triggers remodelling due to the lack of deformation present (Bloomfield 2010; Burr 1997). This altered mechanical environment causes an imbalance in bone's remodelling activity that results in the removal of bone at a rate faster than it can be replaced. Trabecular bone is the first to be affected, and begins to be lost relatively soon after disuse begins. According to studies by Schäfer et al. (2012) and Uhthoff and Jaworski (1978) trabecular changes are evident after approximately two weeks. Cortical bone loses mass more slowly, resulting in thinning of the bone at the endosteal surface, while the outer bone width typically remains relatively unchanged (Lang et al. 2004; Schäfer et al. 2012; Schlecht et al. 2012). The diagnosis of disuse osteoporosis is associated with radiographically observable bone changes including: uniform osteoporosis, spotty osteoporosis, subchondral/metaphyseal radiolucent bands, and cortical changes (Jones 1969; Minaire 1989). Of these radiographic cortical changes, lamellation, a double cortical line parallel to the longitudinal cortical surface, may appear in disuse osteopenia of various bones, but is described most often in the acetabulum (Jones 1969; Minaire 1989; Yagan et al. 1987). Quek and Peh (2002) report that radiographic features indicative of osteopenia and disuse are frequently observable after eight weeks of immobilization.

The location and type of bone involved in disuse will influence its susceptibility to disuse hypotrophy. As trabecular bone is first to be affected by bone loss and is lost rapidly, bone types and locations with greater proportions of trabeculae (e.g., vertebral bodies and long bone ends) are at increased risk for disuse bone loss (Lang et al. 2004; Lau and Guo 2011). Weight bearing bones of the lower limb are also at increased risk as they do not only lose mechanical stimuli from the contraction of muscles during immobilization, but also from the effects of gravity and ground forces related to weight bearing functions (Bloomfield 2010; Lau and Guo 2011; LeBlanc et al. 2000). In instances of disuse hypotrophy associated with fractures, the area affected by disuse hypotrophy is isolated to the injured limb and, more specifically, usually tends to only affect the fracture site and the bone distal to the fracture site (Eyres and Kanis 1995; Quek and Peh 2002).

Over time, bone loss related to disuse will slow and stabilize, but it may persist for months and years after an immobilization event (Schäfer et al. 2012; Takata and Yasui 2001). Some researchers, such as Eyres and Kanis (1995), report that in some cases bone loss may persist indefinitely, even if an individual returns to function; however, other studies found that if function is restored after a period of unloading, the bone may eventually be able to adapt and recover some of the bone lost during the time of disuse (Bloomfield 2010; Minaire 1989; Sibonga et al. 2007). Some individuals may never completely regain lost bone mass, but their return to function certainly helps to instigate bone remodelling for mechanical adaptation. Consequently, radiographic features characteristic of osteopenia at the time of disuse may be obliterated or obscured after function is resumed and bone is remodelled.

2.1.3 Cross-Sectional Studies and Biomechanics in Biological Anthropology

Palaeoanthropologists and biological anthropologists use bone loading responses to comparatively evaluate activity, mobility, and bone loss in skeletal material. These studies employ a variety of methods to assess the cross-sectional properties of limb bones, including radiogrammetry, CT and laser scans, and latex moulds of the outer bone surface. O'Neill and Ruff (2004) remind researchers that not all measurement techniques are equal, but the variety of methods provide biological anthropologists with various options with which to approach biomechanical questions in skeletal remains. As biological anthropologists frequently use biomechanical methods in their research, it is only possible to review a sample of these studies in this section to illustrate the ways in which these methods contribute to broader anthropological questions.

Changes in limb cross-sectional morphology are used to investigate a number of questions about the mobility and activity levels of people in the past. For example, biomechanical studies in bioarchaeology include investigations into bipedalism (e.g., Bleuze 2012), intensity of terrestrial mobility (e.g., Macintosh et al. 2014; Shaw and Stock 2013), activity using the upper limb (e.g., Maggiano et al. 2008; Shaw and Stock 2009), and differences in the sexual division of labour (e.g., Ogilvie and Hilton 2011). These bioarchaeological studies of functional morphology help develop a better understanding of the differences in mechanical loading environments experienced by past peoples, especially in terms of temporal, geographic, and sex-related variability in activities.

Studies of age-related bone loss are also undertaken using cross-sectional measurements. Second metacarpal radiogrammetry is most frequently used to investigate the amount of cortical bone present and is particularly useful as it is a method developed and tested by clinicians to assess bone density and fracture risk (Dequeker 1976; Haara et al. 2006; Ives and Brickley 2004). A number of studies specifically investigated bone loss in Roman-period collections (e.g., Beauchesne and Agarwal 2011; Mays 2006a), a context that is of particular relevance in this thesis research. The studies that use Roman samples identified variable age- and sex-related patterns of bone loss. For example, Mays (2006a) found that the females at Ancaster, UK (one of the sites used in this research), had smaller cortical bone thicknesses, as well as fractures characteristic of osteoporosis. The Roman females at Velia, Italy, lost bone gradually from middle adulthood on, while the males did not lose bone until old adulthood (Beauchesne and Agarwal 2011). At Velia, Cho and Stout (2011) found no differences in bone amounts between the sexes, however at Isola Sacra, another city in Roman Italy, females lost more bone than males.

Sex differences in bone loss have not yet been compared at Roman Ancaster, however Mays (2015a) compared the bone loss in Ancaster males to males of other time periods and found that the risk was similar risk over time.

Palaeoanthropologists and biological anthropologists have, less often, combined functional morphology and biomechanical analyses to understand physical deficits in the past. Some studies found evidence for bone loss and altered cross-sectional properties suggestive of sustained unloading secondary to pathology (e.g., Sparacello et al. 2016; Trinkaus et al. 1994), while other studies argued for evidence supporting a general return to, or maintenance of, altered function (e.g., Cowgill et al. 2012; Holt et al. 2002; Lovell 2016). Still other research, including work by Lieverse et al. (2008) and Oxenham et al. (2009), identified large amounts of asymmetry and bone hypotrophy beyond what could be expected even in normal asymmetric circumstances, leading to interpretations of paralysis (not involving fractured bones). Although biomechanical research pertaining to disuse is not as common as studies of bone loss and habitual activities, this approach to unloading holds great potential for insight into the physical consequences and experiences of injuries in the past.

2.2 Fracture Mechanics

Bone tissue fails and fractures occur when stress and strain is in excess of what the bone can tolerate; the bone's tolerance threshold may be exceeded because the applied force is of high enough magnitude, or because it is prolonged, or applied to structurally compromised bones (Gupta and Zioupos 2008; Wescott 2013). The body can resist skeletal fracture in a variety of ways, ranging from structural adaptation, to soft-tissue cushioning and responses, to the actual organization of the bone matrix itself (Gupta and Zioupos 2008; Wescott 2013). The thickness and geometry of each bone type is tailored to resist the normal strains in an individual's mechanical environment. Additionally, bone is further protected from fracture by the deformation of soft tissues and eccentric contractions of muscles (Martin et al. 2015; Wescott 2013). The instrinsic organization of bone can also prevent a fracture from spreading by diverting and deflecting cracks, as well as responding by bridging cracks with matrix (e.g., cartilage), thus increasing the energy that is needed in order for the fracture to propogate further (Gupta and Zioupos 2008; Martin et al. 2015). However, as Fletcher et al. (2014) note, in instances where microdamage occurs too quickly or frequently, or in the event of advancing age and disease, the bone's ability to successfully repair microfractures is diminished.

In the event that a bone is not able to prevent failure, it will fracture. When this happens, different fracture mechanisms, magnitudes, and forces will result in the formation of differently shaped fracture lines that can then be used to interpret the fracture's cause. The mechanism of fracture, or the manner in which a force is applied to a bone, can include indirect and direct force trauma, as well as injuries related to stress and pathologically weaked bone (Wescott 2013). Catastrophic (i.e., complete) failures of bone are caused by rapid and dynamic loads greater than the bone's toughness, or ability to deform and resist the loads (Martin et al. 2015; McGee et al. 2004). The magnitude of the load applied to bone also influences the way that it breaks; in instances of rapid loading, a bone tends to fail with a comminuted and highly fragmented fracture (Martin et al. 2015; McGee et al. 2004). In contrast, when loads are applied more slowly, fractures are more likely to propogate in a simple, linear fashion (McGee et al. 2004). Fractures will be discussed in the following subsections in regards to the forces and fracture types that they are commonly associated with.

2.2.1 Indirect and Direct Force Fractures

Indirect trauma causes fractures to occur at a location other than where the force was applied and is often associated with oblique, avulsion, and spiral type fractures (Figure 2.2) (Lovell 2008). Direct trauma causes the bone to fail at the site of a direct blunt, penetrating, and/or sharp force blow and can cause transverse and butterfly fracture types, as well as sharp and penetrating injuries such as from a blade or projectile point (Figure 2.3) (Lovell 2008). Crush fractures are technically direct force fracture types, but when caused by instrinsic factors, such as the impact from another bone to a joint surface, they better represent indirect mechanisms.

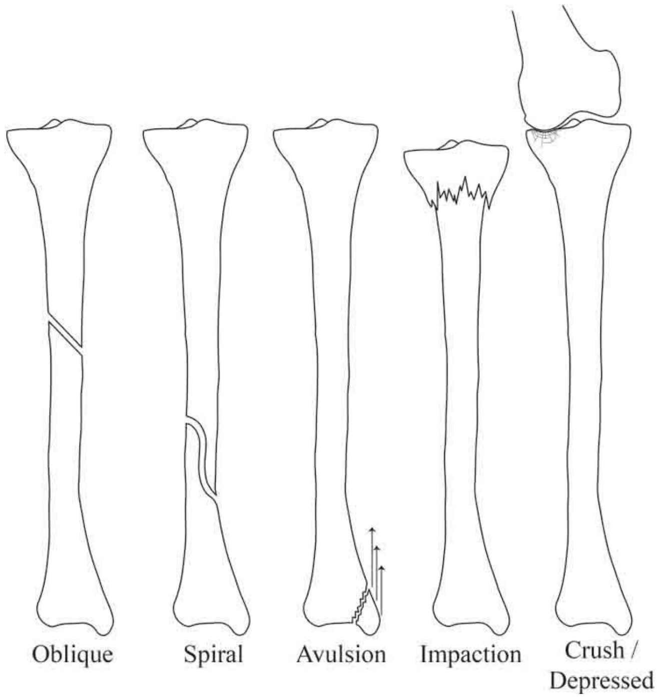

Figure 2.2 – Indirect fracture types. Image based on Lovell (1997: 143, Figure 2)

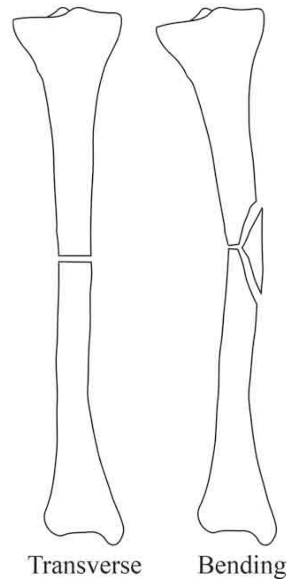

Figure 2.3 – Direct fracture types. Image based on Lovell (2008: 346, Figure 11.2).

Oblique fractures are often produced when a combination of compression, shear, bending, and/or torsion forces are applied from both the proximal and distal ends of the bone (Wescott 2013). These fracture types are situated diagonal to the long bone axis; when greater compression forces are involved, the fracture line exhibits a more obtuse angle (Wescott 2013).

Impacted, avulsion, and crush/depressed fracture types are typically located at the proximal or distal end of a bone and both avulsion and crush fracture types often involve the subchondral surface (Donatto 2001; Egol et al. 2010). Impacted and crush fracture types are generally produced by compression (force applied from two directions) and depression forces (force applied from one direction) (McGee et al. 2004). Impacted fractures are radiographically evident when one fracture segment is driven into the other fracture segment (often a diaphyseal segment is impacted into an epiphyseal segment) (Lovell 2008; McGee et al. 2004). Kobbe and Pape (2014) report that some crush fractures may be caused by a direct trauma blow, but many are caused by bone against bone impact at a joint. Avulsion fractures occur when a piece of bone is pulled off during a sudden tension event (Galloway et al. 2014; Rogers 1992).

Spiral fractures are caused by torsion forces, during which the twisting motion causes tensile and compressive stresses at 45° relative to the longitudinal axis (McGee et al. 2004). The bone fails in a helical shape, with the fracture line twisting around the shaft, the ends of which are usually connected by a longitudinal, shear stress fracture (Martin et al. 2015; McGee et al. 2004; Wescott 2013). Spiral fractures may involve one bone, or paired bones (e.g., both the tibia and fibula). When paired bones are fractured in a spiral manner, the fractures may propagate at opposite ends of the diaphysis (e.g., distal tibia and proximal fibula) (Hamblen et al. 2007).

Bending typically incorporates both compressive and tension forces. The side of the bent bone that is under tensile strain usually fails first, and in the shape of a transverse fracture line (Wescott 2013). When the bones are not under compression (e.g., weight bearing), the fracture line will be simple and transverse. In instances when compression is involved, the fracture line starts as transverse, but then usually splits on an angle to isolate a wedge-shaped fracture segment. This type of fracture is comminuted (i.e., consists of more than two main fracture segments) and referred to as a wedge or butterfly fracture type (Martin et al. 2015; McGee et al. 2004).

2.2.2 Stress, Age-Related, and Pathological Fractures

In addition to fractures caused by direct and indirect trauma, bone can also fail as a result of continued or repeated stress of a magnitude lower than the bone's threshold. Creep and fatigue fractures comprise the two main types of 'stress' fractures. Creep fractures are produced by a continuously applied stress, such as body weight, that causes the bone to deform for an extended period of time, whereas fatigue fractures occur as a result of a dynamic, or changing stress that is applied periodically or cyclically (e.g., walking) (Martin et al. 2015). Matcuk Jr. and colleagues (2016) state that normal loading can also cause stress fractures in osteopenic bone, and when this fracture type occurs in the pathologically weakened bone, it is referred to as an 'insufficiency' fracture. While stress fractures may occur in any bone, they are typically observed in the lower limb and body and are associated with weightbearing; insufficiency fractures frequently occur in the vertebrae, proximal femur, and medial femoral condyle (Matcuk Jr. et al. 2016).

According to Fletcher et al. (2014), creep and fatigue fractures are normal and expected, occurring at the micro-level as a result of repetitive loading from everyday activities such as walking. Bone remodelling can adjust to handle increased loads and damage; however, excessive loading can overwhelm the system (Hazelwood et al. 2001). Additionally, repeated loading can act to degrade bone's mechanical properties over time, making it less able to remodel microfractures (Huang and Ogawa 2010; Turner and Burr 1993). The accumulation and coalescence of microfractures, beyond what the bone can manage to remodel, increases the risk for bone failure (Fletcher et al. 2014; Turner and Burr 1993). Aging bones are particularly susceptible to accumulating microdamage, a fact that alongside bone loss may contribute to increased fragility and fracture risk in older individuals (see Section 2.1). Ensrud (2013b) notes how this combined fracture risk, both compromised bone and a greater propensity to fall, predispose older individuals to fractures. Specific patterns of age-related fracture risks include not only hip fractures related to the bone's inability to withstand loads, but also compression fractures to vertebrae from decreased bone mass, and to the distal radius due to both falls on an outstretched hand and diminished bone amounts (Ensrud 2013b).

It is often difficult to distinguish between fractures caused by bone loss associated with normal aging processes, and bone loss related to pathological processes. Like fractures to thinning and aging bone, pathological fractures also occur as a result of bone that is weakened and less able to resist loads (Derikx et al. 2015; Ensrud 2013b; Raptis et al. 2014). Pathologically weakened bone is associated with either diffuse or localized bone loss and can occur as a result of various diseases, disorders, and deficiencies, including: metabolic bone diseases (e.g., osteomalacia, Paget's disease), bone cysts and tumors, and infection (Derikx et al. 2015; Raptis et al. 2014; Wescott 2013). Despite the difference in the underlying pathological cause for the fracture, bones still respond to forces in the same manner, and are still susceptible to the same fracture types discussed in the previous paragraphs. For example, bone loss associated with advancing age is often associated with fragility fractures of the proximal femur (Kanis et al. 2013). In these fractures, pathologically compromised bone is less able to resist the normal compressive and torsional strains that occur during weight bearing, and frequently results in long spiral fractures caused by torsion and compressive forces (Bedi and Le 2004; Sims 2002).

2.3 Biology of Fracture Healing

Fracture healing is divided into three, overlapping phases: inflammatory, reparative, and remodelling (Claes et al. 2012; Martin et al. 2015). Different fracture types, elements, and locations can heal at variable rates and are dependent on many factors such as: individual age, activity, nutritional status, comorbidities, and mechanical stability of the fractured bone (Claes et al. 2012; Frost 1989; Gaston and Simpson 2007). Although it is possible for some fractures to heal via direct bone healing between fracture ends without an intermediary cartilage callus, fractures more commonly mend by secondary bone healing (i.e., cartilage ossification) (Gaston and Simpson 2007; McKinley 2003). This section covers the stages of secondary bone healing as it relates to fractures, and describes how each stage might be identified in analyses of archaeological skeletal material.

Fractures not only involve a broken bone, but are also associated with various degrees of damage to the surrounding soft tissues and blood vessels. The first stage of fracture healing is the "inflammation" phase. The inflammation phase is primarily anabolic in nature, meaning that new tissues are produced, and is characterized by the formation of a hematoma and fibrous union between fracture fragments (Einhorn and Gerstenfeld 2015). This stage is very important in beginning the cascade of fracture healing. The steps must happen in order in order to initiate the following fracture healing phases; if one stage is improperly realised, fracture healing will be impeded or prevented (Martin et al. 2015).

Tissue damage surrounding a fracture initiates an inflammatory response, and blood from the ruptured blood vessels collects at the fracture site to form a hematoma. By approximately three to seven days after the fracture, these responses provide some immobilization to the fracture site via pain, swelling, and a hydrostatic splint (Martin et al. 2015; McKinley 2003). Current thought is that the cells involved in fracture healing actually originate from the marrow and periosteum, and while the hematoma provides some stability to the fragments, its main function is to activate the stem cells that are responsible for repair (Huang and Ogawa 2010; Martin et al. 2015). Through the process of mechanotransduction (see Section 2.1.1), stem cells are differentiated into osteoblasts or chondroblasts as needed (Huang and Ogawa 2010; Martin et al. 2015). Einhorn and Gerstenfeld (2015) indicate that the tissues from which the stem cells are derived and the amount that will become cartilage or bone cells are influenced by the extent and severity of the trauma and the amount of mechanical strain present at the fracture site.

Once a hematoma is established at the fracture site, a fibrous and cartilaginous connection can begin to form. During the formation of the cartilaginous, soft callus, the anatomical location and the mechanical stability of the fracture greatly influence outcomes (Claes et al. 2012; Einhorn and Gerstenfeld 2015). Wraighte and Scammell (2006) suggest that moderate amounts of movement at the fracture site, as is common in conservative treatments, stimulate the formation of cartilage tissue between the fracture ends. In comparison, low amounts of inter-fragmentary movement can result in the direct formation of bone, while excessive movement can prevent any type of bridge forming between fragments (Claes et al. 2012; Martin et al. 2015). Once a fibrocartilaginous callus has been established and joins the fracture fragments, it is mineralized/calcified, providing the necessary framework for the revascularization necessary for later ossification (Einhorn and Gerstenfeld 2015; McKinley 2003).

Within a few days of the fracture event, the periosteal margins of this fibrocartilaginous callus begin to swell and will form primary new bone (Einhorn and

Gerstenfeld 2015). At the same time, disturbance to the marrow instigates the formation of new woven bone in the medullary canal. The periosteal callus is often more obvious than the endosteal callus, however in terms of initial union, the endosteal callus is thought to be more important (Martin et al. 2015). A study by De Boer et al. (2012) examined the stages of fracture healing evident microscopically and radiographically in archaeological bone. De Boer et al. (2012) found that endosteal callus formation was the first radiographically visible sign of fracture healing, beginning after ten to 12 days, whereas periosteal callus formation was visible after 15 days. New bone associated with the endosteal callus formation therefore represents the first evidence of fracture healing visible in archaeological bone. Prior to this point, the fractures would be identified as perimortem from macroscopic examination.

The next main stage of fracture healing is the reparative phase. Unlike the inflammatory stage that focusses primarily on building new tissue, the reparative stage is mostly catabolic, and involves secondary bone formation (i.e., ossification of the cartilage) and bone remodelling activities (Einhorn and Gerstenfeld 2015). In this stage, a 'provisional' callus is created by replacing the mineralized cartilage with bone (endochondral ossification) (Claes et al. 2012; Einhorn and Gerstenfeld 2015; McKinley 2003). Additionally, the periosteal woven bone is reorganized as trabeculae to bridge the space between fracture fragments (Martin et al. 2015). When the provisional callus unites the fracture fragments and becomes more rigid, it is called a 'bony callus' and signifies the end of the reparative phase (Claes et al. 2012; Martin et al. 2015). At this stage of healing, the material that comprises a bony callus is not as strong as the original cortex, but mechanically, the size and geometric structure of the bony callus means it is often stronger than the original bone itself (Martin et al. 2015).

The final stage of fracture healing is the remodelling phase, in which the bony callus is shaped and converted to lamellar bone. During this stage, the bony callus is remodelled and the periosteal and medullary calluses are replaced with lamellar bone (Martin et al. 2015). Gradually, the bone's original shape, contour, and structure are restored. Some degree of healed angulation can be corrected during this stage, especially in juvenile individuals, but rotational deformities are less correctable (Einhorn and Gerstenfeld 2015; Martin et al. 2015). The trauma is considered fully healed when the bony callus is converted to lamellar bone and the vascular systems are fully restored (Einhorn and Gerstenfeld 2015).

2.4 Fracture Complications

Factors related to the fracture itself, the success of fracture healing, the individual who sustained the fracture, and the socio-cultural environment in which that individual lives, can predispose an individual to injury complications. Complications such as infection and damage to soft tissues may arise immediately as a result of the trauma itself, but others can develop later during or after injury healing, including delayed, non-, and mal-union.

2.4.1 Delayed Union and Non-Union

Clinically, non-union occurs when the ends of fracture segments/fragments fail to bridge and heal between six to eight months after injury, occasionally developing into a pseudoarthrosis, or false joint (McKee 2000; Panagiotis 2005). Delayed union is when fractures have not healed in the time typically expected for that bone type. In archaeological contexts, fractures with delayed union may appear similar to fractures that are still healing; in these instances there is no definitive way to know if a fracture would have healed had the individual survived longer.

According to McKee (2000), delay and/or non-union of fractures is influenced by a number of factors including: vascular damage, an absence of or insufficient stabilization, non-compliance if treatment is attempted, as well as age, diet, and general health of the individual. The risk for delayed and non-united fractures is increased in the event of considerable tissue damage in that damage to the surrounding tissues acts to deplete the available amount of stem cells needed for fracture healing (Einhorn and Gerstenfeld 2015). As outlined in Section 2.3, any interruption to the cascade of fracture healing, such as unavailable stem cells, acts to inhibit the success of fracture bridging and increases the risk for delay and non-union of fractures.

Although bone continuity is not restored in non-united fractures, the ends of these fracture fragments often have evidence of new bone formation and/or remodelling. Hypertrophy at the non-united fracture site is mainly caused by mechanical instability of the fracture whereby movement at the fracture site irritates the periosteum, initiating new bone formation (Harwood et al. 2010; McKee 2000; Panagiotis 2005). Hypertrophic non-unions typically exhibit an elephant foot or horse hoof type shape (McKee 2000; Panagiotis 2005) (Figure 2.4). In contrast, atrophic non-united fractures exhibit little to no new bone formation, frequently related to disturbed vascularization or low-to-absent force transmission at the fracture site (McKee 2000; Panagiotis 2005). McKee (2000) describes non-united fragment ends as typically rounded and note that the distal fragment may become osteopenic due to non-use. Additional features characteristic of non-united fractures include sclerotic bone margins and eburnation at the fracture site (Melenevsky et al. 2011; Panagiotis 2005).

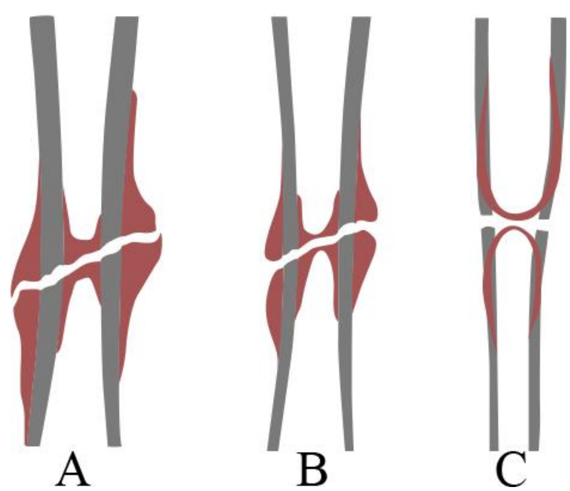

Figure 2.4 – Morphology of non-united fractures. Images A and B depict hypertrophic non-unions. Image C depicts an atrophic non-union. Grey indicates original cortical bone. Red indicates new bone, often sclerotic, that seals the medullary cavity in non-united bones. Image adapted from McKee (2000: 152, Figure 6.2-2).

2.4.2 Malunion

A fracture is malunited when it heals in a less than anatomically optimal position. Types of malunion include displacement (i.e., angulation and/or rotation), poor apposition, and/or overlap of fracture segments, as well as overall shortening of the bone itself (Frost 1989; Lifeso and Younge 1990). Overlap and angulation at a fracture site can alter the length of the bone, and rotation can change the angle of joint surfaces, all of which can negatively influence functional outcome and result in the development of secondary osteoarthritis, dysfunction, and pain (Batra and Gupta 2002; Karnezis et al. 2005; Van Der Schoot et al. 1996). The amount of clinically acceptable malunion is reported for some long bone elements, such as radii, clavicles, and tibiae (e.g., Altissimi et al. 1986; Ledger et al. 2005; Van Der Schoot et al. 1996); however Beerekamp et al. (2011) observe that these values are often derived based on the restoration of anatomical normalcy, rather than their association with functional outcome.

Fracture reduction, or restoration of the fracture to the original alignment, is recommended in modern surgical practice in order to achieve an optimal functional outcome (Beerekamp et al. 2011). Untreated fractures have a tendency to heal with comparably greater amounts of deformity, although it is possible for untreated fractures to heal with minimal malunion (see Lovell's 1990 study of non-human, untreated fractures). Due to the relationship between malunion and a lack of successful treatment, malunited fractures are often used by bioarchaeologists as evidence that treatment was either not sought or was unsuccessful; that is, there was not proper reduction or stabilization of the fractures (e.g., Grauer and Roberts 1996; Roberts 1988a).

To assess unsuccessful fracture healing in the past, Roberts (1988a) suggests a model based on radiographs and patient records of living people in the UK with conservatively treated fractures (i.e., reduced and traditionally splinted using an external cast). This study proposes amounts of displacement, apposition, overlap, and shortening that were associated with fractures that were untreated, or where conservative treatment failed. It can be problematic to use modern clinical data in interpretations of the past as modern groups have different diets and co-morbidities that can affect fracture healing.

However, Roberts (1988a), whose methods were also used by Grauer and Roberts (1996), is currently the only researcher to synthesize and quantify aspects of fracture malunion as it relates to conservative treatment (assumed to be analogous to the past). When Roberts' (1988a) malunion values are used with caution, they are justified in helping to evaluate if a fracture was untreated or if treatment was unsuccessful. The application of Roberts' (1988a) method is further described in Section 4.5.2.

2.4.3 Inflammation and Infection

Open (compound) fracture fragments cause soft tissue wounds that break the skin, allowing infection-causing microorganisms to enter the body. When a pathogenic organism is introduced to the body, an inflammatory response is initiated in order to suppress the foreign organisms. The terms inflammation and infection are not synonymous; inflammation is a complex vascular response to irritations such as those caused by pathogens and trauma, while infection is the invasion of a host organism by microorganisms that cause disease such as bacteria, viruses, fungi, and parasites (Boutin et al. 1998; Signore 2013; Weston 2012). Infection is usually associated with inflammation, but inflammation is not always indicative of infection.

When a pathogenic organism infects and inflames the bone and bone marrow, it results in osteomyelitis. Symptoms of acute osteomyelitis include localized pain, swelling, fever, and necrotic wound edges; these symptoms are more variable and less obvious as the infection becomes chronic (Mouzopoulos et al. 2011). Radiographic changes associated with acute osteomyelitis become apparent after 10 to 15 days, and include hazy, slightly radiolucent localized regions, and some periosteal thickening (Mouzopoulos et al. 2011). Diagnostic features of chronic osteomyelitis include bone sequestration, paired with the formation of an involucrum (new bone formation on the periosteal and endosteal surfaces) and draining sinuses (Boutin et al. 1998; Mouzopoulos et al. 2011). According to Mouzopoulos et al. (2011), only approximately 30% of open fractures may develop osteomyelitis, but when an infection is present, it may cause atrophic non-union of the fracture.

Unlike osteomyelitis, inflammation of the periosteum is not necessarily indicative of infection. When the periosteum becomes inflamed, the inflammation acts to trigger the production of new bone on the periosteal surface (i.e., periostosis) (Weston 2012). This inflammation, and thus the formation of periosteal new bone, can be initiated by various mechanisms that are unrelated to infection; almost anything that irritates or touches the periosteum can instigate the formation of new bone (Chen et al. 2012; Saulacic et al. 2013; Weston 2012). Weston (2012) warns that the many possible aetiologies of periosteal new bone formation mean that caution is required in interpreting its cause; without consideration of the complete skeleton, periosteal new bone should not be used as a reliable indicator of infection. One must be careful in interpreting infection from evidence of periosteal inflammation in skeletal materials; while osteomyelitic lesions may be clear indicators of bone infection, periosteal new bone changes should not immediately be assessed as such.

2.4.4 Osteoarthritis

The understanding of osteoarthritis (OA_x) as simply related to wear and tear and joint degeneration has changed. Researchers now see the process as more complex, involving all the joint tissues (e.g., synovium, bone, and cartilage), as well as an interplay between mechanical, biochemical, genetic, and immunological factors (Berenbaum 2013; Bijlsma et al. 2011; Kohn et al. 2016; Loeser et al. 2012). The pathogenesis of osteoarthritis is still under debate, but Kapoor (2015) suggests that it may begin as a result of mechanical injury, inflammation in the synovium affecting the cartilage, or a problem with cartilage metabolism and homeostasis. Once initiated, the development of osteoarthritis becomes a vicious cycle; degrading cartilage inflames the synovium, the inflamed synovium produces inflammatory mediators that activate chondrocytes and result in further cartilage degradation, more degradation results in more inflammation, and the cycle repeats (Berenbaum 2013).

The risk of osteoarthritis increases with age, after injury to the joint, as a result of obesity, genetic predisposition, and due to other mechanical factors (e.g., malalignment and joint shape) (Loeser et al. 2012). In particular, greater amounts of inflammatory mediators are produced with advancing age, and senescent chondrocytes are less able to keep up with the maintenance and repair of the articular cartilage (Greene and Loeser 2015; Kapoor 2015). In terms of post-traumatic osteoarthritis, the inflammation arising as one of the first stages of healing after trauma can inadvertently contribute to the degradation of the cartilage, thus further predisposing individuals with joint injuries to osteoarthritis (Buckwalter and Felson 2015; Loeser et al. 2012). Although the reasons for insufficient repair of joint tissues differ from trauma to chemical to senescence, the overall commonality among at-risk joints is that they are unable to keep up with the damage caused by mechanical stress (Bijlsma et al. 2011). As such, the abnormal remodelling of joint tissues seen with osteoarthritis are now best interpreted as an injury response (Loeser et al. 2012). According to Anderson et al. (2011), over 40% of individuals with injuries involving the joint and articular surfaces develop osteoarthritis, and 12% of people with osteoarthritis had a previous joint injury.

Most joint tissue is aneural, so the effects of osteoarthritis (pain and stiffness) are typically not noticed by an individual until the condition affects adjacent tissue with nerves (Bijlsma et al. 2011). This means that osteoarthritis is rarely diagnosed early in clinical settings. Once an individual seeks treatment, osteoarthritis can be identified using both clinical and radiological features. Clinical features include pain, limitations in motion, swelling, and joint stiffness and enlargement (Bijlsma et al. 2011). Salat et al. (2015) summarize the radiological features consistent with osteoarthritis, including the narrowing of the joint space, the presence of osteophytes, subchondral sclerosis, subchondral cysts, and deformity of the bone ends. However, approximately half of the individuals with radiological features and structural changes in clinical settings do not actually experience clinical features and vice versa (Bijlsma et al. 2011).

A method for assessing osteoarthritis in dry bone was proposed by Rogers and Waldron (1995) and scores the presence of marginal osteophytes, joint contour changes, porosity, and eburnation. However, the poor association between skeletally observable lesions and the experience of osteoarthritis in clinical settings creates difficulties in interpreting osteoarthritis in the past. Some past individuals with skeletal evidence for osteoarthritis may not have known that they had the disease, just as some individuals with few to no skeletal manifestations may have experienced considerable joint discomfort.

2.4.5 Vascular & Nerve Injury

Soft tissues, such as blood vessels can be damaged during a trauma event or due to the movement of sharp fracture segments. While a certain amount of vascular damage is expected in fracture trauma, and is required for fracture healing, injuries to blood vessels, particularly arteries, can be a severe complication of fracture and may result in loss of the limb, and sometimes result in death due to excessive blood loss (Hamblen et al. 2007; Schlickewei et al. 1992).

Nerve damage can result in complete or partial paralysis (palsy), and can occur either directly as a result of fracture or during the course of treatment and healing (DeFranco and Lawton 2006). The rates of nerve injuries associated with fractures vary, but Taylor et al. (2008) determined that only 1.64% of uncomplicated fractures resulted in nerve injury in a modern sample from the United States. Of the observed nerve injuries associated with fractures, injury to the radial and/or ulnar nerve caused by humeral fractures are the most common (DeFranco and Lawton 2006; Taylor et al. 2008). Additionally, DeFranco and Lawton (2006) found that while secondary palsies often heal, palsies resulting from primary nerve damage may never improve. If peripheral palsies are sustained, decreased mechanical loading will result in muscle atrophy and cause identifiable bone loss over time (Boonyarom and Inui 2006; Giangregorio and McCartney 2006; Takata and Yasui 2001).

Soft tissues are usually absent in archaeological assemblages, so it is not possible to directly identify damage to vasculature or nerves. Individuals that experienced life-threatening blood loss associated with a fracture were unlikely to have survived, and therefore would not have any evidence of new bone indicative of healing. As such, very severe vascular injury that resulted in an individual’s death would be expected to be associated with perimortem fractures. In the case of nerve, or other less life-threatening soft tissue damage, an individual may experience immobility and thus mechanical unloading, which may result in identifiable biomechanical changes associated with disuse (see Section 2.1).

2.5 Risk for Post-Traumatic Functional Complications

In the extremities, functional complications (e.g., dysfunction) may manifest as a total or partial loss of mobility, decreased range of motion, discomfort, and pain. An individual's functional outcome after fracture may be predicted by the severity of the initial fracture, duration of immobility during healing, pre-existing physiological factors (e.g., age), fracture complications (e.g., mal-union, neuropathy), the amount of pain experienced after injury, and how an individual perceives and copes with an injury (Lovgren and Hellstrom 2012; Ponsford et al. 2008).

2.5.1 Fracture Severity & Location

Fracture severity can be assessed based on the type of fracture present, if it is simple (i.e., two fracture fragments) or comminuted (i.e., more than two fracture fragments), if it is open or closed, and the extent of damage to soft tissues and joint surfaces (Baker et al. 1974; Civil and Schwab 1988). A study by Kundel et al. (1996) reports that open fractures often had poorer functional outcomes than closed fractures. Additionally, research by MacDermid et al. (2002) found that greater bone displacement and damage to soft tissues during the trauma event was a better predictor of poorer functional outcomes than fracture reduction. Although some studies identify a relationship between fracture severity and dysfunction, these findings remain contentious. A study by Lin et al. (2009) report that injury variables (e.g., severity) were not predictive of long-term impairment. Furthermore, a study by Ponsford et al. (2008), suggest that non-injury related factors, such as psychological trauma, play a significant role in residual impairments after injury.

In archaeological contexts, it is not usually possible to observe the extent of damage to soft tissues as they are not normally preserved. Additionally, many observed fractures are healed and are affected by some amount of human intervention (i.e., reduction and stabilization). This means that the initial displacement of fragments and the extent of soft tissues cannot be directly assessed in skeletal remains. Beyond consideration of the fracture location, type, and associated infection indicative of an open (i.e., more severe) fracture, the use of fracture severity as a risk factor for impairment is limited in bioarchaeological assessments of trauma.

2.5.2 Immobilization

Physicians and surgeons often prescribe limb immobilization, involving rest and stabilization of the fractured limb (e.g., casting, splinting, surgical fixation), as part of fracture treatment. Although some stabilization is necessary for bones to mend successfully, there is evidence that a long duration of limited activity can be functionally detrimental (Byl et al. 1999; Shaffer et al. 2000). Extended periods of limb immobilization associated with fracture treatments cause mechanical unloading of the immobilized tissues leading to muscle and bone atrophy in the affected limb and impediments in range of motion and muscle strength (see Section 2.1.2).

Clinical studies have found that most musculoskeletal patients respond well to early mobilization, especially of the muscles and joints neighbouring the affected area (Hodgson 2006; Kristiansen et al. 1989; Nash et al. 2004). Returning to function as soon as possible can speed recovery, increase range of motion, reduce pain, and diminish the amount of compensatory movement. Additionally, detrimental effects such as reduced range of movement and muscle weakness that arise secondary to immobility treatments can be mitigated with movement, which acts to reduce swelling and minimize the adhesion of tendons (Millet and Rushton 1995; Simic and Weiland 2003). Consequently, in healthy individuals with normal rates of fracture healing, it is not always necessary to maintain sustained immobilization of the fractured limb, and may in some instances be beneficial in the long term to resume movement earlier.

2.5.3 Anatomical Restoration

Poor anatomical restoration, that is, the lengthening/shortening and the angulation of fracture segments relative to one another, is linked with poor functional outcome in a number of clinical studies (e.g., Batra and Gupta 2002; Engsberg et al. 2014; Greenwood et al. 1997; Ledger et al. 2005). In order to minimize poor functional outcomes (e.g., pain and loss of function), modern orthopaedic practitioners strive to reduce and re-align fracture segments, thus restoring anatomic normalcy to a fractured bone. Unfortunately, it is generally not possible to standardize reduction criteria (e.g., the amount of allowable angulation), as what is considered acceptable varies greatly depending on the age of the individual as well as the type and part of the bone that is involved. According to Frick (2015), it is not considered necessary to achieve perfect restoration in paediatric fractures as the bone usually self-restores with modelling and normal growth. Hartley et al. (2015) report that although anatomical restoration of articular fractures is generally important and encouraged, some joint surfaces, such as tibial plateaus, tolerate greater amounts of malalignment than other joint types. A review of distal radial fracture treatments by Simic and Weiland (2003) notes that when natural anatomical alignment was disrupted, secondary pathology (e.g., osteoarthritis) and biomechanical instability could develop.

Although orthopaedic practitioners strive to return a fractured bone to its anatomically normal state, this does not necessarily guarantee that an individual will have a good functional outcome. That is, the restoration of anatomic ‘normalcy’ in fractured bones does not always correlate with functional outcome. Authors such as Simic and Weiland (2003) and Batra and Gupta (2002), both reporting on distal radial fractures, observe that it is still possible for a ‘poor anatomical result’ to demonstrate exemplary function and vice versa. This variable relationship can likely be extended to all bones of the extremities as other factors, such as pain, coping, fear, and self-efficacy also play an important role in influencing functional outcomes after fracture.

2.5.4 Pain, Coping, & Fear

The ability to feel pain, that is register nociceptive stimuli at the nervous system level, is accepted as a universal human experience (Woolf 1989). In modern, Western clinical contexts, pain and fear can play a significant role in inhibiting function after injury. In the case of fractures, pain may be caused by the injury itself, or as a result of secondary complications that arise after the fracture has healed, such as osteoarthritis. However, how pain is tolerated differs greatly among individuals as well as groups (e.g., cultural, gender), suggesting that socio-cultural norms and individual psychological factors act to influence the reaction to and perception of pain (Bates 1987; Honkasalo 2001). Individuals within the same group will vary in their perception, tolerance, reaction, and overall experience of pain due to complex personal factors such as cognition, personality, gender, and lived/embodied experiences (Honkasalo 2001; Kennedy et al. 2011).

People adopt coping and compensation strategies such as behaviour modification, the use of external supports (e.g., crutches), and/or avoidance of tasks in an effort to alleviate or prevent perceived discomfort. The type of coping strategy that an individual adopts is influenced more by logistical, personal, and socio-cultural factors rooted in past experiences of injury and pain/discomfort, than is correlated with the actual severity of impairment (Tomey and Sowers 2009). Personal coping style (e.g., fear-avoidance tactics) and perceptions of pain play an important role in the maintenance of impairment associated with injury, as well as the development of secondary problems, such disuse and consequent bone atrophy (Crombez et al. 1999; Vlaeyen and Linton 2000; Vlaeyen et al. 1995). Coping strategies focused on physiological alteration of the way in which an activity is undertaken (e.g., gait asymmetry) can result in uneven tissue hypertrophy and possible over-use injuries (Becker et al. 1995; Segal et al. 2014; Wang et al. 2010). In particular, Vlaeyen et al. (1995) and Vlaeyen and Crombez (1999) identify avoidance as an alternative coping method in which the long-term maintenance of protective behaviours will result in disuse of tissues, bone loss, and detrimental functional consequences. Although individual perceptions of pain and chosen coping methods may differ, pain is still part of the injury experience and therefore must be considered as a possible factor in some past impairment. However, this is not to say that through the study of impairment it is possible to know an individual's experience of pain, coping, and fear, but only that these factors may play a role in the post-traumatic risk for dysfunction.

2.6 Asymmetry: Types and Pathology

Various types of asymmetry may manifest in the skeleton, however not all are associated with function and mechanical loading (e.g., directional asymmetry), some skeletal asymmetries are related to developmental stress (e.g., fluctuating asymmetry). Fluctuating asymmetry (FA) is defined as small, random deviations from bilateral symmetry, which are normally distributed around a mean of zero (Palmer and Strobeck 1986; Zaidi 2011). This type of asymmetry is thought to be associated with an individual's inability to adjust to stress during development due to environmental, genetic, physical, and nutritional pressures (Barrett et al. 2012; Zaidi 2011). Anthropological studies of FA often consider dental evidence, such as asymmetric discrepancies in tooth size (e.g., Barrett et al. 2012), but FA is also investigated using human long bone lengths. The random, and normally distributed nature of FA suggests that any asymmetries that it causes will not greatly impact the assessment of the magnitude of other types of asymmetry (Palmer and Strobeck 1986; Zaidi 2011).

Unlike FA, directional asymmetry (DA), also referred to as functional or bilateral asymmetry, is primarily associated with biomechanical adaptation of bone due to functional strain (Palmer and Strobeck 1986; Zaidi 2011). Differences in patterns of loading strains can result in the variation of biomechanical adaptations between right and left sides, allowing directional asymmetry to manifest either through hypertrophy or by atrophy of the bone tissue (Auerbach and Ruff 2006). Investigations of DA are important in anthropology as they contribute to the understanding of human activities and laterality (e.g., Marchi et al. 2006; Rhodes and Knusel 2005; Shaw 2011; Shaw and Stock 2009), as well issues of health and pathology, especially as it relates to physical impairment (e.g., Morbeck et al. 1991; Thompson 2012).

The dominant preference of one side of the body over the other, such as in handedness and activities, is known as laterality. Side-biased increases in loading patterns associated with hand dominance and certain physical activities (e.g., racquet sports) can result in hypertrophy of tissue thickness, asymmetries in cross-sectional shape, and differences in bone mineral density between limb sides (Auerbach and Ruff 2006; Biewener and Bertram 1993; Ducher et al. 2005). A largely right-handed bias is present both in modern and past peoples (Auerbach and Ruff 2006; Steele 2000), but side dominance can vary as a result of activities (Ducher et al. 2005; Jones et al. 1977; Shaw and Stock 2009), as well as the influence of cultural factors, such as those acting to stigmatize left-hand dominant use (Corbeill 2004; Steele 2000).

Asymmetric mechanical adaptations are more prominent in the upper limbs than the lower limbs due to laterality and hand preference, whereas mechanical strains acting on the lower limb are much more uniform and primarily involve stresses associated with locomotion and balance (Auerbach and Ruff 2006; Shaw 2011). Despite more symmetrical forces, lower limbs can still exhibit side-bias, but unlike the predominantly right-biased upper limb asymmetries, the lower limbs are more left-biased, a pattern termed 'crossed symmetry' (Auerbach and Ruff 2006; Ruff and Jones 1981; Shaw 2011). Explanations for crossed symmetry vary from cognitive and developmental concepts, to functional ones that suggest a left lower limb side bias develops due to the greater degree of stabilization needed to perform tasks with the right (e.g., kicking) (Auerbach and Ruff 2006; Ruff and Jones 1981; Shaw 2011).

Limb asymmetry can also develop consequent to pathology, and is linked with diseases such as poliomyelitis (e.g., Morbeck et al. 1991; Thompson 2012), amputations (e.g., Kulkarni et al. 1998; Lazenby and Pfeiffer 1993), and fractures (e.g., Eyres and Kanis 1995). In these cases, paralysis and injuries commonly occur unilaterally, meaning that only one side is likely to experience immobilization and unloading resulting in bone loss. However, the inability to use a limb may result in accentuated compensatory activity by the opposing limb and/or other supporting tissues, resulting in possible bone hypertrophy (Becker et al. 1995; Segal et al. 2014; Wang et al. 2010). Through the combination of bone atrophy consequent to immobilization, and bone hypertrophy through coping and compensatory response, limbs of fractured individuals may develop larger than expected amounts of directional/bilateral asymmetry.

2.7 Disability or Impairment, What's the Difference?

A number of theories have developed to characterize individual experiences of physical differences and 'disability'. The two most frequently applied models of disability, the 'medical' and 'social' models, represent the most extreme ends of disability-oriented theory, differing primarily in their view of the causes of disablement (Palmer and Harley 2012; Shakespeare and Watson 1997). The medical model solely defines disability based on biological dysfunction (i.e., impairment), and implies that individuals need to be treated and cured of their differences (Brandon and Pritchard 2011; Llewellyn and Hogan 2000). As such, supporters of the medical model (primarily physicians, clinicians, as well as some government and insurance officials) tend to use the term 'disability' synonymously with terms such as 'impairment' to describe compromised physical and/or cognitive function (Rothman 2010; Shakespeare 2012). In contrast, the social model of disability, introduced in the 1960s by disability activists, rejects the medical labels and implications that individuals with impairment(s) are less able, less independent, and less healthy than the majority of the population (Gleeson 1997; Oliver 1996; Shakespeare and Watson 1997). Llewellyn and Hogan (2000) summarize that, in the social model, disability is caused solely by exclusionary social and physical structures, that is to say that individuals with impairments are not 'disabled' by their biology, but rather by the discriminatory, oppressive, and stigmatizing behaviours and environments within society.

In the last fifteen years it has become evident that neither the social nor the medical models are sufficient to realistically characterize the scope of disability, prompting the suggestion of a new, more inclusive, 'cultural' model of disability (Shakespeare 2012; Snyder and Mitchell 2010). The 'cultural' model described by Snyder and Mitchell (2010) accounts for both the lived-reality of a compromised biological state as well as the disabling impacts of marginalizing social and physical environments. This approach recognizes "identity and body as constructed", preserving the role of biological impairment, rather than discarding it as the social model does (Snyder and Mitchell 2010: 7). Physiological impairments experienced by people with disabilities likely comprise an important aspect of their embodied identities, which play a role in the disadvantages they encounter, and contribute to how they experience their world (Shakespeare 2012). This revised view of disability, described by Shakespeare (2012) recognizes the role of the biological body as integrated with an individual's greater physical and social environments, the combination of which lead to manifestation of a lived experience of disability.

Interpretations of disability in the past must be grounded in a detailed understanding of a society's culture(s), behaviours, and environments; it is not possible to draw conclusions about disability based on skeletal evidence alone. Often, the socio-cultural information available to bioarchaeologists is insufficient to permit accurate insight into many aspects of social identity, oppression, and exclusion in the past. For the purposes of this research, evidence for physical dysfunction associated with fractures is used to indicate impairment (i.e., biologically compromised function). This use of the term impairment will allow for discussion of the physical, lived experiences of injury, but does not permit interpretation of disability in the social sense.

2.7.1 Bioarchaeological Evidence for Disability and Care

The ability to identify and interpret evidence of past disability, care, and/or compassion based primarily on the assessment of human skeletal remains has been contested over the past 25 years. Working from a social model of disability perspective, Dettwyler (1991) first raised concern about using palaeopathological evidence alone to interpret individual quality of life or the presence of compassion from other group members. Although Dettwyler's (1991) comments on the limitations of bioarchaeological interpretations of past disablement remain valid, there has been a recent renewed interest in individuals of difference (i.e., impaired and/or disabled) and human experience in the past (e.g., Finlay 1999; Hegmon 2016; Lovell 2016; Oxenham et al. 2009; Tilley 2015; Tilley and Oxenham 2011).

Recently, new theoretical approaches have been introduced that strive to understand the human condition in the past. The *Archaeology of Human Experience* works to understand and explain what it was like to actually live in the past (Hegmon 2016), whereas research by Tilley into *the Bioarchaeology of Care* (e.g., Tilley 2015; Tilley and Schrenk 2016) has led to the renewed consideration of physical impairment, specifically in terms of the provision of care in the past. Tilley's (2015) *Bioarchaeology of Care* model does not stand in contradiction to Dettwyler (1991) as this model does not attempt to interpret social perceptions of disability. Instead, the focus in the *Bioarchaeology of Care* is placed on the biological severity of the impairing conditions and the symptoms and consequences that probably would have resulted (Tilley 2015). The functional repercussions of pathological conditions are examined by Tilley (2015) in order to assess the extent of assistance that an individual would have required in order to accomplish certain tasks (e.g., personal hygiene, eating). Although the term 'care' is used in this model, Tilley (2015) makes it clear that this does not necessarily imply that assistance was provided with compassion and kindness.

Tilley's (2015) approach to studying past care provision via evidence for severe impairment provides insight into some aspects of physical function and social response to severe impairment in the past. However, this model is only applicable to individuals with evidence for significant and severe physical impairment (Tilley 2012). It is important that the relationship between pathology and impairment continue to be carefully considered in order to learn as much as possible about the lives of all past peoples, not just those with extreme evidence for pathology.

2.8 Greco-Roman Medicine & Fracture Treatments

Roman medical knowledge and techniques were based on earlier Greek traditions and much of what is currently known about Greco-Roman medicine is interpreted from classical medical texts written by scholars such as Hippocrates (ca. 5th-4th century BC), Celsus (25 BC-50 AD), and Galen (129 AD – ca. 215 AD) (Brorson 2009; King 2001; Nutton 2013). Recognized centres for medical training were not present in the Roman Empire and healers often trained via practical experience and apprenticeship (Cilliers and Retief 2006; Scarborough 1970). Magic and home remedies would have regularly featured in Roman medicine and were used by traditional healers. Traditional healers included medicine makers and magicians, who were considered as alternatives to a doctor's care, especially as a doctor's attention and care may have been expensive, and therefore may not have been affordable to all civilians (Cilliers and Retief 2006; King 2001; Scarborough 1970).

Roman healers, including physicians, surgeons, medics and other individuals practicing health care were frequently associated with the Roman military and are recorded in epigraphs and sculptures (e.g., medics on Trajan's column) (Barnes 1914; Scarborough 1968). 'Hospitals' (*valetudinaria*) have also been identified at some Roman military forts, as well as on large estates (Cilliers and Retief 2006; Davies 1970). Additionally, medical and surgical tools and kits have been recovered from various archaeological contexts, including *valetudinaria* and in burials (Cybulska et al. 2012). It is unclear the extent to which military healers and treatment facilities were available for all community members or just individuals in the army, but evidence for female medical instruments (e.g., gynaecological tools) is used by Baker (2000) to suggest that medical treatment was, at least sometimes, extended to community members.

Extremity fracture treatments were described by Greco-Roman authors such as Hippocrates, Celsus, and Galen. Greco-Roman medical authors wrote about the importance of the fast and correct reduction of fractured bones and recognized complications, such as inflammation, malunion, and impaired mobility (Brorson 2009; Celsus, *Med.* VII; Hippoc. *Fract*.). These texts typically recommend conservative fracture treatments (i.e., non-surgical), however surgical techniques used in the removal of comminuted and dead bone fragments, sharp splintered fragment ends, and amputation are outlined by Celsus (*Med.* VII). External reduction (realignment) of fractured bones can require significant force to return bones to their natural alignment, and Greco-Roman authors report and advise techniques and equipment to assist with the leverage and power required to reduce these fractures (Celsus, *Med*. VII.10; Hippoc. *Fract*.; Redman Coxe 1846). According to classical texts, once fracture segments were reduced, they were stabilized with splints and wrapped with regularly changed bandages and poultices (Brorson 2009; Celsus, *Med.* VII; Hippoc. *Fract*.). Fracture recovery included special diets, relaxation, and rest. Slings were used in the treatment of fractured arms and bed rest was recommended for fractures to the legs (Celsus, *Med.* VII.10; Hippoc. *Fract*. 8-9). Belcastro and Mariotti (2000) also report palaeopathological evidence in the upper limbs and shoulder girdle that are consistent with crutch use in the Roman period.

Due to the predominantly conservative nature of Greco-Roman fracture treatment, it is possible that not all fracture types were successfully reduced, and some may have proven too complex or unstable to maintain alignment even with treatment. Celsus (*Med.* VII) outlined differences in the prognosis and treatment of fractures by location and type. For example, mid-shaft fractures were documented as less painful and difficult to treat than fractures to the bone ends; transverse fractures were believed the simplest to treat, while fractures with pointed fracture ends, such as comminuted and oblique fractures, were more challenging (Celsus, *Med.* VII). Greco-Roman physicians also recognized infection as a serious concern, and the signs of inflammation and gangrene were clearly described by Celsus (*Med.* VII) and Hippocrates (*Fract*. 11). In this pre-antibiotic era, individuals with wounds, especially those with compound fractures, would have been at increased risk for the onset of infection.

As pain and pain response will influence an individual's coping mechanisms after fracture (see Section 2.5.4), it is important to also consider the Roman experience of physical pain. Greco-Roman physicians wrote about the use of physical pain for diagnostic purposes (Wilson 2013), and other authors in antiquity (e.g., Seneca) philosophized about how pain should be addressed and perceived (Edwards 2005). Greco-Roman authors draw a connection between masculinity and the Roman perception of pain. According to Edwards (2005), pain was seen as an opportunity to demonstrate strength of character and mind, and to control and conquer pain without complaint, was to demonstrate great character. Although it is recognized that strength of character was likely unable to eliminate pain, it was used as a tactic to make pain more tolerable (Edwards 2005). As pain was associated with masculinity, this may suggest that the described pain response was a gendered practice, however it is also entirely possible that people of other genders also adopted this attitude to pain.

In the Roman period, successful fracture healing would ultimately have depended on factors that included: the health and nutritional status of the individual, the fracture location and type, the skill of the healer, and individual compliance to treatments. Due to the heterogeneous and unstandardized nature of Roman medicine and the diversity in the Roman world, it would be incorrect to assume that all doctors and healers practiced standardized methods outlined in classical medical texts, or that all people responded to injury and treatments in the same way. Additionally, the cost and/or military affiliation of many Roman medics may have meant that treatment was inaccessible to some members of the civilian population. It is highly probable that the treatment was not consistent or equal among individuals, and even perhaps within communities, throughout the Empire.

2.9 Summary

Biomechanics is a connecting thread in understanding the adaptation of bone to loading forces, why and how it fractures, how it heals, and its associated post-traumatic complications and impairments. This chapter has outlined biomechanical concepts as they are evident in clinical and biological anthropological literature in order to provide a detailed background of fractures and their repercussions. This chapter has also provided insight into the different approaches to understanding fractures and physical differences in the present and the past in order to discuss the treatment and functional consequences of trauma, as well as the physical experience of injury in the Roman world. Moving forward, this thesis combines the biological understanding of fracture production, healing, treatment, and consequences, with an understanding of the cultural contexts in which these fractures occurred, in order to produce an informed interpretation of active life in Roman communities.

Chapter III – MATERIALS

This chapter introduces the site histories, archaeological evidence for activities, and cemetery contexts for the Roman sites of Ancaster (UK) and Vagnari (Italy). Past analyses using the Ancaster and Vagnari skeletal collections are also briefly outlined.

3.1 Ancaster: The site

During the Roman period, Ancaster was a small town in the province of *Britannia*, at the site of modern Ancaster, Lincolnshire, UK (Rivet 1958; Wilson 1968) (Figure 3.1). First described by Marsden (1863) and Trollope (1870), Roman Ancaster has since been the subject of a number of archaeological excavations, including a feature in *Time Team*, a popular archaeological television show in the UK (Douglas M [Director] 2002). While archaeologists and historians once believed that this settlement's Roman name was *Causennæ* (e.g., Marsden 1863; Trollope 1870), this has since been refuted and the name of the

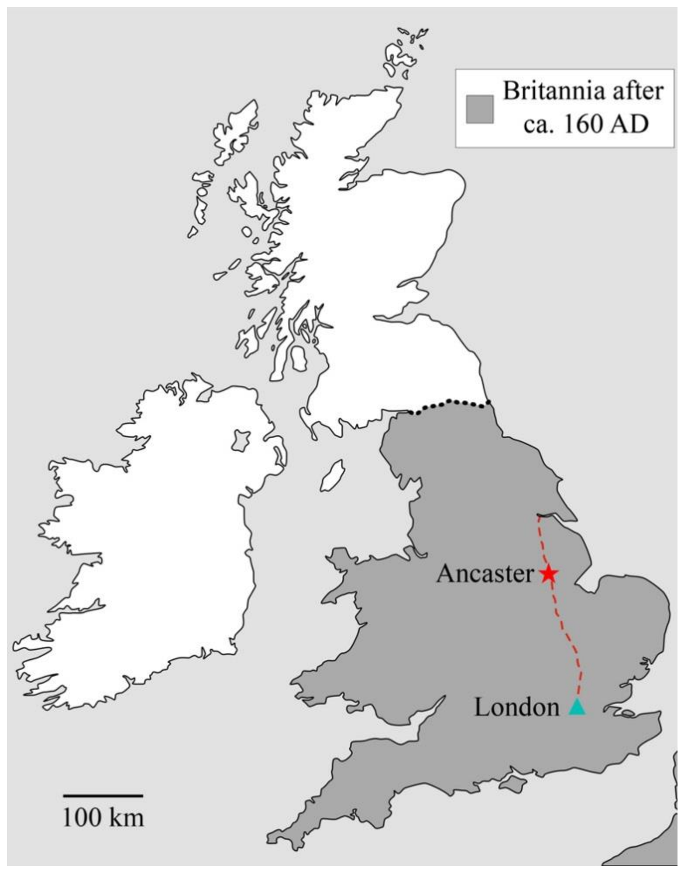

Figure 3.1 – Map of the British Isles showing the limits of Romano-Britain (*Britannia* province) after the early 160s AD. Hadrian's Wall is marked by a dotted black line, Ermine street by a red dashed line, and the location of Ancaster (red star) relative to London (blue triangle) is shown. Location of Hadrian's wall based on Bidwell and Hodgson (2009: 20, Figure 8) and Ermine Street based on Carreras and De Soto (2013: 122, Figure 4).

Roman settlement at Ancaster remains unknown (Historic England 2015); this research refers to the Roman settlement by its modern name (Ancaster).

Established in a natural gap in the Lincoln Edge limestone ridge (Ancaster Gap), Ancaster's location was strategic (Burnham and Wacher 1990). The site was occupied before the Romans, but the first Roman occupation at Ancaster was in the 1st century AD in the form of a small Roman fort, followed by a civilian settlement (Allen 2002; Historic England 2015; Todd 1975). By the 2nd century AD, the Ancaster town walls encircled a sub-rectangular area of approximately 3.7 hectares (9.1 acres), and by the early 3rd century AD it was surrounded by fortifications including a rampart, wall, and ditches (Burnham and Wacher 1990; Todd 1981). Trollope (1870) states that the origins of the modern name 'Ancaster' is likely derived from the Saxon word for *castrum* (Latin), meaning stronghold, which reflects the settlement's history as a fortified location. Although Ancaster was apparently well fortified, it remained a small settlement, especially in comparison with some of the larger contemporaneous settlements in the surrounding area (e.g., *Lindum* [Lincoln, UK]) (Hawkes et al. 1946; Rivet 1958). The presence of fortifications may reflect some danger to, or need for protection, of the town, but they may have also been built, in part, as a demonstration of the town's wealth (Rivet 1958; Timms 1997).

Referred to as a 'posting station' (*strassensiedlung*), a common small roadside settlement type usually associated with an inn or place for travellers to rest, Ancaster was situated astride the main road (Ermine Street) approximately 29 km south of the Roman legionary fortress in Lincoln, UK (Rivet 1958; Todd 1975). Although Ancaster may never have held an official rank, its location straddling Ermine Street suggests it was part of the greater Roman communication system and also controlled or monitored movement along the main road (Allen 2002; Burnham and Wacher 1990). Finds at Ancaster seem to indicate that this settlement had some degree of economic importance and may have housed residents of generally greater wealth; these include a number of coin hoards (Lincolnshire Historic Environment Record 2012b; Wilson and Wright 1968), as well as tessellated mosaic floor fragments and painted plaster (Timms 1997; Webster et al.

2004). Like many Roman settlements, especially small ones, extramural territories and activities were also present at Ancaster. Outside all of Ancaster's walls there is archaeological evidence for not only cemeteries, but also suburbs and agricultural facilities, indicative of population expansion in the 2nd century AD (Burnham and Wacher 1990; Historic England 2015; Todd 1975).

There is archaeological evidence for Roman occupation through at least part of the 4th century, but much about the post-Roman transition of Ancaster (ca. 5th century AD) is unknown (Whitwell et al. 1966). Wilson and Wright (1969) report some archaeological evidence of burning, and rubbish deposits are interpreted as indicative of the abandonment of the fort by the Romans, but there is also some archaeological evidence to suggest that occupation at Ancaster continued (Historic England 2015). For example, some later Anglo-Saxon pottery was recovered in the same stratigraphic layers as late Roman pottery, and a 5th century Anglo-Saxon cremation cemetery was identified to the south east of the Roman walls (Todd 1975). Ancaster remained a relatively important location for quarrying into medieval times and locally quarried limestone is present throughout Lincolnshire (Alexander 1995; Ulmschneider 2000).

3.1.1 Living at Roman Ancaster

As in many Roman civilian towns, various industry and craft activities were likely undertaken at Ancaster. Most published archaeological assessments have concentrated on Ancaster's defensive structures and very little is known about the town's layout and building types, however the available evidence does indicate the presence of agricultural activities, industries, and crafts (Burnham and Wacher 1990; Todd 1970; Todd 1975).

Agriculture played a very important role in the subsistence of small Romano-British communities, such as Ancaster. The soil surrounding Ancaster is of excellent and workable quality, and archaeological evidence for independent farm buildings have been uncovered in the lands immediately surrounding the town (Todd 1970, 1975). Whitwell et al. (1966) and Wilson and May (1965) report one such (3rd to 4th century AD) building located to the south east of Ancaster that contained evidence of ovens, multiple hearths, and corn-dryers. Van der Veen (1989) suggest that corn-dryers would have been used in the Roman period for the preparation of grains for storage and consumption and may have also been used in the production of malt.

Quarrying and stone sculpting were opportune undertakings at Ancaster, due to the close proximity of the community to the Lincoln Edge, a middle Jurassic, oolitic limestone ridge (Burnham and Wacher 1990). Ancaster limestone is a high quality material, mined by the Romans and renowned in the medieval period (Alexander 1995). Archaeological recovery of Roman period stone coffin blanks (uncarved), mile markers, and sculptures made from local, Ancaster stone suggests that members of the community participated in quarrying (Todd 1975; Wilson 1968). Additionally, the prevalence of local limestone carved into altars, sarcophagi, statues, and religious sculptures suggests that Ancaster may have hosted a school of local sculptors (Burnham and Wacher 1990; Frere 1961). Residents at Ancaster apparently benefited from having a quarry and sculptors available, as 70% of the observable graves in the western cemetery included large amounts of local stone masonry (Wilson n.d.). Additionally, at least two individuals were buried in local stone coffins that were reportedly broken before burial and possibly represent discarded material from the local quarries (Wilson and Wright 1969).

In addition to quarrying, there is also archaeological evidence for other crafts and industries at Ancaster. Pottery kilns and indications of ironworking were present outside the settlement walls, suggesting that some of the inhabitants of Ancaster manufactured pottery and worked metal (Lincolnshire Historic Environment Record 2012c; Todd 1975). A number of coin moulds (late 2nd to early 3rd century AD) were also discovered, and may indicate that someone at Ancaster was involved in forging Roman currency (Burnham and Wacher 1990; Hall 2014). Although few buildings have been described from within the town walls, remnants of one foundation suggest that a strip house, commonly used for the sales or manufacturing of goods, faced Ermine Street (Lincolnshire Historic Environment Record 2012a).

3.1.2 The Western Ancaster Cemetery

Ancaster's Roman period cemeteries were first mentioned by Trollope (1870), and since then, both inhumation and cremation cemeteries have been identified outside each of Ancaster's walls (Historic England 2015; Todd 1975; Wilson 1968). During the expansion of a modern churchyard, the Roman cemetery outside the western wall was disturbed and systematic excavations were undertaken by Nottingham University between 1964 and 1969, and in 1971 and 1973 (Wilson 1968, n.d.). While excavations plans are not available, the location of the site can be inferred based on Wilson's (n.d.) description of the excavation in relation to Church Lane, approximately 700 meters north of the church, and at or near the modern cemetery (Figure 3.2).

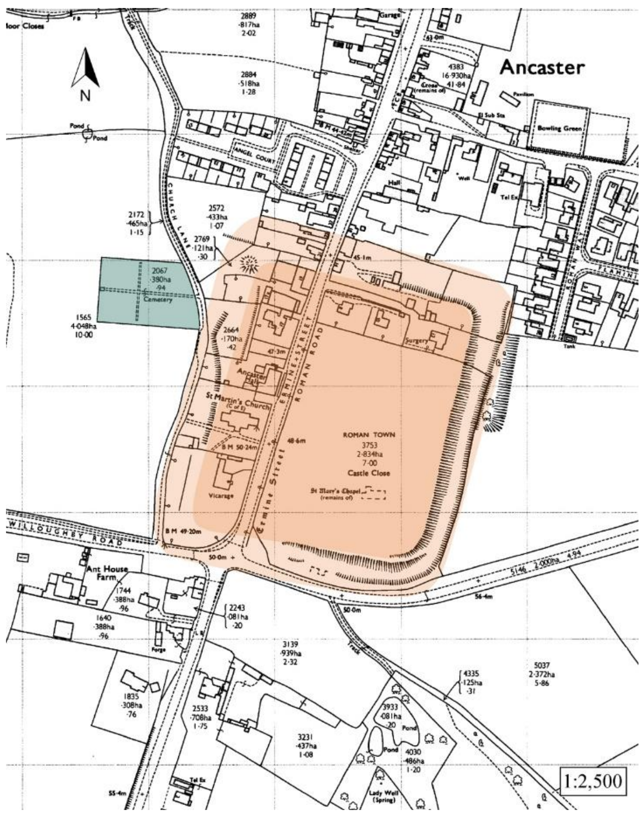

Figure 3.2 – British Ordinance Survey (1980) map showing the approximate location of the Ancaster Roman town and walls (orange shaded areas). The probable excavation area is highlighted in green. Some skeletal material is curated with excavation tags marked "Angel Inn"; this was located north of the cemetery at the modern location of Angel Court. Ordinance Survey (1980) map adapted with permission from Old-Maps.co.uk.

Grave types in the Ancaster western cemetery were varied and included simple earth cut features, stone markers, stone-lined cists or coverings, and stone sarcophagi (Burnham and Wacher 1990; Todd 1975; Wilson 1968; Wilson n.d.). According to Wilson (n.d.), local stone was used in 148 of the 212 assessed burials. Some individuals were buried in wooden coffins, as indicated by iron nails with adhering fragments of preserved wood (Burnham and Wacher 1990; Wilson 1968; Wilson and May 1965). The burials did not often crosscut each other and were predominantly arranged in an east-west orientation (with heads to the west) (Burnham and Wacher 1990; Todd 1975; Wilson and May 1965; Wilson and Wright 1966). Wilson (n.d.) reported body position for 211 burials, in which 197 were laid in an extended supine position with hands at their sides or on their chest or pelvic region, 12 were lain on one side, and three were prone and likely buried without a coffin.

Pitts and Griffin (2012) suggest that grave goods and coffin types are linked with wealth and status, and that individuals buried in later Romano-British rural cemeteries often had fewer grave inclusions (but greater inequality) than urban cemeteries. At Ancaster, grave goods were typically not included in the burials, but when present, they were usually items of personal adornment, such as bracelets (Burnham and Wacher 1990; Wilson n.d.). Some coins, carved local stone, iron nails, and leather were also recovered from burial features (Wilson n.d.). Stone coffins were common, and may have been widely available, at Ancaster; as such, they may not be a reliable indicator of status at this particular site. The status of individuals buried in this cemetery was not interpreted in the archaeological report, but Wilson (1968) suggests that this cemetery exhibited early Christian features given the orientation and nature of the grave inclusions. The relative paucity of grave goods at Ancaster seems consistent with a smaller, more rural settlement, but may also be associated with relatively lower status individuals. Given the incomplete nature of the archaeological report, the relationship between the funerary contexts and possible status at the site remains unclear.

Artifacts and associated features suggest that this cemetery was in use during the late Roman period (3^{rd} - 4^{th} century AD) (Burnham and Wacher 1990; Todd 1975; Wilson n.d.). Archaeological evidence for hearths, wall fragments, and a well that pre-date the cemetery suggest that some parts of the cemetery land were otherwise occupied up until the 3rd century (Wilson 1968). Given the size of the settlement and the close relationship between the city and its neighbouring agricultural lands suggested by Todd (1970), it is feasible that Ancaster's extra-mural cemeteries served individuals from both the town and closely neighbouring countryside. Larger farmsteads (villas) in the surrounding countryside may have had their own cemeteries (e.g., Leech et al. 1981).

3.1.3 Ancaster Skeletal Collection

Initial analysis of the Ancaster skeletons was undertaken in 1989 by Margaret Cox for inclusion in a publication by Wilson (n.d.). Wilson (n.d.) reported the excavation of 238 skeletons, a number revised to total 327 (243 adults and 84 sub-adults) by Cox (1989) during post excavation analysis. The Ancaster skeletal collection is currently curated by Historic England at Fort Cumberland, in Southsea, UK.

Although some information pertaining to the Ancaster excavations has recently become available, such as Wilson's unpublished report, there remain limitations in associating the human remains with excavated features and artifacts. Additionally, it is likely that some pathological bones may have been removed from the collection prior to Cox's analyses (Wilson n.d.); it is not possible to know for certain what elements or pathological bones were removed. To date the skeletons have been the subject of various bioarchaeological studies on age-related bone loss (Mays 2015a; Mays 2006a; Mays 2006b), infant mortality (Gowland and Chamberlain 2002; Mays and Faerman 2001), dental health (Bonsall 2014; Bonsall et al. 2016), frontal sinuses (Buckland-Wright 1970), and other skeletal case studies (e.g., Roberts et al. 2006).

3.2 Vagnari: The Site

The Roman site at Vagnari is located in the Basentello Valley, part of the Fossa Bradanica, 12 km west of the town of Gravina in Puglia, Italy (Small 2011; Small and Small 2007) (Figure 3.3). Vagnari consists of a number of areas, first identified during field surveys in 2000, that formed a large Imperial estate (Small 2011). The entire estate included a village (*vicus*) with an adjacent cemetery; a villa (San Felice), as well as some farms and other smaller villas located in the surrounding territory (Small et al. 2007). Small (2011) noted that the Roman name of this Imperial estate, including the settlement, is currently unknown; the site is currently referred to as 'Vagnari' after the adjacent 18th century farmhouse and estate, the *Masseria Vagnari*.

Figure 3.3 – Map of Italy showing the location of Vagnari (red star) relative to Rome (blue triangle). Route of the *via Appia* marked with a red dashed line, based on Carreras and De Soto (2013: 129, Figure 11). All regions depicted were part of the Roman Empire.

Environmental reconstructions indicate that the Vagnari landscape was more forested in antiquity and was also well suited to rough grazing of livestock (Fiorentino et al. 2011; Small 2011). The Emperor acquired the land in the early 1st century AD, after a series of conflicts between Rome, local populations, Greece, and Carthage (Small 2011).

This territory was at least 25 square kilometres large, privately owned, and located along the *via Appia*, one of the main roads from Rome to Italy's south coast (Figure 3.3) (Small 2011). Droving roads (*tratturi*), thought to have been in use at least since Roman times, also intersected the *via Appia* adjacent to the Vagnari estate (Small and Small 2011). The combination of the *via Appia* and drove roads situated Vagnari ideally for a role in communication, transport, and trade in the south of Roman Italy, and consequently facilitated the movement of goods in and out of the Imperial estate (Small and Small 2011; Small et al. 2007).

The site of the Vagnari *vicus* was occupied intermittently from the 4th century BC, prior to the conquest of this region by the Romans, and comprised an area of approximately 3.5 hectares (8.6 acres) (Small et al. 2007; Small 2011). The Roman *vicus* straddled a small ravine that, according to geomorphological analyses by Campbell et al. (2011), was present with some running water in antiquity. Initially, the settlement was concentrated on the north side of the ravine, however, in the late 1st to 3rd centuries AD, a time that coincides with the land's acquisition by the Emperor early in the 1st century AD, the *vicus* expanded to include the ravine's south side (Small et al. 2007; Small 2011). As a part of the Imperial estate, the *vicus* at Vagnari would have been home to the labour force needed to work the estate, as well as their dependents (Carroll 2013a; Prowse and Small 2009; Small 2011).

Located on a terrace above the *vicus* and cemetery sites, the San Felice villa was likely constructed in the 1st century BC as a higher-status residence (McCallum and vanderLeest 2014; McCallum et al. 2011). Later, during its operation as part of the Imperial estate, the villa's residential purpose shifted to include agricultural, industrial, and artisanal activities, but consistent use of the villa ended by the mid-2nd century AD (McCallum and vanderLeest 2014; McCallum et al. 2011). Archaeological evidence indicates that the villa activities were economically and administratively tied to the Vagnari *vicus* during the time it was affiliated with the Imperial estate (i.e., mainly from the 1st century BC to the end of the 2nd century AD) (McCallum and vanderLeest 2014).

The villa was destroyed, probably by an earthquake or landslide, in the mid-2nd century AD (McCallum and vanderLeest 2014). Occupation of the *vicus* continued in the Imperial period, and shifted toward the south side of the ravine by the middle of the 3rd century AD (Small 2011). During this period, the former-Imperial territories of this large estate were divided into small farms for continued cultivation (Small 2011). Occupation of the Vagnari *vicus* persisted, but was in decline by the Early Medieval period (ca. 6th to 7th centuries AD) (Small 2011).

3.2.1 Living at Roman Vagnari

Slaves, freedmen, and free tenants probably comprised most of the Vagnari population, although there is no clear archaeological evidence for slaves at the site (Prowse et al. 2010; Small 2014a). The residents of Vagnari were predominantly of local origin, according to isotopic and preliminary ancient DNA work on skeletons from the cemetery; however evidence suggests that some individuals were likely from elsewhere in Italy, and some from further away in Asia and Africa (Prowse et al. 2010). Regardless of where they were from, the individuals living in the Vagnari *vicus* would have comprised the estate's work force responsible for agriculture, forestry, as well as pasturage and transhumance activities, among other duties (Small 2011). Additionally, archaeological evidence suggests that like many other Roman communities, economic and commercial endeavours, including a variety of crafts and industries, were also undertaken at the Vagnari *vicus* (Carroll and Prowse 2014).

Charred botanical remains and impressions in building daub provide evidence for a mixed, agricultural economy, milling and baking, forestry management, as well as metallurgy at Vagnari (Carroll 2013a; Carroll 2013b; Fiorentino et al. 2011; Small 2011). Crops including bread and durum wheat, oat, einkorn, and barley were grown by Vagnari residents (Carroll 2013b). Additionally, the recovery of stone milling instruments and a large number of bread baking pots (*clibani*) from the *vicus* and villa, respectively, suggest local grains were milled and baked for individual and commercial purposes at Vagnari (McCallum and vanderLeest 2011; Volterra and Small 2011). Furthermore, identification of what is likely locally-sourced charred wood and charcoal at Vagnari indicates some residents logged and managed the local forest resources for construction materials as well as fuel to power the iron-working and tile kilns (Fiorentino et al. 2011).

Animals were raised and used for subsistence, transportation, draft, and textile purposes. This region has a long history of transhumance practices and the rough pastures of the Vagnari estate would have been ideal for grazing and maintaining herds of sheep and goats, the faunal remains of which have been excavated archaeologically (MacKinnon 2011; Small 2011; Small 2014b). MacKinnon (2011) reports that bones belonging to equids (i.e., donkeys and mules) and pigs were also recovered at Vagnari. Equids were not typically consumed in Roman times, and thus their presence at Vagnari suggests they were probably used for hauling and draught (MacKinnon 2011; Small 2011). For example, draught animals, such as donkeys and oxen, would have been required at Vagnari to assist in ploughing the fields, operating large grain mills, and pulling carts with heavy tile loads (MacKinnon 2011). Buildings with probable stalls, a large stone ‘donkey’ mill, as well as goat/sheep and other animal footprint impressions in tiles identified at Vagnari provide further evidence for the presence of various animals at the *vicus* (Small 2011; Volterra and Small 2011).

In addition to subsistence and work purposes, Small (2014b) argued that there is convincing evidence that sheep/goats were raised for their wool in the Vagnari territories. Large numbers of sheep bones were identified at Vagnari by MacKinnon (2011), suggesting that flocks large enough for wool production were present at this settlement. Additionally, evidence for the preparation of raw materials and textiles were identified at San Felice in the form of large vats possibly used for wool washing, as well as a great number of loom weights and other artifacts used for weaving (McCallum and vanderLeest 2014). Despite the presence of some evidence for weaving at Vagnari, Small (2014b) proposed that this activity was not undertaken at commercial production levels. Instead, Small (2014b) suggested that sheep were likely raised locally for wool, but once shorn, the raw material may have been shipped elsewhere for fulling, spinning, and weaving.

Various other crafts and manufacturing industries were present in Vagnari and are evident archaeologically. Identification of a number of large tile kilns, and compositional similarities between tiles recovered from Vagnari and clay from the adjacent ravine, reveal that individuals in the Vagnari *vicus* manufactured building ceramics (e.g., flat *tegulae* and curved *imbrices*) (Carroll and Prowse 2014; Small 2011; Small et al. 2003). Brent and Prowse (2014) reported that approximately three quarters of identifiable grave types at Vagnari (73.5%, n=72/98) were constructed from these locally-made tiles. Tile graves are not uncommon in the Roman world, but the fact that some of the tiles appear to have been broken prior to deposition suggests that Vagnari individuals were capitalizing on the waste from this local industry for funerary purposes (Small et al. 2007).

There is considerable evidence for metalworking industries (i.e., lead, iron, and bronze) in the 2nd and 3rd centuries at the Vagnari *vicus* (Carroll 2013a; Small et al. 2011). The working of lead at Vagnari is perhaps most noteworthy due to its potential health implications; various lead objects, including the contents of a crucible and production waste, have been documented at Vagnari and indicate that this metal was smelted and probably also recycled in the *vicus* (Carroll and Prowse 2014). In addition to metals, Carroll (2014) reported the recovery of glass slag and sheets of window glass, which provides evidence that glass production was probably also present at Vagnari.

3.2.2 The Vagnari Cemetery

The Roman period cemetery at Vagnari was identified in 2002 on the south side of the ravine, set apart from the majority of the settlement that was situated on the ravine's north side (Small et al. 2007). The Vagnari cemetery served the *vicus*, and possibly also the villa and farms in the surrounding estate (Carroll 2013a; Small 2011). Although most Roman settlements were not divided by ravines, it is nonetheless expected that Roman cemeteries were situated away from the main living areas and/or outside the town walls (Toynbee 1996).

The excavations at the Vagnari cemetery were initiated by Professor Alastair Small, and were continued by Dr. Tracy Prowse from 2003 to the present. Excavations of the cemetery are ongoing, but magnetometry results suggest it is approximately 2000 square meters in size (Small 2011), and is bounded on the north-western side by a road (Small et al. 2007). As of 2014, a total of 107 inhumation burials and three cremation burials have been excavated at the Vagnari cemetery (Prowse, 2016, pers. comm.). Burials were generally oriented from east-west to southeast-northwest (Prowse 2012; Prowse and Small 2009) (Figure 3.4). Most adults were buried in an extended supine position with their arms either at their sides or across their body (Prowse and Small 2009).

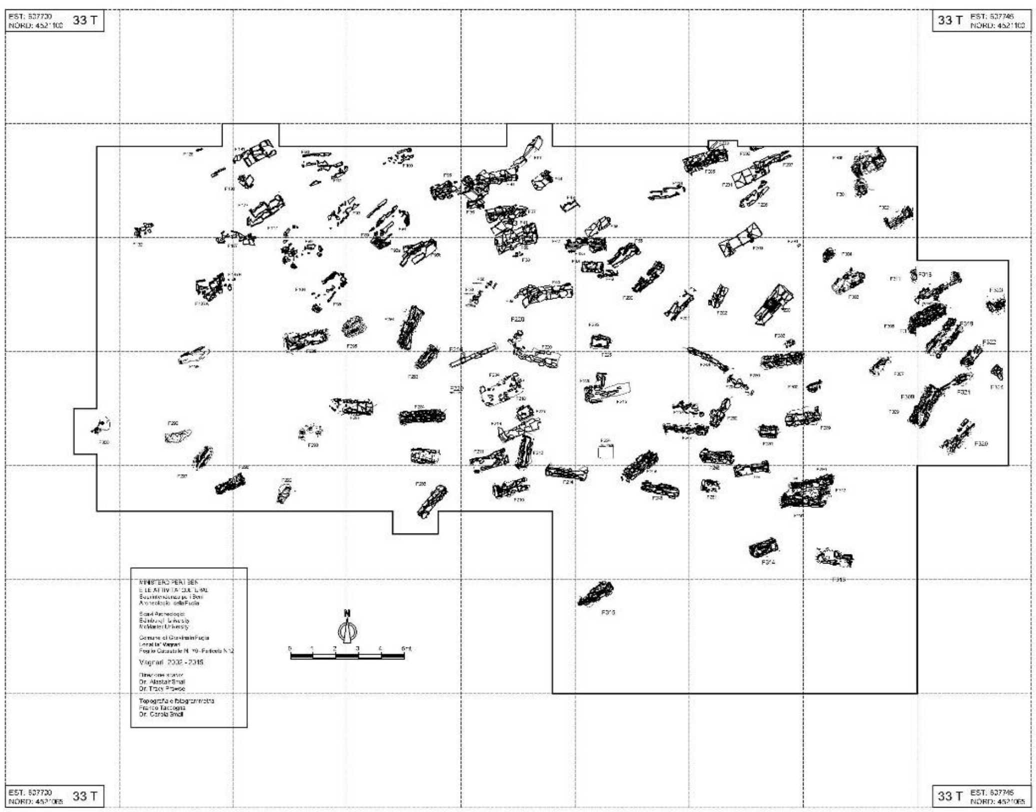

Figure 3.4 – Map of the Vagnari cemetery excavations. Cemetery plan by Franco Taccogno, used with permission by Tracy Prowse.

Most of the burials at Vagnari are *alla cappuccina* burial types, but libation/funnel, cist, and earth cut graves were also identified (Brent and Prowse 2014; Prowse 2012). *Alla cappuccina* burials were constructed from large, locally made tiles (*tegulae*) that were arranged in a tent-shape (inverted 'V') to cover the body (Prowse 2012; Small et al. 2007). In some cases, semi-circular curved tiles (*imbrices*) were placed vertically in the grave as libation tubes to facilitate funerary offerings (Prowse 2012). *Tegulae* were also used to construct cist burials, which were simple, horizontal tile coverings (Prowse and Small 2009). Stone was occasionally used to reinforce *alla cappuccina* burials, or in one case construct a burial cist. Iron nails with some organic matter have also been identified, suggesting that wooden coffins may have been used for some Vagnari residents, mainly for burials of infants and children (Prowse and Small 2009). Still other individuals were interred in simple earth cut graves. Some burials exhibit disturbance caused by intrusion from later burials, or plough and other post-depositional damage (Brent and Prowse 2014; Small et al. 2007). Given the prevalence of grave goods found at Vagnari (see below), it is unlikely that grave robbing was common in the Vagnari cemetery.

At this time, no funerary epigraphs have been recovered at Vagnari, but it seems likely that the position of these graves were known to people in antiquity. This is evidenced by features such as libation tubes in the graves, as well as what has been interpreted as a possible alter within the cemetery limits, suggesting that the living returned to visit the necropolis (Carroll and Prowse 2014). Furthermore, one individual (VA-F312) was interred snugly between two earlier *alla cappuccina* burials (VA-F290 and F291); the precise placement of burial VA-F312 demonstrates that the locations of the other two burials were known (Carroll and Prowse 2014). The close association between these three burials in particular has led Carroll and Prowse (2014) to hypothesize that they may represent familial relationships.

Grave goods are very common at Vagnari and most burials are associated with one or more artifacts (Brent and Prowse 2014; Prowse 2012). Artifacts recovered from burial features indicate that the cemetery was active between the 1st and 4th centuries AD, and most of the graves date to the height of the Vagnari *vicus'* expansion in the 2nd and 3rd centuries AD (Brent and Prowse 2014). Grave goods were typically placed by the feet and legs (with some exceptions) and include: ceramics (e.g., pots and lamps), glass and bronze vessels, coins, hobnails, and iron nails that were often bent (Brent and Prowse 2014; Prowse and Small 2009). Bent iron nails have special significance in antiquity as they were often used in burial rituals "intended probably to prevent the shade of the dead from returning to the world above" (Small et al. 2007: 146). Other items included in the graves include: a bone game piece, iron blades and other tools and weapons, as well as objects of personal adornment made predominantly from iron and bronze (e.g., rings, copper alloy belt buckle, beads, bone pins, bracelets, pendants, fibulae) (Brent and Prowse 2014; Prowse and Small 2009; Prowse et al. 2010).

Patterns in the distribution and prevalence of grave goods at Vagnari can indicate possible social roles and stratification in this community. Brent and Prowse (2014) reported that the simple earth cut burials had the lowest frequency of grave goods, suggesting that these individuals may have had lower socio-economic means, or perhaps did not require more elaborate burials. Additionally, the few cremation burials in the cemetery (*n*=4) contained the greatest number of grave goods, leading Brent and Prowse (2014) to suggest that perhaps wealthier individuals were selecting for cremation over inhumation burials. The number of grave goods deposited increased with age at death, possibly indicating life course changes in social role and/or status (Brent and Prowse 2014). When isotopic evidence for geographic origin is considered relative to the grave goods, there were no indications for different burial treatments, suggesting that individuals from different places were not treated differently in death (Prowse et al. 2010).

3.2.3 Vagnari Skeletal Collection

As of August 2014, when the data for this thesis were collected, a total of 107 skeletons had been excavated from the Vagnari cemetery. This number includes 68 individuals over 15 years old and 39 sub-adults (age and sex estimated by Prowse [2016, pers. comm.]). The Vagnari skeletal collection is split between two curation locations in Gravina in Puglia, Italy; skeletons excavated between 2002 and 2003 are curated at Fondazione Ettore Pomarici Santomasi and the skeletons excavated from 2004 until present are stored at Centro Operativo, Gravina, Soprintendenza per i Beni Culturali e Archeologici della Puglia.

The Vagnari skeletal collection has been the subject of a number of bioarchaeological studies. These studies include isotopic and ancient DNA investigations of geographic origins (Prowse et al. 2010), research on stress evidenced by enamel hypoplasias (Nause 2010; Prowse et al. 2014), isotopic evidence for diet (Semchuk 2016), as well as a preliminary investigation of pathological conditions (Prowse et al. 2014). Ongoing and forthcoming research includes a study of Vitamin D deficiency, dental health and diet, further biomolecular studies of migration and genetics, as well as proposed investigations into the relationship between lead-processing and skeletal lead content at Vagnari (e.g., Prowse and Carroll 2015).

3.3 Summary

From the contextual information available, a number of similarities exist between the Ancaster and Vagnari settlements. The estimated areas of both sites are comparable, cemeteries were in use at overlapping times, both sites were established along important communication routes, and industries and other activities at both locations appear to have been mostly rural and/or industrial in nature. However, while individuals from both communities would have practiced agriculture and animal husbandry, the activities at Vagnari would probably have been expected to create a greater surpluses and profits given the community's Imperial affiliation (Small 2011). Additionally, some differences in industrial specialties likely existed between the two locations. For example, quarrying seems common at Ancaster, compared to forestry, transhumance, and tile manufacturing at Vagnari. It is clear that individuals in both communities were capitalizing on local industry scrap to facilitate funerary needs as tile burials were abundant at Vagnari and stone lined graves were common at Ancaster. Both Ancaster and Vagnari skeletal assemblages have been the subject of a variety of bioarchaeological studies, and continue to be used in ongoing research. While differences in the sample sizes exist, both collections are of sufficient size for evaluation and comparison in this thesis.

Chapter IV – METHODS

4.1 Sex and Age Estimation

4.1.1 Sex Estimation

Pelvic and cranial morphological traits are sexually dimorphic, and are routinely used by biological anthropologists to estimate the sex of an individual. Post-cranial metrics are also dimorphic and reflect sex-related differences in body size. The sex of each adult at Ancaster and Vagnari was estimated through the macroscopic analysis of thirteen pelvic and cranial features, as well as humeral and femoral head diameters. The recording forms used to record skeletal features are presented in Appendix A.

Six pelvic features were examined, including the ventral arc, sub pubic concavity, ischiopubic ramus ridge, the subpubic angle, the greater sciatic notch, and the preauricular sulcus, following methods published by various authors (e.g., Bass 2005; Buikstra and Ubelaker 1994; Milner 1992; Phenice 1969). Seven cranial features were also recorded, including the nuchal crest, mastoid process, supraorbital margin, glabella, and the mental eminence (Acsádi and Nemeskéri 1970, as reported in Buikstra and Ubelaker 1994). Mandibular gonial eversion and ramus flexure were scored after Loth and Henneberg (1996) and Loth and Henneberg (2000).

When preserved, humeral and femoral vertical head diameters were measured to a precision of 0.1mm using Mitutoyo (CD-8"CSX) digital callipers (Kawasaki, Japan) calibrated to 1/100th of a millimetre. Sex categories based on ranges of humeral and femoral diameters were proposed by Stewart (1979) for humeri and Pearson (1917-1919) for femora (both cited by Bass 2005). The diameter ranges that correspond to each sex category were developed for humeri using the Terry collection (Stewart 1979), and for femora based on 17th century archaeological skeletons (Pearson 1917-1919); the ranges are comparable to those proposed for other groups of European and American ancestry.

Each individual was allocated to one of five sex categories: male, probable male, ambiguous, probable female, or female after Buikstra and Ubelaker (1994). The sex of an individual was classed as undetermined when insufficient evidence was available to estimate sex. Multiple pelvic, cranial, and postcranial features were concurrently evaluated in order to determine in which category the features of an individual best fit. Pelvic and cranial features were not always in agreement; in these instances, pelvic features were given precedence. Measurement of humeral and femoral heads were used to estimate sex only in the instances when other features were ambiguous or unclear, or to add additional confidence to the sex estimated using pelvic and cranial features. Skeletal sex was classed as ambiguous when features, or combinations of features, could not be confidently attributed to one male or female sex category. In the Results and Discussion Chapters, the ‘probable’ sex categories were combined with the male and female categories. Individuals of ambiguous and undetermined sex were also combined in these chapters and are referred to as individuals of unknown sex.

4.1.2 Age Estimation

Biological anthropologists estimate skeletal age macroscopically based on developmental and degenerative changes to the skeleton and dentition. The physiological or biological age of an individual is influenced by a variety of factors including their health, diet, and lifestyle, and as such, does not correlate perfectly with chronological age (Mays 2015b). Biological age can be more accurately and precisely estimated in skeletally immature individuals due to well-defined growth events, such as epiphyseal fusion, as well as dental formation and eruption (Buckberry 2015). It becomes more difficult to estimate the age of an individual once they are skeletally mature.

Age was estimated in this research based on characteristics and features outlined in Buikstra and Ubelaker (1994) and by various other authors (e.g., Brooks and Suchey 1990; Brothwell 1981; Íșcan et al. 1985; Íșcan et al. 1984; Lovejoy et al. 1985; Ubelaker 1989). Epiphyseal union, dental formation and eruption, morphology of the pubic symphyseal face, the auricular surface, sternal rib ends, and tooth wear were used to estimate the age of each individual. All indicators of age were scored when present and recorded using the forms presented in Appendix A.

A combination of age-estimation methods were used to assign an age range to each individual based on the overlap of each trait's estimated age range. When present, unfused epiphyses and erupting dentition were most relied on for age estimation. In skeletally mature adults, the pubic symphysis is one of the most favoured indicators of osteological age (Garvin and Passalacqua 2012). Although this part of the pelvis is often damaged postmortem, when the pubic symphysis was present it was given the greatest weight in the estimation of age in skeletally mature adults.

Individuals estimated at 15 years or older were included in this study. Each individual was assigned to an age cohort based on Buikstra and Ubelaker (1994); however, for the purposes of this research, the Buikstra and Ubelaker (1994) adolescent (ADO) age category, which included individuals between 12 and 19, was modified to represent individuals aged 15-19. The age categories used in this research are presented in Table 4.1. Individuals were placed in the age cohort in which the majority of their estimated age range fell. Adult individuals with very broad age ranges (e.g., extending across multiple cohorts) could not be categorized, and were instead labelled as 'Adult'.

Table 4.1 – Age categories used in this research, modified from Buikstra and Ubelaker (1994)

Age category	Age Range	Abbreviation
Adolescent	15-19 years old	ADO
Young Adult	20-34 years old	YA
Middle Adult	35-49 years old	MA
Old Adult	50+ years old	OA

4.2 Inventory & Preservation

The degree of fragmentation and cortical bone weathering of each long bone was scored in order to calculate true prevalence rates of fractures and determine the suitability of bones for radiographic measurements.

The presence of each long bone was recorded using the segment method outlined by Judd (2002b). In this method, each long bone is divided into five sections: one proximal epiphysis, one distal epiphysis, and three equal diaphyseal segments representing the proximal, middle, and distal diaphyseal portions (Figure 4.1). The locations of the proximal and distal epiphyses are devised using the squares method (described in detail by Judd 2002), in which the maximum transverse diameter of the distal and proximal epiphyses are used to delineate a square region around the epiphyseal segment. The completeness of each segment was assigned a number from zero to four that corresponded to the nearest estimated quarter percentile (Table 4.2). Segments that were scored as greater than or equal to 75% (i.e., "4") were included in the analyses. Bones were classed as "complete" when at least three of the five segments were greater than or equal to 75% present.

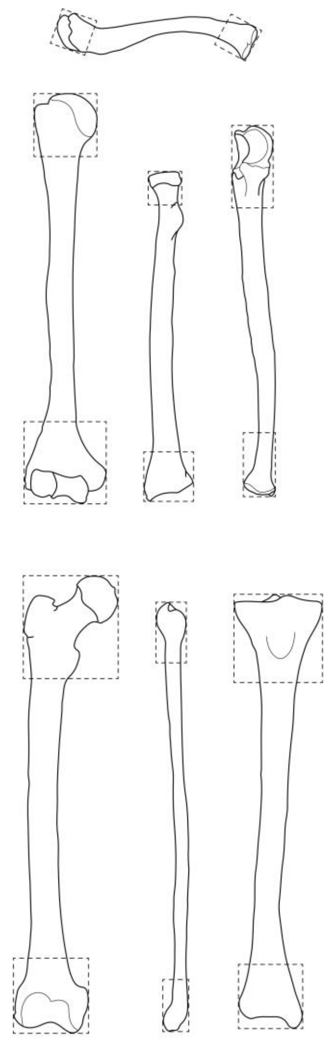

Figure 4.1 – Diagram of the squares method based on Judd (2002b: 1259, Figure 2) and Ruedi et al. (2007: 7). Epiphyseal segments are delineated with dotted lines.

Table 4.2 – The categories for scoring percent long bone segment completeness.

Completeness Category	Completeness Score	Percent Segment Completeness
Absent	0	0%
Incomplete	1	1-24%
Partial	2	25-49%
Present	3	50-74%
Complete	4	75-100%

The completeness of subchondral joint surfaces was scored in order to calculate true prevalence rates of osteoarthritis. The proximal and distal joint surface of each long bone was categorized according to the percent completeness (see Table 4.3). Joints that were at least 50% observable (i.e., "present" and "complete") were included in the analyses.

Table 4.3 – The categories for scoring subchondral surface completeness.

Completeness Category	Percent Segment Completeness
Absent	0-24%
Incomplete	25-49%
Present	50-74%
Complete	75-100%

Abrasion/erosion to cortical bone surfaces was also scored for each radiographed long bone after standards outlined by McKinley (2004) (Table 4.4). Postmortem damage to bone surfaces can include root etching, pitting and etching associated with water and soil action, to flaking often linked with surface exposure. The grade of abrasion/erosion assigned to each element represented the average and predominant amount of postmortem damage to the surface of the entire bone.

Table 4.4 – Grades of abrasion and/or erosion present, after McKinley (2004).

Erosion/Abrasion Grade	Description of Erosion/Abrasion Present
0	No modification to bone surface
1	Slight, patchy erosion
2	Slightly deeper penetration of the surface than phase 1
3	Some detail lost by erosion, but surface morphology still generally present
4	Entire bone surface abraded/eroded, but general bone contour maintained
5	Heavy erosion that masks the surface morphology
5+	Erosion that is extensive and penetrating

Skeletons that had most bones scored as grades three or less were preferentially selected for inclusion in the radiographic analyses as this degree of erosion was less likely to interfere in measurements. However, bones with greater amounts of weathering could still be measured if some original cortical bone surface was present; for example, research by Trinkaus and Ruff (1999) suggests that external contours can be interpolated radiographically by extending surfaces between more well-preserved areas of subperiosteal cortical bone. So although measurements were not ideally taken from bones with weathering scores of four and above, it was still possible to cautiously include these elements when necessary (e.g., when the eroded bone had a fracture). When selecting a comparative sample of individuals for radiographic measurement (see Section 4.3), skeletons with less surface erosion were preferentially chosen in order to simplify measurements.

4.3 Radiography Sample & Method

A portable digital Vidisco X-ray system, consisting of a Golden Engineering XR200 X-Ray Source and a FlashX Pro Digital Detector Array (DDA), was used at each curation location. The Golden XR200 is a pulse-based operating system with a fixed intensity of 150kV and 1.0 mA and variable exposure time settings. A tube with a three millimetre focal point was installed and the DDA had a pixel resolution of approximately 3.5 LP/mm (line pairs per millimetre, a measure of spatial resolution). The distance between the tube and the DDA was set at 120 centimetres.

Safety precautions were taken when working with the portable digital X-ray unit. An *INLIGHT*® OSL dosimeter issued by The National Dosimetry Service, Health Canada, was worn at all times while operating the radiography equipment. Additionally, a Fluke Biomedical 451B-RYR Ion Chamber Survey Meter was used to detect the amount of ionizing radiation in the environment in order to establish and maintain a safe perimeter surrounding the x-ray unit. To carefully monitor exposure and ensure the normal operation of the radiograph unit, the Ion Chamber Survey Meter was kept active and with the x-ray operator at all times while the equipment was in use.

All the long bones and second metacarpals and second metatarsals of individuals with fractures (and suspected fractures), as well as the individuals in the comparative sample, were radiographed. Long bones included clavicles, humeri, radii, ulnae, femora, tibiae, and fibulae. In addition to X-ray images of all long bones in individuals with fractures, a comparative sample of approximately 30% of adults in each collection was selected and radiographed in AP and ML views. For inclusion in the comparative sample, individuals could not exhibit any evidence of trauma and ideally had confident sex and age estimations. For each skeletal assemblage, adults who met these criteria were split into male and female groups and each group was randomized in Microsoft Excel[1]. The random values were sorted from smallest to largest, and equal numbers of males and females (totalling approximately 30% of the entire collection) were selected for use as a comparative sample for each site.

Long bones of similar densities were grouped and radiographed on a single DDA imaging plate; for example, tibiae and humeri; and radii, ulnae, clavicles, and fibulae were imaged together. Antero-posterior (AP) and medio-lateral (ML) views of each bone were obtained. These perpendicular radiographic views are referred to as biplanar radiographs and represent standard and recommended clinical practice necessary to characterize fracture lines, displacement, and deformity as it occurs in different planes (American College of Radiography 2013; Roberts 2000). Femora, tibiae, humeri, radii, and ulnae were oriented according to diagrams in Ruff (2002). Fibulae were oriented relative to the flat, subchondral surface of the distal articular facet; that is, the distal articular surface was positioned parallel to the plate for ML view, and perpendicular to the plate for AP view. Elements were oriented on the DDA in such a way as to minimize the effect of parallax (bone diaphyseal surfaces were placed as close against the DDA as possible). This meant that for AP radiographs, femora were placed with anterior surfaces against the DDA, second metacarpals and second metatarsals were placed dorsal-side

[1] Randomization was completed using the RAND function in Excel. This function randomly assigns a number between zero and one to each cell. The random numbers were sorted from smallest to largest and the first 30% of the individuals with the lowest randomized numbers were included in the comparative sample.

against the DDA, and all other bone types were placed with the posterior surface against the DDA. For ML radiographs, second metacarpals and fibulae were placed medial-side against the DDA, and all other bone types were placed with the lateral aspect against the DDA.

In the Ancaster sample, only paired second metacarpals and metatarsals were x-rayed with the primary objective being to identify asymmetry between the sides. By the time the Vagnari collection was analysed, the additional usefulness of these bone types in non-sided area comparisons was identified. A decision was made to radiograph the Vagnari second metacarpals and second metatarsals regardless of completeness. Second metatarsals were oriented according to the flat, lateral aspect of the proximal end of the bone, which was placed perpendicular to the plate for AP orientations, and parallel for ML orientations. For MC2s, the saddle of the proximal facet was placed perpendicular to the plate for AP radiographs, and parallel to the plate for ML radiographs. Previously published research found that placing the posterior, versus the anterior, side of the second metacarpal against the plate resulted in significantly larger mean total widths (Ives and Brickley 2004). However, the choice of orientation does not significantly affect the medullary width, cortical thickness, or cortical index values (Ives and Brickley 2004).

Three to five morphological features along each bone were indicated on radiographs with lead-markers. A steel ball, measuring 25.4mm (one inch) in diameter, was included in every radiograph and used to calibrate all images and correct for parallax (i.e., image distortion). A variety of exposure times were imaged for each plate to ensure that features, such as the periosteal cortical bone edges and trabecular adhesions to the medullary cortical bone, were clear enough for later measurement. The Vidisco X-ray system was set at 150kV and 1.0 mA, and exposure times were varied for different bone thicknesses; greater exposure times were required for elements with denser/thicker cortical bone, and less exposure time was needed for thinner/less dense bones. Exposure times averaged 1.5s for femora, 1.3s for tibiae and humeri, and 1.2s for radii, ulnae, clavicles, fibulae, metacarpals, and metatarsals.

Each digital X-ray image was analysed using the Vidisco Xbit Pro X-Ray Inspection System software (Version 3.1.1.3 [NDT], Vidisco Ltd). Every radiograph was calibrated using the 25.4mm (1 inch) steel ball. This calibration works to minimize any possible effects of parallax in the radiographs, and allows measurements to be compared across different images. When necessary, images were magnified and "sharpening" effects were applied in order to more clearly define the edges of cortical walls for measurement.

4.4 Fracture Recording & Interpretation

4.4.1 Macroscopic Fracture Recording

Representative "normal" bones and/or bones of the opposite (contralateral) side were used to identify abnormal bone contours that may be indicative of healed fractures. Antemortem fractures occur prior to death and exhibit evidence for new bone formation associated with healing. Individuals who survived for at least a week after injury may exhibit woven bone at the fracture site, indicative of fracture repair (De Boer et al. 2012). Over time, more bone is deposited, and eventually consolidates into organized dense lamellar bone (Wraighte and Scammell 2006). See Section 2.3 for further discussion of fracture healing.

Perimortem fractures occur at or around the time of death and do not exhibit any new bone associated with healing processes (Ubelaker and Adams 1995; Wheatley 2008). Perimortem fractures have unique morphological features, but are often mistaken for postmortem breaks. Living bone has plasticity and elasticity that is absent in dry bone, which results in characteristic smooth-edged breaks, with sharp edges that are typically not at right angles to the outer bone contour (Wheatley 2008). Furthermore, the edges of postmortem breaks are typically a different colour, whereas perimortem broken edges are stained similarly to the rest of the bone (Ubelaker and Adams 1995). All the broken ends of bones were examined for characteristics suggestive of perimortem trauma. Although individuals with perimortem trauma would not have lived long enough to develop a bony response to mechanical unloading, it was necessary to document unhealed traumas in order to accurately calculate fracture prevalence rates.

4.4.2 Fracture Interpretation

Fractured bones were recorded by bone type and side. Every fracture was sketched, photographed, described, and radiographed. Radiography was essential to evaluate type, morphology, and malunion of healed fractures. The location of each fracture was classified according to the segment in which the majority of the fracture line (evident radiographically) was located. When the fracture line was obliterated and could not be located, the fracture position was identified as the segment in which the majority of the bony callus was located.

Radiographic images were necessary to classify fractures by type, that is: comminuted, transverse, oblique, spiral, impaction, avulsion, crush, or incomplete. The appearance of each fracture type are detailed in Section 2.2. Radiographically, transverse and oblique fractures can appear similar. These fracture types were differentiated by the angle of the fracture line; transverse fractures had fracture lines angled less than 45 degrees from the bone's transverse axis, and oblique fractures had lines angled greater than 45 degrees from the bone's transverse axis (Rogers 1992). Fracture line angles were measured digitally using the Vidisco Xbit Pro X-Ray Inspection System software (Version 3.1.1.3 [NDT], Vidisco Ltd), by aligning the angle arms according to the longitudinal and transverse axes of the proximal bone segment (see Figure 4.2). Avulsion and crush fracture types were mainly identified by macroscopic observation as many of the fracture lines were superficial, and were often not radiographically evident (Figures 4.3 and 4.4).

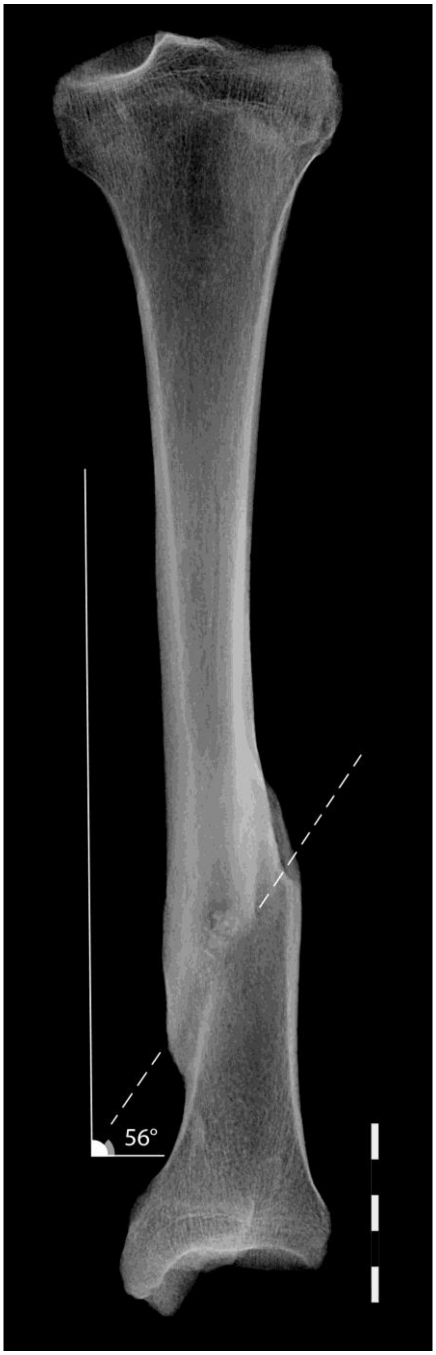

Figure 4.2 – The angle of the fracture line is measured relative to the longitudinal and transverse planes of the bone shaft. The x-ray depicts the anterior view of a spiral fracture belonging to AN-034, however the technique for measuring fracture lines remains the same. Scale bar represents 5cm.

Figure 4.3 – Avulsion fracture to the posterior aspect of the left, lateral malleolus (fibula) of AN-013, leaving a fracture line (marked with an arrow) evident on the subchondral surface. Scale bar represents 3cm.

Figure 4.4 – Crush fracture to the right postero-lateral tibial plateau of AN-062. There is evidence of healing present in the form of remodelled new bone formation, especially evident in the medial part of the lateral condyle. Scale bar represents 5cm.

Incomplete fractures are when the contour of the bone is not completely interrupted (Wraighte and Scammell 2006). These fractures are most common among children whose bones are more pliable than adults, but incomplete fractures sustained during childhood can be difficult to recognize in mature individuals due to thorough remodelling and restoration of the bone contour (Kusaba and Saito 2016). When adults experience an incomplete fracture, it may be related to repetitive stress (fatigue or stress fracture) or weakened bone (insufficiency fractures) (Matcuk Jr. et al. 2016). Stress fractures are most common in the lower limb (Matcuk Jr. et al. 2016; Matheson et al. 1987; Shindle et al. 2012). Incomplete and stress fractures are difficult to identify once healed. While some new bone formation may hint at their presence, these fracture types were only identified with certainty if a fracture line was evident radiographically. Incomplete and stress fractures often heal with minimal deformity and may therefore not be recognizable once the fracture line is healed and obliterated. Due to the difficulties associated with recognizing these fracture types, it is likely that these fracture types are under-represented in most studies of antemortem fractures.

4.4.3 Classification of Fracture Force

In addition to identifying the type of fracture present, the fractures identified were classified according to the type of force that caused the bone to break. Background on fracture force is provided in Section 2.2.1. Differences in direct force and indirect force injuries are often useful in discussing injuries caused by accidents versus those caused by interpersonal violence. However, for the purposes of this research, fractures were also divided according to higher-energy and relatively lower-energy fracture types in order to better address complications related to fracture severity. In this study, higher-energy injuries included transverse, spiral, and comminuted fracture types. Lower-energy injuries included oblique, avulsion, impaction, depression (i.e., articular crush fractures), and incomplete fracture types.

4.5 Fracture Complications

A number of potential complications may arise secondary to an extremity fracture including fractures that have not healed (delayed or non-union); fractures that have healed with poor alignment; infection; and damage to soft tissues (e.g., tendons, blood vessels, nerves). This subsection discusses how these possible complications were recorded.

4.5.1 Delayed Union and Non-Union

In this research, fractures were classified as non-united when the fragment ends remained separate, with dense sclerotic bone, and sealed medullary cavities and/or eburnation (Figure 4.5) (Brickley and Buckberry 2015; Lovell 1997; McKee 2000; Panagiotis 2005).

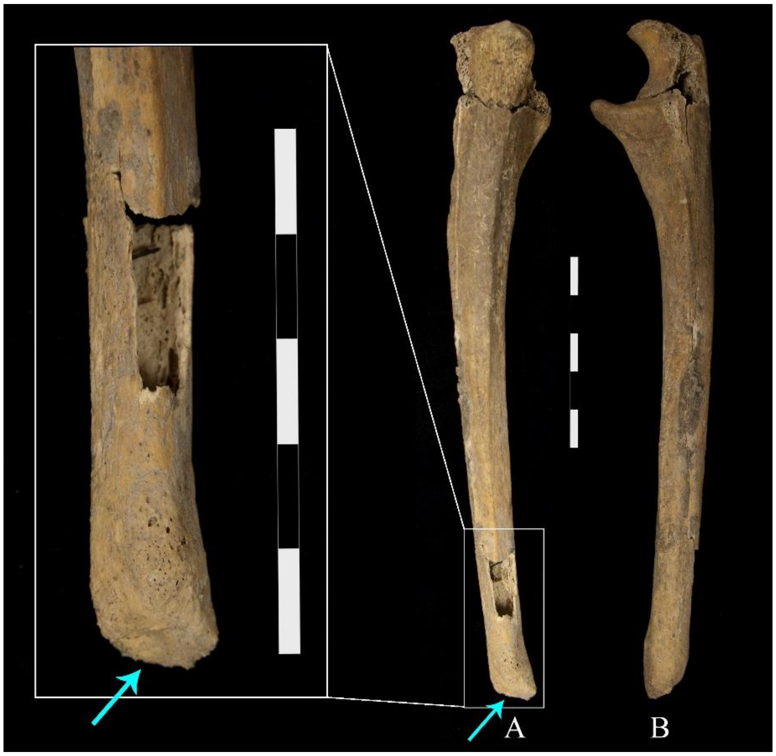

Figure 4.5 – Probable atrophic non-union of the distal left ulna of an individual from Roman *Carnuntum,* Austria (CA-2012.14.140.1192). The medullary cavity is remodelled and infilled (indicated with blue arrows). A) Posterior view with close up of the distal diaphysis with sealed medullary canal. B) Lateral view of the ulna. Scale bars represent 5cm.

4.5.2 Malunion

Fracture malunion was measured based on the position of the distal fracture segment relative to the proximal one. Using the Vidisco Xbit Pro X-Ray Inspection System software (Version 3.1.1.3 [NDT], Vidisco Ltd), the amount of angulation was measured directly on the digital radiograph by aligning angle arms to the medullary cavity mid-line of each fracture fragment (following Grauer and Roberts 1996; Roberts 1988b) (Figure 4.6). Subperiosteal diameters of the fractured bone ends were used to evaluate the percent apposition, which is, the amount that two fracture segment ends were in contact with each other at a fracture site. When two bone fragment ends were in correct anatomical alignment they were considered to be in 100 percent apposition (Equation 4.1) (Grauer and Roberts 1996; Roberts 1988b). Fracture displacement and overlap were digitally measured to the nearest millimetre using the Vidisco Xbit Pro X-Ray Inspection System software (Figure 4.7). When possible, the length of the fractured element was measured and compared to its non-fractured pair. The direction of rotation was described through visual comparison with the non-fractured contralateral element or a normal reference bone, and the degree of rotation was estimated with a protractor (Figure 4.8).

Figure 4.6 – The amount of healed angulation is measured based on the amount that the distal segment is angled away from an anatomically positioned proximal fragment. Image depicts the anterior view of a spiral fracture to AN-210's right tibia with a lateral angulation of 8.3°. Scale bar represents 5cm.

Figure 4.7 – Displacement and overlap measured on the digital radiograph. The distal segment is displaced by 12.7mm laterally, resulting in a calculated apposition of 50.4%. The fracture segments have an overlap of 13.6mm. Depicted is the anterior view of a healed spiral fracture of the left tibia in an Ancaster male (AN-034). Scale bar represents 5cm.

Equation 4.1 – The amount that two bone segments are in good apposition is calculated by dividing the amount of displacement by the total bone diameter.

$$\% \, Apposition = 100\% - \left(100 \times \left[\frac{displacement\ (mm)}{normal\ cortical\ diameter\ (mm)}\right]\right)$$

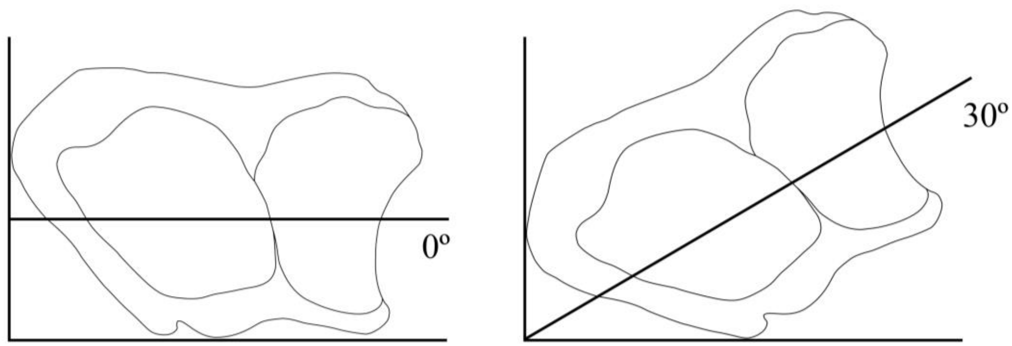

Figure 4.8 – The amount, and direction that the distal fracture segment is rotated is estimated by comparing the fractured with the non-fractured contralateral element. The distal radius depicted represents approximately 30º anterior rotation of the medial aspect of the bone. Image after Gilmour et al. (2015).

4.5.2.1 Deformity & Unsuccessful Healing

The unsuccessful healing of fractures was assessed using a model developed by Roberts (1988a) based on radiographs and patient records of living British people with conservatively treated, simple fractures. Roberts' (1988a) study used modern British patient medical records to determine the amount of displacement, apposition, and overlap of fracture segments, and shortening of the fractured element that were associated with untreated or unsuccessfully treated fractures (Table 4.5). Modern clinical data cannot always be directly applied to people who lived in the past as modern groups experience different diets and co-morbidities that can affect the effectiveness and rate of fracture healing. However, the use of Roberts' (1998a) study can nevertheless help to evaluate failed treatment as it synthesizes and quantifies attributes of fracture malunion as it relates to conservative treatment (analogous to the past).

Table 4.5 – The amount of healed deformity representing unsuccessful healing. Reproduced from Grauer and Roberts (1996).

Element	Degree of deformity constituting unsuccessful healing
Femur	>30 mm shortening >35° linear deformity >50 mm overlap
Tibia	>15° linear deformity >10 mm overlap
Tibia and fibula	>15° linear deformity >35mm overlap
Humerus	>20° linear deformity >15 mm overlap
Radius	>25° linear deformity >15mm overlap
Radius and ulna	>25° linear deformity

Fractures to clavicles, isolated fibular fractures, and isolated ulnar fractures were not included in Roberts' (1988b) classification of unsuccessful healing. To supplement these standards for unsuccessful healing, the published guidelines were adapted to comparatively evaluate healed deformation in these elements. The linear deformity (angulation) and overlap values available from Roberts (1988b) were averaged in order to comparatively assess fracture angulation and overlap in clavicles, fibulae, ulnae, as well as overlap in paired radius and ulna fractures. These adapted guidelines are reported in Table 4.6. Additionally, Roberts (1988b) did not explicitly define the relationship between unsuccessful healing and apposition, rotation, and shortening. As such, an apposition of 50% and a rotation of 25 degrees were selected as guidelines by which to comparatively evaluate healed deformation (Table 4.6). Shortening of more than 30mm was identified as indicative of unsuccessful healing in femora. Although this is a very conservative value, as no other data on shortening were available, 30mm was adopted for comparison among the other element types. It is important to note that while these derived guidelines do not allow definitive identification of unsuccessful healing, they do permit discussion of the degree of difference between a healed fractured bone and the anatomical 'norm'.

Table 4.6 – The amount of healed deformity used to represent comparatively greater amounts of malunion.[1]

Malunion Type	Degree of deformity representing comparatively greater amounts of malunion
Angulation	≥20°
Overlap	≥25mm
Shortening	≥30mm
Apposition	50%
Rotation	25°

[1] Values calculated based on average amounts of unsuccessful healing reported by Roberts (1988b).

4.5.3 Inflammation & Infection

Bony inflammation, characterized by periosteal new bone formation and/or osteomyelitic changes, can be indicative of infection in some cases (Boutin et al. 1998; Lovell 1997; Ortner 2003; Weston 2012). The location and remodelling of any periosteal new bone and osteomyelitic lesions (e.g., sinuses/cloacae) associated with a fracture were recorded and described. When one or both of these skeletal responses was associated with a fractured element it provided evidence for inflammation. Infection was only identified in this research when evidence for osteomyelitis was present. This was necessary as the formation of new bone associated with fracture repair (bony callus formation) is also related to inflammatory processes (Claes et al. 2012), but is not caused by infection.

4.5.4 Osteoarthritis

The presence of osteoarthritis was scored after methods outlined by Rogers and Waldron (1995). In this method, features consistent with osteoarthritis included marginal changes such as osteophytic lipping, as well as changes to the joint surface, including modifications to the joint contour, and porosity and eburnation (Rogers and Waldron 1995). All long bone joint surfaces were observed. Joint surfaces were classified according to shoulder, elbow, wrist, hip, knee, and ankle categories. In this research, shoulder joints included the proximal humerus and distal clavicle articular surfaces, elbow joints included the distal humeral and proximal radial and ulnar articular surfaces, and wrist joints included the distal radial and ulnar articular surfaces. In the lower limb, the femoral head was considered for hip joints, the distal femur and proximal tibial and fibular articular surfaces comprised the knee joint, and the distal tibial and fibular articular surfaces were considered as ankle joints.

The traits associated with osteoarthritis, that is, marginal osteophytes, joint contour changes, porosity, and eburnation, were scored as present or absent based on Rogers and Waldron's (1995) criteria. Osteoarthritis was identified when at least two of the features were present, and always when eburnation was observed (Rogers and Waldron 1995). As multiple articular surfaces comprise a single joint, a joint was deemed to have osteoarthritis when at least one of the subchondral surfaces exhibits the necessary changes outlined by Rogers and Waldron (1995). As osteoarthritic changes can develop naturally with advancing age, it is sometimes not possible to definitively tell if osteoarthritis in an individual with a fracture occurred secondary to the trauma. Only osteoarthritis that was identified in joints adjacent to a fractured element were used to identify possible post traumatic consequences. The age of the individual with the fracture and osteoarthritis was also considered; osteoarthritis is less common in younger individuals and its presence may indicate development of the condition consequent to trauma.

4.5.5 Nerve Injury

Instances of disuse, and therefore possible nerve injury, were identified through analysis of total and cortical cross-sectional areas and total and cortical asymmetries (discussed in detail in Section 4.7). As certain fractures are at greater risk for nerve injury, the affected element was evaluated relative to the type and location of the fracture.

4.6 Fracture Prevalence

Fracture prevalence was calculated according to the number of individuals with trauma (crude prevalence rate [CPR]), as well as according to the total number of elements observed (true prevalence rate [TPR]) (Equations 4.2 and 4.3). Crude prevalence rates are the most commonly applied in bioarchaeological studies, but do not account for differential preservation in archaeological collections. In the calculation of true prevalence rate (TPR), fracture frequency was calculated by comparing the number of fractured elements with the number of observed bones that have at least three segments greater than or equal to 75% complete (after Judd 2002). TPR accounts for the fragmentary nature of many archaeological skeletons and yields a more realistic fracture frequency based on the bones that are actually available for observation. Unfused epiphyses were counted as part of the single element, for example, an unfused radius was not counted as three elements, but as one that included proximal and distal epiphyses and the diaphysis.

Equation 4.2 – The crude prevalence rate of fractures, that is the proportion of individuals with fractures, is calculated by dividing the number of individuals with fractures by the total number of individuals observed.

$$Crude\ Prevalence\ Rate = 100 \times \left(\frac{number\ of\ individuals\ with\ fractures}{Number\ of\ individuals}\right)$$

Equation 4.3 – The true prevalence rate of fractures, that is the proportion of observed elements with fractures, is calculated by dividing the number of fractures observed by the number of elements observed.

$$True\ Prevalence\ Rate = 100 \times \left(\frac{number\ of\ elements\ with\ fractures}{Number\ of\ elements}\right)$$

Every observed fracture lesion was included in the calculations, regardless of preservation, even when multiple fractures occurred in the same element. This was done to account for not only the fragmentary nature of the skeletal collection, but also an individual’s potential for re-injury, in order to ascertain the most accurate trauma frequency possible. If elements that were insufficiently complete to be counted for true prevalence rates exhibited a fracture, they were also included in the counts of the total number of elements; this prevented greater counts of fractured elements than observed elements.

These same prevalence calculations were applied to joint surfaces to determine the prevalence of osteoarthritis (OA_x). The true prevalence rate for osteoarthritis considers the fact that each joint is comprised of two or more subchondral surfaces (e.g., the elbow joint involves humeral, radial, and ulnar subchondral surfaces). The total number of joints that had osteoarthritis were compared to the total number of observed joints (Equation 4.4). A joint was included in the counts if it had at least one subchondral surface that was 50% or more complete (i.e., classified as “present” or “complete”). Evidence of osteoarthritis in the joints adjacent to a fractured element were included in the osteoarthritis prevalence counts as well as the total count of observed joints regardless of the joint’s completeness.

Equation 4.4 – The true prevalence rate of osteoarthritis is calculated by dividing the number of joints with osteoarthritis by the total number of joints present.

$$TPR\ OA_X = 100 \times \left(\frac{number\ of\ joints\ with\ osteoarthritis}{number\ of\ observed\ joints}\right)$$

TPR=True prevalence rate; OA_x=Osteoarthritis

4.6.1 Statistics: Fracture Prevalence Rates

Differences in the prevalence rates of fractures and osteoarthritis were compared within each site and between sites using two-by-two contingency tables (one degree of freedom). SPSS (Version 20 for PC) was used to test for significant differences between groups. Outcomes were considered significant at *p*-values of less than or equal to 0.05.

Odds ratios (OR) with 95% confidence intervals (CI) were used to evaluate the strength of relationships between two groups of binary variables (e.g., male and female). OR values greater or less than 1.0 indicated differences in the probability of fracture; an OR value of 1.0 indicated that there was no difference between the compared groups

(Bland and Altman 2000). Confidence intervals were used to evaluate the precision of the identified difference; a large confidence interval indicates that the difference (or lack of difference) identified may not be precise or reliable (Szumilas 2010).

Differences in fracture counts were also evaluated using chi-square tests. Chi-square does not assume that the data are normally distributed, however it does typically require expected frequencies of greater than five (Field 2009). Yate's corrections were applied to the chi-square tests to account for sample sizes that were small, but greater than five (χ^2_{Yates}). When sample sizes were less than five, Fisher's exact tests (p_{FET}) were instead used to compare groups; Fisher's exact tests are more conservative, and can compare smaller sample sizes, such as those with values less than five.

4.7 Biomechanical Methods

The area of bone present at a single location along a long bone shaft is reflective of the bone's cross-sectional rigidity when in compression or tension (e.g., axial loading) (Marchi et al. 2006; Ruff 2005). The amount of bilateral asymmetry present reflects differences in the mechanical loading strains that were applied to right and left sided bones. In this research, it was necessary to calculate a variety of bone areas and asymmetries for each element type in order to assess the normal mechanical loading experienced by individuals and groups, and to identify functional consequences of fractures. Alone, each area and asymmetry value provides information about the mechanical loading environment. However, the combined presence of both larger than normal amounts of asymmetry, and smaller than normal bone areas, can be used to better deduce fracture complications by identifying asymmetrical unloading indicative of disuse of a fractured limb.

Cross-sectional areas were calculated using biplanar radiographic images (i.e., medio-lateral [ML] and antero-posterior [AP] views). The calculation of cross-sectional areas using biplanar radiographs represents the diaphysis as an ellipse (ellipse model method, or EMM) (O'Neill and Ruff 2004). Other methods, such as the latex cast method (LCM), also exist and allow for the calculation of other biomechanical properties indicative of a bone's ability to resist bending and torsional strain (O'Neill and Ruff 2004). Although these other methods allow for more accurate analyses of the outer bone surface, cross-sectional measurements obtained using the elliptical model method (EMM) nevertheless produce reasonably reliable cortical and total bone areas (O'Neill and Ruff 2004; Stock 2002). As the primary purpose of this research was to identify bone atrophy related to disuse after fracture, which affects the thickness of the cortical bone present, the EMM area measurements were selected to achieve these goals. Area and asymmetry measurements (i.e., cross-sectional measurements for humeri, radii, and tibiae, and region of interest [ROI] measurements for second metacarpals, second metatarsals, and ulnae) were recorded for all radiographed elements, including fragmented bones if the measurement location was preserved and identifiable.

4.7.1 Measurement Locations

Bone areas were calculated using transverse measurements of medullary and subperiosteal diameters. Measurements of the subperiosteal (total) and the medullary width of a bone in both AP and ML views were taken at a single point location on the shafts of humeri, radii, and tibiae. Ulnae, second metacarpals, and second metatarsals were evaluated with the region of interest method (ROI) (see Section 4.7.4). Measurements were oriented transverse to the longitudinal axis of each long bone shaft. Figure 4.9 depicts the longitudinal axes used for each element type for both AP and ML views; midline axes were oriented after Ruff (2002) for humeri, radii, ulnae, and tibiae, and developed for second metacarpals and second metatarsals to follow the bone's normal diaphyseal contour in AP and ML orientations. Measurement locations were not selected for clavicles or fibulae due to the large degree of morphological variability in these bones (see Chapter V). Additionally, because fractures were rarely observed in femora, a decision was made to not include measurements of this bone type.

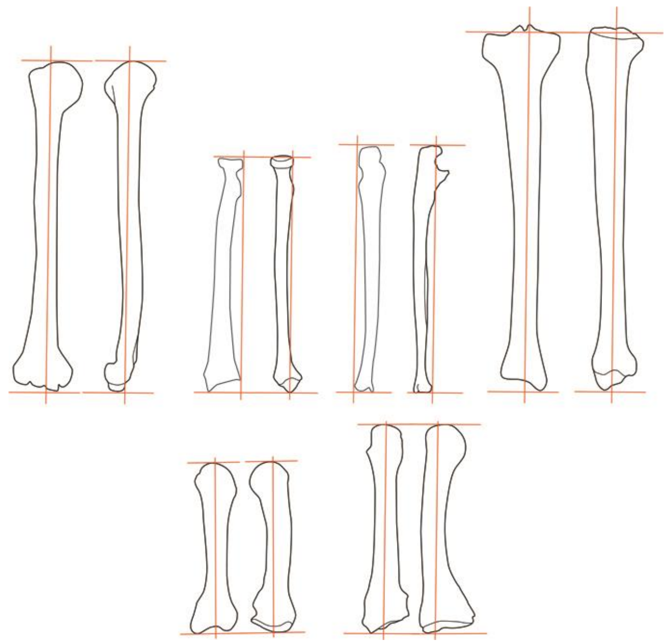

Figure 4.9 – Orientations for total length measurements. Top row from left to right: AP and ML Humerus, AP and ML Radius, AP and ML Ulna, AP and ML tibia. Bottom row from left to right: AP and ML second metacarpal and AP and ML second metatarsal.

Table 4.7 presents the features used to position measurements in this study. Figures 4.10 through 4.12 depict the single-point measurement locations for humeri, radii, and tibiae. Region of interest measurements are depicted in Section 4.7.4.

Table 4.7 – Feature location and type of radiographic, bone area measurement. [1]

Bone Type	Measurement Type	Radiographic Feature Description
Humerus	Single Point	Superior lateral supracondylar crest
Radius	Single Point	Beginning of the interosseous crest, superior to the ulnar notch
Ulna	ROI	Immediately superior to pronator teres attachment where the medullary cortical walls become parallel
MC2	Single Point & ROI	Single Point: Midshaft ROI: Narrowest part of the mid diaphysis (AP view)
Tibia	Single Point	Narrowest part of the mid diaphysis, inferior to nutrient foramen
MT2	ROI	Narrowest part of the mid diaphysis

[1] MC2=second metacarpal; MT2=second metatarsal; ROI=region of interest

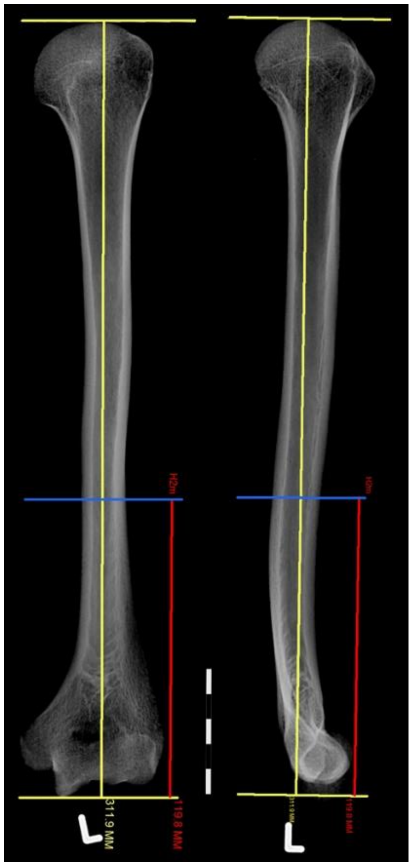

Figure 4.10 – Left humerus of AN-200 demonstrating the placement of the humeral cross-sectional measurement at the supero-lateral supracondylar crest. The bone’s longitudinal axis and maximum/minimum extents identified using perpendicular lines (yellow). AP view on left, ML view on right. Scale represents 5cm.

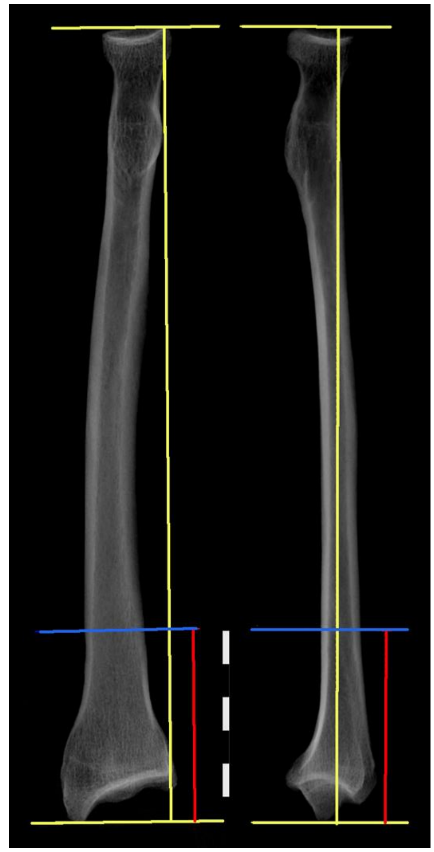

Figure 4.11 – Right radius of AN-034 demonstrates measurement location for the radial measurement, at the beginning of the interosseous crest, superior to the ulnar notch. The bone’s longitudinal axis and maximum/minimum extents identified using perpendicular lines (yellow). AP view on left, ML view on right. Scale represents 5cm.

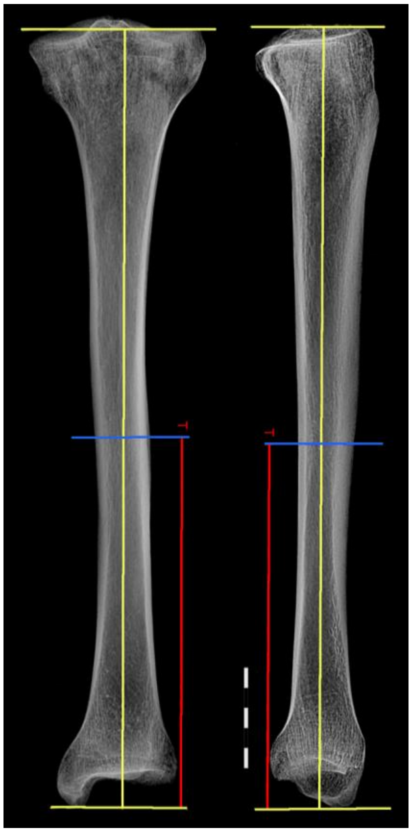

Figure 4.12 – Left tibia of AN-039, showing the placement of the tibial measurement, at the narrowest part of the mid diaphysis, inferior to nutrient foramen. The bone's longitudinal axis and maximum/minimum extents identified using perpendicular lines (yellow). AP view on left, ML view on right. Scale represents 5cm.

4.7.2 Area

Distances between the subperiosteal and the medullary cortical bone walls were measured at the humeral, radial, and tibial morphological features. Radiogrammetric standards outlined by Meema and Meema (1987) and Ives and Brickley (2004) were used to identify the surface of the medullary cortex. When a trabecular-type spur was joined to the cortex on both ends, the spur was included as cortical bone (see Figure 4.13). When a trabecular spur was free on one or both ends, it was not counted as cortical bone and not measured.

Figure 4.13 – Placement of measurements to the outer subperiosteal walls, and the inner medullary walls of the cortical bone. The image depicts the ML view of AN-026's right humerus.

Traditionally, the transverse medullary and subperiosteal (i.e., total) widths are measured on the radiograph film using callipers through an acetate overlay (to protect the original film) (Ives and Brickley 2004; Mays 2002). This research used digital radiographs, meaning that widths were measured digitally with the Vidisco software to the nearest tenth of a millimetre (i.e., 0.1mm). Total subperiosteal cortical width (AP) and medullary width (ap) were measured in antero-posterior view, and the subperiosteal cortical width (ML) and medullary width (ml) were measured at the same location in medio-lateral view. Using the AP and ML subperiosteal and medullary width measurements, the total area (T_A) and cortical area (C_A) of each bone were calculated after O'Neill and Ruff (2004) (Equations 4.5 and 4.6). Medullary areas were calculated (Equation 4.7), but are not reported or discussed further as this cross-sectional attribute was found to be too vulnerable to the positional variation of a morphological feature (see Chapter V)

Equation 4.5 – Total area of a bone is calculated using the subperiosteal widths from two radiographic planes.

$$Total\ area\ (TA) = \pi\left[\frac{(AP \times ML)}{4}\right]$$

AP=subperiosteal width in antero-posterior radiographic view; ML= subperiosteal width in medio-lateral radiographic view

Equation 4.6 – Cortical area of a bone is calculated using the subperiosteal and medullary widths from two radiographic planes.

$$Cortical\ area\ (CA) = \frac{\pi}{4}[(AP \times ML) - (ap \times ml)]$$

AP=subperiosteal width in antero-posterior radiographic view; ML= subperiosteal width in medio-lateral radiographic view; ap=medullary width in antero-posterior radiographic view; ml= medullary width in medio-lateral radiographic view

Equation 4.7 – Medullary area of a bone is calculated using the medullary widths from two radiographic planes.

$$Medullary\ area\ (MA) = \pi\left[\frac{(ap \times ml)}{4}\right]$$

ap=medullary width in antero-posterior radiographic view; ml= medullary width in medio-lateral radiographic view

It was necessary to consider a variety of area measurements for each element type as different area measurements inform different aspects of an individual's active life. Total areas are most greatly affected during mid-adolescence when the subperiosteal surface of bone is expanding; whereas medullary and cortical areas reflect influences on bone amounts after mid-adolescence (Ruff 2005). The relationship between bone areas and age are considered in this research in order to evaluate loading strains, and possible post-traumatic repercussions, throughout the life course.

4.7.3 Bilateral Asymmetry

Skeletal asymmetry provides valuable information about differential mechanical loading of limbs by side. This data, calculated for all measured area types, was assessed in order to determine if some groups were habitually experiencing greater unilateral mechanical loading. Specifically, large amounts of asymmetry associated with a fracture were evaluated to determine if the imbalance in mechanical loading may have been related to disuse or compensation after trauma (see Section 2.6). Asymmetries in total areas may indicate side differences in loading during subadulthood, while cortical and region of interest areas are more indicative of differential loading after skeletal maturity.

Directional and absolute asymmetries were calculated for bones that had both right and left sides preserved. Directional asymmetry (DA) provides information about the size of the bone by side (Equation 4.8): when the right bone is larger, the equation outcome is positive, and when the left is larger the result is a negative number. Directional asymmetry was evaluated within each collection and used to identify possible fracture consequences (e.g., an asymmetrically smaller fractured side). Absolute asymmetry (AA) represents the absolute value of the directional asymmetry (Equation 4.9); this formula does not provide information about which side is larger or smaller, but instead provides a value that represents the absolute amount of (unsided) asymmetry. Directional and absolute asymmetries were calculated for total, cortical, and ROI areas. Absolute asymmetries were used to compare the general amount of asymmetry, regardless of side preference, between Ancaster and Vagnari.

Equation 4.8 – Directional asymmetry was used to indicate which side in a right and left sided bone pair had larger total, cortical, or ROI area.

$$Percent\ Directional\ Asymmetry = 100 \times \frac{(right - left)}{average\ of\ right\ and\ left}$$

Equation 4.9 – Absolute asymmetry was used to indicate the amount of total, cortical, or ROI area asymmetry present and does not indicate which side in a bone pair was larger.

$$Percent\ Absolute\ Asymmetry = 100 \times \frac{(maximum - minimum)}{average\ of\ maximum\ and\ minimum}$$

4.7.4 Region of Interest Method

It was not possible to reliably use single-point measurements for ulnae, second metacarpals, and second metatarsals (see Chapter V), so an alternative method based on the amount of cortical bone within a region was developed to quantify the amount of cortical bone present in these element types.

Rather than measuring the bone present at a single point, this measurement alternative quantifies the amount of cortical bone within a larger zone of fixed size, a region of interest (ROI). The length of each region of interest (ROI) was based on a percentage of the average long bone length. On average, 30% of the second metacarpal total length was 19mm, 36% of the second metatarsal length was 25mm, and 15% of the ulnar total length was 37mm. ROIs for second metacarpals and second metatarsals were placed over the narrowest part of the diaphysis in the AP view (following Hyldstrup and Nielsen 2001; Rosholm et al. 2001). The middle of the ROI was placed over the narrowest transverse part of the medullary canal, the distal and proximal extents of the ROI were placed as close as possible to the locations where the medullary cortical bone walls becomes parallel (see Figures 4.14 and 4.15). For ulnae, the distal edge of the ROI was placed perpendicular to the bone's midline axis, immediately superior to the pronator teres attachment and at the point where the medullary cortical walls become parallel (see Figure 4.16).

Figure 4.14 – Region of interest (ROI) placed on the right second metacarpal of AN-062. The midline is placed on the narrowest part of the mid medullary canal. Image A shows the right second metacarpal with the selected ROI. Image B shows the cortical bone selected for quantification.

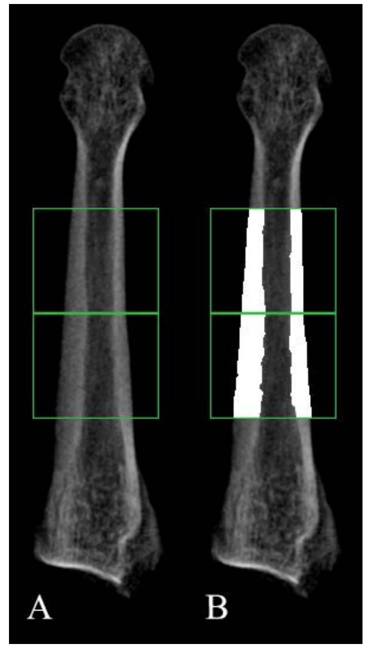

Figure 4.15 – Region of interest (ROI) placed on the left second metatarsal of AN-045. The midline is placed on the narrowest part of the mid medullary canal. Image A shows the left second metatarsal with the selected ROI. Image B shows the cortical bone selected for quantification.

Adobe Photoshop CC (2015) was used to calculate the amount of cortical bone within the second metacarpal, second metatarsal, and ulna ROIs. Each radiographic image was calibrated in millimetres, and a ROI of the correct size was drawn and placed over the appropriate diaphyseal location. The cortical bone within the ROI was selected using the *Quick Selection Tool* in Adobe Photoshop (2015). Using the *Record Measurements* feature in Adobe Photoshop (2015), the area of the selected cortical bone was generated and displayed in the *Measurement Log*; the value was then recorded in millimetres squared.

Figure 4.16 – Region of interest (ROI) placed on the right ulna of AN-001. The ROI is situated immediately superior to the pronator ridge. Image A shows the right ulna with the selected ROI. Image B shows the cortical bone selected for quantification.

4.7.5 Comparison of Cross-Sectional Properties between Sites

In order to evaluate the differences in cross-sectional properties between sites, authors such as Ruff (2005) recommend that biomechanical attributes be corrected for differences in individual body size. This practice is particularly advisable when comparing temporally and geographically disparate populations, as human body size changes over time and in different mechanical environments (Ruff et al. 1993). While uncorrected biomechanical properties were compared within each site, cross-sectional areas were corrected for body size prior to comparisons between Ancaster and Vagnari. It was not necessary to correct asymmetry values for body size as these data reflect percentage differences, rather than raw values.

Various methods for calculating body size and mass exist in the literature and are applied to biomechanical data. As the loading of lower limbs is affected by body mass and gravitational forces, it is advisable to correct for body size in analyses of lower limb bones (Ruff 2005). Studies of upper limb bones frequently use limb bone length to account for body size in biomechanical comparisons (Stock and Pfeiffer 2001). However, Ruff (2000) reports that, like lower limbs, the mechanical properties of bones of the upper limb also scale with body mass. When possible, it is recommended that estimates of body mass as well as bone length are used to correct for body size in biomechanical analyses of both upper and lower limb bones.

In this study, it was not possible to use long bone length as a correction factor due either to length alterations after a healed fracture, or due to fragmentary elements. Instead, mechanical properties were corrected using an estimate of body mass. A femoral head body mass estimation technique from Ruff et al. (1991), as cited by Auerbach and Ruff (2004), was used in this study to estimate body size for males and females; individuals of ambiguous sex were estimated using the ‘combined sex’ formula (Equation 4.10).

Equation 4.10 – Body mass estimations from Ruff et al. (1991) as cited by Auerbach and Ruff (2004).[1]

Males: $BM = (2.741 \times FH - 54.9) \times .90$

Females: $BM = (2.426 \times FH - 35.1) \times .90$

Combined Sex: $BM = (2.160 \times FH - 24.8) \times .90$

[1] BM=Body Mass; FH=femoral head vertical diameter

Vertical femoral head diameter was measured for every preserved femoral head and used to calculate body mass for each individual according to the above formulae. When no femoral head measurement was present or measurable for an individual, the body mass calculations were based on the average femoral head diameter for that site and sex. These calculations of body mass were used to correct for body size for all the element types; given that many individuals had fragmentary elements or bones that were fractured, in this study, it was not feasible to use bone length to account for body size in the upper limb.

4.7.6 Statistics: Cross-Sectional Differences

Differences among the bone cortical and total areas, and asymmetries of individuals without fractures were compared within each site by sex, age, side, and element. Shapiro-Wilks tests of normality were used to determine if area and asymmetry data were normally distributed. As some groups of raw data were not normally distributed, comparisons were made using non-parametric tests. Mann-Whitney U tests (U) were used to evaluate the differences between two groups of data, for example males and females, or upper and lower limbs. Kruskal-Wallis tests (χ^2) were used to test if significant differences among three or more categories were present, for example, among age cohorts (adolescent, young adult, middle adult, old adult); if significant, post-hoc Mann-Whitney U tests were then used to isolate which groups were significantly different. Significance was achieved when *p*-values were less than or equal to .05.

First, differences between and among individuals without fractures were assessed, in order to determine if it was necessary to control for sex and/or age in subsequent comparisons. When significant differences between categories of individuals without fractures were identified, the different categories were separated and considered independently in the following analyses. For example, if male and female humeral cortical areas were significantly different in size, sexes were considered separately in subsequent analyses of humeral cortical bone; if the compared categories were not significantly different, they were combined and considered as a single group. When no significant differences between categories were present, the combination of categories helped to maximize sample sizes for later comparisons with individuals with fractures.

4.7.6.1 Outliers and the Range of 'Normal'

Bone areas and asymmetries of individuals without fractures were used to identify the range of data that was representative of 'normal' for each site and element type. Interquartile ranges (IQR) were calculated for each category of individuals without fractures and were used to determine the normal range of areas and asymmetries of individuals without fractures at each study site. The use of interquartile ranges to identify outliers is common, and is the premise underlying the commonly used box plot to graphically represent the spread of data (Walfish 2006). The median represents the mid-point, or the 50th percentile of the data; 25% of all the data are then less than the median

(Quartile 1), and 25% of all the data are greater than the median (Quartile 3). The difference between Quartiles 1 and 3 represent the 'interquartile range' (IQR), that is, the range within which the middle 50% of the data is represented. Limits of the "normal" spread of data, often referred to as the upper and lower fences, were represented by 1.5 times the IQR (IQRx1.5); the value determined for IQRx1.5 was then added to the third quartile (upper fence) and subtracted from the first quartile (lower fence) (Walfish 2006). Areas and asymmetries located inside the fences were considered 'normal', and data outside the fences were identified as outliers. Bone attributes of individuals both with and without fractures were plotted against their corresponding IQRx1.5 ranges, and the outlying individuals were identified. Only areas and asymmetries belonging to individuals without fractures were used to generate the IQR and its fences.

Factors that could have caused outlying bone areas and asymmetries, such as fractures, laterality, and age were then considered to explain outlying bone areas and asymmetries. In order to explain the relationship between extremity fractures and long-term functional consequences, the location, type, and any secondary complications (e.g., osteoarthritis) of individuals with fractures were considered relative to the bones that exhibited outlying cross-sectional properties.

4.7.6.2 Inter-Site Comparisons

Differences in the normal cross-sectional properties, represented by individuals without fractures, were compared between Ancaster and Vagnari. Shapiro-Wilks tests of normality were used to determine if total and cortical areas corrected by body mass were normally distributed. As some area and asymmetry data were not normally distributed, comparisons were made using non-parametric tests. Mann-Whitney U tests were used to compare the areas and asymmetries for each element type between Ancaster and Vagnari; sex and age were controlled for when these categories had significantly different areas or asymmetries (as previously determined for each site).

4.7.6.3 Differences in the Prevalence of Outliers

The number of outliers were tallied in various ways to determine if the prevalence of outlying cross-sectional attributes were different between age, sex, or site, as well as among fracture types and locations. The prevalence rates of outlying cross-sectional areas were compared using odds ratios (OR). Chi-square tests with Yates corrections (χ^2_{Yates}) or Fisher's Exact tests (p_{FET}) were used to evaluate differences between groups. See Section 4.6.1 for further information on the application of odds ratio, chi-square, and Fisher's Exact tests in this research.

Chapter V – VARIABILITY IN BONE MEASUREMENT LOCATIONS

This study relies on distinctive bone morphological features to place cross-sectional measurements and quantify bone biomechanical properties. As morphological features are not always located at the exact same level along a bone's length, it was necessary to determine how much these features varied in position, and also how much the bone areas varied around a target measurement location. This chapter addresses how much the position of morphological features and cross-sectional areas normally varied along a long bone shaft. The methods used to assess the amount of variability in the location of morphological features are introduced, and the amount that the location of each feature varied along the bone diaphysis is presented. These values are then used to determine the amount that bone areas varied above and below an intended measurement feature in order to select features that were less susceptible to errors associated with inaccurately placed measurements or normal morphological variation of the bone. The features most suitable for use in the cross-sectional analyses of this research are identified as those that had the least change in the location of the feature, as well as the calculated area in the surrounding diaphysis.

Most cross-sectional studies measure bones at locations that correspond to a percentage of the total long bone shaft, so many studies only use complete bones in their assessments (e.g., Mays 2002; Ogilvie and Hilton 2011; Wescott and Cunningham 2006). Consequently, fragmentary and pathological elements are frequently omitted from consideration. Attempts to overcome these measurement limitations include placing measurements at recognizable morphological features and estimating total long bone length from fragmentary elements (e.g., Trinkaus and Ruff 1999). Measurement locations used in this research were placed at radiographically recognizable features. Radiographic, morphological features that were ideally suited for use as measurement locations were:

1. easily identifiable
2. did not vary greatly in position along the long bone's length
3. did not differ significantly in cross-sectional area above or below the selected feature

The suitability of features for use in biomechanical analyses were tested using random selections of complete, radiographed elements from Ancaster. When features were not identifiable or reliable, the region of interest method, an alternative method for quantifying cortical bone within a larger region, was developed and used (Section 5.4)

5.1 Single Point Measurements

A random sample of complete, radiographed bones from Ancaster were used to test the amount that each selected morphological feature varied along the long bone's shaft. Counts for the randomized sample are presented in Table 5.1.

Table 5.1 - Number of complete, radiographed, elements from individuals without fractures used to assess the positional variability of morphological features.

Element	Female	Male	Total
Humerus	56	62	118
Radius	35	42	77
Ulna	41	52	93
Second Metacarpal	37	11	48
Tibia	43	61	104
Second Metatarsal	46	31	77

For each bone type, morphological features were selected for use as measurement locations. The features identified as possible measurement locations are listed in Table 5.2. When possible, selected features avoided large muscle attachments and areas of very thin or convoluted layers of cortical bone such as at the proximal and distal epiphyseal ends. Measurement locations were not selected for clavicles or fibulae due to the large degree of morphological variability in these bones that introduced difficulty in identifying repeatable features. Additionally, because fractures were rarely observed in femora, a decision was made to not include measurements of this bone type.

Table 5.2 – Descriptions and average positions of the morphological features tested for positional variability for each element type. [1]

Bone Type	Radiographic Feature Description	Target TL%	Mean TL% ± 2σ
Humerus	Superior lateral supracondylar crest	35	35.2 ± 3.9
Radius	Just superior to the ulnar notch	25	24.4 ± 3.2
Ulna	Superior to pronator ridge	30	28.9 ± 4.7
MC2	Narrowest part of the mid diaphysis (AP view)	33.3	41.1 ± 4.8
Tibia	Narrowest part of the mid diaphysis, inferior to nutrient foramen	50	49.8 ± 3.9
MT2	Narrowest part of the mid diaphysis	50	48.5 ± 7.6

[1]MC2=second metacarpal; MT2=second metatarsal; TL%=percent total length; 2σ=two standard deviations.

5.2 Positional Variation of Morphological Features

Longitudinal axes of bones were identified (see Section 4.7.1) and each selected feature was marked transverse to the bone's longitudinal midline axis. Total length (TL) was measured radiographically in antero-posterior (AP) view, from the maximum proximal to distal extent of each bone. Medio-lateral (ML) views were used to measure total ulnar lengths; the styloid process was not included in the total length measurement in order to maximize the number of ulnae that could be measured.

The distance from the distal end to the selected morphological feature was measured along the bone's longitudinal axis (L). The location of each feature was represented as a percentage of the long bone's total length (TL%) (see Equation 5.1). The average TL% location was calculated for each feature and two standard deviations from the mean were used to indicate (with 95% confidence) the amount that the position of each feature varied along the long bone's length; the average percent of the total length for each measurement location is reported in Table 5.2. If the standard deviations varied more than five percent (based on error discussed by Sládek et al. 2010), the feature was determined to not have a consistent position along the long bone's shaft, and the measurement location was rejected. With the exception of the second metatarsal, all other morphological features selected had less than 5% positional variation along the long bone shaft (positional variation reported as two standard deviations in Table 5.2). Due to the difficulties in identifying a second metatarsal feature that did not vary considerably in position, this element was instead investigated using a region of interest (ROI) (see Section 5.4).

Equation 5.1 – The location of a feature expressed as a percentage of the long bone's total length.[1]

$$TL\% = 100 \times \left(\frac{L}{TL}\right)$$

[1] TL%=percent total length; L=distance from the distal end of the bone to the feature (mm); TL=total length of the bone (mm).

5.3 Variation of Bone Areas around a Feature

As the position of all the selected features varied slightly along the long bone shaft, it was necessary to quantify the amount that the calculated bone areas changed above and below the target measurement feature. The purpose of this was to assess the effect that an inaccurately positioned cross-sectional measurement would have on the calculated bone area. Studies, such as that by Macintosh et al. (2013), evaluated how cross-sectional properties vary along femoral, tibial, and humeral diaphyses. Tibiae and humeri varied the least in the diaphyseal region distal to the midshaft (Macintosh et al. 2013). These regions of low variability were selected for measurement in the current study.

Randomized samples of roughly 50, non-fractured, complete elements from Ancaster were used to quantify the amount of error associated with inaccurately placed cross-sectional measurements. Table 5.3 presents the sample counts for each element type by sex. Second metatarsals were not included in these analyses as their morphological feature was already eliminated due to excessive positional variation.

Table 5.3 – Number of complete, non-fractured elements used to assess cross-sectional variability around a selected feature.

Element	Female	Male	Total
Humerus	25	29	54
Radius	24	30	54
Ulna	20	35	55
Second Metacarpal	37	11	48
Tibia	23	27	50

For every individual element, the average positional variability indicated by two standard deviations from the mean measurement location (discussed in Section 5.2), was converted to a value in millimetres. ‘Bounding’ measurement slices were then positioned superior and inferior to the ‘target’ morphological feature at a distance equivalent to the amount of positional variability for that element and feature (Figure 5.1). The total and medullary widths were measured at each bounding slice as well as at the target slice, and the total, medullary, and cortical areas for each slice were calculated (see Equations 4.5 through 4.7, in Section 4.7.2). The differences between the bounding and target measurements were compared using mean percent differences (MD%) (Equation 5.2) and Spearman’s rank correlation coefficients (r).

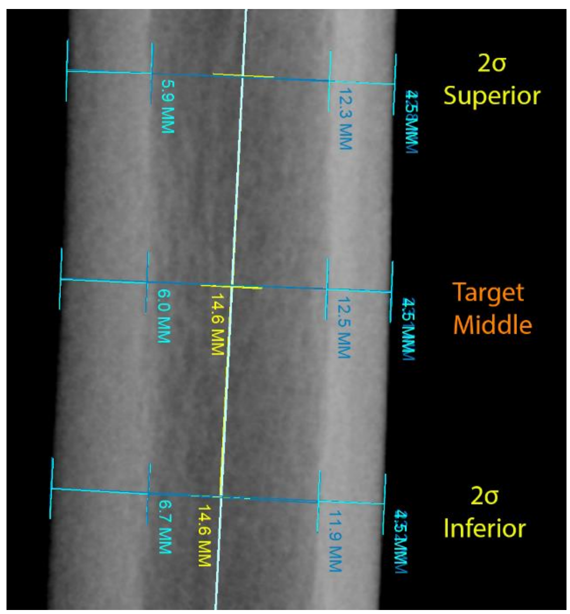

Figure 5.1 –The placement of bounding measurements superior and inferior to the target measurement location are indicated on this antero-posterior view of AN-110’s left tibia.

Equation 5.2 – The mean percent cross-sectional difference between the bounding and target measurements.[1]

$$mean\ percent\ difference\ (MD\%) = 100 \times \left[\frac{(Bounding\ measurement\ - Target\ measurement)}{Target\ measurement}\right]$$

[1] Bounding measurement can refer to either a measurement placed inferior or superior to the target measurement. Measurements can be either the medullary width, total width, or any of the calculated areas.

There are currently no standards that explicitly specify the amount of acceptable variability in cross-sectional studies. However, O'Neill and Ruff (2004) report that the standard error associated with the estimation of true cross-sectional properties using latex cast (LCM) and ellipse model methods (EMM) ranged between 4 and 16%. Compared to ellipse model methods (EMM), which use algebraic assumptions of elliptical shape to infer cross-sectional properties from bilateral X-rays (Lazenby 1998; O'Neill and Ruff 2004; Stock 2002), direct sectioning, CT, and LCM methodologies generally report a lower amount of error in the estimation of cross-sectional shape (≤4 to 9%, as reported by O'Neill and Ruff 2004).

Based on the range of error reported by these other researchers, the acceptable difference between bounding and target feature properties (MD%) was set at less than or equal to eight percent for this research. The allowable range within which 95% of differences fell (i.e., two standard deviations from the mean) was set at 10% above or below the MD%. The relative strength of correlations between the bounding and target measurements, as interpreted from *r* values, are presented in Table 5.4; *p*-values were significant at less than or equal to .05.

Table 5.4 – Strength of correlations interpreted from Spearman's rank correlation coefficients.[1]

r value	Strength of Correlation
0.0 - 0.19	very weak
0.20 – 0.39	weak
0.40 – 0.59	moderate
0.60 – 0.79	strong
0.80 – 1.0	very strong

[1] *r*=Spearman rank correlation coefficient.

The mean percent differences (MD%) and the results of the Spearman's rank correlation coefficients superior and inferior to the target measurement locations are presented in Table 5.5. The results show how much bone areas varied around the target measurement locations, and indicate how inaccurately placed measurements will affect the area outcomes. In the table, results that exceeded the allowable amount (i.e., a mean of 8% and two standard deviations equalling 10%) are presented in bold. Medullary areas were the most vulnerable to positional variability, and were therefore excluded from further consideration in this thesis.

Table 5.5 – Mean percent difference (MD%) and Spearman's rank coefficients (*r*) for bone areas superior and inferior to the target measurement location. Results presented by sex and element.[1]

Cross-Sectional Area	Element	Sex	Superior vs. Target			Inferior vs. Target		
			MD% ± 2σ	*r*	*p*	MD% ± 2σ	*r*	*p*
Total Area	Humerus	F	2.8 ± 4.7	0.975	0.000	2.0 ± 3.4	0.978	0.000
		M	3.0 ± 4.8	0.974	0.000	1.6 ± 3.0	0.974	0.000
	Radius	F	-7.9 ± 6.1	0.933	0.000	**8.3** ± 5.1	0.957	0.000
		M	-6.1 ± 5.0	0.979	0.000	8.0 ± 5.8	0.973	0.000
	Ulna	F	7.0 ± 3.7	0.949	0.000	-2.5 ± 6.1	0.917	0.000
		M	5.3 ± 4.7	0.942	0.000	-4.2 ± 5.1	0.932	0.000
	MC2	F	4.5 ± 7.0	0.966	0.000	-2.3 ± 6.7	0.958	0.000
		M	5.0 ± 7.8	0.973	0.000	-3.0 ± 7.3	0.982	0.000
	Tibia	F	4.1 ± 9.4	0.842	0.000	-4.0 ± 3.4	0.977	0.000
		M	4.8 ± 3.9	0.991	0.000	-4.2 ± 5.5	0.974	0.000
Medullary Area	Humerus	F	2.6 ± **15.2**	0.978	0.000	-0.2 ± **13.7**	0.979	0.000
		M	**5.6 ± 14.7**	0.974	0.000	-1.0 ± **11.4**	0.980	0.000
	Radius	F	**-22.3 ± 13.2**	0.965	0.000	**24.0 ± 26.3**	0.908	0.000
		M	**-18.1 ± 14.5**	0.954	0.000	**18.3 ± 22.6**	0.934	0.000
	Ulna	F	-2.3 ± **15.2**	0.906	0.000	**29.0 ± 23.6**	0.836	0.000
		M	-7.7 ± **15.2**	0.875	0.000	**15.1 ± 19.2**	0.877	0.000
	MC2	F	**23.3 ± 45.2**	0.962	0.000	**-7.3 ± 29.4**	0.969	0.000
		M	**23.1 ± 27.7**	0.938	0.000	**-8.2 ± 28.0**	*0.682*	0.000
	Tibia	F	**13.1 ± 30.2**	0.908	0.000	1.8 ± 23.0	0.934	0.000
		M	**12.3 ± 33.1**	0.962	0.000	3.6 ± **31.2**	0.935	0.000
Cortical Area	Humerus	F	2.8 ± 7.0	0.955	0.000	3.4 ± 5.7	0.949	0.000
		M	2.1 ± 7.8	0.923	0.000	2.5 ± 4.3	0.941	0.000
	Radius	F	-0.7 ± 9.7	0.908	0.000	0.9 ± 8.6	0.937	0.000
		M	0.5 ± 9.4	0.905	0.000	3.0 ± 8.6	0.879	0.000
	Ulna	F	**9.4** ± 5.9	0.899	0.000	**-10.4** ± 7.7	*0.780*	0.000
		M	**8.9** ± 6.7	0.916	0.000	**-9.1** ± 5.8	0.868	0.000
	MC2	F	0.7 ± **12.3**	0.861	0.000	-1.1 ± 9.9	0.878	0.000
		M	-0.1 ± 9.3	0.936	0.000	-1.2 ± **10.1**	0.936	0.000
	Tibia	F	1.2 ± **14.4**	0.953	0.000	-5.1 ± 6.8	0.940	0.000
		M	3.7 ± 7.9	0.946	0.000	-5.3 ± 6.6	0.953	0.000

[1] Bolded values represent the mean percent difference and/or the standard deviations that exceeded the allowable levels variation. Italic font used to indicate correlations less than r=0.85. T_A=total area; M_A=medullary area; C_A=cortical area; MD%=mean percent difference; 2σ=two standard deviations of mean percent difference; *r*=Spearman rank correlation coefficient; *p*=significant at ≤0.05.

The cortical areas of ulnae and second metacarpals routinely exceeded the allowable amounts of variation above and below the target measurement location. Consequently, cortical bone present in ulnae and second metacarpals were evaluated using the region of interest method (see Section 5.4).

Some positional variability existed among female radii and tibiae, but this variability can be explained by the inclusion of identifiable, and avoidable, morphological features. For example, the total areas of female radii were more variable in size inferior to the measurement location, an observation that is explained by normal flaring in the epiphysis near the articular surface. Although this part of the radius fell within the bounding measurement locations, it is recognisable and avoidable; this location would normally not be mistaken for the target measurement location, meaning that this amount of total area variability could be completely avoided. The same is true for female tibiae, which exhibited greater positional error superior to the measurement location. In tibiae, this error is due to the development of the anterior crest, a feature that is very recognisable radiographically and, like the radial epiphysis, can be completely avoided in practice. With an understanding of, and respect for, how the bone morphology influenced the variability in bone areas at each measurement location, the radial and tibial features, along with the humeral feature, were accepted for single-point cross-sectional measurements in this research.

5.4 Region of Interest: Association with Other Techniques

It was not possible to reliably identify morphological features for traditional, single-point, cross-sectional measurements in ulnae, second metacarpals, and second metatarsals. Instead, a method for quantifying the amount of cortical bone present within a larger region of a bone, rather than at a single point, was developed and tested. It was hypothesized that the error associated with positional variation of single-point measurements could be minimized by instead evaluating the amount of bone within a larger diaphyseal zone, or a region of interest (ROI).

Relationships between the amount of cortical bone within a region of interest (ROI) and other methods of measuring the amount of cortical bone were evaluated. Correlations between a standard-sized region of interest and one that is scaled to the total length of each long bone were tested. Comparisons were also made between standard-sized regions and cortical area and cortical index methods, alternative techniques that are often used to measure cortical bone amounts. Comparability between the ROI and other established methods justify the use of this technique, and allow bones without recognizable single-point features or known total lengths to be included in analyses of cortical bone amounts.

Table 5.6 presents the number of elements used to test the standardized regions of interest (ROI) against scaled ROIs, cortical indices, and cortical areas. Approximately 50 ulnae were selected for assessment based on a randomized list of complete non-fractured bones; all complete second metacarpals and metatarsals from individuals without fractures were included. As humeri, radii, and tibiae could be reliably evaluated using single-point measurements, the ROI method was not evaluated for these bone types.

Table 5.6 - Number of complete, non-fractured elements used to evaluate the ROI method.

Element	Female	Male	Total
Ulna	20	35	55
Second Metacarpal	37	11	48
Second Metatarsal	46	31	77

The length of each standardized ROI was based on a percentage of the average total bone length (see Section 4.7.4). The standardized regions were compared to regions scaled to each individual bone length to ensure that standardized regions could be used reliably on bones of differing sizes. Using the total length of each individual bone, the percentages were converted to millimetres to represent the scaled region of interest for every individual bone. In the case of both standard and scaled ROIs, the regions were placed and measured according to the methods outlined in Section 4.7.4.

In order to provide additional confidence in the use of the region of interest method, the standardized and scaled results were compared to cortical indices and cortical areas. Cortical index measurements are calculated based on the relationship between the total and medullary widths (Equation 5.3); this measurement is commonly used in studies of second metacarpals to represent the amount of cortical bone present (e.g., Haara et al. 2006; Ives and Brickley 2004). Cortical areas were calculated using biplanar x-rays using the methods described in Section 4.7.2. Measurements for cortical index and area calculations were placed at the midshaft (i.e., 50% total length) of the second metacarpals, second metatarsals, and ulnae.

Equation 5.3 – Cortical index, a percent value representing the relationship between the total (subperiosteal) and medullary widths. [1]

$$Cortical\ Index = 100\ \times \frac{(TW - MW)}{TW}$$

[1] TW=total width; MW=medullary width.

Spearman's rank correlation coefficient tests were used to compare the relationships between standardized ROIs, scaled ROIs, cortical indices, and cortical areas. Table 5.7 presents the correlations between standard sized ROIs and those that were scaled to the bone's total length, cortical areas, and cortical indices for ulnae, second metacarpals, and second metatarsals.

Table 5.7 – Spearman's rank correlations between standardized ROI areas and ROIs scaled to element length, cortical areas, and cortical indices. [1]

Element Type	Standardized ROI vs. Scaled ROI	Standardized ROI vs. Coritcal Area	Standardized ROI vs. Cortical Index
Ulna	***r*=0.946, p≤0.000**	*r=0.621, p≤0.000*	r=0.438, p=0.001
Second Metacarpal	***r*=0.967, p<0.000**	*r=0.623, p=0.000*	*r=0.698, p<0.000*
Second Metatarsal	***r*=0.937, p≤0.000**	*r=0.733, p≤0.000*	*r=0.616, p≤0.000*

[1] All correlations had significant *p*-values. Very strong correlations indicated with bold text, strong correlations indicated with italic text, and moderate correlations indicated with normal font. ROI=region of interest.

Very strong or strong, significant relationships between standardized ROIs and scaled ROIs, cortical areas, and cortical indices were present for all three bone types. The only exception to this was a moderate relationship identified between ulnar standardized ROI and cortical index values. This moderate, but still significant, correlation can be explained by the location of the cortical index measurement at the ulnar midshaft; this location coincides with marked interosseous crest development, and may not be as representative of the amount of cortical bone present at locations that avoid major soft tissue attachments, such as that selected for the ROI. The strong correlations identified between standardized ROIs and other accepted methods of measuring cortical bone justify the use of standardized ROIs to quantify cortical bone in this research.

5.5 Summary of Variability

This chapter evaluated the error and variability associated with the placement of measurements at morphological locations on a long bone shaft. Features for single-point measurements, exhibiting acceptable levels of error associated with positional variability or inaccurately placed measurements, were identified for humeri, radii, and tibiae. Additionally, the region of interest (ROI) method was assessed and determined to be comparable with other accepted methods of quantifying cortical bone. Cortical bone amounts in ulnae, second metacarpals and second metatarsals did not have reliable single-point features, but can be investigated using the ROI method.

Chapter VI – RESULTS: ANCASTER

This chapter presents the long bone fracture and cross-sectional measurement results for Ancaster. The prevalence and distribution of fractures, fracture types, and complications, are presented by age, sex, and location, in order to elucidate differences in fracture causes and risks between groups at Ancaster. The 'normal' cross-sectional total and cortical area ranges for each bone type are reported, and Ancaster individuals with outlying cross-sectional properties are identified. The chapter concludes by associating the fracture types and complications with the outlying cross-sectional properties in order to identify individuals that may have had altered biomechanical function related to healed fractures.

6.1 Demographic Distribution

A total of 181 adult skeletons were analysed from the Ancaster skeletal collection. The sex and age distribution of the analysed individuals are presented in Table 6.1. Details of each skeleton are reported in Appendix B.

Table 6.1 – Number of observed Ancaster skeletons separated by age and sex.[1]

Age Cohort	Male	Probable Male	Ambiguous Sex	Probable Female	Female	Undetermined Sex	Total
Adolescent (15-19)	1	3	0	0	0	0	4
Young Adult (20-34)	25	17	0	6	27	1	76
Middle Adult (35-49)	33	7	1	9	16	0	66
Old Adult (50+)	3	0	1	0	5	0	9
Adult - Ambiguous	0	0	0	1	4	0	5
Adult - Undetermined	1	5	0	6	1	8	21
Total	63	32	2	22	53	9	181

[1] Ambiguous categories refer to individuals that had observable sex and age features, but could not be classified with certainty. The undetermined categories are individuals that did not have sufficient age or sex features preserved or present to permit classification.

6.2 Fracture Prevalence

The prevalence rates of male and female extremity fractures at Ancaster are presented in Table 6.2 by age; full details for each fracture are provided in Appendix C. Of the 181 Ancaster individuals, 21.5% (*n*=39/181) individuals had fractures. A total of 57 separate fractures were observed among the individuals with fractures; 51 long bone elements had one fracture each and three elements had two fractures each. The true prevalence rate (TPR) of fractures, which compares the total number of fractures to the total number of elements examined, was 3.0% (*n*=57/1905).

Table 6.2 – Ancaster crude and true fracture prevalence rates by age and sex.[1]

Sex	Age Cohort	Individual		Element	
		n/N	CPR (%)	*n/N*	TPR (%)
Male	Adolescent	0/4	0.0	0/49	0.0
	Young Adult	7/42	16.7	9/446	2.0
	Middle Adult	14/40	35.0	23/486	4.7
	Old Adult	1/3	33.3	2/33	6.1
	Adult	0/6	0.0	0/53	0.0
	Total	22/95	23.2	34/1067	3.2
Female	Adolescent	0/0	-	0/0	-
	Young Adult	6/33	18.2	8/378	2.1
	Middle Adult	5/25	20.0	7/261	2.7
	Old Adult	2/5	40.0	3/61	4.9
	Adult	3/12	25.0	4/73	5.5
	Total	16/75	21.3	22/773	2.8
Unknown	Adolescent	0/0	-	0/0	-
	Young Adult	0/1	0.0	0/8	0.0
	Middle Adult	0/1	0.0	0/1	0.0
	Old Adult	1/1	100.0	1/12	8.3
	Adult	0/8	0.0	0/44	0.0
	Total	1/11	8.3	1/65	1.5
Total	Adolescent	0/4	0.0	0/49	0.0
	Young Adult	13/76	17.1	17/832	2.0
	Middle Adult	19/66	28.7	30/748	4.0
	Old Adult	4/9	44.4	6/106	5.7
	Adult	3/26	11.5	4/170	2.4
	Total	39/181	21.5	57/1905	3.0

[1] *n*=number of individuals or elements with fractures, *N*=total number of observed individuals or complete elements (i.e., elements with 3/5 segments that were 75% or more present); CPR=crude prevalence rate; TPR=true prevalence rate; -=no elements or individuals observed.

Fracture prevalence rates (CPR and TPR) were compared between sex and age groups in order to determine if extremity fractures were more common among certain groups. Differences in the true and crude fracture prevalence rates are reported by sex in Table 6.3 and age in Tables 6.4 and 6.5. Both crude and true prevalence rates were slightly greater in middle adult males than females, albeit not significantly. Fracture odds increased slightly with age, a finding that is consistent with the accumulation of injuries over the life course (Glencross 2011), but the differences between Ancaster age groups were typically not significant.

Table 6.3 – Differences between Ancaster male and female crude and true fracture prevalence rates by age.[1]

Age	Crude Prevalence Rate	True Prevalence Rate
Young Adult	*OR=1.1, CI 0.3-3.7* $\chi^2_{Yates}(1, N=75)=0.03, p=.863$	*OR=1.1, CI 0.4-2.7* $\chi^2_{Yates}(1, N=824)=0.01, p=.921$
Middle Adult	OR=2.2, CI 0.7-7.3 $\chi^2_{\mathrm{Yates}}(1, N=64)=1.84$, p=.174	OR=1.9, CI 0.8-4.3 $\chi^2_{\mathrm{Yates}}(1, N=747)=1.97$, p=.160
Old Adult	OR=1.3, CI 0.1-26.6 p_{FET}=1.000	OR=1.2, CI 0.2-7.9 p_{FET}=1.000
Total	OR=1.1, CI 0.5-2.3 $\chi^2_{\mathrm{Yates}}(1, N=169)=0.02$, p=.893	OR=1.1, CI 0.7-1.9 $\chi^2_{\mathrm{Yates}}(1, \mathrm{N}=1840)=0.18$, p=.675

[1] Groups compared using odds ratio, chi-square, and/or Fisher's Exact tests. Bold font indicates that a significant difference is present. Males typically had greater odds of fracture than females, but italic font used to indicate instances when females had greater odds of fracture than males. OR=odds ratio; CI=confidence interval.

Table 6.4 – Age differences in Ancaster crude fracture prevalence rates by sex.[1]

	Young Adult	Middle Adult	Old Adult
		Male	
Young Adult		OR=2.8, CI 1.0-7.9 $\chi^2_{\mathrm{Yates}}(1, N=81)=2.96$, p=.085	OR=2.5, CI 0.2-31.5 p_{FET}=.452
Middle Adult	OR=1.1, CI 0.3-4.2 p_{FET}=1.000		*OR=1.1, CI 0.9-13.5* $p_{FET}=1.000$
Old Adult	OR=3.0, CI 0.4-22.1 p_{FET}=.279	OR=2.7, CI 0.3-20.5 p_{FET}=.565	
	Female		

[1] Groups compared using odds ratio, chi-square, and/or Fisher's Exact tests. Bold font indicates that a significant difference is present. Italic font indicates that compared to an older age category, the younger age category had a greater prevalence of fractures. OR=odds ratio; CI=confidence interval.

Table 6.5 – Age differences in Ancaster true fracture prevalence rates by sex.[1]

	Young Adult	Middle Adult	Old Adult
		Male	
Young Adult		**OR=2.4, CI 1.1-5.3** $\boldsymbol{\chi^2_{Yates}(1, N{=}932){=}5.17, p{=}.023}$	OR=3.1, CI 0.7-15.1 p_{FET} =.171
Middle Adult	OR=1.2, CI 0.5-3.6 $\chi^2_{Yates}(1, N{=}639){=}0.22, p{=}.643$		OR=1.3, CI 0.3-5.8 p_{FET} =.668
Old Adult	OR=2.4, CI 0.6-9.3 p_{FET} =.186	OR=1.8, CI 0.5-7.5 p_{FET}=.408	
	Female		

[1] Groups compared using odds ratio, chi-square, and/or Fisher's Exact tests. Bold font indicates that a significant difference is present. Italic font indicates that compared to an older age category, the younger age category had a greater prevalence of fractures. OR=odds ratio; CI=confidence interval.

The crude prevalence of individuals with multiple trauma were considered in order to examine injury recidivism at Ancaster. Table 6.6 summarizes the number of Ancaster individuals that had one fracture each compared to the number of skeletons that had two or more extremity fractures each (i.e., multiple fractures or polytrauma). Two or more extremity fractures were found in 35.9% (n=14/39) of Ancaster individuals. Males and females had equal odds of polytrauma (OR=1.1, CI 0.3-3.2; $\chi^2_{Yates}(1, N{=}166){=}0.00$, p=1.000). The rate of polytrauma increased with age, as was anticipated given that injuries tend to accumulate over the life course (Glencross 2011), but a chi-square test found that this difference was not significant ($\chi^2(2, N{=}148){=}5.78$, p=.056).

Table 6.6 – The number of Ancaster individuals with either one, or multiple, fractures by age and sex.[1]

Age		One Fracture M	One Fracture F	One Fracture U	One Fracture T	Multiple Fractures* M	Multiple Fractures* F	Multiple Fractures* U	Multiple Fractures* T	Total Fractures M	Total Fractures F	Total Fractures U	Total Fractures T
Adolescent	*n/N*	0/4	0/0	0/0	0/4	0/4	0/0	0/0	0/4	0/4	0/0	0/0	0/4
	%	0.0	-	-	0.0	0.0	-	-	0.0	0.0	-	-	0.0
Young Adult	*n/N*	6/42	4/33	0/1	10/76	1/42	2/33	0/1	3/76	7/42	6/33	0/1	13/76
	%	14.3	12.1	0.0	13.2	2.4	6.1	0.0	3.9	16.7	18.2	0.0	17.1
Middle Adult	*n/N*	8/40	3/25	0/1	11/66	6/40	2/25	0/1	8/66	14/40	5/25	0/1	19/66
	%	20.0	12.0	0.0	16.7	15.0	8.0	0.0	12.1	35.0	20.0	0.0	28.8
Old Adult	*n/N*	0/3	1/5	1/1	1/9	1/3	1/5	0/1	2/9	1/3	2/5	1/1	3/9
	%	0.0	20.0	100.0	11.1	33.3	20.0	0.0	22.2	33.3	40.0	100.0	33.3
Adult	*n/N*	0/6	2/12	0/8	2/26	0/6	1/12	0/8	1/26	0/6	3/12	0/8	3/26
	%	0.0	16.7	0.0	7.7	0.0	8.3	0.0	3.8	0.0	25.0	0.0	11.5
Total	*n/N*	14/95	10/75	1/11	24/181	8/95	6/75	0/11	14/181	22/95	16/75	1/11	39/181
	%	14.7	13.3	9.1	13.3	8.4	8.0	0.0	7.7	23.2	21.3	9.1	21.5

[1] *Multiple fractures include individuals that have two or more fractures each. *n*=number of individuals with fractures; *N*=total number of observed individuals; M=male, F=female, T=total; -=no fractures observed.

6.3 Fracture Distribution

This section reports differences in the fracture prevalence rates between limb and element types by sex and age in order to determine if certain limbs or elements were at increased risk for trauma. Table 6.7 reports the distribution of the Ancaster fractures between the upper and lower limb types by sex and age. Fracture distributions are reported in greater detail in Appendix D. In analyses by limb type, clavicles, humeri, radii, and ulnae were considered bones of the upper limb; bones of the lower limb consisted of femora, tibiae, and fibulae. Fracture prevalence rates were not significantly different between the upper and lower limbs; that is, arms and legs had equal odds of exhibiting trauma (OR=1.1, CI 0.5-2.3; $\chi^2_{\text{Yates}}(1, N=1905)=0.10$, p=.749).

Table 6.7 – Counts and true prevalence rates of Ancaster fractures by limb type, sex, and age.[1]

Limb Type	Age	Female		Male		Unknown Sex		Total	
		n/N	TPR %	*n/N*	TPR %	*n/N*	TPR %	*n/N*	TPR %
Upper Limb	ADO	0/0	-	0/31	0.0	0/0	-	0/31	0.0
	YA	2/201	1.0	3/260	1.2	0/3	0.0	5/464	1.1
	MA	5/143	3.5	13/276	4.7	0/0	-	18/419	4.3
	OA	3/37	8.1	1/21	4.8	1/6	16.7	5/64	7.8
	Adult	1/36	2.8	0/22	0.0	0/15	0.0	1/73	1.4
	Total	11/417	2.6	17/610	2.8	1/24	4.2	29/1051	2.8
Lower Limb	ADO	0/0	-	0/18	0.0	0/0	-	0/18	0.0
	YA	6/177	3.4	6/186	3.2	0/5	0.0	12/368	3.3
	MA	2/118	1.7	10/210	4.8	0/1	0.0	12/329	3.6
	OA	0/24	0.0	1/12	8.3	0/6	0.0	1/42	2.4
	Adult	3/37	8.1	0/31	0.0	0/29	0.0	3/97	3.1
	Total	11/356	3.1	17/457	3.7	0/41	0.0	28/854	3.3
Total	ADO	0/0	-	0/49	0.0	0/0	-	0/49	0.0
	YA	8/378	2.1	9/446	2.0	0/8	0.0	17/832	2.0
	MA	7/261	2.7	23/486	4.7	0/1	0.0	30/748	4.0
	OA	3/61	4.9	2/33	6.1	1/12	8.3	6/106	5.7
	Adult	4/73	5.5	0/53	0.0	0/44	0.0	4/170	2.4
	Total	22/773	2.8	34/1067	3.2	1/65	1.5	57/1905	3.0

[1]*n*=count of all fractures, *N*=count of total observed complete elements (i.e., 3/5 segments 75% or more present); TPR=true prevalence rate; ADO=adolescent; YA=young adult; MA=middle adult; OA=old adult; -=no elements observed.

The distribution of fractures by element type, segment location, sex, and side are depicted in Figure 6.1. Differences in fracture prevalence rates by element, sex, and age are reported in Table 6.8. Supplementary comparisons by age, segment, limb type, and side, are reported in Appendix D. Only males had clavicle fractures, and they fractured this element significantly more than females. Females had significantly greater rates of radial fractures than males. No other element type had fracture frequencies that were significantly different by sex or age. The different rates of fractures to clavicles and radii suggest that Ancaster males and females likely encountered at least some different injury risks that resulted in fractures to different skeletal elements.

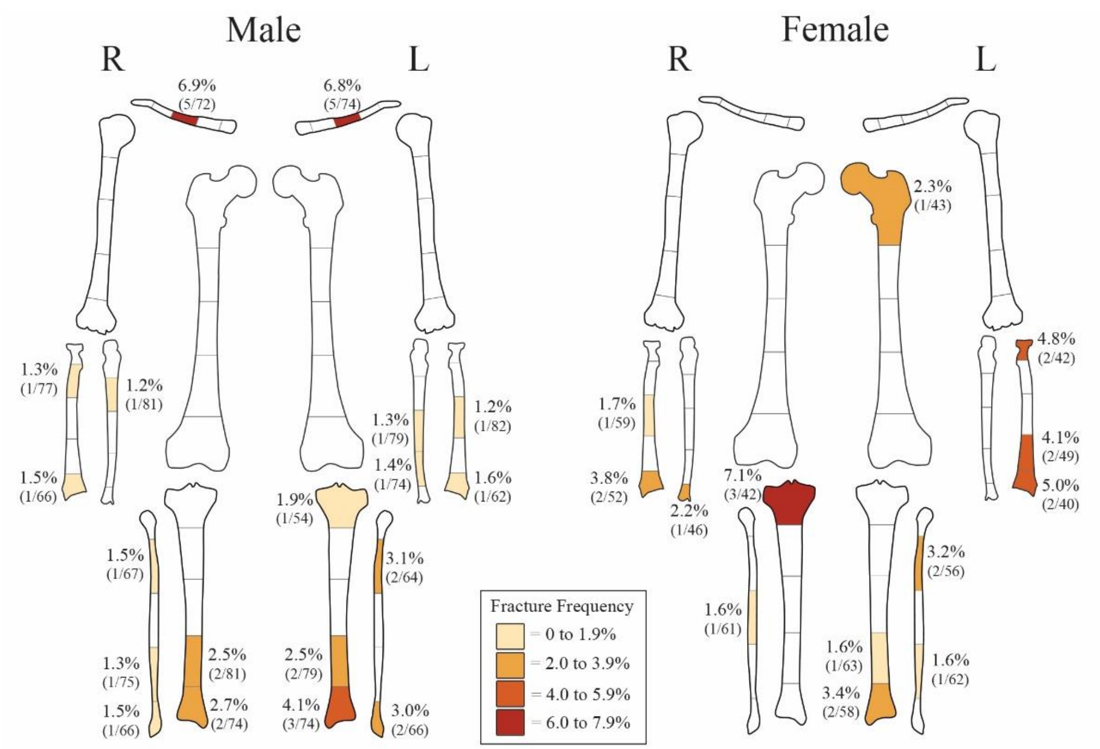

Figure 6.1 – Ancaster fracture true prevalence rates (TPR) by sex, element, segment, and side. Colour coded to represent higher and lower fracture TPRs (see Figure legend). R=Right; L=Left.

Table 6.8 – Counts and differences in Ancaster true fracture prevalence rates between age and sex groups by element type.[1]

Element Type	Male *n/N* %	Male Age Differences	Female *n/N* %	Female Age Differences	Sex Difference (Males vs. Females)
Clavicle	10/140 7.1	$\chi^2(2, N=131)=3.08; p=.215$	0/89 0.0	-	**p_{FET}=.007**
Humerus	0/161 0.0		0/120 0.0	-	-
Radius	4/154 2.6	$\chi^2(2, N=140)=4.24; p=.120$	9/102 8.8	$\chi^2(2, N=95)=3.57; p=.168$	***OR=3.6, CI 1.1-12.1*** ***$\chi^2_{Yates}(1, N=256)=4.94, p=.026$***
Ulna	3/155 1.9	$\chi^2(2, N=140)=0.45; p=.798$	2/106 1.9	$\chi^2(2, N=98)=4.39; p=.111$	OR=1.0, CI 0.2- 6.2 p_{FET}=1.00
Femur	0/161 0.0	-	1/119 0.8	$\chi^2(2, N=108)=1.53; p=.466$	*p_{FET}=.425*
Tibia	10/158 6.3	$\chi^2(2, N=142)=2.78; p=.249$	6/125 4.8	$\chi^2(2, N=110)=3.59; p=.166$	OR=1.3, CI 0.5- 3.8 p_{FET}=.615
Fibula	7/138 5.1	$\chi^2(2, N=122)=0.22; p=.895$	4/112 3.6	$\chi^2(2, N=101)=0.24; p=.889$	OR=1.4, CI 0.4-5.1 p_{FET} =.759

[1] Groups compared using odds ratio, chi-square, and/or Fisher's Exact tests. Bold font indicates that a significant difference is present. Males typically had greater or equal odds of fracture than females; italic font is used to indicate instances that females had greater odds of fracture. TPR=true prevalence rate; *n*=number of fractured elements observed; *N*=total number of elements observed; OR=odds ratio; CI=confidence interval; -=statistical test was unable to be performed because of an absence of fractures.

6.4 Fracture Forces and Types

Fracture types were identified and their prevalence rates compared in order to recognise patterns in the distribution of forces and mechanisms between groups. The Ancaster fractures that could be classified according to mechanism and force type are presented graphically in Figure 6.2 and summarized in Table 6.9 (Appendix C reports fracture details for each analysed individual). Indirect fractures represented 59.3% (*n*=32/54) of the identifiable Ancaster fracture types and included avulsion (Figure 6.3), crush, oblique (Figure 6.4), and stress (Figure 6.5) fracture types. The remaining 40.7% (*n*=22/54) of identifiable fracture types were interpreted as higher energy or direct fracture types and included transverse (Figure 6.6 and 6.7), spiral (Figure 6.8), and comminuted (Figure 6.13) fractures. Three male mid-diaphyseal clavicle fractures could not be classified due either to extensive healing that obliterated the fracture line, or to postmortem damage.

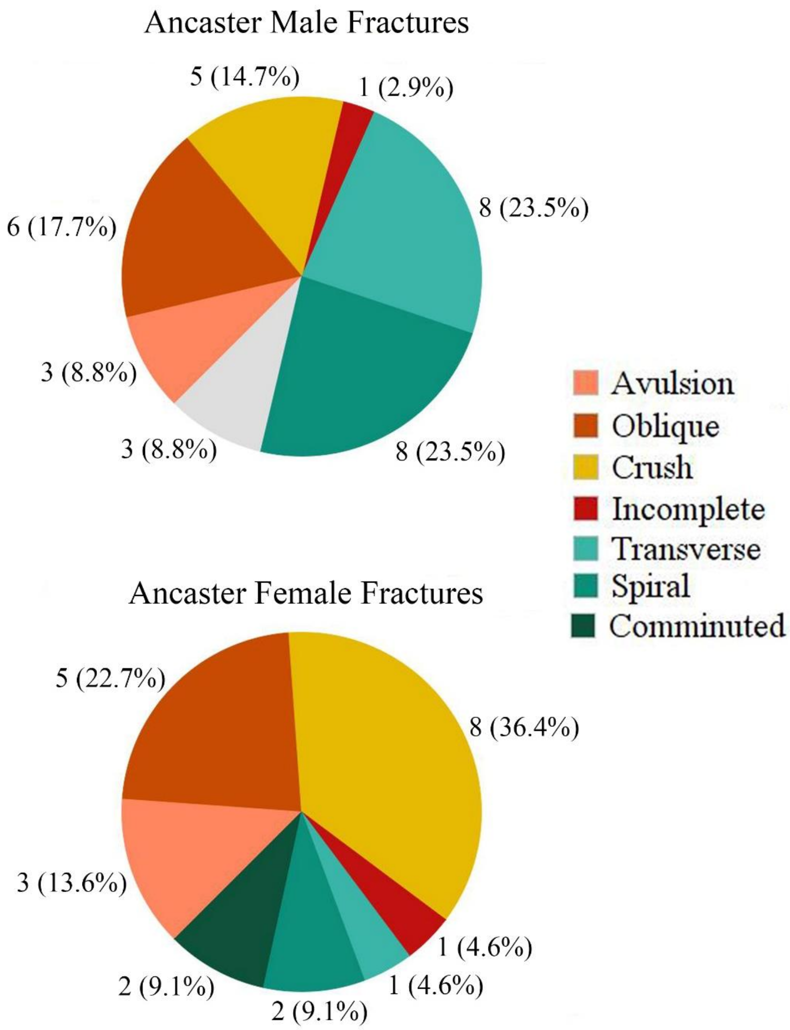

Figure 6.2 – Proportion of Ancaster male and female fracture types. Indirect fracture forces represented by shades of red, orange and yellow, and direct or higher-energy forces represented by green/blue shades (see legend in Figure). Note: AN-155's (Adult female) transverse fibular fracture was classified as an indirect fracture type (avulsion) to reflect the probable causative fracture mechanism.

Table 6.9 – Counts of the Ancaster fractures by force, type, element, and sex.[1]

Force	Mechanism	Clavicle			Radius			Ulna			Femur			Tibia			Fibula			Total		
		M	F	U	M	F	U	M	F	U	M	F	U	M	F	U	M	F	U	M	F	U
Indirect	Avulsion*	-	-	-	-	-	-	-	-	-	-	-	-	2	2	-	1	1*	-	3	3	-
	Oblique	-	-	-	1	3	-	-	-	-	-	-	-	2	-	-	3	2	-	6	5	-
	Crush	-	-	-	1	3	-	-	2	-	-	-	-	4	3	-	-	-	-	5	8	-
	Incomplete**	1	-	-	-	-	-	-	-	-	-	1	-	-	-	-	-	-	-	1	1	-
	Subtotal	1	-	-	2	6	-	-	2	-	-	1	-	8	5	-	4	3	-	15	17	-
Direct / Higher Energy	Transverse	6	-	1	-	1	-	1	-	-	-	-	-	-	-	-	1	-	-	8	1	1
	Spiral	-	-	-	2	-	-	2	-	-	-	-	-	2	1	-	2	1	-	8	2	-
	Comminuted					2															2	
	Subtotal	6	-	1	2	3	-	3	-	-	-	-	-	2	1	-	3	1	-	16	5	1
Unknown		3	-	-	-	-	-	-	-	-	-	-	-	-	-	-	-	-	-	3	-	-
Total		10	-	1	4	9	-	3	2	-	-	1	-	10	6	-	7	4	-	34	22	1

[1] M=male; F=female; U=unknown sex; -=no fractures observed. * includes one fibular fracture (AN-155) identified as transverse, but that was most probably caused by indirect mechanisms. ** Incomplete includes stress/insufficiency fractures.

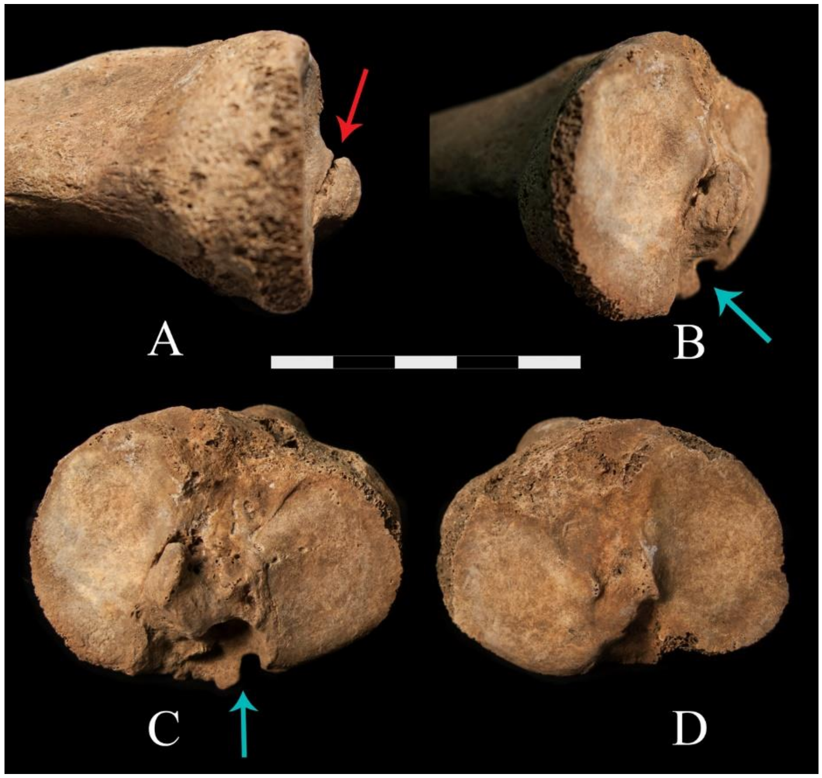

Figure 6.3 – Incompletely avulsed proximal tibial lateral spine (red arrow) in an adult female (AN-154). Also, ossification in the posterior groove corresponding to the posterior cruciate ligament (PCL) (blue arrow). A: Medial view of right tibial plateau; B: Oblique supero-medial view of right tibial plateau; C: Superior view of right tibial plateau; D: Comparative, superior view of left tibial plateau. Scale bar represents 5cm.

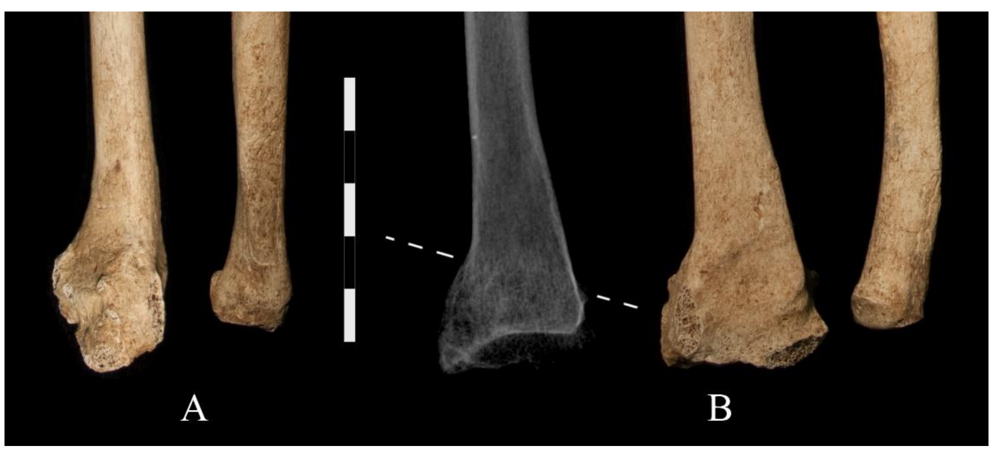

Figure 6.4 – Oblique fracture to the distal radius and a crush fracture to the ulnar styloid process in a middle adult female (AN-053). A: Lateral view, B: Anterior view. Estimated antero-posterior fracture line indicated by dashed line. Not pictured is the steeper (46°) medio-lateral fracture line. Scale bar represents 5cm.

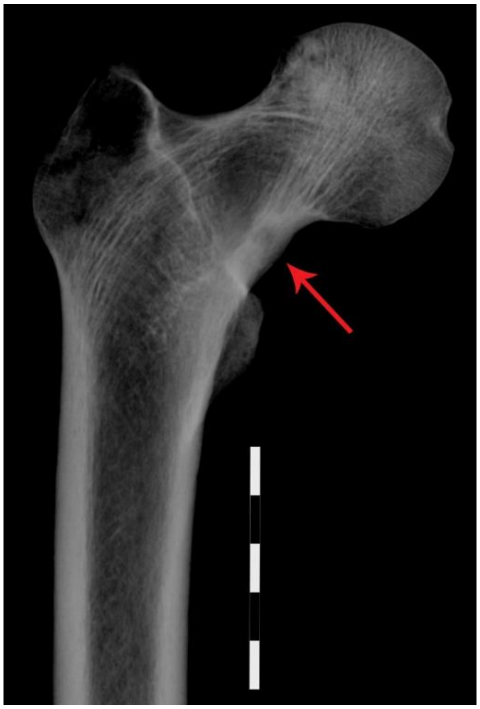

Figure 6.5 – Postero-anterior view of an antemortem insufficiency fracture of the left femoral neck in a middle adult female (AN-113). Location of the fracture is represented by an area of increased opacity and indicated with the red arrow. For additional images of this fracture see Mays (2006a). Scale bar represents 5cm.

Figure 6.6 – Transverse fracture to the distal left ulna of a young adult male (AN-225). A: Anterior view, B: Medial view. Estimated fracture lines indicated with dotted lines. Scale bar represents 5cm.

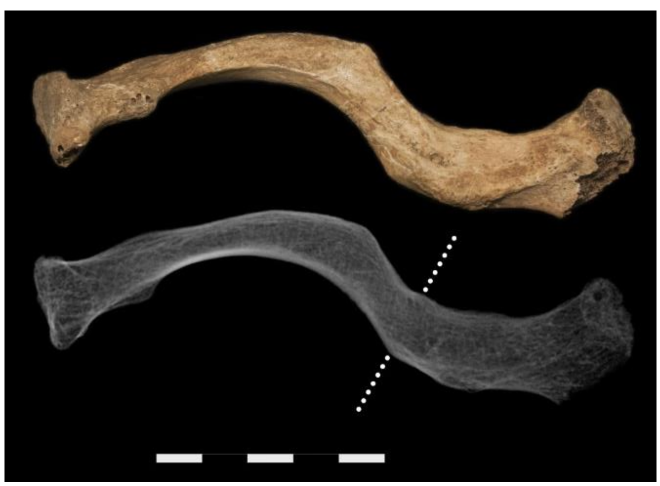

Figure 6.7 – Inferior view of a transverse fracture to the left clavicle of a middle adult (unknown sex, AN-058).. Estimated fracture line marked with dotted line. Scale bar represents 5cm.

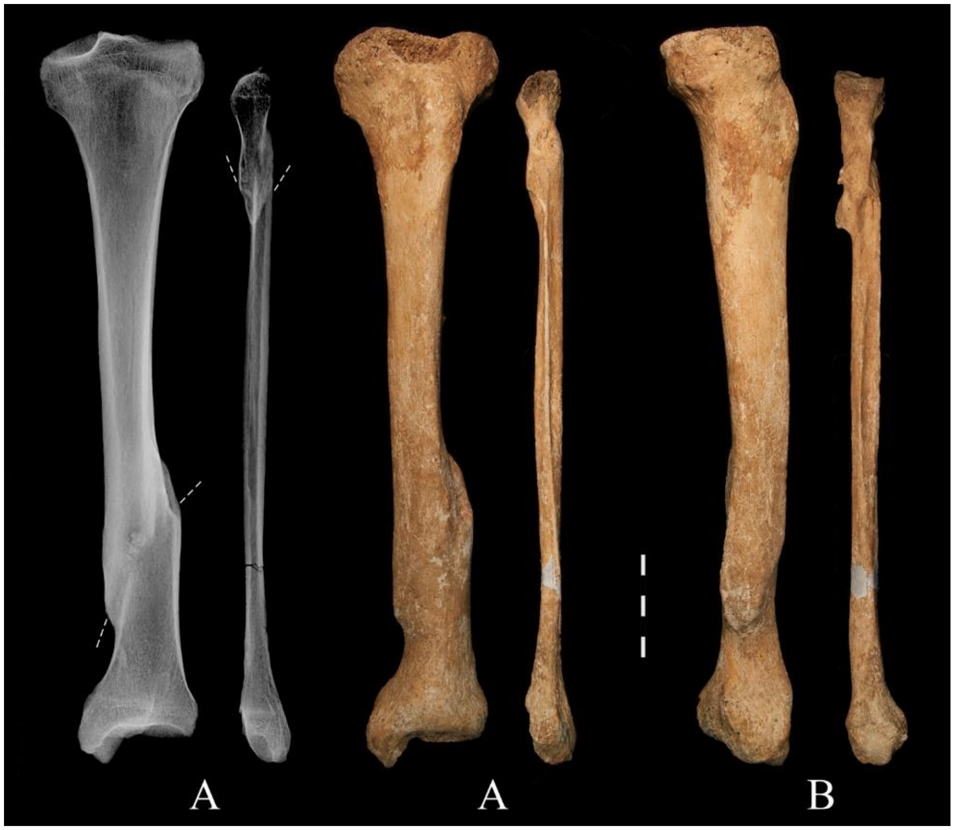

Figure 6.8 – Spiral fractures to the paired left tibia and fibula of a middle adult male (AN-034). A: Anterior view, B: Medial view. Estimated fracture lines marked with dotted lines. Scale bar represents 5cm.

The fracture force and mechanism associated with two of the Ancaster fractures requires further clarification. First, one of the females (AN-155) had an avulsed distal left tibia, paired with a transverse fracture to the distal left fibula (Figure 6.9). While transverse fractures are typically classified as direct injuries, the morphology and pairing of these fracture types suggested they were caused by the same mechanism, that is, over pronation at the ankle (Egol et al. 2010). Both AN-155's fractures, transverse and avulsion, were thus categorized as indirect (avulsion) to account for the probable injury aetiology. Also, one middle adult female (AN-172) had a transverse fracture to the distal aspect of the left radius that bordered on classification as oblique, but as the angle of the fracture line was less than 45 degrees it was categorized as transverse (Figure 6.10).

Figure 6.9 – Avulsed left tibial malleolus paired with a transverse fracture to the distal fibula in an adult female (AN-155). A: Tibia anterior view, B: Fibula anterior view. Estimated fracture lines marked with dotted lines. Scale bar represents 5cm.

Figure 6.10 – Transverse fracture to the distal left radius in a middle adult female (AN-172). A: Anterior view, B: Medial view. Estimated fracture lines marked with dotted lines. Scale bar represents 5cm.

Figures 6.11 and 6.12 illustrate the distribution of indirect and direct force/higher-energy fractures at Ancaster by element, side, and sex. Table 6.10 reports the counts and differences between the prevalence of male and female indirect and direct fracture force types. Ancaster female elements had significantly greater odds of indirect fracture types than males. Females also had significantly more indirect force fractures than they did direct and higher energy indirect fractures, however the large confidence interval suggests a lack of precision in these results. Male elements had four times greater odds of higher energy or direct fracture than females, but this difference was not significant. Male indirect and direct force fracture frequencies were not significantly different. These results suggest that males and females encountered different injury risks that resulted in fractures of differing force types; females were most affected by indirect forces, whereas compared to females, males experienced more direct force and higher-energy injuries.

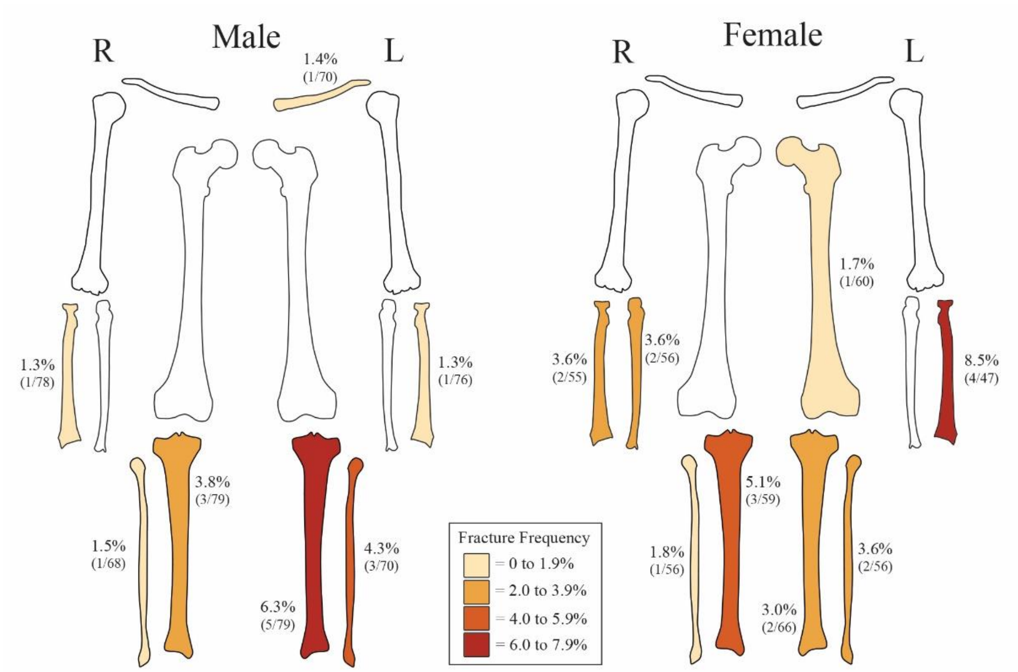

Figure 6.11 – Ancaster indirect fracture true prevalence rates (TPR) by sex, element, side, and segment. Colour coded to represent higher and lower fracture TPRs (see Figure legend). R=Right; L=Left.

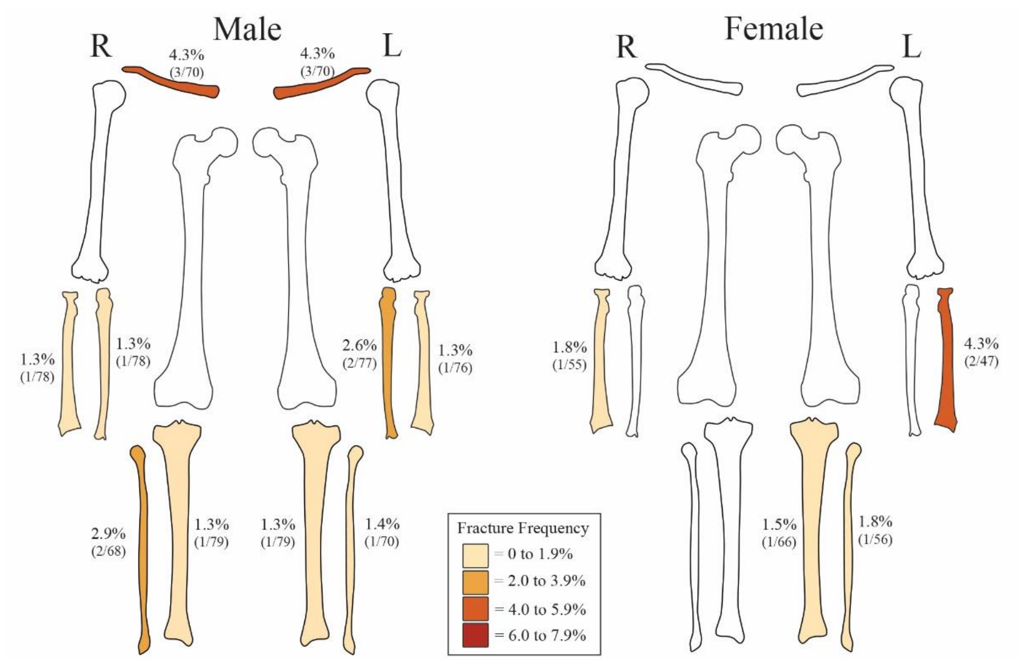

Figure 6.12 – Ancaster direct force and higher-energy fracture true prevalence rates (TPR) by sex, element, side, and segment. Colour coded to represent higher and lower fracture TPRs (see Figure legend). R=Right; L=Left.

Table 6.10 – Fracture counts and differences between the sexes and fracture force types at Ancaster.[1]

Sex	Indirect *n/N* %	Direct/Higher Energy *n/N* %	Indirect vs. Direct
Male	15/34 44.1%	16/34 47.1%	*OR=1.1, CI 0.4-2.9* $\chi^2_{Yates}(1, N=34)=0.00, p=1.000$
Female	17/22 77.3%	5/22 22.7%	**OR=11.6, CI 2.8-47.4;** $\boldsymbol{\chi^2_{Yates}(1, N=22)=11.0, p=.001}$
Male vs Female	***OR=4.3, CI 1.3-14.4*** $\boldsymbol{\chi^2_{Yates}(1, N=56)=4.72, p=.030}$	OR=3.0, CI 0.9-10.1 $\chi^2_{Yates}(1, N=56)=2.42, p=.120$	

[1] Groups compared using odds ratio and chi-square tests. Bold font indicates that a significant difference is present. Italic font used to indicate that females or direct fractures had greater odds of fractures than males or indirect fractures. Counts presented include only those fractures with identifiable force types. *n*=number of fractures of each type; *N*=total number of fractures for each sex; OR=odds ratio; CI=confidence interval.

6.5 Fracture Healing and Complications

With the exception of one perimortem fracture in a distal radius (AN-123), all the other Ancaster fractures exhibited some degree of healing. The one comminuted, perimortem fracture (oblique butterfly) was observed in the left distal radial shaft of a young adult female (AN-123, Figure 6.13). It is possible that this perimortem fracture was sustained shortly before the individual died, however because AN-123 was buried prone and apparently unceremoniously (Wilson n.d.), there is a slight possibility that this fracture occurred after death, during the burial event. No non-union extremity fractures were identified among the Ancaster skeletons.

Figure 6.13 – Young adult female (AN-123) perimortem butterfly fracture to the distal left radius. Butterfly fragment missing. A: Anterior view, B: Medial view; C: Posterior view. Scale bar represents 5cm.

6.5.1 Malunion

The amount of angulation, poor apposition, rotation, shortening, and/or overlap of fracture fragments were recorded for each of the Ancaster fractures. Malunion was classified according to the criteria outlined in Section 4.5.2. Counts and prevalence rates of each kind of malunion observed at Ancaster are reported in Table 6.11 by bone type, limb type, and sex. The amounts of deformation associated with each fracture are reported in Appendix C and the counts and prevalence rates of each type of malunion are reported in Appendix E.

Table 6.11 – Prevalence of fractures with malunion at Ancaster by sex, and element, and limb type.[1]

Element	Male *n/N* %	Female *n/N* %	Unknown Sex *n/N* %	Total *n/N* %	Male vs. Female
Clavicle	4/10 40.0	0/0 -	0/1 0.0	4/11 36.4	
Radius	2/4 50.0	1/9 11.1	0/0 -	3/13 23.1	
Ulna	2/3 66.7	0/2 0.0	0/0 -	2/5 40.0	
Upper Limb Subtotal	8/17 47.1	1/11 9.1	0/1 0.0	9/29 31.0	OR=8.9, CI 0.9-85.7 p_{FET}=.049
Femur	0/0 -	0/1 0.0	0/0 -	0/1 0.0	
Tibia	2/10 20.0	1/6 16.7	0/0 -	2/16 12.5	
Fibula	1/7 14.3	2/4 50.0	0/0 -	2/11 18.2	
Lower Limb Subtotal	3/17 17.6	3/11 27.3	0/0 -	6/28 21.4	*OR=1.8, CI 0.3-10.8* *p_{FET}=.653*
Total	11/34 32.4	4/22 18.2	0/1 0.0	15/57 26.3	

[1] Fracture counts include all lesions with measurable malunion; some fractures were excluded from counts because the fracture type could not exhibit that kind of malunion (e.g., crush fractures cannot be angulated). Shaded rows represent fracture prevalence subtotaled by limb type. Bold font indicates that a significant difference was present. Italic font used to indicate that females had greater odds of malunion than males. *n*=total number of elements with at least one type of malunion, *N*=total number of fractured elements; -=no fractures observed; OR=odds ratio; CI=confidence interval.

In the Ancaster sample, 26.3% (*n*=15/57) of fractures had one or more types of malunion. Rates of malunited fractures were not significantly different between the sexes (OR=2.2, CI 0.6-7.9; $\chi^2_{Yates}(1, N=66)=0.74$, $p=.389$) or between the upper and lower limbs (OR=1.7, CI 0.5-5.5; $\chi^2_{Yates}(1, N=57)=0.27$, $p=.601$). Males at Ancaster had significantly greater rates of malunion in the upper limbs compared to females, however however the large confidence interval suggests a lack of precision in these results. The odds of malunion in the lower limb were not significantly different between the sexes.

Next, the relationship between healed malunions and fracture types were investigated. Counts of fractures that united with one type of malunion, as well as those with multiple types of malunions, are presented by fracture type in Table 6.12. Differences in malunion rates among fracture types are compared in Table 6.13. Higher-energy or direct fracture types accounted for 80.0% (*n*=12/15) of fractures with at least one type of malunion. A significant difference in the types of fractures that were associated with malunion was identified ($\chi^2(4, N=54)=23.18, p<.001$). Spiral fractures had significantly greater odds of having at least one type of malunion, but the large confidence interval suggests a lack of precision in this result (Table 6.13). Of the fractures with multiple malunions, 75% (*n*=3/4) were higher energy or direct types; two were spiral fractures involving paired bones (AN-218 and AN-024), a notoriously unstable fracture type and location (Fabry and Casteleyn 2014) (Figure 6.14). The remaining two fractures with multiple malunions involved clavicles (AN-057, AN-244) that frequently heal with deformity due to difficulties in maintaining reduction (Chan et al. 1999b; McKee et al. 2003) (Figure 6.15).

Figure 6.14 – Spiral fractures to the left tibia and fibula of a young adult female (AN-218). A: Anterior view, B: Medial view. Scale bar represents 5cm.

Table 6.12 – Counts and prevalence rates of malunited fractures at Ancaster by sex and fracture type.[1]

Fracture Type	No Malunion *n/N* %				One Type of Malunion *n/N* %				Multiple Types of Malunion *n/N* %			
	M	F	U	T	M	F	U	T	M	F	U	T
Avulsion	3/3 100.0	2/2 100.0	0/0 -	5/5 100.0	0/3 0.0	0/2 0.0	0/0 -	0/5 0.0	0/3 0.0	0/2 0.0	0/0 -	0/5 0.0
Crush	5/5 100.0	8/8 100.0	0/0 -	13/13 100.0	0/5 0.0	0/8 0.0	0/0 -	0/13 0.0	0/5 0.0	0/8 0.0	0/0 -	0/13 0.0
Oblique	6/6 100.0	4/5 80.0	0/0 -	10/11 90.9	1/6 16.7	1/5 20.0	0/0 -	2/11 18.2	0/6 0.0	0/5 0.0	0/0 -	0/11 0.0
Incomplete	1/1 100.0	1/1 100.0	0/0 -	2/2 100.0	0/1 0.0	0/1 0.0	0/0 -	0/2 0.0	0/1 0.0	0/1 0.0	0/0 -	0/2 0.0
Spiral	2/8 25.0	0/2 0.0	0/0 -	2/10 20.0	5/8 62.5	1/2 50.0	0/0 -	7/10 70.0	1/8 12.5	1/2 50.0	0/0 -	2/10 20.0
Transverse	5/8 62.5	2/2 100.0	1/1 100.0	8/11 72.7	2/8 25.0	0/2 0.0	0/1 0.0	2/11 18.2	1/8 12.5	0/2 0.0	0/1 0.0	1/11 9.1
Comminuted	0/0 -	1/2 50.0	0/0 -	1/2 50.0	0/0 -	1/2 50.0	0/0 -	1/2 50.0	0/0 -	0/0 -	0/0 -	0/0 -
Unknown	2/3 66.7	0/0 -	0/0 -	2/3 66.7	0/3 0.0	0/0 -	0/0 -	0/3 0.0	1/3 33.3	0/0 -	0/0 -	1/3 33.3
Total	24/34 70.6	18/22 81.8	1/1 100.0	43/57 75.4	8/34 23.5	3/22 13.6	0/1 0.0	11/5 7 19.3	3/34 8.8	1/22 4.5	0/1 0.0	4/57 7.0

[1] Malunion types include angulation, poor apposition, rotation, shortening, and overlap of fractured fragments. Multiple malunion includes fractures that had at least two types of malunion (e.g., both angulation and rotation). *n*=number of fractures with malunion; *N*=number of total fractures observed; M=male, F=female, U=unknown sex, T=total; -=no fractures were observed.

Figure 6.15 – Midshaft right clavicle fracture of unknown, but probable oblique fracture, type in a young adult male (AN-244). A: Anterior view, B: Inferior view; C: Posterior view; D: Superior view. Scale bar represents 5cm.

Table 6.13 – Differences in the prevalence of malunion between fracture types at Ancaster.[1]

Fracture Types Compared	Counts *n/N*	Difference
Avulsion, Crush & Incomplete vs All Other Fracture Types	0/20 15/37	**p_{FET}<0.001**
Oblique vs All Other Fracture Types	2/11 13/46	OR=1.8, CI 0.3-9.3 p_{FET}=0.709
Spiral vs All Other Fracture Types	8/10 7/47	***OR=22.9, CI 4.0-130.9*** ***p_{FET}<0.001***
Comminuted vs All Other Fracture Types	1/2 14/55	*OR=2.9, CI 0.2-50.0* *p_{FET}=0.461*
Transverse vs. All Other Fracture Types	3/11 12/46	*OR=1.1, CI 0.2-4.7* *p_{FET}=1.000*
High Energy and Direct Force Fractures vs Indirect Force Fractures	12/23 2/31	**OR=15.8, CI 3.0-82.4** **$\chi^2_{Yates}(1, N=54)=12.1$, p=0.001**
All Fracture Types	-	**$\chi^2(4, N=54)=23.18$, p<.001**

[1] Groups were compared using odds ratio, chi-square, and/or Fisher's Exact tests. Fractures with at least one type of malunion were included in the counts. Bold font indicates that a significant difference is present. Italic font used to indicate that the specific tested fracture type had greater odds of malunion than all other types of fractures combined. *n*=number of fractures with at least one type of malunion; *N*=number of total fractures; OR=odds ratio; CI=confidence interval.

6.5.2 Inflammation & Soft Tissue Injury

None of the fractures at Ancaster presented definitive evidence for infection. Soft tissue injury was identified in one young adult male (AN-047) with an oblique fracture to the left distal fibula, and ossification of the anterior inferior tibiofibular, posterior inferior tibiofibular, and interosseous ligaments (Figure 6.16). Injury to these soft tissues is common in some over-pronation/supination ankle injuries (Donatto 2001).

Figure 6.16 – Left fibular fracture with ossification of the tibiofibular and interosseous ligaments in a middle adult male (AN-047). A: Anterior view of articulated tibia and fibula; B: Medial view of the fibula showing the three ossified ligaments; C: Medio-lateral radiographic view of the fibula (medial against the plate); D: Anterior radiographic view of the fibula. Estimated fracture line indicated with a dotted line. Scale bars represent 5cm.

Additionally, an adult female (AN-154) had an incompletely avulsed right lateral tibial intercondylar eminence, which corresponds to the anterior cruciate ligament (ACL) insertion, and a probable avulsion fracture at the site of the posterior cruciate ligament (PCL) insertion (see Figure 6.3). ACL and PCL avulsions are relatively rare, but both may be caused either by a fall or direct blow to the anterior aspect of a bent knee, possibly with some rotation of the tibia (Allen et al. 2002; Calpur et al. 2002; Egol et al. 2010; Meyers and McKeever 1959). According to Lubowitz et al. (2005), tibial intercondylar eminence avulsions are clinically more often reported in juveniles, and seem predominantly associated with activities that they are undertaking. This, combined with the fact that incomplete fractures are more typical in sub-adults, suggests that the fracture sustained by AN-154 may have occurred during adolescence.

6.5.3 Osteoarthritis

The prevalence rate of osteoarthritis (OA_x) at Ancaster, as well as the prevalence of fractures with osteoarthritis, are reported by age and sex in Table 6.14. Osteoarthritis data are presented for each analysed individual in Appendix F; additional true prevalence rates of osteoarthritis by joint type and age are reported in Appendix G. At Ancaster, 78.1% (*n*=1696/2172) of all expected joint surfaces were present. Of the fractured elements at Ancaster, 92.5% (*n*=50/54) had at least one adjacent articular surface that was sufficiently complete for inclusion in analyses of osteoarthritis.

Table 6.14 – Counts and true prevalence rates of osteoarthritis (OA_x) and fractures with osteoarthritis at Ancaster by sex and age.[1]

Age Category	Total OA_x/*N* joints TPR (%)				Fractured elements with OA_x*/*N* joints TPR (%)			
	Female	Male	Unknown	Total	Female	Male	Unknown	Total
ADO	0/0 -	0/43 0.0%	0/0 -	0/43 0.0%	0/0 -	0/43 0.0%	0/0 -	0/43 0.0%
YA	9/337 2.7%	8/385 2.1%	0/6 0.0%	17/728 2.3%	3/337 0.9%	1/385 0.3%	0/6 0.0%	4/728 0.5%
MA	22/252 8.7%	49/433 11.3%	0/1 0.0%	71/686 10.3%	2/252 0.8%	12/433 2.8%	0/1 0.0%	14/686 2.0%
OA	8/52 14.8%	3/29 10.3%	4/11 36.4%	15/94 16.0%	4/52 7.7%	0/29 0.0%	1/11 9.1%	5/94 5.3%
Adult	7/75 9.3%	5/44 11.4%	2/26 7.7%	14/145 9.7%	0/75 0.0%	0/44 0.0%	0/26 0.0%	0/145 0.0%
Total	46/718 6.4%	65/934 7.0%	6/44 13.6%	117/1696 6.9%	9/718 1.3%	13/934 1.4%	1/44 2.3%	23/1696 1.4%

[1] If osteoarthritis was present in both the proximal and distal joints of the same fractured element, both joint types were recorded. If both bones in a pair (e.g., radii and ulnae) were fractured, the joint with osteoarthritis was only counted once. *N* joints=total number of observable joints; OA_x=osteoarthritis; TPR=true prevalence rate; ADO=adolescent; YA=young adult; MA=middle adult; OA=old adult. *number of fractured elements counted, not the number of fractures total (i.e., some elements had more than one fracture each and were only counted once).

At Ancaster, 32.6% (*n*=59/181) of all analysed individuals and 6.9% (*n*=117/1696) of joints exhibited osteoarthritis. Overall, the rates of osteoarthritis were not different between male and female joints (OR=1.2, CI 0.4-3.3; $\chi^2_{Yates}(1, N=1652)=0.00$, $p=.992$). Of all the joints with osteoarthritis, 19.7% (*n*=23/117) also had fractures in at least one adjacent element. There was also no sex-based difference in the rates of osteoarthritis in individuals with fractures (OR=1.1, CI 0.4-2.6; $\chi^2_{Yates}(1, N=1652)=0.00$, $p=.979$). These results show that males and females were equally susceptible to osteoarthritis at Ancaster; sex did not seem to play a role in the development of osteoarthritis, before or after fracture, at this site.

Table 6.15 reports the difference in osteoarthritis prevalence rates by age. Based on the clinical association between osteoarthritis and advancing age (Loeser 2009), it was hypothesized that older adults would have significantly greater prevalence rates of osteoarthritis than younger adults. This finding was true at Ancaster, and osteoarthritis was significantly more prevalent in middle and/or old adult individuals than young adults.

Table 6.15 – Age differences in the prevalence rates of osteoarthritis at Ancaster overall, as well as the prevalence rates of osteoarthritis among elements with fractures. [1]

	Young Adult	Middle Adult	Old Adult
		Total OA_x/N joints	
Young Adult		**OR=4.8, CI 2.8-8.3 $x^2_{Yates}(1, N=1414)=37.51$, $p=.000$**	**OR=7.9, CI 3.8-16.5 $p_{FET}=.000$**
Middle Adult	OR=3.0, CI 0.9-9.3 $\chi^2_{Yates}(1, N=1414)=2.80$, $p=.094$		OR=1.6, CI 0.9-3.0, $\chi^2_{Yates}(1, N=780)=2.11$, $p=.146$
Old Adult	**OR=8.0, CI 2.0-32.7 $p_{FET}=.008$**	OR=2.7, CI 0.9-8.7 $p_{FET}=.095$	
	Fractures with OA_x/N Joints		

[1] Groups were compared using odds ratios, chi-square, and/or Fisher's exact tests. Bold font indicates that a significant difference is present. In all instances the older age category had greater odds of fracture as the younger age category. OA_x=osteoarthritis; *N* joints= total number of observable joints; OR=odds ratio; CI=confidence interval.

The prevalence of osteoarthritis as it was associated with each fracture type observed at Ancaster is presented in Table 6.16. Sexes were combined, and a chi-square test found that there was no significant difference in the prevalence rates of osteoarthritis among the fracture types ($\chi^2(7, N{=}57){=}10.34$, $p{=}.170$).

Table 6.16 – Counts of osteoarthritis associated with each fracture type at Ancaster by sex.[1]

Force	Fracture Type	Female *n/N* %	Male *n/N* %	Unknown Sex *n/N* %	Total *n/N* %
Indirect	Crush	3/8 37.5	3/5 40.0	0/0 -	6/13 38.5
	Avulsion	0/3 0.0	0/3 0.0	0/0 -	0/6 0.0
	Oblique	3/5 60.0	3/6 50.0	0/0 -	6/11 54.5
	Incomplete	0/1 0.0	0/1 0.0	0/0 -	0/2 0.0
	Subtotal	6/17 35.3	6/15 40.0	0/0 -	12/32 37.5
Higher-Energy and Direct	Spiral	2/2 100.0	2/8 25.0	0/0 -	4/10 40.0
	Transverse	1/1 100.0	3/8 37.5	1/1 100.0	5/10 50.0
	Comminuted	0/2 0.0	0/0 -	0/0 -	0/2 0.0
	Subtotal	3/3 100.0	5/16 31.3	1/1 100.0	9/22 40.1
Unknown		0/0 -	0/3 0.0	0/0 -	0/3 0.0
Total		9/22 40.9	11/34 29.4	1/1 100.0	21/57 35.1

[1] In order to compare against fractured element counts, osteoarthritis was only counted once per element, even if osteoarthritis was present in both proximal and distal articular surfaces. *n*=number of fractures with osteoarthritis; *N*=total number of fractures; -=no fractures observed.

Some clinical research has suggested that fractures can lead to the development of post-traumatic osteoarthritis, particularly when associated with malunion or joint injury (e.g., Anderson et al. 2011; Forward et al. 2008). It was hypothesized that the Ancaster fractures that had healed with greater amounts of deformity (discussed in Section 6.5.1) as well as those fractures that involved joint surfaces, would be at greater risk for developing osteoarthritis.

Table 6.17 presents the counts and prevalence rates of osteoarthritis as it was associated with fractures to joint surfaces and fractures that healed with malunion. Together, fractures to subchondral joint surfaces and fractures with malunion accounted for 54.5% (*n*=12/22) of the fractures with osteoarthritis among Ancaster males and females. When the counts of joint fractures and malunited fractures were combined, this group had significantly greater odds of osteoarthritis than fractures that did not directly involve subchondral surfaces or exhibit large amounts of malunion (OR=5.6, CI 1.7-18.9; $\chi^2_{\mathrm{Yates}}(1, N{=}56){=}6.73$, $p{=}.009$). The results of these tests suggest a relationship between the development of osteoarthritis and trauma to the joint and/or healed fracture malunion. Although the possible development of post-traumatic osteoarthritis is acknowledged in palaeopathological fracture studies, this study is the first known to use a larger collection to investigate the association between the prevalence rates of osteoarthritis, subchondral fractures, and fractures that have healed with malunion.

Table 6.17 – Relationships between the rates of osteoarthritis in fractures to joints and fractures with malunion at Ancaster.[1]

Age	Sex	Malunited fractures	Joint fractures		Both malunited and joint fractures	
		n/N %	n_j/N_j %	*n/N* %	*n/N* %	*n/N* with OA_x %
Adolescent	Male	0/0 -	0/49 0.0	0/11 0.0	0/0 -	0/0 -
	Female	0/0 -	0/0 -	0/0 -	0/0 -	0/0 -
Young Adult	Male	0/2 0.0	3/9 33.3	0/3 0.0	0/5 0.0	0/1 0.0
	Female	2/3 66.6	4/8 50.0	1/4 25.0	3/7 42.9	3/3 100.0
Middle Adult	Male	4/8 50.0	3/23 13.0	3/3 100.0	7/11 63.6	7/12 58.3
	Female	0/1 0.0	3/7 42.9	1/3 33.3	1/4 25.0	1/2 50.0
Old Adult	Male	0/0 -	1/2 50.0	0/1 0.0	0/1 0.0	0/0 -
	Female	0/0 -	1/3 33.3	1/1 100.0	1/1 100.0	1/4 25.0
Adult	Male	0/0 -	0/0 -	0/0 -	0/0 -	0/0 -
	Female	0/0 -	3/4 75.0	0/3 0.0	0/3 0.0	0/0 -
Total	Male	4/10 40.0	7/34 20.6	3/7 42.9	7/17 41.2	7/13 53.8
	Female	2/4 50.0	11/22 50.0	3/11 27.3	5/15 33.3	5/9 55.6

[1] Bold font indicates that a significant difference is present. Italic font used to indicate when the lower limb had greater osteoarthritis frequency than the upper limb. *n*=number of malunited and/or joint fractures with osteoarthritis; *N*=total number of malunited and/or joint fractures observed; n_j=number of joint fractures; N_j=total number of joints observed; OA_x=Osteoarthritis; -=no observed fractures.

6.6 Cross-Sectional Results: Establishing the Cross-Sectional "Norm"

In order to evaluate the bone area and asymmetry changes that were associated with fractures at Ancaster, it was first necessary to determine the normal range of total and cortical areas (T_A, C_A) and total and cortical area directional asymmetries (T_A%DA, C_A%DA) present in this assemblage. The long bones of all the fractured individuals were radiographed, along with a comparative sample of individuals without fractures; the comparative sample represented 33.7% (*n*=61/181) of individuals from the total analysed assemblage. Age and sex differences in cross-sectional properties were tested within the comparative sample in order to determine if groups could be combined in subsequent analyses.

Table 6.18 reports the number of radiographed Ancaster individuals by the total number of individuals observed and total number of individuals with fractures. Some elements were not available for radiography due to differential preservation, fragmentation, or bones being lost or misplaced in the time between excavation and analysis. Table 6.19 reports the number of individuals, elements, and right and left sided element pairs with and without fractures that were measured. The distributions of radiographed individuals with and without fractures are presented in greater detail in Appendix H.

Table 6.18 – Number of Ancaster individuals that were radiographed.[1]

Number of Ancaster Individuals Radiographed	Female *n/N* %	Male *n/N* %	Unknown Sex *n/N* %	Total *n/N* %
n individuals radiographed / Total *N* individuals observed	45/75 60.0	54/95 56.8	1/11 9.1	100/181 55.2
n individuals with fractures radiographed / Total *N* individuals radiographed	16/45 35.6	22/54 40.7	1/1 100.0	39/100 39.0

[1]*n*=number of individuals radiographed; *N*=total number of individuals observed/radiographed.

Table 6.19 – Number of Ancaster individuals, elements, and element pairs with and without fractures that were measured radiographically.[1]

Sex	Element	Individual *n/N*	Element *n/N*	Paired* *n/N*
Female	Humerus	14/42	28/84	14/42
	Radius	14/41	15/63	12/33
	Ulna ROI	11/36	21/69	10/33
	MC2 50%	5/25	10/47	5/22
	MC2 ROI	5/25	10/50	5/25
	Tibia	15/44	28/85	12/42
	MT2 ROI	4/27	8/54	13/36
Male	Humerus	20/51	40/102	20/51
	Radius	18/51	8/69	15/44
	Ulna ROI	18/48	33/90	15/42
	MC2 50%	1/7	2/13	1/6
	MC2 ROI	1/7	2/14	1/7
	Tibia	17/48	34/96	17/48
	MT2 ROI	13/29	26/58	4/19
Unknown Sex	Humerus	0/0	0/0	0/0
	Radius	0/0	0/0	0/0
	Ulna ROI	0/0	0/0	0/0
	MC2 50%	0/0	0/0	0/0
	MC2 ROI	0/0	0/0	0/0
	Tibia	1/2	2/2	1/1
	MT2 ROI	1/2	2/2	1/1
Total	Humerus	34/93	68/186	34/93
	Radius	31/91	60/169	28/78
	Ulna ROI	29/84	54/159	25/75
	MC2 50%	6/32	12/60	6/28
	MC2 ROI	6/32	12/64	6/32
	Tibia	33/93	64/183	30/90
	MT2 ROI	18/57	36/114	18/56

[1] Second metacarpals are reported twice because multiple techniques requiring different bone completeness were used to evaluate the bone amount in this element type. *n*=number of individuals or elements associated with fractured individuals; *N*=total number of radiographed individuals or elements; MC2=second metacarpal; MC2 50%=measurements taken at the second metacarpal midshaft; MT2=second metatarsal; ROI=measurements taken using a standardized region of interest. **number of elements with both right and left sides present and measureable.

6.6.1 Total, Cortical, and Region of Interest Areas:

In order to identify similarities in the cross-sectional properties between groups at Ancaster, the comparative (i.e., ‘normal’) sample was used to determine the average total (T_A) and cortical bone (C_A and ROI) areas for each long bone type. These areas are reported in Table 6.20 along with differences between the sexes. Appendix I reports the raw measurements and calculated areas for each bone type. Data were tested for normality by site, sex, and age; normality tests for each category are reported in Appendix J. The T_A, C_A, and ROIs of each element type were significantly different between males and females. Consequently, each element was divided by sex for all subsequent comparisons of bone area.

Table 6.20 – Average total areas and cortical/ROI areas at Ancaster and the differences between males and females by element type.[1]

Element	Average T_A +/- σ		Average C_A +/- σ	
	Female	Male	Female	Male
Humerus	233.3 ± 24.2	307.1 ± 41.5	167.0 ± 25.7	224.4 ± 28.6
	U=239.5, p≤.001		**U=230, p≤.001**	
Radius	115.8 ± 14.2	156.2 ± 26.7	76.3 ± 9.4	102.3 ± 14.2
	U=227.5, p≤.001		**U=166, p≤.001**	
Ulna ROI	-	-	215.5 ± 39.9	264.9 ± 44.4
	-		**U=554.0, p≤.001**	
MC2 50%	49.4 ± 6.3	60.9 ± 7.8	37.9 ± 4.2	46.5 ± 6.6
	U=45.5, p≤.001		**U=48.0, p≤.001**	
MC2 ROI	-	-	71.1 ± 13.4	80.9 ± 11.1
	-		**U=131.0, p=.018**	
Tibia	385.1 ± 44.7	494.0 ± 66.9	295.5 ± 41.6	405.3 ± 55.4
	U=315.5, p≤.001		**U=178, p≤.001**	
MT2 ROI	-	-	90.4 ± 14.7	101.4 ± 15.1
	-		**U=420.0, p=.002**	

[1] Groups compared using Mann-Whitney U tests. Bold values are significant. T_A=Total area; C_A=Cortical Area; σ=standard deviation; ROI=region of interest; MC2=second metacarpal; MC2 50%=measurement taken at second metacarpal midshaft; MT2=second metatarsal; -=no data available to test.

The total and cortical (C_A and ROI) areas were compared between age categories using Mann-Whitney U tests in Table 6.21. As adult bone loss typically involves resorption on the endosteal bone surface (Schäfer et al. 2012), it was hypothesized that total areas would not exhibit age-related differences, but that cortical areas should decrease with advancing age. At Ancaster, bone total areas did not differ significantly with age for males or females, with the exception of young and middle adult female second metacarpal midshaft (MC2 50%) measurements. These results show that the size of the outer bone area was not typically associated with an individual's age.

Table 6.21 – Age differences in the total and cortical areas at Ancaster by bone type and sex.[1]

Sex	Area	Element	YA vs. MA	YA vs. OA	MA vs. OA
Female	T_A	Humeri	*U*=236.0, *p*=.469	*U*=61.5, *p*=.226	*U*=32.5, *p*=.152
		Radii	*U*=170.5, *p*=.331	*U*=63.5, *p*=.484	*U*=45.5, *p*=.854
		MC2 50%	***U*=75.5, *p*=.029**	*U*=16.5, *p*=.143	*U*=26.5, *p*=.501
		Tibia	*U*=241.5, *p*=.077	*U*=33.0, *p*=.086	*U*=55.0, *p*=.591
	C_A/ROI	Humeri	***U*=143.0, *p*=.007**	***U*=27.0, *p*=.007**	*U*=27.0, *p*=.072
		Radii	***U*=119.0, *p*=.021**	*U*=65.5, *p*=.546	*U*=44.5, *p*=.796
		Ulna ROI	***U*=131.0, *p*=.037**	***U*=33.0, *p*=.035**	*U*=47.0, *p*=.812
		MC2 ROI	***U*=41.0, *p*=.000**	***U*=0.0, *p*=.000**	*U*=26.0, *p*=.620
		MC2 50%	***U*=80.5, *p*=.046**	*U*=12.5, *p*=.065	*U*=21.0, *p*=.244
		Tibia	*U*=305.0, *p*=.546	*U*=56.0, *p*=.629	*U*=50.0, *p*=.420
		MT2 ROI	***U*=55.0, *p*=.000**	***U*=23.0, *p*=.000**	*U*=27.0, *p*=.072
Male	T_A	Humeri	*U*=217.5, *p*=.066	*U*=47.0, *p*=.948	*U*=40.0, *p*=.464
		Radii	*U*=284.5, *p*=.613	*U*=15.0, *p*=.118	*U*=14.0, *p*=.067
		MC2 50%	*U*=4.0, *p*=.380	-	-
		Tibia	*U*=318.0, *p*=.549	*U*=20.0, *p*=.835	*U*=31.0, *p*=.942
	C_A/ROI	Humeri	*U*=241.0, *p*=.168	*U*=39.0, *p*=.555	*U*=31.0, *p*=.200
		Radii	*U*=231.5, *p*=.124	*U*=17.0, *p*=.160	***U*=10.0, *p*=.035**
		Ulna ROI	***U*=152.0, *p*=.008**	*U*=21.0, *p*=.812	*U*=15.0, *p*=.480
		MC2 ROI	*U*=2.0, *p*=.117	-	-
		MC2 50%	***U*=0.0, *p*=.040**	-	-
		Tibia	*U*=351, *p*=.986	*U*=15.0, *p*=.465	*U*=21.0, *p*=.421
		MT2 ROI	*U*=94.5, *p*=.840	-	-

[1] Groups compared using Mann-Whitney U tests. Significant results in bold. -=no test performed due to small sample sizes; YA=young adult; MA=middle adult; OA=old adult; T_A=total area; C_A=cortical area; ROI=region of interest; MC2=second metacarpal; MC2 50%=measurements taken at the second metacarpal midshaft; MT2=second metatarsal; -=no data available to test.

When cortical areas were assessed, significant differences were identified for both male and female elements. Among the males, age-related cortical area differences were only evident between young and middle adult ulnae and second metacarpal midshaft (MC2 50%) locations, as well as middle and old adult radial cortical areas (Table 6.21). In contrast, the cortical areas (C_A and ROI) of all young adult female elements were significantly different from middle and/or old adult females; tibiae were the only exception, and were the only element type that did not exhibit significant age-related differences in cortical area between female age cohorts. These findings indicate that age-related bone loss was present at Ancaster, corroborating Mays' (2006a) findings of age-related bone loss among the second metacarpals of Ancaster females. The absence of age-related bone loss in female tibiae, despite its presence in all other measured elements, may be explained by the maintenance of mobility (e.g., walking) throughout the life course.

In order to maximize the sample sizes for later analyses, the sex and age groups that did not exhibit significant differences in T_A, C_A, and ROI were combined. Appendix K presents the group combinations that were used for later comparison with the fractured individuals. To summarize, all T_A, C_A, and ROI areas were split by sex for the subsequent comparisons. With the exception of female tibial C_A which were combined, all other C_A and ROI measurements among female elements were divided into a young adult category and a combined middle and old adult age category. Most male C_A/ROI and both male and female T_A values could be combined, regardless of age.

6.6.2 Directional Asymmetry

Sex and age differences between total area directional asymmetry (T_A%DA) and cortical area directional asymmetry (C_A%DA) were compared using Mann-Whitney U and Kruskal-Wallis tests and the results are presented in Table 6.22. Asymmetries calculated for each individual are presented in Appendix I. Appendix J reports the tests of normality by site and sex. In the Ancaster comparative sample, no significant differences in either total area directional asymmetry (T_A%DA) or cortical area directional asymmetry (C_A%DA) were identified between males and females or among age categories; additional differences between the age groups when separated by sex are presented in Appendix L. Due to the absence of significant differences between groups, it was not necessary to divide the sample by sex or age in order to compare asymmetry amounts in subsequent analyses.

Table 6.22 – Average directional asymmetry by element, and differences between sexes and among age groups at Ancaster.[1]

Element	Asymmetry Type	Average Asymmetry ± Standard Deviation (%)		Sex Differences (Male vs. Female)	Both Sexes Age Group Differences
		Female	Male		
Humerus	Counts and df			*N*=59	*N*=59, df=4
	T_A%DA	4.2 ± 4.7	3.3 ± 6.9	*U*=421.0, *p*=.844	χ^2=3.34, *p*=.503
	C_A%DA	0.7 ± 6.6	3.6 ± 8.9	*U*=334.0, *p*=.129	χ^2=2.29, *p*=.683
Radius	Counts and df			*N*=50	*N*=50, df=3
	T_A%DA	4.7 ± 7.3	5.7 ± 10.8	*U*=261.5, *p*=.398	χ^2=1.88, *p*=.597
	C_A%DA	5.6 ± 8.8	1.8 ± 10.2	*U*=242.0, *p*=.219	χ^2=1.24, *p*=.743
Ulna ROI	Counts and df			*N*=50	*N*=50, df=3
	ROI%DA	1.8 ± 13.5	5.0 ± 16.4	*U*=265.0, *p*=.376	χ^2=1.89, *p*=.596
MC2 50%	Counts and df			*N*=22	*N*=22, df=3
	T_A%DA	-0.3 ± 5.2	6.7 ± 2.3	*U*=11.0, *p*=.014	χ^2=6.45, *p*=.092
	C_A%DA	-2.1 ± 5.4	-1.6 ± 9.2	*U*=38.0, *p*=.724	χ^2=3.28, *p*=.350
MC2 ROI	Counts and df			*N*=26	*N*=26, df=3
	ROI%DA	-2.7 ± 4.3	-9.1 ± 17.4	*U*=49.0, *p*=.503	χ^2=4.11, *p*=.250
Tibia	Counts and df			*N*=60	*N*=60, df=3
	T_A%DA	-0.0 ± 6.6	-3.3 ± 9.6	*U*=372.5, *p*=.255	χ^2=1.50, *p*=.682
	C_A%DA	-0.0 ± 12.2	-3.5 ± 11.2	*U* =408.0, *p*=.539	χ^2=1.52, *p*=.678
MT2 ROI	Counts and df			*N*=38	*N*=38, df=3
	ROI%DA	-1.7 ± 9.4	2.5 ± 10.6	*U*=314.0, *p*=.281	χ^2=2.35, *p*=.502

[1] Groups compared using Mann-Whitney U and Kruskal-Wallis tests. Bold font indicates significant differences. T_A%DA=total area directional asymmetry; C_A%DA=cortical area directional asymmetry; ROI%DA=region of interest directional asymmetry; MC2 50%=measurement of the second metacarpal midshaft; ROI=region of interest; MC2=second metacarpal; MT2=second metatarsal.

6.7 Outlying Cross-Sectional Properties and Individuals with Fractures

This section identifies individuals with outlying T_A, C_A, and ROI areas and asymmetries. The 'normal' range of areas and asymmetries were determined and reported for each analysed element and group. Individuals with total and/or cortical areas that were above or below the normal range were identified as outliers and those outlying individuals with fractures are specifically addressed. All outliers are listed in Appendix M; outliers with fractures are reported in greater detail in Appendix O.

6.7.1 Total Area

The range of total areas that were considered 'normal' for each element, sex, and age group are reported in Table 6.23. Table 6.24 reports the number of elements that had total areas outside the normal range. Table 6.25 reports the differences between the number of total area outliers by sex and age. At Ancaster, all the outlying total areas were observed in the upper limb. Males and females did not have significantly different rates of outlying total areas (OR=1.0, CI 0.3-4.2; p_{FET}=1.000). The number of outlying total areas increased with age but none of these age-related differences were significant at Ancaster (male: $\chi^2(2, N=280)=0.27$, $p=.875$; female: $\chi^2(2, N=275)=0.94$, $p=.626$). Post-hoc age differences are reported in Appendix N. These findings show that the upper limb is more likely to exhibit outlying total areas, but that the rate of outlying total areas remains relatively unchanged throughout life and between the sexes.

Table 6.23 – 'Normal' range of total areas and number of elements with outlying total areas at Ancaster by element type, sex, and age groups.[1]

Element	Male		Female			Total
	All Ages IQR Range (mm²)	All *n/N* %	YA IQR Range (mm²)	MA/OA IQR Range (mm²)	All *n/N* %	*n/N* %
Humerus	190.0-426.2 (308.6)	0/102 0.0	185.4-282.3 (229.8)		3/84 3.6	3/186 1.6
Radius	98.1-211.3 (155.3)	3/94 3.2	78.6-151.7 (113.7)		1/75 1.3	4/169 2.4
MC2 50%	46.1-73.3 (59.4)	1/13 7.7	32.4-59.2 (44.9)	37.4-68.3 (52.1)	0/47 0.0	1/60 1.7
Tibia	300.1-690.6 (496.9)	0/96 0.0	252.1-519.1 (383.6)		0/85 0.0	0/181 0.0
Total	N/A	4/305 1.3	N/A		4/291 1.4	8/596 1.3

[1] Normal total area range indicated by 1.5 times the calculated interquartile ranges (IQR). Median values reported in brackets. *n*=number of elements with outlying total area; *N*=total number of elements measured; YA=young adult; MA=middle adult; OA=old adult; MC2 50%=second metacarpal midshaft measurement.

Table 6.24 - Prevalence of Ancaster elements with outlying total areas by sex and age.[1]

Age	Male *n/N* %	Female *n/N* %	Total *n/N* %
Young Adult	1/111 0.9	1/126 0.8	2/237 0.8
Middle Adult	3/155 1.9	2/114 1.8	5/269 1.9
Old Adult	0/15 0.0	1/35 2.9	1/50 2.0
Total	4/281 1.4	4/275 1.5	8/556 1.4

[1] Counts include individuals with fractures. *n*=number of elements with outlying total area; *N*=total number of elements measured.

Table 6.25 lists the Ancaster individuals that had outlying total areas and indicates if those total areas were larger or smaller than the normal range. Of the nine Ancaster individuals with outlying total areas, 22.2% (*n*=2/9) also had fractures. One of these individuals with a fracture and outlying total area is worth investigating further. The left humerus of AN-113, a middle adult female with a left femoral fracture, was larger than the norm; while handedness and side dominance is the most likely explanation, an alternative may include enlargement of the upper limb may be associated with the use of a mobility aid (e.g., a crutch). Based on the information currently available it is not possible to know the cause of AN-113's larger, outlying T_A for certain.

Table 6.25 – Ancaster individuals with outlying total areas.[1]

Skeleton Number	Fracture	Sex	Age	Element	Side	Larger (>) or Smaller (<) than Norm	T_A (mm^2)
AN-005	-	M	MA	Radius	L	>	227.6
AN-011	-	M	MA	MC2 50%	R	>	76.8
AN-052		F	MA	Radius	R	>	153.2
AN-058	L Clavicle	F	OA	Tibia	L	>	514.7
AN-093	-	M	MA	Radius	R	>	214.7
AN-102	-	F	YA	Humerus	R	>	316.0
AN-113	L Femur	F	MA	Humerus	L	>	297.8
AN-118	-	M	YA	Radius	R	>	220.5
AN-263	-	F	OA	Humerus	R	>	285.2

[1] >=total area larger than the norm; <=total area smaller than the norm; T_A=total area; - = individuals without fractures; M=male; F=female; YA=young adult; MA=middle adult; OA=old adult; MC2 50%=second metacarpal midshaft measurement; L=left; R=right.

6.7.2 Total Area Directional Asymmetry

The normal range of total area directional asymmetry (T_A%DA), as well as the number of elements with outlying asymmetry levels are presented by bone type and sex in Table 6.26. Table 6.27 reports the number of elements with outlying asymmetry by age and sex. The prevalence of individuals with outlying total area directional asymmetry was not significantly different between males and females (OR=3.4, CI 0.7-16.5; p_{FET}=.175) or between age groups ($\chi^2(2, N=268)=1.69$, p=.430); post-hoc age comparisons are presented in Appendix N.

Table 6.26 – 'Normal' range of total area directional asymmetries at Ancaster and counts of outlying elements by bone type and sex.[1]

Element	T_A%DA Range	Male *n/N* %	Female *n/N* %	Total *n/N* %
Humerus	-10.2-18.9 (3.7)	2/51 3.9	0/42 0.0	2/93 2.2
Radius	-17.1 to 29.7 (6.5)	2/44 4.5	0/34 0.0	2/78 2.6
MC2 50%	-17.2 to 18.7 (2.5)	1/6 16.7	0/22 0.0	1/28 3.6
Tibia	-20.0 to 17.6 (-0.4)	2/48 4.2	2/41 4.9	4/89 4.5
Total	N/A	7/149 4.7	2/139 1.4	9/288 3.1

[1] Normal total area directional asymmetry range indicated by 1.5 times the calculated interquartile range (IQR). Median values are reported in brackets. Counts include fractured individuals. T_A%DA=total area directional asymmetry; *n*=number of elements with outlying total area; *N*=total number of elements measured.

Table 6.27 - Number of Ancaster elements with outlying total area directional asymmetry.[1]

Age	Male *n/N* %	Female *n/N* %	Total *n/N* %
Adolescent	0/12 0.0	0/0 -	0/12 0.0
Young Adult	2/55 3.6	0/61 0.0	2/116 1.7
Middle Adult	5/75 6.7	1/54 1.9	6/129 4.7
Old Adult	0/7 0.0	1/16 6.3	1/23 4.3
Adult	0/0 -	0/8 0.0	0/8 0.0
Total	7/149 4.7	2/139 1.4	9/288 3.1

[1] Counts include fractured individuals. *n*=number of elements with outlying total area; *N*=total number of elements measured.

The eight Ancaster individuals who had outlying levels of total area directional asymmetry are listed in Table 6.28. Fractures are present in 50% (*n*=4/8) of the individuals with outlying total area directional asymmetries. Among these outlying individuals, two skeletons deserve special note. The fractured left radius and ulna of AN-024 was associated with a larger than normal left humerus. Additionally, the left second metatarsal of an individual with a fibular fracture (AN-013) was asymmetrically larger. In both cases, the asymmetry may be best explained by activity or side dominance (Ubelaker and Zarenko 2012) and is probably unrelated to the fracture. No clear patterns in the total area directional asymmetry of the remaining fractured individuals were identified or are explainable at this time.

Table 6.28 - Ancaster individuals with outlying total area directional asymmetry.[1]

Skeleton Number	Fracture	Sex	Age	Element	Larger Side	T_A%DA (%)
AN-006	-	M	MA	Tibia	L	-32.7
AN-013	L Fibula	M	YA	MC2 50%	L	-33.5
AN-024	L Radius & Ulna	M	MA	Humerus	L	-10.5
AN-027	-	M	MA	Tibia	L	-20.8
AN-172	L Radius	F	MA	Tibia	R	21.4
AN-216	-	M	YA	Radius	L	-17.5
AN-241	L Radius	F	OA	Tibia	R	19.2
AN-269	-	M	MA	Radius	L	-22.7
				Humerus	L	-12.8

[1] T_A%DA=total area directional asymmetry; MC2 50%=measurement taken at the second metacarpal midshaft; –=individuals without fractures; M=male, F=female; YA=young adult; MA=middle adult; OA=old adult; L=left, R=right

6.7.3 Cortical Area

The normal ranges of cortical areas for each element type at Ancaster are presented alongside the total number of identified outliers in Table 6.29. Sex differences in the number of larger or smaller cortical area outliers are presented in Table 6.30. The rate of elements with outlying cortical areas was significantly different between females and males. A predominance of females with smaller than normal cortical areas may account for some of this sex difference; females had significantly greater rates of smaller-sized, outlying cortical areas as males.

Table 6.29 - 'Normal' range of male and female cortical areas and counts of all outliers at Ancaster.[1]

Element	Males: All Ages Range (mm^2) (median)	Males: All Male *n/N* %	Females: YA Range (mm^2) (median)	Females: MA/OA Range (mm^2) (median)	Females: All Female *n/N* %	Total *n/N* %
Humerus	138.7-314.8 (222.2)	0/102 0.0	123.6-227.7 (176.4)	115.9-198.9 (160.1)	6/84 7.1	6/186 3.2
Radius	68.9-135.6 (100.3)	1/94 1.1	64.9-93.6 (78.5)	45.1-102.0 (71.7)	3/75 4.0	4/169 2.4
Ulna ROI	YA: 169.5-331.3 (251.1) MA/OA: 147.7-413.3 (279.8)	1/90 1.1	178.1-293.3 (229.8)	46.8-346.8 (201.4)	0/69 0.0	1/126 0.0
MC2 50%	YA: 32.8-49.3 (41.0) MA/OA: 33.8-64.9 (46.9)	1/13 7.7	32.0-45.3 (37.9)	25.9-46.2 (35.1)	4/47 8.5	5/60 8.3
MC2 ROI	60.9-103.2 (85.3)	1/14 7.1	73.3-90.7 (82.5)	45.4-78.1 (61.5)	6/50 12.0	7/64 10.9
Tibia	239.6-574.9 (407.9)	1/96 1.0	190.1-404.0 (298.4)		1/85 1.2	2/181 1.1
MT2 ROI	60.8-143.2 (101.9)	0/58 0.0	79.3-121.9 (98.9)	53.1-114.1 (83.1)	2/54 3.7	2/112 1.8

[1] Normal cortical area range indicated by 1.5 times the calculated interquartile range (mm^2). Counts include individuals with fractures. Median values are presented in brackets below the range. *n*=number of elements with an outlying cross-sectional property; *N*=total number of elements; YA=young adult; MA=middle adult; OA=old adult; ROI=region of interest; MC2 50%=second metacarpal midshaft; MT2=second metatarsal.

Table 6.30 – Sex-based differences between the number of smaller and larger cortical area outliers at Ancaster.[1]

Cortical Area Size	Males *n/N* %	Females *n/N* %	Sex Difference
Smaller Outlier (<)	2/454 0.4	9/417 2.2	**OR=5.0, CI 1.1-23.2; χ^2_{Yates}(1, *N*=871)=3.86, *p*=.050**
Larger Outlier (>)	5/454 1.1	13/417 3.1	OR=2.9, CI 1.0-8.2; χ^2_{Yates}(1, *N*=871)=3.43, *p*=.064
Total	7/454 1.5	22/417 5.3	**OR=3.6, CI 1.5-8.4; χ^2_{Yates}(1, *N*=871)=8.29, *p*=.004**

[1] Bold font indicates significant difference. Italic font indicates males had greater odds of outliers than females. Counts include individuals with fractures. *n*=number of elements with outlying cortical areas; *N*=total number of elements observed; <=smaller outlier; >=larger outlier; OR=odds ratio; CI=confidence interval.

Table 6.31 summarizes the number of elements with larger compared to smaller outlying cortical areas by age. The number of outliers did not increase with age for males (χ^2_{Yates}(2, *N*=422)=0.903, *p*=.637) or females (χ^2_{Yates}(2, *N*=391)=3.07, *p*=.216); supplementary post-hoc tests documenting age group differences are reported in Appendix N. There does seem to be a slight increase in the number of females with smaller outliers with advancing age. These findings, especially when combined with the predominance of females with smaller than normal cortical area outliers, indicate the presence of age-related bone loss that was concentrated among Ancaster females.

Table 6.31 - Number of Ancaster elements with smaller and larger outlying cortical areas.[1]

Age	Male			Female			Total
	n <	*n* >	*n/N* %	*n* <	*n* >	*n/N* %	*n/N* %
Adolescent	0	0	0/45 0.0	0	0	0/47 0.0	0/92 0.0
Young Adult	1	1	2/165 1.2	2	7	9/165 5.5	11/330 3.3
Middle Adult	0	4	4/230 1.7	1	4	5/157 3.2	9/387 2.3
Old Adult	1	0	1/27 3.7	6	0	6/69 8.7	7/96 7.3
Adult	0	0	0/0 -	0	0	0/26 0.0	0/26 0.0
Total	2	5	7/454 1.5	9	11	20/417 4.8	27/871 3.1

[1] Counts of outliers include fractured individuals. <=smaller than the normal cortical area; >=larger than the normal cortical area; *n*=number of outlying total areas; *N*=number of elements measured.

The 16 Ancaster individuals with cortical areas outside the normal range are listed in Table 6.32. Fractures were present in 43.8% (*n*=7/16) of individuals with outlying cortical areas. Three of these individuals (AN-191, 098, 218) merit additional attention as they had lower amounts of outlying C_A on the same side and limb type as the fractured element. Smaller, outlying cortical areas were recorded on the same side as the fracture in AN-191 (fractured right radius and ulna) and AN-098 (fractured right clavicle). AN-218, an individual with a fractured left tibia and fibula, exhibited larger, outlying cortical areas in the contralateral right second metatarsal. The lower, outlying, cortical area amounts of all three individuals represent lower loading forces applied to the fractured limb that may be related to disuse after injury.

Table 6.32 – Ancaster individuals and elements with outlying cortical areas (C_A and ROI).[1]

Skeleton Number	Fracture	Sex	Age	Element	Side	Larger (>) or Smaller (<) than Norm	CA/ROI (mm^2)
AN-001	R Tibia	F	YA	Radius	L&R	>	104.0, 107.0
AN-005	-	M	MA	Radius	R	>	138.5
AN-013	L Fibula	M	YA	MC2 50%	L	>	54.3
AN-026	-	M	YA	MC2 ROI	R	<	57.2
AN-045A	-	F	MA	MC2 ROI	L&R	>	92.3, 88.6
				MC2 50%	L	>	47.0
AN-098	R Clavicle, L Tibia	M	OA	Ulna	R	<	114.5
AN-102	-	F	YA	MC2 ROI	L	>	94.8
				Humerus	L&R	>	236.0, 251.0
				MC2 50%	L	>	45.8
AN-142	-	F	MA	MC2 ROI	R	>	82.6
AN-162	-	F	YA	MC2 ROI	R	<	82.4
AN-177	L Radius	M	MA	Tibia	L	>	575.2
AN-178	-	F	YA	MC2 50%	R	>	47.9
AN-191	R Radius & Ulna	F	OA	MC2 50%	R	<	25.2
AN-218	L Tibia & Fibula	F	YA	MT2 ROI	R	>	122.5
				Radius	L	<	64.0
AN-220	-	F	OA	Humerus	R	<	105.6
AN-241	L Radius	F	OA	Humerus	R	<	99.7
AN-263	-	F	OA	Humerus	L&R	<	110.7, 109.6
				MC2 ROI	L	<	45.3
				MT2 ROI	R	<	52.7
				Tibia	R	<	160.9

[1] <=smaller than normal cortical areas; >=larger than normal cortical areas; C_A=total area directional asymmetry; ROI=region of interest; – = individuals without fractures; L=left, R=right; M=male, F=female; YA=young adult; MA=middle adult; OA=old adult.

6.7.4 Cortical Area Directional Asymmetry

The normal range of cortical area directional asymmetry (C_A%DA) and the number of elements with outlying cortical area asymmetry are presented by element in

Table 6.33 and age in Table 6.34. Age differences in the prevalence of individuals with outlying amounts of cortical area asymmetry are reported in Table 6.35. Males and females had equal rates of elements with outlying cortical area directional asymmetries (OR=1.0, CI 0.4-2.3; $\chi^2_{Yates}(1, N=418)=0.00$, p=1.000). Old adult females had significantly greater rates of elements with outlying cortical area asymmetry compared to young adult females. This observation might be associated with increased bone loss with advancing age, and may, for example, indicate a tendency for older individuals to favour their dominant limb.

Table 6.33 – Normal ranges of male and female cortical area directional asymmetries (C_A%DA) and counts of C_A%DA outliers at Ancaster by bone type and sex.[1]

Element	C_A%DA Range	Male *n/N* %	Female *n/N* %	Total *n/N* %
Humerus	-14.2 to 19.7 (2.2)	5/51 9.8	3/42 7.1	8/93 8.6
Radius	-22.7 to 26.6 (4.6)	1/44 2.3	2/34 5.9	3/78 3.8
Ulna ROI	-40.4 to 47.6 (4.7)	0/42 0.0	0/33 0.0	0/75 0.0
MC2 50%	-14.4 to 9.2 (-2.0)	2/6 33.3	2/22 9.1	4/28 14.3
MC2 ROI	-21.2 to 14.6 (-2.0)	1/6 16.7	0/20 0.0	1/26 3.8
Tibia	-27.4 to 24.7 (-1.9)	2/48 4.2	3/41 7.3	5/89 5.6
MT2 ROI	-28.2 to 26.8 (0.5)	1/28 3.6	1/27 3.7	2/55 3.6
Total	N/A	12/225 5.3	11/219 5.0	23/444 5.2

[1] Normal cortical area directional asymmetry range indicated by 1.5 times the calculated interquartile range. Counts of outliers include individuals with fractures. Median values are reported in brackets. C_A%DA=cortical area directional asymmetry; *n*=number of elements with outlying cross-sectional property; *N*=total number of elements; ROI=region of interest; MC2=second metacarpal; MC2 50%=second metacarpal midshaft; MT2=second metatarsal.

Table 6.34 – Counts and prevalence rates of Ancaster element pairs with outlying cortical area directional asymmetry by age and sex.[1]

Age	Male *n/N* %	Female *n/N* %	Total *n/N* %
Adolescent	0/17 0.0	0/0 -	0/17 0.0
Young Adult	4/80 5.0	2/90 2.2	6/170 3.5
Middle Adult	8/113 7.1	5/75 6.7	13/188 6.9
Old Adult	0/9 0.0	4/25 16.0	4/34 11.8
Adult	0/0 -	0/9 0.0	0/9 0.0
Total	12/219 5.5	11/199 5.5	23/418 5.5

[1] Counts of outliers include individuals with fractures. *n*=number of element pairs with outlying cortical area directional asymmetry; *N*=number of element pairs observed.

Table 6.35 – Age differences in the prevalence of individuals with outlying cortical area directional asymmetries at Ancaster by sex. [1]

	Young Adult	Middle Adult	Old Adult
		Male	
Young Adult		OR=1.4, CI 0.4-5.0 p_{FET}=.764	*p_{FET}=1.000*
Middle Adult	OR=3.1, CI 0.6-16.7 p_{FET}=.247		p_{FET}=1.000
Old Adult	**OR=8.4, CI 1.4-48.9 p_{FET}=.020**	OR=2.7, CI 0.7-10.8 p_{FET}=.222	
	Female		

[1] Groups compared using odds ratio and Fisher's Exact tests. Bold font indicates that a significant difference is present. Italic font is used to indicate instances when the younger age category had greater odds of outlying total areas than the older age category. YA=young adult; MA=middle adult; OA=old adult; OR=odds ratio; CI=confidence interval.

The 17 individuals with outlying cortical area directional asymmetries are listed in Table 6.36. Of the Ancaster individuals with outlying amounts of cortical area asymmetry, 52.9% (*n*=9/17) also had fractured elements. In the case of six individuals with fractures, cortical area asymmetry was identified in the same limb type as the fractured bone. However, only two skeletons, AN-061 and 191, had asymmetrically smaller cortical areas on the same side as the fracture; AN-061, had a fractured left clavicle and humeri that were asymmetrically smaller on the left side, and AN-191 had fractures to the right radius and ulna that were asymmetrically smaller than the contralateral side. While it is possible that the presence of asymmetrically smaller bones predisposed an individual to fracture, in both instances, this cross-sectional evidence may also be indicative of some degree of dysfunction in the fractured limb after the injury. The remaining individuals had either larger cortical areas on the same side arm as the fracture, or asymmetry in a different limb type than the fracture. Of all the fractured individuals with outlying cortical area directional asymmetries in the same limb type, only AN-191 also exhibited outlying cortical areas (C_A or ROI).

Table 6.36 - Ancaster individuals and elements with outlying levels of cortical area directional asymmetry.[1]

Skeleton Number	Fracture	Sex	Age	Element	Larger Side	CA%DA (%)
AN-006	-	M	MA	Tibia	L	-31.1
AN-013	L Fibula	M	YA	MC2 50%	L	-26.4
AN-024	L Radius & Ulna	M	MA	Humerus	L	-31.2
AN-026	-	M	YA	MC2 50%	L	-15.1
				MC2 ROI	L	-38.8
AN-027	-	M	MA	Tibia	L	-28.9
AN-041	-	F	YA	Humerus	L	-12.8
AN-046	L Tibia	M	YA	Humerus	R	24.2
AN-061	L Clavicle	M	MA	Humerus	R	21.2
AN-072	-	F	YA	Tibia	R	25.3
AN-104	R Radius	F	MA	Humerus	R	22.3
AN-172	L Radius	F	MA	Radius	L	-23.6
				Tibia	R	35.3
AN-184	-	M	MA	Humerus	R	22.2
AN-185A	R Clavicle	M	MA	MT2 ROI	R	33.3
AN-191	R Radius & Ulna	F	MA	MC2 50%	L	-16.3
AN-241	L Radius	F	OA	Humerus	L	-18.9
				MT2 ROI	L	-29.6
AN-252	-	M	MA	Humerus	L	-19.3
				Radius	L	-23.9
AN-263	-	F	OA	Radius	R	28.9
				Tibia	L	-32.5

[1] C_A%DA=cortical area directional asymmetry; –=indicates individuals without fractures; M=male, F=female; YA=young adult; MA=middle adult; OA=old adult; ROI=region of interest MC2=second metacarpal; MC2 50%=measurement taken at the second metacarpal midshaft; MT2=second metatarsal; L=left, R=right.

6.8 Cross-Sectional Outliers and Fractured Individuals Compared

This section investigates the relationships between fracture types, complications, and the presence of outlying cross-sectional areas and asymmetries. Connections among these variables are examined in order to better understand the factors that influence the development of outlying cross-sectional areas and asymmetries in fractured elements.

6.8.1 All Fractures with Outlying Cross-Sectional Properties

Table 6.37 summarizes the number of individuals that had both a fracture and at least one outlying cross-sectional property. All fractured individuals with outlying cross-sectional properties were included in these counts, even if the outlying element was located in a different limb type as the fracture (e.g., fractured radius and tibial cortical area asymmetry). All the elements with outlying cross-sectional properties are summarized in Appendix M; each individual with a fracture and an outlying element are detailed in Appendix O.

Table 6.37 - Prevalence of individuals with fractures and outlying cross-sectional properties at Ancaster by sex and age.[1]

Age	Female *n/N* %	Male *n/N* %	Unknown Sex *n/N* %	Total *n/N* %
Young Adult	2/7 28.6	2/5 40.0	0/0 -	4/12 33.3
Middle Adult	4/6 66.7	4/12 33.3	0/0 -	8/18 44.4
Old Adult	1/3 33.3	1/1 100.0	0/1 0.0	2/5 40.0
Total	7/16 43.8	7/18 38.9	0/0 -	14/35 40.0

[1] *n*=number of individuals with fractures; *N*=total number of outlying individuals.

Of the 100 Ancaster individuals randomly selected and radiographed, 35 of those individuals had outlying cross-sectional properties (including individuals with fractures). That means that 65% of all the radiographed individuals (both with and without fractures) had cross-sectional properties that were within the normal range. Of the 35 individuals with outlying cross-sectional properties, 14 individuals had fractures; this means that 64.1% (n=25/39) of the individuals with fractures were within the normal range. The odds of exhibiting outlying cross-sectional properties were compared between individuals with and without fractures; individuals with fractures (n=14/39) had approximately equal odds for outlying cross-sectional properties as individuals without fractures (n=21/61) (OR=1.1, CI 0.5-2.5; $\chi^2_{\text{Yates}}(1, N=100)=0.00$, p=1.000). These findings suggest that the presence of a fracture does not necessarily predict the presence of outlying cross-sectional properties at Ancaster.

Differences in the prevalence of individuals with fractures and associated outlying cross-sectional properties were compared between the sex and age groups at Ancaster. Compared to males, females had only slightly greater odds of having both a fracture and outlying cross-sectional property (OR=1.2, CI 0.3-4.8; $\chi^2_{\text{Yates}}(1, N=34)=0.00$, p=1.000). There was no age-related difference in the prevalence of outlying cross-sectional properties in individuals with fractures ($\chi^2_{\text{Yates}}(2, N=35)=0.37$, p=.831). Post-hoc tests reporting age-related differences for each sex are reported in Appendix N. These results indicate that sex and age do not greatly influence the development of outlying cross-sectional properties in individuals with fractures at Ancaster.

Table 6.38 presents the prevalence of, and differences between, fractured elements associated with outlying cross-sectional properties by fracture force type. Higher energy and indirect fracture force types did not have significantly different rates of cross-sectional outliers at Ancaster. This means that outlying cross-sectional properties were not more likely to be associated with certain fracture force types. However, female higher energy fractures had over four times greater odds of exhibiting outlying cross-sectional properties than male higher energy fractures; although this difference was not significant, the odds suggest that females with higher energy or direct force injuries were more likely than males to greatly deviate from normal loading expectations. This relationship may be related to function after trauma, but could also be explained by activities prior to the injury that caused habitually greater mechanical loading, thus increasing the risk for these types of fractures.

Table 6.38 – Prevalence of, and differences between, outlying Ancaster elements with fractures by fracture force types and sex.[1]

Fracture Force	Female *n/N* %	Male *n/N* %	Ambiguous *n/N* %	Total *n/N* %	Differences Between Females and Males
Indirect	4/15 26.7%	3/13 23.1%	0/0 0.0%	7/28 25.0%	OR=1.2, CI 0.2-6.8 p_{FET}=1.000
Higher Energy/Direct	3/6 50.0%	3/16 18.8%	0/1 0.0%	6/22 27.3%	OR=4.3, CI 0.6-33.1 p_{FET}=.283
Unknown	0/0 0.0%	1/3 33.3%	0/0 0.0%	1/3 33.3%	-
Total	7/21 33.3%	7/32 21.9%	0/1 0.0%	14/54 25.9%	OR=1.8, CI 0.5-6.1 p_{FET}=.525
Differences Between High Energy/Direct and Indirect Fracture Types	OR=2.8, CI 0.4-19.7 p_{FET}=0.354	*OR=1.3, CI 0.2-7.9* *p_{FET}=1.000*	-	OR=1.1, CI 0.3-4.0 x^2_{Yates}=0.000, df=1, p=1.000	

[1] Groups compared using odds ratio, chi-square, and Fisher's Exact tests. Bold font used to indicate significant differences. Italic font used to indicate when indirect or male frequencies had greater prevalence rates than direct and female frequencies. *n*=number of fractures with an outlying cross-sectional property; *N*=total number of fractures in each category; OR=odds ratio; CI=confidence interval.

Counts of individuals who had both outlying cross-sectional properties and fracture complications (i.e., malunion, osteoarthritis, and/or infection) are reported in Table 6.39; differences between the sexes and in the rates of individuals with and without complications are also presented. Individuals with fracture complications were hypothesized to be at greater risk to develop outlying cross-sectional attributes. However, at Ancaster, outlying cross-sectional properties were not significantly associated with fracture complications. Females with fractures and fracture complications did have significantly greater odds of outlying elements than males, but of the six females with outlying cross-sectional properties and fracture complications, only two (AN-191, 218) had evidence for functional repercussions in the same limb and side as a fracture (i.e., smaller than normal bone amounts). As such, the significantly increased rate of female outliers are probably not directly related to injury repercussions, and instead are better explained by other habitual activities. Overall, these results show that fracture complications do not necessarily influence mechanical loading after a fracture.

In adults, mechanical changes and bone loss are more likely to affect the endosteal surface of the bone (Schäfer et al. 2012), so changes to cortical bone area and asymmetry are likely to exhibit the greatest changes following disuse of an injured limb in adulthood. Table 6.40 summarizes the individuals with outlying cortical bone areas and asymmetries in terms of the relationship with the outlying element to the fractured limb side and type.

Table 6.39 – Prevalence of, and differences between, Ancaster fractured individuals with and without outlying cross-sectional properties and fracture complications by sex.[1]

Variables Compared	Female *n/N* %	Male *n/N* %	Unknown *n/N* %	Total *n/N* %	Difference Between Females and Males
Outlying individuals with fractures and complications vs. All fractured individuals with complications	6/8 75.0%	2/12 16.7%	0/1 0.0%	8/21 38.1%	**OR=15.0, CI 1.7-136.2** **$\chi^2_{Yates}(1, N=20)=4.59, p=.032$**
Outlying individuals with fractures but without complications vs. All fractured individuals without complications	1/8 12.5%	5/10 50.0%	0/0 0.0%	6/18 33.3%	*OR=7.0, CI 0.6-79.9* $\chi^2_{Yates}(1, N=18)=1.38, p=.240$
Total individuals with outlying elements associated with fractures vs. All individuals with fractures	7/16 43.8%	7/22 31.8%	0/1 0.0%	14/39 35.9%	OR=1.7, CI 0.4-6.3 $\chi^2_{Yates}(1, N=38)=1.70, p=.680$
Difference Between Outlying Fractures With and Without Complications	OR=1.7, CI 0.2-12.2; $p_{FET}=1.000$	*OR=5.0, CI 0.7-12.3;* $p_{FET}=.172$	-	OR=1.2, CI 0.3-4.6; $\chi^2_{Yates}(1, N=39)=0.00$, $p=1.000$	

[1] Groups compared using odds ratio, chi-square, and Fisher's Exact tests. Bold font used to indicate significant differences. Italic font used to indicate when outliers without fractures and/or males had greater prevalence rates than outliers with fractures and/or females. *n*=number of fractures with an outlying cross-sectional property; *N*=total number of fractures in each category; OR=odds ratio; CI=confidence interval.

Table 6.40 – Counts of Ancaster fractured elements with smaller and larger outlying cortical bone properties organized according to the positional relationship with a fracture.[1]

Age	Sex	Smaller element on fractured limb side	Larger element on fractured limb side	Fracture in lower limb, outlier in upper	Fracture in upper limb, outlier in lower	Total
Young Adult	F	1	-	2	-	3
	M	-	-	2	-	2
Middle Adult	F	1	2	-	1	4
	M	1	1	-	2	4
Old Adult	F	-	1	-	1	2
	M	1	-	-	-	1
Total	F	2	3	2	2	9
	M	2	1	2	2	7
	Total	4	4	4	4	16

[1] F=female; M=male; -=no outlying element associated with a fracture observed.

Twelve of the 14 individuals with fractures and outlying cross-sectional properties had outlying cortical areas and/or cortical area asymmetries; over half (*n*=8/14, 57.1%) of these individuals had outlying cross-sectional properties in the same limb type as the fractured bone. Of these eight, four Ancaster individuals had smaller and/or asymmetric cortical bone areas on the same side as a fracture, all of which were distal to the fracture location, conforming to expectations that dysfunction has the greatest impact in locations distal to the fracture site (Davis 2015; Eyres and Kanis 1995). The cross-sectional properties and patterns in these individuals could be interpreted as indicative of mechanical unloading, and functional disuse, after injury. Specifically, the hand and foot bones exhibited smaller cortical areas in individuals with forearm (AN-191, MA Female) and lower leg (AN-218, YA Female) fractures, and the cortical areas of a humerus (AN-061, MA Male) and an ulna (AN-098, OA Male) were smaller in individuals with clavicle fractures. Additionally, the fractures belonging to two of these individuals (AN-191 and AN-218) were also associated with secondary complications that may have impacted their functional experience of the injury; AN-218 had poor apposition, rotation, overlap, and osteoarthritis, while AN-191 had osteoarthritis.

The Ancaster individuals who had larger cortical areas and/or asymmetries on the same side as the fractured bone all had fractures involving arm bones, specifically radii and ulnae (AN-024, 104, 172, 241). While initially, it was tempting to interpret this finding as indicative of an individual using their dominant, larger side to break a fall or a blow, clinical studies of arm fracture laterality contradict this assumption. Modern clinicians found that arm fractures, especially when located proximal to the wrist, were more likely to occur in the *non*-dominant arm (Borton et al. 1994; Meals 1979). If this modern finding can be applied to a Romano-British context, it suggests that the larger cortical areas should not immediately be explained by handedness. Instead, it may be more reasonable to infer that, in some cases, the outlying cortical properties are indicative of morphological alteration, or perhaps post-injury functional adaptation.

The final two categories include individuals who had cortical bone outliers in the opposite limb type than the fractured limb; that is, upper limb fractures with outlying lower limb cortical properties (n=4/13), or lower limb fractures with outlying upper limb cortical properties (n=4/13). In most cases, it is unlikely that these types of outlying cortical bone areas and asymmetries observed at Ancaster are related to post-injury functional adaptation. One exception may be AN-001, who had a larger right cortical area ipsilateral to a tibial plateau fracture. In addition to the fractured knee, AN-001 also exhibited marked destruction of the ipsilateral hip, interpreted as tuberculosis by Cox (1989). As such, this individual may have experienced impaired mobility, and may have been required to use a mobility aid (e.g., crutch). No distinct patterns in the fractures to the upper limb associated with outlying lower limb elements can be associated with post-injury function at this time. However, as lower limbs typically do not exhibit evidence of laterality, the identification of outlying lower limb cortical properties at Ancaster indicate a relationship with activity.

6.9 Summary

At Ancaster the distribution of fractures differed by sex and skeletal location. Females had significantly greater prevalence rates of indirect fractures and also fractured radii significantly more often as males. In contrast, males had greater odds of direct/higher energy fractures as females and exhibited the only clavicle fractures observed at Ancaster. Although no significant age-related differences in fracture distribution were identified, there was an increase in the prevalence of polytrauma associated with advancing age, a finding that is in agreement with the understanding of fractures as cumulative over the life course (Glencross 2011).

In terms of fracture complications, higher-energy fractures types (i.e., transverse, comminuted, and spiral fractures) were more often associated with fracture malunion than indirect fracture types were. Osteoarthritis was significantly more prevalent in injured joints and malunited fractures, and in some instances may be interpreted as post-traumatic osteoarthritis.

When cross-sectional properties were analysed, cortical areas and asymmetries exhibited the majority of noteworthy changes. Within the comparative sample, it was clear that older adults had significantly smaller upper limb cortical areas than younger adults. In the case of older adult females, greater amounts of cortical bone asymmetry were also observed. These findings corroborate previous research on bone loss at Ancaster by Mays (2006a), and are likely very influential in terms of the types of fractures observed among Ancaster females. The decrease in cortical area predominantly in the upper limbs will be investigated further in Section 9.3.2.

Individuals with and without fractures were found to be at equal risk for exhibiting outlying cross-sectional properties. This research did not identify any significant differences in the presence of outlying cross-sectional properties related to sex, age, fracture force, or fracture complications among individuals with fractures. However, elements belonging to four individuals (AN-061, 098, 191, 218) had smaller than normal cortical areas that were both ipsilateral and distal to the fractured element, and therefore stand out as possible candidates for unloading of a fractured limb after injury.

Chapter VII – RESULTS: VAGNARI

This chapter presents the long bone fracture and cross-sectional measurement results for the Vagnari skeletal collection. The prevalence and distribution of fractures, as well as an analysis of the observed fracture types and complications, are presented by age, sex, and skeletal location. These data are used to help identify differences in fracture causes and risks at Vagnari. The ‘normal’ cross-sectional total and cortical area and asymmetry ranges for each bone type are reported, and the Vagnari individuals with outlying cross-sectional properties are identified. The chapter concludes by associating the fracture types and complications with the outlying cross-sectional properties in order to identify individuals that may have had altered biomechanical function related to healed fractures.

7.1 Demographic Distribution

A total of 66 adult skeletons were analysed from the Vagnari collection. The distribution of the Vagnari skeletons assessed in this research are presented in Table 7.1 by sex and age. Details of each analysed individual are presented in Appendix B.

Table 7.1 – Number of observed Vagnari skeletons separated by age and sex.[1]

Age Category	Male	Possible Male	Ambiguous Sex	Possible Female	Female	Undetermined Sex	Total
Adolescent (15-19)	0	0	1	2	2	1	6
Young Adult (20-34)	6	5	1	6	7	1	26
Middle Adult (35-49)	11	1	0	1	5	0	18
Old Adult (50+)	1	0	0	1	0	0	2
Adult - Ambiguous	0	2	0	2	0	0	4
Adult - Undetermined	1	2	1	2	0	4	10
Total	19	10	3	14	14	6	66

[1] Ambiguous categories refer to individuals that had observable sex and age features, but could not be classified with certainty. The undetermined categories are individuals that did not have sufficient age or sex features preserved to permit classification.

7.2 Fracture Prevalence

The prevalence of extremity fractures in the Vagnari sample is reported in Table 7.2. Full details on each observed fracture are provided in Appendix C. Extremity fractures were recorded in 18.2% (*n*=12/66) of Vagnari individuals. None of the Vagnari skeletons had more than one fracture per long bone element. The true prevalence rate (TPR), or number of observed fracture lesions relative to the total number of complete long bone elements, was 3.1% (*n*=13/425).

Table 7.2 – Vagnari crude and true fracture prevalence rates by sex and age.[1]

Sex	Age Cohort	Individual		Element	
		n/N	CPR (%)	*n/N*	TPR (%)
Male	Adolescent	0/0	-	0/0	-
	Young Adult	5/11	45.5	5/102	4.9
	Middle Adult	3/12	25.0	3/109	2.8
	Old Adult	0/1	0.0	0/9	0.0
	Adult	0/5	0.0	0/16	0.0
	Total	8/29	27.6	8/236	3.4
Female	Adolescent	0/4	0.0	0/35	0.0
	Young Adult	2/13	15.4	2/96	2.1
	Middle Adult	0/6	0.0	0/31	0.0
	Old Adult	0/1	0.0	0/1	0.0
	Adult	1/4	25.0	1/9	11.1
	Total	3/28	10.7	3/172	1.7
Unknown Sex	Adolescent	0/2	0.0	0/6	0.0
	Young Adult	0/2	0.0	0/9	0.0
	Middle Adult	0/0	-	0/0	-
	Old Adult	0/0	-	0/0	-
	Adult	1/5	20.0	2/2	100.0
	Total	1/9	11.1	2/17	11.8
Total	Adolescent	0/6	0.0	0/41	0.0
	Young Adult	7/26	26.9	7/207	3.4
	Middle Adult	3/18	16.7	3/140	2.1
	Old Adult	0/2	0.0	0/10	0.0
	Adult	2/14	14.3	3/27	11.1
	Total	12/66	18.2	13/425	3.1

[1] Element counts include all fractured elements, regardless of their completeness, this means that in two instances it was necessary to include incomplete fractured elements in the element counts. *n*=number of individuals or elements with fractures, *N*=total number of observed individuals or complete elements (i.e., elements with 3/5 segments that were 75% or more present); CPR=crude prevalence rate; TPR=true prevalence rate; -=no individuals or elements observed.

Fracture prevalence rates (CPR and TPR) were compared between sex and age categories in order to determine if certain groups more commonly sustained fractures. Sex and age differences in fracture prevalence rates are presented in Tables 7.3 and 7.4. Males tended to have greater fracture prevalence rates than females, but fracture CPRs and TPRs were not significantly different between the sexes. There was also no difference between age groups, but young adults at Vagnari had greater odds of fracture than the middle adults. This pattern was not expected as older individuals typically have greater fracture prevalence rates due to the accumulation of injuries over the life course (Glencross 2011). The pattern of greater fracture frequencies among younger Vagnari individuals may be partly explained by the small sample of old adults, but might also suggest a more strenuous or risky young adult life at Vagnari. These ideas will be explored further in Chapter IX.

Table 7.3 –Differences between Vagnari male and female crude and true fracture prevalence rates by age.[1]

Age	Crude Prevalence Rate	True Prevalence Rate
Adolescent	-	-
Young Adult	OR=4.5, CI 0.7-31.2; p_{FET}=.182	OR=2.4, CI 0.5-12.8; p_{FET}=.446
Middle Adult	p_{FET}=.515	p_{FET}=1.000
Old Adult	-	-
Adult	-	-
Total	OR=3.2, CI 0.7-13.5 $x^2_{Yates}(1, N=57)=1.63$, p=.201	OR=2.0, CI 0.5-7.6; p_{FET}=.369

[1] Males and females were compared using odds ratio, chi-square, and/or Fisher's Exact tests. Bold font indicates that a significant difference was present. In all cases, males had greater odds of fracture than females. -=no fractures available to compare; OR=odds ratio; CI=confidence interval.

Table 7.4 – Differences between Vagnari young and middle adult fracture prevalence rates by sex.[1]

Sex	Crude Prevalence Rate	True Prevalence Rate
Male	OR=2.5, CI 0.4-14.6; p_{FET}=.400	OR=1.8, CI 0.4-7.8; p_{FET}=.487
Female	p_{FET}=1.000	p_{FET}=1.000
Both Sexes	OR=1.8, CI 0.4-8.4; p_{FET}=.489	OR=1.6, CI 0.4-6.3; p_{FET}=.746

[1] Age groups were compared using odds ratios and Fisher's Exact tests. Bold font indicates that a significant difference was present. In all cases, young adults had greater odds of fracture than middle adults. No fractures were identified in adolescent or old adult individuals, and as such they were not compared or included in this table. OR=odds ratio; CI=confidence interval.

Individuals with two or more fractures (multiple fractures or polytrauma) have been used to recognize cases of injury recidivism in past populations (e.g., Judd 2002a). The number of Vagnari skeletons with evidence for multiple extremity injuries were tallied, and Table 7.5 presents the counts of individuals with polytrauma alongside the counts of individuals with only one fracture. Of the 12 Vagnari individuals with fractures, only one adult of unknown age had more than one fracture (VA-F089, Figure 7.1). Due to the small sample size, rates of multiple fractures could not be compared.

Table 7.5 – The number of Vagnari individuals with either one or multiple fractures by age and sex.[1]

Age	One Fracture				Multiple Fractures*				Total Fractures			
	M *n/N* %	F *n/N* %	U *n/N* %	T *n/N* %	M *n/N* %	F *n/N* %	U *n/N* %	T *n/N* %	M *n/N* %	F *n/N* %	U *n/N* %	T *n/N* %
ADO	0/0 -	0/4 0.0	0/2 0.0	0/6 0.0	0/0 -	0/4 0.0	0/2 0.0	0/6 0.0	0/0 -	0/4 0.0	0/2 0.0	0/6 0.0
YA	5/11 45.4	2/13 15.4	0/2 0.0	7/26 26.9	0/11 0.0	0/13 0.0	0/2 0.0	0/26 0.0	5/11 45.5	2/13 15.4	0/2 0.0	7/26 26.9
MA	3/12 25.0	0/6 0.0	0/0 -	3/18 16.7	0/12 0.0	0/6 0.0	0/0 -	0/18 0.0	3/12 25.0	0/6 0.0	0/0 -	3/18 16.7
OA	0/1 0.0	0/1 0.0	0/0 -	0/2 0.0	0/1 0.0	0/1 0.0	0/0 -	0/2 0.0	0/1 0.0	0/1 0.0	0/0 -	0/2 0.0
Adult	0/5 0.0	1/4 25.0	0/5 0.0	1/14 7.1	0/5 0.0	0/4 0.0	1/5 20.0	1/14 7.1	0/5 0.0	1/4 25.0	1/5 20.0	2/14 14.3
Total	8/29 27.6	3/28 10.7	0/9 0.0	11/66 16.7	0/29 0.0	0/28 0.0	1/9 11.1	1/66 1.5	8/29 27.6	3/28 10.7	1/9 11.1	12/66 18.2

[1] *Multiple fractures include individuals that have two or more fractures each. *n*=number of individuals with fractures; *N*=total number of observed individuals; M=male; F=female; U=unknown sex; T=total; ADO=adolescent; YA=young adult; MA=middle adult; OA=old adult; -=no fractures observed.

Figure 7.1 – Paired fractures to the left radius (oblique fracture) and ulna (transverse fracture) of VA-F089, an adult of unknown sex. A: Ulna anterior view; B: Radius anterior view. Scale bar represents 5cm.

7.3 Fracture Distribution

Differences in the distribution and prevalence rates of fractures were compared in order to identify if certain limbs or elements were at increased risk for fracture at Vagnari. The distribution of fractures between the upper and lower limbs in the Vagnari collection are reported by sex and age in Table 7.6. Appendix D reports the distribution of fractures by element, sex, age, and segment. Bones of the upper limb included clavicles, humeri, radii, and ulnae; the lower limb bones consisted of femora, tibiae, and fibulae. Upper and lower limbs had equal rates of fractures (OR=1.0, CI 0.4-3.1; $\chi^2_{Yates}(1, N=425)=0.00$, $p=1.000$). This means that trauma was not concentrated in either the arms or the legs at Vagnari.

Table 7.6 – Counts and true prevalence rates of Vagnari fractures by limb type, sex, and age. [1]

Limb Type	Age	Female		Male		Unknown Sex		Total	
		n/N	TPR (%)	*n/N*	TPR (%)	*n/N*	TPR (%)	*n/N*	TPR (%)
Upper Limb	ADO	0/23	0.0	0/0	-	0/2	0.0	0/25	0.0
	YA	2/61	3.3	2/52	3.8	0/8	0.0	4/121	3.3
	MA	0/20	0.0	2/59	3.4	0/0	-	2/79	2.5
	OA	0/1	0.0	0/2	0.0	0/0	-	0/3	0.0
	Adult	0/7	0.0	0/10	0.0	2/2	100.0	2/19	10.5
	Total	2/112	1.8	4/123	3.3	2/12	16.7	8/247	3.2
Lower Limb	ADO	0/12	0.0	0/0	-	0/4	0.0	0/16	0.0
	YA	0/35	0.0	3/50	6.0	0/1	0.0	3/86	3.5
	MA	0/11	0.0	2/50	4.0	0/0	-	2/61	3.3
	OA	0/0	-	0/7	0.0	0/0	-	0/7	0.0
	Adult	1/2	50.0	0/6	0.0	0/0	-	1/8	12.5
	Total	1/60	1.7	5/113	4.4	0/5	0.0	6/178	3.4
Total	ADO	0/35	0.0	0/0	-	0/6	0.0	0/41	0.0
	YA	2/96	2.1	5/102	4.9	0/9	0.0	7/207	3.4
	MA	0/31	0.0	4/109	3.7	0/0	-	4/140	2.9
	OA	0/1	0.0	0/9	0.0	0/0	-	0/10	0.0
	Adult	1/9	11.1	0/16	0.0	2/2	100.0	3/27	11.1
	Total	3/172	1.7	9/236	3.8	2/17	11.8	14/425	3.3

[1] Counts include all fractured elements, regardless of their completeness, this means that in two instances it was necessary to include incomplete fractured elements in the element counts. *n*=count of all fractures; *N*=count of total observed complete elements (i.e., 3/5 segments 75% or more present); TPR=true prevalence rate; ADO=adolescent; YA=young adult; MA=middle adult; OA=old adult; -=no elements observed.

The distribution of male and female fractures by element type and segment location are depicted schematically in Figure 7.2. Table 7.7 reports the differences in fracture prevalence rates by bone type, sex, and age. Supplementary comparisons of fracture prevalence by age, segment, limb type, and side are provided in Appendix D. Fracture prevalence rates for the different bone types at Vagnari were not significantly different between the sexes, sides, or age groups. These findings show that an individual's sex or age did not govern the distribution of fractures by bone type at Vagnari.

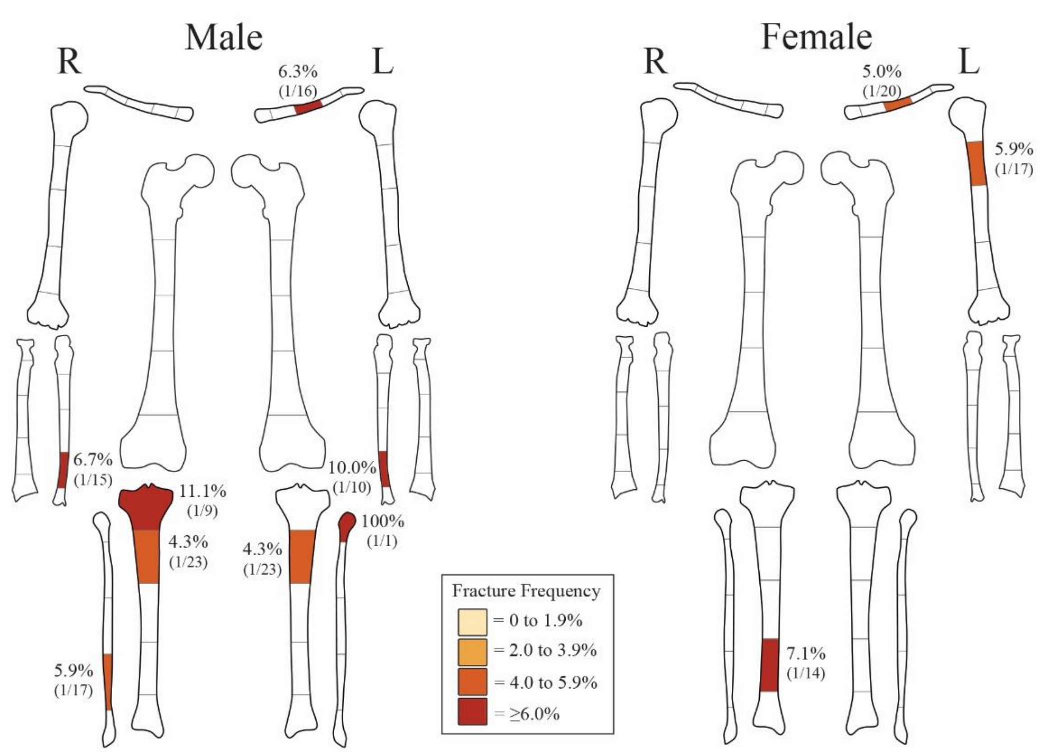

Figure 7.2 – Vagnari fracture true prevalence rates (TPR) by sex, element, segment, and side. Colour coded to represent higher and lower fracture TPRs (see Figure legend). R=Right; L=Left.

Table 7.7 – Counts and differences in Vagnari true fracture prevalence rates between sex groups by bone type.[1]

Element Type	Male		Female		Sex Difference (Male vs. Female)
	n/N %	Age Difference	*n/N* %	Age Difference	
Clavicle	1/23 4.3	*p_{FET}=1.000*	1/21 4.8	p_{FET}=1.000	*OR=1.1, CI 0.1- 18.8; p_{FET}=1.000*
Humerus	0/37 0.0	-	1/34 2.9	p_{FET}=1.000	*p_{FET}=.479*
Radius	0/34 0.0	-	0/30 0.0	-	-
Ulna	2/29 6.9	p_{FET}=0.481	0/27 0.0	-	p_{FET}=.492
Femur	0/41 0.0	-	0/24 0.0	-	-
Tibia	3/43 7.0	OR=1.7, CI 0.1-20.3 p_{FET}=1.000	1/24 4.2	-	OR=1.7, CI 0.2-17.6; p_{FET}=1.000
Fibula	2/29 6.9	OR=1.7 CI 0.1-30.1 p_{FET}=1.000	0/12 0.0	-	p_{FET} =1.000

[1] Groups were compared using odds ratios and Fisher's Exact tests. Bold font indicates that a significant difference was present. Males typically had greater or equal odds of fracture than females. Italic font is used to indicate instances that females or young adults had greater odds of fracture than males or older adults. TPR=true prevalence rate; *n*=number of fractures; *N*=total number of elements observed; OR=odds ratio; CI=confidence interval; -=statistical test was unable to be performed because of an absence of fractures.

7.4 Fracture Forces & Types

The prevalence rates of different fracture types were calculated at Vagnari so that patterns in the distribution of fracture forces and mechanisms could be recognised between groups. Counts of each fracture type identified in the Vagnari sample are presented graphically in Figure 7.3 and summarized in Table 7.8. Appendix C details each fracture type by individual. Direct and higher energy forces represented 38.5% (*n*=5/13) of the Vagnari fractures and included transverse (Figure 7.4), spiral (Figure 7.5), and comminuted fracture types (Figure 7.6). Indirect forces constituted 38.5% (*n*=5/13) of the observed fractures and included oblique (Figure 7.7), crush, and incomplete (Figure 7.8) fracture types. Three fractures could not be classified due either to extensive healing that obliterated the fracture line or postmortem damage. Males appeared to exhibit a wider variety of fracture types than females, but this was likely only because females had fewer fractures, 66.7% (*n*=2/3) of which were unknown types.

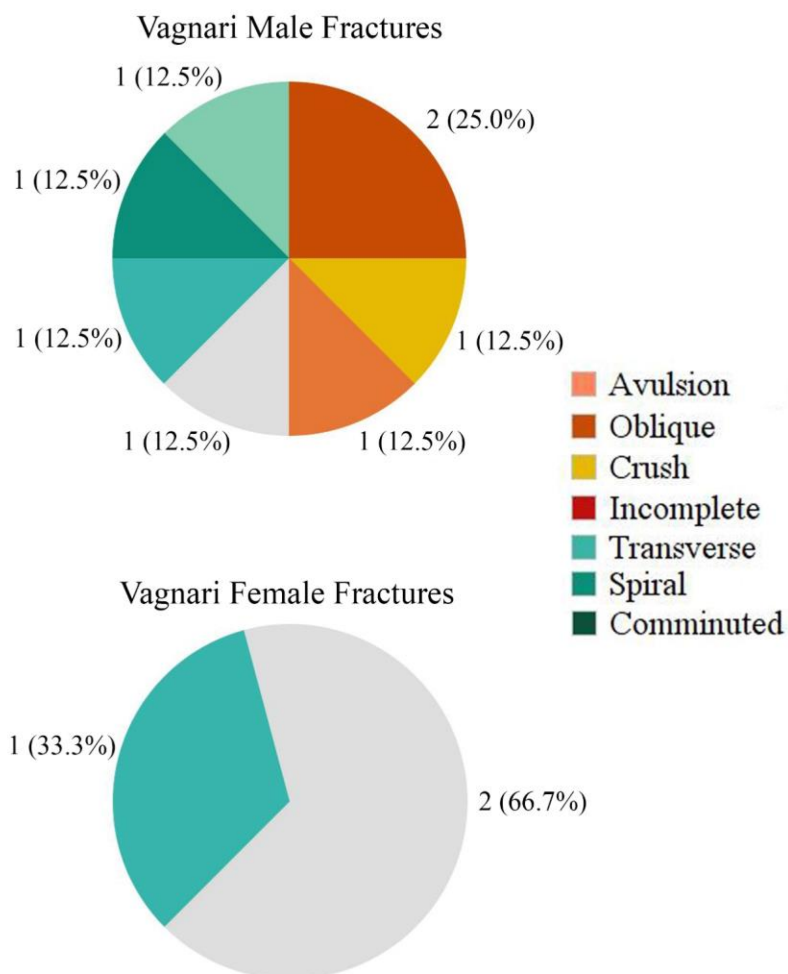

Figure 7.3 – Proportion of Vagnari female and male fracture types. Indirect fracture forces represented by shades of red, orange and yellow, and direct or higher-energy forces represented by green/blue shades (see legend in Figure).

Table 7.8 – Counts of the Vagnari fractures by force, type, element, and sex.[1]

Force	Fracture Type	Clavicle			Humerus			Radius			Ulna			Tibia			Fibula			Total		
		M	F	U	M	F	U	M	F	U	M	F	U	M	F	U	M	F	U	M	F	U
Indirect	Oblique	-	-	-	-	-	-	-	-	1	-	-	-	-	-	-	2	-	-	2	-	1
	Crush	-	-	-	-	-	-	-	-	-	-	-	-	1	-	-	-	-	-	1	-	-
	Incomplete	-	-	-	-	-	-	-	-	-	-	-	-	1	-	-	-	-	-	1	-	-
	Total	-	-	-	-	-	-	-	-	1	-	-	-	2	-	-	2	-	-	4	-	1
Direct / Higher Energy	Transverse	-	1	-	-	-	-	-	-	-	1	-	1	-	-	-	-	-	-	1	1	2
	Spiral	-	-	-	-	-	-	-	-	-	-	-	-	1	-	-	-	-	-	1	-	1
	Comminuted	1	-	-	-	-	-	-	-	-	-	-	-	-	-	-	-	-	-	1	-	-
	Total	1	1	-	-	-	-	-	-	-	1	-	1	1	-	-	-	-	-	3	1	1
Unknown		-	-	-	-	1	-	-	-	-	1	-	-	-	1	-	-	-	-	1	2	-
Total		1	1	-	-	1	-	-	-	1	2	-	1	3	1	-	2	-	-	8	3	2

[1] M=male; F=female; U=unknown sex; -=no fractures observed.

Figure 7.4 – Transverse fracture to the right ulna of a young adult male, VA-F131. Location of the fracture line estimated with a dotted line. A: Ulna anterior view; B: Ulna medial view. Scale bar represents 5cm.

Figure 7.5 – Spiral fracture to the left tibia of a young adult male, VA-F042A. Location of the fracture line estimated with a dotted line on the anterior x-ray view; the fracture line was not clear on the medio-lateral x-ray view. Fragments at the distal end of tibia were re-fit for x-ray but do not appear in the photograph of the actual tibia. A: Tibia anterior view; B: Tibia medial view. Scale bar represents 5cm.

Figure 7.6 – Comminuted fracture to the left clavicle of a middle adult male, VA-F068. Location of the fracture lines estimated with dotted lines on the x-ray views. A: Clavicle inferior view; B: Clavicle posterior view. Scale bar represents 5cm.

Figure 7.7 – Oblique fracture to the right fibula of middle adult male, VA-F216. Fracture line indicated on the medio-lateral view; the fracture line was unclear on the antero-posterior view. A: Fibula lateral view; B: Fibula anterior view. Scale bar represents 5cm.

The incomplete tibial shaft fracture of VA-F231 (Figure 7.8) requires special attention. This fracture was initially recognized based on swelling of the proximal diaphysis and the interpretation was supported by a small linear area of radiolucency that crossed the anterior cortex, localized and sub-linear areas of radiopacity, and a ridge of new bone on the medial surface. Differential diagnosis of the bone characteristics could include infection and osteoid osteoma. However, in the absence of further radiological findings (e.g., cortical lucency), an infection and/or tumour are considered unlikely. The location and appearance of the bony callus and cortex in VA-F231 is consistent with clinical manifestations of stress fractures and is cautiously categorized as such for the purposes of these analyses. Incomplete fracture types, such as that of VA-F231, can be very difficult to recognize and, in adults, may be related to repetitive stress (fatigue or stress fracture) or weakened bone (insufficiency fractures) (Matcuk Jr. et al. 2016). As ambulation places leg bones under repetitive strain, stress fractures are most common in the lower limb, particularly in the proximal, antero-medial tibial diaphysis (Matcuk Jr. et al. 2016; Matheson et al. 1987; Shindle et al. 2012; Swischuk and Jadhav 2014).

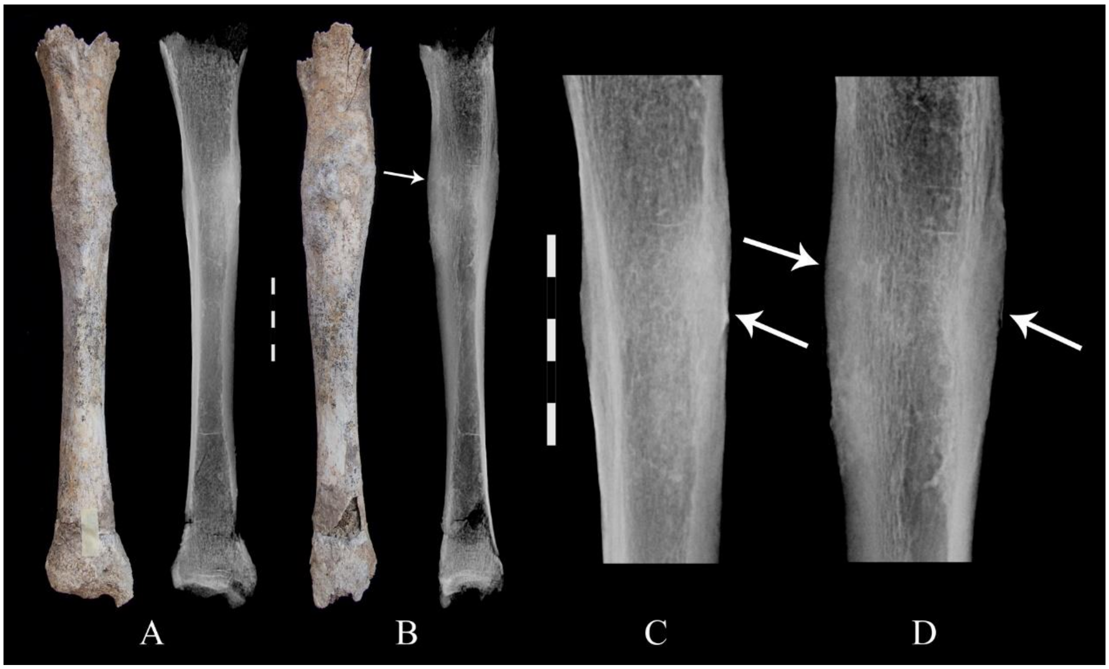

Figure 7.8 – Incomplete stress fracture to the right tibia of a young adult male, VA-F231. Fracture location represented by an area of localized radiopacity and ridge of new bone on the antero-medial and postero-medial surfaces of the tibia, indicated by the arrows. A: Tibia anterior view; B: Tibia medial view; C: Enlarged anterior radiographic view, D: Enlarged medial radiographic view. Scale bar represents 5cm.

Figures 7.9 and 7.10 illustrate the distribution of indirect and direct force fractures at Vagnari by element, side, and sex. Table 7.9 reports the counts and comparisons between force types and sexes. There were no significant differences in the rates of indirect and direct force injuries within or between males and females. Small fracture sample sizes at Vagnari may affect the reliability of these findings, but this result may suggest that males and females encountered similar fracture-causing hazards at Vagnari.

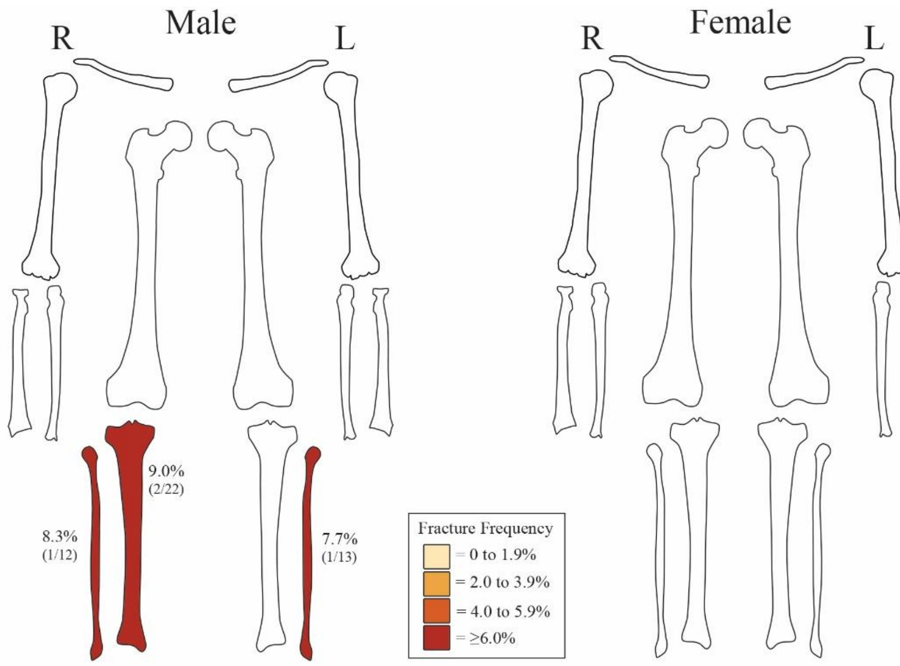

Figure 7.9 – Vagnari indirect fracture true prevalence rates (TPR) by sex, element, side, and segment. Colour coded to represent higher and lower fracture TPRs (see Figure legend). No indirect fractures were observed in female skeletons. R=Right; L=Left.

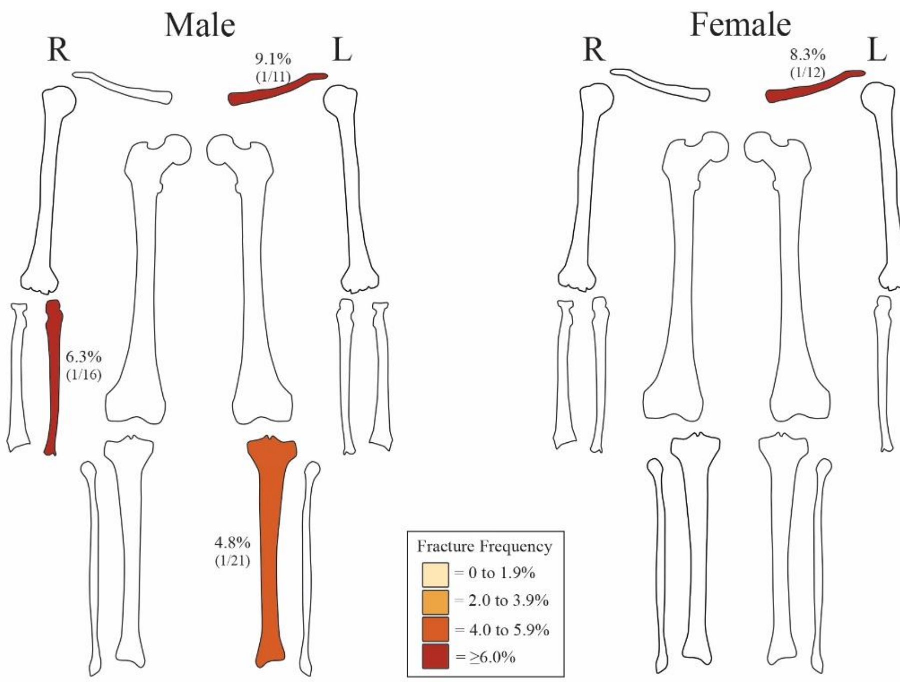

Figure 7.10 – Vagnari direct fracture true prevalence rates (TPR) by sex, element, side, and segment. Colour coded to represent higher and lower fracture TPRs (see Figure legend). R=Right; L=Left.

Table 7.9 – Fracture counts and differences between the sexes and fracture force types at Vagnari.[1]

Sex	Indirect *n/N* %	Direct/Higher Energy *n/N* %	Indirect vs. Direct
Male	4/7 57.1	3/7 42.9	OR=1.7, CI 0.2-14.8 p_{FET}=1.000
Female	0/1 0.0	1/1 100.0	-
Male vs Female	p_{FET}=1.000	*p_{FET}=1.000*	

[1] Groups were compared with odds ratios and Fisher's Exact tests. Bold font indicates that a significant difference was present. Italic font used to indicate that females or direct fractures had greater odds of fractures than males or indirect fractures (depending on the variables being tested). Counts presented are of the fractures with known force types. *n*=number of fractures of each type; *N*=number of total fractures; OR=odds ratio; CI=confidence interval; -=sample sizes too small to test.

7.5 Fracture Healing and Complications

This section presents the complications associated with healed fractures at Vagnari, including malunion, inflammation, and osteoarthritis. All the fractures observed in the Vagnari skeletons occurred antemortem and exhibited some degree of healing. No perimortem or non-union fractures were identified.

7.5.1 Malunion

Healed fractures with malunion were identified and classified according to the criteria outlined in Section 4.5.2. Counts and prevalence rates of malunion observed at Vagnari (i.e., angulation, poor apposition, rotation, and overlap) are reported in Table 7.10 by element, limb type, and sex. The measured amounts of angulation, poor apposition, rotation, shortening, and/or overlap of fracture fragments are reported for each of the Vagnari fractures in Appendix C, and prevalence rates of each type of malunion are summarized in Appendix E. Among the Vagnari fractures, 30.8% (*n*=4/13) had comparatively larger amounts of angulation, apposition, rotation, and/or overlap. Rates of malunion were not significantly different between the sexes (OR=3.5, CI 0.1-84.7, p_{FET}=.491) or between the upper and lower limbs (p_{FET}=.070).

Table 7.10 – Prevalence of fractures with malunion at Vagnari by sex, element type, and limb type.[1]

Element	Male *n/N* %	Female *n/N* %	Unknown Sex *n/N* %	Total *n/N* %	Male vs. Female
Clavicle	1/1 100.0	1/1 100.0	0/0 -	2/2 100.0	
Humerus	0/0 -	0/1 0.0	0/0 -	0/1 0.0	
Radius	0/0 -	0/0 -	1/1 100.0	1/1 100.0	
Ulna	0/2 0.0	0/0 -	1/1 100.0	1/3 33.3	
Upper Limb Subtotal	1/3 33.3	1/2 50.0	2/2 100.0	4/7 57.1	*OR=2.0, CI 0.1-78.3,* p_{FET}*=1.000*
Femur	0/0 -	0/0 -	0/0 -	0/0 -	
Tibia	0/3 0.0	0/1 0.0	0/0 -	0/4 0.0	
Fibula	0/2 0.0	0/0 -	0/0 -	0/2 0.0	
Lower Limb Subtotal	0/5 0.0	0/1 0.0	0/0 -	0/6 0.0	-
Total	1/8 12.5	1/3 33.3	2/2 100.0	4/13 30.8	

[1] Fracture counts include all lesions with measurable malunion; some fractures were excluded from counts because the fracture type could not exhibit that kind of malunion (e.g., crush fractures cannot be angulated). Shaded rows represent fracture prevalence rates subtotalled by limb type. Bold font indicates that a significant difference was present. Italic font used to indicate that females had greater odds of malunion than males. *n*=total number of elements with at least one type of malunion, *N*=total number of fractured elements; -=no fractures observed; OR=odds ratio; CI=confidence interval.

Counts of the Vagnari fractures that had one type of malunion, as well as those that had multiple kinds of malunion are presented by fracture type in Table 7.11. Differences in the rates of malunion associated with different fracture types are reported in Table 7.12. Three of the four malunited fractures at Vagnari were higher-energy or direct force fracture types (i.e., transverse and comminuted). Higher energy/direct force fracture types were more likely to exhibit malunion, albeit not significantly, when compared to the other fracture types, but no one fracture type had significantly greater odds of malunion than any other fracture type. Of the four Vagnari fractures with malunion, one oblique and one transverse fracture affected the paired radius and ulna of a single individual (Figure 7.1). The remaining two malunited fractures were clavicular fractures (Figure 7.11). These fracture types and/or locations are difficult to reduce and stabilize, and often heal with deformity (Chan et al. 1999b; McKee et al. 2003).

Table 7.11 – Counts and prevalence rates of malunited fractures at Vagnari by sex and fracture type.[1]

Fracture Type	No Malunion *n/N* %				One Type of Malunion *n/N* %				Multiple Types of Malunion *n/N* %			
	M	F	U	T	M	F	U	T	M	F	U	T
Crush	1/1 100.0	0/0 -	0/0 -	1/1 100.0	0/1 0.0	0/0 -	0/0 -	0/1 0.0	0/1 0.0	0/0 -	0/0 -	0/1 0.0
Oblique	2/2 100.0	0/0 -	0/0 -	2/2 100.0	0/2 00.0	0/0 -	0/0 -	0/2 0.0	0/2 0.0	0/0 -	1/1 100.0	1/3 33.3
Incomplete	1/1 100.0	0/0 -	0/0 -	1/1 100.0	0/1 0.0	0/0 -	0/0 -	0/1 0.0	0/1 0.0	0/0 -	0/0 -	0/1 0.0
Spiral	1/1 100.0	0/0 -	0/2 0.0	1/3 33.3	0/1 0.0	0/0 -	0/0 -	0/1 0.0	0/1 0.0	0/0 -	0/0 -	0/1 0.0
Transverse	1/1 100.0	0/1 0.0	0/0 -	1/2 50.0	0/1 0.0	1/1 100.0	1/1 100.0	2/3 66.7	0/1 0.0	0/1 0.0	0/0 -	0/2 0.0
Comminuted	0/1 0.0	0/0 -	0/0 -	0/1 0.0	1/1 100.0	0/0 -	0/0 -	1/1 100.0	0/1 0.0	0/0 -	0/0 -	0/1 0.0
Unknown	1/1 100.0	2/2 100.0	0/0 -	3/3 100.0	0/1 0.0	0/2 0.0	0/0 -	0/3 0.0	0/1 0.0	0/2 0.0	0/0 -	0/3 0.0
Total	7/8 87.5	2/3 66.7	0/2 0.0	9/13 69.2	1/8 12.5	1/3 33.3	1/2 50.0	3/13 23.1	0/8 0.0	0/3 0.0	1/2 50.0	1/13 7.7

[1] Malunion types include angulation, poor apposition, rotation, shortening, and overlap of fractured fragments. Multiple malunion includes individuals that have at least two types of malunion (e.g., angulation and rotation). *n*=number of fractures with multiple types of malunion; *N*=number of fractures observed; M=male, F=female, U=unknown sex, T=total; -=no fractures observed.

Table 7.12 –Differences in the prevalence of malunion between fracture types at Vagnari.[1]

Fracture Types Compared	Counts *n/N*	Difference
Avulsion, Crush & Incomplete vs All Other Fracture Types	0/2 4/11	p_{FET}=1.000
Oblique vs All Other Fracture Types	1/3 2/10	*OR=2.0, CI 0.1-34.8* *p_{FET}=1.000*
Spiral vs All Other Fracture Types	0/1 4/12	p_{FET}=1.000
Comminuted vs. All Other Fracture Types	1/1 3/12	*p_{FET}=.308*
Transverse vs. All Other Fracture Types	2/3 2/10	*OR=8.0, CI 0.5-139.3* *p_{FET}=.203*
Direct/High Energy vs. Indirect Trauma	3/5 1/5	*OR=6.0, CI 0.4-101.6* *p_{FET}=.524*
All Fracture Types	-	χ^2(4, N=10)=4.44, *p*=.349

[1] Groups were compared with odds ratios, chi-square, and/or Fisher's Exact tests. Bold font indicates that a significant difference was present. Italic font used to indicate that the specific tested fracture type had greater odds of malunion than all other types of fractures combined. *n*=number of fractures with malunion; *N*=total number of fractures; OR=odds ratio; CI=confidence interval.

Figure 7.11 – Transverse, right clavicle fracture belonging to a young adult female, VA-F249. A: Infero-superior radiograph of the contralateral, left clavicle; B: Infero-superior radiographic and macroscopic view of right clavicle; C: Postero-anterior radiographic and macroscopic posterior view of right clavicle; D: Superior view of right clavicle; E: Anterior view of right clavicle. Scale bar represents 5cm.

7.5.2 Inflammation & Soft Tissue Injury

None of the Vagnari fractures were associated with signs of inflammation indicative of infection or soft tissue ossification suggestive of soft tissue injury.

7.5.3 Osteoarthritis

The prevalence rate of osteoarthritis (OA_x) at Vagnari, as well as the prevalence of Vagnari individuals with both fractures and osteoarthritis, are reported by age and sex in Table 7.13. Osteoarthritis data are reported in full in Appendix F; Appendix G provides additional detail about osteoarthritis true prevalence rates. Compared to the expected number of joints surfaces at Vagnari, only 32.4% (*n*=257/792) joints were present for observation, and only 30.8% (*n*=4/13) of the fractured elements at Vagnari had adjacent articular surfaces that were sufficiently preserved for inclusion in analyses of osteoarthritis.

Table 7.13 – Counts and true prevalence rates of osteoarthritis and fractures with osteoarthritis at Vagnari by sex and age.[1]

Age Category	Total OA_x/N joints TPR (%)				Fractures with OA_x/N joints TPR (%)			
	Female	Male	Unknown Sex	Total	Female	Male	Unknown Sex	Total
ADO	0/23 0.0%	0/0 -	0/4 0.0%	0/27 0.0%	0/23 0.0%	0/0 -	0/4 0.0%	0/27 0.0%
YA	1/44 2.3%	3/73 4.1%	0/6 0.0%	4/123 3.3%	0/44 0.0%	0/73 0.0%	0/6 0.0%	0/123 0.0%
MA	2/25 8.0%	8/66 12.1%	0/0 -	10/91 11.0%	0/25 0.0%	4/66 6.1%	0/0 -	4/91 4.4%
OA	2/6 33.3%	1/4 25.0%	0/0 -	3/10 30.0%	0/6 0.0%	0/4 0.0%	0/0 -	0/10 0.0%
Unknown	1/4 25.0%	0/1 0.0%	0/1 0.0%	1/6 16.7%	1/4 25.0%	0/1 0.0%	0/1 0.0%	1/6 16.7%
Total	5/102 4.9%	11/144 7.6%	0/11 0.0%	16/257 6.2%	1/102 1.0%	4/144 2.8%	0/11 0.0%	5/257 1.9%

[1] Some joints consist of multiple articular surfaces, in these instances any observations of osteoarthritis were only counted once per joint. A joint was determined to have osteoarthritis if at least one of the joint's articular surfaces was affected. In some instances, osteoarthritis was present in both distal and proximal joint surfaces of the same fractured element (e.g., radial fracture with osteoaerthrits in both wrist and elbow), so both were recorded. OA_x=osteoarthritis; *N* joints=total number of observable joints; TPR=true prevalence rate; ADO=adolescent; YA=young adult; MA=middle adult; OA=old adult; -=no joints observed.

Osteoarthritis was identified in 19.7% (*n*=13/66) of Vagnari adults and 6.2% (*n*=16/257) of all preserved joint surfaces. Overall, male and female joints did not have significantly different rates of osteoarthritis (OR=1.6, CI 0.6-4.8, $\chi^2_{Yates}(1, N=246)=0.41$, $p=.523$). Of all the joints with osteoarthritis, 31.3% (*n*=5/16) also had fractures in at least one adjacent element. There was also no sex-related difference in the prevalence of osteoarthritis in individuals with fractures, but males with fractures did have almost three times greater odds of osteoarthritis than females (OR=2.9, CI 0.3-26.2, $p_{FET}=.406$). These findings show that male and female individuals were generally at equal risk for osteoarthritis, but that males with fractures were more likely to have osteoarthritis. This may be explained in two ways: either males with osteoarthritis were at increased risk for fracture, or, after that fracture, males were more susceptible to developing osteoarthritis.

Table 7.14 reports the differences in osteoarthritis frequencies by age. At Vagnari, middle and old adults had significantly more osteoarthritis than young adults. This result is in agreement with the clinical literature that draws an association between osteoarthritis and advancing age (Loeser 2009), and demonstrates that age was influential in the development of osteoarthritis at Vagnari.

Table 7.14 – Age differences in the prevalence rates of osteoarthritis at Vagnari overall, as well as the prevalence rates of osteoarthritis among elements with fractures. [1]

	Young Adult	Middle Adult	Old Adult
		Total OA$_x$/*N* joints	
Young Adult		**OR=3.7, CI 1.1-12.1** **x^2_{Yates}=3.934, df=1, p=0.047**	**OR=12.8, CI 2.4-68.4** **p_{FET}=0.009**
Middle Adult	**p_{FET}=0.031**		OR=3.5, CI 0.8-15.6 p_{FET}=0.118
Old Adult	-	*p_{FET}=1.000*	
	Fractures with OA$_x$/*N* Joints		

[1] Groups were compared using odds ratios, chi-square, and/or Fisher's Exact tests. Bold font indicates that a significant difference is present. The older age category typically had greater odds of fracture than the younger age category; italic font used to indicate when younger age categories had greater osteoarthritis frequencies than older ages. OA$_x$=osteoarthritis; *N* joints=number of observed joints; -=sample sizes too small for comparison; OR=odds ratio; CI=confidence interval.

The prevalence of osteoarthritis in each fracture type observed at Vagnari is presented in Table 7.15 by sex. A chi-square test performed on both sexes combined found no significant differences in the prevalence rates of osteoarthritis among the fracture types ($\chi^2(6, N=13)=5.49$, p=.483).

Table 7.15 – Counts of osteoarthritis as associated with each type of fracture at Vagnari by sex.[1]

Force	Fracture Type	Female *n/N* %	Male *n/N* %	Unknown Sex *n/N* %	Total *n/N* %
Indirect	Crush	0/0	1/1	0/0	1/1
		-	100.0	-	100.0
	Oblique	0/0	1/2	0/1	1/3
		-	50.0	-	33.3
	Incomplete	0/0	0/1	0/0	0/1
		-	0.0	-	0.0
	Subtotal	0/0	1/4	0/0	2/5
		-	25.0	-	40.0
Higher-Energy and Direct	Spiral	0/0	0/1	0/0	0/1
		-	0.0	-	0.0
	Transverse	0/1	0/1	0/1	0/3
		0.0	0.0	-	0.0
	Comminuted	0/0	0/1	0/0	0/1
		-	0.0	-	0.0
	Subtotal	0/1	0/3	0/2	0/5
		0.0	0.0	0.0	0.0
Unknown		1/2	0/1	0/0	1/3
		0.0	0.0	-	33.3
Total		1/3	2/8	0/2	3/13
		33.3	25.0	0.0	23.1

[1] In order to compare against the counts of fractured elements, osteoarthritis was only counted once per element, even if osteoarthritis was present in both proximal and distal articular surfaces. *n*=number of fractures with osteoarthritis; *N*=total number of fractures; -=no fractures observed.

The relationships between malunion, joint fractures, and osteoarthritis could not be reliably investigated at Vagnari due to the relatively poor preservation of joint surfaces in this sample. A fracture involved only one subchondral surface at Vagnari; this joint fracture was also associated with osteoarthritis and represents half (*n*=1/2) of all the fractured elements that were directly associated osteoarthritis at Vagnari. Adjacent joint surfaces were not preserved for any of the malunited fractures in the Vagnari sample, so the relationship between malunion and the development of osteoarthritis could not be assessed.

7.6 Cross-Sectional Results: Establishing the Cross-Sectional 'Norm'

The 'normal' range of total and cortical areas (T_A, C_A), as well as total and cortical area directional asymmetries (T_A%DA, C_A%DA) were determined at Vagnari using radiographs of a comparative sample of individuals without fractured bones. The normal, comparative sample represented 33.3% (*n*=22/66) of all the adults analysed from Vagnari.

Table 7.16 reports the number of Vagnari individuals with and without fractures that were radiographed for cross-sectional analyses. Some individuals were missing elements and were not complete due to differential preservation and fragmentation; Table 7.17 reports counts of the elements and element pairs that were present and measureable. Counts of radiographed bones by element type, age, and sex are presented in greater detail in Appendix H.

Table 7.16 – Counts of radiographed Vagnari individuals.[1]

Number of Vagnari Individuals Radiographed	Female *n/N* %	Male *n/N* %	Unknown Sex *n/N* %	Total *n/N* %
n radiographed individuals / Total N observed	14/28 50.0%	19/29 65.5%	1/9 11.1%	34/66 51.5%
n radiographed individuals with fractures / Total N radiographed	3/14 21.4%	8/19 42.1%	1/1 100.0%	12/34 35.3%

[1] *n*=number of individuals radiographed; *N*=total number of individuals observed/radiographed.

Table 7.17 – Number of radiographed individuals, elements, and element pairs with and without fractures by sex and element measurement type.[1]

Sex	Element	Individual *n/N*	Element *n/N*	Paired* *n/N*
Female	Humerus	2/12	4/24	2/12
	Radius	3/13	5/22	2/9
	Ulna ROI	2/11	4/21	2/10
	MC2 50%	0/2	0/3	-
	MC2 ROI	2/10	2/13	0/4
	Tibia	3/14	6/26	3/12
	MT2 ROI	2/7	2/8	0/1
Male	Humerus	9/18	18/36	9/18
	Radius	9/17	14/27	5/9
	Ulna ROI	7/14	11/23	4/8
	MC2 50%	1/4	1/5	0/1
	MC2 ROI	7/12	8/15	1/3
	Tibia	9/19	17/37	8/18
	MT2 ROI	6/11	7/16	1/5
Unknown Sex	Humerus	1/1	2/2	1/1
	Radius	1/1	2/2	1/1
	Ulna ROI	-	-	-
	MC2 50%	-	-	-
	MC2 ROI	-	-	-
	Tibia	-	-	-
	MT2 ROI	-	-	-
Total	Humerus	12/31	24/62	12/31
	Radius	13/31	21/51	8/19
	Ulna ROI	9/25	15/44	6/18
	MC2 50%	1/5	1/8	0/1
	MC2 ROI	9/21	10/28	1/7
	Tibia	12/33	23/63	11/30
	MT2 ROI	8/18	9/24	1/6

[1] Note: the number of MC2 ROIs is greater than MC2 50% as ROI measurements included additional, incomplete second metacarpals that were omitted from MC2 50% measurements. *n*=number of individuals and elements associated with individuals with fractures; *N*=total number of radiographed individuals or elements; ROI=measurements taken using a standardized region of interest; MC2=second metacarpal; MC2 50%=measurements taken at the second metacarpal midshaft; MT2=second metatarsal; -=no radiographed individuals/elements/pairs available. *number of elements with both right and left sides present and measureable.

7.6.1 Total, Cortical, and Region of Interest Areas:

The average total (T_A) and cortical (C_A and ROI) areas for each long bone type in the Vagnari sample were determined using the comparative (i.e., 'normal') sample. The average bone areas, as well as the differences between the sexes, are reported in Table

7.18. Measured cross-sectional values and calculated areas are presented in Appendix I. Data were tested for normality by site, sex, and age; the normality tests for each category are reported in Appendix J. All male and female total, cortical, and ROI areas were significantly different, with the exception of second metacarpals and metatarsals.

Table 7.18 – Average total and cortical/ROI areas at Vagnari and the differences between males and females by element type.[1]

Element	Average $T_A \pm \sigma$		Average C_A/ROI $\pm \sigma$	
	Female	Male	Female	Male
Humerus	234.0 ± 15.2	310.5 ± 53.7	167.8 ± 23.2	243.7 ± 49.4
	***U*=32.0, *p*≤.001**		***U*=29.0, *p*≤.001**	
Radius	135.2 ± 20.6	158.7 ± 20.5	83.3 ± 14.4	96.7 ± 17.3
	***U*=42.0, *p*=.007**		***U*=57.0, *p*=.048**	
Ulna ROI	-	-	223.2 ± 42.4	262.7 ± 40.7
	-		***U*=51.0, *p*=.024**	
MC2 50%	47.9 ± 6.5	57.3 ± 2.5	37.3 ± 6.5	43.6 ± 4.9
	U=1.0, *p*=.114		*U*=2.0, *p*=.229	
MC2 ROI	-	-	73.4 ± 13.6	84.2 ± 10.7
	-		*U*=21.0, *p*=.126	
Tibia	395.2 ± 68.2	518.5 ± 95.0	304.0 ± 58.6	428.0 ± 88.5
	***U*=57.0, *p*≤.001**		***U*=42.0, *p*≤.001**	
MT2 ROI	-	-	106.6 ± 16.7	114.5 ± 30.6
	-		*U*=26.0, *p*=.955	

[1] Groups compared using Mann-Whitney U tests. Bold values are significant. T_A=total area; C_A=cortical area; ROI=region of interest; σ=standard deviation; MC2=second metacarpal; MC2 50%=measurement taken at second metacarpal midshaft; MT2=second metatarsal; -=no data available.

Age-related differences in T_A and C_A/ROI areas are presented in Table 7.19. At Vagnari, total areas only differed between male middle and old adult tibiae. Cortical areas were significantly different between young and middle adult female upper limb bones (humeri, radii, and ulnae) and middle and old adult male tibiae. In other words, for most bone types at Vagnari, the size of the outer (total) bone area was not associated with adult age, but the cortical area decreased with age. This finding suggests that some age-related bone loss occurred at Vagnari, particularly among the females and in the upper limb. The significant age differences between male tibiae total and cortical area may be due to small sample sizes (old adult male tibiae *n*=2); the absence of differences between young and old adult male tibiae suggests that the difference identified between middle and old adult male tibiae was probably an artifact of very small sample size rather than an actual age difference in total and cortical area.

Table 7.19 – Age differences in the total and cortical areas at Vagnari by sex and bone type.[1]

Sex	Area	Element	YA vs. MA	YA vs. OA	MA vs. OA
Female	T_A	Humeri	*U*=23.5, *p*=.492	-	-
		Radii	*U*=4.0, *p*=.100	*U*=3.0, *p*=.800	*U*=0.0, *p*=.500
		MC2 50%	-	-	-
		Tibia	*U*=18.0, *p*=.839	*U*=8.0, *p*=.758	*U*=2.0, *p*=.533
	C_A/ROI	Humeri	***U*=3.0, *p*=.002**	-	-
		Radii	***U*=0.0, *p*=.009**	*U*=0.0, *p*=.200	*U*=1.0, *p*=1.000
		Ulna ROI	***U*=0.0, *p*=.030**	*U*=2.5, *p*=.121	*U*=2.0, *p*=1.000
		MC2 ROI	*U*=0.0, *p*=.133	*U*=0.0, *p*=.400	*U*=0.0, *p*=.667
		MC2 50%	-	-	-
		Tibia	*U*=12.0, *p*=.304	*U*=7.0, *p*=.606	*U*=3.0, *p*=.800
		MT2 ROI	-	*U*=0.0, *p*=.667	-
Male	T_A	Humeri	*U*=26.0, *p*=.385	-	-
		Radii	*U*=16.0, *p*=.876	-	-
		MC2 50%	*U*=2.0, *p*=1.000	-	-
		Tibia	*U*=21.5, *p*=.180	*U*=0.0, *p*=.071	***U*=0.0, *p*=.022**
	C_A/ROI	Humeri	*U*=24.0, *p*=.291	-	-
		Radii	*U*=15.0, *p*=.755	-	-
		Ulna ROI	*U*=7.0, *p*=.154	-	-
		MC2 ROI	*U*=3.0, *p*=.571	-	-
		MC2 50%	*U*=0.0, *p*=.333	-	-
		Tibia	*U*=23.0, *p*=.250	*U*=1.0, *p*=.143	***U*=0.0, *p*=.022**
		MT2 ROI	*U*=9.0, *p*=.905	-	-

[1] Groups were compared using Mann-Whitney U tests. Significant results in bold. YA=young adult; MA=middle adult; OA=old adult; T_A=total area; C_A=cortical area; ROI=region of interest; MC2=second metacarpal; MC2 50%=measurements taken at the second metacarpal midshaft; MT2=second metatarsal; -=no test performed due to an absence of measurable areas.

In order to maximize the sample sizes for later analyses, the sex and age groups that did not have significantly different total, cortical, and/or ROI areas were combined. The group combinations used for subsequent comparison with individuals with fractures are presented in Appendix K. All total, cortical, and ROI areas were split by sex and were compared separately for males and females in subsequent analyses. All age groups were combined for total area measurements, and only female humeri, radii, and ulnae cortical areas were split into two groups to compare young adults to middle and old adults.

7.6.2 Directional Asymmetry

Sex and age based differences between total area directional asymmetry (T_A%DA) and cortical area directional asymmetry (C_A%DA) were compared and the results are presented in Table 7.20. Appendix I reports the amount of asymmetry in each element for each individual. Appendix J reports the normality of asymmetry data distributions by site and sex. No significant differences in T_A%DA or C_A%DA were identified between Vagnari males and females or among age categories. As no element exhibited significant differences in asymmetry by sex or age, later asymmetry analyses combined these groups to maximize the sample sizes.

Table 7.20 – Average directional asymmetry by element, and differences between sexes and among age groups at Vagnari.[1]

Element	Asymmetry Type	Average Asymmetry ± Standard Deviation (%)		Sex Differences (Male vs. Female)	Both Sexes Age Group Differences
		Female	Male		
Humerus	Counts and df			*N*=19	*N*=19, df=2
	T_A%DA	3.9 ± 5.7	10.0 ± 19.2	*U*=40.0, *p*=.720	χ^2=0.135, *p*=.935
	C_A%DA	4.8 ± 12.1	12.2 ± 25.2	*U*=42.5, *p*=.842	χ^2=3.971, *p*=.137
Radius	Counts and df			*N*=10	*N*=10, df=2
	T_A%DA	8.0 ± 16.0	3.8 ± 10.5	*U*=10.0, *p*=.762	χ^2=0.622, *p*=.733
	C_A%DA	1.2 ± 16.7	7.7 ± 7.9	*U*=7.0, *p*=.352	χ^2=1.595, *p*=.450
Ulna ROI	Counts and df			*N*=12	*N*=12, df=3
	ROI%DA	8.6 ± 19.7	-8.3 ± 4.9	*U*=6.0, *p*=.109	χ^2=3.022, *p*=.388
MC2 ROI	Counts and df			*N*=6	*N*=6, df=2
	ROI%DA	-1.3 ± 16.3	1.8 ± 13.4	*U*=3.0, *p*=.800	χ^2=0.000, *p*=1.000
Tibia	Counts and df			*N*=19	*N*=19, df=3
	T_A%DA	-2.7 ± 8.0	-0.4 ± 15.5	*U*=36.0, *p*=.497	χ^2=1.588, *p*=.662
	C_A%DA	-1.5 ± 9.7	-1.4 ± 18.1	*U* =38.0, *p*=.604	χ^2=2.292, *p*=.514
MT2 ROI	Counts and df			*N*=5	*N*=5, df=2
	ROI%DA	7.6 ± 13.5	4.6*	*U*=1.0, *p*=.800	χ^2=1.400, *p*=.497

[1] Groups compared using Mann-Whitney U and Kruskal-Wallis tests. Midshaft second metacarpal measurements (MC2 50%) were excluded from the table as only one individual had paired second metacarpals. Bolded numbers indicate significant values. ROI=region of interest; MC2=second metacarpal; MT2=second metatarsal; df=degrees of freedom; *N*=number of elements present; T_A%DA=total area directional asymmetry; C_A%DA=cortical area directional asymmetry; ROI%DA=region of interest directional asymmetry. *value derived from a single individual.

7.7 Outlying Cross-Sectional Properties and Individuals with Fractures

This section reports the 'normal' range of areas and asymmetries for each analysed element and group and identifies individuals with outlying total, cortical, and ROI areas and asymmetries. Outliers were identified as individuals with cross-sectional properties that were above or below the normal range. These outliers are reported and discussed in more detail in this section, and are listed in detail in Appendix M; outliers with fractures are reported in Appendix N.

7.7.1 Total Area

Table 7.21 reports the range of total areas considered normal for each element and sex. The number of elements with outlying total areas are reported by age in Table 7.22. As in the Ancaster sample, all the outlying total areas at Vagnari were observed in the upper limb. There was no significant difference in the number of elements with outlying total areas between the Vagnari males and females (OR=2.2, CI 0.4-11.4; p_{FET}=.471). No significant age-related differences in the rates of elements with outlying total areas were observed ($\chi^2(2, N=95)=0.157$, p=.925). Appendix N reports the supplementary post-hoc differences between the Vagnari age groups. Outlying total areas were most common in the upper limb at Ancaster; the frequency of these outlying total areas remains relatively consistent between the sexes and throughout life.

Table 7.21 – Normal range of total areas and number of elements with outlying total areas at Vagnari by sex and element type.[1]

Element	Male		Female		Total
	All Ages IQR Range (mm^2)	All *n/N* %	All Ages IQR Range (mm^2)	All *n/N* %	*n/N* %
Humerus	243.7-383.7 (312.5)	4/36 11.1	196.4-277.2 (233.0)	2/24 8.3	6/60 10.0
Radius	105.3-208.5 (164.3)	0/27 0.0	61.7-207.2 (140.2)	0/22 0.0	0/49 0.0
MC2 50%	54.2-60.6 (57.6)	2/4 50.0	35.2-59.0 (44.8)	0/3 0.0	2/7 28.6
Tibia	306.7-753.7 (507.0)	0/37 0.0	211.2-581.2 (371.4)	0/26 0.0	0/63 0.0
Total	N/A	6/100 6.0	N/A	2/72 2.8	8/172 4.7

[1] Normal total area range indicated by 1.5 times the calculated interquartile ranges (IQR). Median values in brackets. Counts of outliers include individuals with fractures. *n*=number of elements with outlying total area; *N*=total number of elements measured; MC2 50%=measurement taken at the second metacarpal midshaft. *only two non-fractured observations available

Table 7.22 – Counts and prevalence rates of Vagnari elements with outlying total areas by sex and age.[1]

Age	Male *n/N* %	Female *n/N* %	Total *n/N* %
Adolescent	0/0 -	0/12 0.0	0/12 0.0
Young Adult	3/44 6.8	2/40 5.0	5/84 6.0
Middle Adult	3/49 6.1	0/13 0.0	3/62 4.8
Old Adult	0/2 0.0	0/3 0.0	0/5 0.0
Adult	0/5 0.0	0/4 0.0	0/9 0.0
Total	6/100 6.0	2/72 2.8	8/172 4.7

[1] Counts of outliers include individuals with fractures. *n*=number of elements with outlying total area; *N*=total number of elements measured.

The eight Vagnari individuals that had larger or smaller outlying total areas are presented in Table 7.23. Six of the eight outlying total areas at Vagnari were observed in humeri. Half of the elements with outlying total areas belonged to individuals who also had fractures (*n*=4/8). In all four instances, the fracture and outlying T_A were observed in the upper limb elements. In individuals VA-F204 and F249, the relationship between the fractured bone and the element with outlying total area may be indicative of post-injury function. VA-F204 had a fractured left humerus with a smaller than normal total area, while VA-F249 had a fractured left clavicle with a larger outlying right humerus (i.e., the humerus on the same side as the fracture was smaller). The outlying humeral total areas of both VA-F204 and VA-F249 may be explained by laterality. However, VA-F204's smaller, outlying total area may be explained by an interruption of periosteal bone apposition if the injury and unloading occurred during childhood, when bone expansion primarily involves the subperiosteal surface. VA-F249's larger humerus, contralateral to a clavicle fracture in may suggest functional compensation after injury.

Table 7.23 – Vagnari individuals with outlying total areas.[1]

Skeleton Number	Fracture	Sex	Age	Element	Side	Larger (>) or Smaller (<) than Norm	T_A (mm^2)
VA-F042A	L Tibia	M	YA	MC2 50%	R	>	67.1
VA-F062	-	M	MA	Humerus	L	<	170.7
VA-F204	L Humerus	F	YA	Humerus	L	<	196.0
VA-F207	-	M	YA	Humerus	L	<	229.2
VA-F213	-	M	MA	Humerus	L	>	395.6
VA-F214		M	MA	MC2 50%	R	<	54.0
VA-F249	L Clavicle	F?	YA	Humerus	R	>	279.8
VA-F288	L Ulna	M	YA	Humerus	R	<	241.5

[1] >=total area larger than the norm; <=total area smaller than the norm; T_A=total area; -=individuals without fractures; F=female; M=male; YA=young adult; MA=middle adult; OA=old adult; L=left; R=right.

7.7.2 Total Area Directional Asymmetry

The normal ranges of total area directional asymmetry (T_A%DA) are presented by sex and bone type in Table 7.24; Tables 7.24 and 7.25 also present the number of elements with outlying total area directional asymmetry by element and age, respectively. Only two Vagnari males had outlying levels of total area directional asymmetry and the frequency of outlying total area directional asymmetry was not significantly different between sexes (p_{FET}=.505) or between male age groups ($\chi^2(2, N=59)=2.142$, p=.343). Post-hoc age comparisons are reported in Appendix N.

Table 7.24 – Normal range of total area directional asymmetries (T_A%DA) and the number of outliers at Vagnari by bone type and sex.[1]

Element	T_A%DA Range	Male *n/N* %	Female *n/N* %	Total *n/N* %
Humerus	-20.0 to 27.4 (6.0)	1/18 5.6	0/12 0.0	1/30 3.3
Radius	-28.9 to 39.9 (5.4)	0/9 0.0	0/9 0.0	0/18 0.0
MC2 50%	0.2*	0/1 0.0	0/0 -	0/1 0.0
Tibia	-27.7 to 23.6 (-1.5)	1/18 5.6	0/12 0.0	1/30 3.3
Total	N/A	2/45 4.4	0/33 0.0	2/79 2.5

[1] Normal total area directional asymmetry range indicated by 1.5 times the calculated interquartile range (IQR). Median values reported in brackets. Counts of outliers include individuals with fractures. T_A%DA=total area directional asymmetry; *n*=number of elements with outlying total area; *N*=total number of elements measured. MC2 50%=measurement taken at the midshaft of the second metacarpal. *only a single measurement was available.

Table 7.25 – Number of Vagnari elements with outlying total area directional asymmetries (T_A%DA) by age and sex.[1]

Age	Male *n/N* %	Female *n/N* %	Total *n/N* %
Adolescent	0/0 -	0/10 0.0	0/10 0.0
Young Adult	0/29 0.0	0/27 0.0	0/56 0.0
Middle Adult	2/29 6.9	0/7 0.0	2/36 5.6
Old Adult	0/1 0.0	0/2 0.0	0/3 0.0
Adult	0/2 0.0	0/2 0.0	0/4 0.0
Total	2/61 3.3	0/48 0.0	2/109 1.8

[1] Counts of outliers include individuals with fractures. *n*=number of elements with outlying total areas; *N*=total number of elements measured; -=no elements observed.

The Vagnari individuals with outlying levels of total area directional asymmetry are listed in Table 7.26. Neither of the two individuals with outlying total area directional asymmetries had fractures. While these individuals cannot provide insight into functional adaptation to injury, the presence of high amounts of asymmetry suggests that these individuals regularly experienced different right and left limb biomechanical strains.

Table 7.26 – Vagnari individuals with outlying total area directional asymmetry.[1]

Skeleton Number	Fracture	Sex	Age	Element	Larger Side	T_A%DA (%)
VA-F062	-	M	MA	Humerus	R	54.9
VA-F290	-	M	MA	Tibia	L	-31.1

[1] T_A%DA=total area directional asymmetry; –=individuals without fractures; M=male, F=female; MA=middle adult; L=left, R=right.

7.7.3 Cortical Area

The range of normal cortical areas, as well as the number of outlying cortical areas, are presented by element type, sex, and age group in Table 7.27. Table 7.28 reports the number of elements with larger or smaller than normal outlying cortical areas; sex differences in the rates of outliers by size are also reported in this table. The prevalence rates of individuals with outlying cortical areas were not significantly different between the sexes. There were no noteworthy patterns in the size of outliers between males and females. This finding suggests that males were not more likely to have outlying amounts of cortical bone than females, and vice versa.

Table 7.27 – Normal range of male and female cortical areas at Vagnari.[1]

Element	Males		Females			Total *n/N* %
	All Ages Range (mm^2)	All Male *n/N* %	YA Range (mm^2)	MA/OA Range (mm^2)	All Female *n/N* %	
Humerus	153.5-344.4 (248.5)	1/36 2.8	126.7-231.4 (182.4)	88.5-195.5 (141.7)	0/24 0.0	1/60 1.7
Radius	45.8-147.6 (98.0)	0/27 0.0	56.9-115.4 (85.9)	56.6-82.1 (69.9)	0/22 0.0	0/49 0.0
Ulna ROI	174.2-335.1 (258.5)	1/23 4.3	156.7-307.5 (236.0)	127.9-219.7 (173.3)	2/21 9.5	3/44 6.8
MC2 50%	29.5-58.6 (44.5)	0/4 0.0	24.7-48.1 (34.0)		0/3 0.0	0/7 0.0
MC2 ROI	63.4-103.2 (82.7)	1/15 6.7	31.7-114.9 (78.0)		0/13 0.0	1/28 3.6
Tibia	235.8-636.5 (420.8)	0/37 0.0	176.0-413.9 (284.0)		3/26 11.5	3/63 4.8
MT2 ROI	58.6-153.8 (100.6)	1/16 6.3	66.0-148.4 (104.0)		0/8 0.0	1/24 4.2

[1] Normal cortical area range indicated by 1.5 times the calculated interquartile range (IQR) (mm^2). Counts include individuals with fractures. Median values are provided below the ranges in brackets. *n*=number of elements with outlying cross-sectional properties; *N*=total number of elements; YA=young adult; MA=middle adult; OA=old adult; ROI=region of interest; MC2=second metacarpal; MC2 50%=measurement taken at the midshaft of the second metacarpal; MT2=second metatarsal.

Table 7.28 – Sex-based differences between the number of smaller and larger cortical area outliers at Vagnari.[1]

Cortical Area Size	Males *n/N* %	Females *n/N* %	Sex Difference
Smaller Outlier (<)	1/154 0.6	0/114 0.0	p_{FET}=1.000
Larger Outlier (>)	3/154 1.9	5/114 4.4	OR=2.3, CI .5-9.9; p_{FET}=.291
Total	4/154 2.6	5/114 4.4	OR=1.7, CI 0.5-6.6; p_{FET}=.502

[1] *n*=number of elements with outlying cortical areas; *N*=total number of elements observed; <=smaller outlier; >=larger outlier; OR=odds ratio; CI=confidence interval. Bold font indicates significant difference. Italic font indicates males had greater odds of outliers than females.

Age differences in the number of larger and smaller than normal outlying cortical areas were also evaluated and counts of outliers are presented in Table 7.29. The prevalence of individuals with outlying cortical areas were not significantly different among male age groups ($\chi^2(2, N=148)=0.06, p=.972$) or among female age groups ($\chi^2(3, N=108)=3.62, p=.305$). Supplementary post-hoc tests comparing age categories are reported in Appendix N. These findings suggest that age did not strongly govern the number of cortical bone outliers at Vagnari. There is no pattern in the age-related distribution of smaller and larger cortical bone outliers with advancing age; in particular, prevalence rates of outliers do not indicate age-related bone loss at this site.

Table 7.29 – Number of Vagnari elements with smaller and larger outlying cortical areas.[1]

Age	Male			Female			Total
	n <	*n* >	*n/N* %	*n* <	*n* >	*n/N* %	*n/N* %
Adolescent	0	0	0/0 0.0	0	2	2/22 9.1	2/22 9.1
Young Adult	1	1	2/73 2.7	0	2	2/60 3.3	4/133 3.0
Middle Adult	1	1	2/73 2.7	0	0	0/19 0.0	2/92 2.2
Old Adult	0	0	0/2 0.0	0	1	1/7 14.3	1/9 11.1
Adult	0	0	0/6 0.0	0	0	0/6 0.0	0/12 0.0
Total	5	3	4/154 2.6	0	5	5/114 4.4	9/268 3.4

[1] Counts of outliers include individuals with fractures. *n*=number of outlying total areas; *N*=number of elements measured; <=cortical area smaller than normal; >=cortical area larger than normal.

The seven Vagnari individuals with larger or smaller than normal cortical areas are listed in Table 7.30. Of the individuals with outlying cortical areas, 28.6% (*n*=2/7) also had a fracture. Outlying cortical areas were observed in the same limb type as the fracture in one individual with a fracture (VA-F249), but the cortical area of the fractured limb was larger than the contralateral, non-fractured side.

Table 7.30 – Vagnari individuals and elements with outlying cortical areas (C_A and ROI).[1]

Skeleton Number	Fracture	Sex	Age	Element	Side	Larger (>) or Smaller (<) than the Norm	CA/ROI (mm^2)
VA-F062	-	M	MA	Humerus	L	<	118.4
VA-F215	-	F	YA	Tibia	L	>	419.0
VA-F216	Fibula	M	MA	MC2 ROI	R	>	105.6
VA-F234	-	M	YA	MT2 ROI	R	>	178.1
				Ulna	L	>	337.6
VA-F249	Clavicle	F	YA	Ulna	L	>	309.1
VA-F252	-	F	ADO	Tibia	L&R	>	416.1, 421.3
VA-F294	-	F	OA	Ulna	R	>	220.4

[1] <=smaller than normal cortical area; >=larger than normal cortical area; C_A=cortical area; ROI=region of interest; –=individuals without fractures; M=male, F=female; YA=young adult; MA=middle adult; OA=old adult; L=left, R=right.

7.7.4 Cortical Area Directional Asymmetry

The normal range of cortical area directional asymmetry (C_A%DA) is reported by element in Table 7.31. Table 7.32 reports the number of elements with outlying amounts of cortical area directional asymmetry by age and sex. Age differences in the prevalence of outliers are reported in Table 7.33. The rates of cortical area directional asymmetry outliers were not significantly different between males and females (OR=1.3, CI 0.2-9.5; p_{FET}=1.000). There were also no significant differences between the age categories. These findings show that sex and age were not influential in the development of greater rates of elements with outlying cortical area directional asymmetries at Vagnari.

Table 7.31 – Normal ranges of cortical area directional asymmetries (C_A%DA) and the number of outliers at Vagnari by bone type and sex.[1]

Element	C_A%DA Range	Male *n/N* %	Female *n/N* %	Total *n/N* %
Humerus	-19.6 to 31.0 (5.7)	1/18 5.6	1/12 8.3	2/30 6.7
Radius	-24.8 to 33.5 (4.9)	0/9 0.0	0/9 0.0	0/18 0.0
Ulna ROI	-33.8 to 35.7 (-4.3)	0/8 0.0	1/10 10.0	1/18 5.6
MC2 ROI	-36.3 to 34.3 (-5.1)	0/3 0.0	0/4 0.0	0/7 0.0
MC2 50%	0.0*	0/1 0.0	-	0/1 0.0
Tibia	-32.1 to 26.9 (0.4)	1/18 5.6	0/12 0.0	1/30 3.3
MT2 ROI	-12.6 to 33.3 (8.1)	0/5 0/0	0/1 0/0	0/6 0.0
Total	N/A	2/62 3.2	2/48 4.2	4/110 3.6

[1] Normal cortical area directional asymmetry range indicated by 1.5 times the calculated interquartile range (IQR). Median values reported in brackets. Counts of outliers include individuals with fractures. C_A%DA=cortical area directional asymmetry; *n*=number of elements with outlying cortical area directional asymmetries; *N*=total number of elements; ROI=region of interest; MC2=second metacarpal; MC2 50%=measurement location at the second metacarpal midshaft; MT2=second metatarsal. * based on a single measurement.

Table 7.32 – Count and prevalence rates of Vagnari element pairs with outlying cortical area directional asymmetry by age and sex. [1]

Age	Male *n/N* %	Female *n/N* %	Total *n/N* %
Adolescent	0/0 -	0/10 0.0	0/10 0.0
Young Adult	0/30 0.0	0/27 0.0	0/57 0.0
Middle Adult	2/29 6.9	1/7 14.3	3/36 8.3
Old Adult	0/1 0.0	1/2 50.0	1/3 33.3
Adult	0/2 0.0	0/2 0.0	0/4 0.0
Total	2/62 3.2	2/48 4.2	4/110 3.6

[1] Counts of outliers include individuals with fractures. *n*=number of outlying element pairs; *N*=number of element pairs observed; -=no element pairs observed.

Table 7.33 – Age differences in the prevalence of elements with outlying cortical area directional asymmetries at Vagnari by sex. [1]

	Young Adult	Middle Adult	Old Adult
		Male	
Young Adult		p_{FET}=.237	-
Middle Adult	p_{FET}=.206		*p_{FET}=.491*
Old Adult	p_{FET}=.069	OR=6.0, CI 0.2-196.3 p_{FET}=.417	
	Female		

[1] Groups were compared using odds ratios and Fisher's Exact tests. Bold font indicates that a significant difference is present. Italic font is used to indicate instances when greater odds of outlying total areas were present in younger adults, rather than older adults -=no outliers available to compare; OR=odds ratio; CI=confidence interval.

The Vagnari individuals with outlying cortical area directional asymmetries are listed in Table 7.34. None of the individuals with outlying cortical area directional asymmetries had an extremity fracture.

Table 7.34 - Vagnari individuals and elements with outlying levels of cortical area directional asymmetry.[1]

Skeleton Number	Fracture	Sex	Age	Element	Larger Side	C_A%DA (%)
VA-F062	-	M	MA	Humerus	R	72.0
VA-F294	-	F	OA	Ulna	R	51.1
VA-F290	-	M	MA	Tibia	L	-37.8
VA-F306	-	F	MA	Humerus	L	-23.0

[1] C_A%DA=cortical area directional asymmetry; –=individuals without fractures; M=male, F=female; MA=middle adult; OA=old adult; R=right; L=left.

7.8 Cross-Sectional Outliers and Individuals with Fractures Compared

This section investigates the relationships between fracture types, fracture complications, and outlying cross-sectional areas and asymmetries. Connections and interactions among these variables are examined in order to better understand the factors that influence the development of outlying cross-sectional areas and asymmetries in fractured elements.

7.8.1 All Fractures with Outlying Cross-Sectional Properties

Table 7.35 summarizes the counts and prevalence rates of individuals that had both a fracture and at least one outlying cross-sectional property. All individuals with fractures and outlying cross-sectional properties were included in these counts, even if the outlying element was located in a different limb type to the fracture (e.g., fractured radius and tibial cortical area asymmetry). All the elements with outlying cross-sectional properties are summarized in Appendix M and every individual with both a fracture and an outlying element are further detailed in Appendix O.

Table 7.35 – Prevalence of individuals with fractures and outlying cross-sectional properties at Vagnari by sex and age.[1]

Age	Female *n/N* %	Male *n/N* %	Unknown Sex *n/N* %	Total *n/N* %
Adolescent	0/1 0.0	0/0 -	0/0 -	0/1 0.0
Young Adult	2/3 66.7	2/4 50.0	0/0 -	4/7 57.1
Middle Adult	0/1 0.0	1/4 25.0	0/0 -	1/5 20.0
Old Adult	0/1 0.0	0/0 -	0/0 -	0/1 0.0
Total	2/6 33.3	3/8 37.5	0/0 -	5/14 35.7

[1] *n*=number of outlying individuals with fractures; *N*=total number of outlying individuals.

Including both individuals with and without fractures, 34 individuals were radiographed at Vagnari, 14 of which had outlying cross-sectional properties. This means that 58.8% (*n*=20/34) of all the radiographed individuals were within the normal cross-sectional ranges. Of the individuals with fractures, 58.3% (*n*=7/12) also had cross-sectional properties within the normal ranges. The odds of exhibiting outlying cross-sectional properties were compared between individuals with and without fractures. The individuals with fractures (*n*=5/12) had approximately equal odds of outlying cross-sectional properties as individuals without fractured bones (*n*=9/28) (OR=1.5, CI 0.4-6.1; p_{FET}=.720). As individuals with fractures were not at greater risk for developing outlying cross-sectional properties compared to individuals without fractures, these results suggest that the presence of a fracture does not predict outlying cross-sectional properties at Vagnari.

Sex and age differences in the prevalence of individuals with fractures and outlying cross-sectional properties were compared. The rates of outliers did not differ significantly between males and females (OR=1.2, CI 0.1-11.1; p_{FET}=1.000). There were also no significant differences in the counts of outliers among the age categories at Vagnari ($\chi^2(3, N=14)=3.05$, p=.384). Supplementary post-hoc tests reporting differences between each age category are reported in Appendix N. These findings indicate that the presence of outlying cross-sectional properties associated with fractures are not influenced by sex or age-related differences at Vagnari.

Table 7.36 presents the prevalence of, and differences between, elements with fractures that were associated with outlying cross-sectional properties by fracture force type. Although higher energy fractures had slightly greater odds of being associated with outlying cross-sectional properties, there were no significant relationships identified between fracture force type and cross-sectional outliers. That is, neither indirect nor direct/higher energy fractures were significantly more likely to have cross-sectional anomalies.

Table 7.36 – Prevalence of, and differences between, outlying Vagnari elements with fractures by fracture force types and sex.[1]

Fracture Force	Female *n/N* %	Male *n/N* %	Unknown Sex *n/N* %	Total *n/N* %	Differences Between Female and Males
Indirect	0/0 -	1/4 25.0	0/1 -	1/5 20.0	-
Higher Energy/Direct	1/1 100.0	1/3 33.3	0/1 0.0	2/5 40.0	p_{FET}=1.000
Unknown	1/2 50.0	1/1 100.0	0/0 -	2/3 66.7	*p_{FET}=1.000*
Total	2/3 66.7	3/8 37.5	0/2 0.0	5/13 41.7	OR=3.3, CI 0.2-54.5 p_{FET}=.545
Differences Between High Energy/Direct and Indirect Fracture Types	-	OR=1.5, CI 0.1-40.6 p_{FET}=1.000	-	OR=2.7, CI 0.2-45.1 p_{FET}=1.000	

[1] Groups compared using odds ratios and Fisher's Exact tests. Bold font used to indicate statistical significance. Italic font used to indicate when indirect or male frequencies had greater prevalence rates than direct and female frequencies. *n*=number of fractures associated with an outlying cross-sectional property; *N*=total number of fractures in each category; -=no elements or outliers available to compare; OR=odds ratio; CI=confidence interval.

Prevalence rates of individuals that had both outlying cross-sectional properties and fracture complications (i.e., malunion, osteoarthritis, inflammation), as well as differences between the sexes and individuals with and without fracture complications, are reported in Table 7.37. It was hypothesized that individuals with fracture complications would be at greater risk for outlying cross-sectional attributes. However, at Vagnari, males and females with fracture complications did not have significantly greater odds for outlying cross-sectional properties than individuals without fracture complications. These findings demonstrate that fracture complications did not predict the presence of outlying cross-sectional properties.

Table 7.37 – Prevalence of, and differences between, Vagnari individuals with and without outlying cross-sectional properties and fracture complications by sex.[1]

Variables Compared	Female *n/N* %	Male *n/N* %	Unknown Sex *n/N* %	Total *n/N* %	Differences Between Female and Males
Outlying individuals with fractures and complications vs. All individuals with fractures and complications	1/1 100.0	1/3 33.3	0/1 0.0	2/5 40.0	p_{FET}=1.000
Outlying individuals with fractures without complications vs. All individuals with fractures without complications	1/2 50.0	2/5 40.0	0/0 -	3/7 42.9	OR=1.5, CI 0.1-40.6; p_{FET}=1.000
Total individuals with both outlying elements and associated fractures vs. All individuals with fractures	2/3 66.7	3/8 37.5	0/1 0.0	5/12 41.7	OR=5.0, CI 0.3-91.5; p_{FET}=.500
Difference between outlying fractures with complications and outlying fractures without complications	p_{FET}=1.000	*OR=1.3,* *CI 0.1-26.6;* *p_{FET}=1.000*	-	*OR=1.1,* *CI 0.1-11.6;* *p_{FET}=1.000*	

[1] Groups compared using odds ratios and Fisher's Exact tests. Bold font used to indicate statistical significance. Italic font used to indicate when outliers without fractures and/or males had greater prevalence rates than outliers with fractures and/or females. *n*=number of fractures with an outlying cross-sectional property; *N*=total number of fractures in each category; -=no outliers available to compare; OR=odds ratio; CI=confidence interval.

Changes associated with adult bone loss are more likely to affect the endosteal surface of the bone (Schäfer et al. 2012), meaning cortical bone areas and asymmetries are likely to exhibit the greatest changes following disuse of an injured limb. Table 7.38 summarizes the individuals with outlying cortical bone areas and asymmetries in terms of the relationship between the outlying element and the fractured limb type and side.

Table 7.38 – Counts of Vagnari fractured elements with smaller and larger outlying cortical bone properties organized according to the positional relationship with a fracture.[1]

Age	Sex	Smaller element on fractured limb side	Larger element on fractured limb side	Fracture in lower limb, outlier in upper	Fracture in upper limb, outlier in lower	Total
Young Adult	F	-	1	-	-	1
	M	-	-	-	-	-
Middle Adult	F	-	-	-	-	-
	M	-	-	1	-	1
Old Adult	F	-	-	-	-	-
	M	-	-	-	-	-
Total	F	-	1	-	-	1
	M	-	-	1	-	1
	Total	-	1	1	-	2

[1] F=female; M=male; -=no outlying element associated with a fractured element.

Only one of the Vagnari individuals with fractures had outlying cortical areas or asymmetries in the same limb type as the fractured bone. This individual (VA-F249) had elements that were larger in the same limb and on the same side as the fracture; that is, a larger left ulnar cortical area, on the same side as a malunited clavicle fracture. As upper limb fractures (proximal to the wrist) tend to predominantly occur in the non-dominant limb (Borton et al. 1994; Meals 1979), it may not be logical to interpret the ipsilaterally enlarged ulna as indicative of left-sided hand preference. Instead, it is possible that the larger ulna developed as a biomechanical response to the malunited and morphologically altered shoulder girdle.

The final category includes an element that was asymmetric in the opposite limb type than the fractured limb; that is, a lower limb fracture with outlying upper limb cortical properties (n=1/3). This single case at Vagnari involves the fractured right fibula and a larger than normal right second metacarpal cortical area of VA-F216. Although most isolated fibular fractures have limited functional repercussions, in some cases they can cause ankle instability (Bauer et al. 1985; Broos and Bisschop 1991). The fracture exhibited by VA-F216 is associated with osteoarthritis at both the ankle and knee, which may suggest some associated joint instability or discomfort. While it is possible that the outlying second metacarpal cortical area is a result of adaption, perhaps the use of a mobility aid, it may also be better associated with hand preference or accentuated unilateral activity.

7.9 Summary

At Vagnari, very few differences in fracture frequencies were present among the groups analysed. Fracture prevalence rates did not differ significantly between the sexes, age groups, or among bone types, and there were no observable differences in the rates of fracture forces or types. Although it was not significant, a general age-related pattern in the distribution of fractures was observed at Vagnari that suggested young adults had higher fracture prevalence rates than middle or old adults. As older adults are typically expected to have the highest fracture frequencies due to the accumulation of injuries over the life course, the concentration of fractures in younger individuals at Vagnari appears anomalous. While this observation may be explained by issues in preservation, it merits additional discussion in Section 9.3.

In terms of fracture complications, high-energy or direct force fracture types had significantly greater odds of exhibiting malunion than indirect and unknown fracture forces. For the entire Vagnari assemblage, osteoarthritis was more prevalent in older individuals, a finding that is in agreement with the clinically observed increase in osteoarthritis with advancing age (Loeser 2009). Results showed that the joint surfaces of individuals with fractures were not any more likely to have osteoarthritis than those of individuals without fractures. Due to poor preservation, it was not possible to comprehensively investigate the relationships between osteoarthritis, joint fractures, and fracture malunion in the Vagnari sample, but given better joint preservation, consideration of these factors would help to better understand rates of possible post traumatic osteoarthritis in this collection.

When cross-sectional properties were considered among the individuals without fractured bones at Vagnari, significant differences in total and cortical areas between males and females were identified. Additionally, middle adult female upper limb bones (i.e., humeri, radii, and ulnae) tended to have significantly smaller cortical areas than those of young adult females. This pattern in female upper limbs is similar to that observed among the Ancaster skeletal assemblage and will be discussed further in Section 9.3.

Individuals with outlying cross-sectional properties were identified in the Vagnari collection. Individuals both with and without fractured bones were at equal risk for having outlying cross-sectional properties. In other words, individuals with fractures were not at any greater risk for developing outlying cross-sectional properties. Among the individuals with fractured bones, there were no significant differences in the frequency of outliers between the sexes, age groups, fracture force types, or associated fracture complications.

Three of the Vagnari individuals (VA-F204, F249, F216) deserve additional emphasis, as their fractures and cross-sectional properties may provide insight into post-injury biomechanical function and adaptation. The co-occurrence of a thoroughly healed humeral fracture with a smaller than normal total area and absence of outlying cortical areas in a female (VA-F204) suggest that this fracture may be associated biomechanical unloading during childhood when bone apposition on the periosteal surface would be most affected, rather than the endosteal surface as in adults (Ruff et al. 1994; Schäfer et al. 2012). Individuals VA-F249 and VA-F216 provide evidence for mechanical consequences related to altered morphology and perhaps the use of a mobility aid, respectively.

Chapter VIII – RESULTS: COMPARISONS BETWEEN ANCASTER AND VAGNARI

Differences in the fractured bones and biomechanical outliers between Ancaster and Vagnari are reported in this chapter. Fracture prevalence rates and distributions of fractures are compared between the two sites. The outlying cross-sectional properties are also compared according to fracture types, complications, and their anatomical relationship to a fractured element. Biomechanical differences by limb and bone types are presented and provide insight into variable habitual loading forces at Ancaster and Vagnari.

8.1 Demographic Comparison

Figure 8.1 and Table 8.1 report the differences in the prevalence of individuals in each age group at Ancaster and Vagnari. While the proportion of young adult individuals was similar at both sites, adolescents were significantly more prevalent at Vagnari than at Ancaster. Middle and old adult individuals were slightly less prevalent at Vagnari than at Ancaster, but the difference was not significant. Although more adolescents died at Vagnari than at Ancaster, the adult age categories were similar, and should therefore not greatly affect the ability to compare fracture and biomechanical data between the two sites.

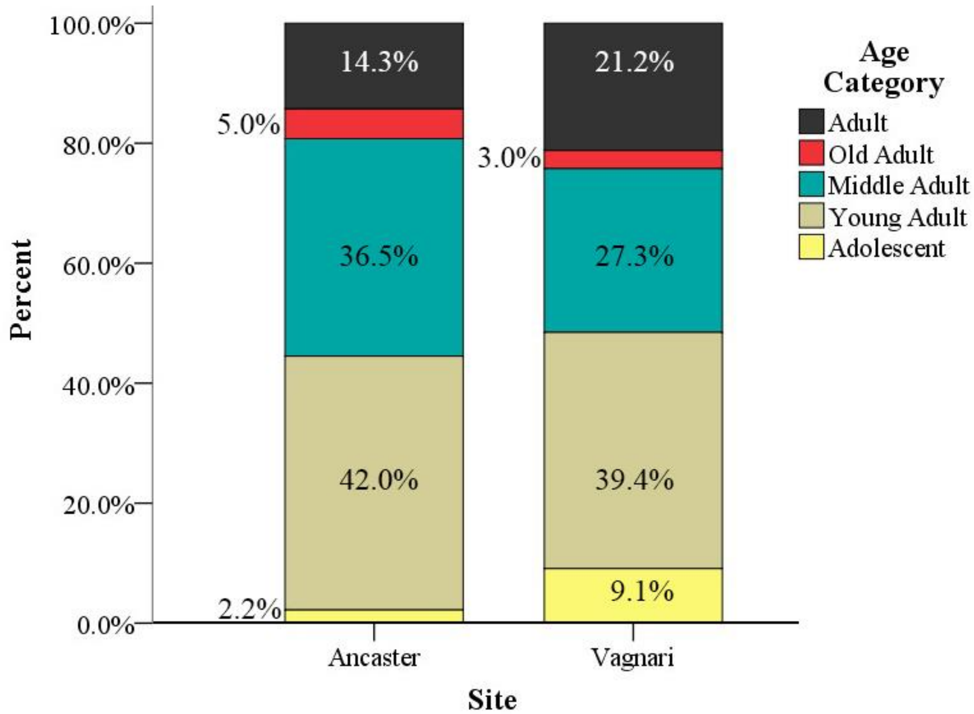

Figure 8.1 – Difference in the proportion of individuals in each age cohort between Ancaster and Vagnari. See Tables 6.1 and 7.1 for counts of individuals in each age category.

Table 8.1 – Difference in the proportion of individuals in each age cohort between Ancaster and Vagnari.[1]

Age	Difference in the number of individuals between sites
Adult	OR=1.6, CI 0.8-3.3, χ^2_{Yates}(1, N=247)=1.20, *p*=.272
Old Adult	OR=1.7, CI 0.4-8.0, p_{FET}=.732
Middle Adult	OR=1.5, CI 0.8-2.8, χ^2_{Yates}(1, N=247)=1.43, *p*=.231
Young Adult	OR=1.1, CI 0.6-2.0, p_{FET}=.771
Adolescent	**OR=4.4, CI 1.2-16.2, p_{FET}=.025**

[1] Age groups compared with odds ratios, chi-square, and/or Fisher's exact tests. Bold font indicates significant difference present. See Tables 6.1 and 7.1 for counts of individuals in each age category. OR=odds ratio; CI=confidence interval.

8.2 Fracture Frequencies and Distribution

The differences between Ancaster and Vagnari fractures by force type, limb type, and age are presented for males in Table 8.2 and females in Table 8.3. While none of the differences between sites were significant, there were a few instances when the odds of fracture were noteworthy and indicate general trends in the distribution of fractures by age, sex, limb, and force type.

Table 8.2 – Difference in male fracture true prevalence rates between Ancaster and Vagnari by limb and force type, age, and sex.[1]

Force Type	Age	Ancaster	Vagnari	Difference Between Ancaster and Vagnari
		Upper Limb		
Indirect	Young Adult	0/260	0/52	-
	Middle Adult	3/276	0/59	p_{FET}=1.000
	Old Adult	0/22	0/2	-
	Subtotal	3/558	0/113	p_{FET}=1.000
High Energy & Direct	Young Adult	2/260	1/52	*OR=2.5, CI 0.2-28.4, p_{FET}=.422*
	Middle Adult	8/276	1/59	OR=1.7, CI 0.2-14.1, p_{FET}=1.000
	Old Adult	1/22	0/2	p_{FET}=1.000
	Subtotal	11/558	1/113	OR=2.3, CI 0.3-17.6, p_{FET}=.701
Total		14/558	1/113	OR=2.9, CI 0.4-22.1, p_{FET}=.486
		Lower Limb		
Indirect	Young Adult	4/186	2/50	*OR=1.9, CI 0.3-10.7, p_{FET}=.610*
	Middle Adult	7/210	2/50	*OR=1.2, CI 0.2-6.0, p_{FET}=.685*
	Old Adult	1/12	0/7	p_{FET}=1.000
	Subtotal	12/408	4/107	*OR=1.3, CI 0.4-4.1, p_{FET}=.753*
High Energy & Direct	Young Adult	2/186	1/50	*OR=1.9, CI 0.2-21.1, p_{FET}=.512*
	Middle Adult	3/210	0/50	p_{FET}=1.000
	Old Adult	0/12	0/7	-
	Subtotal	5/408	1/107	OR=1.3, CI 0.2-11.4, p_{FET}=1.000
Total		17/408	5/107	*OR=1.1, CI 0.4-3.1, p_{FET}=.790*
		Both Limbs		
Indirect	Young Adult	4/446	2/102	*OR=2.2, CI 0.4-12.2, p_{FET}=.310*
	Middle Adult	10/486	2/109	OR=1.1, CI 0.2-5.5, p_{FET}=1.000
	Old Adult	1/34	0/9	p_{FET}=1.000
	Subtotal	15/966	4/220	*OR=1.2, CI 0.4-3.6, p_{FET}=.766*
High Energy & Direct	Young Adult	4/446	2/102	*OR=2.2, CI 0.4-12.2, p_{FET}=.310*
	Middle Adult	11/486	1/109	OR=2.5, CI 0.3-19.6, p_{FET}=.704
	Old Adult	1/34	0/9	p_{FET}=1.000
	Subtotal	16/966	3/220	OR=1.2, CI 0.4-4.2, p_{FET}=1.000
Total	Young Adult	8/446	4/102	*OR=2.2, CI 0.7-7.6, p_{FET}=.250*
	Middle Adult	21/486	3/109	OR=1.6, CI 0.5-5.4, p_{FET}=.596
	Old Adult	2/34	0/9	p_{FET}=1.000
	Total	31/966	7/220	OR=1.0, CI 0.4-2.3, p_{FET}=1.000

[1] Bold indicates a significant value. Italic font indicates that a greater fracture prevalence rate was observed at Vagnari than at Ancaster. OR=odds ratio; CI=confidence interval; p_{FET}=Fisher's Exact Test.

Table 8.3 – Difference in female fracture true prevalence rates between Ancaster and Vagnari by limb and force type, age, and sex.[1]

Force Type	Age	Ancaster	Vagnari	Difference between Ancaster and Vagnari
Upper Limb				
Indirect	Young Adult	1/201	0/61	p_{FET}=1.000
	Middle Adult	3/143	0/20	p_{FET}=1.000
	Old Adult	3/37	0/1	p_{FET}=1.000
	Subtotal	7/381	0/82	p_{FET}=.613
High Energy & Direct	Young Adult	1/201	1/61	*OR=3.3, CI 0.2-54.1, p_{FET}=.412*
	Middle Adult	2/143	0/20	p_{FET}=1.000
	Old Adult	0/37	0/1	-
	Subtotal	3/381	1/82	*OR=1.6, CI 0.2-15.1, p_{FET}=.543*
Total		10/381	1/82	OR=2.2, CI 0.3-17.3, p_{FET}=.698
Lower Limb				
Indirect	Young Adult	4/177	0/35	p_{FET}=1.000
	Middle Adult	2/118	0/11	p_{FET}=1.000
	Old Adult	0/24	0/0	-
	Subtotal	6/319	0/46	p_{FET}=1.000
High Energy & Direct	Young Adult	2/177	0/35	p_{FET}=1.000
	Middle Adult	0/118	0/11	-
	Old Adult	0/24	0/0	-
	Subtotal	2/319	0/46	p_{FET}=1.000
Total		8/319	0/46	p_{FET}=.603
Both Limbs				
Indirect	Young Adult	5/378	0/96	p_{FET}=.588
	Middle Adult	5/261	0/31	p_{FET}=1.000
	Old Adult	3/61	0/1	p_{FET}=1.000
	Subtotal	13/700	0/128	p_{FET}=.238
High Energy & Direct	Young Adult	3/378	1/96	*OR=1.3, CI 0.1-12.8, p_{FET}=1.000*
	Middle Adult	2/261	0/31	p_{FET}=1.000
	Old Adult	0/61	0/1	-
	Subtotal	5/700	1/128	*OR=1.1, CI 0.1-9.4, p_{FET}=1.000*
Total	Young Adult	8/378	1/96	OR=2.1, CI 0.3-16.6, p_{FET}=.694
	Middle Adult	7/261	0/31	p_{FET}=1.000
	Old Adult	3/61	0/1	p_{FET}=1.000
	Total	18/700	1/128	OR=3.3, CI 0.4-25.1, p_{FET}=.337

[1] Bold indicates a significant value. Italic font indicates that a greater fracture prevalence rate was observed at Vagnari than at Ancaster. OR=odds ratio; CI=confidence interval; p_{FET}=Fisher's Exact Test.

Young adult males at Vagnari had greater odds of fractures than the young adult males at Ancaster. The opposite was true for young adult females who had greater odds of fracture at Ancaster than at Vagnari. Small sample sizes of old adults at Vagnari prevented the reliable comparison of this age group, but it was nevertheless clear that fracture prevalence rates increased with age at Ancaster, but decreased with age at Vagnari. This trend was true for both males and females. Although young adults at Vagnari had greater prevalence rates of fractures, because of the accumulation of fractures with age at Ancaster, the overall odds of fracture were equal between the two sites.

Differences in the types of forces that caused the fractures were also present between Ancaster and Vagnari. Young adult female upper limbs and young adult male upper and lower limbs were more likely to have higher energy and direct force fracture types at Vagnari than at Ancaster. However, in all instances, this difference disappears with age due to the increasing fracture frequencies of older Ancaster adults. Indirect force injuries were most common among the Ancaster females; no indirect fracture types were identified among Vagnari females.

8.3 Fractures, Complications, Outliers, & Long-Term Function

The prevalence of outlying elements in individuals without fractures were compared at Ancaster and Vagnari; the site differences in the rates of outliers are presented by limb type in Table 8.4. The rates of outlying upper and lower limb elements in individuals without fractures were similar between Ancaster and Vagnari. At both Ancaster and Vagnari, individuals without fractures were more likely to have outlying elements in their upper limb than the lower limb. The concentration of outliers in the upper limbs at Ancaster and Vagnari may be explained by increased mechanical loading associated with activities that required increased strain on the arms.

Table 8.4 – Differences in the prevalence of elements with outlying cross-sectional properties in individuals without fractures at Ancaster and Vagnari.[1]

Limb Type	Ancaster *n/N* %	Vagnari *n/N* %	Difference Between Ancaster and Vagnari
Upper Limb	26/194 13.4	8/43 18.6	OR=1.4, CI 0.6-3.5, p_{FET}=.470
Lower Limb	6/100 6.0	2/32 6.3	OR=1.0, CI 0.2-5.5, p_{FET}=1.000
Total	32/294 10.9	10/75 13.3	OR=1.3 CI 0.6 -2.7, $\chi^2_{Yates}(1, N=369)=0.15$, p=.695
Difference Between Upper and Lower Limb	OR=2.4, CI=1.0-6.1; $\chi^2_{Yates}(1, N=294)=3.00$, p=0.083	OR=3.4, CI=0.7-17.4; p_{FET}=.174	

[1] Bold indicates a significant value. In all comparisons, Vagnari had greater odds of having outlying cross-sectional properties than Ancaster. Counts of second metacarpal midshaft measurements (MC2 50%) not included in counts so that second metacarpal elements were not counted twice. *n*=number of outlying elements in individuals without fractures; *N*=total number of radiographed elements; OR=odds ratio; CI=confidence interval.

Table 8.5 compares the number of individuals with both fractures and outlying cross-sectional properties to the number of individuals with fractures, as well as the number of individuals with outlying elements. Combined, approximately 40% of the Ancaster and Vagnari individuals with fractures had outlying cross-sectional properties (*n*=19/51, 37.3%). The overall odds that an individual had an element with outlying cross-sectional properties as well as a fracture were approximately equal at Ancaster and Vagnari. However, the upper limbs of Vagnari individuals with fractures had almost four times the odds of exhibiting an element with outlying cross-sectional properties as the upper limbs at Ancaster. In general, these results show that individuals with fractures and outlying cross-sectional properties were not more common at Ancaster or Vagnari. But, the elevated rates of Vagnari individuals with upper limb cross-sectional outliers and fractures suggest that compared to Ancaster, more Vagnari individuals with fractures experienced mechanical loading in the arms that was different than the group norm. Most of the Vagnari outlying upper limb elements are larger than the norm; therefore, it can be deduced that the large number of outliers may have more to do with the participation of these individuals in habitually elevated activities at Vagnari than the fractures.

Table 8.5 – Differences in the prevalence of individuals with fractures that also had elements with outlying cross-sectional properties between Ancaster and Vagnari.[1]

Groups Compared	Limb Type	Ancaster *n/N* %	Vagnari *n/N* %	Difference Between Ancaster and Vagnari
Individuals with fractures and outlying element(s) / Total fractured elements	Upper Limb	11/28 39.3	5/7 71.4	*OR=3.9, CI 0.6-23.5,* p_{FET}*=.207*
	Lower Limb	3/28 10.7	0/6 0.0	p_{FET}=1.000
Individuals with fractures and outlying element(s) / Individuals with fractures	-	14/39 35.9	5/12 41.7	*OR=1.3, CI 0.3-4.8,* p_{FET}*=.743*
Individuals with fractures and outlying element(s) / Total individuals with outliers	-	14/36 38.9	5/14 35.7	OR=1.1, CI 0.3-4.1, $\chi^2_{Yates}(1)=0.00$, *p*=1.000

[1] Bold indicates a significant value. Italics used to indicate when Vagnari had greater odds than Ancaster. Counts of second metacarpal midshaft measurements (MC2 50%) not included in counts so that second metacarpal elements were not counted twice. *n*=number of outlying elements in individuals with fractures; *N*=total number of elements/individuals; OR=odds ratio; CI=confidence interval.

Table 8.6 reports the proportion of outlying individuals with fractures according to the positional relationship between the fracture and the bone with the outlying property. When outliers were identified in the same limb type as a fractured bone, they typically involved the upper limb (Ancaster [*n*=6/7] and Vagnari [*n*=4/4]). However, the proportions of outlying individuals with fractures for each positional relationship were not significantly different between Ancaster and Vagnari.

Table 8.6 – Differences in proportions of fractured and outlying elements according to their anatomical relationship at Ancaster and Vagnari.[1]

Position of fracture relative to outlying bone	Ancaster *n/N* %	Vagnari *n/N* %	Difference Between Ancaster and Vagnari
Smaller on same limb and side as fracture	3/17 17.6	2/6 33.3	OR=2.3, CI 0.3-19.2, p_{FET}=.576
Larger in same limb and side as fracture	4/17 23.5	2/6 33.3	*OR=1.6, CI 0.2-12.4, p_{FET}=.632*
Fractured leg and larger outlying arm	5/17 29.4	2/6 33.3	OR=1.2, CI 0.2-8.8, p_{FET}=1.000
Fractured upper limb and outlying lower limb	5/17 29.4	0/6 0.0	p_{FET}=.272

[1] Bold indicates a significant value. Italics used to indicate when Vagnari had greater odds than Ancaster. *n*=number of outliers associated with a fractured element and a specific position; *N*=number of outliers associated with a fractured element; OR=odds ratios; CI=confidence interval.

8.3.1 Fracture Forces & Types

The prevalence of elements that were fractured and had outlying cross-sectional properties are presented by fracture force type, sex, and site in Table 8.7. Fractured elements at Vagnari were over twice as likely to be associated with outlying cross-sectional properties as the fractured elements at Ancaster. Direct force and higher energy fracture types were associated with elements that had outlying cross-sectional properties more often at Vagnari than at Ancaster. No indirect fractures were observed among Vagnari females, meaning that by default, the Ancaster females had higher rates of outlying cross-sectional properties associated with indirect fractures.

Table 8.7 – Site differences in the prevalence of elements with outlying cross-sectional properties by fracture force type and sex.[1]

Force Type	Males			Females			Total		
	AN *n/N* %	VA *n/N* %	Difference	AN *n/N* %	VA *n/N* %	Difference	AN *n/N* %	VA *n/N* %	Difference
Indirect Force	3/15 20.0	1/4 25.0	*OR=1.3, CI 0.1-17.8 p_{FET}=1.000*	6/18 33.3	0/0 -	-	9/33 27.3	1/4 25.0	OR=1.1 CI 0.1-12.3, p_{FET}=1.000
Direct Force & Higher Energy	2/16 12.5	1/3 33.3	*OR=3.5, CI 0.2-58.8 p_{FET}=.422*	3/4 75.0	1/1 100.0	p_{FET}=1.000	5/20 25.0	2/4 50.0	*OR=3.0, CI 0.3-27.2, p_{FET}=.552*
Unknown Force	1/3 33.3	1/1 100.0	*p_{FET}=1.000*	0/0 -	1/2 50.0	-	1/3 33.3	2/3 66.7	*OR=4.0, CI 0.1-119.2, p_{FET}=1.000*
Total	6/34 17.6	3/8 37.5	*OR=2.8, CI 0.5-15.0, p_{FET}=.336*	7/22 31.8	2/3 66.7	*OR=4.3, CI 0.3-55.6, p_{FET}=.530*	13/56 23.2	5/12 41.7	*OR=2.4, CI 0.6-8.7, p_{FET}=.278*

[1] Bold font indicates a significant difference. Italic font indicates that the prevalence of individuals with outlying cross-sectional properties was greater at Vagnari than at Ancaster. *n*=number of elements with an outlying cross-sectional property; *N*=number of elements with a fracture of the indicated force type; AN=Ancaster, VA=Vagnari; OR=odds ratio; CI=confidence interval.

Table 8.8 combines the Ancaster and Vagnari fracture counts in order to identify if differences in the frequency of outliers were affected by fracture force type. In the combined sample, the direct force and higher energy injuries experienced by females had eight times greater odds for outlying cross-sectional properties than indirect force fracture types, but this difference was not significant. These results show that there was, overall, no significant association between the force causing a fracture and the presence of outlying cross-sectional properties. However, females with higher energy fractures were more likely to have cross-sectional outliers; it remains unclear if these outliers developed before or after an injury.

Table 8.8 – Sex-related differences in the frequency of outlying cross-sectional properties associated with fractured elements at Ancaster and Vagnari combined.[1]

Force Types	Males *n/N* %	Females *n/N* %	Total *n/N* %
Indirect Force	4/19 21.1	6/18 33.3	10/37 27.0
Direct Force & Higher Energy	3/19 15.8	4/5 80.0	7/24 29.2
Difference	OR=1.4, CI 0.3-7.4, p_{FET}=1.000	*OR=8.0, CI 0.7-88.2,* *p_{FET}=.127*	*OR=1.1, CI 0.4 -3.5,* *$\chi^2_{Yates}(1, N=61)=0.00, p=1.000$*

[1] Bold font indicates a significant difference. Italic font indicates that the prevalence of individuals with outlying cross-sectional properties was greater for direct force than indirect force fracture types. *n*=number of outlying elements associated with a fractured element *N*=number of fractured elements of each force type; OR=odds ratio; CI=confidence interval.

8.3.2 Malunion

Table 8.9 reports the differences in the counts of malunited fractures between Ancaster and Vagnari by sex. Most fractured elements, at Ancaster and Vagnari combined, healed without malunion (i.e. *n*=51/70, 72.9%). The overall odds of malunited fractures were approximately equal at Ancaster and Vagnari, but sex differences in the odds of malunion were present between the sites, albeit not significantly. Ancaster males were almost three times as likely as Vagnari males to have malunion. Vagnari females were over twice as likely as Ancaster females to have fractures with malunion.

Table 8.9 –Differences in the number of fractured elements with malunion between Ancaster and Vagnari by sex.[1]

Sex	Ancaster *n/N* %	Vagnari *n/N* %	Site Difference
Male	11/34 32.4	1/8 12.5	OR=3.3, CI 0.4-30.7, p_{FET}=.402
Female	4/22 18.2	1/3 33.3	*OR=2.3, CI 0.2-31.3,* p_{FET}*=.504*
Unknown	0/1 0.0	2/2 100.0	-
Total	15/57 26.3	4/13 30.8	OR=1.2, CI 0.3-4.3, p_{FET}=1.000

[1] Bold font indicates a significant difference. Italic font indicates that the prevalence of individuals with outlying cross-sectional properties was greater at Vagnari than at Ancaster. *n*=number of fractured elements with malunion; *N*=number of fractured elements; OR=odds ratio; CI=confidence interval.

Table 8.10 presents the number of fractures with malunion by fracture type for each site and sex group. Direct force and higher energy fracture types, including spiral, transverse, and comminuted fractures, were most often malunited at Ancaster and Vagnari. Spiral fractures comprised the greatest proportion of malunited fracture types, representing 47.1% (*n*=8/17) of all the malunited fractures at Ancaster and Vagnari combined.

Table 8.10 – Prevalence of malunited fractures by site, type, and sex.[1]

Fracture Type	Ancaster *n/N* %			Vagnari *n/N* %		
	Male	Female	Total	Male	Female	Total
Indirect Force						
Oblique	1/6 16.7	1/5 20.0	2/11 18.2	0/2 0.0	0/0 -	0/2 0.0
Other Lower Energy Fracture Types	0/9 0.0	0/11 0.0	0/19 0.0	0/2 0.0	0/0 -	0/2 0.0
Sub-total	1/15 6.7	1/16 6.3	2/30 6.7	0/4 0.0	0/0 -	0/4 0.0
Direct Force & Higher Energy						
Spiral	6/8 75.0	2/3 66.7	8/11 72.7	0/1 0.0	0/0 -	0/1 0.0
Transverse	3/8 37.5	0/1 0.0	3/9 33.3	0/1 0.0	1/1 100.0	1/2 50.0
Comminuted	0/0 -	1/2 50.0	1/2 50.0	1/1 100.0	0/0 -	1/1 100.0
Sub-total	9/16 56.3	3/6 50.0	12/22 54.5	1/3 33.3	1/1 100.0	2/4 50.0
Unknown Force						
Unknown	1/3 33.3	0/0 -	1/3 33.3	0/1 0.0	0/2 0.0	0/3 0.0
All Force Types						
Total	11/34 32.4	4/22 18.2	15/55 27.3	1/8 12.5	1/3 33.3	2/10 20.0

[1] *n*=number of fractured elements with malunion; *N*=number of fractured elements.

Table 8.11 reports the difference in fractured elements with malunion that were associated with outlying cross-sectional properties between Ancaster and Vagnari. Vagnari had slightly greater odds that malunited fractures were associated with cross-sectional outliers than Ancaster. However, as this difference was not significant, these results suggest that fracture malunion does not necessarily predict the presence or development of outlying cross-sectional properties.

Table 8.11 – Difference in prevalence of fractured elements with malunion and cross-sectional outliers between Ancaster and Vagnari by sex.[1]

Sex	Ancaster *n/N* %	Vagnari *n/N* %	Difference Between Ancaster and Vagnari
Male	1/11 9.1	0/1 0.0	p_{FET}=1.000
Female	1/4 25.0	1/1 100.0	*p_{FET}=.400*
Unknown	0/0 -	0/2 0.0	-
Total	2/15 13.3	1/4 25.0	*OR=2.2, CI 0.1-32.6, p_{FET}=.530*

[1] Bold font indicates a significant difference. Italic font indicates that the prevalence of individuals with outlying cross-sectional properties was greater at Vagnari than at Ancaster. *n*=number of fractured elements with malunion and cross-sectional outliers; *N*=number of fractured elements with malunion; OR=odds ratio; CI=confidence interval.

8.3.3 Osteoarthritis

Table 8.12 presents the differences in rates of fractured elements associated with osteoarthritis by age. Fractured elements at Ancaster and Vagnari were mostly equally associated with osteoarthritis. However, the fractured elements of Vagnari middle adults had twice the odds of having osteoarthritis associated with a fracture than the middle adults at Ancaster. The old adults at Ancaster had more fractures associated with osteoarthritis than the old adults at Vagnari; the dearth of old adults with osteoarthritis at Vagnari may be explained, in part, by the small sample size.

Table 8.12 – Differences in prevalence rates of fractured elements with osteoarthritis between Ancaster and Vagnari by age.[1]

Age Category	Ancaster *n/N* %	Vagnari *n/N* %	Difference Between Ancaster and Vagnari
Adolescent	0/43 0.0	0/27 0.0	-
Young Adult	4/728 0.5	0/123 0.0	p_{FET}=1.000
Middle Adult	14/686 2.0	4/91 4.4	*OR=2.2, CI 0.7-6.9,* p_{FET}*=.149*
Old Adult	5/94 5.3	0/10 0.0	p_{FET}=1.000
Adult	0/145 0.0	1/6 16.7	**p_{FET}=.040**
Total	23/1696 1.4	5/257 1.9	*OR=1.4, CI 0.5-3.8,* p_{FET}*=.404*

[1] Bold font indicates a significant difference. Italic font indicates that the prevalence of individuals with outlying cross-sectional properties was greater at Vagnari than at Ancaster. *n*=number of fractured elements with osteoarthritis; *N*=number of joints observed; OR=odds ratio; CI=confidence interval.

The differences between the Ancaster and Vagnari rates of osteoarthritis and osteoarthritis associated with fractures are presented in Table 8.13. The rates of individuals with fractures and osteoarthritis, as well as individuals with fractures, osteoarthritis, and outlying cross-sectional properties did not differ between Ancaster and Vagnari. These findings suggest that the osteoarthritis associated with a fracture was not predictive of outlying cross-sectional properties.

Table 8.13 – Difference in number of fractured elements with osteoarthritis as well as cross-sectional outliers between Ancaster and Vagnari by sex.[1]

Variables Compared	Males			Females			Total		
	AN *n/N* %	VA *n/N* %	Difference	AN *n/N* %	VA *n/N* %	Difference	AN *n/N* %	VA *n/N* %	Difference
Fractures with osteoarthritis / Total fractures	13/34 38.2	4/8 50.0	*OR=1.6, CI 0.3-7.6,* p_{FET}*=.694*	9/22 40.9	1/3 33.3	OR=1.4, CI 0.1-17.7, p_{FET}=1.000	22/56 39.3	5/12 41.7	OR=1.1, CI 0.3-3.9, p_{FET}=1.000
Number of individuals with fractures, osteoarthritis, and outlying cross-sectional properties / Number of fractures with osteoarthritis	2/13 15.4	1/4 25.0	*OR=1.8, CI 0.1-27.8* p_{FET}*=1.000*	3/9 33.3	0/1 0.0	p_{FET}=1.000	5/23 21.7	1/5 20.0	OR=1.1, CI 0.1-12.3, p_{FET}=1.000

[1] Bold font indicates a significant difference. Italic font indicates that the prevalence of individuals with outlying cross-sectional properties was greater at Vagnari than at Ancaster. *n*=number of fractures with osteoarthritis/outlying cross-sectional properties; *N*=total number of fractures; OR=odds ratio; CI=confidence interval.

8.4 Biomechanical Differences

In order to compare the biomechanical properties of Ancaster and Vagnari, the effect of body size was controlled for by standardizing the areas using body mass estimates, calculated after Auerbach and Ruff (2004). Sex and age were controlled for in comparisons of Ancaster and Vagnari cross-sectional properties based on significant area and asymmetry differences at each site (see Sections 6.6 and 7.6). The normality of body mass corrected area distributions are reported in Appendix J.

8.4.1 Body Mass

Body mass was calculated using femoral head diameters. Average femoral head diameters and estimated body masses for each site and sex are reported in Table 8.14. Appendix B reports the femoral head diameters of each individual. When an individual did not have a femoral head that was sufficiently preserved for measurement, the appropriate average was used to correct the total and cortical areas by body mass.

Table 8.14 – Average body mass by site and sex[1]

	Ancaster			Vagnari		
Sex	Number of Femoral Heads Measured	Average Femoral Head Diameter	Average Body Mass	Number of Femoral Heads Measured	Average Femoral Head Diameter	Average Body Mass
Male	30	48.3 ± 2.0	69.7	14	46.6 ± 1.2	65.5
Female	36	42.2 ± 2.1	60.5	18	41.9 ± 3.0	59.9

[1] Body mass calculated using femoral head diameter.

8.4.2 Total Area

Table 8.15 reports the differences between the Ancaster and Vagnari mean total areas corrected by body size (T_A/BM) for each element and sex; age was controlled for in comparisons of female second metacarpal midshaft areas (MC2 50%) due to the presence of significant age-related differences at Ancaster (see Table 6.34). Figure 8.2 presents the T_A/BM data for each site and element type in a box plot. T_A/BM were routinely larger at Vagnari than at Ancaster. Female radii T_A/BM were significantly larger at Vagnari than at Ancaster; differences between male tibiae total areas were also large, but did not reach significance. The larger total areas at Vagnari can be explained by relatively more intense mechanical loading during subadulthood, as the subperiosteal margin is most affected by strain during growth and development (Ruff et al. 2006).

Table 8.15 – Difference between the average total areas at Ancaster and Vagnari corrected by body size (T_A/BM).[1]

Element	Male			Female			
	Ancaster	Vagnari	Difference		Ancaster	Vagnari	Difference
Humeri	4.4 ± 0.6	4.7 ± 0.9	U=420.5, p=.112		3.8 ± 0.4	3.8 ± 0.4	U=554.5, p=.948
MC2 50%	0.9 ± 0.1	0.8 ± 0.0	U=6.0, p=.410	YA:	0.8 ± 0.1	0.9 ± 0.1	U=17.0, p=.178
				MA/OA:	0.8 ± 0.1	0.8 ± 0.1	U=28.0, p=.805
Radii	2.2 ± 0.4	2.4 ± 0.3	U=277.0, p=.183		1.9 ± 0.2	2.2 ± 0.3	**U=201.0, p=.002**
Tibiae	7.1 ± 1.0	7.8 ± 1.5	U=446.5, p=.061		6.3 ± 0.8	6.3 ± 0.8	U=564.0, p=.944

[1] Groups compared using Mann-Whitney U tests. Bold values indicate a significant difference present between the tested groups. T_A=total area; BM=body mass; MC2 50%=measurement at the second metacarpal midshaft.

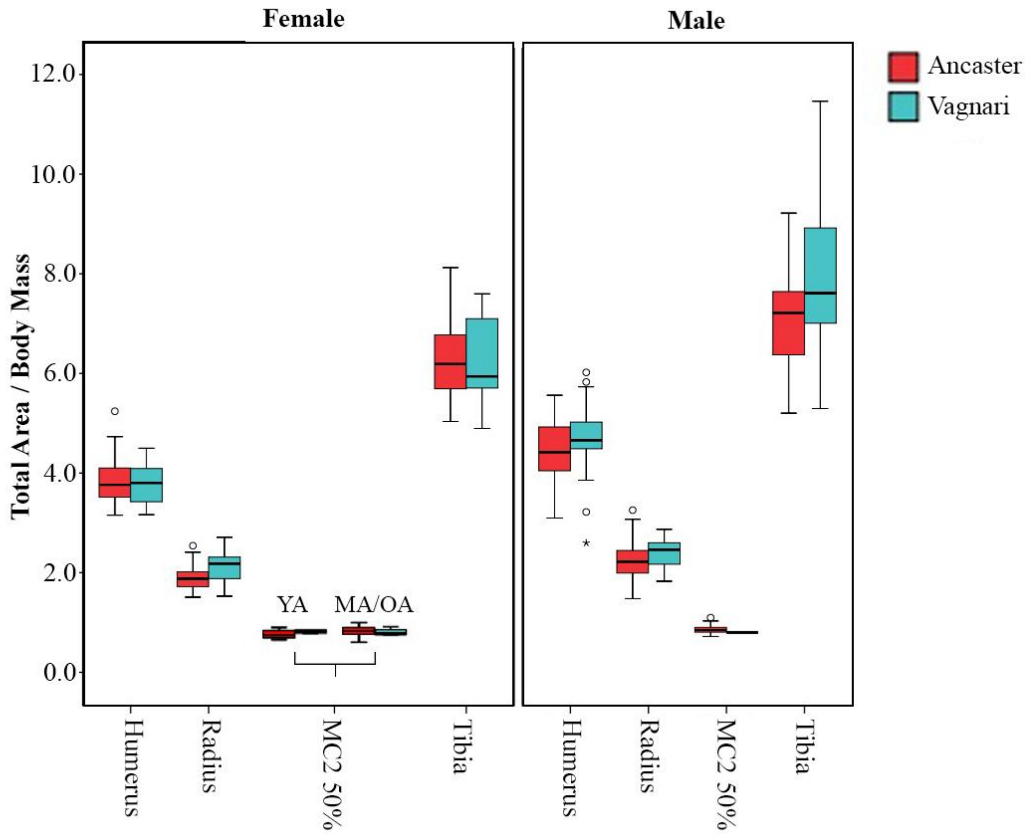

Figure 8.2 – Box plot of total area controlled by body size for each element and sex. ROI=region of interest; YA=young adult; MA=middle adult; OA=old adult; MC2=second metacarpal; MC2 50%=measurement taken at the second metacarpal midshaft; MT2=second metatarsal.

Comparative data were available for mean tibial areas from sites of various time periods in central Europe, and are presented in Table 8.16 after Macintosh et al. (2014). The female tibiae at both Ancaster and Vagnari were very similar in total area to those of all other time periods in central Europe, from the Neolithic to the medieval periods. The males at Ancaster had tibial total areas that were most similar in size to Bronze Age groups. However, the Vagnari males had tibial total areas that were larger than any of the time periods reported by Macintosh et al. (2014). The larger lower limb total areas among Vagnari males show that these individuals were experiencing relatively more strenuous levels of mechanical strain, likely related to physical mobility, than were present at other European sites.

Table 8.16 – Tibial total areas, corrected using estimated body mass, from Ancaster and Vagnari, compared to other central European time periods and activity levels.

Site/Time Period	Male	Female
Roman - Ancaster	7.1 ± 1.0	6.3 ± 0.8
Roman - Vagnari	7.8 ± 1.5	6.3 ± 0.8
Neolithic*	7.4 ± 0.8	6.4 ± 0.8
Bronze Age*	7.0 ± 0.9	6.2 ± 0.8
Iron Age*	6.7 ± 0.6	6.4 ± 0.8
Medieval*	6.5 ± 0.6	6.3 ± 0.9

*Data from Macintosh et al. (2014).

8.4.3 Cortical Area

Table 8.17 reports the mean cortical and region of interest areas controlled for body mass (C_A/BM) for each element type by sex and age; differences between Ancaster and Vagnari are reported in Table 8.18. The C_A/BM data are presented graphically in Figure 8.3. Due to significant differences in the amount of cortical bone present between some age cohorts (see Tables 6.21 and 7.19), age was controlled for in comparisons of female elements, as well as male ulnae and second metacarpal midshaft areas (MC2 50%). Vagnari males and young adult females tended to have larger cortical bone areas than the corresponding groups at Ancaster. In particular, the C_A/BM of male humeri at Vagnari were significantly larger than at Ancaster. When age was controlled for, young adult male ulnae cortical areas, as well as young adult female radii and second metatarsal cortical bone amounts, were also significantly larger at Vagnari than at Ancaster.

Table 8.17 – Average cortical and ROI areas at Ancaster and Vagnari corrected by body size.[1]

Element		Male		YA Female		MA/OA Female	
		Ancaster	Vagnari	Ancaster	Vagnari	Ancaster	Vagnari
Humeri		**3.2 ± 0.4**	**3.7 ± 0.8**	2.9 ± 0.4	2.9 ± 0.4	2.5 ± 0.4	2.3 ± 0.4
Radii		1.5 ± 0.2	1.4 ± 0.3	**1.3 ± 0.1**	**1.4 ± 0.2**	1.2 ± 0.2	1.1 ± 0.2
Ulna ROI	YA:	**3.6 ± 0.4**	**4.3 ± 0.6**	3.8 ± 0.5	3.9 ± 0.6	3.2 ± 0.8	2.6 ± 0.6
	MA/OA:	4.1 ± 0.8	3.8 ± 0.5				
MC2 50%	YA:	0.6 ± 0.0	0.9*	0.7 ± 0.0	0.7 ± 0.1	0.6 ± 0.1	0.6 ± 0.0
	MA/OA:	0.7 ± 0.1	0.7 ± 0.0				
MC2 ROI		1.2 ± 0.2	1.2 ± 0.1	1.4 ± 0.1	1.3 ± 0.1	1.0 ± 0.2	1.0 ± 0.2
Tibiae		5.8 ± 0.8	6.4 ± 1.3	4.9 ± 0.6	5.1 ± 0.8	4.9 ± 0.8	4.4 ± 0.4
MT2 ROI		1.5 ± 0.2	1.7 ± 0.4	**1.7 ± 0.1**	**1.8 ± 0.1**	1.3 ± 0.2	1.3*

[1] Bold values indicate the groups that were identified to be statistically different. YA=young adult, MA=middle adult; OA=old adult; ROI=region of interest; MC2 50%=midshaft second metacarpal; MT2=second metatarsal. *only one element available for observation.

Table 8.18 – Difference in cortical areas and ROIs, controlled for body size (C_A/BM), between Ancaster and Vagnari.[1]

Element		Male	YA Female	MA/OA Female
Humeri		**U=286.0, p=.002**	U=188.0, p=.579	U=58.0, p=.494
Radii		U=345.0, p=0.755	**U=99.0, p=.037**	U=24.0, p=.172
Ulnae	YA:	**U=18.0, p=.017**	U=161.0, p=.976	U=23.0, p=.128
	MA/OA:	U=65.0, p=.150		
MC2 50%	YA	-	U=24.0, p=.494	U=26.0, p=.680
	MA/OA:	U=6.0, p=.889		
MC2 ROI		U=24.0, p=.142	U=36.0, p=.407	U=56.0, p=.845
Tibiae		U=451.0, p=0.068	U=549.0, p=.807	
MT2 ROI		U=89.0, p=0.106	**U=21.0, p=.033**	U=10.0, p=.880

[1] Bold values indicate a significant difference was present. YA=young adult, MA=middle adult; OA=old adult; ROI=region of interest; MC2 50%=midshaft second metacarpal; MT2=second metatarsal; -=insufficient elements available for comparison.

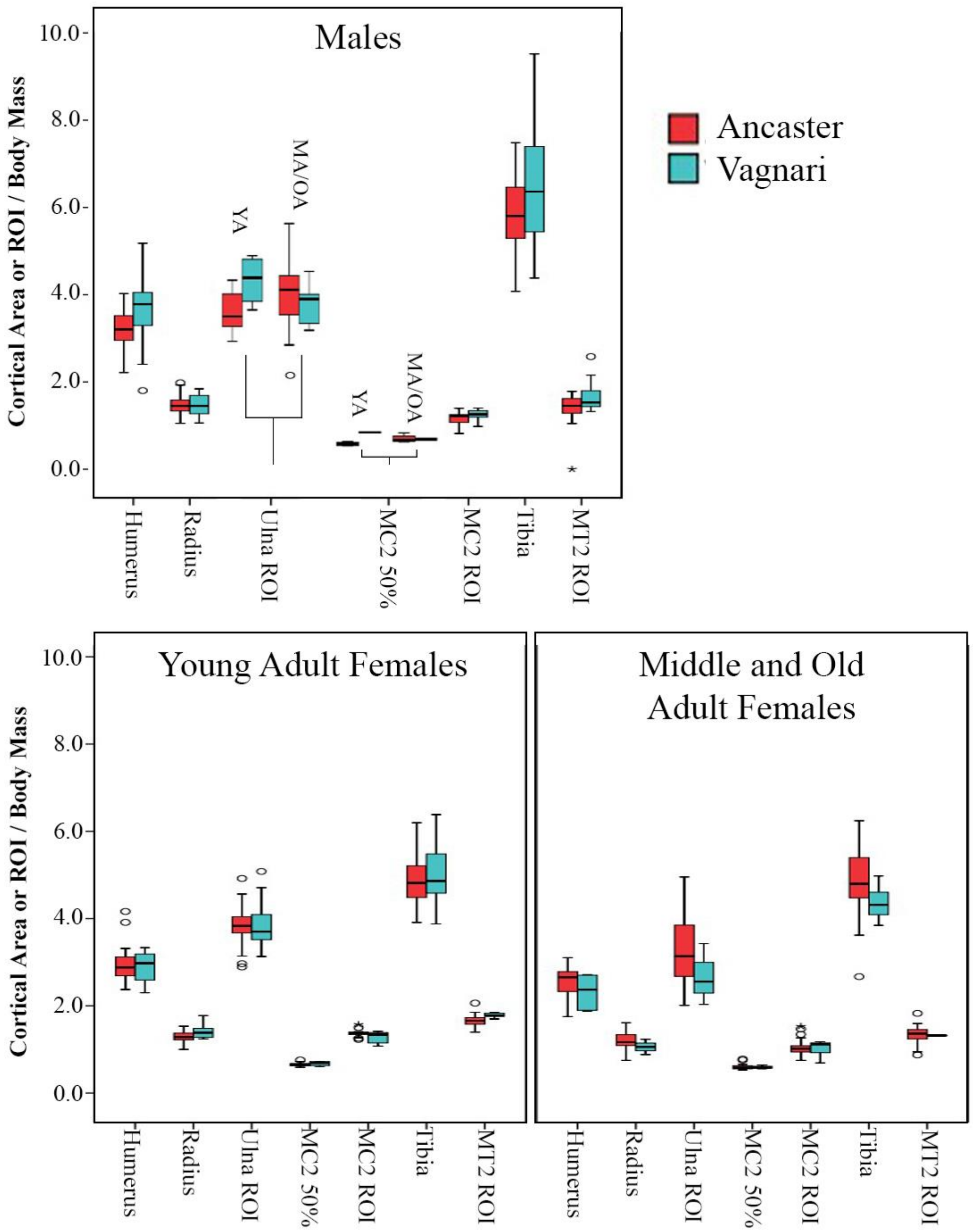

Figure 8.3 – Box plot of cortical area controlled by body size for each element, sex, and age division (when necessary). ROI=region of interest; YA=young adult; MA=middle adult; OA=old adult; MC2=second metacarpal; MC2 50%=measurement taken at the second metacarpal midshaft; MT2=second metatarsal.

8.4.4 Asymmetry

Differences in the amount of absolute asymmetry in each element between Ancaster and Vagnari are presented in Table 8.19. Figures 8.4 and 8.5 graphically present the differences in total and cortical area absolute asymmetry data between Ancaster and Vagnari. No significant differences in the amount of any element's asymmetry were present between Ancaster and Vagnari.

Table 8.19 – Differences between the Ancaster and Vagnari total and cortical area absolute asymmetries by element and limb type.[1]

	Total Area Asymmetry			Cortical Area and Region of Interest Asymmetry		
Element	Ancaster (%)	Vagnari (%)	Difference (%)	Ancaster (%)	Vagnari (%)	Difference (%)
Humerus	5.9 ± 3.8	9.3 ± 12.1	U=533.0, p=.749	6.4 ± 5.1	13.2 ± 16.1	U=433.0, p=.138
Radius	8.7 ± 6.3	11.7 ± 9.4	U=272.0, p=.955	8.2 ± 6.1	10.9 ± 9.0	U=273.0, p=.970
Ulna	-	-	-	12.6 ± 8.8	12.0 ± 13.2	U=268.0, p=.569
MC2 50%	5.1 ± 2.4	0.2*	U=8.0, p=.783	5.2 ± 3.9	0.0*	U=6.0, p=.609
MC2 ROI	-	-	-			U=75.0, p=.906
Tibia	6.1 ± 6.0	9.1 ± 8.0	U=554.0, p=.854	8.8 ± 7.9	10.2 ± 9.8	U=550.0, p=.819
MT2 ROI	-	-	-	8.2 ± 5.6	11.7 ± 5.5	U=57.0, p=.160

[1] Bold font indicates a significant difference between compared groups. T_A=total area; C_A=cortical area; ROI=region of interest; MC2 50%=second metacarpal midshaft measurement; MC2 ROI=second metacarpal region of interest; MT2 ROI=second metatarsal region of interest.
*only one element observed

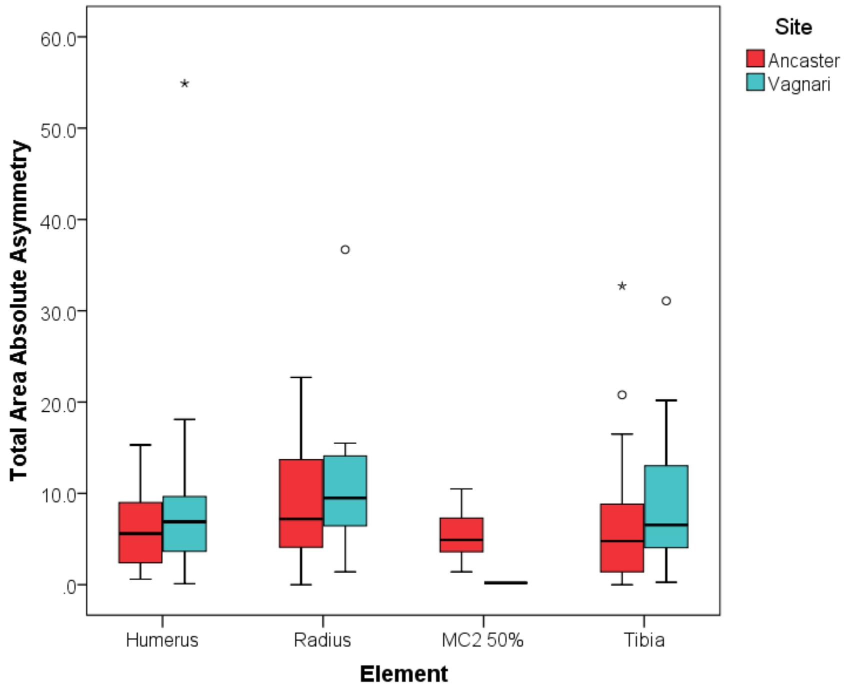

Figure 8.4 – Box plot of total area absolute asymmetry for each element at Ancaster and Vagnari.

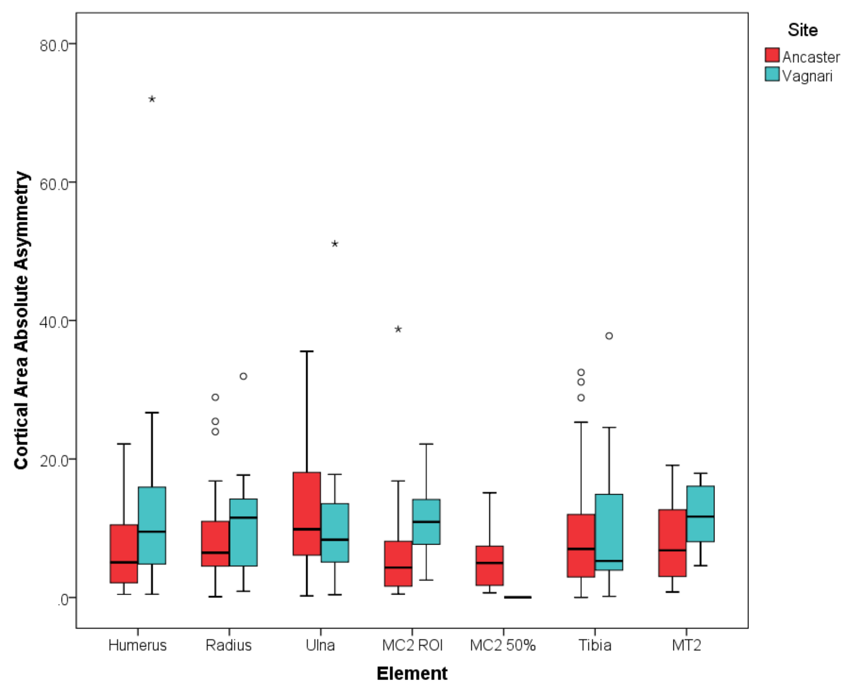

Figure 8.5 – Box plot of cortical area absolute asymmetry for each element at Ancaster and Vagnari.

8.5 Summary

Fractures were distributed differently by sex and age at Ancaster and Vagnari. At Ancaster, fractures were more prevalent among middle and old adult individuals than young adult individuals. The opposite was true at Vagnari where young adult individuals, particularly the males, had the most fractures.

At Ancaster and Vagnari, fractured elements were only associated with outlying cross-sectional properties approximately 40% of the time. When an individual did have both a fracture and an outlying cross-sectional property, the outlying element was most often in the upper limb. The highest rates of outlying cross-sectional properties in individuals with fractured elements were routinely observed among individuals from Vagnari.

The type of fracture force involved may be associated with biomechanical properties in some instances. Direct-force and higher energy injuries were more common at Vagnari than at Ancaster, especially among the young adults. Additionally, direct force or higher energy injuries to female elements were most associated with outlying cross-sectional properties. Direct force or higher-energy traumas were also most commonly associated with fracture malunion, but were not particularly linked with cross-sectional outliers. Osteoarthritis was slightly more common at Vagnari than at Ancaster, but Vagnari males with fractures and osteoarthritis only had slightly greater odds of exhibiting outlying cross-sectional properties.

Finally, bones at Vagnari were typically larger than the elements at Ancaster. Vagnari females had larger radial total areas, and Vagnari males tended to have larger tibial total areas. Cortical areas were larger among the humeri of Vagnari males. In elements where age was controlled for, cortical areas of young adult male ulnae, as well as the radii and second metatarsals of females, were larger at Vagnari than at Ancaster. No differences in the amount of asymmetry present were identified between the two sites.

Chapter IX – DISCUSSION

This chapter unites limb bone biomechanical and fracture data with clinical information, as well as contextual information from historical and archaeological sources in order to describe the nature of physical strains, activities, hazards, and injury repercussions at Ancaster and Vagnari. Patterns in the distribution of fracture types, forces, healing, and complications, are viewed alongside the biomechanical patterns in bone strength and robusticity. When used in combination, these attributes help to deduce the nature of physical strain and discuss the factors that influenced poor functional outcomes after fractures in these Roman communities.

Using clinical knowledge of biomechanical injury responses, the first part of this chapter explores the positional relationships between fractured bones and outlying elements. The location of biomechanical changes relative to a fractured bone provides insight into post-traumatic physical function as certain patterns are associated with particular loading behaviours. For the purposes of this discussion, the locational patterns of outlying elements relative to fractured bones were categorized by their positional relationship in four ways:

1) Outlying element in the same limb type and the same side as a fracture
    a) Smaller outlier
    b) Larger outlier
2) Outlying element in the same limb type, but the opposite side to a fracture
    a) Smaller outlier
    b) Larger outlier
3) Outlying upper extremity element associated with a leg bone fracture
4) Outlying lower extremity element associated with an arm bone fracture

Outliers are discussed in terms of the relative size of their areas, including cortical, total, and region of interest areas (C_A, T_A, ROI), as well as the asymmetries in areas (C_A%DA, T_A%DA, ROI%DA) that were present between the right and left sides. Areas are indicative of the amount of bone present, whereas asymmetries help identify side differences and preferences in habitual loading; both data types were used to identify biomechanical evidence for loading environments. The combination of outlying areas that had a clear side bias helped to identify individuals who were loading, and therefore using, their limbs differently.

Through examination of these patterns, this section discusses the relevance of each positional relationship to functional loss and/or adaptation after injury. The disuse of a limb results in mechanical unloading and may produce smaller bone areas and greater limb asymmetry (Pattern 1a); this concept and possible evidence at Ancaster and Vagnari are discussed in Sections 9.1.1 and 9.1.2. Alternatively, strategies to adapt or compensate for fractures may result in increased loading to limbs, producing identifiably larger (and also perhaps asymmetric) bone areas (Patterns 2b and 3, discussed in Section 9.1.3). Not all biomechanical patterns are easily associated with function after fracture, Section 9.1.4 addresses Patterns 1b, 2a, and 4, which are not easily explained by functional repercussions of fracture.

Relationships were observed between the fracture attributes, their functional consequences, age, and biomechanical evidence for habitual loading. Young adult individuals displayed evidence for functional adaptations to injuries, while disuse of a fractured limb was only present among old adults. Fracture attributes, such as location, type, degree of malunion, and secondary consequences (e.g., osteoarthritis) did not predict poor functional responses. Furthermore, evidence for habitual loading behaviour was indicative of the degree of physical activity common to each site, providing further insight into the hazards, causes, consequences, and response to injuries throughout life at Ancaster and Vagnari. These key findings are discussed and explored in this chapter in order to provide insight into the long-term functional implications of fractures, and injury recovery in the past.

9.1 Long-Term Consequences of Fractures

When limbs are loaded differently after a fracture, the bone thickness and shape changes, and thus provides evidence for post-traumatic, functional consequences.

Functional consequences after a fracture may take the form of limb disuse, but may also include strategies and techniques to adapt and compensate for the injury. These functional responses involve different mechanical loading environments that should be identifiable through cross-sectional analyses.

At Ancaster and Vagnari, biomechanical evidence for altered mechanical loading environments that could be attributed to fractures were relatively rare. Individuals with fractures were not any more likely than individuals without fractures to have outlying bone areas or asymmetries; 39.2% (*n*=20/51) of individuals with fractures also had elements with outlying cross-sectional properties. Post-traumatic impacts to function and loading environments may account for some of the outlying bone properties among individuals with fractures, but the presence of outliers among individuals without fractures demonstrates that outlying bone properties can also be caused in other, very different, ways. Outlying bone properties of individuals without fractures provide evidence for biomechanical changes that were likely caused by habitual loading behaviours that were not routine for most community members. For example, these outlying biomechanical attributes may be related to increased lateralization from habitual activity, or possibly by pathological conditions that were not skeletally evident or were beyond the scope of this research. With respect to these other possible causes of outlying biomechanical properties, and through careful consideration of the biomechanical patterns present in relation to a fractured element, the individuals who exhibit the most probable evidence for post-traumatic functional consequences can be identified.

9.1.1 Unloading of the Fractured Limb after Injury

Diminished limb function, such as caused by immobilization of a fracture during healing, should result in a unilaterally smaller limb on the same side as the fracture. This hypothesis was derived based on the relationship between injury, immobilization, disuse, and unloading; once the limb is immobilized or not used, mechanical loading stimuli are reduced (Schlecht et al. 2012). Over time, a reduction in mechanical loading will result in the atrophy of the muscle and bone tissues in the unloaded limb (Christensen et al. 2008;

van der Poest Clement et al. 1999). Accordingly, bones of the fractured limb that were less robust than normal, and also had outlying cross-sectional areas and asymmetries compared to the contralateral limb, provided the most convincing evidence for unloading or diminished-loading consequent to fracture. The presence of asymmetry and smaller cortical areas on the same side as the fractured limb indicate that loading forces were acting unevenly on the right and left limbs.

Fifty-one individuals at Ancaster (*n*=39) and Vagnari (*n*=12) had fractures; five of which had smaller outlying cross-sectional properties on the same side as a fracture (Table 9.1). In order to identify the presence of disuse, both smaller than normal areas, combined with larger than normal asymmetries were necessary. Of these five outliers, two Ancaster individuals (AN-098 and AN-191) had cortical bone areas and asymmetries that suggested disuse after injury. Individual AN-191 had outlying cortical bone area and greater than normal amounts of asymmetry in the second metacarpal. The ulnae of AN-098 had outlying cortical areas; although the amount of asymmetry exhibited in the ulnae of AN-098 was not outlying, a very large amount of asymmetry was present (i.e., 34.1% difference between the right and left sides).

Table 9.1 – Ancaster and Vagnari individuals with fractured limbs that had smaller outlying elements on the same side and limb type as a fracture.[1]

Skeleton Number	Sex	Age	Fracture	Smaller on the fractured side	Consequent to Fracture?
AN-098	M	OA	Right Clavicle & Left Tibia	Ulna ROI	Possible
AN-191	F	OA	Right Radius & Ulna	MC2 50% C_A & C_A%D_A	Possible
AN-061	M	MA	Left Clavicle	Humerus C_A%DA	Unlikely
AN-218	F	YA	Left Tibia & Fibula	MT2 ROI	Unlikely
VA-F204	F	YA	Left Humerus	Humerus T_A	Unlikely

[1] F=female; M=male; MA=middle adult; OA=old adult; T_A=total area; C_A=cortical area; MC2 50%=measurement taken at the second metacarpal midshaft; MT2=second metatarsal; ROI=region of interest; C_A%DA=cortical area asymmetry.

The outlying cross-sectional properties of the remaining three individuals (AN-061, 218, and VA-F204) do not likely represent post-traumatic disuse. In particular, the cross-sectional properties of VA-F204 emphasize the importance of considering both the size of the bone (in this case, the total area), as well as the asymmetric differences indicative of differential loading, when interpreting post-traumatic unloading. VA-F204 had outlying total areas on the same side as the fracture, but very low amounts of asymmetry, meaning that while the total area of only one side was officially an outlier, both the right and left sides of the bone actually had quite small total areas. Due to the low amount of asymmetry present in this case, the small total area better reflects VA-F204's relatively pronounced gracility, rather than a unilateral response to injury. AN-218 and AN-061 were also removed from further consideration for similar reasons, that is, they had either outlying areas or asymmetries, but not both. The relationships between the biomechanical properties and the fractures of these three individuals were not convincingly indicative of unilateral unloading of the fractured limb, and are listed as 'unlikely' in Table 9.1.

Although a variety of fracture types and locations can have functional consequences in clinical settings, evidence for disuse at Ancaster and Vagnari was only associated with a fractured clavicle (AN-098) and a paired radius and ulna (AN-191). These fractured elements and locations may be difficult to stabilize conservatively, and can sometimes demonstrate dysfunction (e.g., Gabl and Arora 2014; Ledger et al. 2005). Clavicle fractures that heal with shortening (usually greater than 15mm) can decrease the shoulder girdle's mechanical efficiency, increasing the risk for poor functional outcomes (Chan et al. 1999a; Ledger et al. 2005). Distal radial fractures, such as that of AN-191, are one of the most common fracture types and especially prevalent among older females (Sigurdardottir 2014). Orthopaedic guidelines for the acceptable reduction of distal radial fractures exist, but Gabl and Arora (2014) report that morphological and radiographic parameters do not always correlate with functional outcome. In other words, some fractures that heal in a clinically acceptable way may still result in poor functional outcomes, and some unacceptable fracture reductions may nevertheless yield satisfactory functional results.

In addition to the unpredictable relationship between fracture outcome and fracture morphological parameters, functional outcomes of fractures are scored differently among clinical studies. Some studies, such as Batra and Gupta's (2002) work on radial fractures, consider pain, mobility, and grip strength as evidence for an individual's functional capabilities. Other studies of lower limb fracture outcomes evaluated gait, and posed questions about pain, function, sport performance, and quality of life (e.g., Segal et al. 2014). Psychological well-being was even included in the fracture outcome scores of Ponsford et al. (2008). Despite the disagreements in outcome assessment protocols, a "poor" functional outcome typically means that an individual is dissatisfied with their recovery. However, it is important to note that in most scales, individuals with poor outcomes are usually not totally immobile, and can still perform various loading activities with their injured extremity.

Some bioarchaeological studies have worked to traverse the gap between skeletal changes and functional consequences by using clinical samples to develop criteria applicable to archaeological skeletons. For example, a study by Young and Lemaire (2012), uses clinical samples to link osteoarthritic bone changes with functional experiences in order to evaluate the experience of osteoarthritis in the past. Aside from Roberts' (1988a) study on fracture malunion and unsuccessful healing, the clinical links between bone morphology and post-traumatic functional consequences have not been thoroughly investigated in the anthropological literature. However, as dysfunction after injury is undoubtedly influenced by a number of social and cultural, as well personal factors that affect an individual's perception of pain and attitude toward injury (Edwards et al. 2001; Vlaeyen and Linton 2012), injury responses can be expected to vary within and between groups. This, combined with the inconsistencies in how clinicians evaluate the physical repercussions of an injury, and the apparent disparities in the relationship between morphological and radiological parameters and long-term injury experiences, suggest that modern understandings of functional outcomes after trauma should not necessarily be applied to people and function in the past. Instead, biological anthropologists should strive to identify and evaluate the functional repercussions of injuries within their own temporal and cultural contexts.

Although fracture types and locations alone cannot predict disuse, a few bioarchaeological case studies develop their arguments for functional consequences of fractures based on a range of skeletal evidence (e.g., Holt et al. 2002; Knüsel and Goeggel 1993; Lovell 2016). The presence of relatively few bioarchaeological case studies concerning the functional consequences of trauma suggests that long-term dysfunction after a fracture is either not being recognised in archaeological collections, or that it is relatively rare. The evidence in this thesis suggests that both may be true. Of the case studies that discuss the functional consequences of trauma, only Holt et al. (2002) use biomechanical methods that evaluate the endosteal bone margin to determine the amount of cortical bone present. In adults, bone changes predominantly occur on the endosteal bone surface, meaning that it is not possible to identify bone atrophy or hypertrophy based on a bone's appearance. Consequently, it is feasible that instances of disuse-related bone loss are missed in palaeopathological assessments, and could explain why fracture functional consequences are not discussed more regularly in studies of trauma. However, the overall scarcity of long-term disuse identified at Ancaster and Vagnari also supports the argument that long-standing immobility and impairment was probably not a common response to a fracture, at least at the Roman sites investigated in this thesis.

The evidence in this thesis shows how integrated palaeopathological and biomechanical methods have great potential to inform fracture studies. In particular, neither of the Ancaster fractures with disuse stood out upon initial examination, that is, the fractures did not look 'severe' nor were there obvious signs of atrophy. For this reason alone, it is important that palaeopathologists concerned with fracture consequences apply biomechanical methods. An integrated analysis of this nature systematically considers how all individuals with fractures may have experienced functional repercussions, not just those with the most obvious, or severe looking, skeletal evidence. Additionally, the use of biomechanical methods allow arguments for long-term fracture consequences to be based directly on evidence for mechanical loading, rather than only relying on skeletal markers, such as hypertrophied muscle attachments, to infer altered function.

The fact that the only evidence for dysfunction was identified at Ancaster, and none at Vagnari, suggests that differences in the physical, social, and individual behaviours of these two communities may have influenced how individuals recovered from injury. The absence of disuse at Vagnari may be explained by these individuals resuming function sooner after an injury than at Ancaster. Clinically, an early return to function after injury is seen as beneficial to the recovery of function after a fracture. Modern orthopaedic research recommends that individuals with most extremity fractures return to function after the fracture is stabilized (Millet and Rushton 1995; Nash et al. 2004). Resuming physical activity helps to decrease the pain, stiffness, swelling, and discomfort, and increase an individual's range of motion, thus reducing recovery time and the risk of unsatisfactory outcomes (Nash et al. 2004). In the case of conservatively treated fractures, there is a fine line between allowing the fracture sufficient time to heal and resuming physical activities too early. Premature introduction of physical activity can cause excessive movement at an insufficiently healed fracture site. This can result in failed reduction in the fractures that received treatment, as well as the development of complications such as mal- and non-union (McKee 2000). Palaeopathological evidence for fracture treatment is discussed by Grauer and Roberts (1996), however studies of this nature do not integrate biomechanical assessments of disuse. The results of this thesis are the first to suggest the combination of these techniques to inform approaches to recovery and activity after an injury, which are discussed further in Section 9.2.

9.1.2 Positional Patterns in Disuse

The skeletal location and association between an element with an outlying cross-sectional property and a fractured bone is important in interpreting disuse after injury. In all three instances at Ancaster, smaller bones were located distal to the fracture site, and every example of post-traumatic dysfunction was related to fractured arm bones. Bones distal to the fracture site may be affected due, in part, to damaged nerves that impede stimuli transmission from beyond the point of severance or compression (Campbell 2008). However, hand preference, in the form of use avoidance, could also help explain the evidence for decreased loading strains to fractured arms and bones distal to the fracture. Unlike ambulation that usually applies relatively symmetrical forces to the leg bones, an individual with a fractured arm may have been able to choose to engage in, or avoid certain upper-limb activities. In a study of handedness after fracture, Walsh et al. (1993) found that after an arm injury, individuals adopted different patterns in dominant hand use, depending on if fine motor skills were required. For example, with increasing injury severity, in which nerves and soft tissues were affected, patients were more likely to use a different hand (Walsh et al. 1993).

The ease of using the non-injured arm over the fractured arm for at least some tasks may have contributed to asymmetries in mechanical loading at Ancaster and Vagnari. Upper limb asymmetries can be associated with lateralized strains (Ruff 2005), but Danforth and Thompson (2008) and Ubelaker and Zarenko (2012) caution that upper limb skeletal measurements are insufficiently related to handedness in modern populations. Although handedness may not be reliably identifiable, Trinkaus et al. (1994) found that individuals who regularly participated in pronounced lateralized activity with their upper limb had larger cortical area asymmetries than individuals who only did moderate activity. According to Trinkaus et al. (1994), people who engaged in highly lateralized activity had 28 to 57% difference between their left and right sides, compared to individuals of moderate levels of activity who had asymmetries that ranged between five and 14%. The 'normal' upper extremity cortical area asymmetries at Ancaster and Vagnari were well within the range of individuals doing moderate lateralized activity defined by Trinkaus et al. (1994) (see Section 8.4.3). As such, the outliers identified in this research can be confidently identified as individuals who experienced higher or lower than normal amounts of lateralized loading.

Differentiating between upper limb asymmetry caused by increased activity and disuse consequent to trauma may be difficult in some individuals and contexts. This is why this study used evidence for both asymmetry as well as smaller than normal bone area(s) (T_A, C_A, or ROI) in order to interpret disuse after injury. Pronounced asymmetry provided evidence for unequal loading patterns. Smaller than normal bone areas were also required to identify disuse as without clear evidence for relatively less loading, it was difficult to infer that the inequality in loading (asymmetry) was caused by disuse rather than habitual and exaggerated unilateral activity.

The observations at Ancaster conform to the expectation that bones distal to the fracture site will exhibit the greatest evidence for dysfunction (i.e., smaller, outlying bone areas, in this case). Although it is not possible to know how these Ancaster individuals felt about their injuries, it is possible that after a fracture, some may have avoided using their injured arm, or simply found it easier to use their uninjured arm. While lateralized behaviours do play a role in the amount and directionality of asymmetry, the fractured elements of both Ancaster individuals with probable post-traumatic disuse had levels of cortical area asymmetry in excess of the 'normal' 14% suggested by Trinkaus et al. (1994). Specifically, the left ulna of AN-098 was 34.1% smaller than the right, and the left second metacarpal midshaft of AN-191 was 16.3% smaller than the right (see also Table 6.36).

The lower limb typically exhibits lower amounts of asymmetry than the upper limb; however, leg asymmetry is possible in individuals who use their feet or legs unequally in activities (e.g., kicking) (Auerbach and Ruff 2006). Individuals with leg injuries, especially injuries that prevented an individual from using their legs (e.g., paralysis or palsy), would be expected to also exhibit asymmetry of the lower limbs. The absence of large amounts of asymmetry and outlying bone areas among the fractured leg bones at Ancaster and Vagnari may be explained by the fact that, if an individual were physically able, they would have continued to be ambulatory. This may have been especially true at Vagnari, where life and work on the Imperial estate may have required individuals to return to activity in order to earn a wage or subsistence. Regardless of the reason for returning to activity, maintenance of mobility among the injured individuals at Ancaster and Vagnari likely accounts for the absence of evidence for disuse of lower extremity bones at these sites.

9.1.3 Injury Adaptation

An individual's response to a fracture does not always involve disuse of the injured limb; it is also possible that an individual continues to move and function, albeit in an altered or adaptive manner. Some individuals will adopt altered movements in order to alleviate pain or discomfort related to the injury (Lomond and Côté 2011). These adapted movements may take the form of external mobility aids, such as canes and crutches, or may simply be an individual readjusting their own movements to make them more comfortable. A mobility aid, such as a crutch, may be used after a fractured leg to propel the body in locomotion with the arms. The use of this type of mobility aid can place additional strain on the arms, particularly in the carpal tunnel region of the forearms and wrists (Rogers et al. 2016), thereby encouraging the development of larger arm bone(s) in response to the increased mechanical loading. Alternatively, the body may be held in a different position to facilitate movement or compensate for a loss of or altered physical function (Lomond and Côté 2011). In these instances, bones or parts of bones that are compensating for a loss of function may change in size or shape as a result of altered mechanical loading environments.

9.1.3.1 Ambulatory Aids

Archaeological evidence for the use of assistive, external mobility aids has been documented in recent years, and mostly involves evidence for prosthetic use in the past (e.g., Binder et al. 2016; Li et al. 2013; Thurston 2007). Crutch use has also been interpreted in Roman, and other archaeological contexts, based on skeletal evidence such as scapular stress fractures, accentuated upper limb muscle attachments, joint degeneration, and bone hypertrophy (Belcastro and Mariotti 2000; Darton 2010; Knüsel and Goeggel 1993). Iconographic evidence for crutch use during the Greco-Romano period is also available; for example, the Borgia Stele (*No. 6556*), housed at the Naples National Archaeological Museum, is a 5th century BC funerary relief that depicts a man using a crutch (Monaco 1890). The use of crutches as mobility aids is also mentioned by Hippocrates (*Art*. 52) in his descriptions of how patients may adapt to dislocations and fractures. Hippocrates (*Art*. 52) provides some suggestions for the side on which a crutch should be carried, but it is made clear that the crutch can sometimes be used on the same side as the fractured leg, sometimes on the opposite side, and sometimes on both sides, depending on the individual and the injury. Due to the lack of consistency in the side that a crutch is used on, it is not possible to predict which (or both) upper limb(s) may be enlarged relative to a fractured lower limb.

The use of assistive strategies and mobility aids is an important part of understanding individual experiences of injury and can provide insight into how people of the past adjusted to their altered bodies. Modern studies have been undertaken on the effect of crutch use in order to optimize the design and limit the detrimental impacts of ambulatory aids (e.g., Segura and Piazza 2007; Westerhoff et al. 2012). The use of a crutch increases the mechanical loading forces on the shoulder(s) and arm(s), and would theoretically result in the enlargement of the cortical bone in the crutch-arm(s). However, aside from descriptions of the detrimental effects of loading, such as the development of crutch palsy, carpal tunnel syndrome, and joint pain (Rogers et al. 2016), the extent of cross-sectional skeletal changes from crutch use remain unclear. It can be deduced, based on an understanding of biomechanical principles of loading and bone adaptation, that the degree of cross-sectional changes associated with crutch use will vary depending on the intensity of use, force applied (e.g., weight), and the length of time that the ambulatory device is used for. That is, individuals that habitually use crutches for a long period of time should exhibit greater skeletal changes (i.e., larger cortical bone areas in the arms) than individuals who only use the ambulatory aid temporarily.

In this research, four Ancaster individuals and two Vagnari individuals with leg fractures also had enlarged or asymmetric upper limb elements that indicate increased, or unbalanced, loading forces on the upper limb (Table 9.2). Of these six individuals, only two (AN-013 and 046) exhibited evidence for accentuated asymmetry in the upper limb; that is, the application of different loading forces to the right and left arms. The remaining four individuals only had larger than normal total or cortical areas. Asymmetry could not be recorded in individuals VA-F042A and F216, so unilateral loading of the upper arms could not be assessed. Minimal asymmetry was identified in the radii of AN-001, suggesting that this individual was simply more robust than normal. Finally, the outlying total areas of AN-113's humerus are not likely related to the femoral fracture as total areas are shaped most greatly during childhood loading, while the femoral fracture is likely linked with bone fragility and perhaps with advancing age. As such, the humeral properties of AN-113 were likely to have been shaped much before the occurrence of the femoral fracture, and therefore are probably not related.

Table 9.2 – Ancaster and Vagnari individuals with larger, outlying arm bone element(s) associated with a leg fracture.[1]

Skeleton Number	Sex	Age	Fracture	Outlying Element and Side	Use of arms in mobility?
AN-001	F	YA	Right Tibia	Larger right & left radii (C_A)	Unlikely
AN-013	M	YA	Left Fibula	Larger left MC2 50% (C_A, $C_A\%D_A$ & $T_A\%D_A$)	Possible
AN-046	M	YA	Left Tibia	Larger right humerus ($C_A\%D_A$)	Possible
AN-113	F	MA	Left Femur	Larger left humerus (T_A)	Unlikely
VA-F042A	M	YA	Left Tibia	Larger right MC2 50% (T_A)	Unknown
VA-F216	M	MA	Right Fibula	Larger right MC2 ROI (C_A)	Unknown

[1] F=female; M=male; YA=young adult; MA=middle adult; T_A=total area; C_A=cortical area; MC2 50%=measurements taken at the second metacarpal midshaft; MC2 ROI=measurements of the second metacarpal taken within a region of interest; $T_A\%D_A$=total area directional asymmetry, $C_A\%D_A$=cortical area directional asymmetry.

Outlying, upper extremity cross-sectional properties were common among the Ancaster and Vagnari individuals without fractures; a total of 26 individuals (20 at Ancaster and six at Vagnari) had upper limbs with at least one outlying cross-sectional property. In most cases, it is more likely that the upper extremity outliers of individuals with leg fractures usually reflect accentuated and/or unilateral activities than they do adaptations to ambulation strategies. The enlarged upper limbs of four individuals, AN-001, 113, VA-F042A, and F216, likely fall into this category.

The evidence for both upper limb cortical bone enlargement and asymmetries identified in Ancaster individuals AN-013 and 046 provided the only evidence that may be consistent with the use of a mobility aid associated with a leg fracture. Comparatively few individuals without fractures have both outlying cortical area and asymmetry amounts in the upper limb; none of the Ancaster individuals, and only one of the Vagnari individuals without fractures (VA-F294), had larger than normal cortical areas associated with greater than normal levels of asymmetry in the upper limb. While it is possible that these Roman individuals at Ancaster and Vagnari may have had access to, and used, a mobility aid, without additional skeletal or contextual evidence, it is not possible to know for certain. This research cannot suggest the use of assistive aids, such as crutches, based solely on the biomechanical data (i.e., additional data on scapular injuries and muscle attachments would be beneficial). However, thorough biomechanical investigations would complement the other palaeopathological, historical, and archaeological methods for exploring the use of assistive techniques in the past.

9.1.3.2 Compensatory and Adaptive Movement

In addition to the use of external aids for mobility, it is also possible that individuals in the past simply continued moving through the use of physical coping strategies. This type of adaptation is exemplified in some biological archaeological case studies (e.g., Holt et al. 2002, Neri and Lancellotti 2004), including a recent Roman case study by Lovell (2016). In Lovell's (2016) example, she reports an older individual with a healed hip fracture and a shortened leg length with degeneration of the lower limb joints and pathological changes to the foot bones ipsilateral to the fracture (Lovell 2016). These changes, and the lack of other skeletal evidence for crutch use, led Lovell (2016) to suggest that the individual maintained mobility by walking on tiptoe. Lovell's (2016) example provides a temporally relevant, archaeological example of alternative ways that a Roman individual may have responded to changes in body morphology and physiology.

Compensatory and avoidance behaviours are discussed in the clinical literature and can be adopted as a response to injury or fracture. These techniques may be maladaptive in the long term, and allow individuals to develop functional habits that lead to disuse and asymmetry, as well as mechanical limitations and impairments (Lomond and Côté 2011; Vlaeyen et al. 1995). Individuals often initially adopt avoidance behaviours for protective purposes, allowing an injury to heal and preventing re-injury (Vlaeyen et al. 1995). Over time, individuals may avoid physical activity due to fear of re-injury. Although the research by Vlaeyen et al. (1995) refers to complete avoidance of activities, compensatory behaviours that maintain function, but place greater reliance on alternate structures can yield similar detrimental results (e.g., Doherty et al. 2015). Physio- and occupational therapists now work to restore and optimize mobility and prevent maladaptive compensatory strategies in order to help an injured individual return to their original functional capacity (Higgs et al. 2001). This would not have been the case in past societies; in these contexts, the use of compensatory tactics may have helped to preserve or restore at least some degree of acceptable function.

It is possible that some of the outlying elements associated with a fracture at Ancaster and Vagnari represent an individual's attempt to physically compensate for their altered morphology. As individuals can adapt to their altered bodies in diverse ways, a variety of biomechanical changes associated with functional adaptation are possible. This can make it difficult to distinguish between morphological changes that occur as a result of injury adaptation and those that may occur due to other lateralized behaviours or as a result of a pathological condition that does not manifest skeletally. Individuals with larger and asymmetric bones in the same limb type, but contralateral to a fracture, may most convincingly represent an individual's preferential use of the uninjured limb.

No individuals at either Ancaster or Vagnari had larger contralateral limb bones associated with higher amounts of asymmetry, so none represented convincing cases of functional compensation. Despite the absence of extreme evidence for compensation or adaptation at Ancaster and Vagnari, this research nevertheless complements the findings of authors such as Lovell (2016), Neri and Lancellotti (2004), and Holt et al. (2002). As like the individuals in these case studies, the individuals at Ancaster and Vagnari also provide evidence for individuals who persevered after injury, and returned to biomechanically normal physical function.

9.1.4 Other Patterns of Bone Changes Associated with Fractured Elements

Nine Ancaster and Vagnari individuals with fractured limbs exhibited bone areas and asymmetries that could not be readily explained by functional consequences associated with an extremity fracture. These anomalies included fractured limbs that had *larger* cross-sectional areas than the opposing, non-fractured limbs, and individuals with fractured arms but outlying lower extremity bones. Possible explanations for some of these anomalies are discussed below, but in general, these patterns do not appear to be directly related to post-traumatic dysfunction.

Five individuals (AN-024, 104, 241, VA-F249, F288) had larger elements on the same side and limb as a fracture, but that did not involve the fractured element itself. Eighty percent of these individuals (n=4/5) had a left sided, upper extremity that was larger than the right. It is unlikely that all these larger, left-sided, fractured limbs are a consequence of laterality because the left limb was only dominant in one fourth of the upper limb elements belonging to individuals without fractures at Ancaster and Vagnari. As habitual unilateral activity cannot account for such a large proportion of larger left limbs among individuals with fractures, an alternative explanation is that the altered skeletal morphology of a healed fracture changed how mechanical forces were applied to the bones. Although some fractured limbs were larger than non-fractured limbs, this indicates the presence of accentuated, rather than impaired activity, and therefore probably does not indicate the presence of a detrimental functional consequence related to the fracture.

Finally, four Ancaster individuals (AN-172, 177, 185A, 241) had outlying lower extremity elements that were paired with upper limb fractures. Injuries to the upper limb alone should not affect an individual’s ambulation. However it is possible that the individuals also experienced other injuries or conditions throughout their life that did not leave skeletal evidence but nevertheless affected the robusticity of their lower extremity. Alternatively, the outlying leg bones in this category may have arisen due to foot-dominance and/or unilateral activities. Soccer players with a kicking-foot preference are often used as a modern example of foot-dominance (McGrath et al. 2016), however activities in the Roman period could have also resulted in similar unilateral use of the lower limb. For example, Williams and Masseglia (2015) document lower limb laterality among Roman males in Turkey and interpret it as evidence for crouching/kneeling while tending grape vines. Potters, using double, kick-wheel type potters wheels, may also have developed asymmetric lower limbs due to the repetitive, unilateral force required to turn the wheel by kicking it with their foot. This technology was available during the Roman period and is reported in archaeological assemblages from Britain and Belgium (e.g., Borgers 2016; Upex et al. 2008), although not all communities appear to have adopted the kick-wheel (Pena and McCallum 2009).

A study of modern human skeletons by Auerbach and Ruff (2006) reports that compared to upper limb asymmetries, the lower limbs have closer to zero percent directional asymmetry. Of the four Ancaster outliers, the outlying leg elements belonging to one individual (AN-177) do not exhibit outlying levels of asymmetry and are best explained by the individual’s overall robusticity. Furthermore, similar rates of outlying lower limb asymmetry were observed in Ancaster individuals without fractures (*n*=4) as the remaining Ancaster individuals with fractures (*n*=3). No situation is known where legs will develop asymmetrically in response to an upper limb injury, so it is unlikely that the co-occurrence of fractured arm bones and the outlying leg bones represent a functional repercussion of trauma. Additionally, the similar frequency in Ancaster individuals with outlying lower limb asymmetries between individuals with and without fractures suggests that an activity-based explanation is the most probable to explain the lower limb asymmetry in these individuals.

9.2 Fracture Treatments & Complications

Poorly aligned fractures can indicate an absence of, or lack of treatment success, and can lead to the development of osteoarthritis and limb dysfunction due to altered mechanical loading of the malunited bone. In addition to fracture complications, the type and location of fracture may also influence how a bone is mechanically loaded. In order to identify the absence of, or unsuccessful application of treatment at Ancaster and Vagnari, this section evaluates the fracture malunion present. Additionally, relationships between malunion, fracture types, osteoarthritis, and biomechanical evidence for altered loading are investigated in order to determine the factors that affected an individual's physical function at Ancaster and Vagnari.

9.2.1 Fracture Treatments

Untreated fractures can heal with minimal amounts of malunion (Lovell 1990), so the examination of healed mal- and non-united fracture segments can only identify the absence or unsuccessful application of treatment in the past. The majority of fractures at both Ancaster and Vagnari healed with minimal malunion and no non-union fractures were observed at either site. This means that there were relatively few instances at Ancaster and Vagnari when treatment could clearly be recognised as absent or unsuccessful. The absence of evidence for insufficient fracture treatment cannot serve as proof that treatment occurred. However, given the Roman understanding of fracture healing, it is conceivable that fracture treatments were probably attempted and successful in at least some instances. At the very least, it is clear from the low malunion rates, that the healed repercussions of absent or unsuccessful treatment only affected a minority of individuals with fractures at Ancaster and Vagnari. Based on this, it seems that individuals at both sites were probably afforded time to rest and heal after an injury, and before resuming their regular activities.

Fracture treatments have been addressed in the bioarchaeological literature, most notably by Grauer and Roberts (1996). This thesis adds to Grauer and Roberts' (1996) study addressing the possibility of treatment interventions, by also integrating biomechanical assessments of disuse in order to provide insight into behaviours during and after healing. As immobility was often prescribed as part of fracture healing, one might expect evidence for some amount of bone loss associated with prolonged rest. Although most fractured bones at Ancaster and Vagnari were relatively well-aligned, none of these fractures were associated with biomechanical evidence to indicate they spent a long time immobilized (i.e., smaller limb of the same type and side as a fracture, Section 9.1.2). Consequently, it can be argued that individuals with fractures rested only long enough for their fractured bone to sufficiently stabilize before they returned to activity, thus preventing disuse and bone loss.

Malunion was three times more common among Ancaster males with fractures than Vagnari males with fractures. The site differences in malunion rates could be interpreted as evidence for the availability of, or access to, fracture treatments, but in this instance, the higher rates of malunion at Ancaster are best explained by the types of fractures involved. Spiral fractures account for the majority of malunited male fractures at both Ancaster and Vagnari (n=11/19, 57.9%), eight of which were paired, both-bone fractures (e.g., radius and ulna). Using only conservative techniques, spiral fractures can be particularly challenging to reduce and stabilize as the angled fragment edges may easily slip against and past each other (Hamblen et al. 2007). The rate of malunion at Ancaster and Vagnari seems to have more to do with the types of fractures, and therefore the injury hazards encountered, than it does the skill or experience of the person applying treatment, or how long an individual allowed the fracture to heal before returning to function.

The link between malunion and difficult-to-reduce fracture types at Ancaster and Vagnari serves as a cautionary tale in the interpretation of fracture treatment in the past. Although not all fractures may have received treatment, it is apparent from this study that the types of fractures can influence the outcome, regardless of the application of treatment, the skill of the practitioner, or the compliance of the injured individual. Furthermore, just because a fracture exhibits some degree of malunion, this does not mean that dysfunction is certain to follow.

9.2.2 Fracture Types

At Vagnari and Ancaster, fractures caused by direct and higher energy forces were indeed associated with greater prevalence rates of malunion (see Section 9.2.1), but this force category was not generally associated with increased odds for functional consequences (evidenced by outlying bone areas and asymmetries). However, females had a higher prevalence of outlying cross-sectional properties among higher energy fractures than lower energy fractures. This means that at both Ancaster and Vagnari, females who experienced higher-energy traumas had a greater predisposition for altered mechanical loading behaviours. Although this link between fracture force and biomechanical outliers was present among females, there is currently little evidence that their experience of higher force injuries consistently led to the development of dysfunction; none of these females with higher energy fractures demonstrated disuse of the fractured limb.

9.2.3 Osteoarthritis

Trauma is recognised in the bioarchaeological literature as a possible consequence of osteoarthritis, but most studies do not focus on post-traumatic osteoarthritis, and instead examine what overall differences in osteoarthritis rates indicate about behaviour in the past (e.g., Baetsen et al. 1997; Lieverse et al. 2016; Palmer et al. 2014). As osteoarthritis risk increases with age, it is reasonable to expect that some older individuals with fractures may have developed osteoarthritis even if they had not sustained a fracture. Following this, the presence of osteoarthritis in young adults is less common, and when associated with a fracture, is more convincingly indicative of post-traumatic osteoarthritis. By considering individual age at death, as well as the presence of osteoarthritis associated with fractures to articular surfaces, this thesis specifically addresses the osteoarthritis as a post-traumatic consequence in archaeological collections.

At Ancaster, three of the fourteen Ancaster individuals with fractures and osteoarthritis were young adults (AN-152, 218, and 225). When compared with the total rate (including individuals with fractures) of young adults with osteoarthritis at Ancaster (*n*=12/59, 2.0%), the rate of young adults with both osteoarthritis and a fracture is considerably elevated (*n*=3/11, 21.4%). Since osteoarthritis risk increases with age, the fact that such a high rate of young adults with fractures have osteoarthritis is anomalous. Additionally, the fracture types exhibited by these three young adults (articular tibia fracture, paired spiral fractures to the tibia and fibula, and transverse ulna fracture) may have resulted in altered joint mechanics, which may have predisposed these individuals to developing osteoarthritis at a younger age. Based predominantly on the young age of these individuals, but also considering the types of fractures that are present, AN-152, 218, and 225 provide the most convincing evidence for post-traumatic osteoarthritis.

In addition to the presence of osteoarthritis in young adults with fractures, a link between osteoarthritis and fractures involving articular surfaces is also demonstrated in this thesis. This relationship is well-documented in the clinical literature (e.g., Anderson et al. 2011; Buckwalter and Felson 2015), and microtrauma has been implicated in a palaeopathological study by Crubézy et al. (2002), but this study represents the first time that this association is clearly addressed in archaeological skeletal collections. At Ancaster, 33.3% (*n*=6/18) of the individuals with fractures that involved joint surfaces also had evidence of osteoarthritis (see Section 6.5.3). One of these fractures belonged to a young adult (AN-152). Of the five remaining older individuals with osteoarthritis and articular surface fractures, three individuals had unilateral osteoarthritis in the wrist associated with a joint fracture and one individual had bilateral tibial fractures and bilateral knee and ankle osteoarthritis. While it remains possible that these four older individuals with osteoarthritis and articular surface fractures could have developed the condition with age, the unilateral manifestation of osteoarthritis suggests the presence of asymmetric factors that influenced the development of osteoarthritis in these joints. Although the unilateral osteoarthritis may be explained by asymmetric habitual activity, it may also be related to altered joint physiology associated with the trauma.

Finally, links between fracture attributes and malunion and osteoarthritis were evident, especially among females at Ancaster, but these factors were not associated with biomechanical changes. Only four individuals with fractures, two of which were female

(AN-191, 218) and two were male (AN-024, VA-F216), presented with evidence of osteoarthritis and outlying cross-sectional properties. AN-191, a MA female with radial and ulnar fractures, wrist osteoarthritis, and a more gracile and asymmetric fractured limb, provided the only evidence for disuse associated with any of these tested properties. The remaining individuals had patterns of limb robusticity that better represent evidence for functional compensation (e.g., Section 9.1.3).

9.3 Activity, Robusticity, and Relationship to Fractures throughout the Life Course

This section ties the biomechanical and fracture evidence together to outline how the physical environments in which individuals at Ancaster and Vagnari lived influenced their fractures and injury responses. Descriptions of the common levels of activity, based on biomechanical assessments, at Ancaster and Vagnari provide a strong platform from which to discuss the influences on long-term functional consequences of fractures in these Roman contexts. To further elucidate patterns and risks for long-term fracture consequences at Ancaster and Vagnari, this biomechanical evidence is then contextualized and used to interpret the intensity of habitual activities between the sexes and throughout the life course.

9.3.1 Biomechanical Evidence for Activity Intensity

Biomechanical investigations of bone shape and robusticity are used to reconstruct activity in the past. Studies, such as those by Macintosh et al. (2014) and Sparacello and Marchi (2008), investigate biomechanical changes to the lower extremity associated with terrestrial mobility. Other research, such as that by Weiss (2003), as well as Stock and Pfeiffer (2001), use the upper limb to interpret habitual activities such as rowing or paddling; Schmitt et al. (2003) also look at the biomechanical properties of upper limbs to suggest asymmetric behaviours such as spear thrusting in the past. Interpretation of the biomechanical evidence for specific activities at Ancaster and Vagnari is mostly beyond the scope of this thesis. However, the biomechanical evidence for patterns in general strain present between the communities, including a few noteworthy habitual activities, are discussed in order to characterize trends in physical activity that may influence injury responses.

Genetic factors, as well an individual's nutrition, can greatly influence an individual's ability to achieve their maximum potential bone mass (Heaney et al. 2000). However, exercise also plays a very important role in the development of bone. Throughout life, bone is deposited differently in response to strain; recognition of these patterns can help identify if intensive activity was initiated earlier or later during the life course. Prior to mid-adolescence, the diameter and area of the outer periosteal surface is predominantly enlarged via bone apposition (Ruff 2005). Changes to bone thickness are more common on the endosteal surface when amplified loading is continued through adulthood, resulting in larger cortical areas and shrinking medullary areas (Ruff 2005). Accentuated loading that occurs at younger ages enlarges both total and cortical bone areas in growing individuals participating in sports with higher loading requirements, such as the gymnasts described by Dowthwaite and Scerpella (2009). When bone is lost as an adult, it will be lost primarily from the endosteal surface, meaning that bone total areas should remain relatively reliable indicators of physical strain experienced in a person's young life. Based on how bone grows (or is lost) with age, individuals with comparatively larger bone total and cortical areas likely experienced lifelong loading, commencing more intensive habitual activity before skeletal maturity (Ruff 2005).

Male upper and lower limb bones (humeri and tibiae), as well as female forearms (radii) were significantly more robust at Vagnari than Ancaster. The total bone areas, influenced by strains applied prior to skeletal maturity, of male humeri and female radii were different between the two sites. The comparatively larger total areas recorded at Vagnari were likely shaped by heightened loading that began at younger ages than at Ancaster, probably while the individual was still growing. Additionally, the tendency for Vagnari individuals to also have thicker cortical areas means that they probably continued to experience relatively higher levels of activity into adulthood. This section discusses the explanations for the more robust bones at Vagnari and Ancaster, as well as the implications of these biomechanical results at Ancaster and Vagnari.

Agricultural activities may account for some of the robusticity observed, and were practiced at both Ancaster and Vagnari. However, because Vagnari was part of an Imperial estate, it can be expected that the manual labour necessary to create a surplus of goods and revenue would have been in excess of mere subsistence at this site (Small 2011). Females in the Roman world also participated in some manual labour associated with farming (Scheidel 1995). As such, the increased arm robusticity of both sexes may be accounted for by different duties associated with planting, tending, and harvesting of fields.

Alternative explanations for the increased robusticity are also possible. Other activities at Vagnari, such as transhumance, may account for the larger tibial areas, particularly among males. The size and shapes of tibiae have been used in previous bioarchaeological and palaeoanthropological studies to investigate differences in strain associated with terrestrial mobility (e.g., Holt 2003; Macintosh et al. 2014; Shaw and Stock 2013). Tibial areas are comparatively more robust among Vagnari than Ancaster males. This indicates that the Vagnari males experienced relatively more strenuous terrestrial mobility and terrains from younger ages than at Ancaster. Transhumance was a long-standing practice in the Vagnari region (Small 2011). In the Roman period, shepherds were predominantly male (Shaw 1993), meaning that some of the Vagnari males would have moved with their livestock over various types of terrain and considerable distances (Small 2014b).

The larger arm bones of both males and females at Vagnari also suggest that mechanical loading of the upper limb was comparatively greater than at Ancaster. However, as the upper limb bones with biomechanical differences were not the same between males and females, the loads experienced by each sex were probably caused by different activities. In regards to the larger female radii, elevated wrist strain may be associated with spinning or weaving, common domestic chores undertaken by women of antiquity (Moeller 1969; Wild 2002). Weaving is a very repetitive task, and modern studies of musculoskeletal stress on weavers identify accentuated wrist and elbow (Motamedzade and Moghimbeigi 2012). Elevated male humeral robusticity at Vagnari may also be explained by a variety of activities that required heavy, upper body labour, such as construction activities, agricultural practices, tile making, and vineyard work. Pre-industrialized farming and viticulture would have required substantial upper body strength to plant and harvest crops; botanical remains, as well as agricultural implements, recovered at Vagnari confirm agriculture was practiced here (Brent and Prowse 2014; Carroll 2013b). Additionally, tiles were locally manufactured at Vagnari from clay in the adjacent ravine (Small et al. 2003). According to Small (2011), finished tiles weighed between 10 and 20 kg each, meaning tile makers would have had to have some strength to move their goods, as well as to quarry and transport the raw clay. Although some women may have also participated in these jobs, based on Roman notions of gendered labour discussed by Scheidel (1995) (i.e., women's work was domestic and indoors, men worked outside the home), it is likely that these tasks were dominated by men. Accordingly, the physical strains associated with these types of occupations may account for some of the greater mechanical loading forces and identifiable humeral changes among males at Vagnari

Although the level of robusticity present at Ancaster was less than at Vagnari, Ancaster individuals were not gracile enough to suggest that the community would have been completely sedentary and non-active. For example, tibial total areas at Ancaster were of comparable or greater size than other European sites throughout time (see comparison with Macintosh et al. (2014) in Section 8.4.2). This means that although terrestrial mobility strains were especially high at Vagnari, they were not particularly low at Ancaster. The same premise likely applies to male forearm bones at Ancaster; the range of variation in radial and ulnar areas at Ancaster exceeds that at Vagnari, indicating that some Ancaster males were actually experiencing forearm loads of comparatively greater intensity. In particular, three Ancaster males without fractures had larger than normal radial total areas, one of which (AN-005) also had a larger radial cortical area. Based on these results, these individuals experienced increased forearm loading at a young age, which, in the case of AN-005, was continued after skeletal maturity. The elevated forearm strain in some Ancaster individuals may be partly explained by the community's probable association with a sculpting school and a nearby limestone quarry (Burnham and Wacher 1990). Stone working can cause elevated forearm strain due to repetitious activities and percussion vibrations between hammers and chisels (Mukhopadhyay and Srivastava 2010). Participation of a group of Ancaster males in stone working activities could account for some of the more robust, upper range of forearm areas at this site.

Although some of the Ancaster residents clearly also participated in physically strenuous activities, the biomechanical evidence indicates that habitual activities were not initiated as young at Ancaster as they were at Vagnari. As Vagnari was part of an Imperial estate, the presence of elevated activity levels is not entirely surprising. Imperial estates were often worked by slave and lower-socioeconomic groups and involved manual labour in order to produce a surplus for profit (Rosafio 2014). Additionally, in the Roman period, children of lower socio-economic groups would have been expected to have begun work as early as they were able; historic accounts suggest some slaves began work as early as five years old, and were commonly working by ten years old (Bradley 1985; Harvey 2004). Families with the financial means and connections could have arranged to have their child apprentice a craft, trade, or industry, usually beginning around 12 or 13 years of age, but maybe earlier in some cases (Bradley 1985). Children of wealthier families may not have been enrolled in manual occupations at all, instead focussing on more formalized education (Rawson 2003).

While the nature and intensity of the specific activities present in each community influences the robusticity of the bones, the biomechanical evidence does suggest that individuals commenced work at younger ages at Vagnari than at Ancaster. Perhaps, the younger age at which physically strenuous work was begun at Vagnari implies that this community was largely populated by individuals of comparatively lower socio-economic status who had less choice in the age at which they began labour. This interpretation conforms to what we know historically about the composition of Imperial estate populations. This finding also seems to suggest that the status distribution at Ancaster may have been more varied, with some individuals having the option to do less manual labour at a young age.

The association between status and activity has been previously identified in studies, such as that by Ledger et al. (2000), in which greater mechanical loading in the upper limb was identified as indicative of manual labour in a historic slave cemetery. At this time, no biomechanical studies seem to address the relationship between status and biomechanical strain in Roman period collections. It is possible that some relationship between the evidence for mechanical loading, physical activity, and status in these Roman contexts exists, and merits further investigation in future studies.

9.3.2 Over the Life Course: Fractures, Biomechanics, and Changing Roles

Patterns in the distribution of fractures by age at Ancaster and Vagnari provide important insight into the variable nature of injury hazards and strain throughout life in these communities. At Ancaster, fractures were more common among the older adults than the younger adults, while the opposite was true at Vagnari where young adults had greater odds of exhibiting a fracture than the old adults. The age distribution of injuries at Ancaster agrees with the typical accumulation of injuries over the life course. That is, the longer people live, the more hazards and risks they are exposed to, and the greater their potential for injury or multiple injuries (Glencross 2011). In contrast, the frequency of fractures decreases with increasing age at Vagnari. The paucity of fractures among middle and old adults and the concentration of injuries among the young adult age category at Vagnari is not a typical age distribution of fractures and requires further discussion.

The simplest explanation for the scarcity of older adult fractures at Vagnari is related to sample size. It is undeniable that relatively few old adult elements were preserved and available for analysis in this study. However, middle adults were fairly well represented; the number of middle adult elements rivals the number of young adult elements. At Vagnari, middle adults still had lower fracture frequencies than young adults; this was not the case at Ancaster where middle adults demonstrated greater fracture prevalence rates than the young adults. As the age-related trends in fracture accumulation are still evident between the young and middle adults, two groups with comparable sample sizes, it seems likely that the age-related trends evident at Ancaster or at Vagnari are not biased by the poor representation of old adults. As confidence can be had in the trends in fracture distribution at Ancaster and Vagnari, this section investigates the differences in fractures and biomechanical properties among the age groups at each site. Specifically, possible reasons for relationships between age, fracture types, and long-term functional consequences are discussed.

9.3.2.1 Younger Adults

Young adults at Ancaster and Vagnari demonstrated the most notable difference in fracture prevalence rates. Young adult males at Vagnari had greater odds of both high energy and direct force fractures as well as indirect fractures than the young adult males at Ancaster. Combined, the fracture forces represent physical hazards that individuals encountered in the past. However, lower energy and indirect fractures can be particularly useful in interpreting the consequences of physical hazards related to mobility as they are often associated with causes such as slipping, tripping, falling, and unsuccessful jumps.

Biomechanical interpretations made in Section 9.3.1 suggested that individuals at Vagnari were highly physically active from younger ages, especially in terms of terrestrial mobility. With amplified physical activity often comes increased exposure to injury hazards. It is, therefore, not surprising that the young adult males at Vagnari, the group that exhibited the greatest evidence of ambulatory strain, also had some of the highest prevalence rates of fractures that could be best associated with mobility. Elevated rates of indirect force fractures among the young adult males at Vagnari serve as further evidence in support of intensified mechanical strain, indicative of more intense physical activity in younger life at this site. Combined, the biomechanical and fracture evidence suggest that the young adult males at Vagnari were, on average, a highly active and mobile group whose intensified activity resulted in greater risk for fractures.

The young adult males at Vagnari also had greater odds of higher energy fractures than at Ancaster. At Vagnari, these fractures included a transverse fracture to a distal ulna and a comminuted fracture to a midshaft clavicle, both injury types caused by bending forces and usually by direct blows. Although it is tempting to assume that these injuries were sustained during interpersonal conflict, it is just as likely that they were caused by direct impacts during daily life, such as accidental blows from tools, animals, or falling logs and construction materials. Regardless of how the injuries were sustained, the greater odds for higher energy and direct force injuries among young adult males at Vagnari further support an interpretation of activities at Vagnari as more strenuous and potentially hazardous earlier in life.

Based on the evidence available, it is not possible to defend a traditional pattern of injury accumulation over the life course at Vagnari. Young adults at Vagnari were at the greatest risk for fracture, especially fractures caused by direct blows or more serious indirect trauma, and sustained injuries more often than the older age cohorts. The fracture findings complement the cross-sectional evidence that suggests younger individuals experienced relatively greater mechanical stimuli from younger ages than at Ancaster. Due to the higher physical strain and greater fracture risks among the young adults at Vagnari, the highly strenuous lifestyle of this age group likely put them at increased risk for earlier death. Slightly fewer middle and old adults were present at Vagnari, which may help support this suggestion in that fewer young adults lived to be middle and old adults. Together, the biomechanical and fracture evidence indicates that compared to the small town at Ancaster, young adult life was more physically strenuous and hazardous on the Imperial estate at Vagnari, and may have actually contributed to the early death of some of these individuals.

9.3.2.2 Older Adults

According to the biomechanical evidence, mechanical loading strains decreased with advancing age at both Ancaster and Vagnari. While males were minimally affected, female upper limb bones exhibited large age-related decreases in cortical area at both sites. Age-related bone loss is relatively common among modern, older women and results in the deterioration of microarchitecture and the thinning of cortical bone (Seeman 2013). Hormonal changes associated with menopause are an important part of explaining age-related bone loss (Khosla 2012). However, other genetic, nutritional, and lifestyle factors also influence bone health, and may affect bone's biomechanical potential and loss (U.S. Department of Health and Human Services 2004).

Bone loss can be associated with an elevated risk for certain types of extremity fractures associated with lower-energy falls from a standing height or skeletal fragility (Ensrud 2013a). These most commonly include fractures to the proximal femur, as well as fractures to the distal radius and proximal humeri (Ensrud 2013a; Kalia and Agarwal 2014; Wilson et al. 2014). Fragility fractures are most common among older adult females, and are caused not only due to compromised bone structure, but also because most older individuals have a greater propensity to fall (Ensrud 2013a). A low-energy fall, such as a fall from a standing height, accounts for most fragility fracture types. However, some fractures, such as femoral neck fractures, may also result due to spontaneous failure of pathologically weakened bone that is no longer able to resist the gravitational stresses applied by the body (i.e., a type of stress fracture) (Burr et al. 1997). Maintenance of physical activity throughout the life course in order to improve balance, strength, and stability helps to prevent the cause of the fracture in the first place (Gregg et al. 2000).

At Ancaster, a study of second metacarpal cortical thickness by Mays (2006a) found that females had age-related bone loss and reduced amounts of bone compared to modern individuals. This thesis supports Mays (2006a) findings, and also identifies significantly lower cortical bone amounts in all the upper extremity bones of Ancaster older adult females. While males at Ancaster also exhibited some age-related bone loss, female elements were more greatly affected. The patterns in bone loss at Ancaster are comparable to the findings of other studies of bone amounts at Roman period sites. For example, the females at Ancaster lost more bone than the males, much like at the Italian Roman sites of Isola Sacra and Velia, reported by Cho and Stout (2011) and Beauchesne and Agarwal (2011), respectively. Additionally, similar to Velia, Italy, some of the male elements (i.e., radii) at Ancaster did not lose significant amounts of bone until old adulthood, while females began to lose bone from most elements at middle adulthood.

Mays (2006a) also identifies a number of individuals with fractures that commonly predict osteoporosis; these included five females, four of which had distal radial fractures and one (AN-113) that had an incomplete femoral neck fracture. In addition to the female extremity fractures identified and discussed by Mays (2006a), this research also recorded one Colle's fracture to the left radius of a middle adult male (AN-177). It is unlikely that this male radius represents a fragility fracture as radii with 'normal' amounts of cortical bone can still sustain this type of fracture, especially when slightly higher-energy mechanisms are involved (Egol et al. 2010). Additionally, in clinical settings, the occurrence of males with distal radial fractures is relatively constant, and only increases slightly after approximately 70 years of age (Egol et al. 2010).

At Vagnari, the areas of upper extremity bones belonging to older adult females were not only smaller than those of the young adults, but also smaller than the upper limb bones at Ancaster. However, in contrast to Ancaster, where fragility fractures were relatively common among females, none of the fractures at Vagnari were indicative of increased bone loss or osteoporosis. Considering that the amount of cortical bone present decreased with age between young and middle adult females at Vagnari, and that older adult females at Vagnari also tended to have less cortical bone than at Ancaster, the lack of fragility-related fractures was somewhat surprising. However, this absence of fragility fractures among the Vagnari females may be explained due to the smaller sample of middle and old adult females available. Additionally, among Vagnari females, the distal epiphyseal segment, the region most frequently associated with fragility fractures in radii, was often incomplete or absent. Between the small sample size, and the poor preservation of bone ends, if fractures to the distal radii were present in this collection, they were probably damaged postmortem and therefore not observed.

Some age-related decline in strength, and muscle and bone mass is an inevitable part of aging, but this natural progression can be amplified by increasingly sedentary behaviours (Burr 1997; Faulkner et al. 2007). Continued physical function and mechanical loading into old age plays an important role in mediating the loss of bone with advancing age (Muir et al. 2013). While decreased bone amounts are clear in the upper extremity of older individuals at Ancaster and Vagnari, the amount of cortical bone present in the leg bones did not differ significantly with age. The different skeletal distribution of age-related cortical thickness changes suggests that function and mechanical strain played an important role in the maintenance of bone thickness with increasing age at these sites. This finding supports similar results reported by Peck and Stout (2007), who document the heterogeneity of bone mass using modern human cadavers, and explain the intra-skeletal differences as a result of mechanical loading environments for each element type. Conservation of bone in the lower extremity at these Roman sites indicates that older individuals at Ancaster and Vagnari continued to be relatively mobile into old age.

In contrast to the maintenance of bone in the lower limb, the reduced bone amounts in female upper limbs at Ancaster and Vagnari suggest limb specific (i.e., intra-skeletal) differences in loading levels. Based on the biomechanical evidence, it seems that older adult females may not have been required to participate in activities and tasks that involved large amounts of upper limb strain, resulting in reduced mechanical loading forces needed to mediate bone loss. This evidence suggests that females who survived into old age at Ancaster and Vagnari may have been afforded some degree of activity alleviation. Although the concept of retirement is not really applicable to the Roman world, it was socially expected that children support and look after their elderly parents (Harlow and Laurence 2002). Additionally, some older individuals may have been wealthy enough to support themselves and their slaves in old age (Cokayne 2003). However, as a result of financial pressures, individuals of lower status would have been expected to continue working as long as they were able in order to continue to provide for themselves (Cokayne 2003; Parkin 2003). Although the roles of aging women and individuals of lower socio-economic standing are not very well defined in ancient sources, descriptions of the changing roles of wealthier males suggest that, when possible, individuals moved away from physically strenuous activities, instead taking on more executive or philosophical tasks (Harlow and Laurence 2002). As some individuals would not have been financially able to stop working, when confronted with their aging bodies, they may have adopted tasks that were less strenuous, but still profitable.

The evidence for decreased upper body activities among females at both Ancaster and Vagnari seems to indicate that the residents of these communities who reached old age may have been able to reduce or change their workload as they aged. As an Imperial estate, it is unlikely that Vagnari was home to many wealthy people, and it is, therefore, more likely that the bone changes at this site represent age- and sex-related shifts in activities. The economic situation at Ancaster is less well known, but based on archaeological evidence appears to have been more socially stratified. At this site, the age and sex differences could represent a change in activities, like at Vagnari, but may also indicate activity alleviation in the case of wealthier individuals.

The change in, or alleviation of, loading with advancing age may also help to explain the two fractures with possible disuse that were identified at Ancaster. Both cases of disuse involved old adult individuals, whereas instances of possible adaptation or compensation to injury were identified mostly among young adults. The evidence suggests that younger individuals typically found a way to adapt to their altered physiology in order to maintain function and be able to continue to work. A quick return to function may actually have proven beneficial, contributing to the low incidences of functional consequences evident at Vagnari (a discussion of early mobilization after injury is provided in Section 9.1).

It is currently not possible to definitively know how long before an individual's death the two healed, older adult fractures with disuse were sustained. De Boer et al. (2012) present guidelines for determining the time since injury in the earlier stages of fracture healing. Unfortunately, visual methods cannot be used to reliably estimate the time since injury after approximately two to three months after an injury was sustained, when the callus outline becomes smooth radiographically; after one to two years, fracture healing has largely subsided. It is likely that the two individuals with fractures and disuse sustained their fractures at least months, if not years, prior to their deaths.

The concentration of older adults with disuse does suggest that this group was less able to effectively adapt to their injuries and likely experienced some reduction in activity that was associated with the injury. Perhaps some individuals were able to compensate for their injuries as young adults, but as their activity slowed with age, and as other secondary complications developed, the functional repercussions associated with long standing injuries were felt more acutely. Alternatively, if the fracture was experienced as an older individual, perhaps they were unable or unwilling to adjust to their altered body because of physical limitations associated with aging, or due to behavioural and social expectations of an older adult in the Roman period.

9.4 Integrating Stories at Vagnari and Ancaster: Activity, Fractures, Healing, and Impairment

The biomechanical and fracture evidence revealed differences in the patterns of sex- and age-based activity at Ancaster and Vagnari. Additionally, the level of physical activity experienced by the residents at Ancaster and Vagnari likely had an important influence on how individuals in these communities recovered from fracture(s). This section unites and summarizes the various lines of evidence, clarifying the relationships between age, activity, fractures, fracture healing, and long-term consequences of fractures in these communities.

As residents on an Imperial estate, most of the people at Vagnari were likely of lower-socioeconomic status (Rosafio 2014; Small 2011). To date, archaeological evidence suggests that agriculture, viticulture, and transhumance were prevalent, and physically laborious, undertakings in this community (Small 2011). If people of these lower status levels comprised the majority of Vagnari’s labour force, it is unlikely that they could be excused from manual labour for extended periods. The cross-sectional evidence at Vagnari suggests that individuals, especially males, experienced high levels of mechanical loading and increased injury risks, findings that are in agreement with the archaeological evidence for intensified activities at this site. However, the relative absence of healed fracture malunion at Vagnari indicates that although these people worked hard, they were still afforded time to recover and heal in the event of an injury. The nature of the tasks at Vagnari could likely not have been put off for long, and due to the expectations of their occupations, and their need for financial security, the individuals at Vagnari would probably have been expected to quickly return to their original duties after an injury had healed. This quick return to function likely accounts for the absence of disuse among the fractures at Vagnari.

While Vagnari's story is one of highly active, young adult males, the story at Ancaster reveals the changing roles of females with age. Although the evidence suggests that Ancaster was comparatively less physically active, there is no indication that this community was extremely sedentary or inactive. The degree of physical activity present at this site changed with age. While young adults were relatively robust (albeit smaller than Vagnari), bone loss that was likely associated with a reduction in physical activity was apparent among the arms of aging females at this site. The pattern of bone loss among females indicated that they maintained mobility within their environments, but they were evidently no longer required to perform more strenuous activities with their upper limbs. In addition to this trend for bone loss in advancing age, all the individuals with probable post-traumatic functional loss were also older in age. The evidence for diminished activity with increasing age may indicate that, at Ancaster, the elderly and the injured were sufficiently supported by their families or wealth that they were able to reduce their workload.

Overall, at both Ancaster and Vagnari, the absence of disuse associated with fractures in young adults speaks to the resilience and adaptability of these individuals. These findings are reminiscent of a case study by Cowgill et al. (2012) concerning a Palaeolithic juvenile with pathological limb bones but no biomechanical evidence for functional deficit. In this study, Cowgill et al. (2012) interpret the minimal differences between the individual's cross-sectional geometries and those of normal individuals as indicative of persistent mobility and activity. Similar reports of altered, but maintained mobility and activity after a fracture were published by Holt et al. (2002), and Lovell (2016). Much like the individuals reported by these authors, the younger residents at Vagnari and Ancaster clearly resisted dysfunction associated with fractures. Evidence for this behaviour provides valuable insight into how younger people at Ancaster and Vagnari perceived and responded to injuries. It seems that as long as these Roman period individuals were physically capable of activity, they remained active and did not let (or could not let) their healed fractures slow them down.

9.5 Summary & Contributions to Biological Anthropology: Long-Term Functional Consequences of Fractures

This research builds on anthropological case studies concerned with long-term function after injury (e.g., Lovell 2016; Trinkaus et al. 1994), as well as studies that use biomechanical methods to assess the functional impact of other pathological conditions, (e.g., Cowgill et al. 2012; Sparacello et al. 2016). Despite the growing literature on the relationship between function and pathology in the past, no large scale study that considers fracture and complications in relation to biomechanical evidence has yet been published.

The bioarchaeological case studies on function associated with pathological conditions are part of a growing trend in biological anthropology to better understand the human condition and experiences in the past (e.g., Hegmon 2016). The introduction of models, such as the *Bioarchaeology of Care* by Tilley (2015), are part of this movement to understand lived experiences, particularly of individuals with impairment. However, in the case of this model, understanding the provision of care is limited to individuals with evidence for pathology that would clearly have resulted in debilitating functional consequences. The research presented in this thesis demonstrates that the response to fractures can often not be accurately assessed using morphological appearances alone. Fractures that may initially appear to be debilitating often provided little evidence for biomechanical changes in function. Conversely, some injuries that are frequently observed in archaeological assemblages and generally appear to be non-threatening, such as Colle's fractures, may have actually have caused some functional limitations for some individuals in the past. These findings have important implications for how individual experiences of injuries are understood and deciding when models such as the *Bioarchaeology of Care* can be reliably applied. According to the results in this thesis (i.e., the lack of association between lesion appearance and function), it is not always easy and straightforward to identify what constitutes a severe, or functionally impairing, injury.

Although these research findings demonstrate a lack of association between fracture attributes and an individual's physical response to the fracture, this does not undermine the application of new methods and theories used to envision impairment and care in the past. Instead, the results of this research help to advance the understanding of what constitutes a 'severe' injury in terms of its long-term functional repercussions. It is clear that the long-term functional repercussions of fractures cannot be identified based only on a fracture's appearance or the presence of other post-traumatic complications such as osteoarthritis. Some direct force fracture types may heal with malunion and develop osteoarthritis, but not result in physical consequences; some simple, minimally displaced fractures could result in impairment. Not all fractures that appear to be 'severe' are actually impairing, and not all fractures that look non-threatening are without functional complication. It is not possible to assess impairment and disuse based on the outward morphology, characteristics, and complications of a fracture. Although a fracture may look to be grievous, it does not follow that the person necessarily 'suffered' or was greatly impacted by their injury after it had healed. In light of these findings, it is recommended that palaeopathologists wishing to better understand the human experience of impairment resulting from fractures (as well as other pathological conditions) should use caution when making assessments of function based on lesion patterns and morphology.

Through the use of multiple lines of evidence (i.e., biomechanical and palaeopathological fracture analyses), this research has been able to evaluate the habitual mechanical loading environments of individuals with fractures, as well as shed light on the broader group experiences of injuries at Ancaster and Vagnari. While studies focused on individuals with obvious and severe pathological conditions provide important insight about the provision of care in the past, the results of this thesis help further develop the understanding of larger patterns in injury response. The minimal association between fracture forces, types, malunion, osteoarthritis, and long-term disuse support the clinical concept that other, more individual, and perhaps socio-cultural, attitudes toward injury and fracture recovery may influence an individual's risk for developing dysfunction. Additionally, the few examples of post-traumatic dysfunction at Ancaster and the absence of functional consequences at Vagnari indicate that the development of dysfunction, and thus the response to injury, was not universal throughout the Roman world. The type of community in which an individual lived may have influenced if an individual returned quickly to function, thus helping to stave off long-term functional problems associated with post-traumatic disuse. The perseverance and resilience of Roman individuals who experienced fractures at Ancaster and Vagnari is evident.

Chapter X – CONCLUSIONS

The long-term consequences of fractures in Roman period individuals at Ancaster and Vagnari were assessed using a combination of palaeopathological fracture analyses and biomechanical assessments of loading. The outcomes of this research provide valuable insight into how individuals at Ancaster and Vagnari accrued and responded to their injuries, and raise questions about how impairment is associated with, and can be interpreted from, pathological conditions in the past. The conclusions and contributions of this research are summarized below and future research directions are proposed.

10.1 Fractures and Habitual Physical Activity

Biomechanical and fracture analyses helped to identify the habitual loading environments and possible activities that caused fractures and influenced injury responses at Ancaster and Vagnari. The residents at Vagnari, an Imperial estate that was focused on the production of surplus goods for the Emperor's profit, had limb bones that were more robust and indicative of greater mobility and manual labour. While the young adult males at Vagnari also had greater prevalence rates of higher-energy and direct force fracture types, they were also the most likely to adapt and compensate functionally after an injury. In comparison, the extremity elements at the small Roman town of Ancaster were more gracile than at Vagnari; injuries were mostly indirect and included fractures associated with skeletal fragility and age-related bone loss.

These results address the first two questions of this thesis regarding the distribution of trauma and biomechanical evidence for habitual mechanical loading, and provide the base by which physical activities and experiences at Ancaster and Vagnari are understood. The evidence situates Vagnari as the more active of the two communities with injury risks felt most greatly in young adulthood. Although Ancaster was by no means an inactive community, the patterns in fractures and cross-sectional properties establish it as relatively less intensely active than Vagnari, with fracture risks greater among older adults, many of which are best related to bone loss.

10.2 Evidence for Long-Term Fracture Consequences and Impairment

The third research question in this thesis brought together the palaeopathological and biomechanical evidence to assess post-traumatic dysfunction. Of all the individuals with fractures, only two old adult individuals from Ancaster exhibited evidence for dysfunction associated with a fracture.

The prevalence of post-traumatic dysfunction was relatively low at both Ancaster and Vagnari. It is possible that some individuals lost bone as a result of impairment, but did not lose enough bone to be accounted for in this research, thus limiting the recognition of individuals with less obvious functional consequences. Although individuals with more subtle post-traumatic dysfunction may not have been identified in this research, the methods used were able to identify the individuals who reflected the most accentuated evidence for disuse. The low number of individuals with post-traumatic impairment, and the concentration of this dysfunction in older adult individuals, speaks both to the adaptability and perseverance of the younger adult residents in these communities, and to a change in physical roles with advancing age.

As measurable and morphological attributes of fractures were not predictive of the functional outcome at Ancaster and Vagnari, and as the frequency of impairment was evidently low, it seems that individuals at these sites simply carried on with their activities after an injury had healed. The resistance of most Ancaster and Vagnari individuals to functional impairment after injury is in contrast to some modern attitudes to recovery. In clinical settings, an individual's return to function is often greatly mediated by individual and social factors including perceptions of pain, as well as self-efficacy and social attitudes toward injury recovery. The functional perseverance of most residents at Ancaster and Vagnari suggests that a prompt return to function and activity after injury was important, or necessary, in these communities.

10.3 Integrated Evidence: Lived Experiences at Ancaster and Vagnari

Through investigation of these Roman experiences of injury and injury recovery, the hazards, as well as the benefits, of an active and physically strenuous lifestyle for these Roman individuals became apparent. Although individuals who participated in more physically active tasks may have been at greater risk for fracture, it helped them to form more robust bones that were probably protective against fractures as well as later-in-life bone loss. Additionally, more intensive habitual activities also seem to have helped individuals to be more resilient to impairment and poor functional outcomes. Intense physical activities at Vagnari may have encouraged individuals to maintain or regain function quickly after an injury. However, a relatively quick return to function after injury was clearly not at the expense of fracture healing; minimal malunion evident at Ancaster and Vagnari suggests that fractures were provided sufficient time to stabilize before function was fully resumed.

Although the evidence suggests that younger adults were adept at maintaining or resuming function after an injury, the patterns of bone loss in older adults, particularly older adults with fractures at Ancaster, suggest that physical behaviours changed over a person’s life. Bone loss was identified among the older adult individuals at both sites, but evidence for bone loss, fragility fractures, and functional disuse in the older adults from Ancaster, speaks specifically to the age-related impacts of function on fractures and injury recovery at this site. While individuals maintained mobility into old age, the amount of physical activity in the arms decreased, suggesting that manual labour was no longer necessary. As older individuals were evidently able to reduce their upper limb strain, this suggests that although they may have continued less physically demanding tasks, they did not need to do heavy physical labour to support themselves.

The biomechanical evidence for heterogeneous bone loss over the life course indicates the presence of changing physical, and perhaps social roles, in these Roman communities. While continued physical activity helped to resist and protect against functional impairments during younger adulthood, the decreased requirement for physical activity in old adulthood provided an environment that permitted reduced physical activity at this stage of the individual’s life. Therefore, existing trauma and its secondary consequences (e.g., osteoarthritis) may have not only been felt more acutely in older age, but it is also possible that social expectations for decreased physical activity with old age created an environment that was permissive of some degree of impairment.

10.4 Palaeopathological Contributions and Limitations

Although the results of this research found that two individuals had probable disuse of a fractured limb, fractures did not usually provide evidence for impairment. Specifically, there were no associations found between the functional consequences of a fracture, and the fracture type, location, degree of malunion, or presence of osteoarthritis. The lack of correlation between injury attributes and functional repercussions has important implications for understanding the human experience of fractures. In particular, palaeopathologists must be cautious about interpreting a person's experience based on the pattern and morphology of a pathology. Namely, if the morphological appearance of a fracture and its associated complications (e.g., malunion and osteoarthritis) are not predictive of the functional repercussions, it means that physical impairment cannot, and should not, be recognised based solely on these attributes alone. Although it is tempting to infer impairment from how a fracture appears, the pattern of distribution and/or the morphological characteristics of a pathology (in this case, fractures) should not solely be used as the basis for functional assessments in the past.

The integration of biomechanical methods in palaeopathological fracture analyses provided one possible solution to this problem, and was thoroughly explored in this thesis. The use of cross-sectional measurements to account for the amount of bone present, as well as the degree of asymmetry, provided clearer evidence for the degree of functional limitations after an injury, allowing the physical implications of an injury to be more accurately assessed. As biplanar radiographs are, or should be, standard practice in fracture analyses, including cross-sectional methods should not be beyond the capabilities of a simple fracture study. The use of the region of interest method, developed to measure the amount of cortical bone present within a larger area, was tested in this thesis, and may provide an alternative way to account for bone areas in elements that could not be easily assessed using traditional, single point measurements. Consideration of the amount of bone over a larger area, or the placement of multiple single point measurements along the bone diaphysis, are encouraged in future studies in order to characterize the amount of bone present with greater precision.

Biomechanical methods have use in identifying individuals with the most marked evidence for functional disuse and compensation after a fracture. Initially, the identification of only two individuals with post-traumatic disuse may suggest that dysfunction simply rarely occurred. However, it is also possible that some individuals may have had functional consequences, but did not present biomechanical changes to a large enough degree that they were classified as outliers. In other words, there is the possibility that an individual who experienced compromised function lost some bone due changes in mechanical loading, but still remained within the range of normal. In such a case, disuse experienced by this individual would not be identifiable with the current methods. This presents a limitation to biomechanical studies of this nature, but does not invalidate their use; individuals with the most marked biomechanical changes are identifiable, and contribute greatly to identifying and understanding impairment in the past. In order to better elucidate the causes of these outliers, future studies should strive to incorporate methods and skeletal collections that permit investigation of bending and torsional rigidity. Measures of torsional and bending rigidities would also provide additional insight into the mechanical response of bone to loading conditions after trauma.

The relationship between fractures and function provides new insight into the attitudes toward injuries by Roman period individuals at Ancaster and Vagnari. By using a multi-method approach to address the long-term repercussions of fractures (and other pathological conditions), palaeopathologists can more confidently engage with the growing literature concerning impairment and the human experience in the past. Continued physical activity by individuals at Ancaster and Vagnari, despite their injuries, demonstrates a trend for resilience after injury in these Roman communities. Although the residents of Ancaster and Vagnari had few fracture consequences and appeared to be adaptable to their injuries, these findings serve to revitalize trauma studies by encouraging that lived experiences of fractures are considered and evaluated in palaeopathological studies.

10.5 Future Avenues for Consideration

This thesis has approached questions of long-term injury repercussions in small Roman settlements and found a general pattern of resilience, especially among younger individuals. The findings of this research raise other questions about the experience of strains and risks in different types of Roman communities. Settlements are often differentiated, most basically, into urban and rural categories. While such a simplistic division may not always be suitable, Redfern et al. (2015) identified urban-rural differences in mortality, as well as indicators of stress and poor health. Following on from this, future research on trauma and the long-term consequences of extremity fractures should evaluate if patterns, not only in the acquisition of fractures, but also in the responses to injury, are present among settlement types. Through the investigation of different types of Roman communities, and comparison with the results in this thesis, even more can be said about Roman responses to injury and the factors that influenced them.

In this research, a number of individuals with outlying bone areas and/or asymmetries were identified that were not associated with fractured extremity bones. Many of these probably belonged to individuals who were especially active (or inactive), or that had increasingly lateralized occupations, however some individuals may have experienced other pathological conditions not considered in this research. Further investigation of such outliers could help to isolate the effects of other pathological conditions on biomechanical function. Inclusion of comprehensive pathological analyses could help elucidate alternative causes for bone outliers and perhaps identify relationships between function and other pathological conditions that were not considered in this thesis. Additionally, consideration of other measures of bone strength (e.g., bending and torsional rigidity), as well as the inclusion of multiple measurements for each bone, could help to clarify patterns in changing bone amounts.

This thesis, like the biomechanical insight into tuberculosis by Sparacello et al. (2016), demonstrates the important link between functional repercussions and pathological conditions. This thesis has demonstrated a pattern of human resilience and adaptability, while highlighting sex- and age-related changes in functional expectations in two Roman communities. Moving forward, the incorporation of biomechanical techniques in palaeopathological analyses has great potential to further inform bioarchaeological studies of the lived experiences of pathology, impairment, and perhaps even disability.

REFERENCES

Acsádi G, and Nemeskéri J. 1970. *History of Human Life Span and Mortality*. Budapest: Akadémiai Kiadó.

Ahlborg HG, Johnell O, Turner CH, Rannevik G, and Karlsson MK. 2003. Bone Loss and Bone Size after Menopause. *The New England Journal of Medicine* 349:327-334.

Alexander JS. 1995. Building Stone from the East Midlands Quarries: Sources, Transportation and Usage. *Medieval Archaeology* 39:107-135.

Alexandre C, and Vico L. 2011. Pathophysiology of Bone Loss in Disuse Osteoporosis. *Joint Bone Spine* 78:572-576.

Allen CR, Kaplan LD, Fluhme DJ, and Harner CD. 2002. Posterior Cruciate Ligament Injuries. *Current Opinion in Rheumatology* 14:142-149.

Allen M. 2002. *Central Lincolnshire Trunks Main (Phase 3) Archaeological Desk Top Study*. Lincoln: Pre-Construct Archaeology.

Altissimi M, Antenucci R, Fiacca C, and Mancini GB. 1986. Long-Term Results of the Conservative Treatment of Fractures of the Distal Radius. *Clinical Orthopaedics and Related Research* 206:202-210.

American College of Radiography. 2013. *ACR-SPR-SSR Practice Guideline for the Performance of Radiography of the Extremities*. Retrieved 4 June 2014 from www.acr.org.

Anderson DD, Chubinskaya S, Guilak F, Martin JA, Oegema TR, Olson SA, and Buckwalter JA. 2011. Post-Traumatic Osteoarthritis: Improved Understanding and Opportunities for Early Intervention. *Journal of Orthopaedic Research* 29:802-809.

Athanasiou KA, Zhu C-F, Lanctot DR, Agrawal CM, and Wang X. 2000. Fundamentals of Biomechanics in Tissue Engineering of Bone. *Tissue Engineering* 6:361-381.

Auerbach BM, and Ruff C. 2004. Human Body Mass Estimation: A Comparison of "Morphometric" and "Mechanical" Methods. *American Journal of Physical Anthropology* 125:331-342.

Auerbach BM, and Ruff CB. 2006. Limb Bone Bilateral Asymmetry: Variability and Commonality among Modern Humans. *Journal of Human Evolution* 50:203-218.

Baetsen S, Bitter P, and Bruintjes TD. 1997. Hip and Knee Osteoarthritis in an Eighteenth Century Urban Population. *International Journal of Osteoarchaeology* 7:628-630.

Baker PA. 2000. *Medical Care for the Roman Army on the Rhine, Danube and British Frontiers in the First, Second and Early Third Centuries AD* (Unpublished doctoral thesis). University of Newcastle upon Tyne.

Baker SP, O'Neill MPH, Haddon WJ, and Long WB. 1974. The Injury Severity Score: A Method for Describing Patients with Multiple Injuries and Evaluating Emergency Care. *The Journal of Trauma* 14:187-196.

Barnes H. 1914. On Roman Medicine and Roman Medical Inscriptions Found in Britain. *Proceedings of the Royal Society of Medicine* 8:71-87.

Barrett CK, Guatelli-Steinberg D, and Sciulli PW. 2012. Revisiting Dental Fluctuating Asymmetry in Neandertals and Modern Humans. *American Journal of Physical Anthropology* 149:193-204.

Bass SL, Saxon L, Daly R, Turner CH, Robling AG, Seeman E, and Stuckey S. 2002. The Effect of Mechanical Loading on the Size and Shape of Bone in Pre-, Peri-, and Postpubertal Girls: A Study in Tennis Players. *Journal of Bone and Mineral Research* 17:2274-2280.

Bass WM. 2005. *Human Osteology: A Laboratory and Field Manual*. Springfield: Missouri Archaeological Society.

Bates MS. 1987. Ethnicity and Pain: A Biocultural Model. *Social Science and Medicine* 24:47-50.

Batra S, and Gupta A. 2002. The Effect of Fracture-Related Factors on the Functional Outcome at 1 Year in Distal Radius Fractures. *Injury* 33:499-502.

Bauer M, Jonsson K, and Nilsson B. 1985. Thirty-Year Follow-up of Ankle Fractures. *Acta Orthopaedica Scandinavica* 56:103-106.

Beauchesne P, and Agarwal SC. 2011. Age-Related Cortical Bone Maintenance and Loss in an Imperial Roman Population. *International Journal of Osteoarchaeology* 24:15-30.

Becker HP, Rosenbaum D, Kriese T, Gerngro H, and Claes L. 1995. Gait Asymmetry Following Successful Surgical Treatment of Ankle Fractures in Young Adults. *Clinical Orthopaedics and Related Research* 311:262-269.

Bedi A, and Le TT. 2004. Subtrochanteric Femur Fractures. *The Orthopedic Clinics of North America* 35:473-483.

Beerekamp MS, Haverlag R, Ubbink DT, Luitse JS, Ponsen KJ, and Goslings JC. 2011. How to Evaluate the Quality of Fracture Reduction and Fixation of the Wrist and Ankle in Clinical Practice: A Delphi Consensus. *Archives of Orthopaedic and Trauma Surgery* 131:739-746.

Belcastro MG, and Mariotti V. 2000. Morphological and Biomechanical Analysis of a Skeleton from Roman Imperial Necropolis of Casalecchio Di Reno (Bologna, Italy, II-III c. A.D.). A Possible Case of Crutch Use. *Collegium Antropologicum* 24:529-539.

Berenbaum F. 2013. Osteoarthritis as an Inflammatory Disease (Osteoarthritis Is Not Osteoarthrosis!). *Osteoarthritis and Cartilage* 21:16-21.

Bidwell P, and Hodgson N, editors. 2009. *The Roman Army in Northern England*. Newcastle upon Tyne: Arbeia Society.

Biewener AA, and Bertram JEA. 1993. Skeletal Strain Patterns in Relation to Exercise Training During Growth. *Journal of Experimental Biology* 185:51-69.

Bijlsma JW, Berenbaum F, and Lafeber FPJG. 2011. Osteoarthritis: An Update with Relevance for Clinical Practice. *Lancet* 377:2115-2126.

Binder M, Eitler J, Deutschmann J, Ladstätter S, Glaser F, and Fiedler D. 2016. Prosthetics in Antiquity - an Early Medieival Wearer of a Foot Prosthesis (6th Century AD) from Hemmaberg/Austria. *International Journal of Paleopathology* 12:29-40.

Bland JM, and Altman DG. 2000. The Odds Ratio. *British Medical Journal* 320:1468.

Bleuze M. 2012. Proximal Femoral Diaphyseal Cross-Sectional Geometry in Orrorin Tugenensis. *HOMO* 63:153-166.

Bloomfield SA. 2010. Disuse Osteopenia. *Current Osteoporosis Reports* 8:91-97.

Bonsall L. 2014. A Comparison of Female and Male Oral Health in Skeletal Populations from Late Roman Britain: Implications for Diet. *Archives of Oral Biology* 59:1279-1300.

Bonsall L, Ogden AR, and Mays S. 2016. A Case of Early Childhood Caries from Late Roman Ancaster, England. *International Journal of Osteoarchaeology* 26:555-560.

Boonyarom O, and Inui K. 2006. Atrophy and Hypertrophy of Skeletal Muscles: Structural and Functional Aspects. *Acta Physiologica* 188:77-89.

Borgers B. 2016. Roman Pottery Production at the Site of Vervoz, Belgium, between the Mid-First Century AD and the End of the Second Century AD. *Journal of Roman Pottery Studies* 16:54.

Borton D, Masterson E, and O'Brien T. 1994. Distal Forearm Fractures in Children: The Role of Hand Dominance. *Journal of Pediatric Orthopaedics* 14:496-497.

Boutin RD, Brossmann J, Sartoris DJ, Reilly D, and Resnick D. 1998. Update on Imaging of Orthopedic Infections. *Orthopedic Clinics of North America* 29:41-66.

Bradley KR. 1985. Child Labour in the Roman World. *Historical Reflections* 12:311-330.

Brandon T, and Pritchard G. 2011. 'Being Fat': A Conceptual Analysis Using Three Models of Disability. *Disability & Society* 26:79-92.

Brent L, and Prowse T. 2014. Grave Goods, Burial Practices and Patterns of Distribution in the Vagnari Cemetery. In: Small A, editor. *Beyond Vagnari: New Themes in the Study of Roman South Italy* Bari: Edipuglia (pp. 99-109).

Brickley M, and Buckberry J. 2015. Picking up the Pieces: Utilizing the Diagnotic Potential of Poorly Preserved Remains. *International Journal of Paleopathology* 8:51-54.

Brooks S, and Suchey JM. 1990. Skeletal Age Determination Based on the Os Pubis: A Comparison of the Acsádi- Nemeskéri and Suchey-Brooks Methods. *Human Evolution* 5:227-238.

Broos PLO, and Bisschop APG. 1991. Operative Treatment of Ankle Fractures in Adults Correlation between Types of Fracture and Final Results. *Injury* 22:403-406.

Brorson S. 2009. Management of Fractures of the Humerus in Ancient Egypt, Greece, and Rome: An Historical Review. *Clinical Orthopaedics and Related Research* 467:1907-1914.

Brothwell D. 1981. *Digging up Bones*. Oxford: Oxford University Press.

Buckberry J. 2015. The (Mis)Use of Adult Age Estimates in Osteology. *Annals of Human Biology* 42:323-331.

Buckland-Wright JC. 1970. A Radiographic Examination of Frontal Sinuses in Early British Populations. *Man, New Series* 5:512-517.

Buckwalter JA, and Felson DT. 2015. Post-Traumatic Arthritis: Definitions and Burden of Disease. In: Olson SA, and Guilak F, editors. *Post-Traumatic Arthritis: Pathogenesis, Diagnosis and Management*. New York: Springer (pp. 7-15).

Buikstra JE, and Ubelaker DH, editors. 1994. *Standards for Data Collection from Human Skeletal Remains: Proceedings of a Seminar at the Field Museum of Natural History*. Fayetteville: Arkansas Archaeological Survey.

Burnham BC, and Wacher J. 1990. *The 'Small Towns' of Roman Britain*. London: B.T. Batsford Ltd.

Burr DB. 1997. Muscle Strength, Bone Mass, and Age-Related Bone Loss. *Journal of Bone and Mineral Research* 12:1547-1551.

Burr DB, Forwood MR, Fyhrie DP, Martin RB, Schaffler MB, and Turner CH. 1997. Bone Microdamage and Skeletal Fragility in Osteoporotic and Stress Fractures. *Journal of Bone and Mineral Research* 12:6-15.

Byl NN, Kohlhase W, and Engel G. 1999. Functional Limitation Immediately after Cast Immobilization and Closed Reduction of Distal Radius Fractures: Preliminary Report. *Journal of Hand Therapy* 12:201-211.

Calpur OU, Copuroglu C, and Ozcan M. 2002. Avulsion Fractures of Both Anterior and Posterior Cruciate Ligament Tibial Insertions. *Knee Surgery, Sports Traumatology, Arthroscopy* 10:223-225.

Campbell I, Bicket A, Sanderson DCW, and Whitelaw L. 2011. Geomorphology. In: Small A, editor. *Vagnari: The Village, the Industries, the Imperial Property*. Bari: Edipuglia (pp. 37-51).

Campbell WW. 2008. Evaluation and Management of Peripheral Nerve Injury. *Clinical Neurophysiology* 119:1951-1965.

Carreras C, and De Soto P. 2013. The Roman Transport Network: A Precedent for the Integration of the European Mobility. *Historical Methods: A Journal of Quantitative and Interdisciplinary History* 46:117-133.

Carroll M. 2013a. Exploring the Vicus at the Roman Imperial Estate at Vagnari (Comune Di Irsina, Provincia Di Matera, Regione Basilicata). *Papers of the British School at Rome* 81:381-384.

Carroll M. 2013b. *Investigating Agricultural Activities at the Roman Imperial Estate at Vagnari (Puglia) in 2013*. Retrieved April 26, 2016 from www.romansociety.org/fileadmin/documents/pdf/M_Carroll_2013.pdf.

Carroll M. 2014. Vagnari 2012: New Work in the Vicus by the University of Sheffield. In: Small A, editor. *Beyond Vagnari: New Themes in the Study of Roman South Italy* Bari: Edipuglia (pp. 79-87).

Carroll M, and Prowse T. 2014. Exploring the Vicus and the Necropolis at the Roman Imperial Estate at Vagnari (Comune Di Gravina in Puglia, Provincia Di Bari, Regione Puglia). *Papers of the British School at Rome* 82:353-356.

Celsus. 1961. De Medicina. Translated By: Spencer W. Cambridge, MA: Harvard University Press.

Chan K, Jupiter J, Leffert R, and Marti R. 1999a. Clavicle Malunion. *Journal of Shoulder and Elbow Surgery* 8:287-290.

Chan KY, Jupiter JB, Leffert RD, and Marti R. 1999b. Clavicle Malunion. *Journal of Shoulder and Elbow Surgery* 8:287-290.

Chen EM, Masih S, Chow K, Matcuk G, and Patel D. 2012. Periosteal Reaction: Review of Various Patterns Associated with Specific Pathology. *Contemporary Diagnostic Radiology* 35:1-5.

Cho H, and Stout SD. 2011. Age-Associated Bone Loss and Intraskeletal Variability in the Imperial Romans. *Journal of Anthropological Sciences* 89:109-125.

Christensen B, Dyrberg E, Aagaard P, Kjaer M, and Langberg H. 2008. Short-Term Immobilization and Recovery Affect Skeletal Muscle but Not Collagen Tissue Turnover in Humans. *Journal of Applied Physiology* 105:1845-1851.

Cilliers L, and Retief FP. 2006. Medical Practice in Graeco-Roman Antiquity. *Curationis* 29:34-40.

Civil ID, and Schwab CW. 1988. The Abbreviated Injury Scale, 1985 Revision: A Condensed Chart for Clinical Use. *The Journal of Trauma* 28:87-90.

Claes L, Recknagel S, and Ignatius A. 2012. Fracture Healing under Healthy and Inflammatory Conditions. *Nature Reviews Rheumatology* 8:133-143.

Cokayne K. 2003. *Experiencing Old Age in Ancient Rome*. London: Routledge.

Corbeill A. 2004. *Nature Embodied: Gesture in Ancient Rome*: Princeton University Press.

Cowgill LW, Mednikova MB, Buzhilova AP, and Trinkaus E. 2012. The Sunghir 3 Upper Paleolithic Juvenile: Pathology Versus Persistence in the Paleolithic. *International Journal of Osteoarchaeology* 25:176-187.

Cox M. 1989. *The Human Bones from Ancaster. Ancient Monuments Laboratory Report 93/89*. London: Historic Buildings and Monuments Commission for England.

Crombez G, Vlaeyen JWS, Heuts PHTG, and Lysens R. 1999. Pain-Related Fear Is More Disabling Than Pain Itself: Evidence on the Role of Pain-Related Fear in Chronic Back Pain Disability. *Pain* 80:329-339.

Crubézy E, Goulet J, Jaruslav B, Jan J, Daniel R, and Bertrand L. 2002. Epidemiology of Osteoarthritis and Enthesopathies in a European Population Dating Back 7700 Years. *Joint Bone Spine* 69:580-588.

Cybulska M, Jesman C, Mludzik A, and Kula A. 2012. On Roman Military Doctors and Their Medical Instruments. *Military Pharmacy and Medicine* 2:1-8.

Danforth ME, and Thompson A. 2008. An Evaluation of Determination of Handedness Using Standard Osteological Measurements. *Journal of Forensic Sciences* 53:777-781.

Darton Y. 2010. Scapular Stress Fracture: A Palaeopathological Case Consistent with Crutch Use. *International Journal of Osteoarchaeology* 20:113-121.

Davies RW. 1970. Some Roman Medicine. *Medical History* 14:101-106.

Davis LE. 2015. Disorders of Peripheral Nerves. In: Davis LE, and Richardson SP, editors. *Fundamentals of Neurologic Disease*. New York: Springer (pp. 63-72).

De Boer HH, Merwe AE, Hammer S, Steyn M, and Maat GJR. 2012. Assessing Post-Traumatic Time Interval in Human Dry Bone. *International Journal of Osteoarchaeology* 25:98-109.

DeFranco MJ, and Lawton JN. 2006. Radial Nerve Injuries Associated with Humeral Fractures. *The Journal of Hand Surgery* 31:655-663.

Dequeker J. 1976. Quantitative Radiology: Radiogrammetry of Cortical Bone. *British Journal of Radiology* 1976:912-920.

Derikx LC, Verdonschot N, and Tanck E. 2015. Towards Clinical Application of Biomechanical Tools for the Prediction of Fracture Risk in Metastaic Bone Disease. *Journal of Biomechanics* 48:761-766.

Dettwyler KA. 1991. Can Palaeopathology Provide Evidence for "Compassion"? *American Journal of Physical Anthropology* 84:375-384.

Doherty C, Bleakley C, Hertel J, Caulfield B, Ryan J, and Delahunt E. 2015. Lower Extremity Function During Gait in Participants with First Time Acute Lateral

Ankle Sprain Compared to Controls. *Journal of Electromyography and Kinesiology* 25:182-192.

Donatto KC. 2001. Ankle Fractures and Syndesmosis Injuries. *Orthopedic Clinics of North America* 32:79-90.

Douglas (Director). 2002. The Roman's Panic (Ancaster, Lincolnshire) [Television Series Episode]. *Time Team*. UK: Channel 4. 55 min.

Dowthwaite JN, and Scerpella TA. 2009. Skeletal Geometry and Indicies of Bone Strength in Artistic Gymnasts. *Journal of Musculoskeletal Neuronal Interactions* 9:198-214.

Ducher G, Courteix D, Meme S, Magni C, Viala JF, and Benhamou CL. 2005. Bone Geometry in Response to Long-Term Tennis Playing and Its Relationship with Muscle Volume: A Quantitative Magnetic Resonance Imaging Study in Tennis Players. *Bone* 37:457-466.

Edwards C. 2005. The Suffering Body: Philosophy and Pain in Seneca's Letters. In: Porter JI, editor. *Constructions of the Classical Body*. Ann Arbor: The University of Michigan Press (pp. 252-268).

Edwards RR, Doleys DM, Fillingim RB, and Lowery D. 2001. Ethnic Differences in Pain Tolerance: Clinical Implications in a Chronic Pain Population. *Psychosomatic Medicine* 63:316-323.

Egol KA, Koval KJ, and Zuckerman JD. 2010. *Handbook of Fractures*. Philadelphia: Lippincott Williams & Wilkins.

Einhorn TA. 1992. Bone Strength: The Bottom Line. *Calcified tissue international* 51:333-339.

Einhorn TA, and Gerstenfeld LC. 2015. Fracture Healing: Mechanisms and Interventions. *Nature Reviews Rheumatology* 11:45-54.

Engsberg J, Leduc S, Ricci W, and Borrelli Jr J. 2014. Improved Function and Joint Kinematics after Correction of Tibial Malalignment. *American Journal of Orthopedics* 43:E313-318.

Ensrud KE. 2013a. Epidemiology of Fracture Risk with Advancing Age. *The Journals of Gerontology Series A: Biological Sciences and Medical Sciences* 68:1236-1242.

Ensrud KE. 2013b. Epidemiology of Fracture Risk with Advancing Age. *Journals of Gerontology Medical Sciences* 68:1236-1242.

Eyres KS, and Kanis JA. 1995. Bone Loss after Tibial Fracture: Evaluated by Dual-Energy X-Ray Absorptiometry. *Journal of Bone and Joint Surgery (Br)* 77-B:473-478.

Fabry J, and Casteleyn P-P. 2014. Non-Operative Treatment of Long Bone Fractures in Adults. In: Bentley G, editor. *European Surgical Orthopaedics and Traumatology*. Berlin: Springer-Verlag (pp. 139-158).

Faulkner JA, Larkin LM, Claflin DR, and Brooks SV. 2007. Age-Related Changes in the Structure and Function of Skeletal Muscles. *Clinical and Experimental Pharmacology and Physiology* 34:1091-1096.

Field A. 2009. *Discovering Statistics Using SPSS*. Los Angeles: Sage Publications.

Finlay N, editor. 1999. *Disability and Archaeology*. Cambridge: The Department of Archaeology.

Fiorentino G, Primavera M, Dand A, and Monckton S. 2011. L'analisi Dei Resti Vegetali Carbonizzati. In: Small A, editor. *Vagnari: The Village, the Industries, the Imperial Property*. Bari: Edupuglia (pp. 329-343).

Fletcher L, Codrington J, and Parkinson I. 2014. Effects of Fatigue Induced Damage on the Longitudinal Fracture Resistance of Cortical Bone. *Journal of Materials Science: Materials in Medicine* 25:1661-1670.

Forward DP, Davis TRC, and Sithole JS. 2008. Do Young Patients with Malunited Fractures of the Distal Radius Inevitably Develop Symptomatic Post-Traumatic Osteoarthritis? *The Journal of Bone and Joint Surgery* 90-B:629-637.

Frere SS. 1961. Some Romano-British Sculptures from Ancaster and Wilsford, Lincolnshire. *The Antiquaries Journal* 41:229-231.

Frick SL. 2015. Skeletal Growth, Development, and Healing as Related to Pediatric Trauma. In: Mencio GA, and Swiontkowski MF, editors. *Green's Skeletal Trauma in Children*. Philadelphia: Elsevier (pp. 1-15).

Frost HM. 1989. The Biology of Fracture Healing: An Overview for Clinicians. Part II. *Clinical Orthopaedics and Related Research* 248:294-309.

Frost HM. 1990. Skeletal Structural Adaptations to Mechanical Useage (Satmu): 1. Redefining Wolff's Law: The Bone Modeling Problem. *The Anatomical Record* 226:403-413.

Gabl M, and Arora R. 2014. Outcome Assessment after Distal Radius Fractures. In: Hove LM, Lindau T, and Holmer P, editors. *Distal Radius Fractures*. Heidelberg: Springer (pp. 53-59).

Galloway A, Zephro L, and Wedel VL. 2014. Classification of Fractures. In: Wedel VL, and Galloway A, editors. *Broken Bones*. 2nd ed. Springfield: Charles C. Thomas (pp. 59-72).

Garvin HM, and Passalacqua NV. 2012. Current Practices by Forensic Anthropologists in Adult Skeletal Age Estimation. *Journal of Forensic Sciences* 57:427-433.

Gaston MS, and Simpson AHR. 2007. Inhibition of Fracture Healing. *The Bone & Joint Journal* 89-B:1553-1560.

Giangregorio L, and McCartney N. 2006. Bone Loss and Muscle Atrophy in Spinal Cord Injury: Epidemiology, Fracture Prediction, and Rehabilitation Strategies. *Journal of Spinal Cord Medicine* 29:489-500.

Gilmour RJ, Gowland R, Roberts C, Bernert Z, Kiss KK, and Lassányi G. 2015. Gendered Differences in Accidental Trauma to Upper and Lower Limb Bones at Aquincum, Roman Hungary. *International Journal of Paleopathology* 11:1-17.

Gleeson BJ. 1997. Disability Studies: A Historical Materialist View. *Disability & Society* 12:179-202.

Glencross B. 2011. Skeletal Injury across the Life Course: Towards Understanding Social Agency. In: Agarwal SC, and Glencross B, editors. *Social Bioarchaeology*. Chichester: Wiley-Blackwell (pp. 390-409).

Goodman CA, Hornberger TA, and Robling AG. 2015. Bone and Skeletal Muscle: Key Players in Mechanotransduction and Potential Overlapping Mechanisms. *Bone* 80:24-36.

Gowland RL, and Chamberlain AT. 2002. A Bayesian Approach to Ageing Perinatal Skeletal Material from Archaeological Sites: Implications for the Evidence for Infanticide in Roman-Britain. *Journal of Archaeological Science* 29:677-685.

Grauer AL, and Roberts CA. 1996. Paleoepidemiology, Healing, and Possible Treatment of Trauma in the Medieval Cemetery Population of St. Helen-on-the-Walls, York, England. *American Journal of Physical Anthropology* 100:531-544.

Greene MA, and Loeser RF. 2015. Aging-Related Inflammation in Osteoarthritis. *Osteoarthritis and Cartilage* 23:1966-1971.

Greenwood D, Muir K, Doherty M, Milner S, Stevens M, and Davis T. 1997. Conservatively Managed Tibial Shaft Fractures in Nottingham, UK: Are Pain, Osteoarthritis, and Disability Long-Term Complications? *Journal of Epidemiology and Community Health* 51:701-704.

Gregg EW, Pereira MA, and Caspersen CJ. 2000. Physical Activity, Falls, and Fractures among Older Adults: A Review of the Epidemiologic Evidence. *Journal of the American Geriatrics Society* 48:883-893.

Gupta HS, and Zioupos P. 2008. Fracture of Bone Tissue: The 'Hows' and the 'Whys'. *Medical Engineering & Physics* 30:1209-1226.

Haara M, Heliövaara M, Impivaara O, Arokoski JPA, Manninen P, Knekt P, Kärkkäinen A, Reunanen A, Aromaa A, and Kröger H. 2006. Low Metacarpal Index Predicts Hip Fracture: A Prospective Population Study of 3,561 Subjects with 15 Years of Follow-Up. *Acta Orthopaedica* 77:9-14.

Hall J. 2014. With Criminal Intent? Forgers at Work in Roman London. *Britannia* 45:165-194.

Hamblen DL, Simpson AHR, and Adams JC. 2007. *Adams's Outline of Fractures, Including Joint Injuries*. Edinburgh: Churchill Livingstone Elsevier.

Harlow M, and Laurence R. 2002. *Growing up and Growing Old in Ancient Rome: A Life Course Approach*. London: Routledge.

Hartley BR, Roberts CS, and Giannoudis PV. 2015. Current Treatment and Outcomes of Intra-Articular Fractures. *Post-Traumatic Arthritis*. Springer (pp. 269-283).

Harvey BK. 2004. *Roman Lives: Ancient Roman Life as Illustrated by Latin Inscriptions*. Newburyport: Focus Publishing.

Harwood PJ, Newman JB, and Michael ALR. 2010. An Update on Fracture Healing and Non-Union. *Orhopaedics and Trauma* 21:9-23.

Hawkes CFC, Richmond IA, and Nash-Williams VE. 1946. The Roman Occupation. *Archaeology Journal* 103:110-136.

Hazelwood SJ, Martin RB, Rashid MM, and Rodrigo JJ. 2001. A Mechanistic Model for Internal Bone Remodeling Exhibits Different Dynamic Responses in Disuse and Overload. *Journal of Biomechanics* 34:299-308.

Heaney R, Abrams S, Dawson-Hughes B, Looker A, Looker A, Marcus R, Matkovic V, and Weaver C. 2000. Peak Bone Mass. *Osteoporosis international* 11:985-1009.

Hegmon M. 2016. Archaeology of the Human Experience: An Introduction. *Archaeological Papers of the American Anthropological Association* 27:7-21.

Higgs J, Refshauge KM, and Ellis E. 2001. Portrait of the Physiotherapy Profession. *Journal of Interprofessional Care* 15:79-89.

Hippocrates. 1849a. On Fractures. *In: The Genuine Works of Hippocrates*. Translated By: Adams F. London: Sydenham Society (pp. 489-552).

Hippocrates. 1849b. On the Articulations. *In: The Genuine Works of Hippocrates*. Translated By: Adams F. London: Sydenham Society (pp. 553-654).

Historic England. 2015. *Causennae Roman Town*. Retrieved November 29, 2015 from http://www.pastscape.org.uk/hob.aspx?hob_id=325933.

Hodgson S. 2006. Proximal Humerus Fracture Rehabilitation. *Clinical Orthopaedics and Related Research* 442:131-138.

Holt BM. 2003. Mobility in Upper Paleolithic and Mesolithic Europe: Evidence from the Lower Limb. *American Journal of Physical Anthropology* 122:200-215.

Holt BM, Fornaciari G, and Formicola V. 2002. Bone Remodelling Following a Lower Leg Fracture in the 11,000-Year-Old Hunter-Gatherer from Vado All' Arancio (Italy). *International Journal of Osteoarchaeology* 12:402-406.

Honkasalo ML. 2001. Vicissitudes of Pain and Suffering: Chronic Pain and Liminality. *Medical Anthropology* 19:319-353.

Huang C, and Ogawa R. 2010. Mechanotransduction in Bone Repair and Regeneration. *The FASEB Journal* 24:3625-3632.

Hyldstrup L, and Nielsen SP. 2001. Metacarpal Index by Digital X-Ray Radiogrammetry. *Journal of Clinical Densitometry* 4:299-306.

Íșcan M, Loth S, and Wright R. 1985. Age Estimation from the Rib by Phase Analysis: White Females. *Journal of Forensic Sciences* 30:853-863.

Íșcan YM, Loth SR, and Wright RK. 1984. Metamorphosis at the Sternal Rib End: A New Method to Estimate Age at Death in White Males. *American Journal of Physical Anthropology* 65:147-156.

Ives R, and Brickley MB. 2004. A Procedural Guide to Metacarpal Radiogrammetry in Archaeology. *International Journal of Osteoarchaeology* 14:7-17.

Jones G. 1969. Radiological Appearances of Disuse Osteoporosis. *Clinical Radiology* 20:345-353.

Jones HH, Priest JD, Hayes WC, Tichenor CC, and Nagel DA. 1977. Humeral Hypertrophy in Response to Exercise. *The Journal of Bone and Joint Surgery* 59-A:204-208.

Judd M. 2002a. Ancient Injury Recidivism: An Example from the Kerma Period of Ancient Nubia. *International Journal of Osteoarchaeology* 12:89-106.

Judd MA. 2002b. Comparison of Long Bone Trauma Recording Methods. *Journal of Archaeological Science* 29:1255-1265.

Kalia RB, and Agarwal AC. 2014. Fragility Fractures of the Distal Radius. *Journal of Orthopedics, Traumatology and Rehabilitation* 7:113.

Kanis J, McCloskey E, Johansson H, Cooper C, Rizzoli R, and Reginster J-Y. 2013. European Guidance for the Diagnosis and Management of Osteoporosis in Postmenopausal Women. *Osteoporosis international* 24:23-57.

Kapoor M. 2015. Pathogenesis of Osteoarthritis. In: Kapoor M, and Mahomed NN, editors. *Osteoarthritis: Pathogenesis, Diagnosis, Available Treatments, Drug Safety, Regenerative and Precision Medicine*. Switzerland: Springer (pp. 1-28).

Karnezis IA, Panagiotopoulous E, Tyllianakis M, Megas P, and Lambiris E. 2005. Correlation between Radiological Parameters and Patient-Rated Wrist Dysfunction Following Fractures of the Distal Radius. *Injury* 36:1435-1439.

Kennedy CE, Moore PJ, Peterson RA, Katzman MA, Vermani M, and Charmak WD. 2011. What Makes People Anxious About Pain? How Personality and Perception Combine to Determine Pain Anxiety Responses in Clinical and Non-Clinical Populations. *Anxiety, Stress, and Coping* 24:179-200.

Khosla S. 2012. Pathogenesis of Age-Related Bone Loss in Humans. *Journals of Gerontology Medical Sciences* 68:1226-1235.

King H. 2001. *Greek and Roman Medicine*. London: Bristol Classical Press.

Knudson D. 2007. *Fundamentals of Biomechanics*. New York: Springer.

Knüsel CJ, and Goeggel S. 1993. A Cripple from the Medieval Hospital of Sts James and Mary Magdalen, Chichester. *International Journal of Osteoarchaeology* 3:155-165.

Kobbe P, and Pape H-C. 2014. Tibial Plateau Fractures. In: Oestern H-J, Trentz O, and Uranues S, editors. *Bone and Joint Injuries*. Berlin Springer (pp. 333-339).

Kohn MD, Sassoon AA, and Fernando ND. 2016. Classifications in Brief: Kellgren-Lawrence Classification of Osteoarthritis. *Clinical Orthopaedics and Related Research* Early View:1-8.

Kristiansen B, Angermann P, and Larsen TK. 1989. Functional Results Following Fractures of the Proximal Humerus a Controlled Clinical Study Comparing Two Periods of Immobilization. *Archives of Orthopaedic and Trauma Surgery* 108:339-341.

Kulkarni J, Adams J, Thomas E, and Silman A. 1998. Association between Amputation, Arthritis and Osteopenia in British Male War Veterans with Major Lower Limb Amputations. *Clinical Rehabilitation* 12:348-353.

Kundel K, Braun W, Wieberneit J, and Rüter A. 1996. Intraarticular Distal Humerus Fractures: Factors Affecting Functional Outcome. *Clinical Orthopaedics and Related Research* 332:200-208.

Kusaba A, and Saito S. 2016. Biomechanics of Fracture in Growth Period. *Biomechanics and Biomaterials in Orthopedics*. London: Springer (pp. 307-310).

Lang T, LeBlanc A, Evans H, Lu Y, Genant H, and Yu A. 2004. Cortical and Trabecular Bone Mineral Loss from the Spine and Hip in Long-Duration Spaceflight. *Journal of Bone and Mineral Research* 19:1006-1012.

Lau RY-c, and Guo X. 2011. A Review on Current Osteoporosis Research: With Special Focus on Disuse Bone Loss. *Journal of Osteoporosis* 2011:1-6.

Lazenby RA. 1990. Continuing Periosteal Apposition II: The Significance of Peak Bone Mass, Strain Equilibrium, and Age-Related Activity Differentials for Mechanical Compensation in Human Tubular Bones. *American journal of physical anthropology* 82:473-484.

Lazenby RA. 1998. Second Metacarpal Cross-Sectional Geometry: Rehabiliting a Circular Argument. *American Journal of Human Biology* 10:747-756.

Lazenby RA, and Pfeiffer SK. 1993. Effects of a Nineteenth Century Below-Knee Amputation and Prosthesis on Femoral Morphology. *International Journal of Osteoarchaeology* 3:19-28.

LeBlanc A, Schneider V, Shackelford L, Oganov V, Bakulin A, and Voronin L. 2000. Bone Mineral and Lean Tissue Loss after Long Duration Space Flight. *Journal of Musculoskeletal Neuronal Interactions* 1:157-160.

Leblanc AD, Schneider VS, Evans HJ, Engelbretson DA, and Krebs JM. 1990. Bone Mineral Loss and Recovery after 17 Weeks of Bed Rest. *Journal of Bone and Mineral Research* 5:843-850.

Ledger M, Holtzhausen LM, Constant D, and Morris AG. 2000. Biomechanical Beam Analysis of Long Bones from a Late 18th Century Slave Cemetery in Cape Town, South Africa. *American Journal of Physical Anthropology* 112:207-216.

Ledger M, Leeks N, Ackland T, and Wang A. 2005. Short Malunions of the Clavicle: An Anatomic and Functional Study. *Journal of Shoulder and Elbow Surgery* 14:349-354.

Leech R, Besly EM, Everton RF, and Fowler E. 1981. The Excavation of a Romano-British Farmstead and Cemetery on Bradley Hill, Somerton, Somerset. *Britannia* 12:177-122.

Li X, Wagner M, Wu X, Tarasov P, Zhang Y, Schmidt A, Goslar T, and Gresky J. 2013. Archaeological and Palaeopathological Study on the Third/Second Century BC Grave from Turfan, China: Individual Health History and Regional Implications. *Quaternary International* 290:335-343.

Lieverse AR, Mack B, Bazaliiskii VI, and Weber AW. 2016. Revisiting Osteoarthritis in the Cis-Baikal: Understanding Behavioral Variability and Adaptation among Middle Holocene Foragers. *Quaternary International* 405:160-171.

Lieverse AR, Metcalf MA, Bazaliiskii VI, and Weber AW. 2008. Pronounced Bilateral Asymmetry of the Complete Upper Extremity: A Case from the Early Neolithic Baikal, Siberia. *International Journal of Osteoarchaeology* 18:219-239.

Lifeso R, and Younge D. 1990. The Neglected Hip Fracture. *Journal of Orthopaedic Trauma* 4:287-292.

Lin C-WC, Moseley AM, Herbert RD, and Refshauge KM. 2009. Pain and Dorsiflexion Range of Motion Predict Short- and Medium-Term Activity Limitation in People Receiving Physiotherapy Intervention after Ankle Fracture: An Observational Study. *Australian Journal of Physiotherapy* 55:31-37.

Lincolnshire Historic Environment Record. 2012a. Roman Building on Land at 1 Ermine Street, Ancaster. Monument Report. HER#: 38964. Heritage Gateway. Retrieved December 27, 2015 from http://www.heritagegateway.org.uk/Gateway/Results_Single.aspx?uid=MLI97541&resourceID=1006

Lincolnshire Historic Environment Record. 2012b. Roman Coin Hoard, Ancaster. Find Spot Record. HER#: 30325. Retrieved December 27, 2015 from http://www.heritagegateway.org.uk/Gateway/Results_Single.aspx?uid=MLI30325&resourceID=1006

Lincolnshire Historic Environment Record. 2012c. Roman Kiln and Cemetery. Monument Report. HER#: 30341. Heritage Gateway. Retrieved December 27, 2015 from http://www.heritagegateway.org.uk/Gateway/Results_Single.aspx?uid=MLI30341&resourceID=1006

Llewellyn A, and Hogan K. 2000. The Use and Abuse of Models of Disability. *Disability & Society* 15:157-165.

Loeser RF. 2009. Aging and Osteoarthritis: The Role of Chondrocyte Senescence and Aging Changes in the Cartilage Matrix. *Osteoarthritis and Cartilage* 17:971-979.

Loeser RF, Goldring SR, Scanzello CR, and Goldring MB. 2012. Osteoarthritis: A Disease of the Joint as an Organ. *Arthritis & Rheumatism* 64:1697-1707.

Lomond KV, and Côté JN. 2011. Differences in Posture–Movement Changes Induced by Repetitive Arm Motion in Healthy and Shoulder-Injured Individuals. *Clinical Biomechanics* 26:123-129.

Loth SR, and Henneberg M. 1996. Mandibular Ramus Flexure: A New Morphologic Indicator of Sexual Dimorphism in the Human Skeleton. *American Journal of Physical Anthropology* 99:473-485.

Loth SR, and Henneberg M. 2000. Gonial Eversion: Facial Architecture, Not Sex. *HOMO* 51:81-89.

Lovejoy CO, Meindl RS, Pryzbeck TR, and Mensforth RP. 1985. Chronological Metamorphosis of the Auricular Surface of the Ilium: A New Method for the Determination of Adult Skeletal Age at Death. *American Journal of Physical Anthropology* 68:15-28.

Lovell NC. 1990. *Patterns of Injury and Illness in Great Apes*. Washington, D.C.: Smithsonian Institution Press.

Lovell NC. 1997. Trauma Analysis in Paleopathology. *Yearbook of Physical Anthropology* 40:139-170.

Lovell NC. 2008. Analysis and Interpretation of Skeletal Trauma. In: Katzenberg MA, and Saunders SR, editors. *Biological Anthropology of the Human Skeleton*. 2nd Ed. ed. Hoboken, NJ: John Wiley & Sons, Inc. (pp. 341-386).

Lovell NC. 2016. Tiptoeing through the Rest of His Life: A Functional Adaptation to a Leg Shortened by Femoral Neck Fracture. *International Journal of Paleopathology* 13:91-95.

Lovgren A, and Hellstrom K. 2012. Reliability and Validity of Measurement and Associations between Disability and Behavioural Factors in Patients with Colles' Fracture. *Physiotherapy Theory and Practice* 28:188-197.

Lubowitz JH, Elson WS, and Guttmann D. 2005. Part II: Arthroscopic Treatment of Tibial Plateau Fractures: Intercondylar Eminence Avulsion Fractures. *Arthroscopy: The Journal of Arthroscopic and Related Surgery* 21:86-92.

MacDermid JC, Donner A, Richards RS, and Roth JH. 2002. Patient Versus Injury Factors as Predictors of Pain and Disability Six Months after a Distal Radius Fracture. *Journal of Clinical Epidemiology* 55:849-854.

Macintosh AA, Davies TG, Ryan TM, Shaw CN, and Stock JT. 2013. Periosteal Versus True Cross-Sectional Geometry: A Comparison Along Humeral, Femoral, and Tibial Diaphyses. *American Journal of Physical Anthropology* 150:442-452.

Macintosh AA, Pinhasi R, and Stock JT. 2014. Lower Limb Skeletal Biomechanics Track Long-Term Decline in Mobility across ~6150 Years of Agriculture in Central Europe. *Journal of Archaeological Science* 52:376-390.

MacKinnon M. 2011. The Faunal Remains. In: Small A, editor. *Vagnari: The Village, the Industries, the Imperial Property*. Bari: Edipuglia (pp. 305-328).

Maggiano IS, Schultz M, Kierdorf H, Sosa TS, Maggiano CM, and Tiesler Blos V. 2008. Cross-Sectional Analysis of Long Bones, Occupational Activities and Long-Distance Trade of the Classic Maya from Xcambo--Archaeological and Osteological Evidence. *American Journal of Physical Anthropology* 136:470-477.

Marchi D, Sparacello VS, Holt BM, and Formicola V. 2006. Biomechanical Approach to the Reconstruction of Activity Patterns in Neolithic Western Liguria, Italy. *American Journal of Physical Anthropology* 131:447-455.

Marsden JH. 1863. Observations on Certain Roman Remains at Ancaster. *Reports and Papers of the Architectural and Archaeological Societies of the Counties of Lincoln and Northampton*. Sleaford.

Martin RB, Burr DB, Sharkey NA, and Fyhrie DP. 2015. *Skeletal Tissue Mechanics*. New York: Springer.

Matcuk Jr. GR, Mahanty SR, Skalski MR, Patel DB, White EA, and Gottsegen CJ. 2016. Stress Fractures: Pathophysiology, Clinical Presentation, Imaging Features, and Treatment Options. *Emergency Radiology* 23:365-375.

Matheson GO, Clement DB, McKenzie DC, Taunton JE, Lloyd-Smith DR, and MacIntyre JG. 1987. Stress Fractures in Atheletes: A Study of 320 Cases. *The American Journal of Sports Medicine* 15:46-58.

Mays S. 2015a. Age-Associated Reduction in Cortical Bone in Males, Trends from the Third Century AD to the Present Day. *Calcified Tissue International* 96:370-371.

Mays S. 2015b. The Effect of Factors Other Than Age Upon Skeletal Age Indicators in the Adult. *Annals of Human Biology* 42:332-341.

Mays S, and Faerman M. 2001. Sex Identification in Some Putative Infanticide Victims from Roman Britain Using Ancient DNA. *Journal of Archaeological Science* 28:555-559.

Mays SA. 2002. Asymmetry in Metacarpal Cortical Bone in a Collection of British Post-Mediaeval Human Skeletons. *Journal of Archaeological Science* 29:435-441.

Mays SA. 2006a. Age-Related Cortical Bone Loss in Women from a 3rd-4th Century AD Population from England. *American Journal of Physical Anthropology* 129:518-528.

Mays SA. 2006b. A Palaeopathological Study of Colles' Fracture. *International Journal of Osteoarchaeology* 16:415-428.

McCallum M, and vanderLeest H. 2011. Archaeological Fieldwork Reports: Excavations at San Felice, June-July 2009. *Papers of the British School at Rome* 78:334-336.

McCallum M, and vanderLeest H. 2014. Research at San Felice: The Villa on the Imperial Estate. In: Small A, editor. *Beyond Vagnari: New Themes in the Study of Roman South Italy*. Bari: Edipuglia (pp. 123-134).

McCallum M, vanderLeest H, Veal R, Taylor A, Cooney L, Brown L, and Munro M. 2011. The Roman Villa at San Felice: Investigations, 2004–2010. *Mouseion: Journal of the Classical Association of Canada* 11:25-108.

McGee AM, Qureshi AA, and Porter KM. 2004. Review of the Biomechanics and Patterns of Limb Fractures. *Trauma* 6:29-40.

McGrath TM, Waddington G, Scarvell JM, Ball NB, Creer R, Woods K, and Smith D. 2016. The Effect of Limb Dominance on Lower Limb Functional Performance – a Systematic Review. *Journal of Sports Sciences* 34:289-302.

McKee M. 2000. Aseptic Non-Union. In: Rüedi TP, and Murphy WM, editors. *AO Principles of Fracture Management*. Stuttgart: Thieme (pp. 748-762).

McKee MD, Wild LM, and Schemitsch EH. 2003. Midshaft Malunions of the Clavicle. *Journal of Bone and Joint Surgery* 85:790-797.

McKinley JI. 2004. Compiling a Skeletal Inventory: Disarticulated and Co-Mingled Remains. In: Brickley M, and McKinley JI, editors. *Guidelines to the Standards for Recording Human Remains*. Southampton: British Association for Biological Anthropology and Osteoarchaeology and the Institute of Field Archaeologists (pp. 14-17).

McKinley T. 2003. Principles of Fracture Healing. *Surgery (Oxford)* 21:209-212.

Meals RA. 1979. The Laterality of Fractures and Dislocations with Respect to Handedness. *Clinical Orthopaedics and Related Research* 143:158-161.

Meema HE, and Meema S. 1987. Postmenopausal Osteoporosis: Simple Screening Method for Diagnosis before Structural Failure. *Radiology* 164:405-410.

Melenevsky Y, Yablon CM, Ramappa A, and Hochman MG. 2011. Clavicle and Acromioclavicular Joint Injuries: A Review of Imaging, Treatment, and Complications. *Skeletal Radiology* 40:831-842.

Meyers MH, and McKeever FM. 1959. Fracture of the Intercondylar Eminence of the Tibia. *The Journal of Bone and Joint Surgery* 41-A:209-222.

Millet PJ, and Rushton N. 1995. Early Mobilization in the Treatment of Colles' Fracture: A 3 Year Prospective Study. *Injury* 26:671-675.

Milner GR. 1992. Determination of Skeletal Age and Sex. *A Manual Prepared for the Dickson Mounds Reburial Team*. Lewiston, Illinois: Dickson Mounds Museum.

Minaire P. 1989. Immobilization Osteoporosis: A Review. *Clinical Rheumatology* 8:95-103.

Moeller WO. 1969. The Male Weavers at Pompeii. *Technology and Culture* 10:561-566.

Monaco D. 1890. *Guide Général Du Musée National De Naples Suivant La Nouvelle Numération D'après Le Dernier Classement*. Naples: Imprimerie E. Pietrocola.

Morbeck ME, Zihlman AL, Sumner DR, and Galloway A. 1991. Poliomyelitis and Skeletal Asymmetry in Gombe Chimpanzees. *Primates* 32:77-91.

Motamedzade M, and Moghimbeigi A. 2012. Musculoskeletal Disorders Amoung Female Carpet Weavers in Iran. *Ergonomics* 55:229-236.

Mouzopoulos G, Kanakaris NK, Kontakis G, Obakponovwe O, Townsend R, and Giannoudis PV. 2011. Managment of Bone Infections in Adults: The Surgeon's and Microbiologist's Perspectives. *Injury* 42:S18-S23.

Muir JM, Ye C, Bhandari M, Adachi JD, and Thabane L. 2013. The Effect of Regular Physical Activity on Bone Mineral Density in Post-Menopausal Women Aged 75 and Over: A Retrospective Analysis from the Canadian Multicentre Osteoporosis Study. *BMC Musculoskeletal Disorders* 14:1.

Mukhopadhyay P, and Srivastava S. 2010. Evaluating Ergonomic Risk Factors in Non-Regulated Stone Carving Units of Jaipur. *Work* 35:87-99.

Nash CE, Mickan SM, Del Mar CB, and Glasziou PP. 2004. Resting Injured Limbs Delays Recovery: A Systematic Review. *Journal of Family Practice* 53:706-706.

Nause CL. 2010. *Prevalence and Timing of Enamel Hypoplasias in the Vagnari Skeletal Sample (1st - 4th Centuries A.D.)* (Unpublished masters thesis). Southern Illinois University Carbondale.

Neri R, and Lancellotti L. 2004. Fractures of the Lower Limbs and Their Secondary Skeletal Adaptations: A 20th Century Example of Pre-Modern Healing. *International Journal of Osteoarchaeology* 14:60-66.

Nutton V. 2013. *Ancient Medicine*. Abingdon: Routledge.

O'Neill MC, and Ruff CB. 2004. Estimating Human Long Bone Cross-Sectional Geometric Properties: A Comparison of Noninvasive Methods. *Journal of Human Evolution* 47:221-235.

Ogilvie MD, and Hilton CE. 2011. Cross-Sectional Geometry in the Humeri of Foragers and Farmers from the Prehispanic American Southwest: Exploring Patterns in the Sexual Division of Labor. *American Journal of Physical Anthropology* 144:11-21.

Oliver M. 1996. Defining Impairment and Disability: Issues at Stake. In: Barnes C, and Mercer G, editors. *Exploring the Divide*. Leeds: The Disability Press (pp. 29-54).

Ordinance Survey. 1980. *Ancaster, Lincolnshire, UK [Map]*. Retrieved 7 December 2015 from Old-Maps.co.uk.

Ortner DJ. 2003. *Identification of Pathological Conditions in Human Skeletal Remains*. San Diego: Academic Press.

Oxenham MF, Tilley L, Matsumura H, Nguyen LC, Nguyen KT, Nguyen KD, Domett K, and Huffer D. 2009. Paralysis and Severe Disability Requiring Intensive Care in Neolithic Asia. *Anthropological Science* 117:107-112.

Palmer AR, and Strobeck C. 1986. Fluctuating Asymmetry: Measurement, Analysis, Patterns. *Annual Review of Ecology and Systematics* 17:391-421.

Palmer J, Hoogland M, and Waters-Rist A. 2014. Activity Reconstruction of Post-Medieval Dutch Rural Villagers from Upper Limb Osteoarthritis and Entheseal Changes. *International Journal of Osteoarchaeology* 26:78-92.

Palmer M, and Harley D. 2012. Models and Measurement in Disability: An International Review. *Health Policy and Planning* 27:357-364.

Panagiotis M. 2005. Classification of Non-Union. *Injury, International Journal of the Care of the Injured* 365:530-537.

Parkin TG. 2003. *Old Age in the Roman World: A Cultural and Social History*. Baltimore: The Johns Hopkins University Press.

Pearson K. 1917-1919. *A Study of the Long Bones of the English Skeleton I: The Femur*. London: Cambridge University Press.

Pearson OM, and Lieberman DE. 2004. The Aging of Wolff's "Law": Ontogeny and Responses to Mechanical Loading in Cortical Bone. *American Journal of Physical Anthropology* Suppl 39:63-99.

Peck JJ, and Stout SD. 2007. Intraskeletal Variability in Bone Mass. *American Journal of Physical Anthropology* 132:89-97.

Pena JT, and McCallum M. 2009. The Production and Distribution of Pottery at Pompeii: A Review of the Evidence; Part 1, Production. *American Journal of Archaeology*:57-79.

Phenice TW. 1969. A Newly Developed Visual Method of Sexing the Os Pubis. *American Journal of Physical Anthropology* 30:297-302.

Pitts M, and Griffin R. 2012. Exploring Health and Social Well-Being in Late Roman Britain: An Intercemetery Approach. *American Journal of Archaeology* 116:253-276.

Ponsford J, Hill B, Karamitsios M, and Bahar-Fuchs A. 2008. Factors Influencing Outcome after Orthopedic Trauma. *The Journal of Trauma: Injury, Infection, and Critical Care* 64:1001-1009.

Prowse T. 2012. Archaeological Fieldwork Reports: Excavations at Vagnari, 2011. *Papers of the British School at Rome* 80:378-380.

Prowse T, Nause C, and Ledger M. 2014. Growing up and Growing Old on an Imperial Estate: Preliminary Palaeopathological Analysis of Skeletal Remains from

Vagnari. In: Small A, editor. *Beyond Vagnari: New Themes in the Study of Roman South Italy*. Bari: Edipuglia (pp. 111-122).

Prowse T, and Small A. 2009. *Excavations in the Roman Cemetery at Vagnari, 2008 Preliminary Report*. The Journal of Fasti Online: Retrieved 9 December 2016 from http://www.fastionline.org/docs/FOLDER-it-2009-131.pdf.

Prowse TL, Barta JL, von Hunnius TE, and Small AM. 2010. Stable Isotope and Ancient DNA Evidence for Geographic Origins at the Site of Vagnari (2nd-4th Centuries AD), Italy. *Roman Diasporas: Archaeological Approaches to Mobility and Diversity in the Roman Empire, Journal of Roman Archaeology* Supplement 78:175-198.

Prowse TL, and Carroll M. 2015. Research at Vagnari (Comune Di Gravina in Puglia, Provincia Di Bari, Regione Puglia). *Papers of the British School at Rome* 83:324-326.

Quek S-T, and Peh WCG. 2002. Radiology of Osteoporosis. *Seminars in Musculoskeletal Radiology* 6:197-206.

Raptis K, Ballas EG, Stathopoulos IP, Mari A, and Tournis S. 2014. Conservative Treatment of Humeral Fracture in a Patient with Paget's Disease of Bone. *Journal of Musculoskeletal and Neuronal Interactions* 14:484-487.

Rawson B. 2003. *Children and Childhood in Roman Italy*. Oxford: Oxford University Press.

Redfern RC, DeWitte SN, Pearce J, Hamlin C, and Dinwiddy KE. 2015. Urban-Rural Differences in Roman Dorset, England: A Bioarchaeological Perspective on Roman Settlements. *American Journal of Physical Anthropology*.

Redman Coxe J. 1846. *The Writings of Hippocrates and Galen: Epitomised from the Original Latin Translations*. Philadelphia: Lindsay and Blakiston.

Rhodes JA, and Knusel CJ. 2005. Activity-Related Skeletal Change in Medieval Humeri: Cross-Sectional and Architectural Alterations. *American Journal of Physical Anthropology* 128:536-546.

Rivet ALF. 1958. *Town and Country in Roman Britain*. London: Hutchinson University Library.

Roberts AM, Robson-Brown K, Musgrave JH, and Leslie I. 2006. A Case of Bilateral Scapholunate Advanced Collapse in a Romano-British Skeleton from Ancaster. *International Journal of Osteoarchaeology* 16:208-220.

Roberts C. 2000. Trauma in Biocultural Perspective: Past, Present and Future. In: Cox M, and Mays S, editors. *Human Osteology in Archaeology and Forensic Science*. London: Greenwich Medical Media Ltd. (pp. 337-356).

Roberts CA. 1988a. *Trauma and Its Treatment in British Antiquity: An Osteoarchaeological Study of Macroscopic and Radiological Features of Long Bone Fractures from the Historic Period with a Comparative Study of Clinical Radiographs, Supplemented by Contemporary Documentary, Iconographical and Archaeological Evidence* (Unpublished doctoral thesis). University of Bradford, Bradford.

Roberts CA. 1988b. Trauma and Treatment in British Antiquity: A Radiographic Study. In: Slater EA, and Tate JO, editors. *Science and Archaeology Glasgow 1987: Proceedings of a Conference on the Application of Scientific Techniques to Archaeology*. Oxford: BAR British Series (pp. 339-360).

Rogers E, Leineweber MJ, and Andrysek J. 2016. Analysis of Terrain Effects on the Interfacial Force Distribution at the Hand and Forearm During Crutch Gait. *Assistive Technology*.

Rogers J, and Waldron T. 1995. *A Field Guide to Joint Disease in Archaeology*. Chichester: John Wiley & Sons.

Rogers L. 1992. *Radiology of Skeletal Trauma*. New York: Churchill Livingstone.

Rosafio P. 2014. Vagnari, an Outline of the Imperial Estate. In: Small AM, editor. Small C, Trans. *Beyond Vagnari: New Themes in the Study of Roman South Italy*. Bari: Edipuglia (pp. 277-283).

Rosholm A, Hyldstrup L, Baeksgaard L, Grunkin M, and Thodberg HH. 2001. Estimation of Bone Mineral Density by Digital X-Ray Radiogrammetry: Theoretical Background and Clinical Testing. *Osteoporosis International* 12:961-969.

Rothman JC. 2010. The Challenge of Disability and Access: Reconceptualizing the Role of the Medical Model. *Journal of Social Work in Disability & Rehabilitation* 9:194-222.

Ruedi TP, Buckley RE, and Moran CG. 2007. *AO Principles of Fracture Management*. New York: Thieme.

Ruff C, Holt B, and Trinkaus E. 2006. Who's Afraid of the Big Bad Wolff?: "Wolff's Law" and Bone Functional Adaptation. *American Journal of Physical Anthropology* 129:484-498.

Ruff C, Trinkaus E, Walker A, and Spencer Larsen C. 1993. Postcranial Robusticity in Homo I: Temporal Trends and Mechanical Interpretation. *American Journal of Physical Anthropology* 91:21-53.

Ruff CB. 2000. Body Size, Body Shape, and Long Bone Strength in Modern Humans. *Journal of Human Evolution* 38:269-290.

Ruff CB. 2002. Long Bone Articular and Diaphyseal Structure in Old World Monkeys and Apes. I: Locomotor Effects. *American Journal of Physical Anthropology* 119:305-342.

Ruff CB. 2005. Mechanical Determinants of Bone Form: Insights from Skeletal Remains. *Journal of Musculoskeletal and Neuronal Interactions* 5:202.

Ruff CB, and Jones HH. 1981. Bilateral Asymmetry in Cortical Bone of the Humerus and Tibia--Sex and Age Factors. *Human Biology* 53:69-86.

Ruff CB, Scott WW, and Liu AYC. 1991. Articular and Diaphyseal Remodeling of the Proximal Femur with Changes in Body Mass in Adults. *American Journal of Physical Anthropology* 86:397-413.

Ruff CB, Walker A, and Trinkaus E. 1994. Postcranial Robusticity in Homo. III: Ontogeny. *American Journal of Physical Anthropology* 93:35-54.

Russo CR, Lauretani F, Seeman E, Bartali B, Bandinelli S, Di Iorio A, Guralnik J, and Ferrucci L. 2006. Structural Adpatations to Bone Loss in Aging Men and Women. *Bone* 38:113-118.

Salat P, Salonen D, and Veljkovic AN. 2015. Imaging in Osteoarthritis. In: Kapoor m, editor. *Osteoarthritis*. Switzerland: Springer (pp. 131-154).

Saulacic N, Schaller B, Iizuka T, Buser D, Hug C, and Bosshardt DD. 2013. Analysis of New Bone Formation Induced by Periosteal Distraction in a Rat Calvarium Model. *Clinical Implant Dentistry and Related Research* 15:283-291.

Scarborough J. 1968. Roman Medicine and the Legions: A Reconsideration. *Medical History* 12:254-261.

Scarborough J. 1970. Romans and Physicians. *The Classical Journal* 65:296-306.

Schäfer ML, Böttcher J, Pfeil A, Hansch A, Malich A, Maurer MH, Streitparth F, Röttgen R, and Renz DM. 2012. Comparison between Amputation-Induced Demineralization and Age-Related Bone Loss Using Digital X-Ray Radiogrammetry. *Journal of Clinical Densitometry* 15:135-145.

Scheidel W. 1995. The Most Silent Women of Greece and Rome: Rural Labour and Women's Life in the Ancient World (I). *Greece & Rome* 42:202-217.

Schlecht SH, Pinto DC, Agnew AM, and Stout SD. 2012. Brief Communication: The Effects of Disuse on the Mechanical Properties of Bone: What Unloading Tells Us About the Adaptive Nature of Skeletal Tissue. *American Journal of Physical Anthropology* 149:599-605.

Schlickewei W, Kuner EH, Mullaji AB, and Götze B. 1992. Upper and Lower Limb Fractures with Concomitant Arterial Injury. *Journal of Bone and Joint Surgery [Br]* 74-B:181-188.

Schmitt D, Churchill SE, and Hylander WL. 2003. Experimental Evidence Concerning Spear Use in Neandertals and Early Modern Humans. *Journal of Archaeological Science* 30:103-114.

Seeman E. 2008. Bone Quality: The Material and Structural Basis of Bone Strength. *Journal of Bone and Mineral Metabolism* 26:1-8.

Seeman E. 2013. Age-and Menopause-Related Bone Loss Compromise Cortical and Trabecular Microstructure. *The Journals of Gerontology Series A: Biological Sciences and Medical Sciences* 68:1218-1225.

Segal G, Elbaz A, Parsi A, Heller Z, Palmanovich E, Nyska M, Feldbrin Z, and Kish B. 2014. Clinical Outcomes Following Ankle Fracture: A Cross-Sectional Observational Study. *Journal of Foot and Ankle Research* 7:50.

Segura A, and Piazza SJ. 2007. Mechanics of Ambulation with Standard and Spring-Loaded Crutches. *Archives of Physical Medicine and Rehabilitation* 88:1159-1163.

Semchuk L. 2016. *A Stable Isotope Investigation of Diet in the Vagnari Cemetery* (Unpublished masters thesis). McMaster University, Hamilton.

Shaffer MA, Okereke E, Esterhai JLJ, Elliott MA, Walter GA, Yim SH, and Vandenborne K. 2000. Effects of Immobilization on Plantar-Flexion Torque, Fatigue Resistance, and Functional Ability Following an Ankle Fracture. *Physical Therapy* 80:769-780.

Shakespeare T. 2012. Still a Health Issue. *Disability and Health Journal* 5:129-131.

Shakespeare TOM, and Watson N. 1997. Defending the Social Model. *Disability & Society* 12:293-300.

Shaw BD. 1993. The Bandit. In: Giardina A, editor. *The Romans*. Chicago: The University of Chicago Press (pp. 300-341).

Shaw CN. 2011. Is 'Hand Preference' Coded in the Hominin Skeleton? An in-Vivo Study of Bilateral Morphological Variation. *Journal of Human Evolution* 61:480-487.

Shaw CN, and Stock JT. 2009. Habitual Throwing and Swimming Correspond with Upper Limb Diaphyseal Strength and Shape in Modern Human Athletes. *American Journal of Physical Anthropology* 140:160-172.

Shaw CN, and Stock JT. 2013. Extreme Mobility in the Late Pleistocene? Comparing Limb Biomechanics among Fossil Homo, Varsity Athletes and Holocene Foragers. *Journal of Human Evolution* 64:242-249.

Shindle MK, Endo Y, Warren RF, Lane JM, Helfet DL, Schwartz EN, and Ellis SJ. 2012. Stress Fractures About the Tibia, Foot, and Ankle. *Journal of the American Academy of Orthopaedic Surgeons* 20:167-176.

Sibonga JD, Evans HJ, Sung HG, Spector ER, Lang TF, Oganov VS, Bakulin AV, Shackelford LC, and LeBlanc AD. 2007. Recovery of Spaceflight-Induced Bone Loss: Bone Mineral Density after Long-Duration Missions as Fitted with an Exponential Function. *Bone* 41:973-978.

Signore A. 2013. About Inflammation and Infection. *European Journal of Nuclear Medicine and Molecular Imaging* 3:1-2.

Sigurdardottir K. 2014. Epidemiology. In: Hove LM, Lindau T, and Holmer P, editors. *Distal Radius Fractures*. Heidelberg: Springer (pp. 37-44).

Simic PM, and Weiland AJ. 2003. Fractures of the Distal Aspect of the Radius: Changes in Treatment over the Past Two Decades. *The Journal of Bone and Joint Surgery* 85-A:552-564.

Sims SH. 2002. Subtrochanteric Femoral Fractures. *Orthopedic Clinics of North America* 33:113-126.

Sládek V, Berner M, Galeta P, Friedl L, and Kudrnová Š. 2010. The Effect of Midshaft Location on the Error Ranges of Femoral and Tibial Cross-Sectional Parameters. *American Journal of Physical Anthropology* 141:325-332.

Small A, McLaren D, and Heald A. 2011. Iron-Working at Vagnari. In: Small A, editor. *Vagnari: The Village, the Industries, the Imperial Property*. Bari: Edipuglia (pp. 279-285).

Small A, and Small C. 2011. The Via Appia and Vagnari. In: Small A, editor. *Vagnari: The Village, the Industries, the Imperial Property*. Bari: Edupuglia (pp. 383-386).

Small A, Small C, Abdy R, De Stefano A, Giuliani R, Henig M, Johnson K, Kenrick P, Prowse T, Small A et al. . 2007. Excavation in the Roman Cemetery at Vagnari, in the Territory of Gravina in Puglia, 2002. *Papers of the British School at Rome* 75:123-229.

Small AM. 2011. *Vagnari: The Village, the Industries, the Imperial Property*. Bari: Edipuglia.

Small AM. 2014a. *Beyond Vagnari: New Themes in the Study of Roman South Italy*. Bari: Edipuglia.

Small AM. 2014b. From *Silvium* to Vagnari: Sheep, Wool and Weaving on the *Saltus*. In: Small AM, editor. *Beyond Vagnari: New Themes in the Study of Roman Italy*. Bari: Edipuglia (pp. 53-63).

Small AM, Volterra V, and Hancock RGV. 2003. New Evidence from Tile-Stamps for Imperial Properties near Gravina, and the Topography of Imperial Estates in SE Italy. *Journal of Roman Archaeology* 16:179-199.

Small C, and Small A. 2007. Archaeological Field Survey at San Felice in Apulia. *Mouseion: Journal of the Classical Association of Canada* 7:101-122.

Snyder SL, and Mitchell DT. 2010. *Cultural Locations of Disability*. Chicago: University of Chicago Press.

Sparacello V, and Marchi D. 2008. Mobility and Subsistence Economy: A Diachronic Comparison between Two Groups Settled in the Same Geographical Area (Liguria, Italy). *American Journal of Physical Anthropology* 136:485-495.

Sparacello VS, Roberts CA, Canci A, Moggi-Cecchi J, and Marchi D. 2016. Insights on the Paleoepidemiology of Ancient Tuberculosis from the Structural Analysis of Postcranial Remains from the Ligurian Neolithic (Northwestern Italy). *International Journal of Paleopathology* 15:50-64.

Steele J. 2000. Handedness in Past Human Populations: Skeletal Markers. *Laterality* 5:193-220.

Stewart TD. 1979. *Essentials of Forensic Anthropology*. Springfield, Il: Thomas.

Stock J, and Pfeiffer S. 2001. Linking Structural Variability in Long Bone Diaphyses to Habitual Behaviors: Foragers from the Southern African Later Stone Age and the Andaman Islands. *American Journal of Physical Anthropology* 115:337-348.

Stock JT. 2002. A Test of Two Methods of Radiographically Deriving Long Bone Cross-Sectional Properties Compared to Direct Sectioning of the Diaphysis. *International Journal of Osteoarchaeology* 12:335-342.

Swischuk LE, and Jadhav SP. 2014. Tibial Stress Phenomena and Fractures: Imaging Evaluation. *Emergency Radiology* 21:173-177.

Szumilas M. 2010. Explaining Odds Ratios. *Journal of the Canadian Academy of Child and Adolescent Psychiatry* 19:227-229.

Takata S, and Yasui N. 2001. Disuse Osteoporosis. *Journal of Medical Investigation* 48:147-156.

Taylor CA, Braza D, Rice JB, and Dillingham T. 2008. The Incidence of Peripheral Nerve Injury in Exremity Trauma. *American Journal of Physical Medicine & Rehabilitation* 87:381-385.

Thompson AR. 2012. Differential Diagnosis of Limb Length Discrepancy in a 19th Century Burial from Southwest Mississippi. *International Journal of Osteoarchaeology* 24:517-530.

Thurston AJ. 2007. Paré and Prosthetics: The Early History of Artificial Limbs. *ANZ Journal of Surgery* 77:1114-1119.

Tilley L. 2012. The Bioarchaeology of Care. *The SAA Archaeological Record*. Chicago: Society for American Archaeology (pp. 39-41).

Tilley L. 2015. *Theory and Practice in the Bioarchaeology of Care*. Switzerland: Springer.

Tilley L, and Oxenham MF. 2011. Survival against the Odds: Modeling the Social Implications of Care Provision to Seriously Disabled Individuals. *International Journal of Paleopathology* 1:35-42.

Tilley L, and Schrenk AA. 2016. *New Developments in the Bioarchaeology of Care: Further Case Studies and Expanded Theory*: Springer.

Timms S. 1997. *Archaeological Watching Brief Report: Ermine Street, Ancaster*. Lincoln: Pre-Construct Archaeology.

Todd M. 1970. The Small Towns of Roman Britain. *Britannia* 1:114-130.

Todd M. 1975. The 'Small Towns' of Roman Britain: Papers Presented to a Conference, Oxford 1975. In: Rodwell W, and Rowley T, editors. *British Archaeological Reports 15*. Oxford: Oxford University Department for External Studies (pp. 211-223).

Todd M. 1981. *The Roman Town at Ancaster: The Excavations of 1955-1971*. Nottingham: Univeristy of Nottingham.

Tomey KM, and Sowers MR. 2009. Assessment of Physical Functioning: A Conceptual Model Encompassing Environmental Factors and Individual Compensation Strategies. *Physical Therapy* 89:705-714.

Toynbee JM. 1996. *Death and Burial in the Roman World*. Baltimore: Johns Hopkins University Press.

Trinkaus E, Churchill SE, and Ruff CB. 1994. Postcranial Robusticity in *Homo*. II: Humeral Bilateral Asymmetry and Bone Plasticity. *American Journal of Physical Anthropology* 93:1-34.

Trinkaus E, and Ruff CB. 1999. Diaphyseal Cross-Sectional Geometry of near Eastern Middle Palaeolithic Humans: The Tibia. *Journal of Archaeological Science* 26:1289-1300.

Trollope E. 1870. Ancaster, the Roman Causennae. *The Archaeological Journal* 27:1-15.

Turner CH. 1998. Three Rules for Bone Adaptation to Mechanical Stimuli. *Bone* 23:399-407.

Turner CH, and Burr DB. 1993. Basic Biomechanical Measurements of Bone: A Tutorial. *Bone* 14:595-608.

U.S. Department of Health and Human Services. 2004. Determinants of Bone Health. *Bone Health and Osteoporosis: A Report of the Surgeon General*. Rockville: Office of the Surgeon General (pp. 110-157).

Ubelaker DH. 1989. *Human Skeletal Remains*. Washington, D.C.: Taraxacum Press.

Ubelaker DH, and Adams BJ. 1995. Differentiation of Perimortem and Postmortem Trauma Using Taphonomic Indicators. *Journal of Forensic Sciences* 40:509-512.

Ubelaker DH, and Zarenko KM. 2012. Can Handedness Be Determined from Skeletal Remains? A Chronological Review of the Literature. *Journal of Forensic Sciences* 57:1421-1426.

Uhthoff HK, and Jaworski ZFG. 1978. Bone Loss in Response to Long-Term Immobilization. *The Journal of Bone and Joint Surgery* 60-B:420-429.

Ulmschneider K. 2000. Settlement, Economy, and the 'Productive' Site: Middle Anglo-Saxon Lincolnshire A.D. 650-780. *Medieval Archaeology* 44:53-79.

Umemura Y, Ishiko T, Yamauchi T, Kurono M, and Mashiko S. 1997. Five Jumps Per Day Increase Bone Mass and Breaking Force in Rats. *Journal of Bone and Mineral Research* 12:1480-1485.

Upex SG, Challands A, Patterson E, Perrin R, and Todd M. 2008. The Excavation of a Fourth-Century Roman Pottery Production Unit at Stibbington, Cambridgeshire. *Archaeological Journal* 165:265-333.

van der Poest Clement E, van der Wiel H, Patka P, Roos JC, and Lips P. 1999. Long-Term Consequences of Fracture of the Lower Leg: Cross-Sectional Study and Long-Term Longitudinal Follow-up of Bone Mineral Density in the Hip after Fracture of Lower Leg. *Bone* 24:131-134.

Van Der Schoot DKE, Den Outer AJ, Bode PJ, Obermann WR, and Van Vugt AB. 1996. Degenerative Changes at the Knee and Ankle Related to Malunion of Tibial Fractures. *Journal of Bone and Joint Surgery (Br)* 78B:722-725.

Van der Veen M. 1989. Charred Grain Assemblages from Roman-Period Corn Driers in Britain. *Archaeology Journal* 146:302-319.

Vlaeyen JW, and Linton SJ. 2000. Fear-Avoidance and Its Consequences in Chronic Musculoskeletal Pain: A State of the Art. *Pain* 85:317-332.

Vlaeyen JW, and Linton SJ. 2012. Fear-Avoidance Model of Chronic Musculoskeletal Pain: 12 Years On. *Pain* 153:1144-1147.

Vlaeyen JWS, and Crombez G. 1999. Fear of Movement/(Re)Injury, Avoidance and Pain Disability in Chronic Low Back Pain Patients. *Manual Therapy* 4:187-195.

Vlaeyen JWS, Kole-Snijders AMJ, Rotteveel AM, Ruesink R, and Huets PHTG. 1995. The Role of Fear of Movement/(Re)Injury in Pain Disability. *Journal of Occupational Rehabilitation* 5:235-252.

Volterra V, and Small A. 2011. Millstones. In: Small A, editor. *Vagnari: The Village, the Industries, the Imperial Property*. Bari: Edipuglia (pp. 417-427).

Walfish S. 2006. A Review of Statistical Outlier Methods. *Pharmaceutical Technology* 30:82-88.

Walsh WW, Belding NN, Taylor E, and Nunley JA. 1993. The Effect of Upper Extremity Trauma on Handedness. *The American Journal of Occupational Therapy* 47:787-795.

Wang R, Thur CK, Gutierrez-Farewik EM, Wretenberg P, and Broström E. 2010. One Year Follow-up after Operative Ankle Fractures: A Prospective Gait Analysis Study with a Multi-Segment Foot Model. *Gait & Posture* 31:234-240.

Warden SJ, Bogenschutz ED, Smith HD, and Gutierrez AR. 2009. Throwing Induces Substantial Torsional Adaptation within the Midshaft Humerus of Male Baseball Players. *Bone* 45:931-941.

Weaver CM, Gordon CM, Janz KF, Kalkwarf HJ, Lappe JM, Lewis R, O'Karma M, Wallace TC, and Zemel BS. 2016. The National Osteoporosis Foundation's Position Statement on Peak Bone Mass Development and Lifestyle Factors: A Systematic Review and Implementation Record. *Osteoporosis International* 27:1281-1386.

Webster T, Butler A, and Yates A. 2004. *An Archaeological Trial Trench Evaluation at 5 Paddock Close, Ancaster, Lincolnshire*. Northamptonshire: Northamptonshire Archaeology.

Weiss E. 2003. Effects of Rowing on Humeral Strength. *American Journal of Physical Anthropology* 121:293-302.

Wescott DJ. 2013. Biomechanics of Bone Trauma. In: Siegel J, Saukko PJ, and Houck MM, editors. *Encyclopedia of Forensic Sciences*. 2nd ed. New York: Elsevier (pp. 83-88).

Wescott DJ, and Cunningham DL. 2006. Temporal Changes in Arikara Humeral and Femoral Cross-Sectional Geometry Associated with Horticultural Intensification. *Journal of Archaeological Science* 33:1022-1036.

Westerhoff P, Graichen F, Bender A, Halder A, Beier A, Rohlmann A, and Bergmann G. 2012. In Vivo Measurement of Shoulder Joint Loads During Walking with Crutches. *Clinical Biomechanics* 27:711-718.

Weston DA. 2012. Nonspecific Infection in Paleopathology: Interpreting Periosteal Reactions. In: Grauer AL, editor. *A Companion to Paleopathology*. Chichester: Blackwell Publishing Ltd. (pp. 492-512).

Wheatley BP. 2008. Perimortem or Postmortem Bone Fractures? An Experimental Study of Fracture Patterns in Deer Femora. *Journal of Forensic Sciences* 53:69-72.

Whitwell JB, Todd M, and Ponsford M. 1966. Ancaster - Miscellaneous Excavations. *East Midland Archaeological Bulletin* 9:10-13.

Wild J. 2002. The Textile Industries of Roman Britain. *Britannia* 33:1-42.

Williams L, and Masseglia J. 2015. Tending the Vines: Biomechanical Evidence of Laterality and Gendered Labor Division in Viticulture at Pessinus, Turkey [Abstract]. *American Journal of Physical Anthropology* S60:325.

Wilson DR. 1968. An Early Christian Cemetery at Ancaster. In: Barley MW, and Hanson RPC, editors. *Christianity in Britain, 300-700*. Leicester: Leicester University Press (pp. 197-200).

Wilson DR. n.d. *Ancaster Excavations, Vol. 2. [Unfinished Manuscript]*. Unpublished: University of Nottingham.

Wilson DR, and May J. 1965. Ancaster - Miscellaneous Excavations. *East Midland Archaeological Bulletin* 8:13-14.

Wilson DR, and Wright RP. 1966. Roman Britain in 1965. *The Journal of Roman Studies* 56:196-225.

Wilson DR, and Wright RP. 1968. Roman Britain in 1967. *The Journal of Roman Studies* 58:176-214.

Wilson DR, and Wright RP. 1969. Roman Britain in 1968. *The Journal of Roman Studies* 59:198-246.

Wilson LA, Gooding BW, Manning PA, Wallace WA, and Geoghegan JM. 2014. Risk Factors and Predictors of Mortality for Proximal Humeral Fractures. *Shoulder & Elbow* 6:95-99.

Wilson N. 2013. The Semantics of Pain in Greco-Roman Antiquity. *Journal of the History of Neurosciences* 22:129-143.

Woolf C. 1989. Recent Advances in the Pathophysiology of Acute Pain. *British Journal of Anaesthesia* 63:139-146.

Wraighte PJ, and Scammell BE. 2006. Principles of Fracture Healing. *Surgery (Oxford)* 24:198-207.

Yagan R, Radivoyevitch M, and Khan MA. 1987. Double Cortical Line in the Acetabular Roof: A Sign of Disuse Osteoporosis. *Radiology* 165:171-175.

Young JL, and Lemaire ED. 2012. Linking Bone Changes in the Distal Femur to Functional Deficits. *International Journal of Osteoarchaeology*:1-13.

Zaidi ZF. 2011. Body Asymmetries: Incidence, Etiology and Clinical Implications. *Australian Journal of Basic and Applied Sciences* 5:2157-2191.

Appendix A: Recording Forms

The forms used to record the data for this thesis are presented in this appendix. Most forms were fillable in Adobe Acrobat, but some sketch forms were also used to illustrate bone preservation and fracture morphology. Adobe Acrobat fillable forms helped to keep recording consistent among sites and individuals, and were also directly exportable to Microsoft Excel. The recording forms in this appendix, in the order of appearance, include:

- Sex and age estimation recording form (Figure A.1)
- Long bone preservation sketch form (Figure A.2)
- Long bone inventory, erosion & abrasion grade, and joint surface preservation fillable form (Figure A.3)
- Osteoarthritis recording form (Figure A.4)
- Trauma recording form (Figure A.5)
- Right and left clavicle fracture sketch forms (Figure A.6)
- Right and left humerus fracture sketch forms (Figure A.7)
- Right and left radius fracture sketch forms (Figure A.8)
- Right and left ulna fracture sketch forms (Figure A.9)
- Right and left femur fracture sketch forms (Figure A.10)
- Right and left tibia fracture sketch forms (Figure A.11)
- Right and left fibula fracture sketch forms (Figure A.12)

Sex/Age Estimation Date: ______________________________ Site______________________________

Observer:______________________________ Sk #______________________________

Sex Estimation

Pelvis	**Left**	**Right**
Ventral Arc (0-3) *		
Subpubic Concavity (0-3) *		
Ischiopubic Ramus Ridge (0-3) *		
Greater Sciatic Notch (0-5) *		
Preauricular Sulcus (0-4) *		
Subpubic Angle (0-3)		
Estimated Sex		

Skull	**Left**	**Right**
Nuchal Crest (0-5) *		
Mastoid Process (0-5) *		
Supraorbital Margin (0-5) *		
Glabella (0-5) *		
Mental Eminence (0-5) *		
Gonial Eversion (flare) (-1,0,+1) **		
Ramus Flexure (-1,0,+1) **		
Estimated Sex		

* after observations described in Buikstra & Ubelaker 1994 (0-3 and 0-5 scales [1 = more feminine])
** after Loth & Henneberg 1996, 2000 (+1 = flexure; -1 = straight; 0 = neither flexed or straight)

Age Estimation

Age Scores	**Left**	**Right**
Pubic Symphysis[+]		
Auricular Surface[++]		
Sternal 4th Rib Ends[°]		
3rd Molars		
Osteological Age Range		
Age Category		

Epiphyseal Union[¶]

Location	**Element**	**Left**	**L Age Range**	**Right**	**R Age Range**

[+] Suchey-Brooks scoring system; [++] after methods outlined by Lovejoy et al. 1985; [°] after İşcan et al. (1984); [¶] Un-united epiphyses listed here, all others assumed fused

Notes:

Figure A.1 – Adobe Acrobat fillable form used to record skeletal features for sex and age estimation.

Long Bone Inventory Date: ______________________________ Site________________________________

Observer:____________________________ Sk #_______________________________

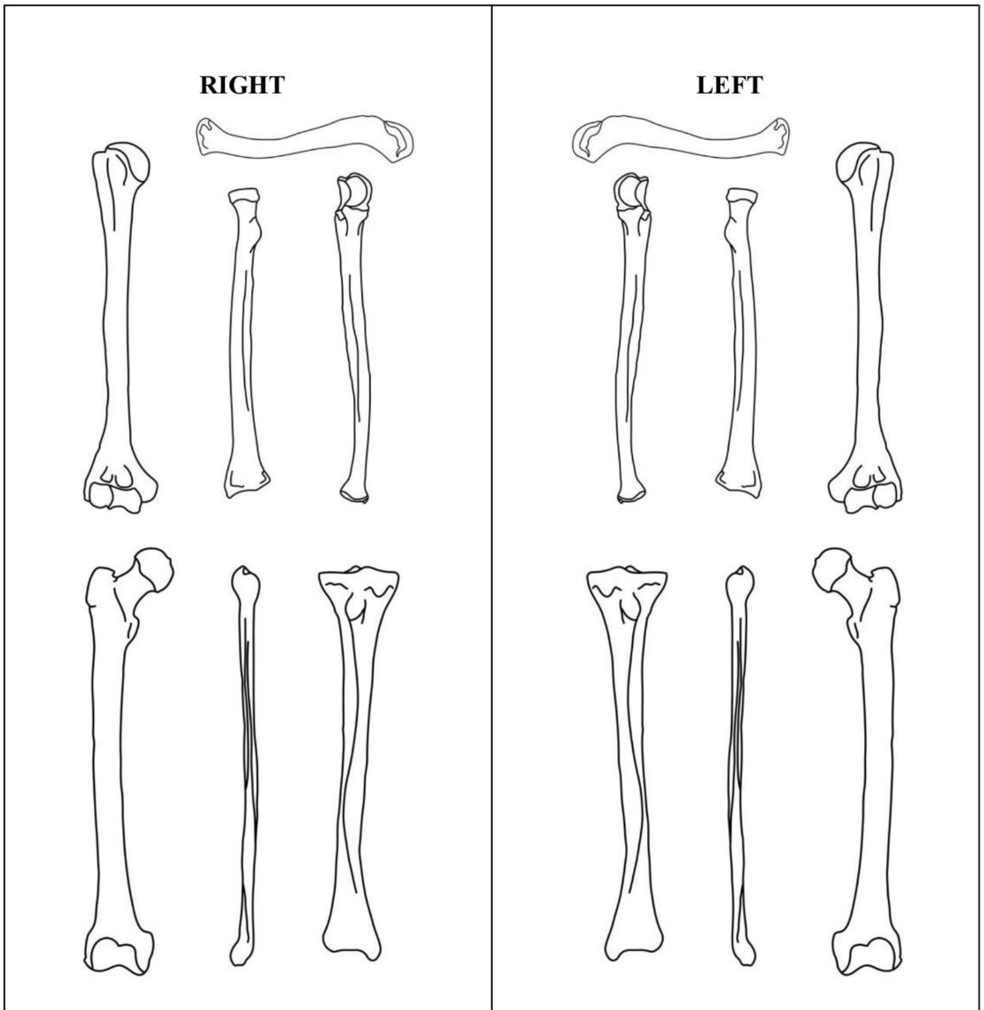

Notes:

Figure A.2 – Sketch recording form used to visually document the presence of each long bone.

Long Bone Inventory & Preservation

Date: ____________ Site____________

Observer:____________ Sk #____________

Sex: ________

Osteo Age Range: ________

Age Category: ________

Trauma: ________

Side: ________

Bone(s): ________

Approx. cortical bone quality (for use in X-ray eligibility selection)*

*score 1-3; 1 = excellent, 3 = very poor preservation

Long Bone Inventory*

Element	LEFT								RIGHT							
	Taph**	Prox. Joint Surf.§	1 Proximal Epiphysis	2 Proximal 1/3	3 Mid 1/3	4 Distal 1/3	5 Distal Epiphysis	Dist. Joint Surf.§	Taph**	Prox. Joint Surf.§	1 Proximal Epiphysis	2 Proximal 1/3	3 Mid 1/3	4 Distal 1/3	5 Distal Epiphysis	Dist. Joint Surf.§
Clavicle																
Humerus																
Radius																
Ulna																
Femur																
Tibia																
Fibula																

* segment preservation estimated on a scale of 1-4; 1 = ~0-25% , 2 = ~25-50%; 3 = ~50-75%; 4 = ~75-100%
** taphonomic/weathering scores assigned to entire element based on method outlined in Brickley & McKinley (2004:14). (Ranges from 0 = no weathering to 5+ = extensive erosion)
§ joint completeness scores are as follows: complete (C) ≥90%; present (P) 50-89%, incomplete (I) 25-49%, absent (A) <25%

Notes:

Figure A.3 – Adobe Acrobat fillable form used to document the preservation and erosion of each long bone and joint surface.

Joint Disease

Date: ______________________ Site______________________

Observer:______________________ Sk #______________________

DJD	Clavicle				Humerus				Radius				Ulna			
	Left		**Right**		**Left**		**Right**		**Left**		**Right**		**Left**		**Right**	
	Prox	Dist	Prox	Dist	Prox	Dist	Prox	Dist	Prox	Dist	Prox	Dist	Prox	Dist	Prox	Dist
Joint Completeness¶																
Marginal Osteophyte *																
New bone on joint surface																
Pitting on joint surface **																
Alteration of bony contour																
Eburnation																
OA §																

DJD	Femur				Tibia				Fibula			
	Left		**Right**		**Left**		**Right**		**Left**		**Right**	
	Prox	Dist	Prox	Dist	Prox	Dist	Prox	Dist	Prox	Dist	Prox	Dist
Joint Completeness¶												
Marginal Osteophyte *												
New bone on joint surface												
Pitting on joint surface **												
Alteration of bony contour												
Eburnation												
OA §												

Observations:

* Maximum marginal osteophyte measured and classified as ≤2mm and >2mm.
** Pitting and porosity scored as micro (m) (<1mm) or macro (M) (≥1mm); when observed, subchondral cysts indicated by 'S'.
¶ joint completeness scores are as follows: complete (C) ≥90%; present (P) 50-89%, incomplete (I) 25-49%, absent (A) <25%
§ OA classified according to Rogers and Waldron (1995). Eburnation or at least 2 other observations must be present to qualify as OA. NOTE: in pitting & osteophyte categories, OA identified when M and > 2mm present; OA selected when only m and/or ≤2mm were

Figure A.4 – Adobe Acrobat fillable form used to record osteoarthritis and joint surface completeness for each long bone observed.

Trauma Recording   Date: ____________________________ Site________________________________

Observer:___________________________ Sk #________________________________

Sex: ______________________________

Osteo Age Range: ____________________

Age Category: _______________________

Element: ___________________________

Side: ______________________________

Fracture Pattern: ____________________

Fracture Location: ___________________

Fracture Description:

Length		
Side	**Length (mm)**	**Fractured +**
Left		
Right		

	Actual					**X-Ray**			
	AP		**ML**			**AP**		**ML**	
	mm	**%**	**mm**	**%**		**mm**	**%**	**mm**	**%**
Displacement/ Apposition +									
Shortening					**Overlap**				
	Degree	**Direction**	**Degree**	**Direction**		**Degree**	**Direction**	**Degree**	**Direction**
Angulation*									
Rotation **									

+ also known as translation. Typically expressed as a percent relative to the diameter of the bone.
* direction distal fragment points relative to the long bone axis
** distal fragment relative to proximal (when proximal in anatomical position)

Multiple Injuries+

+ Checked when present

Sketch+

+ Checked when present

Complications:	**X+**	**Description**
Non-union		
Periostitis		
Osteomyelitis		
DJD		
Myostisis ossificans traumatica		
Osteochondritis dissecans (OD)		
Asymmetry		

+ Checked when present

Figure A.5 – Adobe Acrobat fillable form used to record the long bone trauma.

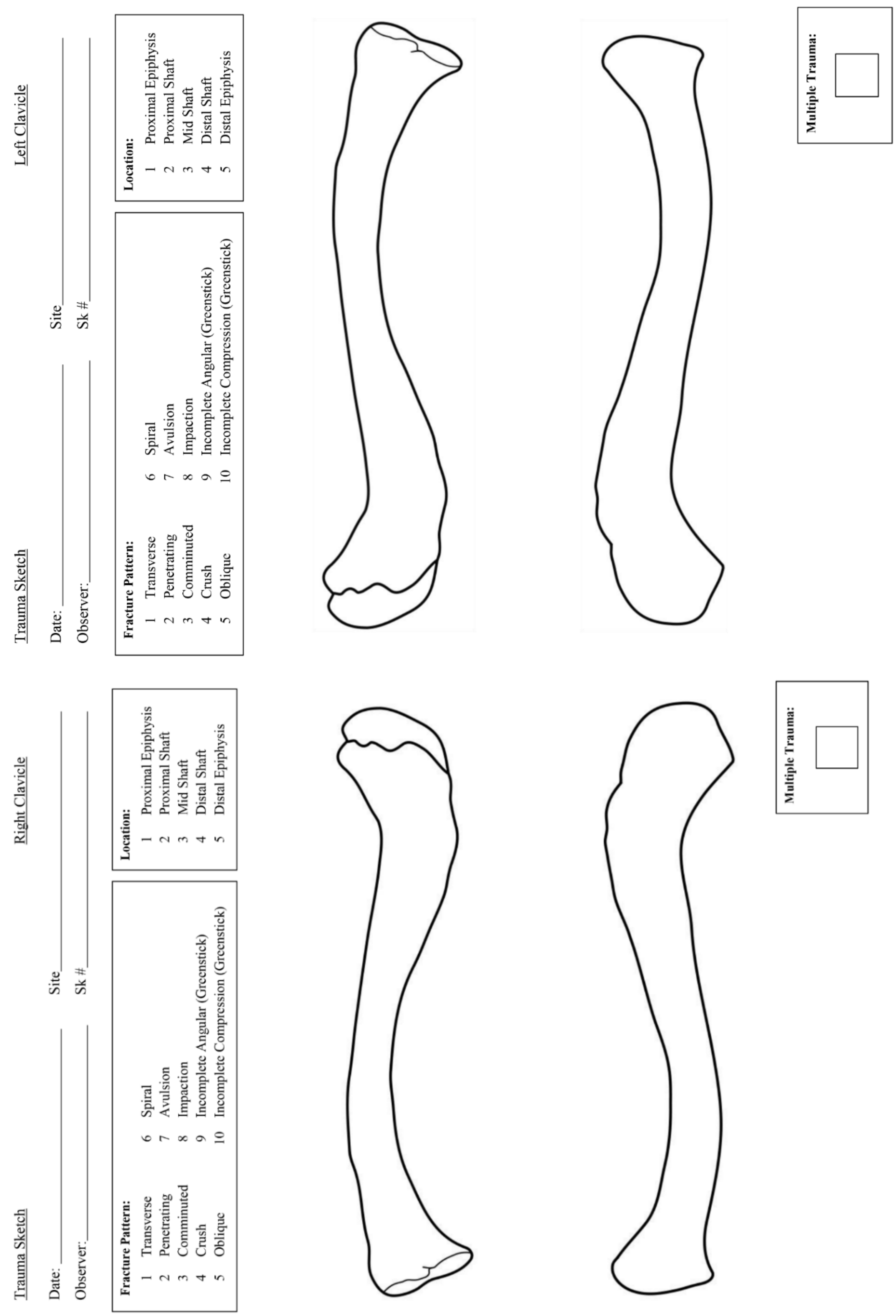

Figure A.6 – Sketch forms for documenting fractures to right and left clavicles.

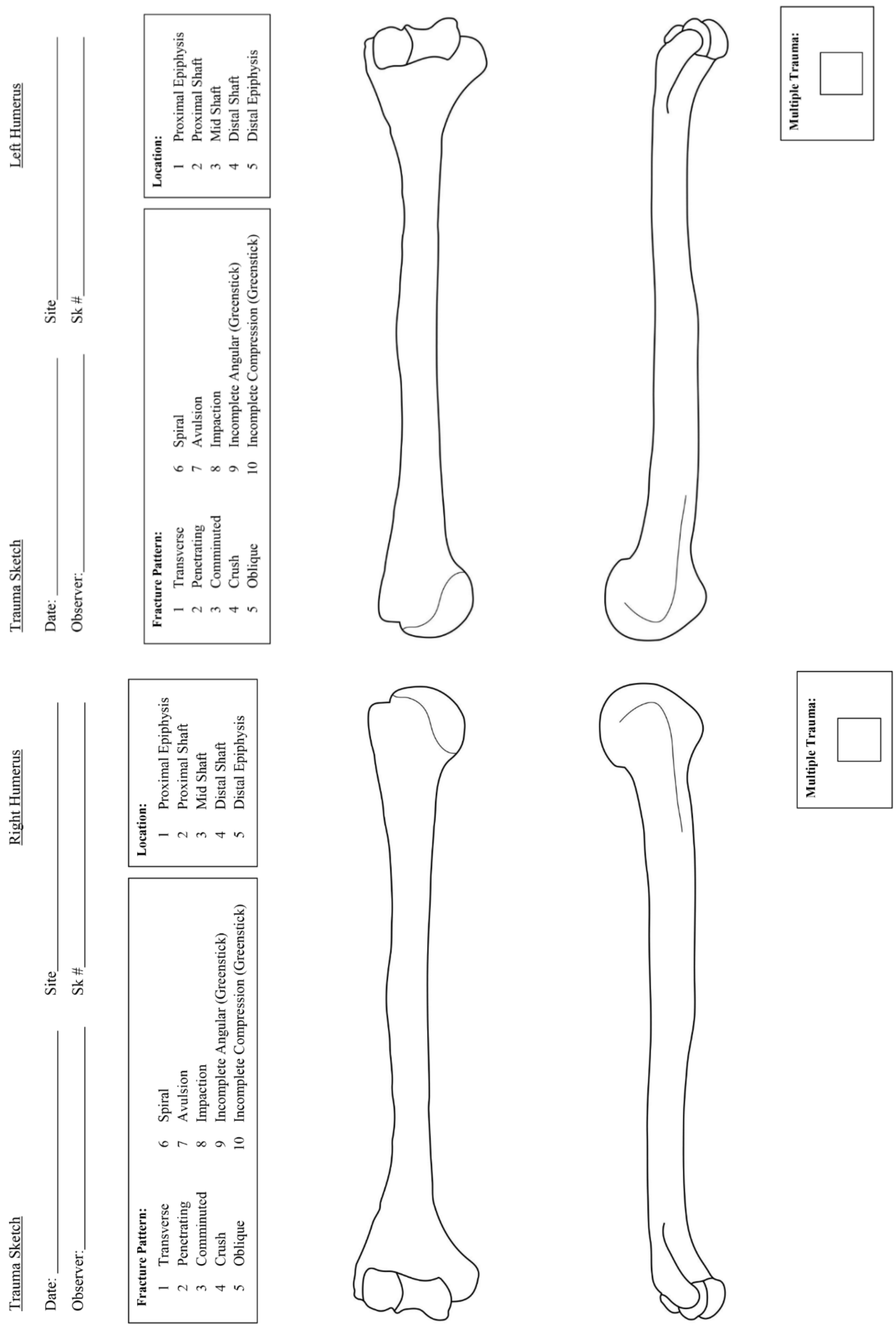

Figure A.7 – Sketch forms for documenting fractures to right and left humeri.

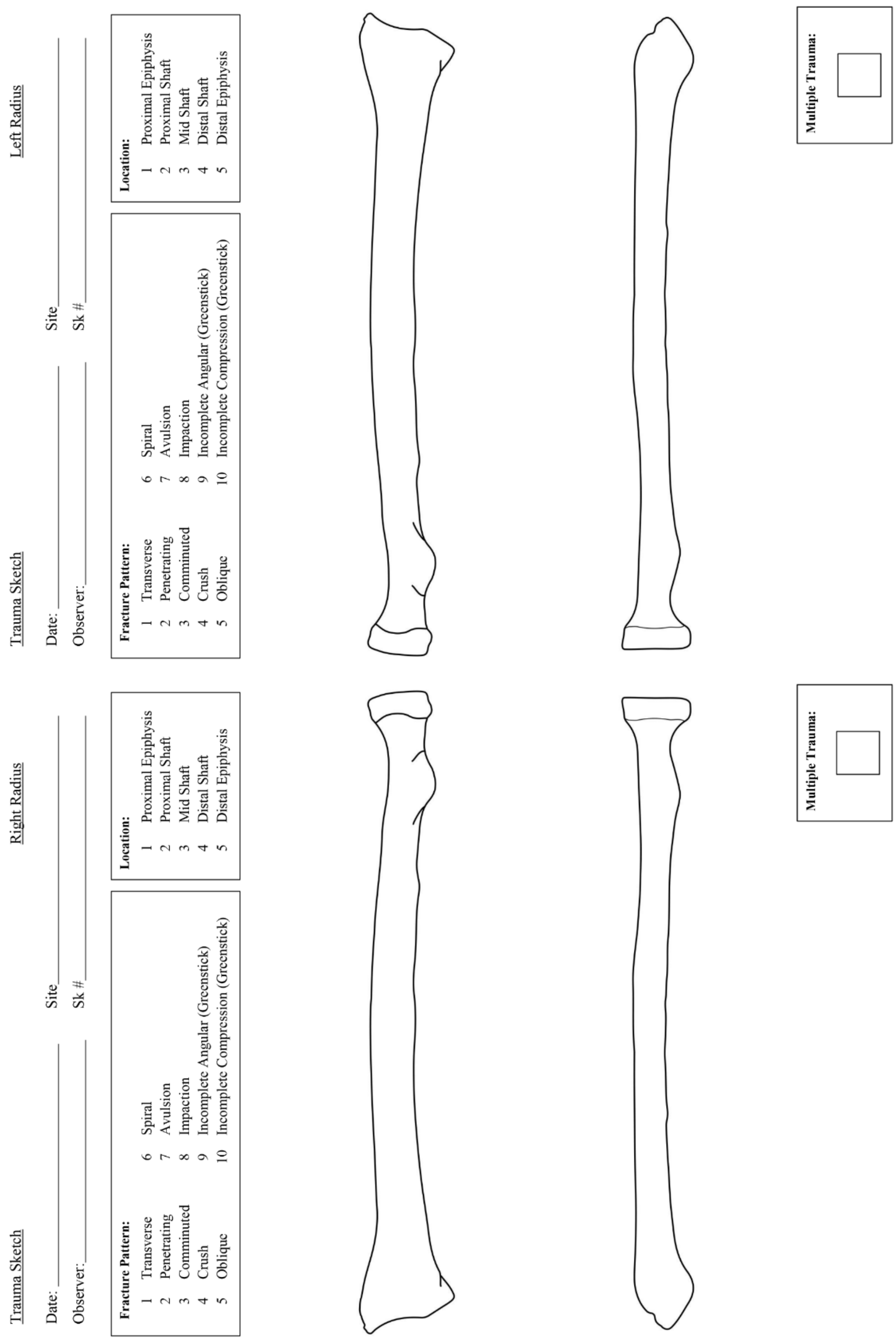

Figure A.8 – Sketch forms for documenting fractures to right and left radii.

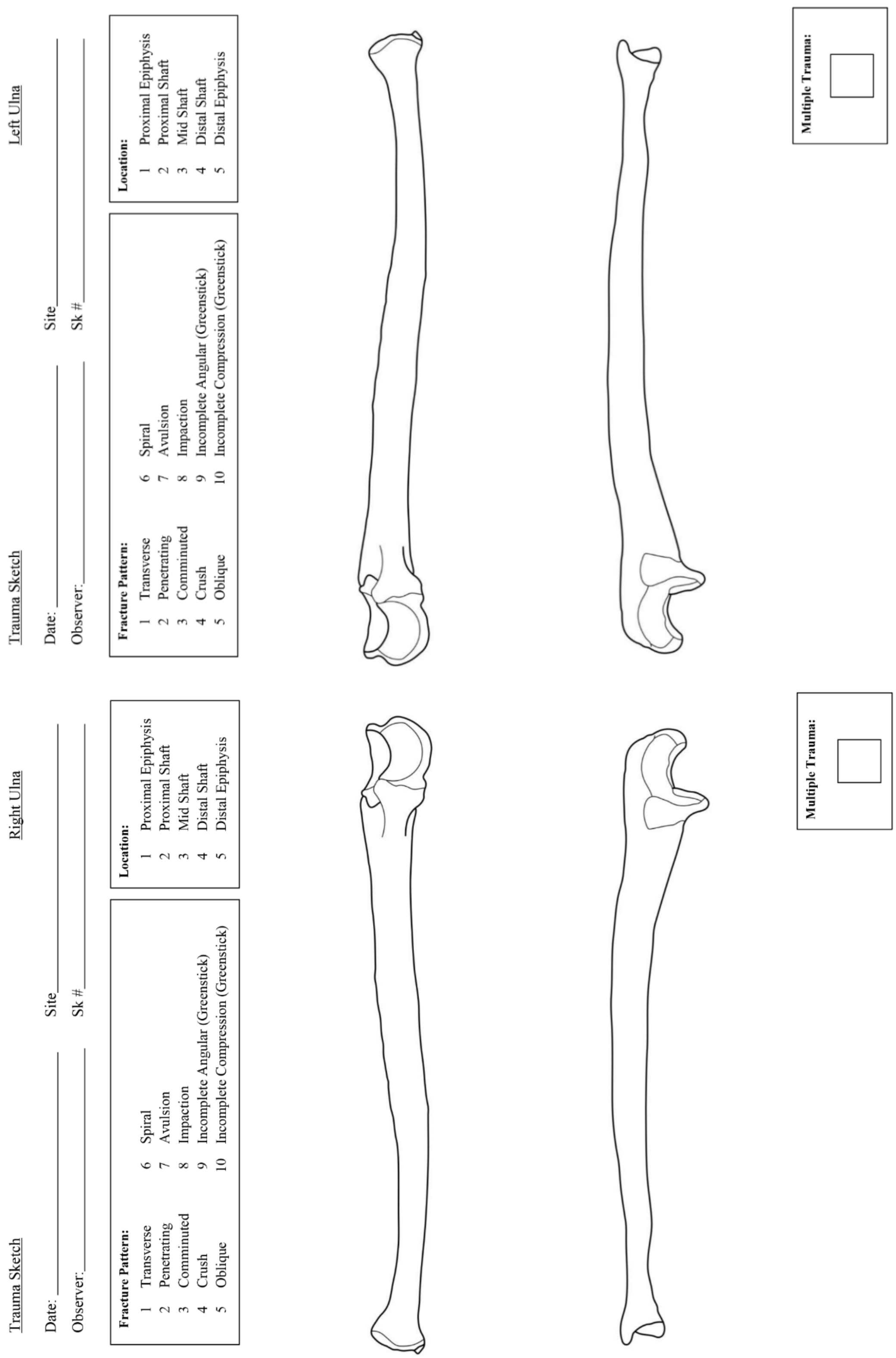

Figure A.9 – Sketch forms for documenting fractures to right and left ulnae.

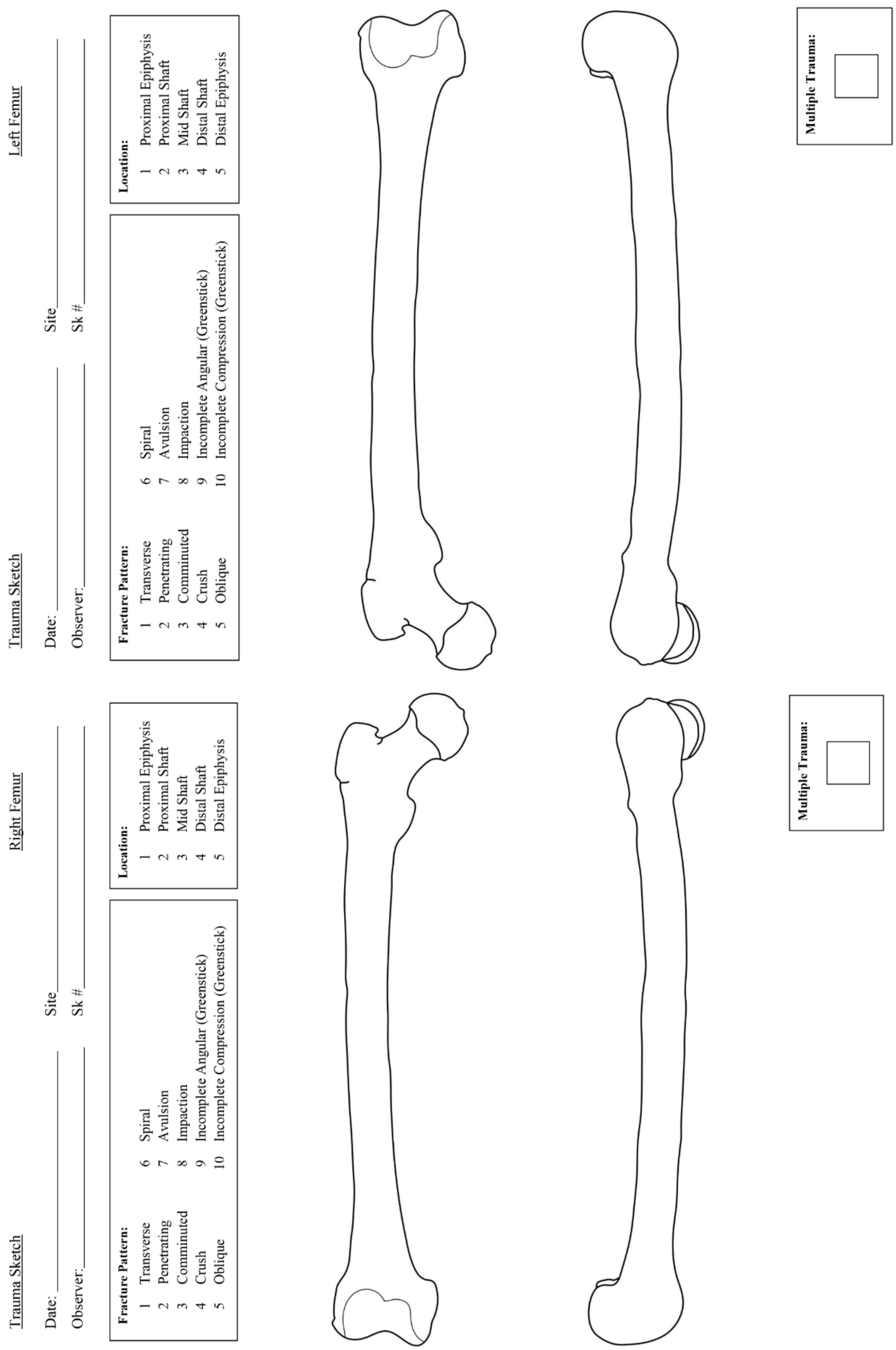

Figure A.10 – Sketch forms for documenting fractures to right and left femora.

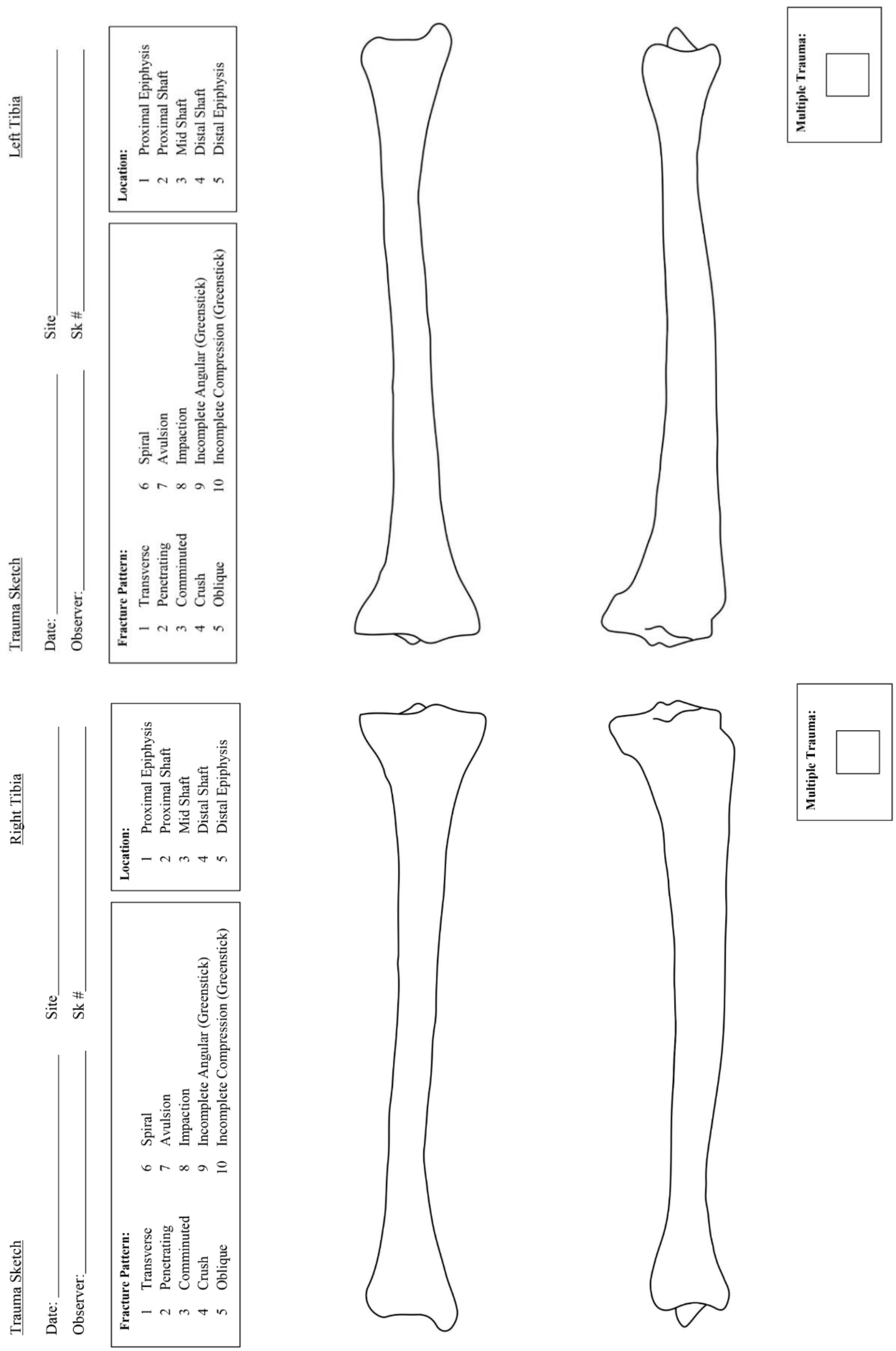

Figure A.11 – Sketch forms for documenting fractures to right and left tibiae.

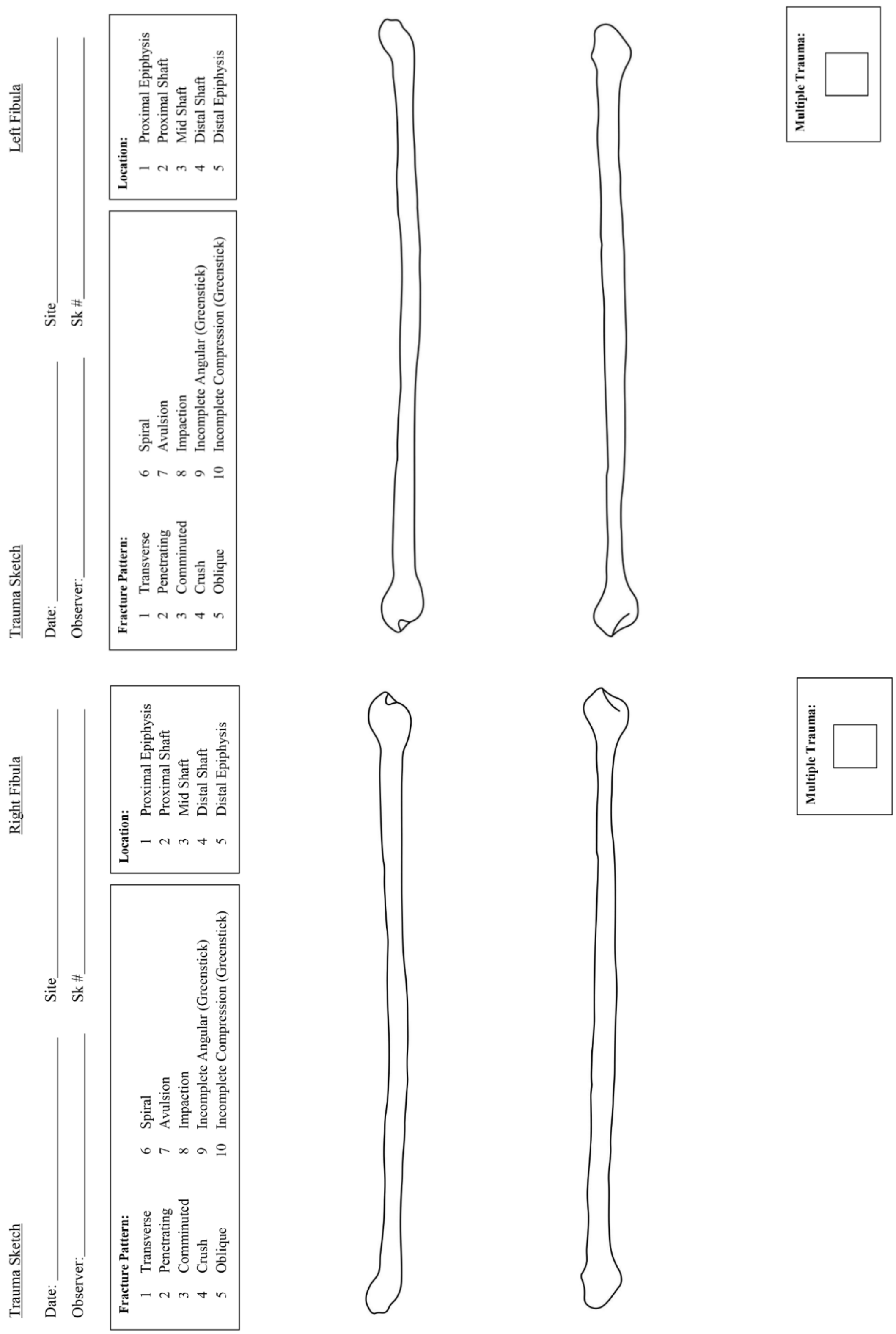
Trauma Sketch — Right Fibula

Date: ____________ Site ____________

Observer: ____________ Sk # ____________

Fracture Pattern:
1 Transverse
2 Penetrating
3 Comminuted
4 Crush
5 Oblique
6 Spiral
7 Avulsion
8 Impaction
9 Incomplete Angular (Greenstick)
10 Incomplete Compression (Greenstick)

Location:
1 Proximal Epiphysis
2 Proximal Shaft
3 Mid Shaft
4 Distal Shaft
5 Distal Epiphysis

Multiple Trauma:

Trauma Sketch — Left Fibula

Date: ____________ Site ____________

Observer: ____________ Sk # ____________

Fracture Pattern:
1 Transverse
2 Penetrating
3 Comminuted
4 Crush
5 Oblique
6 Spiral
7 Avulsion
8 Impaction
9 Incomplete Angular (Greenstick)
10 Incomplete Compression (Greenstick)

Location:
1 Proximal Epiphysis
2 Proximal Shaft
3 Mid Shaft
4 Distal Shaft
5 Distal Epiphysis

Multiple Trauma:

Figure A.12 – Sketch forms for documenting fractures to right and left fibulae.

Appendix B: Each Analysed Individual

This appendix reports the information recorded for each individual at Ancaster and Vagnari in Tables B.1 and B.2, respectively. The estimated sex, age category, and age range are presented for every individual analysed. Fractures are indicated when they were observed, as are the individuals that were included in the radiographic analysis. The number of bones that were considered 'complete' are presented (a total of eight upper limb and six lower limb bones were possibly present). Femoral head diameters are reported when they were present and measurable. Additionally, the erosion & abrasion grade assigned to each long bone for each individual are recorded.

Abbreviations used in the tables are as follows:

F – Female
F? – Possible Female
M – Male
M? – Possible Male
U – Undetermined
A – Ambiguous
ADO – Adolescent (15-19 years old)
YA – Young Adult (20-34 years old)
MA – Middle Adult (35-49 years old)
OA – Old Adult (50+ years old)
UL – Upper limb
LL – Lower limb
C – Clavicle
H – Humerus
Rad – Radius
Ul – Ulna
MC2 – Second metacarpal
Fem – Femur
T – Tibia
Fib – Fibula
MT2 – Second metatarsal
Y – 'Yes' (i.e., was individual radiographed or a fracture was present)
- – observation absent (e.g., not radiographed, not fractured, element not preserved and no erosion & abrasion score was assigned)

Table B.1 – The sex, age, and skeletal inventory details for each individual at Ancaster.

Skeleton Number	Sex	Age	Age Range	Fracture	X-ray	Number of 'Complete' Bones		Femur Head Diameter	Erosion & Abrasion Grade (Right / Left)								
						UL	LL		C	H	Rad	Ul	MC2	Fem	T	Fib	MT2
AN-001	F?	YA	18-25	Y	Y	7	6	44.6	-/-	3/3	3/1	3/3	-/-	1/1	1/2	3/2	-/-
AN-002*	F	MA	35-50	-	Y	7	4	-	2/1	2/3	1/2	1/2	2/1	4/3	2/3	-/-	-/-
AN-002A	F	MA	40-50	-	-	6	0	-	-/-	-/-	-/-	-/-	-/-	-/-	-/-	-/-	-/-
AN-003	M?	YA	25-35	-	-	4	1	-	-/-	-/-	-/-	-/-	-/-	-/-	-/-	-/-	-/-
AN-003A	F	YA	26-31	-	Y	8	6	-	0/0	2/1	3/2	2/2	-/-	2/2	2/2	3/3	1/1
AN-004	M	OA	45-60	-	Y	8	1	-	1/1	2/1	2/1	1/2	-/-	1/2	-/-	-/-	-/-
AN-005	M	MA	35-46	-	Y	8	6	-	1/0	3/4	3/3	2/3	-/-	3/3	1/2	2/1	-/-
AN-006	M	MA	35-46	-	Y	8	6	-	3/2	2/2	2/2	2/2	2/1	2/3	1/1	2/1	-/-
AN-010	F	MA	40-50	-	Y	8	6	-	2/1	2/2	1/2	2/1	1/2	3/3	1/2	2/1	3/3
AN-011	M	MA	30-42	-	Y	8	6	-	1/0	1/1	1/0	0/0	3/1	1/1	2/1	1/0	0/0
AN-012	M	YA	21-30	-	-	8	5	-	-/-	-/-	-/-	-/-	-/-	-/-	-/-	-/-	-/-
AN-012B	M	MA	40-55	Y	Y	8	6	-	-/-	1/1	1/1	1/1	-/-	0/0	0/0	1/1	-/-
AN-013	M	YA	25-39	Y	Y	8	6	-	0/0	1/1	1/1	1/1	0/0	1/1	1/1	1/1	0/0
AN-014	M?	YA	25-30	-	-	7	0	-	-/-	-/-	-/-	-/-	-/-	-/-	-/-	-/-	-/-
AN-021	F	A	Adult	-	-	6	3	-	-/-	-/-	-/-	-/-	-/-	-/-	-/-	-/-	-/-
AN-022	M	MA	35-45	-	-	7	5	-	-/-	-/-	-/-	-/-	-/-	-/-	-/-	-/-	-/-
AN-023	M	MA	30-40	Y	Y	8	4	-	3/2	1/1	2/2	2/2	-/-	2/3	1/1	-/-	-/-
AN-024	M	MA	30-40	Y	Y	8	4	-	1/1	1/1	1/1	1/1	-/-	1/1	-/-	2/2	-/-
AN-025	F?	MA	35-40	-	-	1	0	-	-/-	-/-	-/-	-/-	-/-	-/-	-/-	-/-	-/-
AN-026	M	YA	25-35	-	Y	8	6	-	1/1	1/1	1/1	2/1	1/1	3/1	1/1	2/3	1/1
AN-027	M	MA	30-44	-	Y	0	6	-	-/-	-/-	1/1	-/-	1/1	1/1	1/1	1/2	1/2
AN-028	M	MA	30-40	-	-	5	6	-	-/-	-/-	-/-	-/-	-/-	-/-	-/-	-/-	-/-
AN-032B	U	U	Adult	-	-	0	6	-	-/-	-/-	-/-	-/-	-/-	-/-	-/-	-/-	-/-

Sk #	Sex	Age	Age Range	Fracture	X-Ray	UL	LL	Femur Head Diameter	C	H	Rad	Ul	MC2	Fem	T	Fib	MT2
AN-034	M	MA	35-50	Y	Y	8	6	-	0/0	0/1	0/0	0/1	-/-	1/1	1/0	2/1	-/-
AN-035	M?	YA	25-35	-	-	8	6	-	2/1	4/4	2/3	2/3	-/-	2/2	3/3	4/4	3/3
AN-038	F	YA	25-34	-	-	5	5	-	-/-	-/-	-/-	-/-	-/-	-/-	-/-	-/-	-/-
AN-039	M?	YA	26-39	-	Y	7	6	-	-/1	1/2	1/0	1/1	-/-	1/2	2/2	2/3	2/1
AN-041	F	YA	20-26	-	Y	7	6	-	-/-	3/3	1/1	1/4	-/-	2/2	1/2	1/1	1/1
AN-042	F	YA	25-34	-	-	8	6	-	-/-	-/-	-/-	-/-	-/-	-/-	-/-	-/-	-/-
AN-043	M	YA	23-34	-	-	6	6	-	-/-	-/-	-/-	-/-	-/-	-/-	-/-	-/-	-/-
AN-045	F?	A	Adult	-	-	6	0	-	-/-	-/-	-/-	-/-	-/-	-/-	-/-	-/-	-/-
AN-045A	F?	MA	21-44	-	Y	5	5	-	2/2	2/3	-/-	-/-	1/2	2/3	2/1	-/-	0/1
AN-046	M?	YA	18-30	Y	Y	8	4	-	1/2	2/2	1/1	1/2	-/-	2/3	2/2	-/-	-/-
AN-047	M	MA	27-49	Y	Y	8	6	-	2/0	1/1	0/0	0/1	-/-	1/2	1/1	2/2	0/0
AN-048B	M?	AD O	17-20	-	Y	8	6	-	0/0	0/1	0/1	1/0	-/-	0/0	1/1	2/1	-/-
AN-049	M	YA	25-34	-	-	0	1	-	-/-	-/-	-/-	-/-	-/-	-/-	-/-	-/-	-/-
AN-050	M	OA	50-59	-	Y	5	5	-	1/-	2/4	2/1	-/-	-/-	2/2	2/3	3/3	-/-
AN-052	F	MA	28-51	-	Y	4	5	-	1/1	3/2	3/3	3/4	-/-	2/3	2/2	3/4	-/-
AN-053	F	MA	35-50	Y	Y	7	5	-	1/0	1/1	0/0	0/0	0/0	1/1	1/0	-/-	-/-
AN-056	M	MA	30-45	Y	Y	7	6	-	1/0	1/1	0/1	-/-	-/-	1/1	1/1	2/1	0/0
AN-057	M	MA	40-44	Y	Y	6	4	-	1/1	1/2	-/-	-/-	-/-	1/1	1/1	-/-	-/-
AN-058	A	OA	40-60	Y	Y	6	6	44.3	1/1	-/-	-/-	1/0	-/-	1/1	1/1	1/1	0/0
AN-061	M	MA	35-46	Y	Y	8	6	-	1/1	1/2	1/1	1/2	-/-	1/1	1/1	1/0	1/1
AN-062	F	YA	26-45	Y	Y	8	3	-	1/1	1/1	1/1	1/1	1/0	-/-	-/-	-/-	-/-
AN-063	M	MA	35-50	-	-	8	0	-	-/-	-/-	-/-	-/-	-/-	-/-	-/-	-/-	-/-
AN-064	M?	MA	40-45	Y	Y	2	3	-	-/-	5/3	2/3	-/-	-/-	2/2	2/1	-/-	2/1
AN-065	M	MA	26-40	-	Y	8	6	-	3/1	2/3	2/2	2/2	-/-	3/4	1/2	-/-	2/2

Sk #	Sex	Age	Age Range	Fracture	X-Ray	UL	LL	Femur Head Diameter	C	H	Rad	Ul	MC2	Fem	T	Fib	MT2
AN-066	F	YA	23-34	-	Y	8	6	-	1/2	1/4	2/2	2/2	-/-	2/4	1/0	1/1	1/1
AN-067	F	MA	40-44	-	Y	2	6	40.8	-/-	-/-	1/-	1/-	2/1	1/1	1/1	2/1	1/1
AN-068	M	MA	40-44	-	-	2	6	-	-/-	-/-	-/-	-/-	-/-	-/-	-/-	-/-	-/-
AN-069	F?	U	Adult	-	-	3	0	-	-/-	-/-	-/-	-/-	-/-	-/-	-/-	-/-	-/-
AN-072	F	YA	30-34	-	Y	5	6	-	1/2	1/1	2/2	1/0	-/-	-/-	1/2	2/2	-/-
AN-077	M?	YA	25-35	-	-	8	5	-	-/-	-/-	-/-	-/-	-/-	-/-	-/-	-/-	-/-
AN-078	F	YA	22-29	-	-	4	6	40.3, 41.9	-/-	-/-	-/-	-/-	-/-	-/-	-/-	-/-	-/-
AN-080	U	U	Adult	-	-	3	0	-	-/-	-/-	-/-	-/-	-/-	-/-	-/-	-/-	-/-
AN-081	F	MA	40-44	-	-	2	1	-	-/-	-/-	-/-	-/-	-/-	-/-	-/-	-/-	-/-
AN-082	M	ADO	16-22	-	Y	8	1	-	2/3	3/3	2/3	1/3	-/-	2/3	-/-	-/-	-/-
AN-092	M	YA	25-32	-	Y	8	6	-	3/4	3/3	4/2	4/2	-/-	4/2	2/2	1/1	-/-
AN-093	M	MA	28-45	-	Y	8	6	-	1/1	2/1	3/2	3/2	-/-	1/2	3/2	2/2	1/1
AN-096	F	YA	25-35	-	-	1	2	45.4	-/-	-/-	-/-	-/-	-/-	-/-	-/-	-/-	-/-
AN-098	M	OA	50+	Y	Y	8	6	-	1/0	1/1	1/1	1/1	-/-	1/1	1/1	1/0	-/-
AN-102	F	YA	26-34	-	Y	2	2	-	-/-	3/3	-/-	-/-	0/0	2/3	-/-	-/-	-/-
AN-104	F?	MA	30-40	Y	Y	7	6	-	0/1	0/1	0/1	0/1	-/-	1/1	1/1	0/0	-/-
AN-106	M	MA	30-44	-	-	8	6	-	-/-	-/-	-/-	-/-	-/-	-/-	-/-	-/-	-/-
AN-107	M?	ADO	15-19	-	Y	7	5	-	3/5+	4/2	2/4	4/3	2/3	-/2	1/3	1/2	2/2
AN-108	M?	ADO	17-22	-	Y	8	6	-	1/4	2/3	2/2	3/3	-/-	2/1	1/1	1/1	-/-
AN-109	F	MA	35-61	-	Y	7	4	-	1/0	2/2	1/-	1/1	1/0	2/3	1/1	-/-	1/1
AN-110	M?	YA	26-34	-	Y	6	6	-	2/2	1/2	2/2	1/1	-/-	3/2	1/2	2/1	2/2
AN-111	M	YA	18-30	-	-	8	6	44.8	-/-	-/-	-/-	-/-	-/-	-/-	-/-	-/-	-/-
AN-112	F	YA	30-39	-	Y	7	6	-	3/3	2/3	2/1	1/2	1/2	3/-	3/3	2/4	2/2
AN-112A	U	U	Adult	-	-	4	0	-	-/-	-/-	-/-	-/-	-/-	-/-	-/-	-/-	-/-

Sk #	Sex	Age	Age Range	Fracture	X-Ray	UL	LL	Femur Head Diameter	C	H	Rad	Ul	MC2	Fem	T	Fib	MT2
AN-113	F	MA	35-46	Y	Y	8	6	-	0/0	2/2	2/1	1/0	1/1	1/1	1/1	1/0	-/-
AN-115	F	MA	35-50	-	Y	8	5	-	1/1	1/1	1/1	2/2	3/1	2/1	1/1	-/-	-/-
AN-116	F?	MA	26-44	Y	Y	8	6	44.8	0/1	2/2	1/1	1/2	-/-	1/1	1/1	1/1	2/1
AN-117	M?	MA	30-50	Y	Y	8	5	49.8	1/1	1/2	2/2	2/2	-/-	1/2	2/2	1/2	1/1
AN-118	M?	YA	25-39	-	Y	6	6	50.2	4/1	4/2	3/2	3/3	-/-	2/2	3/2	1/1	-/-
AN-119	M?	YA	18-30	-	-	8	0	-	-/-	-/-	-/-	-/-	-/-	-/-	-/-	-/-	-/-
AN-120	M	YA	25-34	Y	Y	8	6	49.7	1/1	2/3	2/2	2/2	-/-	2/2	2/1	2/1	1/1
AN-121	M	U	Adult	-	-	8	6	-	-/-	-/-	-/-	-/-	-/-	-/-	-/-	-/-	-/-
AN-122	M	MA	35-46	-	-	8	6	51.4	-/-	-/-	-/-	-/-	-/-	-/-	-/-	-/-	-/-
AN-123	F	YA	25-34	Y	Y	8	6	42	0/0	1/1	1/1	1/1	-/-	1/1	1/1	1/0	-/-
AN-128	F	YA	25-34	-	-	8	6	40.5	-/-	-/-	-/-	-/-	-/-	-/-	-/-	-/-	-/-
AN-133	F	YA	21-34	-	-	8	6	39.8	-/-	-/-	-/-	-/-	-/-	-/-	-/-	-/-	-/-
AN-134	F?	MA	35-40	-	Y	0	5	41.3, 41.2	-/-	-/-	-/-	-/-	-/-	3/2	1/2	-/3	-/-
AN-135	M?	MA	30-60	-	-	7	6	-	-/-	-/-	-/-	-/-	-/-	-/-	-/-	-/-	-/-
AN-136	M	YA	24-39	-	Y	7	6	49.9	0/0	-/1	0/0	1/0	-/-	1/1	2/1	1/0	1/1
AN-140	M?	YA	25-39	-	-	7	6	-	-/-	-/-	-/-	-/-	-/-	-/-	-/-	-/-	-/-
AN-141	M?	MA	35-50	-	-	8	6	-	-/-	-/-	-/-	-/-	-/-	-/-	-/-	-/-	-/-
AN-142	F	MA	35-45	-	Y	7	6	42.6	1/0	3/3	1/2	1/1	1/0	2/3	1/2	2/4	1/0
AN-143	M	YA	20-34	-	Y	8	6	-	1/1	3/3	1/1	1/1	-/-	2/4	3/2	3/3	1/0
AN-144	M	YA	25-39	-	Y	6	6	46.8	4/4	3/1	3/0	3/1	-/-	3/2	2/2	3/4	-/-
AN-147	M	MA	35-50	-	-	8	4	48.6	-/-	-/-	-/-	-/-	-/-	-/-	-/-	-/-	-/-
AN-152	F	MA	30-44	Y	Y	8	6	37.6	0/0	1/1	1/1	1/1	0/0	1/1	0/0	0/1	1/1
AN-154	F	A	Adult	-	Y	4	6	39.4	2/2	1/1	1/2	-/-	-/-	1/1	2/2	2/2	-/-
AN-155	F?	U	Adult	-	Y	0	0	-	-/-	-/-	-/-	-/-	-/-	-/-	3/3	-/3	-/-
AN-156	M	MA	35-44	-	-	8	6	44.8	-/-	-/-	-/-	-/-	-/-	-/-	-/-	-/-	-/-
AN-157	F	YA	26-34	-	Y	8	5	45.4	0/0	1/0	0/0	0/1	-/-	0/0	0/0	-/-	-/-

Sk #	Sex	Age	Age Range	Fracture	X-Ray	UL	LL	Femur Head Diameter	C	H	Rad	Ul	MC2	Fem	T	Fib	MT2
AN-158	M?	U	Adult	-	-	0	6	48.2	-/-	-/-	-/-	-/-	-/-	-/-	-/-	-/-	-/-
AN-159	U	U	Adult	-	-	0	4	-	-/-	-/-	-/-	-/-	-/-	-/-	-/-	-/-	-/-
AN-160	F?	YA	18-22	-	-	5	3	-	-/-	-/-	-/-	-/-	-/-	-/-	-/-	-/-	-/-
AN-161A	M?	MA	40-44	-	-	0	2	-	-/-	-/-	-/-	-/-	-/-	-/-	-/-	-/-	-/-
AN-162	F?	YA	17-22	-	Y	8	6	39.9	4/4	3/4	3/3	2/2	4/3	2/2	1/1	1/2	4/3
AN-165	M	YA	20-30	Y	Y	8	6	49.6	1/1	1/2	1/1	2/1	1/1	1/1	0/1	1/1	1/1
AN-167	M?	YA	18-25	-	Y	7	5	49.8	1/1	2/1	1/0	1/1	-/-	1/1	1/1	3/3	-/-
AN-168	F	YA	21-30	-	Y	8	6	42.1	2/2	2/2	1/1	1/1	1/1	1/1	1/1	1/1	1/1
AN-170	M	MA	35-45	-	Y	8	6	47.2	2/2	4/1	1/2	2/3	-/-	3/2	0/1	1/4	0/0
AN-171	F	MA	30-45	-	Y	7	6	42.9	0/1	3/2	0/1	0/0	1/1	4/3	3/2	3/3	2/1
AN-172	F?	MA	30-55	Y	Y	8	6	43.2	2/1	1/1	1/1	1/1	-/-	1/2	2/2	2/2	-/-
AN-173	F?	MA	30-45	-	-	4	6	-	-/-	-/-	-/-	-/-	-/-	-/-	-/-	-/-	-/-
AN-175	M	YA	26-34	-	-	3	5	-	-/-	-/-	-/-	-/-	-/-	-/-	-/-	-/-	-/-
AN-177	M	MA	35-46	Y	Y	8	6	-	1/1	1/2	1/0	1/1	-/-	2/2	2/2	2/2	-/-
AN-178	F?	YA	26-39	-	Y	8	6	44.8	4/3	4/4	2/2	1/4	1/1	4/3	4/1	3/2	3/2
AN-179	M	YA	25-34	-	-	8	6	43.5	-/-	-/-	-/-	-/-	-/-	-/-	-/-	-/-	-/-
AN-182	F	YA	20-25	-	-	6	6	40.5	-/-	-/-	-/-	-/-	-/-	-/-	-/-	-/-	-/-
AN-183	F?	MA	35-46	-	-	7	5	44	-/-	-/-	-/-	-/-	-/-	-/-	-/-	-/-	-/-
AN-184	M	MA	35-50	-	Y	8	5	48.7	2/1	2/4	2/2	2/4	-/-	1/1	1/1	-/-	1/1
AN-185	F	YA	19-25	-	-	5	6	39.6	-/-	-/-	-/-	-/-	-/-	-/-	-/-	-/-	-/-
AN-185A	M	MA	34-42	Y	Y	8	6	-	2/2	2/1	3/3	3/3	2/1	3/2	2/3	4/2	1/2
AN-188	M?	YA	26-35	-	-	7	5	-	-/-	-/-	-/-	-/-	-/-	-/-	-/-	-/-	-/-
AN-190	F	MA	25-59	-	-	3	5	-	-/-	-/-	-/-	-/-	-/-	-/-	-/-	-/-	-/-
AN-191	F	OA	40-60	Y	Y	8	5	-	1/1	1/2	0/0	1/1	0/1	2/2	2/2	4/2	-/-
AN-193	F	A	Adult	-	-	1	3	41.7	-/-	-/-	-/-	-/-	-/-	-/-	-/-	-/-	-/-
AN-198	U	U	Adult	-	-	0	3	-	-/-	-/-	-/-	-/-	-/-	-/-	-/-	-/-	-/-

Sk #	Sex	Age	Age Range	Fracture	X-Ray	UL	LL	Femur Head Diameter	C	H	Rad	Ul	MC2	Fem	T	Fib	MT2
AN-199	U	U	Adult	-	-	0	4	-	-/-	-/-	-/-	-/-	-/-	-/-	-/-	-/-	-/-
AN-200	M	YA	20-30	-	Y	8	4	-	2/1	1/2	2/0	0/0	-/-	1/1	-/1	-/-	-/-
AN-201	M	MA	35-50	-	-	8	6	-	-/-	-/-	-/-	-/-	-/-	-/-	-/-	-/-	-/-
AN-202	F	YA	25-34	-	Y	8	6	-	1/2	1/1	0/0	0/3	1/1	0/1	0/0	1/0	1/1
AN-204A	M	MA	35-46	Y	Y	8	6	-	2/1	2/1	2/1	2/2	-/-	2/1	1/1	2/3	1/1
AN-205	F	YA	20-26	-	-	4	5	41.3	-/-	-/-	-/-	-/-	-/-	-/-	-/-	-/-	-/-
AN-209	M?	U	Adult	-	-	6	6	-	-/-	-/-	-/-	-/-	-/-	-/-	-/-	-/-	-/-
AN-210	M?	YA	25-35	Y	Y	4	6	-	1/1	1/2	-/-	-/-	-/-	1/2	1/1	2/2	1/1
AN-211	M?	YA	25-42	-	Y	7	6	47.3	0/0	1/4	5/5	5/3	-/-	4/3	1/2	2/2	-/-
AN-212	F	YA	26-34	-	-	6	6	-	-/-	-/-	-/-	-/-	-/-	-/-	-/-	-/-	-/-
AN-213	M?	U	Adult	-	-	6	6	49.1	-/-	-/-	-/-	-/-	-/-	-/-	-/-	-/-	-/-
AN-214	M	YA	19-25	-	-	2	1	-	-/-	-/-	-/-	-/-	-/-	-/-	-/-	-/-	-/-
AN-216	M?	YA	20-34	-	Y	8	6	47.3, 45.7	2/1	5/2	4/3	4/4	-/-	2/2	2/3	1/2	0/0
AN-217	F	MA	35-39	-	Y	7	5	46.1, 45.3	2/4	5/5	3/3	3/4	2/3	5/4	2/5	4/5	2/4
AN-217A	M	YA	25-29	-	-	1	0	-	-/-	-/-	-/-	-/-	-/-	-/-	-/-	-/-	-/-
AN-218	F	YA	25-34	Y	Y	8	6	-	1/1	1/1	1/0	1/1	1/1	1/1	1/1	1/1	1/1
AN-220	F	OA	50+	-	Y	5	4	-	3/2	5/5+	5/2	2/2	1/0	3/2	3/3	-/-	0/1
AN-221	M	YA	30-34	-	-	0	5	47.3	-/-	-/-	-/-	-/-	-/-	-/-	-/-	-/-	-/-
AN-222	M?	U	Adult	-	-	2	6	-	-/-	-/-	-/-	-/-	-/-	-/-	-/-	-/-	-/-
AN-223	U	U	Adult	-	-	0	4	-	-/-	-/-	-/-	-/-	-/-	-/-	-/-	-/-	-/-
AN-224	F	U	Adult	-	-	2	4	-	-/-	-/-	-/-	-/-	-/-	-/-	-/-	-/-	-/-
AN-225	M	YA	24-29	Y	Y	8	6	48.5	1/1	1/1	1/1	1/0	-/-	2/2	2/2	1/1	0/0
AN-226	F	YA	30-39	-	Y	8	6	40.5	1/1	3/1	1/1	2/2	1/1	3/2	2/2	2/2	0/0
AN-229	M	MA	35-45	-	Y	8	6	48.3	1/2	2/2	4/1	4/1	-/-	1/2	1/0	0/0	-/-
AN-230	M?	YA	20-29	-	-	4	3	48.4	-/-	-/-	-/-	-/-	-/-	-/-	-/-	-/-	-/-
AN-230A	M	MA	40-56	Y	Y	8	6	-	1/1	2/3	2/2	2/3	-/-	2/1	0/1	2/5	1/1

Sk #	Sex	Age	Age Range	Fracture	X-Ray	UL	LL	Femur Head Diameter	C	H	Rad	Ul	MC2	Fem	T	Fib	MT2
AN-234	U	YA	25-34	-	-	3	5	-	-/-	-/-	-/-	-/-	-/-	-/-	-/-	-/-	-/-
AN-235	M?	YA	25-29	-	Y	6	0	49.5	-/-	1/1	2/2	4/3	-/-	-/-	-/-	-/-	-/-
AN-235B	M	YA	25-34	-	-	0	1	-	-/-	-/-	-/-	-/-	-/-	-/-	-/-	-/-	-/-
AN-237	F?	MA	35-50+	-	-	4	3	-	-/-	-/-	-/-	-/-	-/-	-/-	-/-	-/-	-/-
AN-238	M	MA	25-55	-	Y	8	6	-	0/1	1/1	0/0	0/0	-/-	1/1	1/1	1/1	-/-
AN-240	M	YA	26-34	-	-	7	6	-	-/-	-/-	-/-	-/-	-/-	-/-	-/-	-/-	-/-
AN-241	F	OA	45+	Y	Y	8	6	-	1/1	2/3	3/2	3/2	-/-	1/2	2/2	3/3	1/1
AN-242	F	OA	40-49	-	Y	8	4	-	1/1	2/3	2/2	2/2	1/1	5/3	1/2	3/3	1/2
AN-243	F	YA	25-34	-	Y	8	6	42.4	2/2	1/1	1/1	2/2	-/-	1/1			
AN-244	M	YA	25-35	Y	Y	8	6	49.9	3/1	0/0	2/1	1/1	-/-	0/1	0/1	0/1	0/0
AN-247	F	YA	30-39	Y	Y	2	6	42.4	-/-	1/1	-/-	-/-	-/-	3/0	1/0	1/1	2/2
AN-248	A	MA	25-45	-	-	0	1	-	-/-	-/-	-/-	-/-	-/-	-/-	-/-	-/-	-/-
AN-252	M	MA	35-46	-	Y	8	6	-	0/1	1/1	1/2	4/4	-/-	1/1	1/1	1/1	2/1
AN-256	F?	U	Adult	-	-	1	4	45	-/-	-/-	-/-	-/-	-/-	-/-	-/-	-/-	-/-
AN-257	M?	MA	35-57	-	-	8	6	-	-/-	-/-	-/-	-/-	-/-	-/-	-/-	-/-	-/-
AN-259	F	YA	20-29	-	Y	8	6	-	4/4	4/3	2/2	4/3	2/1	3/4	2/0	2/1	1/1
AN-262A	F	MA	35-39	-	Y	8	6	-	3/2	3/1	3/1	3/2	-/-	3/2	1/2	1/1	0/0
AN-263	F	OA	60+	-	Y	8	5	-	1/1	1/1	2/3	1/1	1/1	1/1	2/1	1/1	1/1
AN-263A	F?	U	Adult	-	-	0	6	42.0, 42.2	-/-	-/-	-/-	-/-	-/-	-/-	-/-	-/-	-/-
AN-266	M?	MA	40-46	-	Y	8	6	45.1	1/2	2/2	1/2	1/1	-/-	2/2	1/1	1/2	0/1
AN-267	F?	YA	25-35	-	-	0	4	-	-/-	-/-	-/-	-/-	-/-	-/-	-/-	-/-	-/-
AN-269	M	MA	35-44	-	Y	8	6	47.9	1/2	4/4	3/3	3/3	-/-	4/3	5/4	5+/5+	2/0
AN-270	F?	YA	25-35	-	-	7	4	-	-/-	-/-	-/-	-/-	-/-	-/-	-/-	-/-	-/-
AN-271	F?	U	Adult	-	-	5	0	-	-/-	-/-	-/-	-/-	-/-	-/-	-/-	-/-	-/-
AN-272	U	U	Adult	-	-	0	2	-	-/-	-/-	-/-	-/-	-/-	-/-	-/-	-/-	-/-
AN-274	F	YA	20-25	-	-	0	6	41.6	-/-	-/-	-/-	-/-	-/-	-/-	-/-	-/-	-/-

Sk #	Sex	Age	Age Range	Fracture	X-Ray	UL	LL	Femur Head Diameter	C	H	Rad	Ul	MC2	Fem	T	Fib	MT2
AN-276	F	A	Adult	-	-	0	6	39.5	-/-	-/-	-/-	-/-	-/-	-/-	-/-	-/-	-/-
AN-277	F?	U	Adult	Y	Y	8	5	42.9	2/4	2/1	2/3	3/3	-/-	2/1	1/1	2/2	-/-
AN-278	M	YA	30-34	-	-	8	0	-	-/-	-/-	-/-	-/-	-/-	-/-	-/-	-/-	-/-
AN-280	M	YA	20-34	-	-	7	6	50.5	-/-	-/-	-/-	-/-	-/-	-/-	-/-	-/-	-/-
AN-282	M	YA	21-34	-	-	5	3	-	-/-	-/-	-/-	-/-	-/-	-/-	-/-	-/-	-/-
AN-282B*	M?	U	Adult	-	-	0	1	51.2	-/-	-/-	-/-	-/-	-/-	-/-	-/-	-/-	-/-

F=Female; F?=Possible Female; M=Male; M?=Possible Male; U=Undetermined; A=Ambiguous; ADO=Adolescent (15-19 years old); YA=Young Adult (20-34 years old); MA=Middle Adult (35-49 years old); OA=Old Adult (50+ years old); UL=Upper limb; LL=Lower limb; C=Clavicle; H=Humerus; Rad=Radius; Ul=Ulna; MC2=Second metacarpal; Fem=Femur; T=Tibia; Fib=Fibula; MT2=Second metatarsal; Y='Yes' (i.e., was individual radiographed or a fracture was present); - – observation absent (e.g., not radiographed, not fractured, femoral head absent/damaged and not measured, no erosion & abrasion score was assigned); blank=erosion score not recorded.

Table B.2 – The sex, age, and skeletal inventory details for each individual at Vagnari.

Skeleton Number	Sex	Age	Age Range	Fracture	X-ray	Number of 'Complete' Bones		Femur Head Diameter	Erosion & Abrasion Grade Right/Left								
						UL	LL		C	H	Rad	Ul	MC2	Fem	T	Fib	MT2
VA-F034	M?	U	35-50+	-	Y	5	4	-	3/-	3/3	4/3	3/3	-/-	5/4	2/4	3/4	-/-
VA-F035	M	MA	30-50	-	-	5	4	-	3/4	3/4	3/4	3/3	-/-	4/4	4/3	3/4	-/-
VA-F037	F	MA	25-35	-	-	6	4	40.3, 36.8	3/3	3/3	2/3	2/2	-/1	3/3	4/3	4/3	3/-
VA-F040	F	ADO	15-17	-	Y	8	6	40.3, 39.1	3/3	3/2	1/1	2/2	2/2	2/2	3/2	2/3	4/1
VA-F042	M	YA	20-30	-	-	8	5	45.0	3/2	4/3	3/3	3/2	3/2	4/4	5/3	3/4	-/-
VA-F042A	M	YA	25-35	Y	Y	5	4	46.1, 47.1	3/2	4/4	3/3	3/3	3/-	3/3	3/3	-/-	-/-
VA-F062	M?	MA	35-45	-	Y	5	5	-	-/3	4/5	5/3	4/3	2/3	4/5	5/4	4/4	5/5
VA-F067	M	YA	25-45	Y	Y	7	6	44.5	3/3	3/3	3/2	3/2	-/3	4/3	3/3	4/3	-/3
VA-F068	M	MA	35-45	Y	Y	7	6	45.1	2/2	4/3	2/2	2/2	-/-	3/3	4/2	4/2	-/2
VA-F086	M?	U	Adult	-	-	0	0	-	-/-	-/-	-/-	-/-	-/-	-/-	-/-	-/-	-/-
VA-F089	U	U	Adult	Y	Y	1	0	-	4/5	4/4	4/4	4/4	-/-	4/5	-/-	4/-	-/-
VA-F092	M	MA	35-45	-	Y	4	3	-	3/3	3/3	4/3	4/3	2/-	3/3	3/3	2/3	-/-
VA-F093	F	YA	20-30	-	-	3	4	-	3/3	3/4	3/3	3/3	-/-	3/4	3/5	4/4	-/-
VA-F094	F	MA	30-45	-	-	0	2	-	2/3	3/3	4/4	-/3	-/-	4/-	3/4	-/-	-/2
VA-F095	F?	U	Adult	-	-	0	0	-	-/4	-/-	-/5	-/4	-/-	-/-	4/4	3/4	-/-
VA-F096A	F?	U	Adult	-	-	6	1	-	2/3	4/3	2/3	-/2	-/-	4/4	3/3	-/4	-/-
VA-F096B	F?	U	Adult	Y	Y	1	1	-	-/-	-/5	4/5	4/5	-/2	3/3	3/3	-/-	-/3
VA-F098	F?	U	Adult	-	-	0	0	-	-/-	5/5	5/4	4/4	-/-	5/4	-/-	-/-	-/-
VA-F100	M?	U	Adult	-	-	0	1	-	-/-	-/-	3/3	4/4	-/-	3/3	4/4	3/3	-/-
VA-F117	F?	YA	20-26	-	-	8	5	-	2/4	2/4	3/3	3/3	-/4	3/3	2/4	2/3	-/4
VA-F126	M?	YA	25-30	-	-	1	2	-	3/-	3/3	4/3	3/3	-/-	3/4	3/4	3/3	3/-
VA-F127	A	YA	22-30	-	-	6	1	38.0	3/3	3/3	4/3	4/2	-/-	-/3	3/5	4/4	-/2
VA-F130	F?	ADO	15-19	-	-	2	1	39.7, 39.1	3/2	3/3	3/3	2/3	-/2	3/3	3/4	3/3	-/-

Sk #	Sex	Age	Age Range	Fracture	X-Ray	UL	LL	Femur Head Diameter	C	H	Rad	Ul	MC2	Fem	T	Fib	MT2
VA-F131	M	YA	25-35	Y	Y	6	5	-	3/3	2/2	3/3	3/3	3/-	3/3	3/3	3/3	3/-
VA-F132	F	YA	26-45	-	-	2	0	-	3/4	4/4	3/3	2/3	-/-	3/3	3/4	-/-	-/-
VA-F137A	F?	YA	20-30	-	-	6	1	46.1	3/3	3/3	4/4	4/4	4/-	3/3	3/-	3/-	-/-
VA-F137B	A	U	Adult	-	-	0	0	-	-/-	-/-	-/-	-/-	-/-	3/3	-/-	-/-	-/-
VA-F200	F	MA	40-45	-	Y	6	1	45.5, 44.8	3/2	3/3	2/3	2/3	4/3	3/3	3/3	-/3	-/-
VA-F204	F	YA	25-35+	Y	Y	5	4	-	2/2	2/2	3/2	2/2	-/3	4/5	3/3	4/-	-/3
VA-F205	F	MA	35-50	-	Y	2	3	40.7, 40.0	-/-	3/2	-/3	-/3	-/-	4/4	4/4	-/-	-/-
VA-F206	F	MA	35-45+	-	-	0	0	-	-/-	4/-	3/-	4/-	-/-	4/5	4/4	4/-	-/-
VA-F207	M?	YA	19-25	-	Y	1	5	48.9	4/4	3/3	4/4	4/4	-/-	4/4	4/4	5/5	-/3
VA-F208	U	ADO	17-Dec	-	-	0	1	-	-/-	-/3	-/3	-/4	5/-	5+/5+	5+/5+	-/-	-/-
VA-F211	F	YA	25-35	-	Y	8	2	-	2/2	3/2	2/3	2/3	-/-	2/2	2/2	2/3	-/-
VA-F212	U	U	Adult	-	-	0	0	-	-/-	-/-	-/-	-/-	-/-	-/-	-/-	-/-	-/-
VA-F213	M	MA	27-57	-	Y	1	4	-	-/5	4/4	4/4	4/4	-/3	5/4	2/3	3/3	-/-
VA-F214	M	MA	35-45	-	Y	8	6	-	2/3	4/3	2/2	4/3	2/-	3/3	3/2	3/2	2/2
VA-F215	F	YA	30-40	-	Y	5	2	46.7, 45.7	3/3	3/4	3/3	3/2	2/2	3/2	2/3	3/3	2/-
VA-F216	M	MA	30-40	Y	Y	7	6	47.4	3/2	3/4	2/4	2/4	1/-	3/3	3/3	2/4	-/2
VA-F220	M	MA	35-45	Y	Y	4	5	46.7	3/3	3/3	3/3	3/3	-/2	4/3	3/3	3/2	-/3
VA-F229	M	U	35+	-	-	3	2	47.5	3/4	3/4	3/5	4/4	3/-	4/5+	5+/5+	3/5	-/-
VA-F231	M?	YA	27-37	Y	Y	2	4	46.5	4/3	5/3	3/3	3/3	3/-	3/3	3/4	3/3	-/-
VA-F234	M	YA	25-35	-	Y	8	6	48.0	4/3	4/5	5/3	4/3	3/3	4/4	3/3	3/5	3/4
VA-F235	M	OA	40-60+	-	Y	2	5	-	-/3	4/4	4/4	3/4	-/-	3/3	3/3	2/3	-/-
VA-F245	F	ADO	17-21	-	-	5	0	-	-/3	5/4	4/3	5/3	-/-	4/4	4/4	3/4	-/-
VA-F246	F?	YA	20-25	-	-	0	1	-	-/-	5/5	4/3	4/5	-/-	5/5	5+/5	5/5	-/-
VA-F247	M	MA	30-50	-	-	3	3	-	2/3	3/3	2/2	-/2	-/-	3/3	3/3	2/2	-/-
VA-F248	F?	YA	20-35	-	-	0	0	-	2/-	4/-	-/-	2/-	2/2	4/4	4/3	4/3	3/-
VA-F249	F?	YA	25-35	Y	Y	2	2	39.2	2/3	2/3	2/3	2/2	-/-	3/3	3/3	-/3	-/-

Sk #	Sex	Age	Age Range	Fracture	X-Ray	UL	LL	Femur Head Diameter	C	H	Rad	Ul	MC2	Fem	T	Fib	MT2
VA-F250	M?	YA	25-30	-	Y	6	5	-	3/2	3/3	3/4	4/3	3/-	4/4	4/3	4/2	2/2
VA-F252	F?	ADO	17-22	-	Y	8	5	44.7	3/4	3/4	3/3	3/3	2/2	3/3	3/3	3/3	3/4
VA-F253	M?	U	Adult	-	-	2	1	-	4/-	4/3	3/5	3/4	-/-	5/3	3/3	3/3	-/-
VA-F254	M	MA	30-40	-	-	1	1	45.7	-/2	4/3	2/2	3/2	-/-	3/4	3/2	2/-	-/-
VA-F280	U	YA	20-25	-	-	2	0	-	2/4	3/4	2/2	3/3	-/-	5/4	5/-	4/4	-/-
VA-F284	F	YA	20-25	-	Y	8	2	-	3/3	3/4	3/4	3/4	-/-	3/4	3/3	4/3	-/-
VA-F287	M	MA	35-50	-	Y	6	3	-	5/-	3/3	3/3	3/3	-/-	3/3	3/3	2/3	-/-
VA-F288	M?	YA	25-35	Y	Y	8	6	46.9, 47.5	5/3	5/5	4/3	3/4	-/3	4/4	4/3	5/4	5/4
VA-F289	A	ADO	16-19	-	-	2	3	-	4/-	5/3	4/3	5/-	-/-	4/4	3/3	3/3	-/-
VA-F290	M	MA	30-60	-	Y	8	4	-	3/3	4/3	3/3	3/4	-/-	3/3	3/4	3/2	4/4
VA-F291	M	YA	25-35	-	-	0	2	-	-/-	3/3	2/3	2/3	-/-	3/3	3/2	2/3	-/-
VA-F293	U	U	Adult	-	-	0	0	-	-/-	-/-	-/-	-/-	-/-	-/-	-/-	-/-	-/-
VA-F294	F?	OA	50+	-	Y	1	0	43.9	3/-	-/4	4/4	3/3	3/4	5/4	4/3	3/2	-/2
VA-F296	F	YA	18-25	-	Y	8	6	41.1, 41.1	3/2	3/3	2/3	2/3	2/-	2/2	2/3	3/3	-/-
VA-F298	U	U	Adult	-	-	0	0	-	-/-	-/-	-/-	-/-	-/-	-/-	-/-	-/-	-/-
VA-F306	F?	MA	35-50	-	Y	6	1	-	3/2	4/3	2/3	2/2	-/-	3/3	3/3	-/-	-/-
VA-F312	F?	YA	25-35	-	Y	5	6	-	3/3	3/3	4/2	3/2	2/-	3/3	3/3	4/3	-/2

F=Female; F?=Possible Female; M=Male; M?=Possible Male; U=Undetermined; A=Ambiguous; ADO=Adolescent (15-19 years old); YA=Young Adult (20-34 years old); MA=Middle Adult (35-49 years old); OA=Old Adult (50+ years old); UL=Upper limb; LL=Lower limb; C=Clavicle; H=Humerus; Rad=Radius; Ul=Ulna; MC2=Second metacarpal; Fem=Femur; T=Tibia; Fib=Fibula; MT2=Second metatarsal; Y='Yes' (i.e., was individual radiographed or a fracture was present); - – observation absent (e.g., not radiographed, not fractured, femoral head absent/damaged and not measured, no erosion & abrasion score was assigned); blank=erosion score not recorded.

Appendix C: Fracture Attributes

Each fracture observed at Ancaster and Vagnari are detailed in this Appendix. The attributes reported for each fracture include the bone and segment location, the element type, and side. Additionally, the type of fracture and its timing (i.e., antemortem, perimortem) are presented; the prevalence of osteoarthritis, angulation, poor apposition, rotation, overlap, and shortening are also recorded. Table C.1 reports the fractures observed at Ancaster and Table C.2 presents the fractures observed at Vagnari.

Abbreviations used in the charts include:

OA_x – Osteoarthritis
ANG – Angulation
APP – Amount of poor apposition
RO – Rotation
/ – Attribute not observable
- – Attribute not applicable to this fracture type
U – Unknown Sex
F – Female
F? – Possible Female
M – Male
M? – Possible Male
YA – Young Adult (20-34 years old)
MA – Middle Adult (35-49 years old)
OA – Old Adult (50+ years old)
L – Left
R – Right
A – Antemortem
P – Perimortem
N – No osteoarthritis observed
PE – Proximal epiphysis
PD – Proximal diaphysis
MD – Middle diaphysis
DD – Distal diaphysis
DE – Distal epiphysis

Table C.1 – Attributes of each fracture observed at Ancaster.

Skeleton Number	Sex	Age	Element	Side	Fracture Type	Timing	Segment	OA_x	ANG (°)	APP (%)	RO (°)	Overlap (mm)	Shortening (mm)
AN-001	F?	YA	Tibia	R	Crush	A	PE	N	-	-	-	-	/
AN-012B	M	MA	Clavicle	L	Unknown	A	MD	N	/	/	/	/	/
			Radius	R	Crush	A	DE	N	-	-	-	-	/
			Tibia	R	Oblique (possible spiral)	A	DD	Knee	5.2	93.2	5	/	-6
AN-013	M	YA	Fibula	L	Avulsion	A	DE	N	0	100	0	0	/
AN-023	M	MA	Radius	R	Spiral	A	PD	N	9.3	44.9	19	7.7	/
			Ulna	R	Spiral	A	PD	N	6.9	34.5	6	5.4	/
AN-024	M	MA	Radius	L	Spiral	A	MD	Elbow	12.9	-9	90	4.7	/
			Ulna	L	Spiral	A	MD	Elbow	9.6	-10.8	3	14.2	/
AN-034	M	MA	Fibula	L	Spiral	A	PD	N	1.3	43.2	0	6.4	/
			Tibia	L	Spiral	A	DD	N	3.9	50.4	0	13.6	-18
AN-046	M?	YA	Tibia	L	Avulsion	A	DE	N	/	/	/	/	9
AN-047	M	MA	Fibula	L	Oblique	A	DE	N	0	100	0	/	/
AN-053	F	MA	Radius	R	Oblique	A	DE	N	6.8	100	0	/	/
			Ulna	R	Crush	A	DE	N	-	-	-	-	/
AN-056	M	MA	Clavicle	R	Incomplete – possible oblique	A	MD	N	5.4	82.5	/	-	-10
AN-057	M	MA	Clavicle	L	Transverse	A	MD	N	16.7	40	30	0	-2
AN-058	U	OA	Clavicle	L	Transverse	A	MD	Shoulder	13.2	70	5	-2.1	-14
AN-061	M	MA	Clavicle	L	Transverse	A	MD	N	17	100	5	/	-1
AN-062	F	YA	Tibia	R	Crush	A	PE	N	-	-	-	-	/

Skeleton Number	Sex	Age	Element	Side	Fracture Type	Timing	Segment	OA_x	ANG (º)	APP (%)	RO (º)	Overlap (mm)	Shortening (mm)
AN-064	M?	MA	Tibia	L	Oblique	A	DD	N	4.4	69.2	/	23.5	/
AN-098	M	OA	Clavicle	R	Transverse	A	MD	N	12.7	86.5	0	/	-4
			Tibia	L	Avulsion	A	DE	N	/	/	/	/	-3
AN-104	F?	MA	Radius	R	Spiral Butterfly Comminuted	A	MD	N	7.1	100	55	/	0
AN-113	F	MA	Femur	L	Incomplete - Stress.	A	PE	N	-	-	-	-	-
AN-116	F	MA	Fibula	L	Oblique	A	PD	Knee	0	60.8	/	0	/
AN-117	M?	MA	Tibia	L	Crush	A	PE	Knee, Ankle	-	-	-	-	/
				L	Crush	A	DE	Knee, Ankle	-	-	-	-	/
			Tibia	R	Avulsion, Crush	A	DE	Knee, Ankle	/	/	0	0	4
			Fibula	R	Oblique	A	DD	Knee, Ankle	4.1	61.7	0	9.6	/
AN-120A	M	YA	Clavicle	L	Transverse (probable)	A	MD	N	17.1	100	23	/	-14
AN-123	F	YA	Radius	L	Oblique Butterfly	P	DD	N	/	/	/	/	/
AN-152	F	YA	Radius	L	Crush	A	PE	N	13.7	-	-	-	-1
			Tibia	L	Crush	A	DE	Knee	-	-	-	-	-1
AN-154	F	Adult	Tibia	R	Avulsion	A	PE	N	/	/	/	/	/
AN-155	F?	Adult	Fibula	L	Transverse	A	DD	N	16.6	100	/	3.7	/
			Tibia	L	Avulsion	A	DE	N	/	/	/	5.3	/
AN-165	M	YA	Fibula	L	Oblique	A	PD	N	2.8	69.5	/	0	/

Skeleton Number	Sex	Age	Element	Side	Fracture Type	Timing	Segment	OA_x	ANG (º)	APP (%)	RO (º)	Overlap (mm)	Shortening (mm)
AN-172	F?	MA	Radius	L	Transverse	A	DD	Wrist	11	92.9	4	2.1	-18
					Crush	A	DE	Wrist	-	-	-	-	/
AN-177	M	MA	Radius	L	Oblique	A	DE	Wrist	13.9	88	12	10	-8
AN-185A	M	MA	Clavicle	R	Unknown	A	MD	N	14.3	100	4	/	-6
AN-191	F	OA	Radius	R	Oblique	A	DE	Wrist	14.3	100	10	/	-6
			Ulna	R	Crush	A	DE	Wrist	-	-	-	-	/
AN-204A	M	MA	Clavicle	R	Transverse	A	MD	N	22.9	100	6	/	/
			Fibula	R	Transverse	A	PD	Knee	0	100	/	1.3	/
AN-210	M?	YA	Fibula	R	Spiral	A	DE	N	11.4	65.4	0	21.5	/
			Tibia	R	Spiral	A	DD	N	8.3	68.2	30	19	-19
			Tibia	R	Crush	A	DE	N	-	-	-	-	/
AN-218	F	YA	Fibula	L	Spiral	A	PD	Knee	5.3	28.3	0	26.1	-9
			Tibia	L	Spiral	A	DD	Knee	3.6	52.6	30	10.2	-13
AN-225	M	YA	Ulna	L	Transverse	A	DD	Wrist	16.2	50.5	5	3.1	-9
AN-230A	M	MA	Clavicle	L	Transverse	A	MD	Shoulder	5.2	15.1	10	0	/
AN-241	F	OA	Radius	L	Oblique	A	DE	Elbow, Wrist	13.2	74.3	18	3.1	/
AN-244	M	YA	Clavicle	R	Unknown	A	MD	N	13.9	-41	10	28.5	/
AN-247	F	YA	Fibula	R	Oblique	A	MD	N	2.7	41.6	0	7.6	4
AN-277	F?	Adult	Radius	L	Crush	A	PE	N	-	-	-	-	-2

OA_x=Osteoarthritis; ANG=Angulation; APP=Amount of poor apposition; RO=Rotation; /=Attribute not observable; -=Attribute not applicable to this fracture type; U=Unknown Sex; F=Female; F?=Possible Female; M=Male; M?=Possible Male; YA=Young Adult (20-34 years old); MA=Middle Adult (35-49 years old); OA=Old Adult (50+ years old); L=Left; R=Right ; A=Antemortem; P=Perimortem; N=No osteoarthritis observed; PE=Proximal epiphysis; PD=Proximal diaphysis; MD=Middle diaphysis; DD=Distal diaphysis; DE=Distal epiphysis

Table C.2 – Attributes of each fracture observed at Vagnari.

Skeleton Number	Sex	Age	Element	Side	Fracture Type	Timing	Segment	OA$_x$	ANG (º)	APP (%)	RO (º)	Overlap (mm)	Shortening (mm)
VA-F042A	M	YA	Tibia	L	Spiral	A	PD	N	4	56.5	0	3.1	/
VA-F068	M	MA	Clavicle	L	Butterfly	A	MD	N	12.8	-127.5	0	4.8	/
VA-F089	U	Adult	Radius	L	Oblique	A	MD	N	5.4	48.5	40	5.4	/
			Ulna	L	Transverse	A	DD	N	16.5	58.6	30	5.5	/
VA-F096B	F?	Adult	Tibia	R	Unknown	A	DD	N	1.7	100	0	0	/
VA-F067	M	YA	Fibula	L	Oblique with impaction	A	PE	N	-	-	/	-	/
VA-F131	M	YA	Ulna	R	Transverse	A	DD	N	3.6	69.5	3	5.7	/
VA-F204	F	YA	Humerus	L	Unknown	A	PD	N	11.1	/	0	/	/
VA-F231	M?	YA	Tibia	R	Incomplete - Stress	A	PD	N	0	100	0	0	/
VA-F216	M	MA	Fibula	R	Oblique	A	DD	Knee, Ankle	4.5	53.5	5	4.8	/
VA-F220	M	MA	Tibia	R	Crush	A	PE	Knee	-	-	-	-	/
VA-F249	F?	YA	Clavicle	L	Transverse	A	MD	N	36.2	79.6	0	4.7	/
VA-F288	M?	YA	Ulna	L	Unknown	A	DD	N	/	/	0	/	/

OA$_x$=Osteoarthritis; ANG=Angulation; APP=Amount of poor apposition; RO=Rotation; /=Attribute not observable; -=Attribute not applicable to this fracture type; U=Unknown Sex; F=Female; F?=Possible Female; M=Male; M?=Possible Male; YA=Young Adult (20-34 years old); MA=Middle Adult (35-49 years old); OA=Old Adult (50+ years old); L=Left; R=Right ; A=Antemortem; P=Perimortem; N=No osteoarthritis observed; PE=Proximal epiphysis; PD=Proximal diaphysis; MD=Middle diaphysis; DD=Distal diaphysis; DE=Distal epiphysis

Appendix D: Fracture Distribution & Prevalence

This appendix reports the counts and true prevalence rates of fractures by element and by bone segment; supplementary statistical comparisons are also presented here. Section D.1 presents the distribution and true prevalence rates of fractures by sex, element, limb type, and age at Ancaster and Vagnari. Section D.2 reports the prevalence of fractures by element and bone segment for Ancaster and Vagnari. In the calculation of prevalence by bone segment, segments were included when they were >75% present. Sections D.3 through D.6 report additional differences (post-hoc tests) between the fracture prevalence rates by age, segment, limb type, and side.

Abbreviations used in the tables are as follows:

n – number of elements or segments with fractures
N – number of observed elements or segments
TPR – true prevalence rate
F – Female
F? – Possible Female
M – Male
M? – Possible Male
U – Unknown sex
ADO – Adolescent (15-19 years old)
YA – Young Adult (20-34 years old)
MA – Middle Adult (35-49 years old)
OA – Old Adult (50+ years old)
A – Adult (unknown age)
PE – proximal epiphysis segment
PD – proximal diaphysis segment
MD – middle diaphysis segment
DD – distal diaphysis segment
DE – distal epiphysis segment

D.1 – Counts and True Prevalence Rates: Element, Age, Sex

Table D.1 – Counts and true prevalence rate of fractures by element type, limb type, age, and sex at Ancaster.

Element	Age Cohort	Female			Male			Unknown			Total		
		n	*N*	TPR (%)	*n*	*N*	TPR (%)	*n*	*N*	TPR (%)	*n*	*N*	TPR (%)
Clavicle	ADO	0	0	-	0	7	0.0	0	0	-	0	7	0.0
	YA	0	38	0.0	2	57	3.5	0	0	-	2	95	2.1
	MA	0	34	0.0	7	69	10.1	0	0	-	7	103	6.8
	OA	0	9	0.0	1	5	20.0	1	2	50.0	2	16	12.5
	A	0	8	0.0	0	2	0.0	0	4	0.0	0	14	0.0
	Total	0	89	0.0	10	140	7.1	1	6	16.7	11	235	4.7
Humerus	ADO	0	0	-	0	8	0.0	0	0	-	0	8	0.0
	YA	0	59	0.0	0	70	0.0	0	1	0.0	0	130	0.0
	MA	0	40	0.0	0	70	0.0	0	0	-	0	110	0.0
	OA	0	8	0.0	0	6	0.0	0	1	0.0	0	15	0.0
	A	0	13	0.0	0	7	0.0	0	4	0.0	0	24	0.0
	Total	0	120	0.0	0	161	0.0	0	6	0.0	0	287	0.0
Radius	ADO	0	0	-	0	8	0.0	0	0	-	0	8	0.0
	YA	2	51	3.9	0	66	0.0	0	1	0.0	2	118	1.7
	MA	4	34	11.8	4	69	5.8	0	0	-	8	103	7.8
	OA	2	10	20.0	0	5	0.0	0	1	0.0	2	16	12.5
	A	1	7	14.3	0	6	0.0	0	4	0.0	1	17	5.9
	Total	9	102	8.8	4	154	2.6	0	6	0.0	13	262	5.0
Ulna	ADO	0	0	-	0	8	0.0	0	0	-	0	8	0.0
	YA	0	53	0.0	1	67	1.5	0	1	0.0	1	121	0.8
	MA	1	35	2.9	2	68	2.9	0	0	-	3	103	2.9
	OA	1	10	10.0	0	5	0.0	0	2	0.0	1	17	5.9
	A	0	8	0.0	0	7	0.0	0	3	0.0	0	18	0.0
	Total	2	106	1.9	3	155	1.9	0	6	0.0	5	267	1.9
Upper Limb	ADO	0	0	-	0	31	0.0	0	0	-	0	31	0.0
	YA	2	201	1.0	3	260	1.2	0	3	0.0	5	464	1.1
	MA	5	143	3.5	13	276	4.7	0	0	-	18	419	4.3
	OA	3	37	8.1	1	21	4.8	1	6	16.7	5	64	7.8
	A	1	36	2.8	0	22	0.0	0	15	0.0	1	73	1.4
	Total	11	417	2.6	17	610	2.8	1	24	4.2	29	1051	2.8
Femur	ADO	0	0	-	0	6	0.0	0	0	-	0	6	0.0
	YA	0	57	0.0	0	65	0.0	0	1	0.0	0	123	0.0
	MA	1	43	2.3	0	74	0.0	0	0	-	1	117	0.9
	OA	0	8	0.0	0	5	0.0	0	2	0.0	0	15	0.0
	A	0	11	0.0	0	11	0.0	0	5	0.0	0	27	0.0
	Total	1	119	0.8	0	161	0.0	0	8	0.0	1	288	0.3

Element	Age Cohort	Female			Male			Unknown			Total		
		n	*N*	TPR (%)	*n*	*N*	TPR (%)	*n*	*N*	TPR (%)	*n*	*N*	TPR (%)
Tibia	ADO	0	0	-	0	6	0.0	0	0	-	0	6	0.0
	YA	4	59	6.8	3	66	4.5	0	2	0.0	7	127	5.5
	MA	0	42	0.0	6	72	8.3	0	1	0.0	6	115	5.2
	OA	0	9	0.0	1	4	25.0	0	2	0.0	1	15	6.7
	A	2	15	13.3	0	10	0.0	0	14	0.0	2	39	5.1
	Total	6	125	4.8	10	158	6.3	0	19	0.0	16	302	5.3
Fibula	ADO	0	0	-	0	6	0.0	0	0	-	0	6	0.0
	YA	2	61	3.3	3	55	5.5	0	2	0.0	5	118	4.2
	MA	1	33	3.0	4	64	6.3	0	0	-	5	97	5.2
	OA	0	7	0.0	0	3	0.0	0	2	0.0	0	12	0.0
	A	1	11	9.1	0	10	0.0	0	10	0.0	1	31	3.2
	Total	4	112	3.6	7	138	5.1	0	14	0.0	11	264	4.2
Lower Limb	ADO	0	0	-	0	18	0.0	0	0	-	0	18	0.0
	YA	6	177	3.4	6	186	3.2	0	5	0.0	12	368	3.3
	MA	2	118	1.7	10	210	4.8	0	1	0.0	12	329	3.6
	OA	0	24	0.0	1	12	8.3	0	6	0.0	1	42	2.4
	A	3	37	8.1	0	31	0.0	0	29	0.0	3	97	3.1
	Total	11	356	3.1	17	457	3.7	0	41	0.0	28	854	3.3
Total	ADO	0	0	-	0	49	0.0	0	0	-	0	49	0.0
	YA	8	378	2.1	9	446	2.0	0	8	0.0	17	832	2.0
	MA	7	261	2.7	23	486	4.7	0	1	0.0	30	748	4.0
	OA	3	61	4.9	2	33	6.1	1	12	8.3	6	106	5.7
	A	4	73	5.5	0	53	0.0	0	44	0.0	4	170	2.4
	Total	22	773	2.8	34	1067	3.2	1	65	1.5	57	1905	3.0

n=number of elements with fractures; *N*=number of observed elements; TPR=true prevalence rate; ADO=Adolescent (15-19 years old); YA=Young Adult (20-34 years old); MA=Middle Adult (35-49 years old); OA=Old Adult (50+ years old); A=Adult (unknown age).

Table D.2 – Counts and true prevalence rate of fractures by element type, limb type, age, and sex at Vagnari.

Element	Age Cohort	Female			Male			Unknown			Total		
		n	*N*	TPR (%)	*n*	*N*	TPR (%)	*n*	*N*	TPR (%)	*n*	*N*	TPR (%)
Clavicle	ADO	0	5	0.0	0	0	-	0	0	-	0	5	0.0
	YA	1	10	10.0	0	11	0.0	0	1	0.0	1	22	4.5
	MA	0	4	0.0	1	11	9.1	0	0	-	1	15	6.7
	OA	0	0	-	0	0	-	0	0	-	0	0	-
	A	0	2	0.0	0	1	0.0	0	0	-	0	3	0.0
	Total	1	21	4.8	1	23	4.3	0	1	0.0	2	45	4.4
Humerus	ADO	0	8	0.0	0	0	-	0	1	0.0	0	9	0.0
	YA	1	16	6.3	0	15	0.0	0	2	0.0	1	33	3.0
	MA	0	8	0.0	0	15	0.0	0	0	-	0	23	0.0
	OA	0	0	-	0	1	0.0	0	0	-	0	1	0.0
	A	0	2	0.0	0	6	0.0	0	0	-	0	8	0.0
	Total	1	34	2.9	0	37	0.0	0	3	0.0	1	74	1.4
Radius	ADO	0	5	0.0	0	0	-	0	1	0.0	0	6	0.0
	YA	0	17	0.0	0	12	0.0	0	3	0.0	0	32	0.0
	MA	0	5	0.0	0	19	0.0	0	0	-	0	24	0.0
	OA	0	1	0.0	0	1	0.0	0	0	-	0	2	0.0
	A	0	2	0.0	0	2	0.0	1	1	100.0	1	5	20.0
	Total	0	30	0.0	0	34	0.0	1	5	20.0	1	69	1.4
Ulna	ADO	0	5	0.0	0	0	-	0	0	-	0	5	0.0
	YA	0	18	0.0	2	14	14.3	0	2	0.0	2	34	5.9
	MA	0	3	0.0	0	14	0.0	0	0	-	0	17	0.0
	OA	0	0	-	0	0	-	0	0	-	0	0	-
	A	0	1	0.0	0	1	0.0	1	1	100.0	1	3	33.3
	Total	0	27	0.0	2	29	6.9	1	3	33.3	3	59	5.1
Upper Limb	ADO	0	23	0.0	0	0	-	0	2	0.0	0	25	0.0
	YA	2	61	3.3	2	52	3.8	0	8	0.0	4	121	3.3
	MA	0	20	0.0	1	59	1.7	0	0	-	1	79	1.3
	OA	0	1	0.0	0	2	0.0	0	0	-	0	3	0.0
	A	0	7	0.0	0	10	0.0	2	2	100.0	2	19	10.5
	Total	2	112	1.8	3	123	2.4	2	12	16.7	7	248	2.8
Femur	ADO	0	5	0.0	0	0	-	0	3	0.0	0	8	0.0
	YA	0	15	0.0	0	19	0.0	0	0	-	0	34	0.0
	MA	0	4	0.0	0	17	0.0	0	0	-	0	21	0.0
	OA	0	0	-	0	2	0.0	0	0	-	0	2	0.0
	A	0	0	-	0	3	0.0	0	0	-	0	3	0.0
	Total	0	24	0.0	0	41	0.0	0	3	0.0	0	68	0.0

Element	Age Cohort	Female			Male			Unknown			Total		
		n	*N*	TPR (%)	*n*	*N*	TPR (%)	*n*	*N*	TPR (%)	*n*	*N*	TPR (%)
Tibia	ADO	0	4	0.0	0	0	0.0	0	1	0.0	0	5	0.0
	YA	0	12	0.0	2	21	9.5	0	0	-	2	33	6.1
	MA	0	6	0.0	1	17	5.9	0	0	-	1	23	4.3
	OA	0	0	-	0	2	0.0	0	0	-	0	2	0.0
	A	1	2	50.0	0	3	0.0	0	0	-	1	5	20.0
	Total	1	24	4.2	3	43	7.0	0	1	0.0	4	68	5.9
Fibula	ADO	0	3	0.0	0	0	-	0	0	-	0	3	0.0
	YA	0	8	0.0	1	10	10.0	0	1	0.0	1	19	5.3
	MA	0	1	0.0	1	16	6.3	0	0	-	1	17	5.9
	OA	0	0	-	0	3	0.0	0	0	-	0	3	0.0
	A	0	0	-	0	0	-	0	0	-	0	0	-
	Total	0	12	0.0	2	29	6.9	0	1	0.0	2	42	4.8
Lower Limb	ADO	0	12	0.0	0	0	-	0	4	0.0	0	16	0.0
	YA	0	35	0.0	3	50	6.0	0	1	0.0	3	86	3.5
	MA	0	11	0.0	2	50	4.0	0	0	-	2	61	3.3
	OA	0	0	-	0	7	0.0	0	0	-	0	7	0.0
	A	1	2	50.0	0	6	0.0	0	0	-	1	8	12.5
	Total	1	60	1.7	5	113	4.4	0	5	0.0	6	178	3.4
Total	ADO	0	35	0.0	0	0	-	0	6	0.0	0	41	0.0
	YA	2	96	2.1	5	102	4.9	0	9	0.0	7	207	3.4
	MA	0	31	0.0	3	109	2.8	0	0	-	3	140	2.1
	OA	0	1	0.0	0	9	0.0	0	0	-	0	10	0.0
	A	1	9	11.1	0	16	0.0	2	2	100.0	3	27	11.1
	Total	3	172	1.7	8	236	3.4	2	17	11.8	13	425	3.1

n=number of elements with fractures; *N*=number of observed elements; TPR=true prevalence rate; ADO=Adolescent (15-19 years old); YA=Young Adult (20-34 years old); MA=Middle Adult (35-49 years old); OA=Old Adult (50+ years old); A=Adult (unknown age).

D.2 – Counts and True Prevalence Rates: Element, Segment, Side

Table D.3 – Counts and true prevalence rate of fractures by element type, bone segment, side, and sex at Ancaster.

Sex	Element Type	Right						Left					
		Element *n/N* %	PE *n/N* %	PD *n/N* %	MD *n/N* %	DD *n/N* %	DE *n/N* %	Element *n/N* %	PE *n/N* %	PD *n/N* %	MD *n/N* %	DD *n/N* %	DE *n/N* %
Male	Clavicle	5/70 7.1	0/63 0.0	0/70 0.0	5/72 6.9	0/72 0.0	0/60 0.0	5/70 7.1	0/59 0.0	0/69 0.0	5/74 6.8	0/73 0.0	0/61 0.0
	Humerus	0/80 0.0	0/58 0.0	0/78 0.0	0/84 0.0	0/82 0.0	0/66 0.0	0/81 0.0	0/66 0.0	0/78 0.0	0/82 0.0	0/80 0.0	0/72 0.0
	Radius	2/78 2.6	0/70 0.0	1/77 1.3	0/81 0.0	0/73 0.0	1/66 1.5	2/76 2.6	0/70 0.0	0/76 0.0	1/82 1.2	0/74 0.0	1/62 1.6
	Ulna	1/78 1.3	0/65 0.0	1/81 1.2	0/81 0.0	0/68 0.0	0/57 0.0	2/77 2.6	0/70 0.0	0/79 0.0	1/79 1.3	1/74 1.4	0/63 0.0
	Femur	0/82 0.0	0/62 0.0	0/81 0.0	0/84 0.0	0/80 0.0	0/55 0.0	0/79 0.0	0/61 0.0	0/80 0.0	0/82 0.0	0/77 0.0	0/53 0.0
	Tibia	4/79 5.1	0/53 0.0	0/75 0.0	0/81 0.0	2/81 2.5	2/74 2.7	6/79 7.6	1/54 1.9	0/77 0.0	0/80 0.0	2/79 2.5	3/74 4.1
	Fibula	3/68 4.4	0/28 0.0	1/67 1.5	0/71 0.0	1/75 1.3	1/66 1.5	4/70 5.7	0/31 0.0	2/64 3.1	0/74 0.0	0/74 0.0	2/66 3.0
	Total	15/535 2.8	0/399 0.0	3/529 0.6	5/554 0.9	3/531 0.6	4/444 0.9	19/532 3.6	1/411 0.2	2/523 0.4	7/553 1.3	3/531 0.6	6/451 1.3
Female	Clavicle	0/46 0.0	0/39 0.0	0/47 0.0	0/49 0.0	0/51 0.0	0/38 0.0	0/43 0.0	0/37 0.0	0/43 0.0	0/50 0.0	0/48 0.0	0/33 0.0
	Humerus	0/60 0.0	0/40 0.0	0/56 0.0	0/64 0.0	0/62 0.0	0/48 0.0	0/60 0.0	0/42 0.0	0/58 0.0	0/64 0.0	0/60 0.0	0/48 0.0
	Radius	3/55 5.5	0/51 0.0	0/54 0.0	1/59 1.7	0/56 0.0	2/52 3.8	6/47 12.8	2/42 4.8	0/47 0.0	0/56 0.0	2/49 4.1	2/40 5.0
	Ulna	2/56 3.6	0/50 0.0	0/60 0.0	0/60 0.0	0/55 0.0	2/46 4.3	0/50 0.0	0/40 0.0	0/53 0.0	0/57 0.0	0/47 0.0	0/40 0.0

Sex	Element Type	Right						Left					
		Element	PE	PD	MD	DD	DE	Element	PE	PD	MD	DD	DE
Female cont.	Femur	0/59 0.0	0/44 0.0	0/61 0.0	0/66 0.0	0/61 0.0	0/41 0.0	1/60 1.7	1/43 2.3	0/60 0.0	0/67 0.0	0/62 0.0	0/43 0.0
	Tibia	3/59 5.1	3/42 7.1	0/56 0.0	0/63 0.0	0/60 0.0	0/55 0.0	3/66 4.5	0/48 0.0	0/65 0.0	0/68 0.0	1/63 1.6	2/58 3.4
	Fibula	1/56 1.8	0/26 0.0	0/52 0.0	1/61 1.6	0/60 0.0	0/55 0.0	3/56 5.4	0/26 0.0	2/56 3.6	0/64 0.0	1/62 1.6	0/51 0.0
	Total	9/391 2.3	3/292 1.0	0/386 0.0	2/422 0.5	0/405 0.0	4/335 1.2	13/382 3.4	3/278 1.1	2/382 0.5	0/426 0.0	4/391 1.0	4/313 1.3
Unknown Sex	Clavicle	0/3 0.0	0/1 0.0	0/2 0.0	0/2 0.0	0/2 0.0	0/0 -	1/3 33.3	0/1 0.0	0/2 0.0	1/3 33.3	0/2 0.0	0/0 -
	Humerus	0/4 0.0	0/2 0.0	0/3 0.0	0/4 0.0	0/4 0.0	0/2 0.0	0/2 0.0	0/0 -	0/1 0.0	0/4 0.0	0/4 0.0	0/0 -
	Radius	0/3 0.0	0/1 0.0	0/2 0.0	0/2 0.0	0/2 0.0	0/0 -	0/3 0.0	0/1 0.0	0/2 0.0	0/3 0.0	0/2 0.0	0/1 0.0
	Ulna	0/3 0.0	0/2 0.0	0/2 0.0	0/4 0.0	0/1 0.0	0/0 -	0/3 0.0	0/1 0.0	0/3 0.0	0/3 0.0	0/2 0.0	0/1 0.0
	Femur	0/4 0.0	0/1 0.0	0/4 0.0	0/5 0.0	0/4 0.0	0/2 0.0	0/4 0.0	0/0 -	0/3 0.0	0/6 0.0	0/5 0.0	0/3 0.0
	Tibia	0/9 0.0	0/7 0.0	0/7 0.0	0/9 0.0	0/9 0.0	0/7 0.0	0/10 0.0	0/6 0.0	0/7 0.0	0/9 0.0	0/9 0.0	0/9 0.0
	Fibula	0/7 0.0	0/3 0.0	0/5 0.0	0/7 0.0	0/6 0.0	0/6 0.0	0/7 0.0	0/2 0.0	0/6 0.0	0/7 0.0	0/7 0.0	0/7 0.0
	Total	0/33 0.0	0/17 0.0	0/25 0.0	0/31 0.0	0/28 0.0	0/17 0.0	1/32 3.1	0/11 0.0	0/24 0.0	1/35 2.9	0/31 0.0	0/21 0.0

n=number of elements or segments with fractures; *N*=number of observed elements or segments; PE=Proximal epiphysis; PD=Proximal diaphysis; MD=Middle diaphysis; DD=Distal diaphysis; DE=Distal epiphysis.

Table D.4 – Counts and true prevalence rate of fractures by element type, bone segment, side, and sex at Vagnari.

Sex	Element Type	Right Element *n/N* %	Right PE *n/N* %	Right PD *n/N* %	Right MD *n/N* %	Right DD *n/N* %	Right DE *n/N* %	Left Element *n/N* %	Left PE *n/N* %	Left PD *n/N* %	Left MD *n/N* %	Left DD *n/N* %	Left DE *n/N* %
Male	Clavicle	0/12 0.0	0/4 0.0	0/13 0.0	0/16 0.0	0/17 0.0	0/0 -	1/11 9.1	0/5 0.0	0/12 0.0	1/16 6.3	0/13 0.0	0/2 0.0
	Humerus	0/21 0.0	0/5 0.0	0/21 0.0	0/24 0.0	0/26 0.0	0/7 0.0	0/16 0.0	0/0 -	0/16 0.0	0/23 0.0	0/27 0.0	0/6 0.0
	Radius	0/18 0.0	0/4 0.0	0/20 0.0	0/25 0.0	0/19 0.0	0/8 0.0	0/16 0.0	0/7 0.0	0/22 0.0	0/27 0.0	0/16 0.0	0/10 0.0
	Ulna	1/16 6.3	0/8 0.0	0/22 0.0	0/24 0.0	1/15 6.7	0/4 0.0	1/13 7.7	0/8 0.0	0/24 0.0	0/27 0.0	1/10 10.0	0/6 0.0
	Femur	0/23 0.0	0/15 0.0	0/24 0.0	0/19 0.0	0/23 0.0	0/7 0.0	0/18 0.0	0/11 0.0	0/25 0.0	0/17 0.0	0/22 0.0	0/8 0.0
	Tibia	2/22 9.1	1/9 11.1	1/23 4.4	0/28 0.0	0/25 0.0	0/7 0.0	1/21 4.8	0/7 0.0	1/23 4.3	0/28 0.0	0/25 0.0	0/8 0.0
	Fibula	1/16 6.3	0/1 0.0	0/19 0.0	0/25 0.0	1/17 5.9	0/4 0.0	1/13 7.7	1/1 100.0	0/16 0.0	0/22 0.0	0/15 0.0	0/6 0.0
	Total	4/128 3.1	1/46 2.2	1/142 0.7	0/161 0.0	2/142 1.4	0/37 0.0	4/108 3.7	1/39 2.6	1/138 0.7	1/160 0.6	1/128 0.8	0/46 0.0
Female	Clavicle	0/9 0.0	0/3 0.0	0/11 0.0	0/15 0.0	0/13 0.0	0/2 0.0	1/11 9.1	0/3 0.0	0/14 0.0	1/20 5.0	0/16 0.0	0/2 0.0
	Humerus	0/17 0.0	0/3 0.0	0/17 0.0	0/22 0.0	0/25 0.0	0/4 0.0	1/17 5.9	0/1 0.0	1/17 5.9	0/22 0.0	0/22 0.0	0/6 0.0
	Radius	0/14 0.0	0/5 0.0	0/17 0.0	0/22 0.0	0/15 0.0	0/5 0.0	0/16 0.0	0/7 0.0	0/15 0.0	0/23 0.0	0/20 0.0	0/6 0.0
	Ulna	0/12 0.0	0/8 0.0	0/18 0.0	0/17 0.0	0/13 0.0	0/4 0.0	0/15 0.0	0/6 0.0	0/20 0.0	0/20 0.0	0/18 0.0	0/3 0.0
	Femur	0/11 0.0	0/9 0.0	0/21 0.0	0/20 0.0	0/15 0.0	0/4 0.0	0/13 0.0	0/10 0.0	0/26 0.0	0/14 0.0	0/12 0.0	0/4 0.0

Sex	Element Type	Right						Left					
		Element	PE	PD	MD	DD	DE	Element	PE	PD	MD	DD	DE
Female cont.	Tibia	1/13 7.7	0/7 0.0	0/17 0.0	0/24 0.0	1/14 7.1	0/4 0.0	0/11 0.0	0/2 0.0	0/17 0.0	0/24 0.0	0/17 0.0	0/3 0.0
	Fibula	0/6 0.0	0/1 0.0	0/8 0.0	0/15 0.0	0/7 0.0	0/4 0.0	0/6 0.0	0/1 0.0	0/9 0.0	0/17 0.0	0/8 0.0	0/1 0.0
	Total	1/82 1.2	0/36 0.0	0/109 0.0	0/135 0.0	1/102 1.0	0/27 0.0	2/89 2.2	0/30 0.0	1/118 0.8	1/140 0.7	0/113 0.0	0/25 0.0
Unknown Sex	Clavicle	0/2 0.0	0/0 -	0/2 0.0	0/2 0.0	0/2 0.0	0/0 -	0/1 0.0	0/0 -	0/1 0.0	0/1 0.0	0/2 0.0	0/0 -
	Humerus	0/2 0.0	0/0 -	0/2 0.0	0/3 0.0	0/3 0.0	0/2 0.0	0/1 0.0	0/0 -	0/1 0.0	0/5 0.0	0/4 0.0	0/1 0.0
	Radius	0/2 0.0	0/0 -	0/2 0.0	0/4 0.0	0/1 0.0	0/1 0.0	1/2 50.0	0/1 0.0	0/4 0.0	1/4 25.0	0/1 0.0	0/2 0.0
	Ulna	0/1 0.0	0/1 0.0	0/3 0.0	0/3 0.0	0/0 0.0	0/1 0.0	1/2 50.0	0/1 0.0	0/3 0.0	0/2 0.0	1/2 50.0	0/0 -
	Femur	0/2 0.0	0/0 -	0/4 0.0	0/4 0.0	0/2 0.0	0/1 0.0	0/1 0.0	0/1 0.0	0/4 0.0	0/3 0.0	0/1 0.0	0/0 -
	Tibia	0/0 -	0/0 -	0/2 0.0	0/3 0.0	0/1 0.0	0/0 -	0/1 0.0	0/0 -	0/1 0.0	0/3 0.0	0/1 0.0	0/0 -
	Fibula	0/0 -	0/0 -	0/0 -	0/3 0.0	0/2 0.0	0/0 -	0/1 0.0	0/0 -	0/1 0.0	0/3 0.0	0/1 0.0	0/0 -
	Total	0/9 0.0	0/1 0.0	0/15 0.0	0/22 0.0	0/11 0.0	0/5 0.0	2/9 22.2	0/3 0.0	0/15 0.0	1/21 4.8	1/12 8.3	0/3 0.0

n=number of elements or segments with fractures; *N*=number of observed elements or segments; PE=Proximal epiphysis; PD=Proximal diaphysis; MD=Middle diaphysis; DD=Distal diaphysis; DE=Distal epiphysis.

D.3 – Supplemental Fracture Prevalence Rate Comparisons: Age

Table D.5 –Post-hoc age group comparisons of Ancaster fracture true prevalence rates by element type and sex.[1]

Element	Sex	YA vs. MA	YA vs OA	MA vs. OA
Clavicle	M	OR=3.1, CI 0.6-15.6 p_{FET}=0.182	OR=6.9, CI 0.5-93.1 p_{FET}=0.226	OR=2.2, CI 0.2-22.7 p_{FET}=0.445
	F	-	-	-
Radius	M	p_{FET}=0.120	-	*p_{FET}=1.000*
	F	OR=3.3, CI 0.6-18.9 p_{FET}=0.212	OR=6.1, CI 0.8-49.9 p_{FET}=0.122	OR=1.9, CI 0.3-12.1 p_{FET}=0.606
Ulna	M	OR=2.0 CI 0.2-22.6 p_{FET}=1.000	*p_{FET}=1.000*	*p_{FET}=1.000*
	F	p_{FET}=0.398	p_{FET}=0.159	OR=3.8, CI 0.2-66.5 p_{FET}=0.399
Femur	M	-	-	-
	F	p_{FET}=0.430	-	*p_{FET}=1.000*
Tibia	M	OR=2.0 CI 0.5-8.2 p_{FET}=0.495	OR=7.0, CI 0.6-89.0 p_{FET}=0.214	OR=3.6 CI 0.3-39.7 p_{FET}=0.334
	F	*p_{FET}=0.139*	*p_{FET}=1.000*	-
Fibula	M	OR=1.2 CI 0.3-5.4 p_{FET}=1.000	*p_{FET}=1.000*	*p_{FET}=1.000*
	F	*OR=1.1 CI 0.1-12.4* *p_{FET}=1.000*	*p_{FET}=1.000*	*p_{FET}=1.000*

[1] Groups compared using odds ratio, chi-square, and Fisher's Exact tests. No humeral fractures were observed so this bone type was excluded from this table. Bold font indicates that a significant difference is present. Italic font indicates that compared to an older age category, the younger age category had a greater prevalence of fractures. -=statistical test was unable to be performed because of an absence of fractures; M=male; F=female; OR=odds ratio; CI=confidence interval.

D.4 – Supplemental Fracture Prevalence Rate Comparisons: Segment

Table D.6 – Differences in Ancaster fracture prevalence rates between bone segment locations by sex.[1]

Segments compared	Male		Female	
	n/N	Difference	*n/N*	Difference
PE	1/810	OR=6.5, CI 0.9-47.9	6/570	*OR=2.0, CI 0.8-5.2*
PD, MD, DD, DE	33/4116	χ^2_{Yates}=3.607, df=1, p=0.058	16/3060	*χ^2_{Yates}=1.445, df=1, p=0.229*
PD	5/1052	OR=1.6, CI 0.6-4.1	2/768	OR=2.7, CI 0.6-11.6
PE, MD, DD, DE	29/3874	χ^2_{Yates}=0.547, df=1, p=0.460	20/2862	p_{FET}=0.199
MD	12/1107	*OR=1.9, CI 0.9-3.8*	2/848	OR=3.1, CI 0.7-13.1
PE, PD, DD, DE	22/3819	*χ^2_{Yates}=2.532, df=1, p=0.460*	20/2782	χ^2_{Yates}=1.779, df=1, p=0.182
DD	6/1062	OR=1.3, CI 0.5-3.1	7/796	*OR=1.7, CI 0.7-4.1*
PE, PD, MD, DE	28/3864	χ^2_{Yates}=0.121, df=1, p=0.728	15/2834	*p_{FET}=0.298*
DE	10/895	*OR=1.9, CI 0.9-4.0*	8/648	***OR=2.7, CI 1.1-6.3***
PE, PD, MD, DD	24/4031	*χ^2_{Yates}=2.199, df=1, p=0.138*	14/2982	***p_{FET}=0.043***

[1] Groups compared using odds ratio, chi-square, and Fisher's Exact tests. Bold font indicates that a significant difference is present. Italic font used to indicate that the single tested segment had greater odds of fractures than all the other segments combined. *n*=number of fractured segments, *N*=total number of observed segments, PE=proximal epiphysis, PD=proximal diaphysis, MD=middle diaphysis, DD=distal diaphysis, DE=distal epiphysis; OR=odds ratio; CI=confidence interval.

Table D.7 – Differences in Vagnari fracture prevalence rates between bone segment locations by sex.[1]

Segments compared	Male		Female	
	n/N	Difference	*n/N*	Difference
PE	2/85	*OR=3.8, CI 0.8-19.2*	0/66	p_{FET}=1.000
PD, MD, DD, DE	6/954	*p_{FET}=0.134*	3/769	
PD	2/280	OR=1.1, CI 0.2-5.5	1/227	*OR=1.3, CI 0.1-14.9*
PE, MD, DD, DE	6/759	p_{FET}=1.000	2/608	*p_{FET}=1.000*
MD	1/321	OR=3.2, CI 0.4-25.7	1/275	*OR=1.0, CI 0.1-11.3*
PE, PD, DD, DE	7/718	p_{FET}=0.447	2/560	*p_{FET}=1.000*
DD	3/270	*OR=1.7, CI 0.4-7.2*	1/215	*OR=1.4, CI 0.1-16.0*
PE, PD, MD, DE	5/769	*p_{FET}=0.435*	2/620	*p_{FET}=1.000*
DE	0/83	p_{FET}=1.000	0/52	p_{FET}=1.000
PE, PD, MD, DD	8/956		3/783	
All Segments	-	χ^2=4.737, df=4, p=0.315	-	χ^2=0.535, df=4, p=0.970

[1] Segment groups were compared using Fisher's Exact tests; all the segments were compared using chi-square tests. Bold font indicates that a significant difference was present. Italic font used to indicate that the single tested segment had greater odds of fractures than all other segments combined. *n*=number of fractured segments, *N*=total number of observed segments, PE=proximal epiphysis, PD=proximal diaphysis, MD=middle diaphysis, DD=distal diaphysis, DE=distal epiphysis; OR=odds ratio; CI=confidence interval.

D.5 – Supplemental Fracture Prevalence Rate Comparisons: Limb Type

Table D.8 – Differences between the upper and lower limb fracture prevalence rates by sex at Ancaster and Vagnari.[1]

Variables Compared	Ancaster Upper vs. Lower Limb	Vagnari Upper vs. Lower Limb
Males	*OR=1.3, CI 0.6-2.5* *χ^2_{Yates}=0.238, df=1, p=.625*	*OR=1.4, CI 0.4-5.3* *p_{FET}=1.000*
Females	OR=1.2, CI 0.5-2.7 χ^2_{Yates}=0.026, df=1, p=.873	OR=1.1, CI 0.1-12.1 p_{FET}=.741
Unknown	p_{FET}=.369	p_{FET}=1.000
Total	*OR=1.2, CI 0.7-2.0* *χ^2_{Yates}=0.277, df=1, p=.599*	*OR=1.0, CI 0.4-3.1* *χ^2_{Yates}=0.000, df=1, p=1.000*

[1] Groups compared using odds ratio, chi-square, and Fisher's exact tests. Bold font indicates that a significant difference is present. Italic font used to indicate instances when lower limbs had greater fracture odds than upper limbs. OR=odds ratio; CI=confidence interval.

Table D.9 – Differences between the Ancaster male and female true fracture prevalence rates by limb type and age.[1]

Age	Upper Limb	Lower Limb
Adolescent	-	-
Young Adult	OR=1.2, CI 0.2-7.0 p_{FET}=1.000	OR=1.0, CI 0.4-2.5 x^2_{Yates}=0.000, df=1, p=1.000
Middle Adult	OR=1.4, CI 0.5-3.9 x^2_{Yates}= 0.107, df=1, p=.744	OR=1.8, CI 0.8-4.3 x^2_{Yates}=1.358, df=1, p=.244
Old Adult	*OR=1.8, CI 0.2-18.1* *p_{FET}=1.000*	OR=1.2, CI 0.2-7.9 p_{FET}=1.000
Total	OR=1.1, CI 0.5-2.3 x^2_{Yates}=0.021, df=1, p=.886	OR=1.2, CI 0.6-2.6 x^2_{Yates}=0.239, df=1, p=.625

[1] Groups compared using odds ratio, chi-square, and Fisher's Exact tests. Bold font indicates that a significant difference is present. Males typically had greater fracture odds than females, but italic font is used to indicate instances that females had greater odds of fracture than males. OR=odds ratio; CI=confidence interval.

Table D.10 – Differences between the male and female upper and lower limb fracture frequencies at Vagnari by age.[1]

Age	Upper Limb	Lower Limb
Adolescent	-	-
Young Adult	OR=1.2, CI 0.2-8.7 p_{FET}=1.00	p_{FET}=0.265
Middle Adult	p_{FET}=1.00	p_{FET}=1.000
Old Adult	-	-
Total	-	-
Adolescent	OR=1.8, CI 0.3-10.3 p_{FET}=0.686	OR=2.7, CI 0.3-23.9 p_{FET}=0.666

[1] Males and females were compared using Fisher's Exact tests. Bold font indicates that a significant difference was present. In all cases, males had greater odds of fracture than females. -=no fractures available to compare; OR=odds ratio; CI=confidence interval.

Table D.11 – Differences between the Ancaster upper limb fracture true prevalence rates by sex and age.[1]

	Young Adult	Middle Adult	Old Adult
		Male	
Young Adult		OR=4.2, CI 1.2-15.0 χ^2_{Yates}=4.683, df=1, p=0.300	OR=4.3, CI 0.4-43.1 p_{FET}=0.268
Middle Adult	OR=3.6, CI 0.7-18.9 p_{FET}=0.132		OR=1.0, CI 0.1-8.1 p_{FET}=1.000
Old Adult	OR=8.8, CI 1.4-54.5 p_{FET}=0.280	OR=2.4, CI 0.6-10.7 p_{FET}=0.364	
	Female		

[1] Groups compared using odds ratio, chi-square, and Fisher's Exact tests. Bold font indicates that a significant difference is present. Italic font indicates that compared to an older age category, the younger age category had a greater prevalence of fractures. OR=odds ratio; CI=confidence interval.

Table D.12 – Differences between the Ancaster lower limb fracture true prevalence rates by sex and age.[1]

	Young Adult	Middle Adult	Old Adult
		Male	
Young Adult		OR=1.5, CI 0.5-4.2, x^2_{Yates} =0.269, df=1, p=0.604	OR=2.7, CI 0.3-24.7 p_{FET}=0.359
Middle Adult	*OR=2.0 CI 0.4-10.3 p_{FET}=0.483*		-
Old Adult	*OR=1.1 CI 1.0-1.2 p_{FET}=1.000*	OR=1.8, CI 0.2-15.5 p_{FET}=0.465	
	Female		

[1] Groups compared using odds ratio, chi-square, and Fisher's Exact tests. Bold font indicates that a significant difference is present. Italic font indicates that compared to an older age category, the younger age category had a greater prevalence of fractures. OR=odds ratio; CI=confidence interval; - = no fractures observed and statistical test unable to be performed.

Table D.13 – Differences between upper and lower limb fracture frequencies at Vagnari by sex and age.[1]

Variables compared	Limb Type	Male	Female	Both Sexes
Upper vs. Lower Limb	N/A	OR=1.4, CI 0.4-5.3 p_{FET}=0.741	*OR=1.1, CI 0.1-12.1 p_{FET}=1.000*	OR=1.0, CI 0.4-3.1 x^2_{Yates}=0.000, df=1, p=1.000
YA vs. MA	Upper	OR=1.1, CI 0.2-8.4 p_{FET}=1.000	p_{FET}=1.000	OR=1.3, CI 0.2-7.4 p_{FET}=1.000
	Lower	OR=1.5, CI 0.2-9.6 p_{FET}=1.000	-	OR=1.1, CI 0.2-6.6 p_{FET}=1.000

[1] Groups were compared using chi-square and Fisher's Exact tests. Bold font indicates that a significant difference was present. Italic font used to indicate instances when upper limbs or middle adults had greater fracture odds than lower limbs or young adults. No fractures were identified in adolescent or old adult individuals, and as such, they were not compared or included in this table. YA=young adult; MA=middle adult; OR=odds ratio; CI=confidence interval; -=no fractures available to compare.

D.6 – Supplemental Fracture Prevalence Rate Comparisons: Side

Table D.14 –Differences in Ancaster fracture true prevalence rates between sex and side groups by element type.[1]

Element Type	Side Comparison (Left vs. Right)	
	Male	Female
Clavicle	OR=1.0, CI 0.3, 3.6 χ^2_{Yates}=0.000, df=1 p=1.000	-
Radius	OR=1.0, CI 0.1, 7.5 p_{FET}=1.000	OR=2.5, CI 0.6, 10.8 p_{FET}=.295
Ulna	OR=2.1, CI 0.2, 23.1 p_{FET}=.620	*p_{FET}=.497*
Femur	-	p_{FET}=1.000
Tibia	OR=1.5, CI 0.4, 5.7 χ^2_{Yates}=0.427, df=1, p=0.513	*OR=1.1, CI 0.2-5.8* *p_{FET}=1.000*
Fibula	OR=1.0, CI 0.2, 5.9 p_{FET}=1.000	OR=3.1, CI 0.3, 30.9 p_{FET}=.618

[1] Groups compared using odds ratio, chi-square, and Fisher's Exact tests. No humeral fractures were observed so this bone type was excluded from this table. Bold font indicates that a significant difference is present. Males and left sided elements typically had greater or equal odds of fracture than females and the right side; italic font is used to indicate instances that females or the right side had greater odds of fracture. -=statistical test was unable to be performed because of an absence of fractures. OR=odds ratio; CI=confidence interval

Table D.15 – Differences in Vagnari fracture true prevalence rates between sex and side groups by element type.[1]

Element Type	Side Comparison (Left vs. Right)	
	Male	Female
Clavicle	p_{FET}=0.478	p_{FET}=1.000
Humerus	-	p_{FET}=1.000
Ulna	OR=1.3, CI 0.1-22.1 p_{FET} = 1.000	-
Tibia	*OR=2.0, CI 0.2-23.9* *p_{FET}=1.00*	*p_{FET}=1.00*
Fibula	OR=1.3, CI 0.1-22.1 p_{FET} = 1.00	-

[1] No radial or femoral fractures were observed in individuals of known sex, so these bone types were excluded from this table. Groups were compared using Fisher's Exact tests. Bold font indicates that a significant difference was present. Males and the left side typically had greater or equal odds of fracture than females and the right side; italic font is used to indicate instances that females or the right side had greater odds of fracture than males or the left side. -=statistical test was unable to be performed because of an absence of fractures; OR=odds ratio; CI=confidence interval.

Appendix E: Fracture Malunion

The prevalence of fractures with malunion are detailed in this appendix. Counts of each type of malunion are presented by element type, sex, limb type, and site. Table E.1 reports the prevalence of fracture malunion at Ancaster. Table E.2 reports the prevalence of fracture malunion at Vagnari.

Abbreviations used in the charts include:

n – total number of elements with at least one type of malunion
N – total number of fractured elements
- – no fractures observed

Table E.1 – Prevalence rates of each type of malunion at Ancaster by sex and element type, and subtotalled for limb type, and sex[1].

Element	Sex	Total Fractures with Malunion		Angulation ≥20 degrees		Apposition ≥50%		Rotation ≥25 degrees		Overlap ≥25mm	
		n/N	%	*n/N*	%	*n/N*	%	*n/N*	%	*n/N*	%
Clavicle	Male	4/10	40.0	1/9	11.1	3/9	33.3	1/8	12.5	1/3	33.3
	Female	0/0	-	0/0	-	0/0	-	0/0	-	0/0	-
	Unknown Sex	0/1	0.0	0/1	0.0	0/1	0.0	0/1	0.0	0/1	0.0
	Total	4/11	36.4	1/10	10.0	3/10	30.0	1/9	11.1	1/3	33.3
Radius	Male	2/4	50.0	0/3	0.0	2/3	66.7	1/3	33.3	0/3	0.0
	Female	1/9	11.1	0/6	0.0	0/5	0.0	1/7	14.3	0/3	0.0
	Total	3/13	23.1	0/9	0.0	2/8	25.0	2/10	20.0	0/6	0.0
Ulna	Male	2/3	66.7	0/3	0.0	2/3	66.7	0/3	0.0	0/3	0.0
	Female	0/2	0.0	0/0	-	0/0	-	0/0	-	0/0	-
	Total	2/5	40.0	0/3	0.0	2/3	66.7	0/3	0.0	0/3	0.0
Upper Limb Subtotal	Male	8/17	47.1	1/15	6.7	7/15	46.7	2/14	14.3	1/9	11.1
	Female	1/11	9.1	0/6	0.0	0/5	0.0	1/7	14.3	0/3	0.0
	Unknown Sex	0/1	0.0	0/1	0.0	0/1	0.0	0/1	0.0	0/0	-
	Total	9/29	31.0	1/22	4.5	7/21	33.3	3/22	13.6	1/12	8.3
Femur	Male	0/0	-	0/0	-	0/0	-	0/0	-	0/0	-
	Female	0/1	0.0	0/0	-	0/0	-	0/0	-	0/0	-
	Total	0/1	0.0	0/0	-	0/0	-	0/0	-	0/0	-
Tibia	Male	2/10	20.0	0/4	0.0	0/4	0.0	1/4	25.0	1/5	20.0
	Female	1/6	16.7	0/1	0.0	0/1	0.0	1/1	100	0/2	0.0
	Total	2/16	12.5	0/5	0.0	0/5	0.0	2/5	40.0	0/7	0.0
Fibula	Male	1/7	14.3	0/7	0.0	1/7	14.3	0/5	0.0	0/6	0.0
	Female	2/4	50.0	0/4	0.0	2/4	50.0	0/2	0.0	1/4	25.0
	Total	2/11	18.2	0/11	0.0	3/11	27.3	0/7	0.0	1/10	10.0
Lower Limb Subtotal	Male	3/17	17.6	0/11	0.0	1/11	9.1	1/9	11.1	1/11	9.1
	Female	3/11	27.3	0/5	0.0	2/5	40.0	1/3	33.3	1/6	16.7
	Total	6/28	21.4	0/16	0.0	3/16	18.8	2/12	16.7	2/17	11.8

Element	Sex	Total Fractures with Malunion		Angulation ≥20 degrees		Apposition ≥50%		Rotation ≥25 degrees		Overlap ≥25mm	
		n/N	%	*n/N*	%	*n/N*	%	*n/N*	%	*n/N*	%
Total	Male	11/34	32.4	1/26	3.8	8/26	30.8	3/23	13.0	2/20	10.0
	Female	4/22	18.2	0/11	0.0	2/10	20.0	2/10	20.0	1/9	11.1
	Unknown Sex	0/1	0.0	0/1	0.0	0/1	0.0	0/1	0.0	0/0	-
	Total	15/57	26.3	1/38	2.6	10/37	27.0	5/34	14.7	3/29	10.3

[1] Fracture counts include all lesions with measurable malunion; some fractures were excluded from counts because the fracture type could not exhibit that kind of malunion (e.g., crush fractures cannot be angulated). Shaded rows represent fracture frequency subtotals by limb type. *n*=total number of elements with at least one type of malunion, *N*=total number of fractured elements; -=no fractures observed

Table E.2 – Prevalence rates of each type of malunion at Vagnari by sex and element type, and subtotalled for limb type, and sex[1].

Element	Sex	Total Fractures with Malunion		Angulation ≥20 degrees		Apposition ≤50%		Rotation ≥25 degrees		Overlap ≥25mm	
		n/N	%	*n/N*	%	*n/N*	%	*n/N*	%	*n/N*	%
Clavicle	Male	1/1	100.0	0/1	0.0	1/1	100.0	0/1	12.5	0/1	0.0
	Female	1/1	100.0	1/1	100.0	0/1	0.0	0/1	0.0	0/1	0.0
	Total	2/2	100.0	1/2	50.0	1/2	50.0	0/2	11.1	0/2	0.0
Humerus	Male	0/0	-	0/0	-	0/0	-	0/0	-	0/0	-
	Female	0/1	0.0	0/1	0.0	0/0	-	0/1	0.0	0/0	-
	Total	0/1	0.0	0/1	0.0	0/0	-	0/1	0.0	0/0	-
Radius	Male	0/0	-	0/0	-	0/0	-	0/0	-	0/0	-
	Female	0/0	-	0/0	-	0/0	-	0/0	-	0/0	-
	Unknown Sex	1/1	100.0	0/1	0.0	1/1	100.0	1/1	100.0	0/1	0.0
	Total	1/1	100.0	0/1	0.0	1/1	100.0	1/1	100.0	0/1	0.0
Ulna	Male	0/2	0.0	0/1	0.0	0/1	0.0	0/1	0.0	0/1	0.0
	Female	0/0	-	0/0	-	0/0	-	0/0	-	0/0	-
	Unknown Sex	1/1	100.0	0/1	0.0	0/1	0.0	1/1	100.0	0/1	0.0
	Total	1/3	33.3	0/2	0.0	0/2	0.0	1/2	33.3	0/2	0.0

Element	Sex	Total Fractures with Malunion		Angulation ≥20 degrees		Apposition ≤50%		Rotation ≥25 degrees		Overlap ≥25mm	
		n/N	%	*n/N*	%	*n/N*	%	*n/N*	%	*n/N*	%
Upper Limb Subtotal	Male	1/3	33.3	0/2	0.0	1/2	50.0	0/2	0.0	0/2	0.0
	Female	1/2	50.0	1/2	50.0	0/1	0.0	0/2	0.0	0/1	0.0
	Unknown Sex	2/2	100.0	0/2	0.0	1/2	50.0	2/2	100.0	0/2	0.0
	Total	4/7	57.1	1/6	16.7	2/5	40.0	2/6	33.3	0/5	0.0
Tibia	Male	0/3	0.0	0/2	0.0	0/2	0.0	0/2	0.0	0/2	0.0
	Female	0/1	0.0	0/1	0.0	0/1	0.0	0/1	0.0	0/1	0.0
	Total	0/4	0.0	0/3	0.0	0/3	0.0	0/3	0.0	0/3	0.0
Fibula	Male	0/2	0.0	0/2	0.0	0/2	0.0	0/1	0.0	0/2	0.0
	Female	0/0	-	0/0	-	0/0	-	0/0	-	0/0	-
	Total	0/2	0.0	0/2	0.0	0/2	0.0	0/1	0.0	0/2	0.0
Lower Limb Subtotal	Male	0/5	0.0	0/4	0.0	0/4	0.0	0/3	0.0	0/4	0.0
	Female	0/1	0.0	0/1	0.0	0/1	0.0	0/1	0.0	0/1	0.0
	Total	0/6	0.0	0/5	0.0	0/5	0.0	0/4	0.0	0/5	0.0
Total	Male	1/8	12.5	0/6	0.0	1/6	16.7	0/5	0.0	0/6	0.0
	Female	1/3	33.3	1/3	33.3	0/2	0.0	0/3	0.0	0/2	0.0
	Unknown Sex	2/2	100.0	0/2	0.0	1/2	50.0	2/2	100.0	0/2	0.0
	Total	4/13	30.8	1/11	9.1	2/10	20.0	2/10	20.0	0/10	0.0

[1] Fracture counts include all lesions with measurable malunion; some fractures were excluded from counts because the fracture type could not exhibit that kind of malunion (e.g., crush fractures cannot be angulated). Shaded rows represent fracture frequency subtotals by limb type. *n*=total number of elements with at least one type of malunion, *N*=total number of fractured elements; -=no fractures observed

Appendix F: Osteoarthritis & Joint Preservation

This appendix reports the osteoarthritis recorded for each individual at Ancaster and Vagnari. The charts below record the number of joints with osteoarthritis relative to the actual number of joints that were present and observable. Shaded cells represent the joints that were complete and that had osteoarthritis. Table F.1 reports the osteoarthritis observed in Ancaster individuals and Table F.2 reports the osteoarthritis observed in Vagnari individuals.

Abbreviations used in these tables include:

F - Female
F? – Probable female
U – Unknown sex
M? – Probable male
M - Male
ADO - Adolescent
YA – Young adult
MA – Middle adult
OA – Old adult
A – Adult (unknown age)
OA_x – Osteoarthritis
UL – Upper Limb
LL – Lower Limb
R - Right
L - Left
Y – Yes, a fracture or osteoarthritis was observed
C – joint was more than 50% present
I – joint was less than 50% present
- – no osteoarthritis
+ – osteoarthritis present
.

Table F.1 – Osteoarthritis recorded among individuals at Ancaster by joint type and side.

Skeleton Number	Sex	Age	Fracture		OA_x Present	Shoulder		Elbow		Wrist		Hip		Knee		Ankle	
			UL	LL		R	L	R	L	R	L	R	L	R	L	R	L
AN-001	F?	YA	-	Y	-	-/C	-/I	-/C	-/C	-/C	-/C	-/C	-/C	-/C	-/C	-/C	-/C
AN-002*	F	MA	-	-	Y	-/C	-/C	-/C	-/C	-/C	-/C	-/C	-/C	-/C	-/C	-/C	-/C
AN-002A	F	MA	-	-	Y	+/C	-/C	-/C	-/C	+/C	-/I	-/I	-/I	-/I	-/I	-/I	-/I
AN-003	M?	YA	-	-	-	-/C	-/C	-/C	-/C	-/I	-/I	-/C	-/I	-/I	-/C	-/I	-/I
AN-003A	F	YA	-	-	Y	+/C	+/C	-/C	-/C	-/C	-/C	-/C	-/C	-/C	-/C	-/C	-/C
AN-004	M	OA	-	-	Y	-/C	-/C	-/C	-/C	-/C	+/C	-/C	-/C	-/I	-/I	-/I	-/I
AN-005	M	MA	-	-	Y	-/C	-/C	-/I	-/C	+/C	-/C	-/C	-/C	-/C	-/C	-/C	-/C
AN-006	M	MA	-	-	Y	+/C	+/C	-/C	-/C	-/C	-/C	-/C	-/C	-/C	-/C	-/C	-/C
AN-010	F	MA	-	-	Y	+/C	+/C	-/C	+/C	-/C	-/C	+/C	-/C	-/C	-/C	-/C	-/C
AN-011	M	MA	-	-	Y	-/C	-/C	+/C	+/C	+/C	-/C	-/C	-/C	+/C	-/C	-/C	-/C
AN-012	M	YA	-	-	-	-/C	-/C	-/C	-/C	-/I	-/C	-/C	-/C	-/C	-/C	-/C	-/C
AN-012B	M	MA	Y	Y	Y	-/C	-/C	-/C	+/C	-/C	-/C	-/C	-/C	+/C	-/C	-/C	-/C
AN-013	M	YA	-	Y	-	-/C	-/C	-/C	-/C	-/C	-/C	-/C	-/C	-/C	-/C	-/C	-/C
AN-014	M?	YA	-	-	-	-/C	-/I	-/C	-/C	-/I	-/C	-/I	-/I	-/I	-/I	-/I	-/I
AN-021	F	A	-	-	-	-/I	-/C	-/C	-/C	-/I	-/C	-/C	-/C	-/I	-/I	-/C	-/C
AN-022	M	MA	-	-	-	-/C	-/C	-/C	-/C	-/C	-/C	-/C	-/I	-/C	-/C	-/C	-/C
AN-023	M	MA	Y	-	Y	-/C	-/C	-/C	-/C	-/C	-/C	+/C	-/C	-/C	-/C	-/C	-/C
AN-024	M	MA	Y	-	Y	+/C	-/C	-/C	+/C	-/I	-/C	-/C	-/C	-/C	-/C	-/I	-/C
AN-025	F?	MA	-	-	Y	-/I	+/C	-/C	-/C	-/I	-/I	-/I	-/C	-/I	+/C	-/C	-/I
AN-026	M	YA	-	-	-	-/C	-/C	-/C	-/C	-/C	-/I	-/C	-/C	-/C	-/C	-/C	-/C
AN-027	M	MA	-	-	Y	-/I	-/I	-/I	-/I	-/I	-/C	-/C	+/C	-/C	-/C	-/C	-/C
AN-028	M	MA	-	-	Y	-/C	-/C	-/C	-/C	-/I	-/C	+/C	+/C	-/C	-/C	-/C	-/C
AN-032B	U	A	-	-	-	-/I	-/I	-/I	-/I	-/I	-/I	-/I	-/I	-/C	-/C	-/C	-/C
AN-034	M	MA	-	Y	Y	+/C	+/C	-/C	-/C	-/C	-/C	-/C	-/C	-/C	-/C	-/C	-/C

Skeleton Number	Sex	Age	Fracture		OA_x Present	Shoulder		Elbow		Wrist		Hip		Knee		Ankle	
			UL	LL		R	L	R	L	R	L	R	L	R	L	R	L
AN-035	M?	YA	-	-	-	-/C	-/C	-/C	-/C	-/C	-/C	-/C	-/C	-/C	-/C	-/C	-/C
AN-038	F	YA	-	-	Y	-/C	-/C	-/C	-/C	-/I	+/C	-/C	-/C	-/C	-/C	-/C	-/C
AN-039	M?	YA	-	-	-	-/C	-/C	-/C	-/C	-/C	-/C	-/C	-/C	-/C	-/C	-/C	-/C
AN-041	F	YA	-	-	-	-/C	-/I	-/C	-/C	-/C	-/C	-/C	-/C	-/C	-/C	-/C	-/C
AN-042	F	YA	-	-	-	-/C	-/C	-/C	-/C	-/C	-/C	-/C	-/C	-/C	-/C	-/C	-/C
AN-043	M	YA	-	-	-	-/C	-/C	-/C	-/C	-/C	-/C	-/I	-/C	-/C	-/C	-/C	-/C
AN-045	F?	A	-	-	Y	-/C	-/I	+/C	-/C	-/I	-/C	-/I	-/I	-/I	-/I	-/I	-/I
AN-045A	F?	MA	-	-	-	-/C	-/C	-/C	-/C	-/C	-/I	-/I	-/C	-/C	-/C	-/C	-/C
AN-046	M?	YA	-	Y	-	-/C	-/C	-/C	-/C	-/C	-/C	-/C	-/C	-/C	-/C	-/C	-/C
AN-047	M	MA	-	Y	-	-/C	-/C	-/C	-/C	-/C	-/C	-/C	-/C	-/C	-/C	-/C	-/C
AN-048B	M?	ADO	-	-	-	-/C	-/C	-/C	-/C	-/C	-/C	-/C	-/C	-/C	-/C	-/C	-/C
AN-049	M	YA	-	-	Y	-/I	-/I	-/I	-/I	-/I	-/I	-/I	+/C	-/I	-/C	-/I	-/I
AN-050	M	OA	-	-	-	-/C	-/C	-/C	-/C	-/I	-/C	-/C	-/C	-/C	-/C	-/C	-/C
AN-052	F	MA	-	-	Y	-/C	-/C	-/I	-/I	-/C	-/I	-/C	-/C	+/C	-/C	-/C	-/C
AN-053	F	MA	Y	-	-	-/C	+/C	-/C	-/C	-/C	-/I	-/I	-/C	-/C	-/C	-/C	-/C
AN-056	M	MA	Y	-	-	-/C	-/C	-/C	-/C	-/C	-/C	-/C	-/C	-/C	-/C	-/C	-/C
AN-057	M	MA	Y	-	-	-/C	-/C	-/C	-/C	-/I	-/C	-/I	-/C	-/C	-/C	-/C	-/C
AN-058	U	OA	Y	-	Y	+/C	+/C	-/C	-/C	-/I	-/C	-/C	-/C	+/C	+/C	-/C	-/C
AN-061	M	MA	Y	-	-	-/C	+/C	-/C	-/C	-/C	-/C	-/C	-/C	-/I	-/I	-/C	-/C
AN-062	F	YA	-	Y	Y	+/C	-/C	-/C	-/C	-/C	-/C	-/I	-/C	-/I	-/C	-/I	-/C
AN-063	M	MA	-	-	Y	+/C	+/C	-/C	-/C	-/C	-/C	-/I	-/I	-/I	-/I	-/I	-/I
AN-064	M?	MA	-	Y	-	-/I	-/I	-/I	-/I	-/C	-/I	-/I	-/C	-/I	-/I	-/C	-/I
AN-065	M	MA	-	-	-	-/C	-/C	-/C	-/C	-/C	-/C	-/C	-/C	-/C	-/C	-/C	-/C
AN-066	F	YA	-	-	-	-/C	-/C	-/C	-/C	-/C	-/C	-/C	-/C	-/C	-/C	-/C	-/C
AN-067	F	MA	-	-	-	-/I	-/I	-/C	-/I	-/C	-/I	-/C	-/C	-/C	-/C	-/C	-/C
AN-068	M	MA	-	-	-	-/I	-/I	-/C	-/I	-/C	-/I	-/C	-/C	-/C	-/C	-/C	-/C
AN-069	F?	A	-	-	-	-/C	-/C	-/C	-/C	-/I	-/I	-/I	-/I	-/I	-/I	-/I	-/I

Skeleton Number	Sex	Age	Fracture		OA_x Present	Shoulder		Elbow		Wrist		Hip		Knee		Ankle	
			UL	LL		R	L	R	L	R	L	R	L	R	L	R	L
AN-072	F	YA	-	-	-	-/C	-/C	-/C	-/C	-/C	-/I	-/C	-/C	-/C	-/C	-/C	-/C
AN-077	M?	YA	-	-	-	-/C	-/C	-/C	-/C	-/I	-/I	-/I	-/C	-/C	-/C	-/C	-/C
AN-078	F	YA	-	-	-	-/I	-/I	-/C	-/C	-/C	-/C	-/C	-/C	-/C	-/C	-/C	-/C
AN-080	U	A	-	-	-	-/I	-/I	-/I	-/I	-/C	-/I	-/C	-/I	-/I	-/I	-/I	-/I
AN-081	F	MA	-	-	Y	-/I	-/I	-/C	-/I	-/C	-/I	+/C	-/I	-/C	-/C	-/I	-/I
AN-082	M	ADO	-	-	-	-/C	-/C	-/C	-/C	-/C	-/C	-/C	-/C	-/I	-/I	-/I	-/I
AN-092	M	YA	-	-	-	-/C	-/C	-/C	-/C	-/C	-/C	-/C	-/C	-/C	-/C	-/C	-/C
AN-093	M	MA	-	-	Y	-/C	-/C	-/C	-/C	+/C	-/C	-/C	-/C	+/C	-/C	-/C	-/C
AN-096	F	YA	-	-	-	-/I	-/I	-/I	-/I	-/C	-/I	-/C	-/C	-/C	-/C	-/I	-/I
AN-098	M	OA	Y	-	Y	-/C	-/C	-/C	-/C	+/C	+/C	-/C	-/I	-/C	-/I	-/C	-/C
AN-102	F	YA	-	-	Y	-/C	-/I	-/C	-/C	-/I	-/I	-/C	-/C	+/C	-/C	-/I	-/I
AN-104	F?	MA	Y	-	-	-/C	-/C	-/C	-/C	-/C	-/C	-/C	-/C	-/C	-/C	-/C	-/C
AN-106	M	MA	-	-	-	-/C	-/C	-/C	-/C	-/C	-/C	-/C	-/C	-/C	-/C	-/C	-/C
AN-107	M?	ADO	-	-	-	-/C	-/C	-/C	-/C	-/C	-/C	-/I	-/C	-/C	-/C	-/C	-/C
AN-108	M?	ADO	-	-	-	-/C	-/C	-/C	-/C	-/C	-/C	-/C	-/C	-/C	-/C	-/C	-/C
AN-109	F	MA	-	-	-	-/C	-/C	-/C	-/C	-/C	-/C	-/C	-/C	-/C	-/C	-/C	-/C
AN-110	M?	YA	-	-	Y	-/C	-/C	-/C	-/C	+/C	-/C	-/C	-/C	-/C	-/C	-/C	-/C
AN-111	M	YA	-	-	-	-/C	-/C	-/C	-/C	-/C	-/C	-/C	-/C	-/C	-/C	-/C	-/C
AN-112	F	YA	-	-	-	-/C	-/C	-/C	-/C	-/C	-/C	-/C	-/C	-/C	-/C	-/C	-/C
AN-112A	U	A	-	-	-	-/I	-/I	-/C	-/I	-/I	-/I	-/I	-/I	-/I	-/I	-/I	-/I
AN-113	F	MA	-	Y	Y	-/C	-/C	-/C	-/C	+/C	+/C	-/C	-/C	-/C	-/C	-/C	-/C
AN-115	F	MA	-	-	-	-/C	-/C	-/C	-/C	-/C	-/C	-/C	-/C	-/C	-/C	-/C	-/C
AN-116	F?	MA	-	Y	Y	-/C	-/C	-/C	-/C	-/C	-/C	-/C	-/C	+/C	+/C	-/C	-/C
AN-117	M?	MA	-	Y	Y	-/C	-/C	+/C	-/C	+/C	-/C	-/C	-/C	+/C	+/C	+/C	+/C
AN-118	M?	YA	-	-	Y	-/C	-/C	-/C	-/C	-/C	-/C	+/C	+/C	-/C	-/C	-/C	-/C
AN-119	M?	YA	-	-	-	-/C	-/C	-/C	-/C	-/C	-/C	-/I	-/I	-/I	-/I	-/I	-/I
AN-120	M	YA	Y	-	-	-/C	-/C	-/C	-/C	-/C	-/C	-/C	-/C	-/C	-/C	-/C	-/C

Skeleton Number	Sex	Age	Fracture		OA_x Present	Shoulder		Elbow		Wrist		Hip		Knee		Ankle	
			UL	LL		R	L	R	L	R	L	R	L	R	L	R	L
AN-121	M	A	-	-	Y	-/C	-/C	-/C	-/C	+/C	-/C	-/I	+/C	+/C	+/C	-/C	-/C
AN-122	M	MA	-	-	-	-/C	-/C	-/C	-/C	-/C	-/C	-/C	-/C	-/C	-/C	-/C	-/C
AN-123	F	YA	Y	-	-	-/C	-/C	-/C	-/C	-/C	-/C	-/C	-/C	-/C	-/C	-/C	-/C
AN-128	F	YA	-	-	-	-/C	-/C	-/C	-/C	-/C	-/C	-/C	-/C	-/C	-/C	-/C	-/C
AN-133	F	YA	-	-	-	-/I	-/C	-/C	-/I	-/C	-/C	-/C	-/C	-/C	-/C	-/C	-/C
AN-134	F?	MA	-	-	-	-/I	-/I	-/I	-/C	-/I	-/I	-/C	-/C	-/C	-/C	-/C	-/C
AN-135	M?	MA	-	-	Y	+/C	-/C	-/C	-/C	-/C	+/C	-/C	-/C	-/C	-/I	-/C	-/C
AN-136	M	YA	-	-	Y	-/C	-/C	-/C	-/C	+/C	-/C	-/C	-/C	-/C	-/C	-/C	-/C
AN-140	M?	YA	-	-	-	-/I	-/C	-/I	-/C	-/C	-/C	-/C	-/C	-/C	-/C	-/C	-/C
AN-141	M?	MA	-	-	Y	-/I	-/I	-/C	-/C	-/C	-/C	-/C	-/C	-/C	-/C	-/C	-/C
AN-142	F	MA	-	-	-	-/C	-/C	-/C	-/C	-/C	-/C	-/C	-/C	-/C	-/C	-/C	-/C
AN-143	M	YA	-	-	-	-/C	-/C	-/C	-/C	-/C	-/C	-/C	-/C	-/C	-/C	-/C	-/C
AN-144	M	YA	-	-	Y	-/I	-/C	-/C	-/C	-/C	+/C	-/C	-/C	-/C	-/C	-/C	-/C
AN-147	M	MA	-	-	Y	-/C	-/C	-/C	-/C	-/C	-/C	-/C	-/C	-/C	-/C	-/C	-/C
AN-152	F	MA	Y	Y	Y	+/C	+/C	-/C	-/C	-/C	-/C	-/C	-/C	-/C	+/C	-/C	-/C
AN-154	F	A	-	Y	-	-/I	-/I	-/C	-/C	-/I	-/C	-/C	-/C	-/C	-/C	-/C	-/C
AN-155	F?	A	-	Y	-	-/I	-/I	-/C	-/C	-/C	-/I	-/I	-/C	-/C	-/I	-/I	-/C
AN-156	M	MA	-	-	-	-/C	-/C	-/C	-/C	-/C	-/C	-/C	-/C	-/C	-/C	-/C	-/C
AN-157	F	YA	-	-	-	-/C	-/C	-/C	-/C	-/C	-/C	-/C	-/C	-/C	-/C	-/C	-/C
AN-158	M?	A	-	-	-	-/I	-/I	-/I	-/I	-/I	-/I	-/C	-/C	-/C	-/C	-/C	-/C
AN-159	U	A	-	-	-	-/I	-/I	-/I	-/I	-/I	-/I	-/I	-/I	-/C	-/C	-/C	-/C
AN-160	F?	YA	-	-	-	-/C	-/C	-/C	-/C	-/C	-/C	-/I	-/I	-/C	-/C	-/C	-/C
AN-161A	M?	MA	-	-	-	-/I	-/I	-/I	-/I	-/I	-/I	-/I	-/I	-/C	-/I	-/C	-/I
AN-162	F?	YA	-	-	-	-/C	-/C	-/C	-/C	-/C	-/I	-/C	-/C	-/C	-/C	-/C	-/C
AN-165	M	YA	-	Y	-	-/C	-/C	-/C	-/C	-/C	-/C	-/C	-/C	-/C	-/C	-/C	-/C
AN-167	M?	YA	-	-	-	-/I	-/C	-/I	-/C	-/I	-/C	-/C	-/C	-/C	-/C	-/C	-/C
AN-168	F	YA	-	-	-	-/C	-/C	-/C	-/C	-/C	-/C	-/C	-/C	-/C	-/C	-/C	-/C

Skeleton Number	Sex	Age	Fracture		OA_x Present	Shoulder		Elbow		Wrist		Hip		Knee		Ankle	
			UL	LL		R	L	R	L	R	L	R	L	R	L	R	L
AN-170	M	MA	-	-	Y	+/C	+/C	+/C	+/C	-/C	-/C	-/C	-/C	-/C	-/C	-/C	-/C
AN-171	F	MA	-	-	-	-/C	-/C	-/C	-/C	-/C	-/C	-/C	-/C	-/C	-/C	-/C	-/C
AN-172	F?	MA	Y	-	Y	-/C	-/C	-/C	-/C	-/C	+/C	-/C	-/C	+/C	+/C	-/C	-/C
AN-173	F?	MA	-	-	-	-/C	-/C	-/C	-/C	-/I	-/I	-/C	-/C	-/C	-/C	-/C	-/C
AN-175	M	YA	-	-	-	-/C	-/I	-/I	-/I	-/C	-/I	-/C	-/I	-/I	-/I	-/C	-/C
AN-177	M	MA	Y	-	Y	-/C	-/C	-/C	-/C	-/C	+/C	-/C	-/C	-/C	-/C	-/C	-/C
AN-178	F?	YA	-	-	-	-/C	-/C	-/C	-/C	-/C	-/C	-/C	-/C	-/C	-/C	-/C	-/C
AN-179	M	YA	-	-	-	-/C	-/C	-/C	-/C	-/C	-/C	-/C	-/C	-/C	-/C	-/C	-/C
AN-182	F	YA	-	-	-	-/I	-/I	-/C	-/I	-/C	-/C	-/C	-/C	-/C	-/C	-/C	-/C
AN-183	F?	MA	-	-	-	-/C	-/C	-/C	-/C	-/C	-/I	-/C	-/C	-/C	-/C	-/C	-/C
AN-184	M	MA	-	-	-	-/C	-/C	-/C	-/C	-/C	-/C	-/C	-/C	-/C	-/C	-/C	-/C
AN-185	F	YA	-	-	-	-/I	-/I	-/I	-/I	-/C	-/C	-/C	-/C	-/C	-/C	-/C	-/C
AN-185A	M	MA	Y	-	-	-/C	-/C	-/C	-/C	-/C	-/C	-/C	-/C	-/C	-/C	-/C	-/C
AN-188	M?	YA	-	-	Y	-/C	-/C	-/I	-/C	-/C	-/C	-/C	+/C	-/C	-/C	-/C	-/C
AN-190	F	MA	-	-	-	-/C	-/C	-/I	-/I	-/C	-/C	-/C	-/I	-/C	-/C	-/C	-/C
AN-191	F	OA	Y	-	Y	+/C	-/I	-/C	-/C	+/C	-/C	-/C	+/C	-/C	-/C	-/C	-/C
AN-193	F	A	-	-	Y	-/I	-/I	+/C	-/I	-/I	-/I	-/C	-/I	+/C	+/C	-/C	-/C
AN-198	U	A	-	-	Y	-/I	-/I	-/I	-/I	-/I	-/I	-/I	-/I	-/I	+/C	-/C	-/C
AN-199	U	A	-	-	-	-/I	-/I	-/I	-/I	-/I	-/I	-/I	-/I	-/C	-/C	-/C	-/C
AN-200	M	YA	-	-	-	-/C	-/C	-/C	-/C	-/C	-/C	-/C	-/C	-/C	-/C	-/I	-/C
AN-201	M	MA	-	-	-	-/C	-/C	-/C	-/I	-/C	-/C	-/C	-/C	-/C	-/C	-/C	-/C
AN-202	F	YA	-	-	-	-/C	-/C	-/C	-/C	-/C	-/C	-/C	-/C	-/C	-/C	-/C	-/C
AN-204A	M	MA	Y	Y	Y	-/C	-/C	-/C	-/C	-/C	-/C	-/C	-/C	+/C	-/C	-/C	-/C
AN-205	F	YA	-	-	-	-/I	-/I	-/I	-/I	-/C	-/C	-/C	-/C	-/C	-/C	-/C	-/C
AN-209	M?	A	-	-	Y	+/C	-/C	-/C	-/C	-/I	-/I	-/C	-/I	-/C	-/C	-/C	-/C
AN-210	M?	YA	-	Y	-	-/C	-/C	-/I	-/I	-/I	-/I	-/I	-/I	-/C	-/C	-/C	-/C
AN-211	M?	YA	-	-	-	-/C	-/C	-/C	-/C	-/I	-/I	-/I	-/C	-/C	-/C	-/C	-/C

Skeleton Number	Sex	Age	Fracture		OA_x Present	Shoulder		Elbow		Wrist		Hip		Knee		Ankle	
			UL	LL		R	L	R	L	R	L	R	L	R	L	R	L
AN-212	F	YA	-	-	-	-/C	-/C	-/C	-/C	-/C	-/C	-/C	-/C	-/C	-/C	-/C	-/C
AN-213	M?	A	-	-	-	-/I	-/C	-/C	-/C	-/I	-/C	-/C	-/C	-/C	-/C	-/C	-/C
AN-214	M	YA	-	-	-	-/C	-/C	-/I	-/I	-/I	-/I	-/I	-/I	-/I	-/I	-/C	-/C
AN-216	M?	YA	-	-	-	-/I	-/C	-/C	-/C	-/C	-/C	-/C	-/C	-/C	-/C	-/C	-/C
AN-217	F	MA	-	-	-	-/C	-/I	-/C	-/C	-/C	-/C	-/C	-/C	-/C	-/C	-/C	-/C
AN-217A	M	YA	-	-	-	-/I	-/I	-/I	-/I	-/I	-/I	-/I	-/I	-/I	-/I	-/I	-/I
AN-218	F	YA	-	Y	Y	-/C	-/C	-/C	-/C	-/C	-/C	+/C	+/C	+/C	+/C	-/C	-/C
AN-220	F	OA	-	-	-	-/I	-/I	-/I	-/C	-/C	-/C	-/C	-/C	-/I	-/C	-/C	-/C
AN-221	M	YA	-	-	-	-/I	-/I	-/I	-/I	-/I	-/I	-/C	-/C	-/C	-/C	-/C	-/I
AN-222	M?	A	-	-	-	-/I	-/C	-/I	-/I	-/I	-/C	-/I	-/I	-/C	-/C	-/C	-/C
AN-223	U	A	-	-	-	-/I	-/I	-/I	-/I	-/I	-/I	-/I	-/I	-/C	-/C	-/C	-/C
AN-224	F	A	-	-	Y	-/C	-/I	-/C	-/I	-/I	-/I	+/C	-/I	-/C	-/C	-/C	-/C
AN-225	M	YA	Y	-	Y	-/C	-/C	-/C	-/C	-/C	+/C	-/C	-/C	-/C	-/C	-/C	-/C
AN-226	F	YA	-	-	-	-/C	-/C	-/C	-/C	-/C	-/C	-/C	-/C	-/C	-/C	-/C	-/C
AN-229	M	MA	-	-	Y	-/C	-/C	-/C	-/C	-/C	-/C	-/C	-/C	+/C	+/C	-/C	-/C
AN-230	M?	YA	-	-	-	-/I	-/I	-/C	-/I	-/C	-/I	-/C	-/C	-/C	-/I	-/C	-/C
AN-230A	M	MA	Y	-	Y	-/C	+/C	-/C	+/C	-/C	-/C	-/C	-/C	+/C	-/C	-/C	-/C
AN-234	U	YA	-	-	-	-/C	-/I	-/C	-/I	-/I	-/I	-/I	-/I	-/C	-/C	-/C	-/C
AN-235	M?	YA	-	-	-	-/C	-/C	-/C	-/C	-/C	-/I	-/C	-/C	-/I	-/I	-/I	-/I
AN-235B	M	YA	-	-	-	-/I	-/I	-/I	-/I	-/I	-/I	-/I	-/I	-/I	-/C	-/I	-/C
AN-237	F?	MA	-	-	Y	-/I	-/C	-/I	-/I	-/C	-/C	-/C	-/C	+/C	-/C	-/C	-/C
AN-238	M	MA	-	-	Y	-/C	-/C	-/C	-/C	-/C	-/C	-/C	-/C	-/C	+/C	-/C	-/C
AN-240	M	YA	-	-	-	-/C	-/C	-/C	-/C	-/C	-/C	-/I	-/I	-/C	-/C	-/C	-/C
AN-241	F	OA	Y	-	Y	+/C	+/C	+/C	+/C	-/C	+/C	-/C	-/C	-/C	-/C	-/C	-/C
AN-242	F	OA	-	-	-	-/C	-/C	-/C	-/C	-/C	-/C	-/C	-/C	-/C	-/C	-/C	-/C
AN-243	F	YA	-	-	-	-/C	-/C	-/C	-/C	-/C	-/C	-/C	-/C	-/C	-/C	-/C	-/C
AN-244	M	YA	Y	-	-	-/C	-/C	-/C	-/C	-/C	-/C	-/C	-/C	-/C	-/C	-/C	-/C

Skeleton Number	Sex	Age	Fracture		OA_x Present	Shoulder		Elbow		Wrist		Hip		Knee		Ankle	
			UL	LL		R	L	R	L	R	L	R	L	R	L	R	L
AN-247	F	YA	-	Y	-	-/C	-/C	-/I	-/C	-/I	-/I	-/I	-/I	-/C	-/C	-/C	-/C
AN-248	U	MA	-	-	-	-/I	-/I	-/I	-/I	-/I	-/I	-/I	-/I	-/I	-/I	-/I	-/C
AN-252	M	MA	-	-	Y	+/C	+/C	-/C	-/C	+/C	+/C	-/C	-/C	-/C	-/C	+/C	+/C
AN-256	F?	A	-	-	-	-/I	-/I	-/I	-/I	-/I	-/I	-/I	-/C	-/I	-/I	-/C	-/C
AN-257	M?	MA	-	-	Y	+/C	-/C	-/C	-/C	-/C	-/C	-/C	-/C	-/C	-/C	-/C	-/C
AN-259	F	YA	-	-	-	-/C	-/C	-/C	-/C	-/C	-/C	-/C	-/C	-/C	-/C	-/C	-/C
AN-262A	F	MA	-	-	-	-/C	-/C	-/C	-/C	-/C	-/C	-/C	-/C	-/C	-/C	-/C	-/C
AN-263	F	OA	-	-	-	-/I	-/C	-/C	-/C	-/C	-/C	-/C	-/C	-/C	-/C	-/C	-/C
AN-263A	F?	A	-	-	-	-/I	-/I	-/I	-/I	-/I	-/I	-/C	-/C	-/C	-/C	-/C	-/C
AN-266	M?	MA	-	-	-	-/C	-/C	-/C	-/C	-/C	-/C	-/C	-/C	-/C	-/C	-/C	-/C
AN-267	F?	YA	-	-	-	-/I	-/I	-/I	-/I	-/I	-/I	-/I	-/I	-/C	-/C	-/C	-/C
AN-269	M	MA	-	-	-	-/C	+/C	-/C	-/C	-/C	-/C	-/C	-/C	-/C	-/C	-/C	-/C
AN-270	F?	YA	-	-	-	-/C	-/C	-/I	-/C	-/C	-/C	-/I	-/I	-/I	-/I	-/C	-/C
AN-271	F?	A	-	-	-	-/C	-/C	-/C	-/C	-/C	-/I	-/I	-/I	-/I	-/I	-/I	-/I
AN-272	U	A	-	-	Y	-/I	-/I	-/I	-/I	-/I	-/I	-/I	-/I	+/C	-/C	-/C	-/C
AN-274	F	YA	-	-	-	-/I	-/I	-/I	-/I	-/I	-/I	-/C	-/C	-/C	-/C	-/C	-/C
AN-276	F	A	-	-	Y	-/I	-/I	-/I	-/I	-/I	-/I	-/C	-/C	+/C	+/C	-/C	-/C
AN-277	F?	A	Y	-	-	-/C	-/C	-/C	-/C	-/C	-/C	-/C	-/C	-/C	-/C	-/C	-/C
AN-278	M	YA	-	-	-	-/C	-/C	-/C	-/C	-/C	-/C	-/I	-/I	-/I	-/I	-/I	-/I
AN-280	M	YA	-	-	-	-/C	-/C	-/C	-/C	-/C	-/C	-/C	-/C	-/C	-/C	-/C	-/C
AN-282	M	YA	-	-	-	-/I	-/I	-/C	-/C	-/C	-/C	-/I	-/I	-/C	-/C	-/C	-/C
AN-282B*	M?	A	-	-	-	-/I	-/I	-/I	-/I	-/I	-/I	-/C	-/I	-/C	-/I	-/I	-/I

F=Female; F?=Probable female; U=Unknown sex; M?=Probable male; M=Male; ADO=Adolescent; YA=Young adult; MA=Middle adult; OA=Old adult; A=Adult (unknown age); OA_x=Osteoarthritis; UL=Upper Limb; LL=Lower Limb; R=Right; L=Left; Y=Yes, a fracture or osteoarthritis was observed; C=joint was more than 50% present; I=joint was less than 50% present; -=no osteoarthritis; +=osteoarthritis present. Shaded cells represent the joints that were complete with osteoarthritis.

Table F.2 – Osteoarthritis recorded among individuals at Vagnari by joint type and side.

Skeleton Number	Sex	Age	Fracture		OA_x Present	Shoulder		Elbow		Wrist		Hip		Knee		Ankle	
			UL	LL		R	L	R	L	R	L	R	L	R	L	R	L
VA-F034	M?	A	-	-	-	-/I	-/I	-/I	-/I	-/I	-/I	-/I	-/I	-/I	-/I	-/I	-/I
VA-F035	M	MA	-	-	-	-/I	-/I	-/I	-/C	-/I	-/I	-/I	-/I	-/I	-/I	-/I	-/I
VA-F037	F	MA	-	-	-	-/I	-/C	-/I	-/I	-/I	-/I	-/C	-/C	-/I	-/I	-/C	-/C
VA-F040	F	ADO	-	-	-	-/C	-/C	-/C	-/C	-/C	-/C	-/C	-/C	-/C	-/C	-/C	-/C
VA-F042	M	YA	-	-	-	-/I	-/C	-/I	-/C	-/I	-/C	-/C	-/C	-/I	-/C	-/I	-/I
VA-F042A	M	YA	-	Y	-	-/C	-/I	-/C	-/C	-/I	-/C	-/C	-/C	-/I	-/C	-/C	-/I
VA-F062	M?	MA	-	-	-	-/I	-/I	-/C	-/I	-/C	-/C	-/I	-/I	-/I	-/C	-/C	-/C
VA-F067	M	YA	-	Y	-	-/I	-/I	-/C	-/I	-/I	-/C	-/C	-/I	-/C	-/C	-/I	-/C
VA-F068	M	MA	Y	-	-	-/I	-/I	-/C	-/I	-/C	-/C	-/C	-/I	-/I	-/I	-/I	-/I
VA-F086	M?	A	-	-	-	-/I	-/I	-/I	-/I	-/I	-/I	-/I	-/I	-/I	-/I	-/I	-/I
VA-F089	U	A	Y	-	-	-/I	-/I	-/I	-/I	-/I	-/I	-/I	-/I	-/I	-/I	-/I	-/I
VA-F092	M	MA	-	-	-	-/I	-/I	-/I	-/I	-/I	-/I	-/I	-/I	-/I	-/I	-/I	-/C
VA-F093	F	YA	-	-	-	-/I	-/I	-/I	-/I	-/I	-/I	-/I	-/I	-/I	-/I	-/I	-/I
VA-F094	F	MA	-	-	-	-/I	-/I	-/I	-/I	-/I	-/C	-/I	-/I	-/I	-/I	-/I	-/I
VA-F095	F?	A	-	-	-	-/I	-/I	-/I	-/I	-/I	-/I	-/I	-/I	-/I	-/I	-/I	-/I
VA-F096A	F?	A	-	-	-	-/I	-/C	-/I	-/C	-/C	-/I	-/I	-/I	-/I	-/I	-/I	-/I
VA-F096B	F?	A	-	Y	Y	-/I	-/I	-/I	-/I	-/I	+/C	-/I	-/I	-/I	-/I	-/I	-/I
VA-F098	F?	A	-	-	-	-/I	-/I	-/I	-/I	-/I	-/I	-/I	-/I	-/I	-/I	-/I	-/I
VA-F100	M?	A	-	-	-	-/I	-/I	-/I	-/I	-/I	-/I	-/I	-/I	-/I	-/I	-/I	-/I
VA-F117	F?	YA	-	-	-	-/I	-/I	-/I	-/C	-/C	-/I	-/I	-/I	-/C	-/I	-/C	-/I
VA-F126	M?	YA	-	-	Y	-/C	-/I	-/I	+/C	-/I	-/C	+/C	-/I	-/C	-/C	-/C	-/C
VA-F127	A	YA	-	-	-	-/I	-/C	-/C	-/C	-/I	-/I	-/I	-/C	-/I	-/C	-/I	-/I
VA-F130	F?	ADO	-	-	-	-/I	-/C	-/I	-/C	-/I	-/I	-/C	-/C	-/I	-/C	-/I	-/C
VA-F131	M	YA	Y	-	-	-/I	-/I	-/C	-/C	-/I	-/C	-/I	-/C	-/C	-/C	-/C	-/C
VA-F132	F	YA	-	-	-	-/I	-/I	-/I	-/I	-/C	-/I	-/C	-/I	-/I	-/I	-/I	-/I

Skeleton Number	Sex	Age	Fracture		OA_x Present	Shoulder		Elbow		Wrist		Hip		Knee		Ankle	
			UL	LL		R	L	R	L	R	L	R	L	R	L	R	L
VA-F137A	F?	YA	-	-	-	-/I	-/I	-/C	-/C	-/I	-/C	-/C	-/C	-/C	-/I	-/I	-/I
VA-F137B	A	A	-	-	-	-/I	-/I	-/I	-/I	-/I	-/I	-/I	-/I	-/I	-/I	-/I	-/I
VA-F200	F	MA	-	-	Y	-/I	-/C	-/C	-/I	-/C	+/C	-/C	-/I	-/I	-/C	-/C	-/I
VA-F204	F	YA	Y	-	-	-/C	-/I	-/I	-/I	-/I	-/I	-/I	-/I	-/I	-/I	-/I	-/I
VA-F205	F	MA	-	-	-	-/I	-/I	-/C	-/I	-/I	-/I	-/C	-/C	-/I	-/C	-/C	-/I
VA-F206	F	MA	-	-	-	-/I	-/I	-/I	-/I	-/I	-/I	-/I	-/I	-/I	-/I	-/I	-/I
VA-F207	M?	YA	-	-	-	-/C	-/I	-/I	-/I	-/I	-/I	-/C	-/C	-/C	-/C	-/I	-/C
VA-F208	U	ADO	-	-	-	-/I	-/I	-/I	-/I	-/I	-/I	-/I	-/I	-/I	-/I	-/I	-/I
VA-F211	F	YA	-	-	-	-/I	-/I	-/I	-/I	-/I	-/I	-/I	-/I	-/I	-/I	-/I	-/I
VA-F212	U	A	-	-	-	-/I	-/I	-/I	-/I	-/I	-/I	-/I	-/I	-/I	-/I	-/I	-/I
VA-F213	M	MA	-	-	-	-/I	-/I	-/I	-/I	-/I	-/I	-/I	-/C	-/I	-/C	-/I	-/C
VA-F214	M	MA	-	-	Y	-/C	-/I	-/C	-/C	-/C	-/C	+/C	+/C	-/C	-/C	-/C	-/C
VA-F215	F	YA	-	-	-	-/C	-/I	-/I	-/I	-/I	-/I	-/C	-/C	-/C	-/I	-/I	-/I
VA-F216	M	MA	-	Y	Y	-/I	-/I	-/I	-/C	-/C	-/C	-/C	-/C	+/C	-/C	+/C	-/C
VA-F220	M	MA	-	Y	Y	-/I	-/I	-/I	-/C	-/I	-/C	-/C	-/C	+/C	+/C	-/C	-/C
VA-F229	M	A	-	-	-	-/I	-/I	-/I	-/I	-/I	-/I	-/C	-/I	-/I	-/I	-/I	-/I
VA-F231	M?	YA	-	Y	-	-/I	-/I	-/C	-/I	-/I	-/I	-/C	-/I	-/I	-/I	-/C	-/I
VA-F234	M	YA	-	-	-	-/I	-/I	-/C	-/C	-/C	-/C	-/C	-/I	-/C	-/C	-/C	-/C
VA-F235	M	OA	-	-	Y	-/I	-/I	-/C	-/I	-/I	-/I	-/C	-/I	+/C	-/C	-/I	-/I
VA-F245	F	ADO	-	-	-	-/I	-/I	-/I	-/C	-/I	-/I	-/I	-/I	-/I	-/I	-/I	-/I
VA-F246	F?	YA	-	-	-	-/C	-/I	-/I	-/I	-/I	-/I	-/I	-/I	-/I	-/I	-/I	-/I
VA-F247	M	MA	-	-	-	-/I	-/C	-/I	-/I	-/C	-/C	-/C	-/I	-/C	-/C	-/I	-/I
VA-F248	F?	YA	-	-	-	-/I	-/I	-/C	-/I	-/C	-/I	-/C	-/C	-/I	-/I	-/I	-/I
VA-F249	F?	YA	Y	-	-	-/I	-/I	-/C	-/I	-/I	-/I	-/I	-/C	-/I	-/C	-/I	-/I
VA-F250	M?	YA	-	-	-	-/C	-/I	-/C	-/C	-/I	-/I	-/C	-/C	-/C	-/C	-/C	-/I
VA-F252	F?	ADO	-	-	-	-/I	-/I	-/C	-/I	-/C	-/I	-/C	-/I	-/C	-/I	-/I	-/I

Skeleton Number	Sex	Age	Fracture		OA_x Present	Shoulder		Elbow		Wrist		Hip		Knee		Ankle	
			UL	LL		R	L	R	L	R	L	R	L	R	L	R	L
VA-F253	M?	A	-	-	-	-/I	-/I	-/I	-/I	-/I	-/I	-/I	-/I	-/I	-/I	-/I	-/I
VA-F254	M	MA	-	-	-	-/I	-/I	-/C	-/C	-/I	-/C	-/C	-/C	-/C	-/C	-/I	-/I
VA-F280	U	YA	-	-	-	-/I	-/I	-/I	-/C	-/I	-/I	-/I	-/I	-/I	-/I	-/I	-/I
VA-F284	F	YA	-	-	-	-/I	-/I	-/I	-/I	-/I	-/I	-/I	-/I	-/I	-/C	-/I	-/I
VA-F287	M	MA	-	-	-	-/I	-/I	-/I	-/I	-/I	-/I	-/I	-/I	-/I	-/I	-/I	-/I
VA-F288	M?	YA	Y	-	-	-/I	-/I	-/C	-/C	-/I	-/I	-/C	-/C	-/C	-/C	-/I	-/C
VA-F289	A	ADO	-	-	-	-/C	-/I	-/I	-/I	-/C	-/I	-/I	-/I	-/C	-/C	-/I	-/I
VA-F290	M	MA	-	-	Y	-/I	-/C	-/C	-/C	-/C	-/C	+/C	+/C	-/C	-/C	-/C	-/I
VA-F291	M	YA	-	-	-	-/I	-/I	-/C	-/C	-/I	-/I	-/I	-/C	-/C	-/I	-/I	-/I
VA-F293	U	A	-	-	-	-/I	-/I	-/I	-/I	-/I	-/I	-/I	-/I	-/I	-/I	-/I	-/I
VA-F294	F?	OA	-	-	Y	-/I	-/I	-/I	-/C	-/I	+/C	+/C	-/I	-/C	-/I	-/C	-/C
VA-F296	F	YA	-	-	-	-/C	-/C	-/C	-/C	-/C	-/C	-/C	-/C	-/C	-/C	-/C	-/C
VA-F298	U	A	-	-	-	-/I	-/I	-/I	-/I	-/I	-/I	-/I	-/I	-/I	-/I	-/I	-/I
VA-F306	F?	MA	-	-	Y	-/C	+/C	-/C	-/C	-/I	-/I	-/C	-/I	-/C	-/C	-/I	-/I
VA-F312	F?	YA	-	-	-	-/I	-/I	-/C	-/C	-/I	-/I	-/I	-/I	-/C	-/C	-/C	-/C

F=Female; F?=Probable female; U=Unknown sex; M?=Probable male; M=Male; ADO=Adolescent; YA=Young adult; MA=Middle adult; OA=Old adult; A=Adult (unknown age); OA_x=Osteoarthritis; UL=Upper Limb; LL=Lower Limb; R=Right; L=Left; Y=Yes, a fracture or osteoarthritis was observed; C=joint was more than 50% present; I=joint was less than 50% present; -=no osteoarthritis; +=osteoarthritis present. Shaded cells represent the joints that were complete with osteoarthritis.

Appendix G: Osteoarthritis True Prevalence Rates

Table G.1 reports the true prevalence rates of osteoarthritis by joint type, age, and sex; the prevalence of osteoarthritis for all individuals at Ancaster and Vagnari is reported, as is the prevalence of osteoarthritis in individuals with fractures. If osteoarthritis was present in both proximal and distal joints of the same fractured element (e.g., shoulder and elbow), both were counted separately. If both bones in a pair (e.g., radii and ulnae) were fractured, the joint with osteoarthritis was only counted once.

Abbreviations used in this table includes:

F - Female
U – Unknown sex
M - Male
ADO - Adolescent
YA – Young adult
MA – Middle adult
OA – Old adult
Sub – Subtotal
A – Adult (unknown age)
OA_x – Osteoarthritis
n OA_x – Number of joints with osteoarthritis
N joints– Total number of joints observed
TPR – True prevalence rate

Table G.1 – True prevalence rates of osteoarthritis at Ancaster and Vagnari for all joints, as well as the joints associated with a fractured bone. True prevalence rates reported by joint type, age, and sex.

Joint	Age	Ancaster						Vagnari					
		Total joints with OA_x / N joints TPR (%)			OA_x in joints associated with a fracture / N joints TPR (%)			Total joints with OA_x / N joints TPR (%)			OA_x in joints associated with a fracture / N joints TPR (%)		
		F	M	U	F	M	U	F	M	U	F	M	U
Shoulder	ADO	0/0	0/8	0/0	0/0	0/8	0/0	0/1	0/0	0/2	0/1	0/0	0/2
		-	0.0	-	-	0.0	-	0.0	-	0.0	0.0	-	0.0
	YA	3/48	0/66	0/1	0/48	0/66	0/1	1/10	0/1	0/1	0/10	0/1	0/1
		6.3	0.0	0.0	0.0	0.0	0.0	10.0	0.0	0.0	0.0	0.0	0.0
	MA	7/41	15/70	0/0	0/41	1/70	0/0	1/1	0/4	0/0	0/1	0/4	0/0
		17.1	21.4	-	0.0	1.4	-	100.0	0.0	-	0.0	0.0	-
	OA	3/6	0/6	2/2	0/6	0/6	1/2	0/1	0/1	0/0	0/1	0/1	0/0
		50.0	0.0	100	0.0	0.0	50.0	0.0	0.0	-	0.0	0.0	-
	A	0/9	1/6	0/0	0/9	0/6	0/0	0/1	0/0	0/2	0/1	0/0	0/2
		0.0	16.7	-	0.0	0.0	-	0.0	-	0.0	0.0	-	0.0
	Sub	13/104	16/156	2/3	0/104	1/156	1/3	2/14	0/6	0/5	0/14	0/6	0/5
		12.5	10.3	66.7	0.0	0.6	33.3	14.3	0.0	0.0	0.0	0.0	0.0
Elbow	ADO	0/0	0/8	0/0	0/0	0/8	0/0	0/3	0/0	0/4	0/3	0/0	0/4
		-	0.0	-	-	0.0	-	0.0	-	0.0	0.0	-	0.0
	YA	0/53	0/66	0/1	0/53	0/66	0/1	0/11	1/5	0/2	0/11	0/5	0/2
		0.0	0.0	0.0	0.0	0.0	0.0	0.0	20.0	0.0	0.0	0.0	0.0
	MA	1/41	8/71	0/0	0/41	1/71	0/0	0/6	0/11	0/0	0/6	0/11	0/0
		2.4	11.3	-	0.0	1.4	-	0.0	0.0	-	0.0	0.0	-
	OA	2/9	0/6	0/2	1/9	0/6	0/2	0/0	0/1	0/0	0/0	0/1	0/0
		22.2	0.0	0.0	11.1	0.0	0.0	-	0.0	-	-	0.0	-
	A	2/16	0/6	0/1	0/16	0/6	0/1	0/0	0/3	0/5	0/0	0/3	0/5
		12.5	0.0	0.0	0.0	0.0	0.0	-	0.0	0.0	-	0.0	0.0
	Sub	5/119	8/157	0/4	1/119	1/157	0/4	0/20	1/20	0/11	0/20	0/20	0/11
		4.2	5.1	0.0	0.8	0.6	0.0	0.0	5.0	0.0	0.0	0.0	0.0
Wrist	ADO	0/0	0/8	0/0	0/0	0/8	0/0	0/1	0/0	0/3	0/1	0/0	0/3
		-	0.0	-	-	0.0	-	0.0	-	0.0	0.0	-	0.0

Joint	Age	Ancaster: Total joints with OA_x / N joints TPR (%)			Ancaster: OA_x in joints associated with a fracture / N joints TPR (%)			Vagnari: Total joints with OA_x / N joints TPR (%)			Vagnari: OA_x in joints associated with a fracture / N joints TPR (%)		
		F	M	U	F	M	U	F	M	U	F	M	U
Wrist	YA	1/54	4/60	0/0	0/54	1/60	0/0	0/10	0/6	0/3	0/10	0/6	0/3
cont.		1.9	6.7	-	0.0	1.7	-	0.0	0.0	0.0	0.0	0.0	0.0
	MA	4/37	8/72	0/0	1/37	1/72	0/0	1/1	0/7	0/0	0/1	0/7	0/0
		10.8	11.1	-	2.7	1.4	-	100.0	0.0	-	0.0	0.0	-
	OA	2/10	3/5	0/1	2/10	0/5	0/1	1/1	0/1	0/0	0/1	0/1	0/0
		20.0	60.0	0.0	20.0	0.0	0.0	100.0	0.0	-	0.0	0.0	-
	A	0/7	1/4	0/1	0/7	0/4	0/1	1/1	0/0	0/4	0/1	0/0	0/4
		0.0	25.0	0.0	0.0	0.0	0.0	100.0	-	0.0	0.0	-	0.0
	Sub	7/108	16/149	0/2	3/108	2/149	0/2	3/14	0/14	0/10	0/14	0/14	0/10
		6.5	10.7	0.0	2.8	1.3	0.0	21.4	0.0	0.0	0.0	0.0	0.0
Hip	ADO	0/0	0/7	0/0	0/0	0/7	0/0	0/3	0/0	0/4	0/3	0/0	0/4
		-	0.0	-	-	0.0	-	0.0	-	0.0	0.0	-	0.0
	YA	2/57	4/60	0/0	0/57	0/60	0/0	0/13	1/6	0/2	0/13	0/6	0/2
		3.5	6.7	-	0.0	0.0	-	0.0	16.7	0.0	0.0	0.0	0.0
	MA	2/42	4/73	0/0	0/42	0/73	0/0	0/2	4/12	0/0	0/2	0/12	0/0
		4.8	5.5	-	0.0	0.0	-	0.0	33.3	-	0.0	0.0	-
	OA	1/10	0/5	0/2	0/10	0/5	0/2	2/2	0/2	0/0	0/2	0/2	0/0
		10.0	0.0	0.0	0.0	0.0	0.0	100.0	0.0	-	0.0	0.0	-
	A	1/14	1/7	0/1	0/14	0/7	0/1	0/0	0/2	0/6	0/0	0/2	0/6
		7.1	14.3	0.0	0.0	0.0	0.0	-	0.0	0.0	-	0.0	0.0
	Sub	6/123	9/152	0/3	0/123	0/152	0/3	2/20	5/22	0/12	0/20	0/22	0/12
		4.9	5.9	0.0	0.0	0.0	0.0	10.0	22.7	0.0	0.0	0.0	0.0
Knee	ADO	0/0	0/6	0/0	0/0	0/6	0/0	0/1	0/0	0/4	0/1	0/0	0/4
		-	0.0	-	-	0.0	-	0.0	-	0.0	0.0	-	0.0
	YA	3/64	0/66	0/2	1/64	0/66	0/2	0/15	1/6	0/2	0/15	0/6	0/2
		4.7	0.0	0.0	1.6	0.0	0.0	0.0	16.7	0.0	0.0	0.0	0.0
	MA	8/46	10/72	0/0	1/46	3/72	0/0	0/7	3/11	0/0	0/7	2/11	0/0
		17.4	13.9	0.0	2.2	4.2	0.0	0.0	27.3	-	0.0	1.8	-
	OA	0/9	0/3	2/2	0/9	0/3	0/2	0/0	1/1	0/0	0/0	0/1	0/0
		0.0	0.0	100	0.0	0.0	0.0	-	100.0	-	-	0.0	-

Joint	Age	Ancaster: Total joints with OA_x / N joints TPR (%)			Ancaster: OA_x in joints associated with a fracture / N joints TPR (%)			Vagnari: Total joints with OA_x / N joints TPR (%)			Vagnari: OA_x in joints associated with a fracture / N joints TPR (%)		
		F	M	U	F	M	U	F	M	U	F	M	U
Knee cont.	A	4/12	2/11	2/11	0/12	0/11	0/11	0/0	0/2	0/5	0/0	0/2	0/5
		33.3	18.2	18.2	0.0	0.0	0.0	-	0.0	0.0	-	0.0	0.0
	Sub	15/131	12/158	4/15	2/131	3/158	0/15	0/23	5/20	0/11	0/23	2/20	0/11
		11.5	7.6	26.7	1.5	1.9	0.0	0.0	25.0	0.0	0.0	10.0	0.0
Ankle	ADO	0/0	0/6	0/0	0/0	0/6	0/0	0/1	0/0	0/2	0/1	0/0	0/2
		-	0.0	-	-	0.0	-	0.0	-	0.0	0.0	-	0.0
	YA	0/61	0/67	0/2	0/61	0/67	0/2	0/7	0/4	0/2	0/7	0/4	0/2
		0.0	0.0	0.0	0.0	0.0	0.0	0.0	0.0	0.0	0.0	0.0	0.0
	MA	0/45	4/75	0/1	0/45	2/75	0/1	0/2	1/10	0/0	0/2	1/10	0/0
		0.0	5.3	0.0	0.0	2.7	0.0	0.0	10.0	-	0.0	10.0	-
	OA	0/10	0/4	0/2	0/10	0/4	0/2	0/2	0/0	0/0	0/2	0/0	0/0
		0.0	0.0	0.0	0.0	0.0	0.0	0.0	-	-	0.0	-	-
	A	0/17	0/10	0/12	0/17	0/10	0/12	0/0	0/1	0/5	0/0	0/1	0/5
		0.0	0.0	0.0	0.0	0.0	0.0	-	0.0	0.0	-	0.0	0.0
	Sub	0/133	4/162	0/17	0/133	2/162	0/17	0/12	1/15	0/9	0/12	1/15	0/9
		0.0	2.5	0.0	0.0	1.5	0.0	0.0	6.7	0.0	0.0	6.7	0.0
Total	ADO	0/0	0/43	0/0	0/0	0/43	0/0	0/10	0/0	0/19	0/10	0/0	0/19
		-	0.0	-	-	0.0	-	0.0	-	0.0	0.0	-	0.0
	YA	9/337	8/385	0/6	1/337	1/385	0/6	1/66	3/28	0/12	0/66	0/28	0/12
		2.7	2.1	0.0	0.3	0.3	0.0	1.5	10.7	0.0	0.0	0.0	0.0
	MA	22/252	49/433	0/1	3/252	8/433	0/1	2/19	8/55	0/0	0/19	3/55	0/0
		8.7	11.3	0.0	1.2	1.8	0.0	10.5	14.5	-	0.0	5.5	-
	OA	8/52	3/29	4/11	2/52	0/29	1/11	3/5	1/6	0/0	0/5	0/6	0/0
		14.8	10.3	36.4	3.8	0.0	9.1	60.0	16.7	-	0.0	0.0	-
	A	7/75	5/44	2/26	0/75	0/44	0/26	1/2	0/8	0/27	0/2	0/8	0/27
		9.3	11.4	7.7	0.0	0.0	0.0	50.0	0.0	0/0	0.0	0.0	0/0
	Sub	46/718	65/934	6/44	6/718	9/934	1/44	7/102	12/97	0/58	0/102	3/97	0/58
		6.4	7.0	13.6	0.8	1.0	2.3	6.9	12.4	0.0	0.0	3.1	0.0

F=Female; M=Male; U=Unknown sex; ADO=Adolescent; YA=Young adult; MA=Middle adult; OA=Old adult; Sub=Subtotal; A=Adult (unknown age); OA_x=Osteoarthritis; n OA_x=Number of joints with osteoarthritis; N joints=Total number of joints observed; TPR=True prevalence rate

Appendix H: Elements Radiographed For Cross-Sectional Analyses

Table H.1 presents the number of elements from individuals with fractures relative to the total number of elements that were radiographed for cross-sectional analyses. The number of element pairs radiographed for cross-sectional analyses of area asymmetries are reported for Ancaster and Vagnari in Table H.2. These counts are divided by site, element type, individual age, and sex. Separate counts are provided for second metacarpal midshaft areas and region of interests as not all bones were able to be measured using both techniques.

Abbreviations used in these tables include:

F - Female
U – Unknown sex
M – Male
T – Total
ADO - Adolescent
YA – Young adult
MA – Middle adult
OA – Old adult
Adult – Unknown age
ROI – Region of interest
MC2 – Second metacarpal
MC2 50% - Second metacarpal midshaft
MT2 – Second metatarsal

Table H.1 – Number of radiographed elements from individuals with fractures compared to the total number of elements radiographed for cross-sectional measurement.

Element	Age	Ancaster				Vagnari			
		F	M	U	T	F	M	U	T
Humerus	ADO	0/0	0/8	0/0	0/8	0/4	0/0	0/0	0/4
	YA	8/38	12/36	0/0	20/74	4/14	10/16	0/0	14/30
	MA	12/30	26/52	0/0	38/82	0/6	6/18	0/0	6/24
	OA	4/10	2/6	0/0	6/16	0/0	0/0	0/0	0/0
	Adult	4/6	0/0	0/0	4/6	0/0	0/2	2/2	2/4
	Total	28/84	40/102	0/0	68/186	4/24	16/36	2/2	22/62

Element	Age	Ancaster				Vagnari			
		F	M	U	T	F	M	U	T
Radius	ADO	0/0	0/8	0/0	0/8	0/4	0/0	0/0	0/4
	YA	8/34	12/35	0/0	20/69	3/12	7/12	0/0	10/24
	MA	11/27	19/46	0/0	30/73	0/3	5/13	0/0	5/16
	OA	4/10	2/5	0/0	6/15	0/1	0/0	0/0	0/1
	Adult	4/4	0/0	0/0	4/4	2/2	0/2	2/2	4/6
	Total	27/75	33/94	0/0	60/169	5/22	12/27	2/2	19/51
Ulna ROI	ADO	0/0	0/8	0/0	0/8	0/3	0/0	0/0	0/3
	YA	8/33	8/32	0/0	16/65	4/14	6/10	0/0	10/24
	MA	7/24	23/46	0/0	30/70	0/2	4/12	0/0	4/14
	OA	4/10	2/4	0/0	6/14	0/2	0/0	0/0	0/2
	Adult	2/2	0/0	0/0	2/2	0/0	0/1	0/0	0/1
	Total	21/69	33/90	0/0	54/159	4/21	10/23	0/0	14/44
MC2 50%	ADO	0/0	0/2	0/0	0/2	0/2	0/0	0/0	0/2
	YA	4/20	2/4	0/0	6/24	0/2	1/1	0/0	1/3
	MA	4/21	0/7	0/0	4/28	0/3	0/2	0/0	0/5
	OA	2/6	0/0	0/0	2/6	0/0	0/0	0/0	0/0
	Total	10/47	2/13	0/0	12/60	0/7	1/3	0/0	1/10
MC2 ROI	ADO	0/0	0/2	0/0	0/2	0/4	0/0	0/0	0/4
	YA	4/20	2/4	0/0	6/24	1/3	6/10	0/0	7/13
	MA	4/22	0/8	0/0	4/30	0/4	2/5	0/0	2/9
	OA	2/8	0/0	0/0	2/8	0/1	0/0	0/0	0/1
	Adult	0/0	0/0	0/0	0/0	1/1	0/0	0/0	1/1
	Total	10/50	2/14	0/0	12/64	2/13	8/15	0/0	10/28
Tibia	ADO	0/0	0/6	0/0	0/6	0/4	0/0	0/0	0/4
	YA	3/34	4/36	0/0	7/70	4/14	10/16	0/0	14/30
	MA	2/36	4/50	0/0	6/86	0/4	6/18	0/0	6/22
	OA	0/9	1/4	2/2	1/15	0/2	0/2	0/0	0/4
	Adult	2/6	0/0	0/0	2/6	2/2	0/1	0/0	2/3
	Total	7/85	9/96	2/2	16/183	6/26	16/37	0/0	22/63
MT2 ROI	ADO	0/0	0/2	0/0	0/2	0/3	0/0	0/0	0/3
	YA	4/26	12/24	0/0	16/50	1/3	5/9	0/0	6/12
	MA	2/20	14/32	0/0	16/52	0/0	2/7	0/0	2/7
	OA	2/8	0/0	2/2	4/10	0/1	0/0	0/0	0/1
	Adult	0/0	0/0	0/0	0/0	1/1	0/0	0/0	1/1
	Total	8/54	26/58	2/2	36/114	2/8	7/16	0/0	9/24

F=Female; M=Male; U=Unknown sex; T=Total; ADO=Adolescent; YA=Young adult; MA=Middle adult; OA=Old adult; Adult=Unknown age; ROI=Region of interest; MC2 50%=Measurement at the second metacarpal midshaft; MT2=Second metatarsal.

Table H.2 – Number of radiographed element pairs from individuals with fractures compared to the total number of element pairs radiographed for cross-sectional measurement.

Element	Age	Ancaster				Vagnari			
		F	M	U	T	F	M	U	T
Humerus	ADO	0/0	0/4	0/0	0/4	0/2	0/0	0/0	0/2
	YA	4/19	6/18	0/0	10/37	2/7	5/8	0/0	7/15
	MA	6/15	13/26	0/0	19/41	0/3	3/9	0/0	3/12
	OA	2/5	1/3	0/0	3/8	0/0	0/0	0/0	1/1
	Adult	2/3	0/0	0/0	2/3	0/0	1/1	1/1	1/1
	Total	14/42	20/51	0/0	34/93	2/12	9/18	1/1	12/31
Radii	ADO	0/0	0/4	0/0	0/4	0/2	0/0	0/0	0/2
	YA	4/16	6/17	0/0	10/33	1/5	2/4	0/0	3/9
	MA	5/11	8/21	0/0	13/32	0/1	2/4	0/0	2/5
	OA	2/5	1/2	0/0	3/7	0/0	0/0	0/0	1/2
	Adult	2/2	0/0	0/0	2/2	1/1	1/1	1/1	2/2
	Total	13/34	15/44	0/0	28/78	2/9	5/9	1/1	8/19
Ulna ROI	ADO	0/0	0/4	0/0	0/4	0/1	0/0	0/0	0/1
	YA	4/16	3/14	0/0	7/30	2/7	2/4	0/0	4/11
	MA	3/11	11/22	0/0	14/33	0/1	2/4	0/0	2/5
	OA	2/5	1/2	0/0	3/7	0/1	0/0	0/0	0/1
	Adult	1/1	0/0	0/0	1/1	0/0	0/0	0/0	0/0
	Total	10/33	15/42	0/0	25/75	2/10	4/8	0/0	6/18
MC2 50% & ROI	ADO	0/0	0/1	0/0	0/1	0/2	0/0	0/0	0/2
	YA	2/10	1/2	0/0	3/12	0/1	1/2	0/0	1/3
	MA	2/10	0/3	0/0	2/13	0/1	0/1	0/0	0/2
	OA	1/2	0/0	0/0	1/2	0/0	0/0	0/0	0/0
	Adult	0/0	0/0	0/0	0/0	0/0	0/0	0/0	0/0
	Total	5/22	1/6	0/0	6/28	0/4	1/3	0/0	1/7
Tibia	ADO	0/0	0/3	0/0	0/3	0/2	0/0	0/0	0/2
	YA	3/16	7/18	0/0	10/34	2/7	5/8	0/0	7/15
	MA	4/18	9/25	0/0	13/43	0/1	3/9	0/0	3/10
	OA	2/4	1/2	1/1	4/7	0/1	0/1	0/0	0/2
	Adult	3/3	0/0	0/0	3/3	1/1	0/0	0/0	1/1
	Total	12/41	17/48	1/1	30/90	3/12	8/18	0/0	11/30
MT2 ROI	ADO	0/0	0/1	0/0	0/1	0/1	0/0	0/0	0/1
	YA	4/15	12/17	0/0	16/32	0/0	1/3	0/0	1/3
	MA	2/11	14/23	0/0	16/34	0/0	0/2	0/0	0/2
	OA	2/5	0/0	2/2	4/7	0/0	0/0	0/0	0/0
	Adult	0/0	0/0	0/0	0/0	0/0	0/0	0/0	0/0
	Total	8/31	26/41	2/2	36/74	0/1	1/5	0/0	1/6

F=Female; M=Male; U=Unknown sex; T=Total; ADO=Adolescent; YA=Young adult; MA=Middle adult; OA=Old adult; Adult=Unknown age; ROI=Region of interest; MC2 50%=Measurement at the second metacarpal midshaft; MT2=Second metatarsal.

Appendix I: Measured Cross-Sectional Values

This appendix presents the measured subperiosteal and medullary diameter measurements for each element type by site, individual, and bone side. The calculated bone total, medullary, and cortical areas are also presented, as are the calculated degrees of asymmetry for each area type. This appendix is divided first by site, followed by bone type. Graphs of individual areas and asymmetries are provided following the raw data tables; these graphs include the ranges of normal for each group (determined using 1.5 times the interquartile range), allowing outliers to be identified.

Abbreviations used in the following tables are as follows:

F – Female
F? – Possible Female
M – Male
M? – Possible Male
U – Undetermined Sex
ADO – Adolescent (15-19 years old)
YA – Young Adult (20-34 years old)
MA – Middle Adult (35-49 years old)
OA – Old Adult (50+ years old)
L – Left
R – Right
AP – Antero-posterior total width
ap – Antero-posterior medullary width
ML – Medio-lateral total width
ml – Medio-lateral medullary width
T_A – Total area
M_A – Medullary area
C_A – Cortical area
T_A%DA – Total area directional asymmetry
M_A%DA – Medullary area directional asymmetry
C_A%DA – Cortical area directional asymmetry
ROI%DA – Region of interest area directional asymmetry

I.1 – Ancaster Cross-Sectional Properties

I.1.1 - Humerus

Table I.1 – Radiographically measured bone diameters, and calculated bone areas and asymmetries for humeri at Ancaster.

Skeleton Number	Sex	Age	Side	AP	ap	ML	ml	T_A	M_A	C_A	T_A %DA	M_A %DA	C_A %DA
AN-001	F?	YA	L	17.7	5.3	18.3	6.7	254.4	27.9	226.5	-3.3	3.0	-4.1
			R	17.6	6.1	17.8	6.0	246.0	28.7	217.3			
AN-002*	F	MA	L	17.2	9.1	18.3	10.5	247.2	75.0	172.2	-0.7	10.7	-6.1
			R	16.9	9.5	18.5	11.2	245.6	83.6	162.0			
AN-003A	F	YA	L	16.5	8.9	17.1	11	221.6	76.9	144.7	6.5	19.3	-1.1
			R	17.3	10.7	17.4	11.1	236.4	93.3	143.1			
AN-004	M	OA	L	17.2	9.6	19.5	10.2	263.4	76.9	186.5	1.8	-4.2	4.1
			R	17.6	10.1	19.4	9.3	268.2	73.8	194.4			
AN-005	M	MA	L	21.2	10.6	20.9	10.6	348.0	88.2	259.7	-3.8	-13.1	-0.9
			R	20.7	10.6	20.6	9.3	334.9	77.4	257.5			
AN-006	M	MA	L	19.7	10.8	21.5	12.1	332.7	102.6	230.0	10.1	8.7	10.7
			R	21.3	11.5	22.0	12.4	368.0	112.0	256.0			
AN-010	F	MA	L	16.2	10.2	17.7	9.2	225.2	73.7	151.5	-1.2	-2.9	-0.5
			R	16.0	9.7	17.7	9.4	222.4	71.6	150.8			
AN-011	M	MA	L	19.3	8.5	20.6	10.9	312.3	72.8	239.5	8.4	-26.1	16.8
			R	20.2	8.1	21.4	8.8	339.5	56.0	283.5			
AN-012B	M	MA	L	20.7	10.2	22.5	11.6	365.8	92.9	272.9	-5.0	7.6	-9.7
			R	20.8	11.2	21.3	11.4	348.0	100.3	247.7			
AN-013	M	YA	L	18.5	8.8	23.2	11.4	337.1	78.8	258.3	-7.5	-10.5	-6.6
			R	18.1	8.6	22.0	10.5	312.7	70.9	241.8			
AN-023	M	MA	L	16.5	7.7	19.5	9.0	252.7	54.4	198.3	7.6	13.1	6.0
			R	17.1	7.6	20.3	10.4	272.6	62.1	210.6			
AN-024	M	MA	L	18.1	7.4	20.3	9.7	288.6	56.4	232.2	-10.5	46.2	-31.2
			R	17.5	9.5	18.9	12.1	259.8	90.3	169.5			
AN-026	M	YA	L	17.2	9.0	21.2	11.3	286.4	79.9	206.5	-5.6	13.1	-13.8
			R	16.5	9.2	20.9	12.6	270.8	91.0	179.8			

Skeleton Number	Sex	Age	Side	AP	ap	ML	ml	T_A	M_A	C_A	T_A %DA	M_A %DA	C_A %DA
AN-034	M	MA	L	18.6	9.6	23.5	12.0	343.3	90.5	252.8	3.1	3.1	3.1
			R	19.6	9.9	23.0	12.0	354.1	93.3	260.8			
AN-039	M?	YA	L	20.4	12.4	21.7	12.4	347.7	120.8	226.9	6.5	16.0	1.1
			R	21.0	12.8	22.5	14.1	371.1	141.7	229.4			
AN-041	F	YA	L	16.1	7.0	19.1	8.8	241.5	48.4	193.1	-5.9	17.6	-12.8
			R	16.1	7.5	18.0	9.8	227.6	57.7	169.9			
AN-045	F?	Adult	L	16.4	9.5	19.4	11.0	249.9	82.1	167.8	3.7	-12.6	10.8
			R	17.2	9.4	19.2	9.8	259.4	72.4	187.0			
AN-046	M?	YA	L	19.3	9.5	20.2	10.0	306.2	74.6	231.6	18.4	-5.1	24.8
			R	21.9	9.5	21.4	9.5	368.1	70.9	297.2			
AN-047	M	MA	L	20.7	14.3	21.5	13.5	349.5	151.6	197.9	9.6	-2.1	17.7
			R	21.4	13.8	22.9	13.7	384.9	148.5	236.4			
AN-048B	M?	ADO	L	19.9	11.4	21.0	12.5	328.2	111.9	216.3	7.7	20.0	0.7
			R	20.8	12.9	21.7	13.5	354.5	136.8	217.7			
AN-050	M	OA	L	19.2	10.1	21.4	12.5	322.7	99.2	223.5	7.8	4.5	9.2
			R	20.1	11.0	22.1	12.0	348.9	103.7	245.2			
AN-052	F	MA	L	15.9	8.1	18.0	9.7	224.8	61.7	163.1	9.6	7.3	10.5
			R	16.5	8.9	19.1	9.5	247.5	66.4	181.1			
AN-053	F	MA	L	15.5	9.2	16.7	9.9	203.3	71.5	131.8	-0.5	6.3	-4.4
			R	15.7	9.7	16.4	10.0	202.2	76.2	126.0			
AN-056	M	MA	L	18.3	9.9	21.3	10.8	306.1	84.0	222.2	-6.8	-44.3	4.6
			R	18.4	7.1	19.8	9.6	286.1	53.5	232.6			
AN-057	M	MA	L	17.4	11.3	19.1	11.5	261.0	102.1	159.0	12.8	26.2	3.0
			R	18.7	12.0	20.2	14.1	296.7	132.9	163.8			
AN-061	M	MA	L	19.4	10.6	19.4	9.4	295.6	78.3	217.3	15.8	-0.8	21.2
			R	21.0	9.5	21.0	10.4	346.4	77.6	268.8			
AN-062	F	YA	L	16.3	9.7	17.7	11.3	226.6	86.1	140.5	-4.0	-25.7	7.4
			R	16.5	9.3	16.8	9.1	217.7	66.5	151.2			
AN-064	M?	MA	L	18.7	10.5	20.4	11.9	299.6	98.1	201.5	4.4	-9.6	10.6
			R	18.9	9.7	21.1	11.7	313.2	89.1	224.1			

Skeleton Number	Sex	Age	Side	AP	ap	ML	ml	T_A	M_A	C_A	T_A %DA	M_A %DA	C_A %DA
AN-065	M	MA	L	16.6	7.5	18.5	7.9	241.2	46.5	194.7	6.9	-21.8	12.7
			R	17.5	6.9	18.8	6.9	258.4	37.4	221.0			
AN-066	F	YA	L	17.1	8.5	17.5	9.2	235.0	61.4	173.6	2.2	23.1	-6.5
			R	16.8	9.3	18.2	10.6	240.1	77.4	162.7			
AN-072	F	YA	L	16.6	9.0	18.3	12.7	238.6	89.8	148.8	2.4	-6.5	7.4
			R	17.0	10.2	18.3	10.5	244.3	84.1	160.2			
AN-082	M	ADO	L	15.6	7.1	18.1	7.8	221.8	43.5	178.3	-2.4	-16.8	0.8
			R	16.5	7.2	16.7	6.5	216.4	36.8	179.7			
AN-092	M	YA	L	17.4	6.5	20.7	8.1	282.9	41.4	241.5	9.1	0.0	10.6
			R	18.7	6.5	21.1	8.1	309.9	41.4	268.5			
AN-093	M	MA	L	20.0	10.7	22.0	11.7	345.6	98.3	247.3	11.8	8.9	12.9
			R	22.0	11.4	22.5	12.0	388.8	107.4	281.3			
AN-098	M	OA	L	18.7	12.9	21.7	14.4	318.7	145.9	172.8	15.7	29.9	1.7
			R	21.2	15.5	22.4	16.2	373.0	197.2	175.8			
AN-102	F	YA	L	17.1	6.5	20.8	8.5	279.4	43.4	236.0	12.3	39.8	6.2
			R	18.8	7.8	21.4	10.6	316.0	64.9	251.0			
AN-104	F?	MA	L	16.8	11.7	18.7	11.7	246.7	107.5	139.2	7.6	-15.3	22.3
			R	17.3	10.3	19.6	11.4	266.3	92.2	174.1			
AN-107	M?	ADO	L	16.6	7.5	20.2	9.4	263.4	55.4	208.0	7.7	18.8	4.5
			R	17.0	7.6	21.3	11.2	284.4	66.9	217.5			
AN-108	M?	ADO	L	20.1	8.5	20.2	10.0	318.9	66.8	252.1	-4.5	-12.7	-2.4
			R	19.7	8.6	19.7	8.7	304.8	58.8	246.0			
AN-109	F	MA	L	16.6	10.8	20.0	12.1	260.8	102.6	158.1	5.9	18.6	-3.3
			R	17.7	12.3	19.9	12.8	276.6	123.7	153.0			
AN-110	M?	YA	L	18.5	9.6	19.9	9.6	289.1	72.4	216.8	2.7	12.8	-0.9
			R	19.3	10.8	19.6	9.7	297.1	82.3	214.8			
AN-112	F	YA	L	15.0	6.0	16.6	7.9	195.6	37.2	158.3	7.6	15.5	5.6
			R	15.8	7.1	17.0	7.8	211.0	43.5	167.5			
AN-113	F	MA	L	18.5	12.1	20.5	15.2	297.9	144.5	153.4	-8.3	-5.4	-11.2
			R	17.8	13.3	19.6	13.1	274.0	136.8	137.2			

Skeleton Number	Sex	Age	Side	AP	ap	ML	ml	T_A	M_A	C_A	T_A %DA	M_A %DA	C_A %DA
AN-115	F	MA	L	14.5	5.7	16.7	7.4	190.2	33.1	157.1	9.6	26.5	5.6
			R	15.5	6.8	17.2	8.1	209.4	43.3	166.1			
AN-116	F?	MA	L	15.9	7.6	18.7	8.9	233.5	53.1	180.4	4.1	7.6	3.0
			R	17.5	8.2	17.7	8.9	243.3	57.3	186.0			
AN-117	M?	MA	L	18.0	7.5	20.9	9.0	295.5	53.0	242.5	-1.5	-15.8	1.3
			R	18.9	7.2	19.6	8.0	290.9	45.2	245.7			
AN-118	M?	YA	L	19.4	10.9	21.0	11.5	320.0	98.4	221.5	8.9	23.8	1.4
			R	20.9	12.7	21.3	12.5	349.6	125.1	224.6			
AN-120	M	YA	L	18.3	9.4	20.2	9.9	290.3	73.1	217.2	2.8	-4.5	5.1
			R	19.3	8.9	19.7	10.0	298.6	69.9	228.7			
AN-123	F	YA	L	15.5	6.3	16.0	6.5	194.8	32.2	162.6	11.7	17.8	10.5
			R	16.7	6.8	16.7	7.2	219.0	38.5	180.6			
AN-142	F	MA	L	15.8	6.3	16.1	6.5	199.8	32.2	167.6	3.1	21.7	-0.9
			R	16.0	6.7	16.4	7.6	206.1	40.0	166.1			
AN-143	M	YA	L	17.3	7.3	17.8	8.0	241.9	45.9	196.0	7.3	-12.2	11.3
			R	18.4	6.8	18.0	7.6	260.1	40.6	219.5			
AN-144	M	YA	L	18.9	9.3	19.6	10.8	290.9	78.9	212.1	8.2	-7.2	13.3
			R	19.8	8.9	20.3	10.5	315.7	73.4	242.3			
AN-152	F	MA	L	16.8	9.2	16.3	8.8	215.1	63.6	151.5	7.7	18.0	3.0
			R	17.6	9.8	16.8	9.9	232.2	76.2	156.0			
AN-154	F	Adult	L	16.3	10.5	18.3	11.5	234.3	94.8	139.4	5.9	8.2	4.4
			R	17.2	11.2	18.4	11.7	248.6	102.9	145.6			
AN-157	F	YA	L	17.0	6.9	17.1	7.0	228.3	37.9	190.4	-2.4	9.8	-5.1
			R	17.3	7.2	16.4	7.4	222.8	41.8	181.0			
AN-162	F?	YA	L	15.6	7.1	19.4	10.9	237.7	60.8	176.9	1.5	3.1	1.0
			R	15.6	7.0	19.7	11.4	241.4	62.7	178.7			
AN-165	M	YA	L	20.5	11.1	20.8	11.6	334.9	101.1	233.8	6.6	2.6	8.2
			R	20.7	11.3	22.0	11.7	357.7	103.8	253.8			
AN-167	M?	YA	L	19.6	9.4	19.8	11.4	304.8	84.2	220.6	-9.5	-10.1	-9.3
			R	18.0	9.4	19.6	10.3	277.1	76.0	201.0			

Skeleton Number	Sex	Age	Side	AP	ap	ML	ml	T_A	M_A	C_A	T_A %DA	M_A %DA	C_A %DA
AN-168	F	YA	L	17.3	8.5	18.4	9.4	250.0	62.8	187.3	3.4	-6.6	6.5
			R	17.9	8.5	18.4	8.8	258.7	58.7	199.9			
AN-170	M	MA	L	20.5	10.3	21.2	10.0	341.3	80.9	260.4	-3.4	-8.1	-1.9
			R	20.5	10.1	20.5	9.4	330.1	74.6	255.5			
AN-171	F	MA	L	16.4	10.4	18.1	10.7	233.1	87.4	145.7	1.6	5.5	-0.8
			R	16.3	10.4	18.5	11.3	236.8	92.3	144.5			
AN-172	F?	MA	L	15.0	9.6	18.1	11.7	213.2	88.2	125.0	11.2	18.5	5.7
			R	15.9	10.4	19.1	13.0	238.5	106.2	132.3			
AN-177	M	MA	L	18.3	9.2	20.6	9.9	296.1	71.5	224.5	1.8	1.1	2.0
			R	18.9	9.8	20.3	9.4	301.3	72.4	229.0			
AN-178	F?	YA	L	16.6	6.4	18.2	8.2	237.3	41.2	196.1	5.2	17.9	2.3
			R	17.2	7.3	18.5	8.6	249.9	49.3	200.6			
AN-184	M	MA	L	18.1	11.3	22.2	14.3	315.6	126.9	188.7	15.3	3.9	22.2
			R	20.9	12.0	22.4	14.0	367.7	131.9	235.7			
AN-185A	M	MA	L	17.9	6.9	19.4	7.5	272.7	40.6	232.1	1.1	-11.3	3.2
			R	18.2	6.0	19.3	7.7	275.9	36.3	239.6			
AN-191	F	OA	L	15.8	9.3	16.4	9.9	203.5	72.3	131.2	7.9	34.8	-11.0
			R	16.6	11.0	16.9	11.9	220.3	102.8	117.5			
AN-200	M	YA	L	18.3	8.6	19.7	9.8	283.1	66.2	217.0	2.6	4.0	2.2
			R	18.6	8.6	19.9	10.2	290.7	68.9	221.8			
AN-202	F	YA	L	15.6	6.2	17.4	7.3	213.2	35.5	177.6	6.0	4.5	6.3
			R	16.1	6.4	17.9	7.4	226.3	37.2	189.1			
AN-204	M	MA	L	18.7	10.9	21.8	13.4	320.2	114.7	205.5	7.5	0.0	11.4
			R	19.7	11.5	22.3	12.7	345.0	114.7	230.3			
AN-211	M?	YA	L	15.9	7.7	19.1	10.6	238.5	64.1	174.4	3.3	-2.0	5.2
			R	16.1	8.6	19.5	9.3	246.6	62.8	183.8			
AN-216	M?	YA	L	18.7	8.6	22.5	11.9	330.5	80.4	250.1	2.3	2.2	2.4
			R	19.4	9.1	22.2	11.5	338.3	82.2	256.1			
AN-217	F	MA	L	15.7	9.2	17.9	10.4	220.7	75.1	145.6	0.8	-5.0	3.7
			R	15.4	9.1	18.4	10.0	222.6	71.5	151.1			

Skeleton Number	Sex	Age	Side	AP	ap	ML	ml	T_A	M_A	C_A	T_A %DA	M_A %DA	C_A %DA
AN-218	F	YA	L	15.1	5.3	16.6	6.0	196.9	25.0	171.9	7.8	25.9	4.9
			R	15.4	5.5	17.6	7.5	212.9	32.4	180.5			
AN-220	F	OA	L	15.1	10.1	17.1	10.3	202.8	81.7	121.1	11.0	38.5	-13.6
			R	16.1	10.9	17.9	14.1	226.3	120.7	105.6			
AN-225	M	YA	L	18.7	10.9	21.4	12.8	314.3	109.6	204.7	13.9	5.6	18.0
			R	21.0	12.2	21.9	12.1	361.2	115.9	245.3			
AN-226	F	YA	L	16.9	7.2	17.0	7.9	225.6	44.7	181.0	2.2	25.8	-4.6
			R	16.6	8.1	17.7	9.1	230.8	57.9	172.9			
AN-229	M	MA	L	19.5	8.1	20.8	8.8	318.6	56.0	262.6	5.2	9.3	4.3
			R	19.6	8.5	21.8	9.2	335.6	61.4	274.2			
AN-230a	M	MA	L	18.4	7.3	20.9	8.6	302.0	49.3	252.7	4.7	22.7	0.8
			R	19.2	8.3	21.0	9.5	316.7	61.9	254.7			
AN-235	M?	YA	L	19.4	9.5	22.0	11.3	335.2	84.3	250.9	-1.7	-24.1	4.9
			R	19.7	8.6	21.3	9.8	329.6	66.2	263.4			
AN-238	M	MA	L	18.7	7.7	20.8	9.3	305.5	56.2	249.2	0.6	-0.9	0.9
			R	18.9	7.8	20.7	9.1	307.3	55.7	251.5			
AN-241	F	OA	L	16.4	10.9	18.0	13.0	231.8	111.3	120.6	7.3	29.5	-18.9
			R	16.9	12.8	18.8	14.9	249.5	149.8	99.7			
AN-242	F	OA	L	15.7	8.8	19.2	10.4	236.8	71.9	164.9	9.3	11.8	8.3
			R	16.8	9.9	19.7	10.4	259.9	80.9	179.1			
AN-243	F	YA	L	16.1	7.5	18.1	9.0	228.9	53.0	175.9	-2.0	7.4	-5.0
			R	15.7	7.9	18.2	9.2	224.4	57.1	167.3			
AN-244	M	YA	L	18.4	8.4	19.8	9.1	286.1	60.0	226.1	2.5	12.9	-0.5
			R	18.4	8.7	20.3	10.0	293.4	68.3	225.0			
AN-247	F	YA	L	16.1	7.9	15.9	8.1	201.1	50.3	150.8	-4.4	4.9	-7.8
			R	15.5	8.3	15.8	8.1	192.3	52.8	139.5			
AN-252	M	MA	L	20.0	12.4	22.0	16.2	345.6	157.8	187.8	3.9	25.9	-19.3
			R	20.8	15.6	22.0	16.7	359.4	204.6	154.8			
AN-259	F	YA	L	14.4	6.5	16.9	8.8	191.1	44.9	146.2	4.6	12.6	2.0
			R	14.9	6.9	17.1	9.4	200.1	50.9	149.2			

Skeleton Number	Sex	Age	Side	AP	ap	ML	ml	T_A	M_A	C_A	T_A %DA	M_A %DA	C_A %DA
AN-262A	F	MA	L	15.1	6.3	18.7	8.6	221.8	42.6	179.2	0.9	22.2	-4.9
			R	15.4	7.2	18.5	9.4	223.8	53.2	170.6			
AN-263	F	OA	L	16.1	12.3	20.6	15.5	260.5	149.7	110.7	9.1	15.9	-1.0
			R	17.8	13.8	20.4	16.2	285.2	175.6	109.6			
AN-266	M?	MA	L	16.0	7.8	19.2	9.8	241.3	60.0	181.2	13.8	19.4	11.9
			R	18.0	8.6	19.6	10.8	277.1	72.9	204.1			
AN-269	M	MA	L	18.6	7.8	20.0	8.2	292.2	50.2	241.9	-12.8	-36.5	-8.5
			R	17.5	6.7	18.7	6.6	257.0	34.7	222.3			
AN-277	F?	Adult	L	16.8	8.4	16.5	8.0	217.7	52.8	164.9	0.6	-12.5	4.4
			R	17.0	7.8	16.4	7.6	219.0	46.6	172.4			

F=Female; F?=Probable female; U=Unknown sex; M?=Probable male; M=Male; ADO=Adolescent; YA=Young adult; MA=Middle adult; OA=Old adult; L=Left; R=Right; AP=Antero-posterior total width; ap=Antero-posterior medullary width; ML=Medio-lateral total width; ml=Medio-lateral medullary width; T_A=Total area; M_A=Medullary area; C_A=Cortical area; T_A%DA=Total area directional asymmetry; M_A%DA=Medullary area directional asymmetry; C_A%DA=Cortical area directional asymmetry.

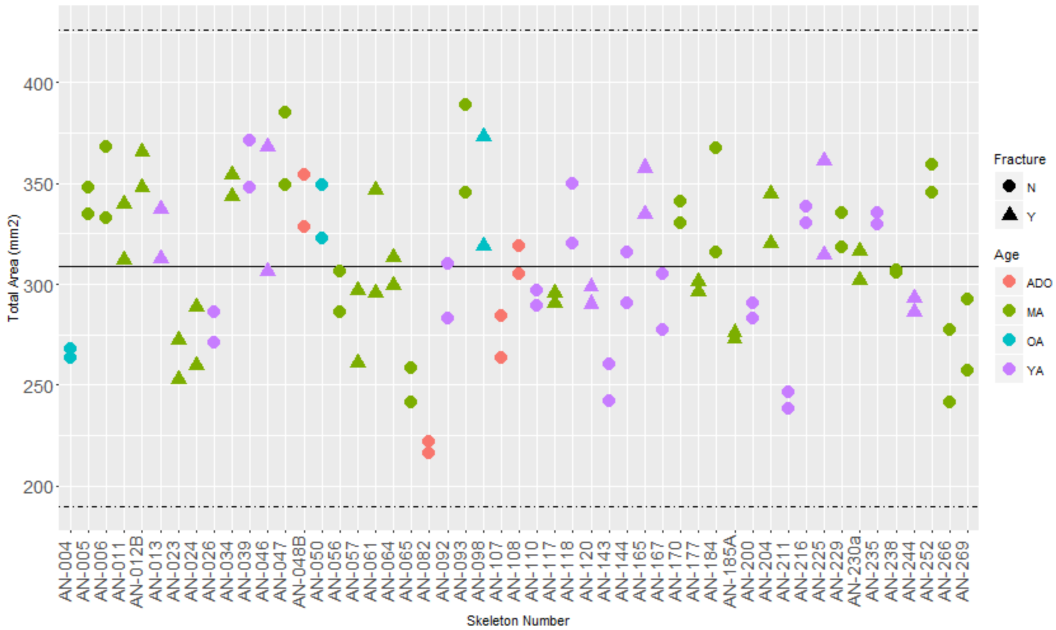

Figure I.1 – Ancaster male humeral total areas (mm²).

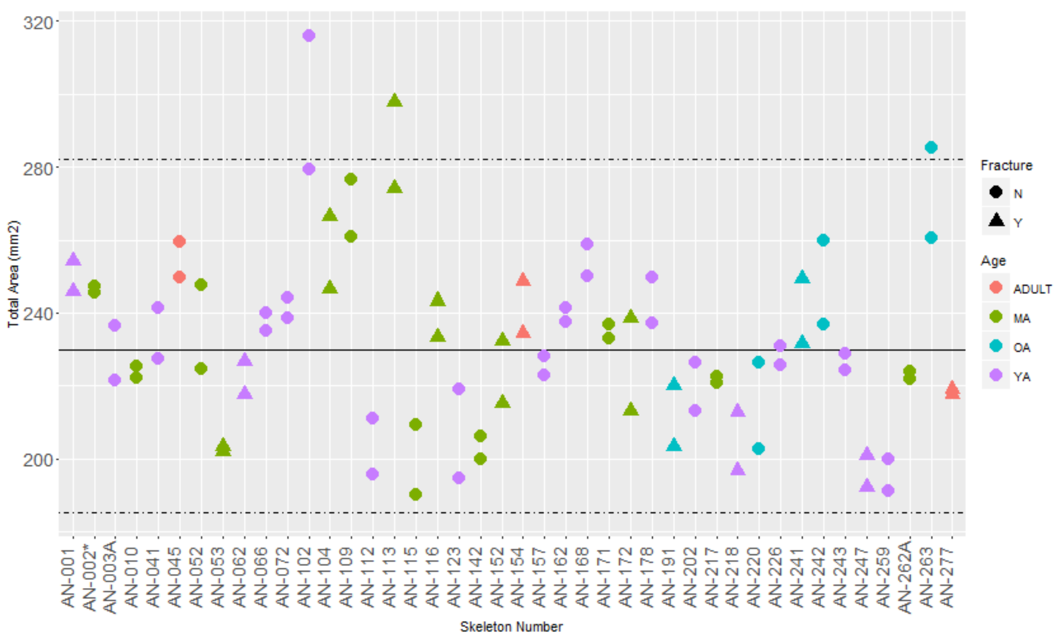

Figure I.2 – Ancaster female humeral total areas (mm²).

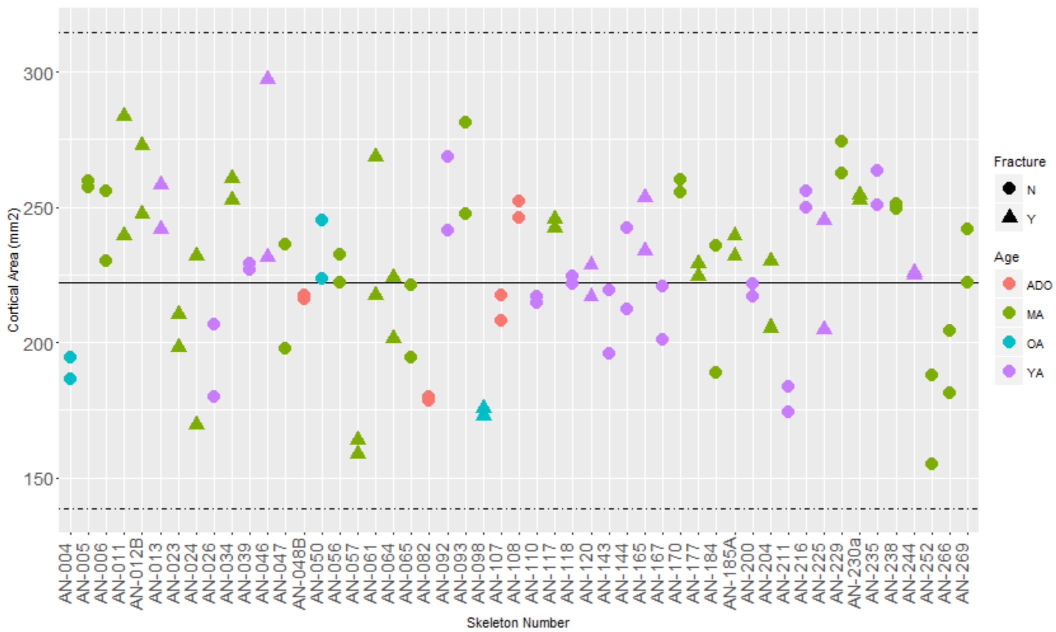

Figure I.3 – Ancaster male humeral cortical areas (mm^2).

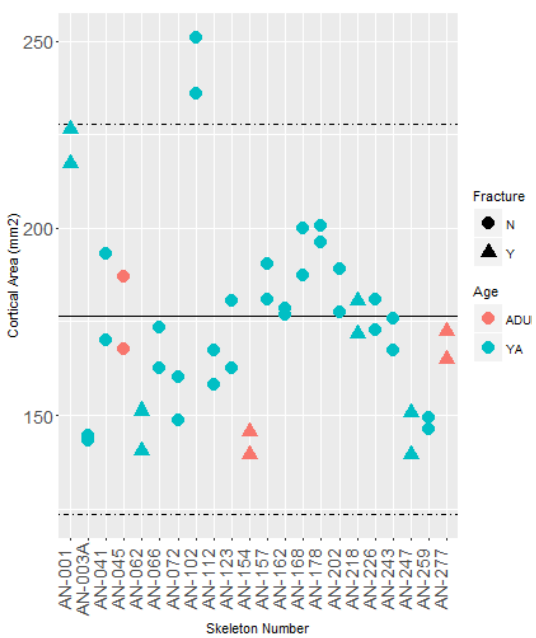

Figure I.4 – Ancaster young adult female humeral cortical areas (mm^2).

Figure I.5 – Ancaster middle and old adult female humeral cortical areas (mm^2).

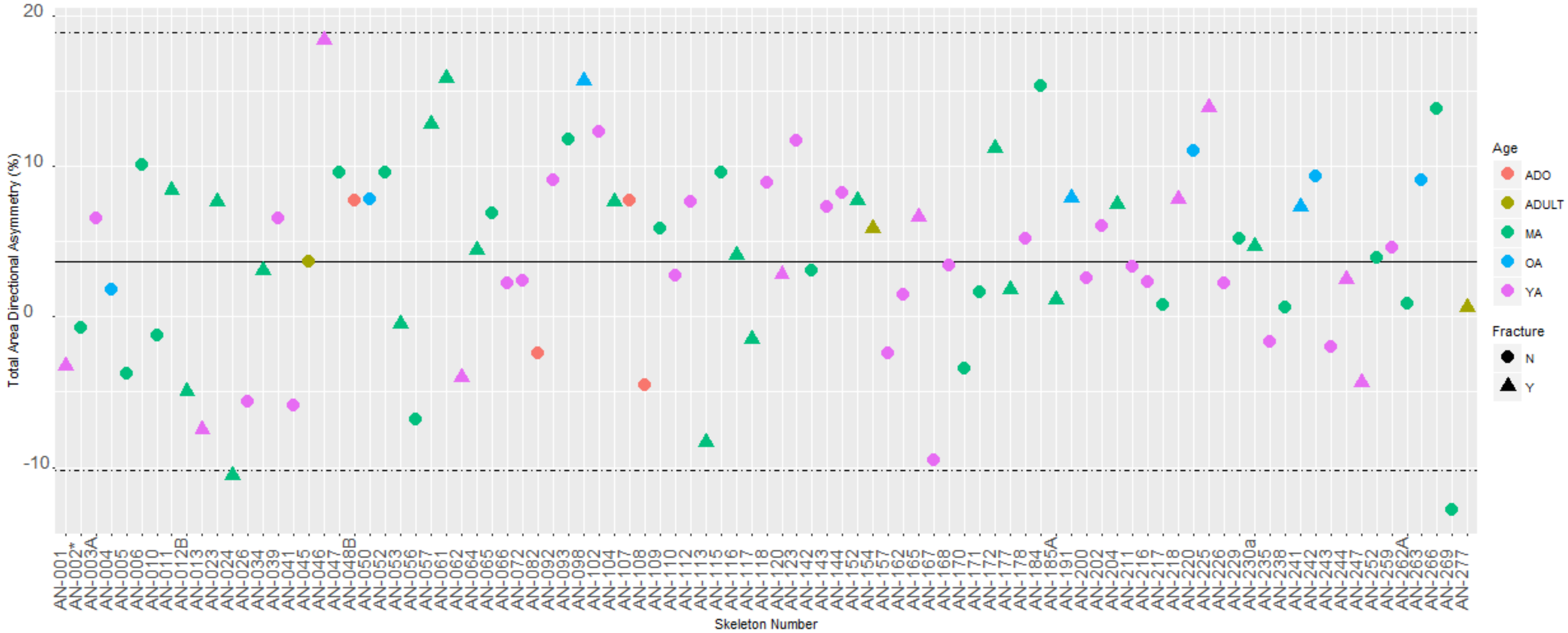

Figure I.6 – Ancaster humeral total area directional asymmetry (%).

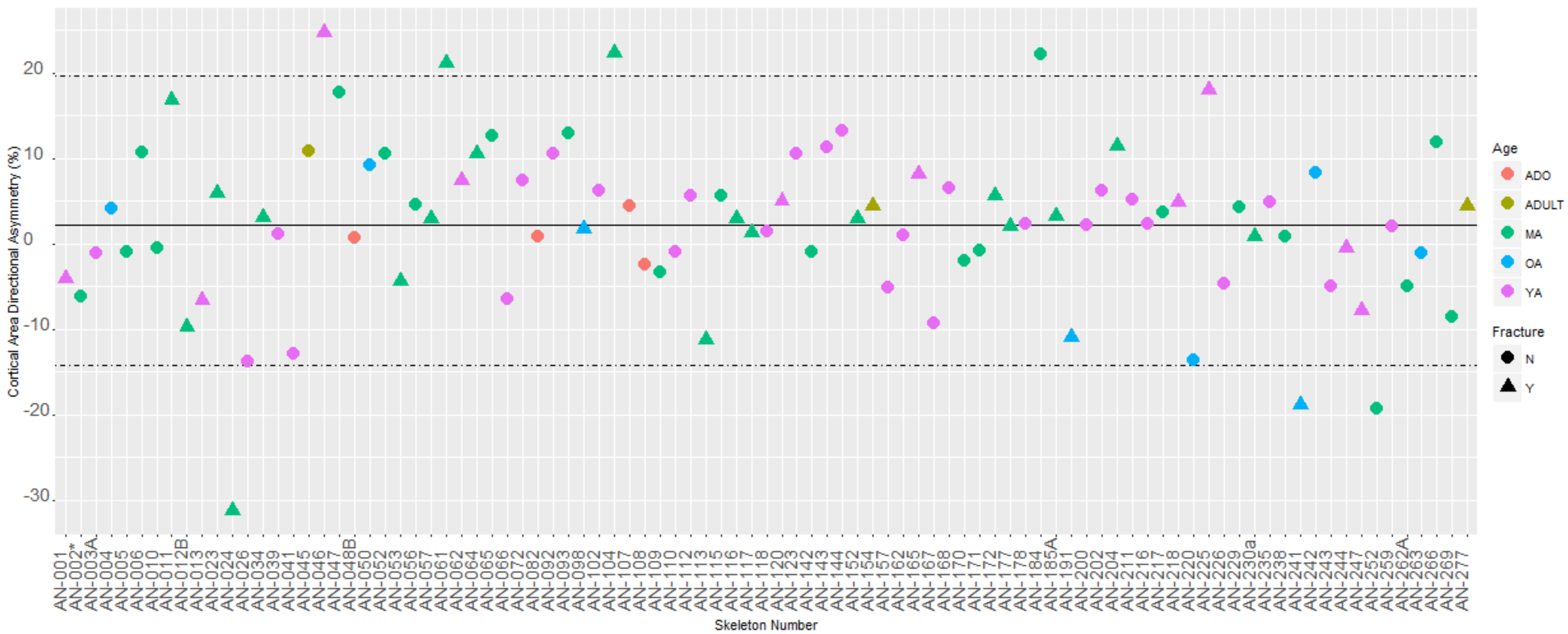

Figure I.7 – Ancaster humeral cortical area directional asymmetry (%).

I.1.2 - Radius

Table I.2 – Radiographically measured bone diameters, and calculated bone areas and asymmetries for radii at Ancaster.

Skeleton Number	Sex	Age	Side	AP	ap	ML	ml	T_A	M_A	C_A	T_A %DA	M_A %DA	C_A %DA
AN-001	F	YA	L	15.6	8.3	11.2	5.1	137.2	33.2	104.0	9.6	28.0	2.9
			R	16.3	9.2	11.8	6.1	151.1	44.1	107.0			
AN-002*	F	MA	L	15.0	10.0	11.5	7.0	135.5	55.0	80.5	7.1	10.4	4.7
			R	16.1	11.1	11.5	7.0	145.4	61.0	84.4			
AN-003A	F	YA	L	14.1	9.9	10.0	5.5	110.7	42.8	68.0	20.5	26.0	16.8
			R	15.6	10.4	11.1	6.8	136.0	55.5	80.5			
AN-004	M	OA	L	14.6	8.2	10.3	4.3	118.1	27.7	90.4	0.4	26.6	-9.3
			R	15.1	9.6	10.0	4.8	118.6	36.2	82.4			
AN-005	M	MA	L	20.7	14.4	14.0	8.2	227.6	92.7	134.9	-8.9	-28.3	2.7
			R	19.5	12.0	13.6	7.4	208.3	69.7	138.5			
AN-006	M	MA	L	17.1	11.7	12.7	7.0	170.6	64.3	106.2	6.4	-3.9	12.2
			R	16.9	10.5	13.7	7.5	181.8	61.9	120.0			
AN-010	F	MA	L	14.6	9.7	9.5	5.0	108.9	38.1	70.8	7.0	-3.1	12.0
			R	15.5	9.8	9.6	4.8	116.9	36.9	79.9			
AN-011	M	MA	L	15.7	9.7	11.0	5.1	135.6	38.9	96.8	-8.7	-29.1	-1.4
			R	14.8	8.2	10.7	4.5	124.4	29.0	95.4			
AN-012B	M	MA	L	18.5	10.8	12.4	6.9	180.2	58.5	121.6	-4.1	13.5	-13.8
			R	17.9	10.8	12.3	7.9	172.9	67.0	105.9			
AN-013	M	YA	L	17.0	11.5	12.7	7.4	169.6	66.8	102.7	-11.2	-33.2	1.0
			R	15.2	8.7	12.7	7.0	151.6	47.8	103.8			
AN-023	M	MA	L	-	-	-	-	-	-	-	-	-	-
			R	16.1	10.0	11.4	5.6	144.2	44.0	100.2			
AN-024	M	MA	L	14.6	8.2	11.0	5.2	126.1	33.5	92.6	-	-	-
			R	-	-	-	-	-	-	-			
AN-026	M	YA	L	14.6	8.3	11.5	5.2	131.9	33.9	98.0	18.7	63.7	-4.7
			R	16.6	12.1	12.2	6.9	159.1	65.6	93.5			
AN-027	M	MA	L	15.6	10.1	12.0	6.1	147.0	48.4	98.6	-	-	-
			R	-	-	-	-	-	-	-			

Skeleton Number	Sex	Age	Side	AP	ap	ML	ml	T_A	M_A	C_A	T_A %DA	M_A %DA	C_A %DA
AN-034	M	MA	L	17.9	11.9	11.6	6.4	163.1	59.8	103.3	13.7	25.6	6.0
			R	18.9	12.8	12.6	7.7	187.0	77.4	109.6			
AN-039	M	YA	L	17.3	10.8	12.8	6.7	173.9	56.8	117.1	14.1	14.6	13.9
			R	18.9	11.8	13.5	7.1	200.4	65.8	134.6			
AN-041	F	YA	L	15.0	9.1	9.1	4.4	107.2	31.4	75.8	6.5	0.7	8.8
			R	15.5	9.6	9.4	4.2	114.4	31.7	82.8			
AN-046	M	YA	L	15.0	9.1	13.9	8.2	163.8	58.6	105.1	10.0	11.8	9.0
			R	16.7	10.5	13.8	8.0	181.0	66.0	115.0			
AN-047	M	MA	L	16.5	10.7	12.3	6.8	159.4	57.1	102.3	4.2	2.0	5.4
			R	16.8	10.6	12.6	7.0	166.3	58.3	108.0			
AN-048B	M	ADO	L	18.8	13.5	12.4	6.1	183.1	64.7	118.4	2.6	14.5	-4.5
			R	19.3	13.8	12.4	6.9	188.0	74.8	113.2			
AN-050	M	OA	L	16.1	9.8	12.1	7.0	153.0	53.9	99.1	-	-	-
			R	-	-	-	-	-	-	-			
AN-052	F	MA	L	-	-	-	-	-	-	-	-	-	-
			R	17.9	12.3	10.9	5.8	153.2	56.0	97.2			
AN-053	F	MA	L	12.8	8.7	9.8	5.6	98.5	38.3	60.3	6.3	12.9	1.9
			R	13.1	8.8	10.2	6.3	104.9	43.5	61.4			
AN-056	M	MA	L	16.9	9.6	11.7	6.0	155.3	45.2	110.1	3.2	23.0	-6.3
			R	17.6	11.7	11.6	6.2	160.3	57.0	103.4			
AN-061	M	MA	L	16.2	9.6	12.4	6.7	157.8	50.5	107.3	0.6	8.5	-3.4
			R	16.7	10.3	12.1	6.8	158.7	55.0	103.7			
AN-062	F	YA	L	14.7	9.1	10.3	5.1	118.9	36.5	82.5	-3.0	11.2	-10.1
			R	14.4	9.8	10.2	5.3	115.4	40.8	74.6			
AN-064	M	MA	L	-	-	-	-	-	-	-	-	-	-
			R	17.5	11.3	12.5	6.6	171.8	58.6	113.2			
AN-065	M	MA	L	14.3	8.5	10.4	4.8	116.8	32.0	84.8	21.6	44.6	11.0
			R	16.2	10.7	11.4	6.0	145.0	50.4	94.6			
AN-066	F	YA	L	14.5	6.6	10.0	4.3	113.9	22.3	91.6	-5.5	-4.2	-5.8
			R	14.0	6.8	9.8	4.0	107.8	21.4	86.4			

Skeleton Number	Sex	Age	Side	AP	ap	ML	ml	T_A	M_A	C_A	T_A %DA	M_A %DA	C_A %DA
AN-067	F	MA	L	-	-	-	-	-	-	-	-	-	-
			R	13.0	6.3	11.0	4.9	112.3	24.2	88.1			
AN-072	F	YA	L	-	-	-	-	-	-	-	-	-	-
			R	15.1	10.0	10.0	5.4	118.6	42.4	76.2			
AN-082	M	ADO	L	15.8	11.6	10.4	6.1	129.1	55.6	73.5	14.1	23.1	6.7
			R	16.9	12.4	11.2	7.2	148.7	70.1	78.5			
AN-092	M	YA	L	15.5	8.8	13.2	6.3	160.7	43.5	117.1	-2.7	4.9	-5.7
			R	15.8	9.7	12.6	6.0	156.4	45.7	110.6			
AN-093	M	MA	L	18.2	12.1	13.1	6.9	187.3	65.6	121.7	13.7	47.8	-12.0
			R	20.4	16.0	13.4	8.5	214.7	106.8	107.9			
AN-098	M	OA	L	14.7	10.0	12.4	8.2	143.2	64.4	78.8	15.1	24.0	7.1
			R	16.7	12.0	12.7	8.7	166.6	82.0	84.6			
AN-104	F	MA	L	15.8	12.1	10.8	6.7	134.0	63.7	70.3	-3.1	0.4	-6.5
			R	15.6	11.8	10.6	6.9	129.9	63.9	65.9			
AN-107	M	ADO	L	17.3	12.7	11.7	7.3	159.0	72.8	86.2	7.3	8.1	6.7
			R	18.0	13.4	12.1	7.5	171.1	78.9	92.1			
AN-108	M	ADO	L	15.7	10.1	11.6	5.7	143.0	45.2	97.8	8.1	10.6	6.9
			R	15.8	9.7	12.5	6.6	155.1	50.3	104.8			
AN-109	F	MA	L	-	-	-	-	-	-	-	-	-	-
			R	15.9	13.2	11.2	7.3	139.9	75.7	64.2			
AN-110	M	YA	L	15.3	9.2	11.6	6.1	139.4	44.1	95.3	18.7	41.5	5.8
			R	17.7	11.4	12.1	7.5	168.2	67.2	101.1			
AN-112	F	YA	L	13.1	7.7	9.3	4.1	95.7	24.8	70.9	16.4	44.8	3.8
			R	14.5	9.4	9.9	5.3	112.7	39.1	73.6			
AN-113	F	MA	L	-	-	-	-	-	-	-	-	-	-
			R	15.5	8.8	10.8	6.1	131.5	42.2	89.3			
AN-115	F	MA	L	13.8	8.8	9.5	4.8	103.0	33.2	69.8	-8.1	-39.2	4.0
			R	13.0	7.1	9.3	4.0	95.0	22.3	72.6			
AN-116	F	MA	L	15.0	10.7	9.8	5.3	115.5	44.5	70.9	0.0	-26.0	13.5
			R	14.7	8.4	10.0	5.2	115.5	34.3	81.1			

Skeleton Number	Sex	Age	Side	AP	ap	ML	ml	T_A	M_A	C_A	T_A %DA	M_A %DA	C_A %DA
AN-117	M	MA	L	14.5	10.0	10.8	6.5	123.0	51.1	71.9	21.5	17.0	24.6
			R	16.9	10.7	11.5	7.2	152.6	60.5	92.1			
AN-118	M	YA	L	17.2	12.0	14.4	8.5	194.5	80.1	114.4	12.5	22.8	4.6
			R	19.5	14.1	14.4	9.1	220.5	100.8	119.8			
AN-120	M	YA	L	14.6	8.8	11.2	5.7	128.4	39.4	89.0	13.3	3.4	17.4
			R	15.7	9.1	11.9	5.7	146.7	40.7	106.0			
AN-123	F	YA	L	-	-	-	-	-	-	-	-	-	-
			R	14.9	9.4	9.1	3.6	106.5	26.6	79.9			
AN-136	M	YA	L	16.6	11.2	11.4	5.7	148.6	50.1	98.5	12.7	22.3	7.5
			R	17.2	12.1	12.5	6.6	168.9	62.7	106.1			
AN-142	F	MA	L	11.8	7.7	10.0	5.5	92.7	33.3	59.4	-	-	-
			R	-	-	-	-	-	-	-			
AN-143	M	YA	L	14.2	7.1	10.7	4.7	119.3	26.2	93.1	-5.9	6.8	-9.8
			R	13.9	7.6	10.3	4.7	112.4	28.1	84.4			
AN-144	M	YA	L	16.3	10.3	11.6	6.8	148.5	55.0	93.5	-5.0	-18.9	2.4
			R	16.5	9.5	10.9	6.1	141.3	45.5	95.7			
AN-152	F	MA	L	13.0	8.8	9.4	5.1	96.0	35.2	60.7	12.3	0.5	18.5
			R	14.7	9.6	9.4	4.7	108.5	35.4	73.1			
AN-154	F	Adult	L	12.6	8.2	9.5	5.8	94.0	37.4	56.7	9.2	11.4	7.8
			R	13.0	8.6	10.1	6.2	103.1	41.9	61.2			
AN-157	F	YA	L	14.6	10.1	9.9	5.8	113.5	46.0	67.5	9.0	1.4	13.8
			R	15.5	9.9	10.2	6.0	124.2	46.7	77.5			
AN-162	F	YA	L	14.3	7.9	11.0	6.2	123.5	38.5	85.1	-8.5	-12.6	-6.7
			R	14.3	8.3	10.1	5.2	113.4	33.9	79.5			
AN-165	M	YA	L	13.3	6.9	10.5	4.4	109.7	23.8	85.8	7.4	27.5	1.0
			R	13.8	7.7	10.9	5.2	118.1	31.4	86.7			
AN-167	M	YA	L	17.1	11.5	11.7	6.7	157.1	60.5	96.6	-0.3	-0.3	-0.4
			R	16.9	11.3	11.8	6.8	156.6	60.3	96.3			
AN-168	F	YA	L	14.3	9.4	10.3	5.2	115.7	38.4	77.3	6.4	5.2	7.0
			R	15.1	10.3	10.4	5.0	123.3	40.4	82.9			

Skeleton Number	Sex	Age	Side	AP	ap	ML	ml	T_A	M_A	C_A	T_A %DA	M_A %DA	C_A %DA
AN-170	M	MA	L	15.7	9.6	12.7	6.1	156.6	46.0	110.6	6.8	28.3	-3.9
			R	16.8	11.8	12.7	6.6	167.6	61.2	106.4			
AN-171	F	MA	L	13.7	8.7	9.4	4.9	101.1	33.5	67.7	10.3	22.8	3.5
			R	14.0	9.4	10.2	5.7	112.2	42.1	70.1			
AN-172	F	MA	L	15.3	11.8	10.3	6.2	123.8	57.5	66.3	12.9	42.5	-23.6
			R	16.3	13.1	11.0	8.6	140.8	88.5	52.3			
AN-177	M	MA	L	14.7	7.6	11.2	5.2	129.3	31.0	98.3	14.3	13.5	14.5
			R	16.1	8.7	11.8	5.2	149.2	35.5	113.7			
AN-178	F	YA	L	14.9	9.6	10.7	5.3	125.2	40.0	85.3	2.4	-6.1	6.1
			R	15.4	8.7	10.6	5.5	128.2	37.6	90.6			
AN-184	M	MA	L	16.6	9.7	12.1	7.1	157.8	54.1	103.7	14.2	11.5	15.6
			R	16.9	9.2	13.7	8.4	181.8	60.7	121.1			
AN-185A	F	YA	L	12.7	5.9	9.3	3.5	92.8	16.2	76.5	13.1	17.1	12.2
			R	13.6	7.0	9.9	3.5	105.7	19.2	86.5			
AN-191	F	OA	L	13.1	6.8	8.8	3.9	90.5	20.8	69.7	10.8	41.2	-0.7
			R	13.1	7.6	9.8	5.3	100.8	31.6	69.2			
AN-200	M	YA	L	15.2	10.3	11.6	6.6	138.5	53.4	85.1	-0.9	-20.8	9.9
			R	15.2	9.2	11.5	6.0	137.3	43.4	93.9			
AN-202	F	YA	L	12.6	6.9	9.8	4.7	97.0	25.5	71.5	4.1	-1.6	6.0
			R	13.4	7.6	9.6	4.2	101.0	25.1	76.0			
AN-204A	M	MA	L	16.0	10.2	10.8	5.2	135.7	41.7	94.1	8.1	13.0	5.9
			R	16.3	10.6	11.5	5.7	147.2	47.5	99.8			
AN-211	M	YA	L	12.3	7.4	10.3	4.7	99.5	27.3	72.2	-	-	-
			R	-	-	-	-	-	-	-			
AN-216	M	YA	L	17.0	11.4	13.3	6.8	177.6	60.9	116.7	-17.5	-25.7	-13.4
			R	14.6	8.8	13.0	6.8	149.1	47.0	102.1			
AN-217	F	MA	L	15.3	11.7	10.7	6.9	128.6	63.4	65.2	6.9	-1.7	14.7
			R	16.1	11.5	10.9	6.9	137.8	62.3	75.5			
AN-218	F	YA	L	12.6	7.5	9.5	5.1	94.0	30.0	64.0	2.6	-6.9	6.8
			R	13.5	8.3	9.1	4.3	96.5	28.0	68.5			

Skeleton Number	Sex	Age	Side	AP	ap	ML	ml	T_A	M_A	C_A	T_A %DA	M_A %DA	C_A %DA
AN-220	F	OA	L	14.0	9.1	10.2	5.3	112.2	37.9	74.3	1.6	-13.1	8.3
			R	14.8	9.0	9.8	4.7	113.9	33.2	80.7			
AN-225	M	YA	L	13.9	5.3	10.8	3.9	117.9	16.2	101.7	15.8	35.3	12.2
			R	15.7	7.2	11.2	4.1	138.1	23.2	114.9			
AN-226	F	YA	L	15.6	10.8	10.1	4.7	123.7	39.9	83.9	0.5	10.1	-4.4
			R	16.0	10.4	9.9	5.4	124.4	44.1	80.3			
AN-229	M	MA	L	14.5	6.6	11.1	3.9	126.4	20.2	106.2	10.8	50.0	0.9
			R	14.7	7.8	12.2	5.5	140.9	33.7	107.2			
AN-230A	M	MA	L	14.2	7.1	10.9	5.2	121.6	29.0	92.6	8.9	28.2	1.9
			R	15.1	8.6	11.2	5.7	132.8	38.5	94.3			
AN-238	M	MA	L	15.7	10.0	11.4	5.8	140.6	45.6	95.0	7.6	12.0	5.4
			R	16.5	10.9	11.7	6.0	151.6	51.4	100.3			
AN-241	F	OA	L	13.2	9.9	8.8	5.4	91.2	42.0	49.2	23.4	26.1	21.1
			R	15.0	11.4	9.8	6.1	115.5	54.6	60.8			
AN-242	F	OA	L	13.8	7.6	11.5	7.0	124.6	41.8	82.9	13.9	27.6	6.2
			R	15.2	9.0	12.0	7.8	143.3	55.1	88.1			
AN-243	F	YA	L	13.2	6.3	10.0	4.5	103.7	22.3	81.4	0.0	27.1	-9.0
			R	13.2	7.6	10.0	4.9	103.7	29.2	74.4			
AN-244	M	YA	L	15.0	7.9	11.6	7.0	136.7	43.4	93.2	-0.9	-32.1	11.0
			R	15.4	8.0	11.2	5.0	135.5	31.4	104.0			
AN-252	M	MA	L	15.5	7.9	11.0	5.6	133.9	34.7	99.2	11.0	69.3	-23.9
			R	16.7	13.6	11.4	6.7	149.5	71.6	78.0			
AN-259	F	YA	L	12.3	6.5	10.0	4.1	96.6	20.9	75.7	1.4	6.0	0.1
			R	12.6	6.9	9.9	4.1	98.0	22.2	75.8			
AN-262A	F	MA	L	13.5	9.3	10.8	6.5	114.5	47.5	67.0	1.1	4.2	-1.2
			R	13.9	9.7	10.6	6.5	115.7	49.5	66.2			
AN-263	F	OA	L	13.7	11.6	9.7	6.5	104.4	59.2	45.2	6.0	-16.0	28.9
			R	14.4	10.7	9.8	6.0	110.8	50.4	60.4			
AN-266	M	MA	L	14.8	7.7	10.5	5.0	122.1	30.2	91.8	21.4	7.7	25.4
			R	16.6	8.0	11.6	5.2	151.2	32.7	118.6			

Skeleton Number	Sex	Age	Side	AP	ap	ML	ml	T_A	M_A	C_A	T_A %DA	M_A %DA	C_A %DA
AN-269	M	MA	L	18.0	12.2	11.2	6.4	158.3	61.3	97.0	-22.7	-80.9	3.1
			R	15.0	7.7	10.7	4.3	126.1	26.0	100.1			
AN-277	F	Adult	L	16.5	12.0	10.1	6.2	130.9	58.4	72.5	7.3	-9.0	18.6
			R	16.0	10.3	11.2	6.6	140.7	53.4	87.4			

F=Female; F?=Probable female; U=Unknown sex; M?=Probable male; M=Male; ADO=Adolescent; YA=Young adult; MA=Middle adult; OA=Old adult; L=Left; R=Right; AP=Antero-posterior total width; ap=Antero-posterior medullary width; ML=Medio-lateral total width; ml=Medio-lateral medullary width; T_A=Total area; M_A=Medullary area; C_A=Cortical area; T_A%DA=Total area directional asymmetry; M_A%DA=Medullary area directional asymmetry; C_A%DA=Cortical area directional asymmetry.

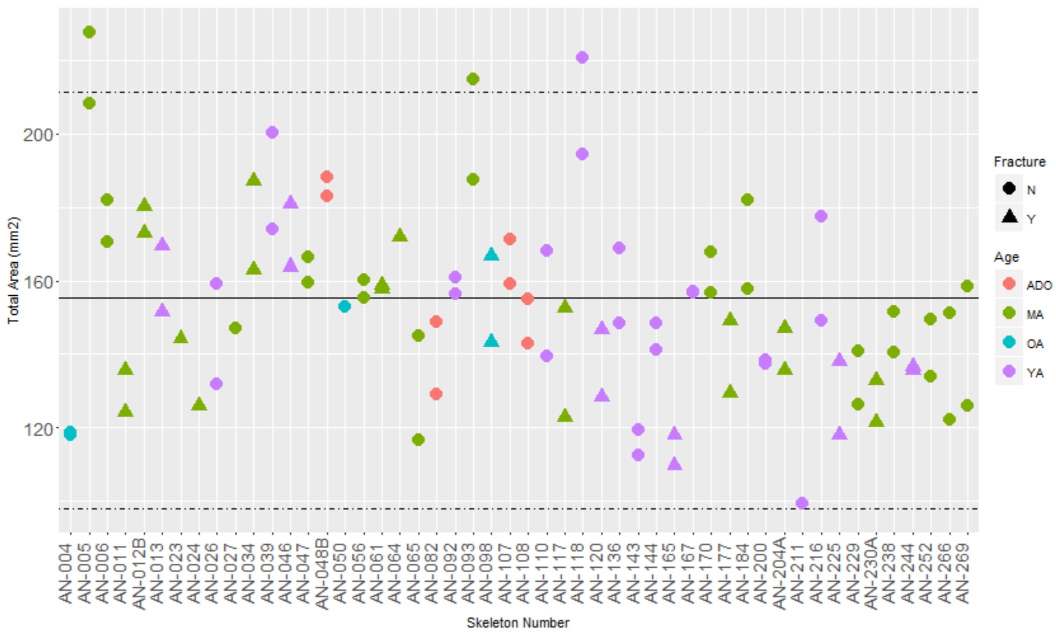

Figure I.8 – Ancaster male radius total areas (mm^2).

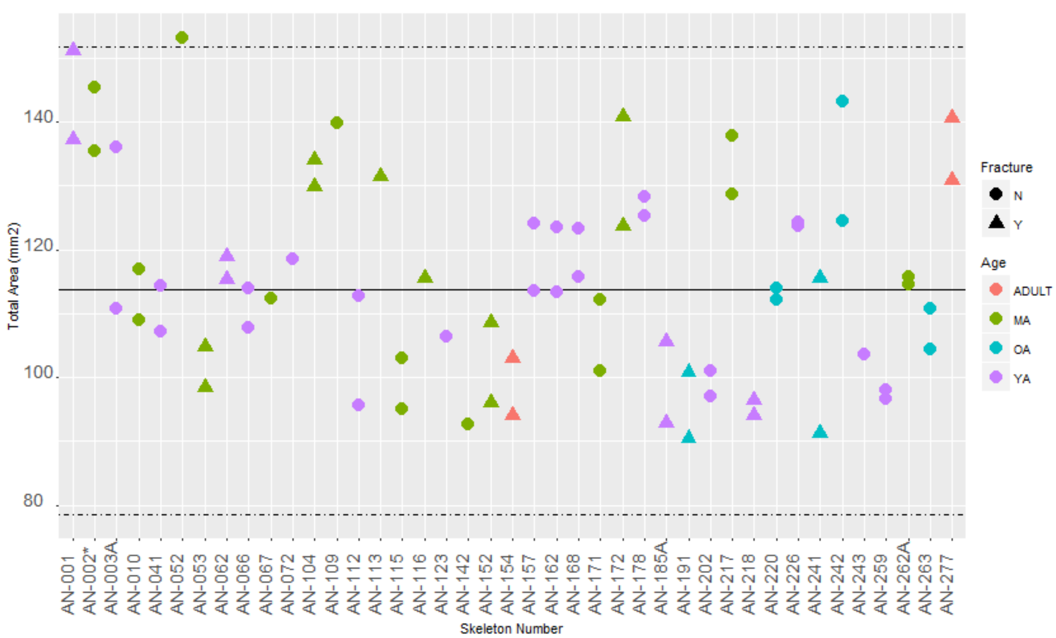

Figure I.9 – Ancaster female radius total areas (mm^2).

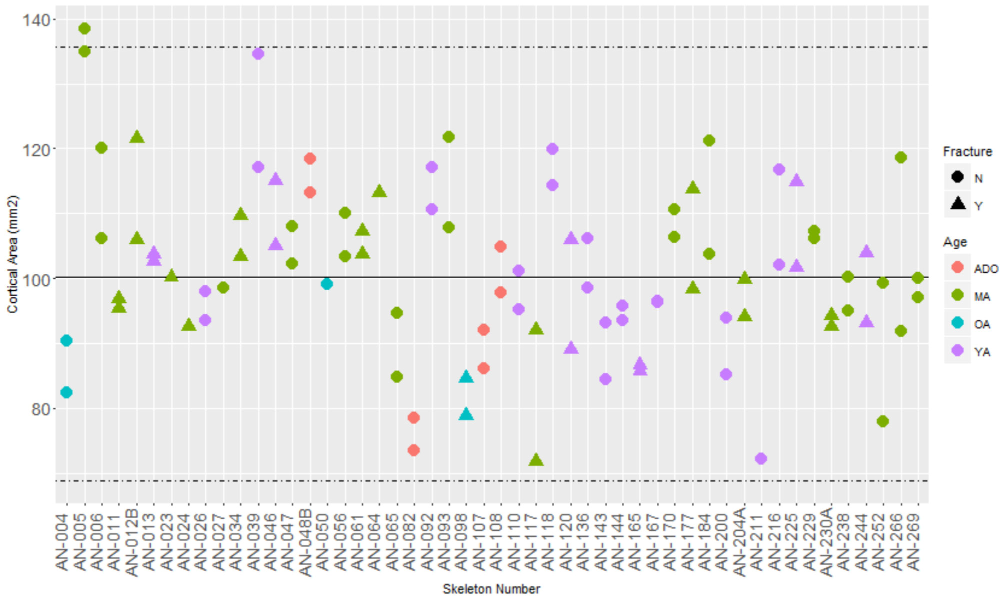

Figure I.10 – Ancaster male radius cortical areas (mm^2).

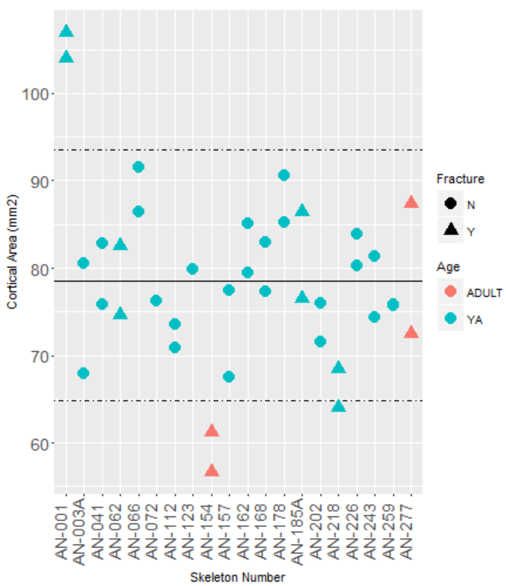

Figure I.11 – Ancaster young adult female radial cortical areas (mm^2). Two outliers (AN-154) belong to an individual of unknown age, but fall within the range of normal for middle and old adult females. As such, they were not considered true outliers.

Figure I.12 – Ancaster young adult female radial cortical areas (mm^2).

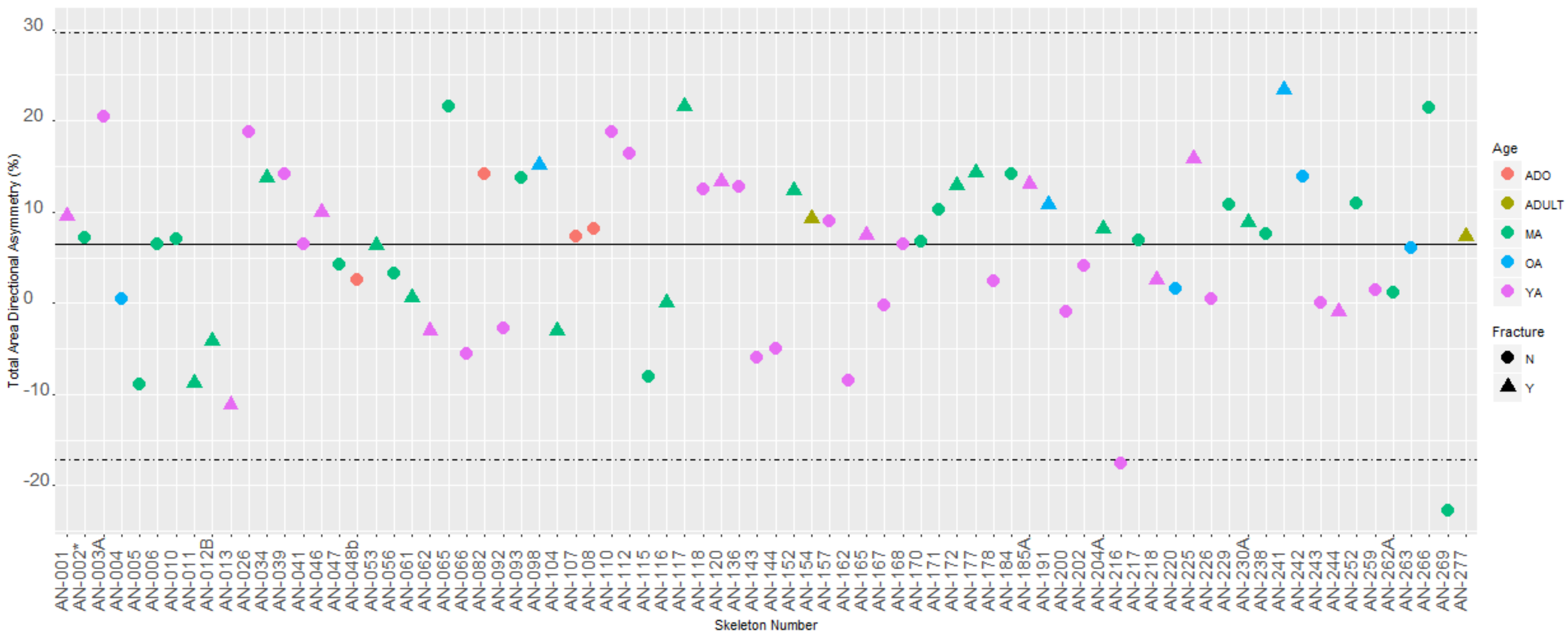

Figure I.13 – Ancaster radial total area directional asymmetry (%).

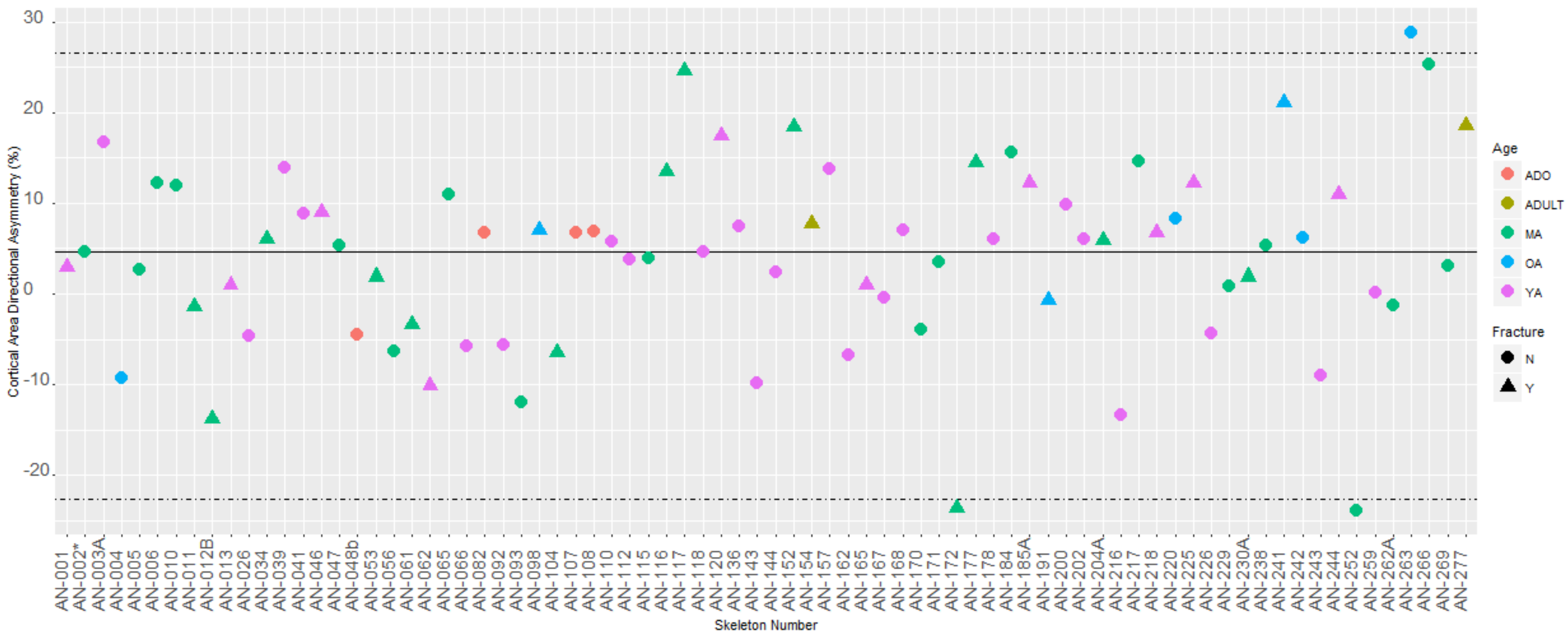

Figure I.14 – Ancaster radial cortical area directional asymmetry (%).

I.1.3 - Ulna

Table I.3 – Radiographically measured bone diameters, and calculated bone areas and asymmetries for ulnae at Ancaster.

Skeleton Number	Sex	Age	L ROI	R ROI	ROI %DA
AN-001	F?	YA	270.3	247.6	-8.8
AN-002	F	MA	180.0	242.9	29.7
AN-003A	F	YA	178.8	189.4	5.8
AN-004	M	OA	231.8	279.8	18.8
AN-005	M	MA	358.1	-	-
AN-006	M	MA	229.0	328.0	35.5
AN-010	F	MA	163.7	150.9	-8.1
AN-011	M	MA	241.2	326.6	30.1
AN-012B	M	MA	238.0	233.5	-1.9
AN-013	M	YA	269.9	-	-
AN-023	M	MA	236.5	200.6	-16.4
AN-024	M	MA	278.0	-	-
AN-026	M	YA	251.7	210.8	-17.7
AN-034	M	MA	258.0	290.0	11.7
AN-039	M?	YA	240.3	227.9	-5.3
AN-041	F	YA	221.3	263.1	17.3
AN-046	M?	YA	257.2	-	-
AN-047	M	MA	213.6	223.8	4.7
AN-048B	M?	ADO	295.1	265.0	-10.7
AN-053	F	MA	171.5	-	-
AN-061	M	MA	252.0	235.4	-6.8
AN-062	F	YA	204.5	210.0	2.7
AN-065	M	MA	247.3	287.1	14.9
AN-066	F	YA	250.1	226.4	-9.9
AN-067	F	MA	-	154.8	-
AN-072	F	YA	-	192.0	-
AN-082	M	ADO	228.8	233.4	2.0
AN-092	M	YA	251.0	298.4	17.3
AN-093	M	MA	317.9	393.6	21.3
AN-098	M	OA	161.5	114.5	-34.1
AN-107	M?	ADO	227.0	272.1	18.1
AN-108	M?	ADO	253.5	296.7	15.7
AN-109	F	MA	121.3	136.4	11.7
AN-110	M?	YA	204.6	221.2	7.8
AN-112	F	YA	240.5	223.3	-7.4

Skeleton Number	Sex	Age	L ROI	R ROI	ROI %DA
AN-113	F	MA	183.3	195.1	6.2
AN-115	F	MA	298.7	222.5	-29.2
AN-116	F?	MA	218.4	241.1	9.9
AN-117	M?	MA	263.8	281.3	6.4
AN-118	M?	YA	250.4	275.5	9.5
AN-120	M	YA	237.0	293.7	21.4
AN-123	F	YA	253.6	250.9	-1.1
AN-136	M	YA	251.2	262.1	4.2
AN-142	F	MA	241.6	239.4	-0.9
AN-143	M	YA	235.8	240.4	1.9
AN-144	M	YA	202.3	267.5	27.8
AN-152	F	MA	162.1	192.2	17.0
AN-157	F	YA	219.6	195.4	-11.7
AN-162	F?	YA	253.3	273.2	7.6
AN-165	M	YA	219.8	261.3	17.3
AN-167	M?	YA	230.6	216.6	-6.3
AN-168	F	YA	228.1	243.8	6.7
AN-170	M	MA	297.1	279.6	-6.1
AN-171	F	MA	180.8	224.6	21.6
AN-177	M	MA	286.8	302.6	5.4
AN-178	F?	YA	254.6	263.0	3.2
AN-184	M	MA	304.2	282.9	-7.3
AN-185A	M	MA	275.7	259.8	-5.9
AN-191	F	OA	210.3	272.2	25.7
AN-200	M	YA	286.0	238.4	-18.2
AN-202	F	YA	236.9	245.8	3.7
AN-204A	M	MA	195.4	169.9	-14.0
AN-211	M?	YA	291.3	-	-
AN-216	M?	YA	269.5	270.1	0.2
AN-217	F	MA	183.7	201.4	9.2
AN-218	F	YA	195.1	236.5	19.2
AN-220	F	OA	226.8	244.4	7.5
AN-225	M	YA	265.6	293.8	10.1
AN-226	F	YA	209.5	222.7	6.1
AN-229	M	MA	265.9	305.2	13.8
AN-230A	M	MA	241.6	239.4	-0.9
AN-235	M?	YA	302.6	-	-
AN-238	M	MA	313.7	373.8	17.5

Skeleton Number	Sex	Age	L ROI	R ROI	ROI %DA
AN-241	F	OA	137.0	141.9	3.5
AN-242	F	OA	208.5	189.1	-9.8
AN-243	F	YA	221.7	233.6	5.2
AN-244	M	MA	274.0	314.5	13.8
AN-252	M	MA	198.7	148.5	-28.9
AN-259	F	YA	252.3	229.8	-9.3
AN-262A	F	MA	229.1	258.0	11.9
AN-263	F	OA	151.5	123.7	-20.2
AN-266	M?	MA	258.9	211.5	-20.2
AN-269	M	MA	275.8	274.6	-0.4
AN-277	F?	Adult	209.5	269.0	24.9

F=Female; F?=Probable female; U=Unknown sex; M?=Probable male; M=Male; ADO=Adolescent; YA=Young adult; MA=Middle adult; OA=Old adult; L=Left; R=Right; ROI=Region of interest; directional asymmetry; ROI%DA=Region of interest area directional asymmetry

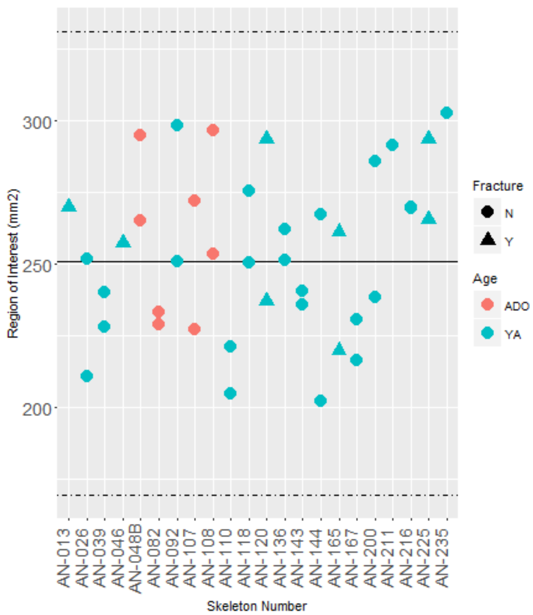

Figure I.15 – Ancaster young adult male ulna region of interest areas (mm^2).

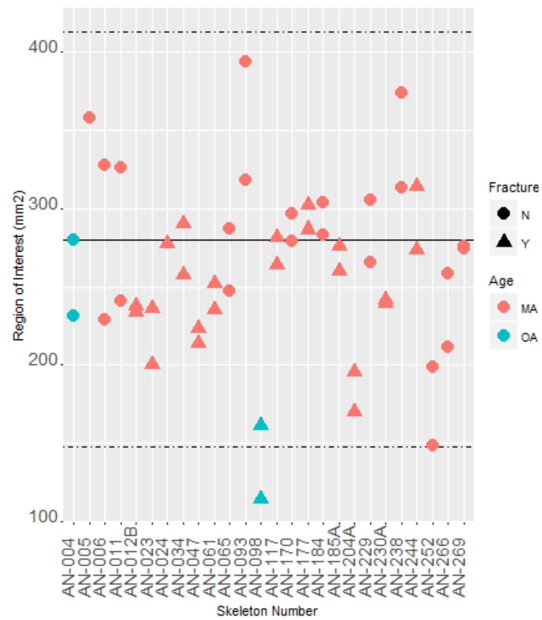

Figure I.16 – Ancaster middle and old adult male ulna region of interest areas (mm^2).

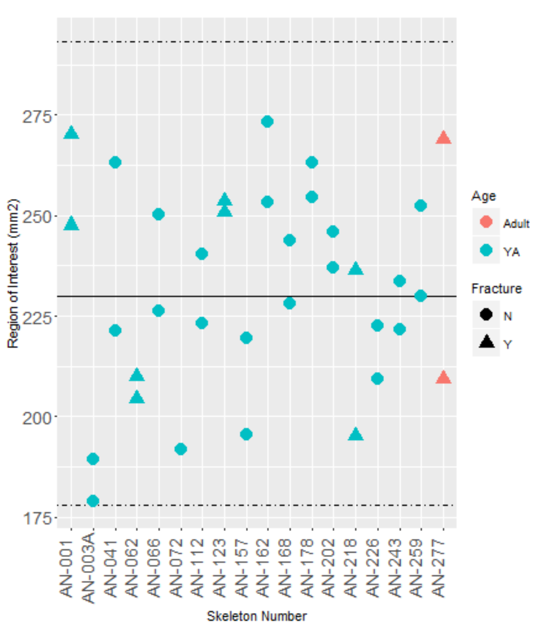

Figure I.17 – Ancaster young adult female ulna region of interest areas (mm^2).

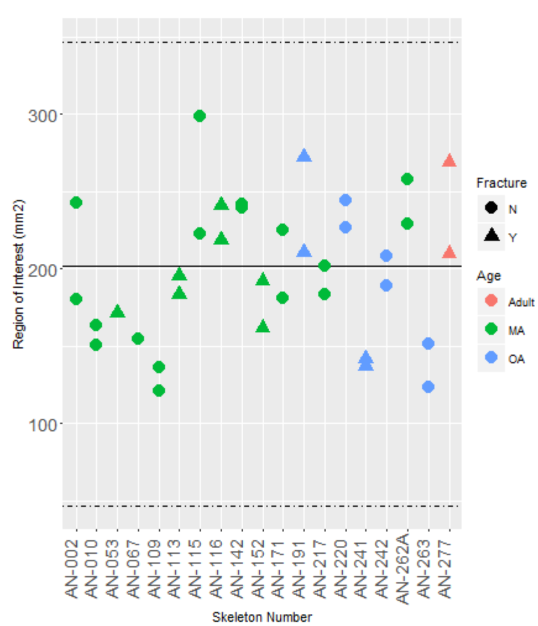

Figure I.18 – Ancaster middle and old adult female ulna region of interest areas (mm^2).

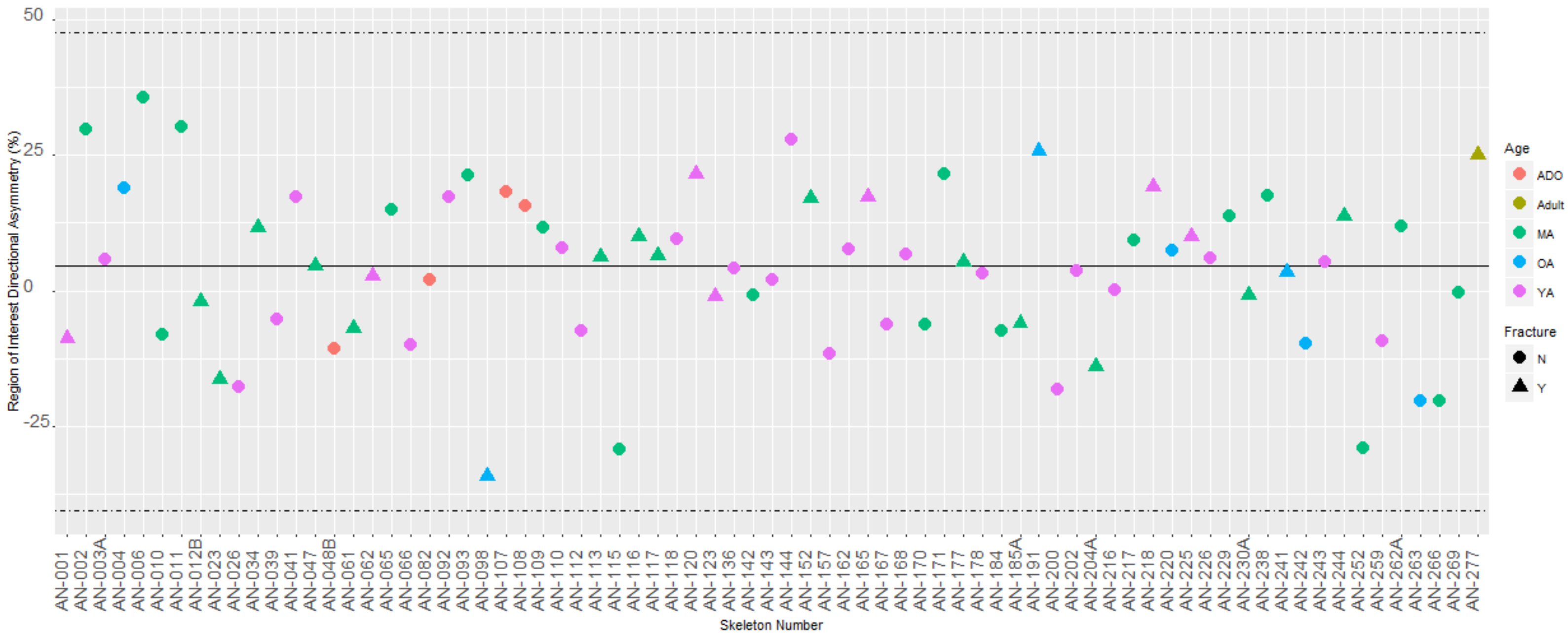

Figure I.19 – Ancaster ulna region of interest area directional asymmetry (%).

I.1.4 – Second Metacarpal Midshaft

Table I.4 – Radiographically measured bone diameters, and calculated bone areas and asymmetries for second metacarpal midshafts at Ancaster.

Skeleton Number	Sex	Age	Side	AP	ap	ML	ml	T_A	M_A	C_A	T_A %DA	M_A %DA	C_A %DA
AN-002*	F	MA	L	8.3	5.1	8.7	5.3	56.7	21.2	35.5	-3.6	-0.1	-5.7
			R	8.1	5.0	8.6	5.4	54.7	21.2	33.5			
AN-006	M	MA	L	8.2	4.0	9.3	4.4	59.9	13.8	46.1	7.8	16.1	5.2
			R	8.5	4.4	9.7	4.7	64.8	16.2	48.5			
AN-010	F	MA	L	7.5	3.9	7.5	3.5	44.2	10.7	33.5	7.8	27.2	0.7
			R	7.7	4.6	7.9	3.9	47.8	14.1	33.7			
AN-011	M	MA	L	9.1	4.2	10.1	4.1	72.2	13.5	58.7	6.2	32.9	-1.3
			R	9.4	4.8	10.4	5.0	76.8	18.8	57.9			
AN-013	M	YA	L	9.9	5.2	9.4	4.6	73.1	18.8	54.3	-33.5	-56.9	-26.4
			R	8.4	3.6	7.9	3.7	52.1	10.5	41.7			
AN-026	M	YA	L	8.1	3.9	9.0	4.3	57.3	13.2	44.1	3.6	48.0	-15.1
			R	8.4	4.8	9.0	5.7	59.4	21.5	37.9			
AN-027	M	MA	L	8.2	4.0	8.6	2.7	55.4	8.5	46.9	10.5	66.7	-5.2
			R	8.7	4.8	9.0	4.5	61.5	17.0	44.5			
AN-045a	F?	MA	L	8.1	3.6	9.3	4.3	59.2	12.2	47.0	-3.8	-6.4	-3.1
			R	7.8	3.3	9.3	4.4	57.0	11.4	45.6			
AN-053	F	MA	L	7.4	4.5	8.6	4.8	50.0	17.0	33.0	2.3	22.2	-9.8
			R	7.4	4.5	8.8	6.0	51.1	21.2	29.9			
AN-062	F	YA	L	7.5	2.8	7.1	3.2	41.8	7.0	34.8	5.4	25.3	0.8
			R	7.7	3.3	7.3	3.5	44.1	9.1	35.1			
AN-067	F	MA	L	8.0	4.8	8.4	5.1	52.8	19.2	33.6	-7.5	-19.1	-1.3
			R	7.7	4.3	8.1	4.7	49.0	15.9	33.1			

Skeleton Number	Sex	Age	Side	AP	ap	ML	ml	T_A	M_A	C_A	T_A %DA	M_A %DA	C_A %DA
AN-102	F	YA	L	8.3	3.5	8.5	3.5	55.4	9.6	45.8	-7.3	-6.6	-7.4
			R	8.0	3.1	8.2	3.7	51.5	9.0	42.5			
AN-107	M?	ADO	L	7.8	4.5	8.9	4.3	54.5	15.2	39.3	5.5	-2.5	8.4
			R	7.8	3.7	9.4	5.1	57.6	14.8	42.8			
AN-109	F	MA	L	8.3	4.4	9.0	5.8	58.7	20.0	38.6	4.6	27.2	-9.7
			R	8.5	5.5	9.2	6.1	61.4	26.4	35.1			
AN-112	F	YA	L	6.8	2.4	8.4	2.8	44.9	5.3	39.6	-5.4	25.0	-10.3
			R	6.6	2.4	8.2	3.6	42.5	6.8	35.7			
AN-113	F	MA	L	8.6	4.0	7.5	3.5	50.7	11.0	39.7	1.7	15.1	-2.3
			R	8.1	3.7	8.1	4.4	51.5	12.8	38.7			
AN-142	F	MA	L	6.9	2.1	7.1	2.4	38.5	4.0	34.5	4.0	46.6	-2.4
			R	6.8	2.7	7.5	3.0	40.1	6.4	33.7			
AN-152	F	MA	L	7.3	3.1	7.5	4.1	43.0	10.0	33.0	4.9	12.1	2.6
			R	7.1	3.5	8.1	4.1	45.2	11.3	33.9			
AN-162	F?	YA	L	7.9	3.5	7.8	3.8	48.4	10.4	38.0	-5.2	-2.7	-5.9
			R	7.5	3.5	7.8	3.7	45.9	10.2	35.8			
AN-168	F	YA	L	6.6	1.8	8.3	2.5	43.0	3.5	39.5	-3.4	10.5	-4.8
			R	6.7	2.0	7.9	2.5	41.6	3.9	37.6			
AN-171	F	MA	L	-	-	-	-	-	-	-	-	-	-
			R	8.0	4.3	7.8	4.2	49.0	14.2	34.8			
AN-178	F?	YA	L	8.4	4.1	8.6	3.8	56.7	12.2	44.5	3.3	-13.0	7.4
			R	8.3	3.8	9.0	3.6	58.7	10.7	47.9			
AN-185a	M	MA	L	-	-	-	-	-	-	-	-	-	-
			R	7.2	2.0	8.9	3.5	50.3	5.5	44.8			
AN-191	F	OA	L	7.0	3.4	7.2	3.7	39.6	9.9	29.7	-8.8	11.0	-16.3
			R	6.5	3.6	7.1	3.9	36.2	11.0	25.2			

Skeleton Number	Sex	Age	Side	AP	ap	ML	ml	T_A	M_A	C_A	T_A %DA	M_A %DA	C_A %DA
AN-202	F	YA	L	7.4	3.0	7.7	2.9	44.8	6.8	37.9	1.4	-10.5	3.4
			R	7.6	2.9	7.6	2.7	45.4	6.1	39.2			
AN-217	F	MA	L	7.6	4.2	8.8	4.3	52.5	14.2	38.3	8.1	2.1	10.2
			R	7.8	4.1	9.3	4.5	57.0	14.5	42.5			
AN-218	F	YA	L	7.1	2.1	7.1	2.3	39.6	3.8	35.8	6.9	32.7	3.7
			R	7.4	2.4	7.3	2.8	42.4	5.3	37.1			
AN-220	F	OA	L	7.5	4.0	7.7	3.8	45.4	11.9	33.4	-	-	-
			R	-	-	-	-	-	-	-			
AN-226	F	YA	L	7.6	3.2	7.5	3.3	44.8	8.3	36.5	-5.5	-23.7	-1.7
			R	7.1	2.6	7.6	3.2	42.4	6.5	35.8			
AN-242	F	OA	L	7.8	3.6	8.2	4.4	50.2	12.4	37.8	3.7	17.1	-1.2
			R	7.9	4.0	8.4	4.7	52.1	14.8	37.4			
AN-259	F	YA	L	6.6	2.0	7.8	1.9	40.4	3.0	37.4	1.5	26.1	-0.8
			R	6.7	1.9	7.8	2.6	41.0	3.9	37.2			
AN-263	F	OA	L	-	-	-	-	-	-	-	-	-	-
			R	7.0	4.4	9.6	6.0	52.8	20.7	32.0			

F=Female; F?=Probable female; U=Unknown sex; M?=Probable male; M=Male; ADO=Adolescent; YA=Young adult; MA=Middle adult; OA=Old adult; L=Left; R=Right; AP=Antero-posterior total width; ap=Antero-posterior medullary width; ML=Medio-lateral total width; ml=Medio-lateral medullary width; T_A=Total area; M_A=Medullary area; C_A=Cortical area; T_A%DA=Total area directional asymmetry; M_A%DA=Medullary area directional asymmetry; C_A%DA=Cortical area directional asymmetry.

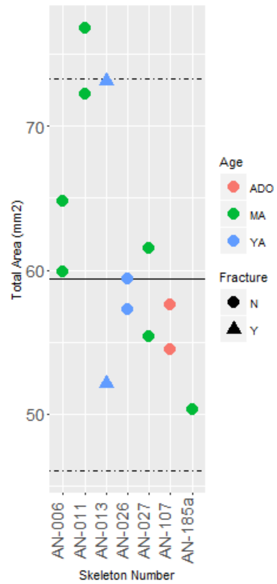

Figure I.20 – Ancaster male MC2 midshaft total areas (mm^2).

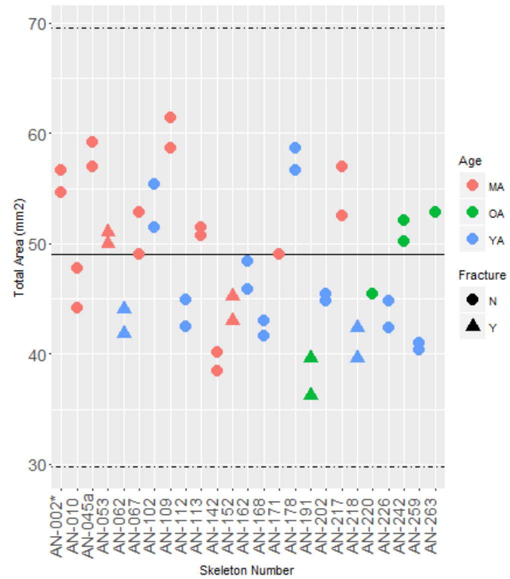

Figure I.21 – Ancaster female MC2 midshaft total areas (mm^2).

Figure I.22 – Ancaster male MC2 midshaft cortical areas (mm^2).

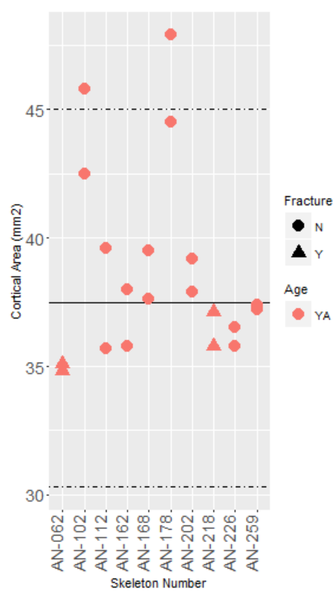

Figure I.23 – Ancaster young adult female MC2 midshaft cortical areas (mm^2).

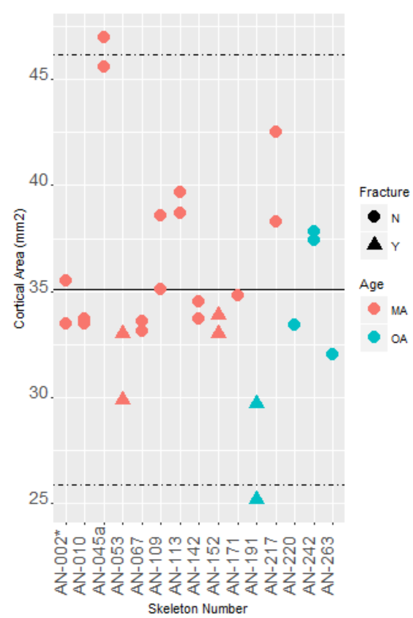

Figure I.24 – Ancaster middle and old adult female MC2 midshaft cortical areas (mm^2).

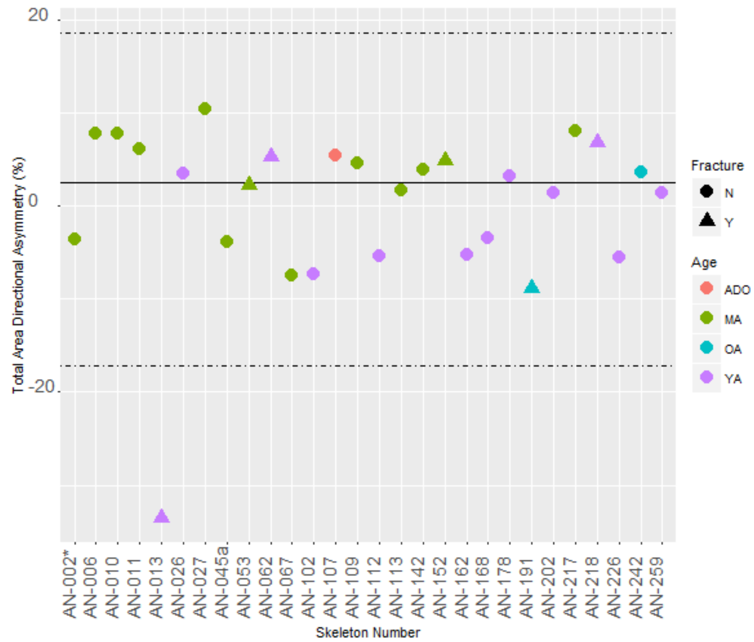

Figure I.25 – Ancaster second metacarpal midshaft total area directional asymmetry (%).

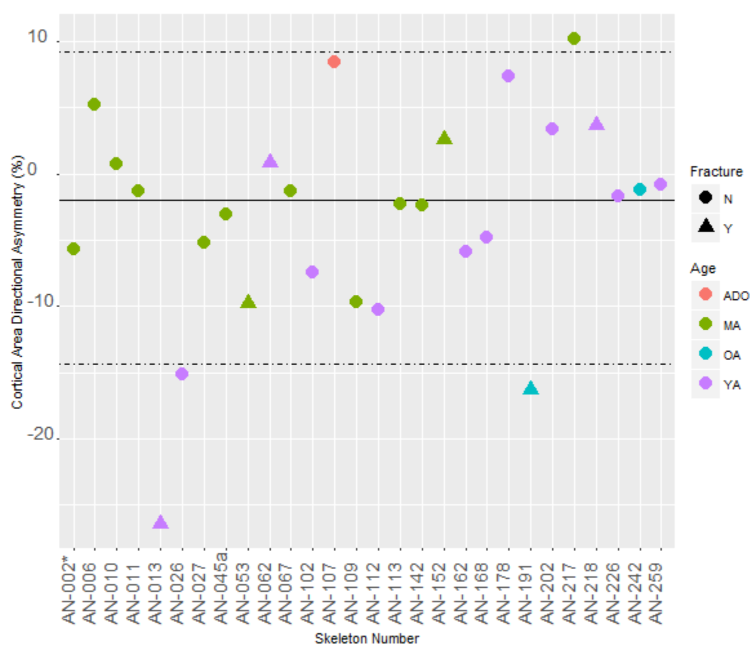

Figure I.26 – Ancaster second metacarpal midshaft cortical area directional asymmetry (%).

I.1.5 – Second Metacarpal Region of Interest

Table I.5 – Radiographically measured bone diameters, and calculated bone areas and asymmetries for second metacarpal region of interests at Ancaster.

Skeleton Number	Sex	Age	L ROI	R ROI	ROI %DA
AN-002*	F	MA	59.5	64.4	-7.9
AN-006	M	MA	85.8	87.2	-1.6
AN-010	F	MA	61.3	61.6	-0.5
AN-011	M	MA	88.2	97.7	-10.2
AN-013	M	YA	88.7	85.1	4.1
AN-026	M	YA	57.2	84.7	-38.8
AN-027	M	MA	66.4	78.6	-16.8
AN-045a	F?	MA	88.6	92.3	-4.1
AN-053	F	MA	52.5	60.4	-14.0
AN-062	F	YA	76.7	84.6	-9.8
AN-067	F	MA	62.1	61.1	1.6
AN-102	F	YA	94.8	90.6	4.5
AN-107	M?	ADO	79.4	71.3	10.7
AN-109	F	MA	50.8	55.1	-8.1
AN-112	F	YA	82.7	84.3	-1.9
AN-113	F	MA	63.6	70.2	-9.9
AN-142	F	MA	77.8	82.6	-6.0
AN-152	F	MA	62.6	61.9	1.1
AN-162	F?	YA	69.8	77.1	-9.9
AN-168	F	YA	83.0	82.0	1.2
AN-171	F	MA	61.8	66.5	-7.3
AN-178	F?	YA	81.4	84.1	-3.3
AN-185a	M	MA	87.8	85.9	2.2
AN-191	F	OA	51.9	58.1	-11.3
AN-202	F	YA	84.8	80.0	5.8
AN-217	F	MA	55.1	55.4	-0.5
AN-218	F	YA	82.4	85.8	-4.0
AN-220	F	OA	61.2	65.6	-6.9
AN-226	F	YA	77.6	79.2	-2.0
AN-242	F	OA	58.4	59.3	-1.5
AN-259	F	YA	83.2	82.2	1.2
AN-263	F	OA	45.8	45.3	1.1

F=Female; F?=Probable female; U=Unknown sex; M?=Probable male; M=Male; ADO=Adolescent; YA=Young adult; MA=Middle adult; OA=Old adult; L=Left; R=Right; ROI=Region of interest; directional asymmetry; ROI%DA=Region of interest area directional asymmetry

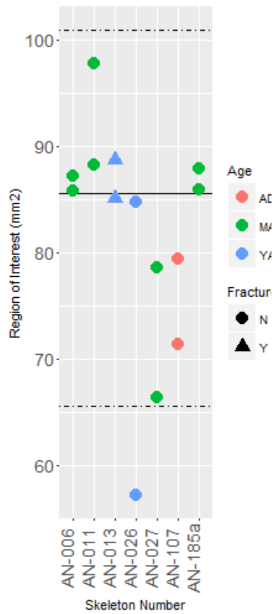

Figure I.27 – Ancaster male MC2 region of interest areas (mm^2).

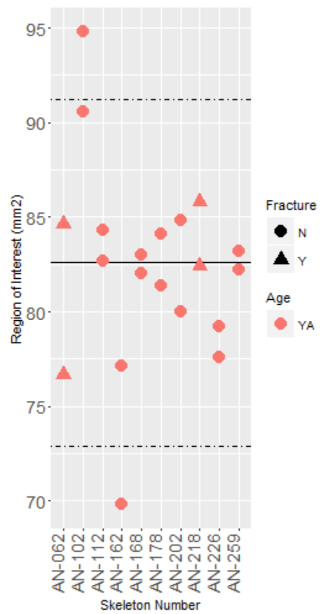

Figure I.28 – Ancaster young adult female MC2 region of interest areas (mm^2).

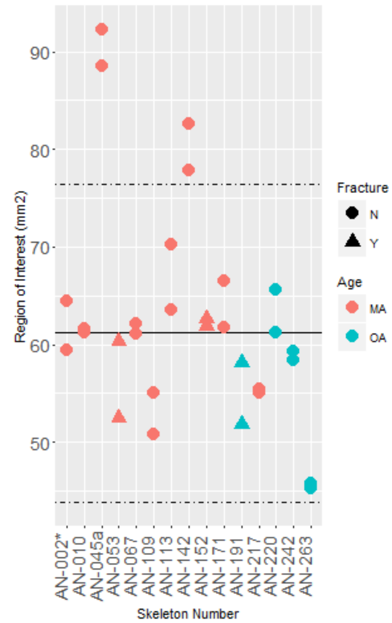

Figure I.29 – Ancaster middle and old adult female MC2 region of interest areas (mm^2).

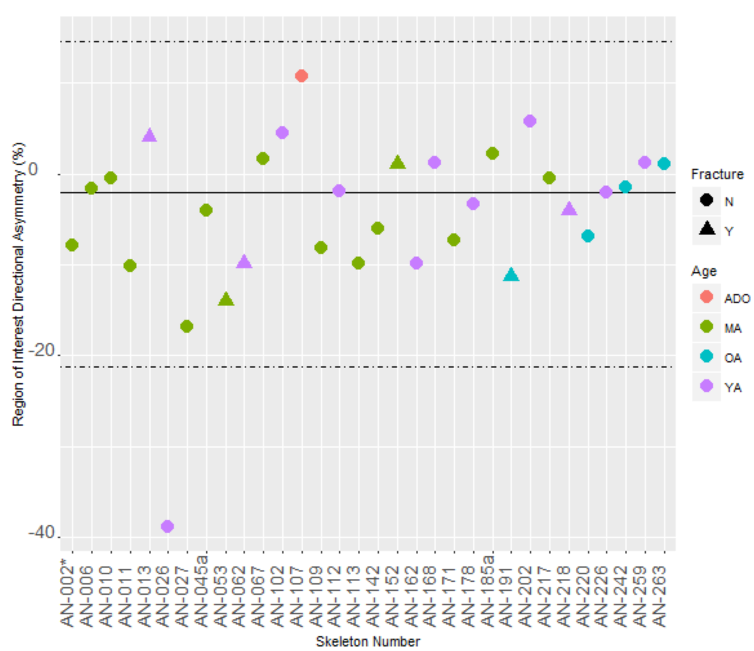

Figure I.30 – Ancaster second metacarpal region of interest area directional asymmetry (%).

I.1.6 - Tibia

Table I.6 – Radiographically measured bone diameters, and calculated bone areas and asymmetries for tibiae at Ancaster.

Skeleton Number	Sex	Age	Side	AP	ap	ML	ml	T_A	M_A	C_A	T_A %DA	M_A %DA	C_A %DA
AN-001	F?	YA	L	19.9	7.7	24.0	6.8	375.1	41.1	334.0	3.7	54.3	-5.0
			R	20.4	10.5	24.3	8.7	389.3	71.7	317.6			
AN-002*	F	MA	L	20.8	11.2	22.3	10.5	364.3	92.4	271.9	-0.5	2.3	-1.5
			R	20.6	12.8	22.4	9.4	362.4	94.5	267.9			
AN-003A	F	YA	L	21.8	11.9	22.8	11.2	390.4	104.7	285.7	-1.3	0.1	-1.9
			R	21.7	11.6	22.6	11.5	385.2	104.8	280.4			
AN-005	M	MA	L	28.6	14.0	25.0	9.3	561.6	102.3	459.3	-11.5	-10.0	-11.9
			R	27.7	12.8	23.0	9.2	500.4	92.5	407.9			
AN-006	M	MA	L	26.2	13.2	28.0	11.9	576.2	123.4	452.8	-32.7	-38.8	-31.1
			R	25.6	10.3	20.6	10.3	414.2	83.3	330.9			
AN-010	F	MA	L	20.0	13.6	20.9	10.3	328.3	110.0	218.3	1.0	0.5	1.2
			R	19.1	12.8	22.1	11.0	331.5	110.6	220.9			
AN-011	M	MA	L	24.5	8.5	26.7	7.5	513.8	50.1	463.7	2.8	13.3	1.6
			R	25.1	10.4	26.8	7.0	528.3	57.2	471.1			
AN-012B	M	MA	L	29.0	12.3	27.5	11.0	626.4	106.3	520.1	-5.0	14.9	-9.6
			R	26.8	13.2	28.3	11.9	595.7	123.4	472.3			
AN-013	M	YA	L	20.8	10.8	29.2	11.2	477.0	95.0	382.0	14.4	19.8	13.0
			R	23.0	11.8	30.5	12.5	551.0	115.8	435.1			
AN-023	M	MA	L	19.0	8.5	22.8	7.9	340.2	52.7	287.5	-1.9	16.3	-5.7
			R	18.8	8.5	22.6	9.3	333.7	62.1	271.6			
AN-026	M	YA	L	21.8	11.9	26.7	10.5	457.1	98.1	359.0	-11.3	-1.8	-14.1
			R	21.3	11.8	24.4	10.4	408.2	96.4	311.8			
AN-027	M	MA	L	21.9	10.5	26.9	9.9	462.7	81.6	381.0	-20.8	10.4	-28.9
			R	20.7	11.2	23.1	10.3	375.6	90.6	285.0			
AN-039	M?	YA	L	28.1	13.8	29.2	11.2	644.4	121.4	523.0	-0.6	2.0	-1.2
			R	27.2	14.6	30.0	10.8	640.9	123.8	517.0			
AN-041	F	YA	L	20.2	9.7	24.0	9.3	380.8	70.9	309.9	5.1	8.7	4.2
			R	20.9	10.7	24.4	9.2	400.5	77.3	323.2			

Skeleton Number	Sex	Age	Side	AP	ap	ML	ml	T_A	M_A	C_A	T_A %DA	M_A %DA	C_A %DA
AN-045A	F?	MA	L	23.5	12.8	24.7	7.9	455.9	79.4	376.5	-1.7	7.3	-3.8
			R	24.8	12.5	23.0	8.7	448.0	85.4	362.6			
AN-046	M?	YA	L	25.4	9.4	29.3	11.0	584.5	81.2	503.3	3.5	-10.6	5.6
			R	24.4	10.0	31.6	9.3	605.6	73.0	532.5			
AN-047	M	MA	L	22.8	12.4	30.4	11.8	516.5	100.3	416.2	0.0	0.0	0.0
			R	22.6	11.3	29.1	11.3	516.5	100.3	416.2			
AN-048B	M?	ADO	L	24.7	11.0	27.6	9.3	510.2	81.2	429.0	-8.4	-11.5	-7.9
			R	22.7	9.8	26.3	9.4	468.9	72.4	396.5			
AN-050	M	OA	L	24.8	14.1	24.2	10.4	471.4	115.2	356.2	9.4	10.3	9.1
			R	23.8	13.0	27.7	12.5	517.8	127.6	390.2			
AN-052	F	MA	L	19.5	9.7	22.4	8.5	343.1	64.8	278.3	4.2	9.0	3.1
			R	21.0	11.0	21.7	8.2	357.9	70.8	287.1			
AN-053	F	MA	L	18.9	11.8	21.9	9.9	325.1	91.8	233.3	8.1	24.1	1.0
			R	18.7	12.2	24.0	12.2	352.5	116.9	235.6			
AN-056	M	MA	L	23.5	8.6	28.1	9.9	518.6	66.9	451.8	-16.5	3.7	-19.8
			R	22.3	9.3	25.1	9.5	439.6	69.4	370.2			
AN-057	M	MA	L	22.5	10.9	26.7	10.4	471.8	89.0	382.8	-3.5	17.5	-9.1
			R	23.3	12.4	24.9	10.9	455.7	106.2	349.5			
AN-058	?	OA	L	25.9	9.4	25.3	11.3	514.6	83.4	431.2	-3.6	-9.2	-2.5
			R	24.8	10.2	25.5	9.5	496.7	76.1	420.6			
AN-061	M	MA	L	19.8	9.9	28.2	8.7	438.5	67.6	370.9	5.5	-54.4	13.5
			R	21.0	7.7	28.1	6.4	463.5	38.7	424.8			
AN-062	F	YA	L	-	-	-	-	-	-	-	-	-	-
			R	22.0	11.7	22.4	10.3	387.0	94.6	292.4			
AN-064	M?	MA	L	21.1	9.8	29.3	9.8	485.6	75.4	410.1	-11.5	-31.8	-8.2
			R	21.6	8.4	25.5	8.3	432.6	54.8	377.8			
AN-065	M	MA	L	25.1	11.1	22.6	7.9	445.5	68.9	376.7	-0.2	8.5	-1.9
			R	26.2	11.1	21.6	8.6	444.5	75.0	369.5			
AN-066	F	YA	L	20.2	9.8	19.5	7.4	309.4	57.0	252.4	6.1	2.6	6.8
			R	19.2	9.3	21.8	8.0	328.7	58.4	270.3			

Skeleton Number	Sex	Age	Side	AP	ap	ML	ml	T_A	M_A	C_A	T_A %DA	M_A %DA	C_A %DA
AN-067	F	MA	L	25.6	13.5	22.6	10.2	454.4	108.1	346.3	1.5	31.0	-10.0
			R	25.2	14.7	23.3	12.8	461.2	147.8	313.4			
AN-072	F	YA	L	18.6	12.1	24.4	12.7	356.4	120.7	235.8	13.6	-14.5	25.3
			R	20.0	12.9	26.0	10.3	408.4	104.4	304.1			
AN-092	M	YA	L	22.8	8.5	23.0	7.3	411.9	48.7	363.1	-5.6	32.4	-12.1
			R	21.0	8.6	23.6	10.0	389.2	67.5	321.7			
AN-093	M	MA	L	26.9	11.0	27.6	9.7	583.1	83.8	499.3	7.9	55.7	-3.4
			R	28.3	13.6	28.4	13.9	631.2	148.5	482.8			
AN-098	M	OA	L	23.6	11.2	26.5	12.0	491.2	105.6	385.6	13.4	1.4	16.5
			R	24.5	10.9	29.2	12.5	561.9	107.0	454.9			
AN-104	F?	MA	L	21.4	9.8	22.9	10.9	384.9	83.9	301.0	3.3	10.6	1.1
			R	21.1	10.9	24.0	10.9	397.7	93.3	304.4			
AN-107	M?	ADO	L	23.9	9.5	26.5	10.3	497.4	76.9	420.6	-5.8	-14.9	-4.2
			R	24.2	8.1	24.7	10.4	469.5	66.2	403.3			
AN-108	M?	ADO	L	23.0	11.0	26.1	9.6	471.5	82.9	388.5	0.4	-23.6	4.8
			R	24.2	9.8	24.9	8.5	473.3	65.4	407.8			
AN-109	F	MA	L	22.1	14.3	25.0	11.0	433.9	123.5	310.4	12.1	4.0	15.2
			R	23.9	14.0	26.1	11.7	489.9	128.6	361.3			
AN-110	M?	YA	L	23.1	12.5	26.8	11.6	486.2	113.9	372.3	3.9	-18.2	9.8
			R	24.1	12.2	26.7	9.9	505.4	94.9	410.5			
AN-112	F	YA	L	19.5	7.8	22.3	6.9	341.5	42.3	299.3	-4.9	-16.9	-3.3
			R	20.1	7.7	20.6	5.9	325.2	35.7	289.5			
AN-113	F	MA	L	23.9	16.7	24.1	15.1	452.4	198.1	254.3	1.7	-29.4	20.5
			R	24.0	15.9	24.4	11.8	459.9	147.4	312.6			
AN-115	F	MA	L	20.7	8.9	23.4	7.9	380.4	55.2	325.2	4.6	21.5	1.5
			R	23.6	9.8	21.5	8.9	398.5	68.5	330.0			
AN-116	F?	MA	L	21.7	9.7	24.3	8.0	414.1	60.9	353.2	3.9	-22.5	7.8
			R	21.0	8.6	26.1	7.2	430.5	48.6	381.8			
AN-117	M?	MA	L	23.1	9.0	27.5	8.8	498.9	62.2	436.7	2.6	-0.8	3.1
			R	21.8	7.7	29.9	10.2	511.9	61.7	450.3			
AN-118	M?	YA	L	23.8	12.2	31.6	12.4	590.7	118.8	471.9	-6.2	4.2	-9.0
			R	22.8	11.6	31.0	13.6	555.1	123.9	431.2			

Skeleton Number	Sex	Age	Side	AP	ap	ML	ml	T_A	M_A	C_A	T_A %DA	M_A %DA	C_A %DA
AN-120	M	YA	L	25.4	10.2	28.6	8.0	570.5	64.1	506.5	-9.8	60.6	-24.1
			R	22.1	12.3	29.8	12.4	517.2	119.8	397.5			
AN-123	F	YA	L	20.9	9.1	21.5	7.4	352.9	52.9	300.0	6.0	18.0	3.8
			R	21.6	9.6	22.1	8.4	374.9	63.3	311.6			
AN-134	F?	MA	L	23.3	8.8	22.6	8.5	413.6	58.7	354.8	-9.0	49.3	-23.3
			R	22.6	11.9	21.3	10.4	378.1	97.2	280.9			
AN-136	M	YA	L	25.3	12.2	26.7	9.5	530.5	91.0	439.5	2.7	24.5	-2.5
			R	24.1	10.9	28.8	13.6	545.1	116.4	428.7			
AN-142	F	MA	L	20.2	8.9	22.2	8.5	352.2	59.4	292.8	-1.3	6.6	-3.0
			R	20.3	9.4	21.8	8.6	347.6	63.5	284.1			
AN-143	M	YA	L	21.0	11.0	23.9	10.1	394.2	87.3	306.9	13.1	-9.1	18.6
			R	22.8	11.8	25.1	8.6	449.5	79.7	369.8			
AN-144	M	YA	L	24.8	10.3	28.2	10.1	549.3	81.7	467.6	-11.4	-8.2	-12.0
			R	23.9	9.4	26.1	10.2	489.9	75.3	414.6			
AN-152	F	MA	L	21.6	9.3	21.8	10.0	369.8	73.0	296.8	-0.1	-6.3	1.3
			R	20.9	9.7	22.5	9.0	369.3	68.6	300.8			
AN-154	F	ADULT	L	17.7	10.3	21.6	9.2	300.3	74.4	225.8	6.8	23.4	0.6
			R	18.6	11.2	22.0	10.7	321.4	94.1	227.3			
AN-155	F?	ADULT	L	21.5	12.7	26.0	13.9	439.0	138.6	300.4	-15.8	3.1	-25.7
			R	21.4	13.0	22.3	14.0	374.8	142.9	231.9			
AN-157	F	YA	L	23.2	10.3	22.6	8.3	411.8	67.1	344.7	-15.7	-22.7	-14.4
			R	22.4	8.3	20.0	8.2	351.9	53.5	298.4			
AN-162	F?	YA	L	23.6	12.9	23.7	9.4	439.3	95.2	344.1	-0.9	4.1	-2.3
			R	23.7	13.3	23.4	9.5	435.6	99.2	336.3			
AN-165	M	YA	L	23.3	12.2	23.3	10.4	426.4	99.7	326.7	0.0	-0.3	0.1
			R	23.4	12.4	23.2	10.2	426.4	99.3	327.0			
AN-167	M?	YA	L	21.7	11.7	26.9	11.6	458.5	106.6	351.9	-5.5	-30.0	0.9
			R	23.4	9.2	23.6	10.9	433.7	78.8	355.0			
AN-168	F	YA	L	19.7	9.9	24.8	7.9	383.7	61.4	322.3	-7.4	-18.9	-5.3
			R	21.4	8.4	21.2	7.7	356.3	50.8	305.5			

Skeleton Number	Sex	Age	Side	AP	ap	ML	ml	T_A	M_A	C_A	T_A %DA	M_A %DA	C_A %DA
AN-170	M	MA	L	22.9	8.4	27.6	9.4	496.4	62.0	434.4	9.4	18.9	8.0
			R	24.9	10.6	27.9	9.0	545.6	74.9	470.7			
AN-171	F	MA	L	21.9	12.3	20.1	8.8	345.7	85.0	260.7	5.3	-10.5	10.0
			R	21.8	11.2	21.3	8.7	364.7	76.5	288.2			
AN-172	F?	MA	L	20.9	11.7	22.8	11.9	374.3	109.4	264.9	21.4	-24.2	35.3
			R	21.8	10.7	27.1	10.2	464.0	85.7	378.3			
AN-177	M	MA	L	27.6	12.4	29.5	6.6	639.5	64.3	575.2	-16.7	-11.8	-17.3
			R	26.8	10.1	25.7	7.2	541.0	57.1	483.8			
AN-178	F?	YA	L	20.7	11.3	26.3	9.3	427.6	82.5	345.0	-7.4	-7.0	-7.5
			R	21.6	11.8	23.4	8.3	397.0	76.9	320.0			
AN-184	M	MA	L	28.0	12.0	25.6	12.9	563.0	121.6	441.4	-4.1	-1.1	-4.9
			R	27.2	13.2	25.3	11.6	540.5	120.3	420.2			
AN-185A	M	MA	L	19.4	6.1	24.1	7.2	367.2	34.5	332.7	-1.0	7.9	-1.9
			R	18.3	7.2	25.3	6.6	363.6	37.3	326.3			
AN-191	F	OA	L	17.2	9.0	25.6	8.9	345.8	62.9	282.9	3.8	27.2	-2.2
			R	17.6	9.4	26.0	11.2	359.4	82.7	276.7			
AN-202	F	YA	L	20.5	11.7	24.3	7.8	391.2	71.7	319.6	1.5	-16.7	5.1
			R	20.3	9.3	24.9	8.3	397.0	60.6	336.4			
AN-204A	M	MA	L	27.1	12.3	26.9	10.1	572.5	97.6	475.0	-8.4	-14.0	-7.3
			R	25.2	12.7	26.6	8.5	526.5	84.8	441.7			
AN-210	M?	YA	L	26.5	11.9	26.6	9.3	553.6	86.9	466.7	3.9	5.7	3.6
			R	25.1	12.6	29.2	9.3	575.6	92.0	483.6			
AN-211	M?	YA	L	26.5	13.2	26.0	11.7	541.1	121.3	419.8	-8.7	-11.6	-7.9
			R	26.1	12.5	24.2	11.0	496.1	108.0	388.1			
AN-216	M?	YA	L	26.6	9.1	26.3	12.3	549.4	87.9	461.5	3.4	5.8	2.9
			R	26.9	10.5	26.9	11.3	568.3	93.2	475.1			
AN-217	F	MA	L	22.2	14.0	22.3	11.6	388.8	127.5	261.3	7.5	-23.8	19.7
			R	22.7	12.3	23.5	10.4	419.0	100.5	318.5			
AN-218	F	YA	L	-	-	-	-	-	-	-	-	-	-
			R	17.9	8.7	21.8	6.2	306.5	42.4	264.1			

Skeleton Number	Sex	Age	Side	AP	ap	ML	ml	T_A	M_A	C_A	T_A %DA	M_A %DA	C_A %DA
AN-220	F	OA	L	21.6	12.1	24.8	10.2	420.7	96.9	323.8	-13.3	-25.0	-10.1
			R	21.7	10.0	21.6	9.6	368.1	75.4	292.7			
AN-225	M	YA	L	24.9	13.0	29.3	9.9	573.0	101.1	471.9	13.1	9.1	14.0
			R	27.1	13.3	30.7	10.6	653.4	110.7	542.7			
AN-226	F	YA	L	20.4	10.0	20.0	8.5	320.4	66.8	253.7	1.0	-17.4	5.3
			R	20.7	8.5	19.9	8.4	323.5	56.1	267.5			
AN-229	M	MA	L	27.7	13.5	25.5	8.7	554.8	92.2	462.5	2.0	-29.0	7.2
			R	27.5	10.2	26.2	8.6	565.9	68.9	497.0			
AN-230A	M	MA	L	25.2	11.5	26.1	9.8	516.6	88.5	428.1	4.1	-8.7	6.5
			R	29.4	12.6	23.3	8.2	538.0	81.1	456.9			
AN-238	M	MA	L	22.0	11.8	25.3	10.1	437.2	93.6	343.5	5.8	-20.6	12.0
			R	22.1	10.2	26.7	9.5	463.4	76.1	387.3			
AN-241	F	OA	L	18.8	9.5	25.7	10.3	379.5	76.9	302.6	19.2	40.5	12.9
			R	21.7	12.0	27.0	12.3	460.2	115.9	344.2			
AN-242	F	OA	L	21.8	8.2	21.8	7.5	373.3	48.3	325.0	-	-	-
			R	-	-	-	-	-	-	-			
AN-243	F	YA	L	21.1	11.5	22.2	10.1	367.9	91.2	276.7	-0.3	-2.9	0.6
			R	22.9	12.4	20.4	9.1	366.9	88.6	278.3			
AN-244	M	YA	L	26.2	10.1	23.9	9.3	491.8	73.8	418.0	-6.4	-3.8	-6.8
			R	24.9	10.9	23.6	8.3	461.5	71.1	390.5			
AN-247	F	YA	L	21.3	11.9	22.1	8.4	369.7	78.5	291.2	7.7	-5.2	10.9
			R	23.0	10.1	22.1	9.4	399.2	74.6	324.7			
AN-252	M	MA	L	24.9	13.2	26.6	14.4	520.2	149.3	370.9	-0.4	-25.2	8.2
			R	24.0	11.8	27.5	12.5	518.4	115.8	402.5			
AN-259	F	YA	L	18.3	7.3	21.9	10.7	314.8	61.3	253.4	-3.6	3.6	-5.4
			R	17.9	8.1	21.6	10.0	303.7	63.6	240.0			
AN-262A	F	MA	L	21.8	9.5	22.8	8.7	390.4	64.9	325.5	-1.8	-0.4	-2.0
			R	22.1	8.4	22.1	9.8	383.6	64.7	318.9			
AN-263	F	OA	L	19.9	15.1	27.8	17.8	434.5	211.1	223.4	-0.8	24.6	-32.5
			R	22.5	18.6	24.4	18.5	431.2	270.3	160.9			

Skeleton Number	Sex	Age	Side	AP	ap	ML	ml	T_A	M_A	C_A	T_A %DA	M_A %DA	C_A %DA
AN-266	M?	MA	L	22.1	10.7	23.3	7.4	404.4	62.2	342.2	0.1	19.5	-3.9
			R	22.6	10.7	22.8	9.0	404.7	75.6	329.1			
AN-269	M	MA	L	24.1	11.2	24.7	6.0	467.5	52.8	414.7	-13.0	-12.5	-13.0
			R	24.2	7.8	21.6	7.6	410.5	46.6	364.0			
AN-277	F?	ADULT	L	22.1	11.8	23.3	7.8	404.4	72.3	332.1	-14.5	-7.6	-16.0
			R	19.8	10.4	22.5	8.2	349.9	67.0	282.9			

F=Female; F?=Probable female; U=Unknown sex; M?=Probable male; M=Male; ADO=Adolescent; YA=Young adult; MA=Middle adult; OA=Old adult; L=Left; R=Right; AP=Antero-posterior total width; ap=Antero-posterior medullary width; ML=Medio-lateral total width; ml=Medio-lateral medullary width; T_A=Total area; M_A=Medullary area; C_A=Cortical area; T_A%DA=Total area directional asymmetry; M_A%DA=Medullary area directional asymmetry; C_A%DA=Cortical area directional asymmetry.

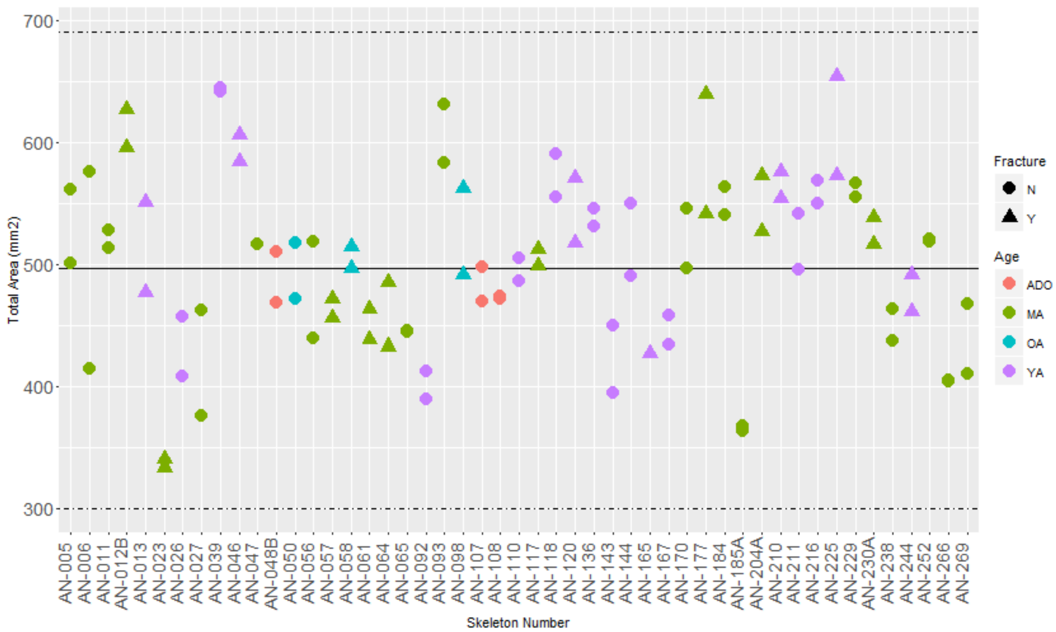

Figure I.31 – Ancaster male tibial total areas (mm^2).

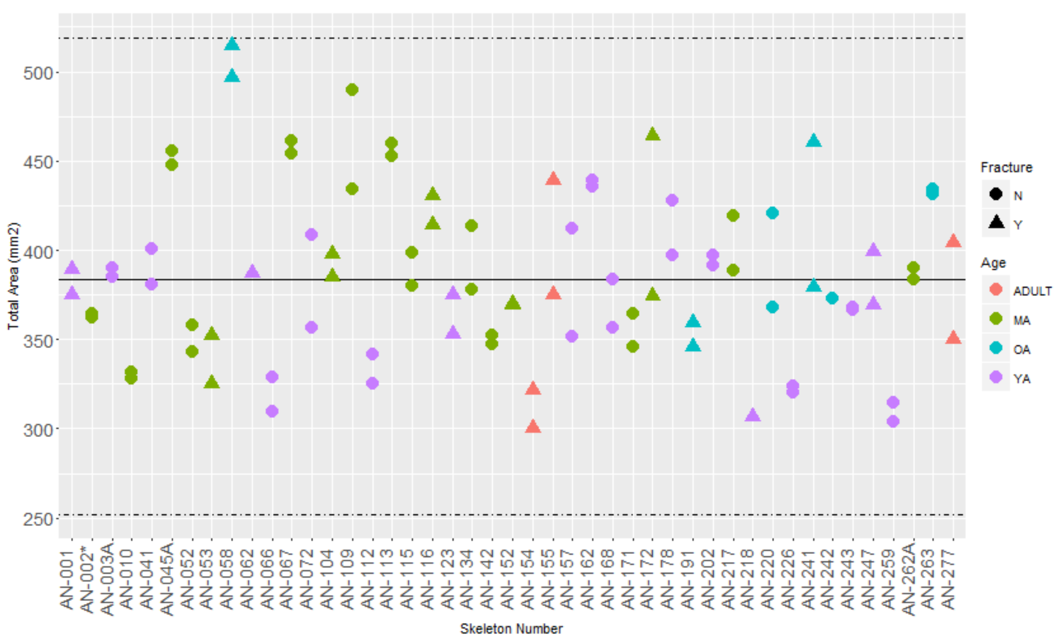

Figure I.32 – Ancaster female tibial total areas (mm^2).

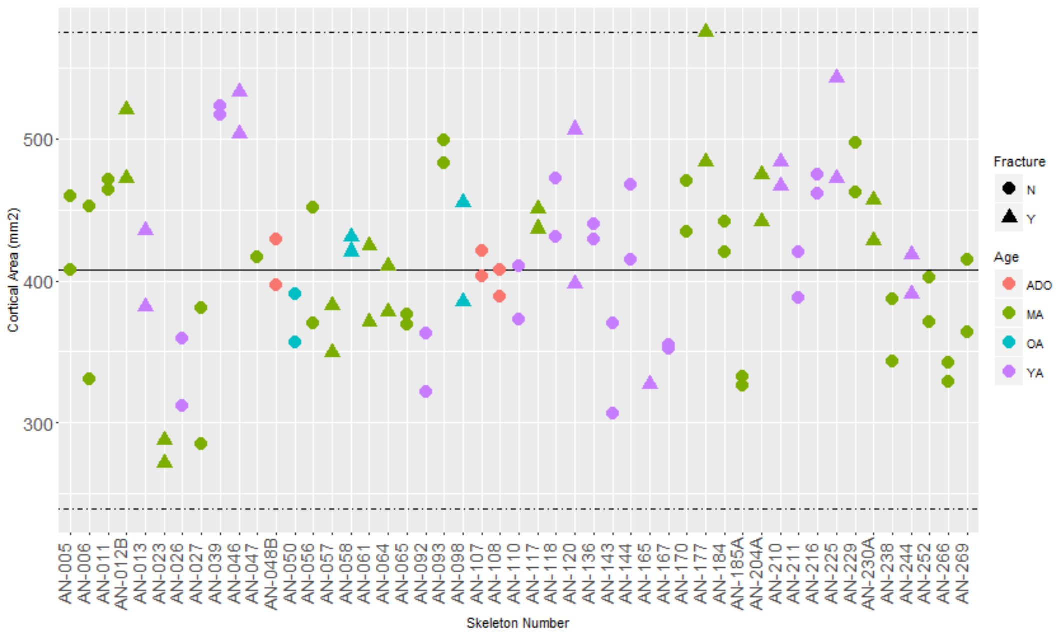

Figure I.33 – Ancaster male tibial cortical areas (mm^2).

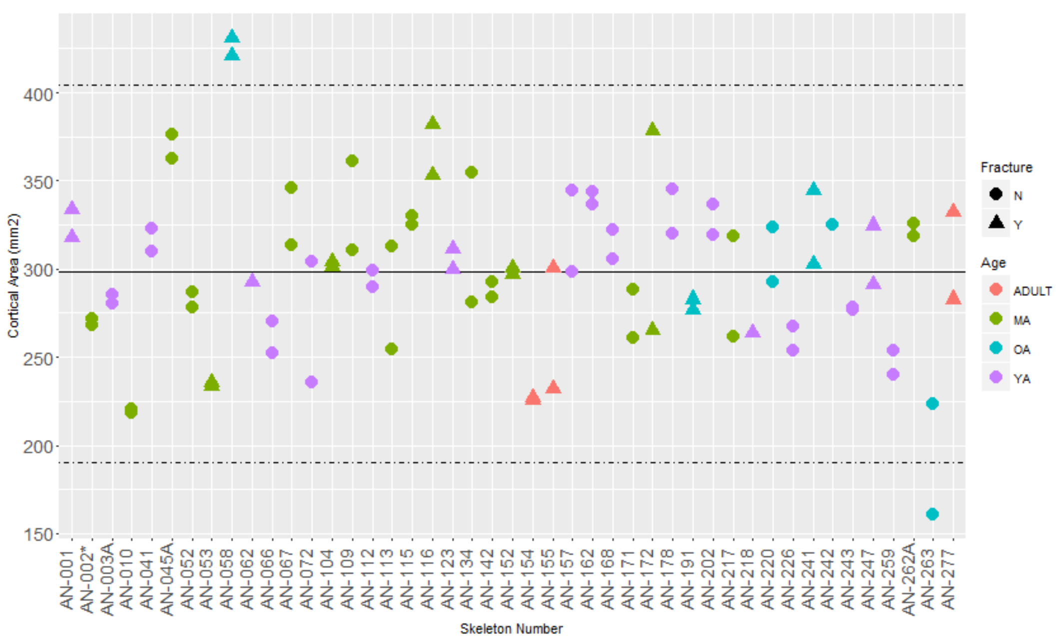

Figure I.34 – Ancaster female tibial cortical areas (mm^2). Individual AN-058 is of unknown sex, because the cortical areas fall within the range of normal for males this individual was not considered an outlier.

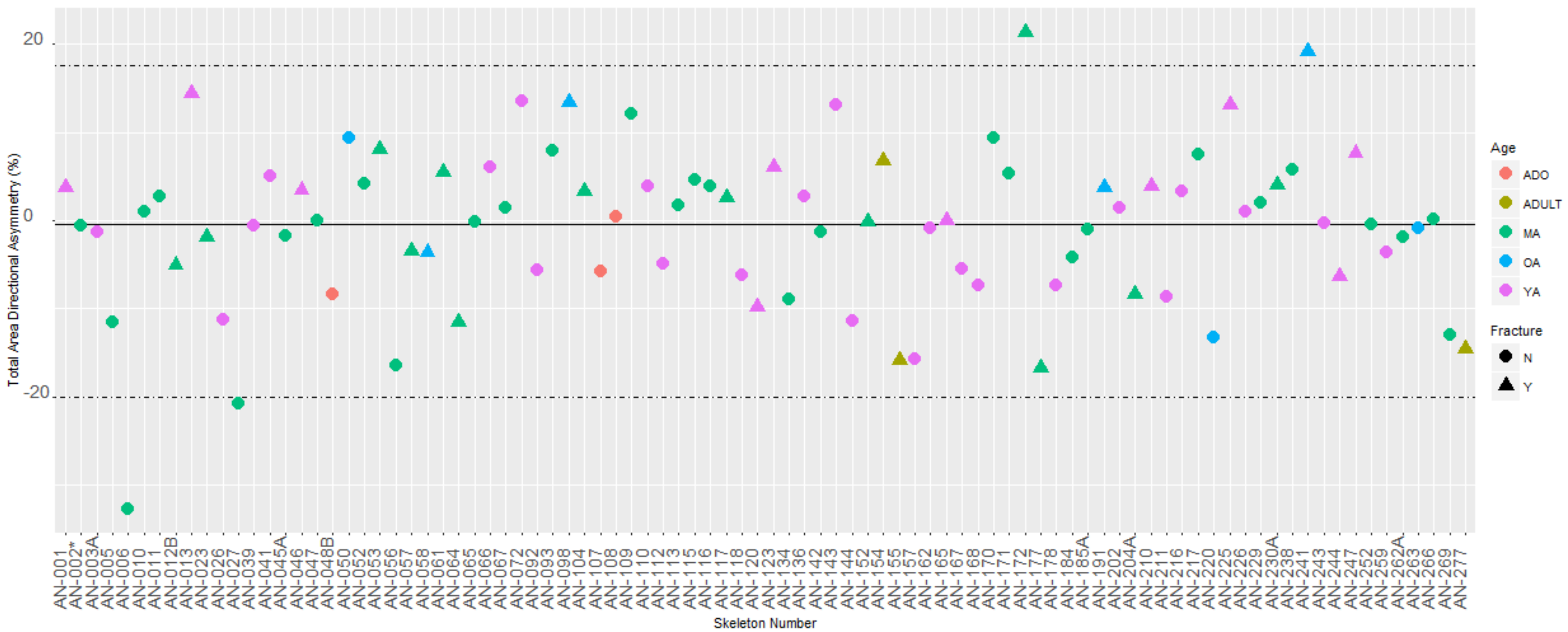

Figure I.35 – Ancaster tibial total area directional asymmetry (%).

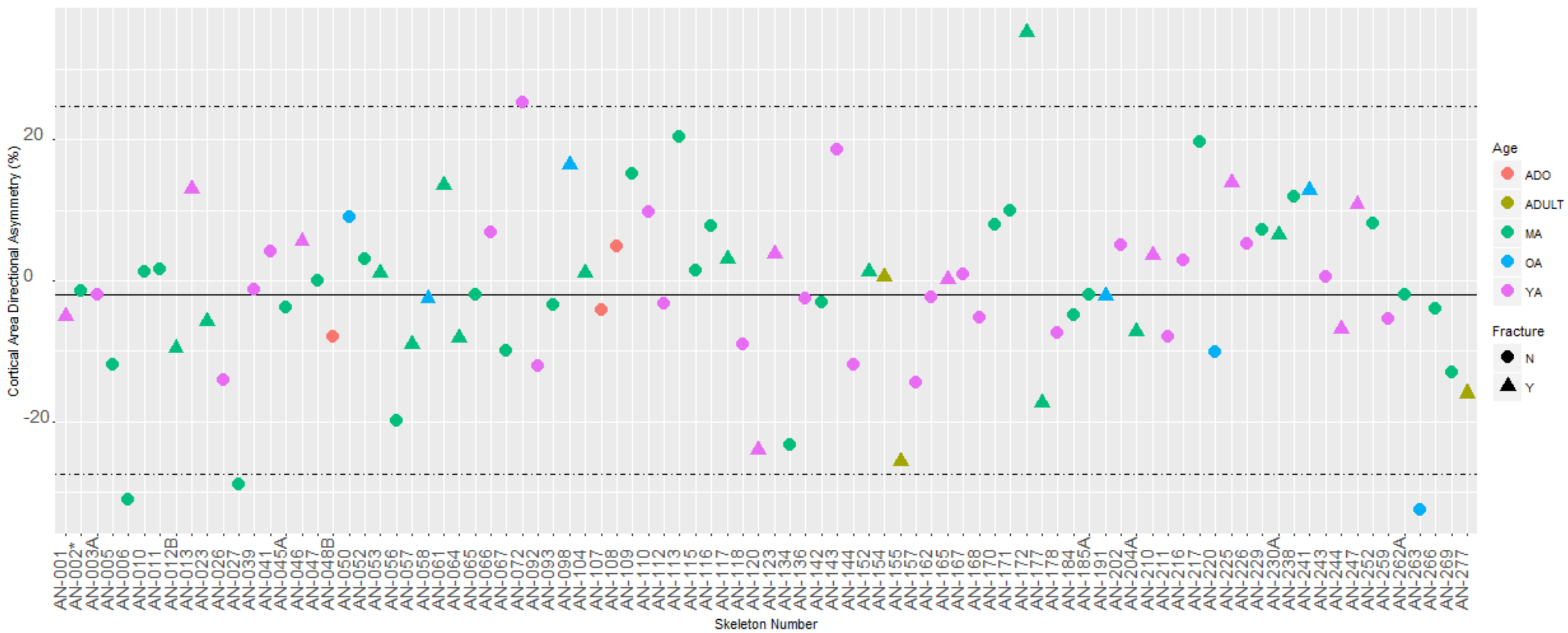

Figure I.36 – Ancaster tibial cortical area directional asymmetry (%).

I.1.7 – Second Metatarsal Region of Interest

Table I.7 – Radiographically measured bone diameters, and calculated bone areas and asymmetries for second metatarsal region of interests at Ancaster.

Skeleton Number	Sex	Age	L ROI	R ROI	ROI %DA
AN-003A	F	YA	90.1	91.8	1.9
AN-010	F	MA	67.9	72.9	7.1
AN-011	M	MA	107.6	114.7	6.4
AN-013	M	YA	105.7	93.3	-12.5
AN-026	M	YA	101.4	121.4	18.0
AN-027	M	MA	124.6	120.9	-3.0
AN-039	M?	YA	106.6	101.9	-4.5
AN-041	F	YA	102.2	104.3	2.0
AN-045A	F?	MA	110.2	96.1	-13.7
AN-056	M	MA	95.8	99.7	4.0
AN-058	?	OA	84.7	85.8	1.3
AN-061	M	MA	96.1	96.5	0.4
AN-064	M?	MA	80.8	88.2	8.8
AN-065	M	MA	96.8	91.0	-6.2
AN-066	F	YA	99.9	97.3	-2.6
AN-067	F	MA	57.7	68.1	16.5
AN-093	M	MA	101.4	122.8	19.1
AN-107	M?	ADO	102.8	116.7	12.7
AN-109	F	MA	91.6	83.1	-9.7
AN-110	M?	YA	86.6	-	-
AN-112	F	YA	84.3	87.9	4.2
AN-113	F	MA	83.1	81.5	-1.9
AN-116	F?	MA	95.6	87.2	-9.2
AN-117	M?	MA	99.5	94.9	-4.7
AN-120	M	YA	85.1	90.1	5.7
AN-136	M	YA	92.4	103.9	11.7
AN-142	F	MA	80.7	95.7	17.0
AN-143	M	YA	111.0	95.3	-15.2
AN-152	F	MA	65.4	68.7	4.9
AN-162	F?	YA	114.5	95.5	-18.1
AN-165	M	YA	111.2	113.0	1.6
AN-168	F	YA	111.2	103.8	-6.9
AN-170	M	MA	89.7	75.9	-16.7
AN-171	F	MA	91.1	87.2	-4.4
AN-178	F?	YA	105.4	109.7	4.0

Skeleton Number	Sex	Age	L ROI	R ROI	ROI %DA
AN-184	M	MA	89.7	89.0	-0.8
AN-185A	M	MA	94.4	132.1	33.3
AN-202	F	YA	95.2	97.2	2.1
AN-204A	M	MA	95.2	83.6	-13.0
AN-210	M?	YA	98.3	96.0	-2.4
AN-216	M?	YA	95.9	98.6	2.8
AN-218	F	YA	107.1	122.5	13.4
AN-220	F	OA	79.9	84.4	5.5
AN-225	M	YA	92.3	100.1	8.1
AN-226	F	YA	97.9	89.7	-8.7
AN-230A	M	MA	105.2	105.7	0.5
AN-241	F	OA	88.3	65.5	-29.6
AN-242	F	OA	77.0	84.8	9.6
AN-243	F	YA	106.1	97.7	-8.2
AN-244	M	YA	98.5	102.0	3.5
AN-247	F	YA	80.2	94.7	16.6
AN-252	M	MA	108.7	111.8	2.8
AN-259	F	YA	111.7	109.0	-2.4
AN-262A	F	MA	92.0	78.2	-16.2
AN-263	F	OA	57.0	52.7	-7.8
AN-266	M?	MA	64.7	69.2	6.7
AN-269	M	MA	112.8	117.4	4.0

F=Female; F?=Probable female; U=Unknown sex; M?=Probable male; M=Male; ADO=Adolescent; YA=Young adult; MA=Middle adult; OA=Old adult; L=Left; R=Right; ROI=Region of interest; directional asymmetry; ROI%DA=Region of interest area directional asymmetry

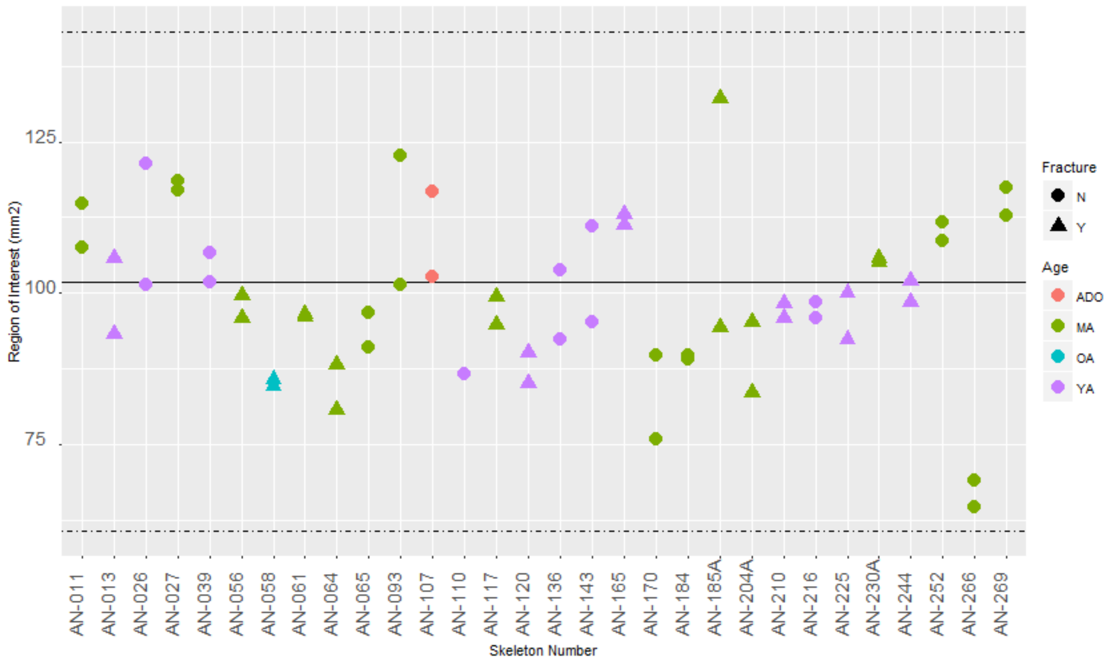

Figure I.37 – Ancaster male second metatarsal region of interest areas (mm^2).

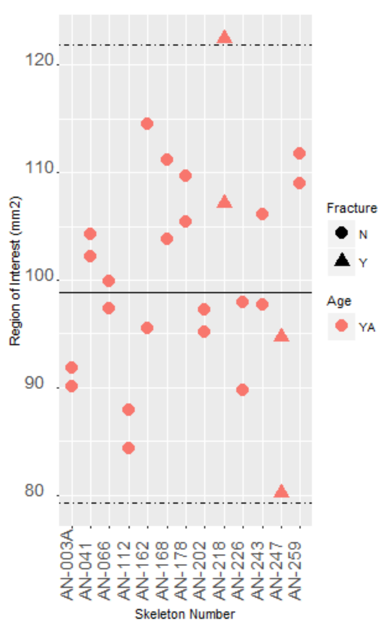

Figure I.38 – Ancaster young adult female second metatarsal region of interest areas (mm^2).

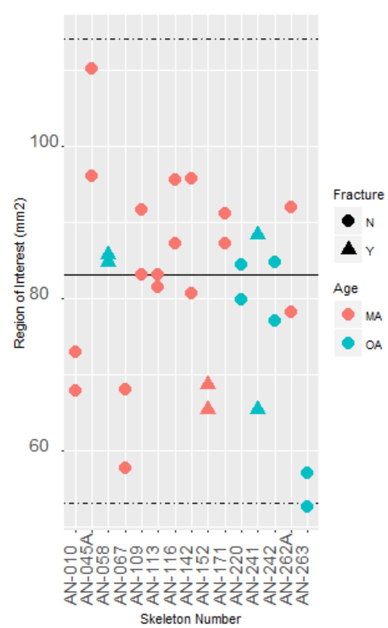

Figure I.39 – Ancaster young adult female second metatarsal region of interest areas (mm^2).

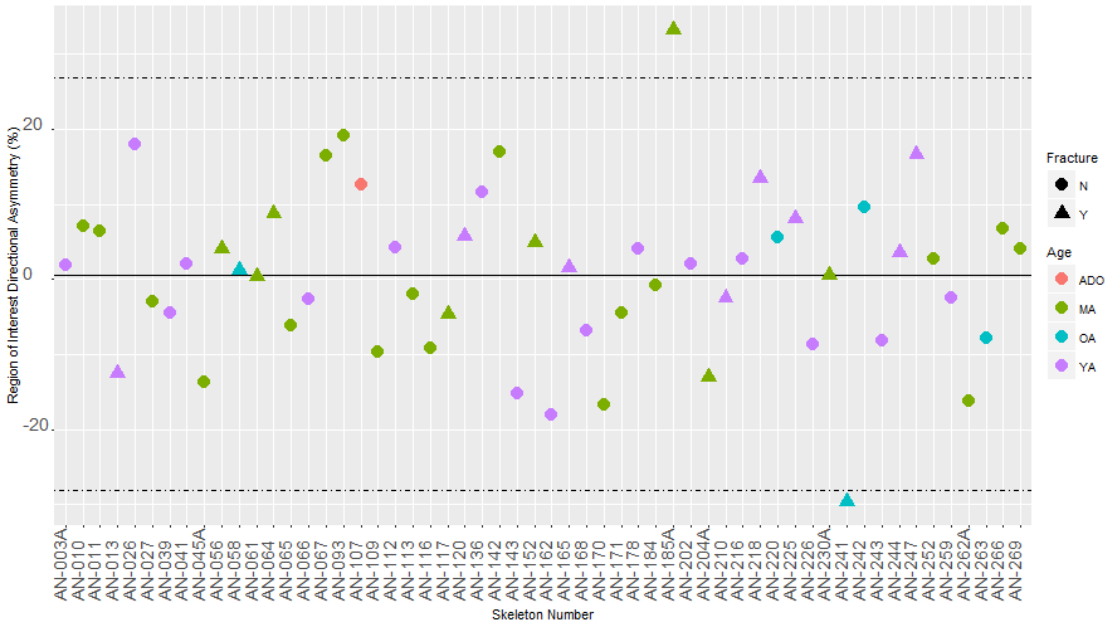

Figure I.40 – Ancaster second metatarsal region of interest areas directional asymmetry (%)

I.2 – Vagnari Cross-Sectional Properties

I.2.1 - Humerus

Table I.8 – Radiographically measured bone diameters, and calculated bone areas and asymmetries for humeri at Vagnari.

Skeleton Number	Sex	Age	Side	AP	ap	ML	ml	T_A	M_A	C_A	T_A %DA	M_A %DA	C_A %DA
VA-F034	M?	Adult	L	19.2	7.5	19.1	7.0	288.0	41.2	246.8	-2.6	27.4	-8.7
			R	19.0	7.6	18.8	9.1	280.5	54.3	226.2			
VA-F040	F	ADO	L	16.3	7.7	18.3	9.0	234.3	54.4	179.8	6.0	-15.3	13.5
			R	15.6	8.0	18.0	10.1	220.5	63.5	157.1			
VA-F042A	M	YA	L	17.2	7.1	18.8	8.2	254.0	45.7	208.2	9.1	-6.1	12.2
			R	17.8	6.6	19.9	8.3	278.2	43.0	235.2			
VA-F062	M?	MA	L	19.0	7.7	20.1	8.0	299.9	48.4	251.6	54.9	-7.9	72.0
			R	14.3	6.8	15.2	9.8	170.7	52.3	118.4			
VA-F067	M	YA	L	18.4	7.8	21.5	10.8	310.7	66.2	244.5	-9.3	-40.3	-2.3
			R	18.2	7.0	19.8	8.0	283.0	44.0	239.0			
VA-F068	M	MA	L	18.4	9.4	21.2	11.4	306.4	84.2	222.2	-7.5	-7.0	-7.6
			R	18.1	9.7	20.0	10.3	284.3	78.5	205.8			
VA-F089	U	Adult	L	16.7	8.5	19.1	9.8	250.5	65.4	185.1	0.5	33.1	-14.4
			R	17.9	11.3	17.9	10.3	251.6	91.4	160.2			
VA-F092	M	MA	L	19.0	7.7	20.2	7.7	301.4	46.6	254.9	10.1	13.4	9.5
			R	17.7	7.2	19.6	7.2	272.5	40.7	231.8			
VA-F131	M	YA	L	18.9	7.1	20.4	7.3	302.8	40.7	262.1	-6.3	31.5	-13.7
			R	18.1	8.0	20.0	8.9	284.3	55.9	228.4			
VA-F200	F	MA	L	16.1	9.6	18.2	13.6	230.1	102.5	127.6	1.4	4.3	-0.8
			R	16.6	10.6	17.4	11.8	226.9	98.2	128.6			
VA-F204	F	YA	L	15.6	7.6	16.0	8.5	196.0	50.7	145.3	2.5	-9.9	6.5
			R	15.6	6.8	16.4	8.6	200.9	45.9	155.0			

Skeleton Number	Sex	Age	Side	AP	ap	ML	ml	T_A	M_A	C_A	T_A %DA	M_A %DA	C_A %DA
VA-F205	F	MA	L	17.5	9.5	17.4	11.3	239.2	84.3	154.8	-4.0	-10.1	-0.5
			R	17.8	10.7	17.8	11.1	248.8	93.3	155.6			
VA-F207	M?	YA	L	18.7	7.6	18.7	8.5	274.6	50.7	223.9	18.1	-13.3	26.7
			R	16.3	8.2	17.9	9.0	229.2	58.0	171.2			
VA-F211	F	YA	L	16.5	6.9	18.2	7.9	235.9	42.8	193.0	8.8	24.3	5.7
			R	15.8	6.1	17.4	7.0	215.9	33.5	182.4			
VA-F213	M	MA	L	21.7	10.4	22.1	9.9	376.7	80.9	295.8	-4.9	37.4	-14.0
			R	23.0	8.2	21.9	8.6	395.6	55.4	340.2			
VA-F214	M	MA	L	19.4	9.5	21.4	10.8	326.1	80.6	245.5	-6.9	-8.2	-6.5
			R	19.6	9.2	22.7	12.1	349.4	87.4	262.0			
VA-F215	F	YA	L	17.5	9.6	18.1	8.8	248.8	66.4	182.4	8.6	4.2	10.3
			R	16.7	9.0	17.4	9.0	228.2	63.6	164.6			
VA-F216	M	MA	L	18.2	7.3	20.2	7.4	288.7	42.4	246.3	1.3	11.8	-0.6
			R	19.1	8.0	19.5	7.6	292.5	47.8	244.8			
VA-F220	M	MA	L	20.6	9.0	20.6	9.2	333.3	65.0	268.3	-0.7	4.9	-2.1
			R	19.7	8.7	21.4	10.0	331.1	68.3	262.8			
VA-F231	M?	YA	L	20.5	6.2	19.6	6.0	315.6	29.2	286.4	-10.5	-6.6	-11.0
			R	20.9	6.7	17.3	5.2	284.0	27.4	256.6			
VA-F234	M	YA	L	20.0	6.9	20.2	7.9	317.3	42.8	274.5	-4.4	-19.4	-1.8
			R	20.9	7.7	20.2	8.6	331.6	52.0	279.6			
VA-F249	F?	YA	L	16.7	6.4	20.7	11.2	271.5	56.3	215.2	3.0	4.1	2.7
			R	17.9	7.7	19.9	9.7	279.8	58.7	221.1			
VA-F250	M?	YA	L	20.6	10.8	18.8	8.9	304.2	75.5	228.7	-1.2	-29.9	10.5
			R	19.4	11.7	20.2	11.1	307.8	102.0	205.8			
VA-F252	F?	ADO	L	16.4	5.7	17.7	7.0	228.0	31.3	196.6	8.7	-35.0	17.9
			R	15.2	7.1	17.5	8.0	208.9	44.6	164.3			

Skeleton Number	Sex	Age	Side	AP	ap	ML	ml	T_A	M_A	C_A	T_A %DA	M_A %DA	C_A %DA
VA-F284	F	YA	L	17.0	8.7	17.4	9.1	232.3	62.2	170.1	12.0	-4.5	18.7
			R	16.5	9.0	15.9	9.2	206.0	65.0	141.0			
VA-F287	M	MA	L	21.2	10.0	23.0	12.0	383.0	94.2	288.7	14.8	41.0	7.5
			R	19.1	7.4	22.0	10.7	330.0	62.2	267.8			
VA-F288	M?	YA	L	18.0	8.7	18.5	10.8	261.5	73.8	187.7	-8.0	2.7	-12.5
			R	16.8	8.7	18.3	11.1	241.5	75.8	165.6			
VA-F290	M	MA	L	19.6	9.9	21.0	12.1	323.3	94.1	229.2	9.2	18.0	5.7
			R	18.5	9.8	20.3	10.2	295.0	78.5	216.4			
VA-F296	F	YA	L	17.7	7.7	18.8	11.2	261.3	67.7	193.6	0.2	-5.2	2.1
			R	17.3	7.7	19.2	11.8	260.9	71.4	189.5			
VA-F306	F?	MA	L	16.0	10.1	18.0	12.3	226.2	97.6	128.6	-3.3	30.7	-23.0
			R	16.0	9.7	18.6	9.4	233.7	71.6	162.1			
VA-F312	F?	YA	L	18.6	7.9	16.9	8.3	246.9	51.5	195.4	-0.1	-14.0	4.0
			R	17.0	8.2	18.5	9.2	247.0	59.3	187.8			

F=Female; F?=Probable female; U=Unknown sex; M?=Probable male; M=Male; ADO=Adolescent; YA=Young adult; MA=Middle adult; OA=Old adult; L=Left; R=Right; AP=Antero-posterior total width; ap=Antero-posterior medullary width; ML=Medio-lateral total width; ml=Medio-lateral medullary width; T_A=Total area; M_A=Medullary area; C_A=Cortical area; T_A%DA=Total area directional asymmetry; M_A%DA=Medullary area directional asymmetry; C_A%DA=Cortical area directional asymmetry.

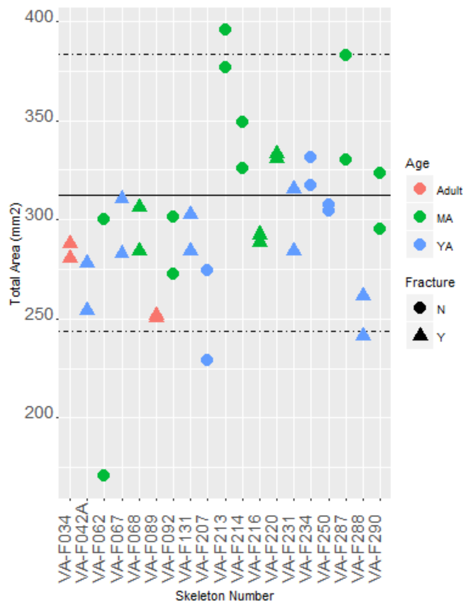

Figure I.41 – Vagnari male humeral total areas (mm²).

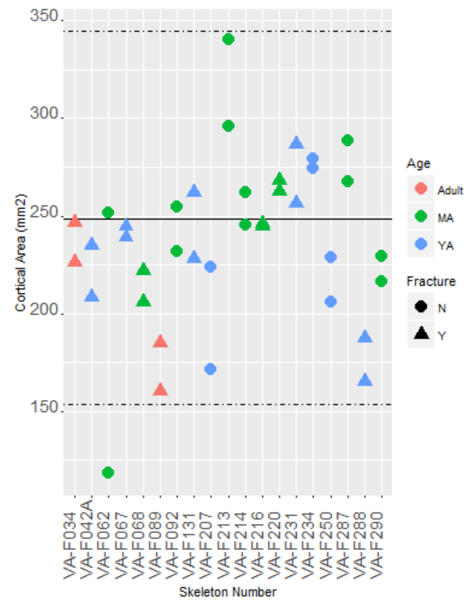

Figure I.42 – Vagnari male humeral cortical areas (mm²).

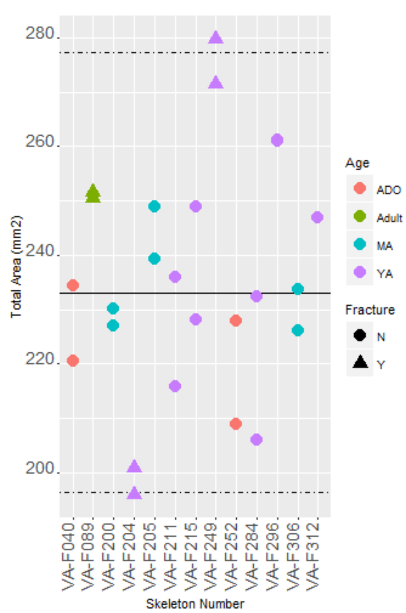

Figure I.43 – Vagnari female humeral total areas (mm²).

Figure I.44 – Vagnari young adult female humeral cortical areas (mm²).

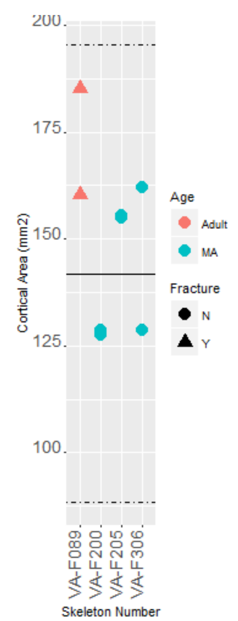

Figure I.45 – Vagnari middle adult female humeral cortical areas (mm²).

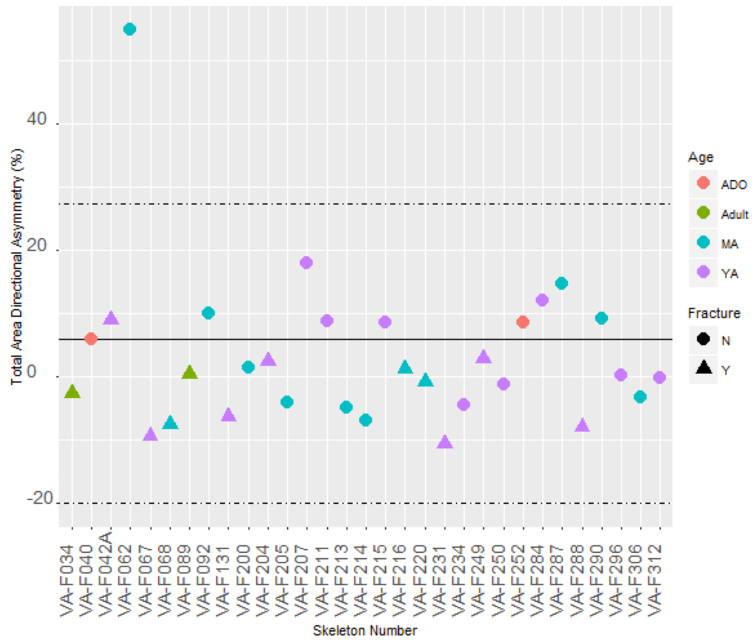

Figure I.46 – Vagnari humeral total area directional asymmetry (%).

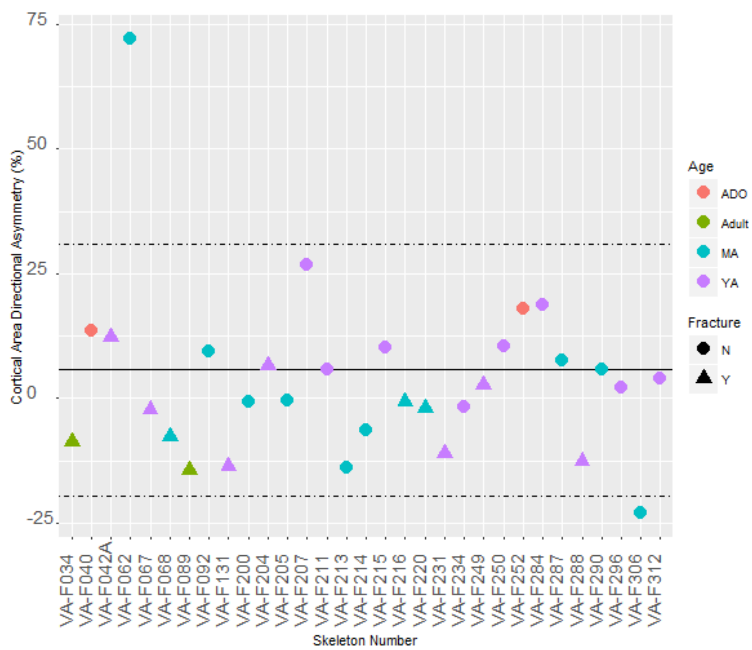

Figure I.47 – Vagnari humeral cortical area directional asymmetry (%).

I.2.2 - Radius

Table I.9 – Radiographically measured bone diameters, and calculated bone areas and asymmetries for radii at Vagnari.

Skeleton Number	Sex	Age	Side	AP	ap	ML	ml	T_A	M_A	C_A	T_A %DA	M_A %DA	C_A %DA
VA-F034	M?	Adult	L	15.2	7.5	11.8	4.1	140.9	24.2	116.7	23.8	86.8	0.9
			R	17.8	11.8	12.8	6.6	178.9	61.2	117.8			
VA-F040	F	ADO	L	13.5	8.5	10.0	5.2	106.0	34.7	71.3	15.5	39.6	0.9
			R	14.2	10.0	11.1	6.6	123.8	51.8	72.0			
VA-F042A	M	YA	L	15.8	10.1	11.5	6.3	142.7	50.0	92.7	1.7	-9.0	7.0
			R	16.5	10.2	11.2	5.7	145.1	45.7	99.5			
VA-F062	M?	MA	L	14.3	10.1	10.7	6.0	120.2	47.6	72.6	15.1	38.5	-4.2
			R	16.8	12.6	10.6	7.1	139.9	70.3	69.6			
VA-F067	M	YA	L	17.1	12.4	13.8	8.3	185.3	80.8	104.5	-	-	-
			R	-	-	-	-	-	-	-			
VA-F068	M	MA	L	15.1	9.0	12.2	6.3	144.7	44.5	100.2	-5.3	2.7	-9.1
			R	15.6	9.4	11.2	6.2	137.2	45.8	91.5			
VA-F089	U	Adult	L	13.6	8.3	10.3	4.8	110.0	31.3	78.7	17.4	-5.4	25.1
			R	15.3	7.7	10.9	4.9	131.0	29.6	101.3			
VA-F096B	F?	Adult	L	15.2	9.2	10.8	5.1	128.9	36.9	92.1	5.4	-4.1	8.9
			R	16.5	7.9	10.5	5.7	136.1	35.4	100.7			
VA-F131	M	YA	L	-	-	-	-	-	-	-	-	-	-
			R	15.0	10.2	11.6	6.7	136.7	53.7	83.0			
VA-F200	F	MA	L	14.1	8.9	10.5	6.4	116.3	44.7	71.5	-11.5	-2.3	-17.7
			R	14.5	10.5	9.1	5.3	103.6	43.7	59.9			
VA-F204	F	YA	L	14.8	7.0	11.3	7.2	131.3	39.6	91.8	-8.2	-34.3	1.3
			R	15.4	8.1	10.0	4.4	121.0	28.0	93.0			
VA-F207	M?	YA	L	13.7	7.6	12.5	5.2	134.5	31.0	103.5	-	-	-
			R	-	-	-	-	-	-	-			

Skeleton Number	Sex	Age	Side	AP	ap	ML	ml	T_A	M_A	C_A	T_A %DA	M_A %DA	C_A %DA
VA-F211	F	YA	L	14.9	9.5	9.8	4.8	114.7	35.8	78.9	36.7	46.2	31.9
			R	16.4	9.6	12.9	7.6	166.2	57.3	108.9			
VA-F213	M	MA	L	16.1	7.4	11.5	4.6	145.4	26.7	118.7	-	-	-
			R	-	-	-	-	-	-	-			
VA-F214	M	MA	L	17.7	11.7	13.2	7.5	183.5	68.9	114.6	-	-	-
			R	19.1	14.2	-	-	-	-	-			
VA-F215	F	YA	L	16.6	8.9	12.7	7.2	165.6	50.3	115.2	-7.5	10.8	-16.7
			R	17.0	11.7	11.5	6.1	153.5	56.1	97.5			
VA-F216	M	MA	L	17.3	10.1	12.8	7.0	173.9	55.5	118.4	5.9	34.8	-11.4
			R	18.8	13.4	12.5	7.5	184.6	78.9	105.6			
VA-F220	M	MA	L	19.1	13.4	13.0	8.3	195	87.4	107.7	-	-	-
			R	-	-	-	-	-	-	-			
VA-F231	M?	YA	L	-	-	-	-	-	-	-	-	-	-
			R	17.9	10.6	11.6	7.0	163.1	58.3	104.8			
VA-F249	F?	YA	L	16.0	10.5	11.0	6.2	138.2	51.1	87.1	-	-	-
			R	-	-	-	-	-	-	-			
VA-F288	M?	YA	L	16.4	8.8	11.6	4.9	149.4	33.9	115.5	5.3	25.3	-1.4
			R	17.6	10.9	11.4	5.1	157.6	43.7	113.9			
VA-F234	M	YA	L	17.6	13.9	12.2	7.2	168.6	78.6	90.0	-9.5	-40.3	11.5
			R	16.4	10.9	11.9	6.1	153.3	52.2	101.1			
VA-F250	M?	YA	L	17.9	12.8	11.8	8.1	165.9	81.4	84.5	1.4	-10.7	11.7
			R	18.3	13.5	11.7	6.9	168.2	73.2	95.0			
VA-F252	F?	ADO	L	15.6	10.8	11.8	7.4	144.6	62.8	81.8	5.4	6.1	4.9
			R	15.8	11.8	12.3	7.2	152.6	66.7	85.9			
VA-F284	F	YA	L	14.1	7.8	10.4	4.5	115.2	27.6	87.6	13.1	31.4	6.5
			R	15.2	8.6	11.0	5.6	131.3	37.8	93.5			

Skeleton Number	Sex	Age	Side	AP	ap	ML	ml	T_A	M_A	C_A	T_A %DA	M_A %DA	C_A %DA
VA-F287	M	MA	L	17.8	11.3	12.4	7.4	173.4	65.7	107.7	8.4	2.6	11.7
			R	19.2	11.0	12.5	7.8	188.5	67.4	121.1			
VA-F290	M	MA	L	-	-	-	-	-	-	-	-	-	-
			R	19.0	14.8	10.9	6.9	162.7	80.2	82.5			
VA-F294	F?	OA	L	17.5	12.9	10.2	7.1	140.2	71.9	68.3	-	-	-
			R	-	-	-	-	-	-	-			
VA-F296	F	YA	L	16.7	11.5	11.4	7	149.5	63.2	86.3	4.4	12.1	-1.7
			R	17.3	12.8	11.5	7.1	156.3	71.4	84.9			
VA-F306	F?	MA	L	14.5	10.1	10.4	5.4	118.4	42.8	75.6	-	-	-
			R	-	-	-	-	-	-	-			
VA-F312	F?	YA	L	-	-	-	-	-	-	-	-	-	-
			R	17.1	13.1	10.5	6.3	141.0	64.8	76.2			

F=Female; F?=Probable female; U=Unknown sex; M?=Probable male; M=Male; ADO=Adolescent; YA=Young adult; MA=Middle adult; OA=Old adult; L=Left; R=Right; AP=Antero-posterior total width; ap=Antero-posterior medullary width; ML=Medio-lateral total width; ml=Medio-lateral medullary width; T_A=Total area; M_A=Medullary area; C_A=Cortical area; T_A%DA=Total area directional asymmetry; M_A%DA=Medullary area directional asymmetry; C_A%DA=Cortical area directional asymmetry.

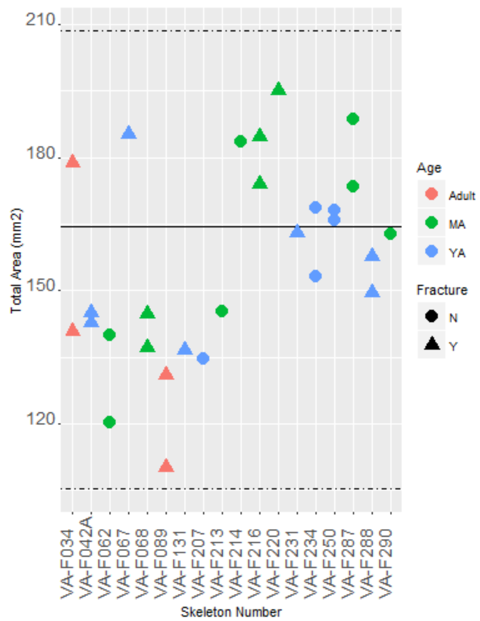

Figure I.48 – Vagnari male radial total areas (mm^2).

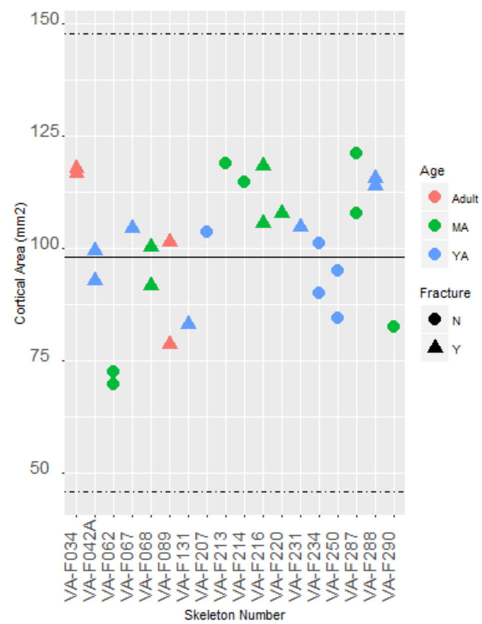

Figure I.49 – Vagnari male radial cortical areas (mm^2).

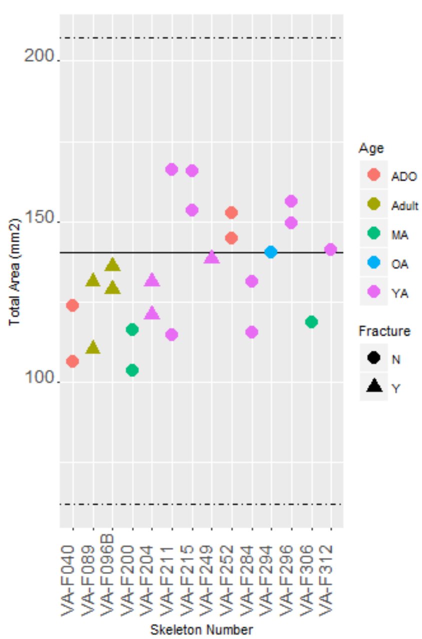

Figure I.50 – Vagnari female radial total areas (mm^2).

Figure I.51 – Vagnari young adult female radial cortical areas (mm^2).

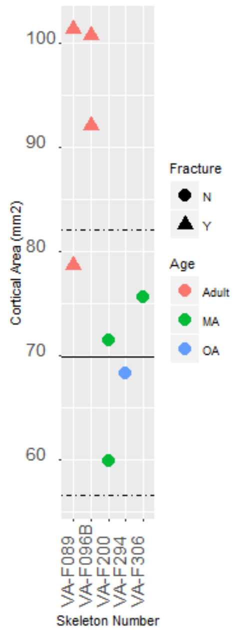

Figure I.52 – Vagnari middle adult female radial cortical areas (mm^2). Individuals VA-F089 and F096B are of unknown age; their areas fall within the range of young adult females and, as such, they were not considered outliers.

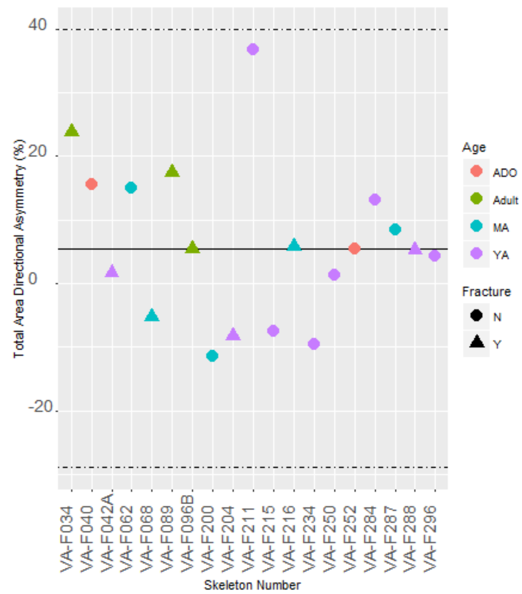

Figure I.53 – Vagnari radial total area directional asymmetry (%).

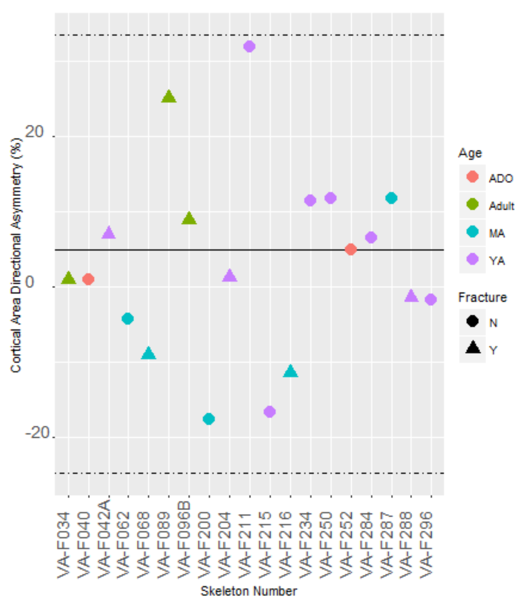

Figure I.54 – Vagnari radial cortical area directional asymmetry (%).

I.2.3 - Ulna

Table I.10 – Radiographically measured bone diameters, and calculated bone areas and asymmetries for ulnae at Vagnari.

Skeleton Number	Sex	Age	L ROI	R ROI	ROI %DA
VA-F034	M?	Adult	-	276.4	-
VA-F040	F	ADO	208.8	198.3	-5.2
VA-F062	M?	MA	218.8	219.5	-
VA-F042A	M	YA	237.5	241.5	1.7
VA-F068	M	MA	252.8	249.6	-1.3
VA-F067	M	YA	237.0	270.7	13.3
VA-F092	M	MA	297.6	258	-14.3
VA-F131	M	YA	233.8	-	-
VA-F200	F	MA	173.6	172.9	-0.4
VA-F204	F	YA	232.5	223.9	-3.8
VA-F211	F	YA	238.4	284.9	17.8
VA-F214	M	MA	267.2	254.0	-5.1
VA-F231	M?	YA	-	314.8	-
VA-F215	F	YA	220.4	250.7	12.9
VA-F216	M	MA	295.1	304.9	3.3
VA-F234	M	YA	337.6	326.2	-3.4
VA-F249	F?	YA	309.1	277	-11.0
VA-F250	M?	YA	265.5	239.6	-10.3
VA-F252	F?	ADO	236.0	-	-
VA-F284	F	YA	195.7	213.2	8.6
VA-F287	M	MA	-	258.9	-
VA-F294	F?	OA	130.7	220.4	51.1
VA-F296	F	YA	295.2	273.6	-7.6
VA-F290	M	MA	-	208.9	-
VA-F312	F?	YA	250.9	231.3	-8.1

F=Female; F?=Probable female; U=Unknown sex; M?=Probable male; M=Male; ADO=Adolescent; YA=Young adult; MA=Middle adult; OA=Old adult; L=Left; R=Right; ROI=Region of interest; directional asymmetry; ROI%DA=Region of interest area directional asymmetry

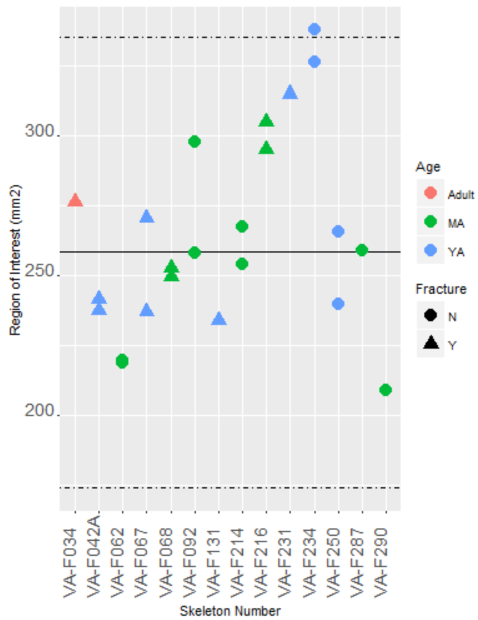

Figure I.55 – Vagnari male ulna region of interest areas (mm^2).

Figure I.56 – Vagnari young adult female ulna region of interest areas (mm^2).

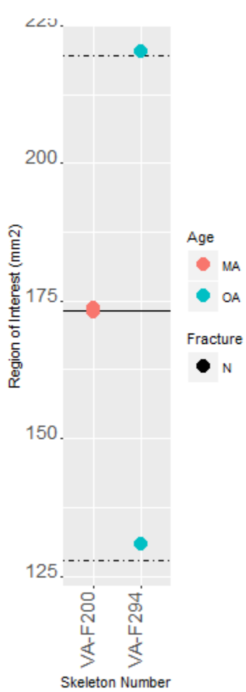

Figure I.57 – Vagnari middle adult female ulna region of interest areas (mm^2).

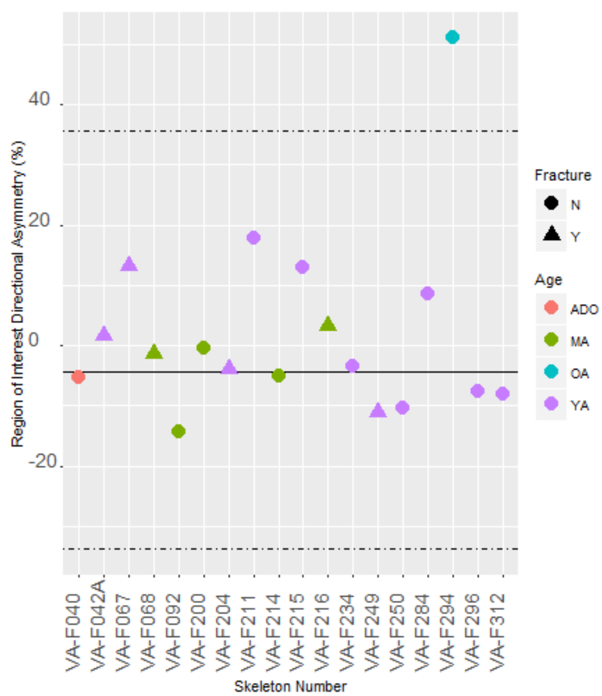

Figure I.58 – Vagnari male ulna region of interest directional asymmetry (%).

I.2.4 – Second Metacarpal Midshaft

Table I.11 – Radiographically measured bone diameters, and calculated bone areas and asymmetries for second metacarpal midshafts at Vagnari.

Skeleton Number	Sex	Age	Side	AP	ap	ML	ml	T_A	M_A	C_A	T_A %DA	M_A %DA	C_A %DA
VA-F040	F	ADO	L	-	-	-	-	-	-	-	-	-	-
			R	7.5	3.6	7.6	3.8	44.8	10.7	34.0	-	-	-
VA-F042A	M	YA	L	-	-	-	-	-	-	-	-	-	-
			R	8.3	3.3	10.3	4.3	67.1	11.1	56.0	-	-	-
VA-F062	M?	MA	L	-	-	-	-	-	-	-	-	-	-
			R	8.7	5.2	8.8	4.6	60.1	18.8	41.3	-	-	-
VA-F200	F	MA	L	7.1	3.5	7.8	3.8	43.5	10.4	33.0	-	-	-
			R	-	-	-	-	-	-	-	-	-	-
VA-F214	M	MA	L	-	-	-	-	-	-	-	-	-	-
			R	7.9	4.2	8.7	4.9	54.0	16.2	37.8	-	-	-
VA-F234	M	YA	L	7.7	3.1	9.5	4	57.5	9.7	47.7	0.2	1.4	0.0
			R	7.8	3.4	9.4	3.7	57.6	9.9	47.7	-	-	-
VA-F252	F?	ADO	L	7.5	3.3	9.4	4.1	55.4	10.6	44.7	-	-	-
			R	-	-	-	-	-	-	-	-	-	-

F=Female; F?=Probable female; U=Unknown sex; M?=Probable male; M=Male; ADO=Adolescent; YA=Young adult; MA=Middle adult; OA=Old adult; L=Left; R=Right; AP=Antero-posterior total width; ap=Antero-posterior medullary width; ML=Medio-lateral total width; ml=Medio-lateral medullary width; T_A=Total area; M_A=Medullary area; C_A=Cortical area; T_A%DA=Total area directional asymmetry; M_A%DA=Medullary area directional asymmetry; C_A%DA=Cortical area directional asymmetry

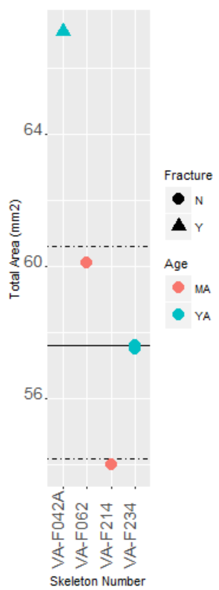

Figure I.59 – Vagnari male second metacarpal midshaft total areas (mm^2).

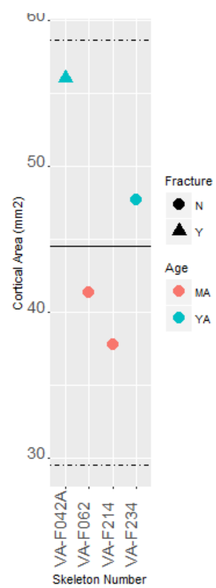

Figure I.60 – Vagnari male second metacarpal midshaft cortical areas (mm^2).

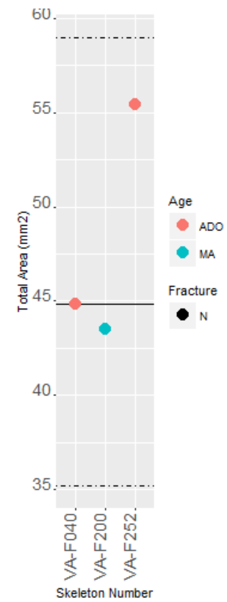

Figure I.61 – Vagnari female second metacarpal midshaft total areas (mm^2).

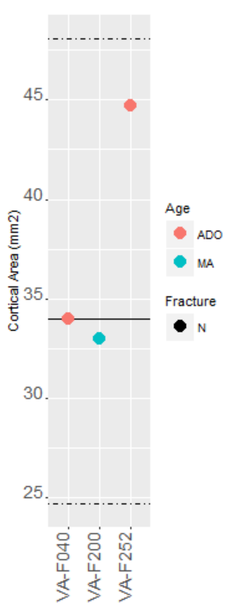

Figure I.62 – Vagnari female second metacarpal midshaft cortical areas (mm^2).

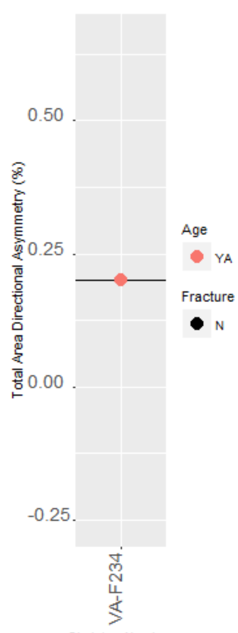

Figure I.63 – Vagnari second metacarpal midshaft total area directional asymmetry (%).

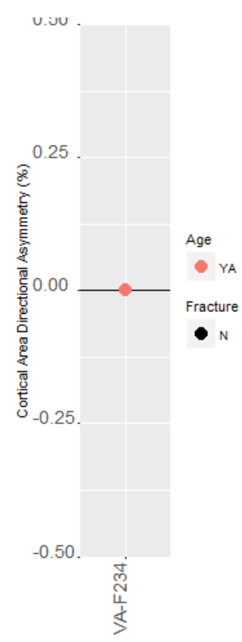

Figure I.64 – Vagnari second metacarpal midshaft cortical area directional asymmetry (%).

I.2.5 – Second Metacarpal Region of Interest

Table I.12 – Radiographically measured bone diameters, and calculated bone areas and asymmetries for second metacarpal region of interests at Vagnari.

Skeleton Number	Sex	Age	L ROI	R ROI	ROI %DA
VA-F040	F	ADO	62.6	78.2	22.2
VA-F042A	M	YA	-	97.2	-
VA-F062	M?	MA	67.6	75.7	11.3
VA-F067	M	YA	92.0	-	-
VA-F092	M	MA	96.7	-	-
VA-F096B	F?	Adult	75.6	-	-
VA-F131	M	YA	83.6	80.0	-4.4
VA-F200	F	MA	63.1	56.8	-10.5
VA-F204	F	YA	87.7	-	-
VA-F213	M	MA	91.8	-	-
VA-F214	M	MA	-	78.0	-
VA-F215	F	YA	84.8	82.7	-2.5
VA-F216	M	MA	-	105.6	-
VA-F220	M	MA	87.8	-	-
VA-F231	M?	YA	-	72.9	-
VA-F234	M	YA	93.4	86.5	-7.7
VA-F252	F?	ADO	93.1	80.8	-14.1
VA-F288	M?	YA	97.0	-	-
VA-F294	F?	OA	48.7	-	-
VA-F296	F	YA	-	75.3	-
VA-F312	F?	YA	-	81.4	-

F=Female; F?=Probable female; U=Unknown sex; M?=Probable male; M=Male; ADO=Adolescent; YA=Young adult; MA=Middle adult; OA=Old adult; L=Left; R=Right; ROI=Region of interest; directional asymmetry; ROI%DA=Region of interest area directional asymmetry

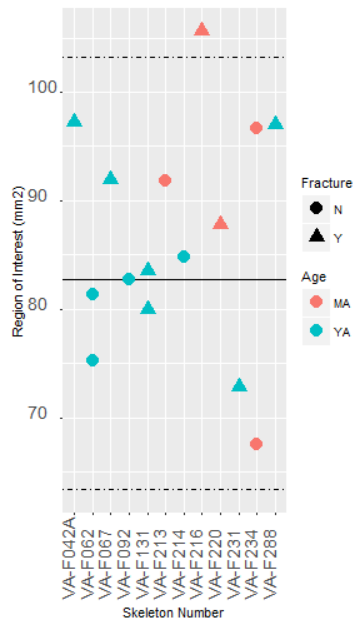

Figure I.65 – Vagnari male second metacarpal region of interest areas (mm²).

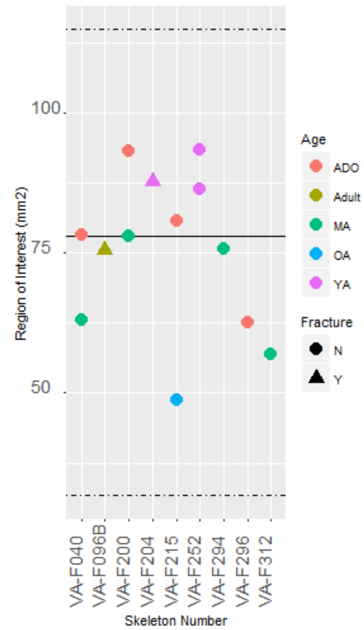

Figure I.66 – Vagnari female second metacarpal region of interest areas (mm²).

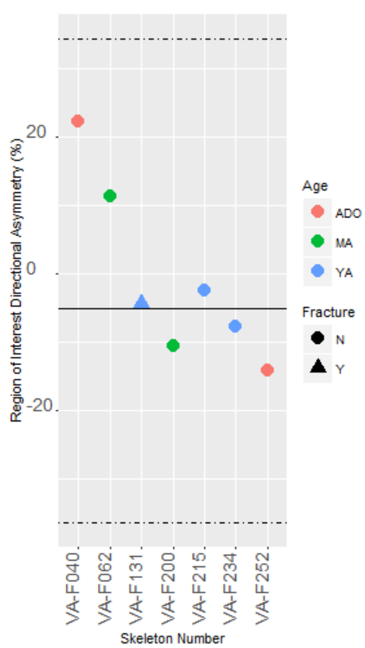

Figure I.67 – Vagnari second metacarpal region of interest area directional asymmetry (%).

I.2.6 - Tibia

Table I.13 – Radiographically measured bone diameters, and calculated bone areas and asymmetries for tibiae at Vagnari.

Skeleton Number	Sex	Age	Side	AP	ap	ML	ml	T_A	M_A	C_A	T_A %DA	M_A %DA	C_A %DA
VA-F034	M?	Adult	L	-	-	-	-	-	-	-	-	-	-
			R	22.0	10.9	29.1	10.7	502.8	91.6	411.2			
VA-F040	F	ADO	L	19.5	10.0	20.7	9.2	317.0	72.3	244.8	-4.1	-5.0	-3.9
			R	18.8	10.3	20.6	8.5	304.2	68.8	235.4			
VA-F042A	M	YA	L	22.1	10.4	24.5	9.6	425.3	78.4	346.8	-6.7	8.0	-10.4
			R	21.0	10.5	24.1	10.3	397.5	84.9	312.5			
VA-F062	M?	MA	L	24.5	9.6	24.8	9.1	477.2	68.6	408.6	7.7	21.3	5.3
			R	23.2	10.4	28.3	10.4	515.7	84.9	430.7			
VA-F067	M	YA	L	24.2	10.3	25.2	7.2	479.0	58.2	420.7	-6.2	-14.7	-5.1
			R	23.2	9.7	24.7	6.6	450.1	50.3	399.8			
VA-F068	M	MA	L	22.2	11.9	24.8	8.0	432.4	74.8	357.6	-1.6	13.6	-5.0
			R	22.4	11.6	24.2	9.4	425.7	85.6	340.1			
VA-F092	M	MA	L	24.3	11.9	31.1	12.0	593.5	112.2	481.4	-0.9	-24.8	4.0
			R	24.4	10.5	30.7	10.6	588.3	87.4	500.9			
VA-F096B	F?	Adult	L	21.7	12.8	24.3	11.8	414.1	118.6	295.5	3.8	-2.3	6.2
			R	19.5	12.4	28.1	11.9	430.4	115.9	314.5			
VA-F131	M	YA	L	26.4	10.5	24.2	9.1	501.8	75.0	426.7	-14.4	9.5	-19.2
			R	22.3	10.2	24.8	10.3	434.4	82.5	351.8			
VA-F200	F	MA	L	20.5	11.9	24.4	10.9	392.9	101.9	291.0	-6.5	5.3	-11.0
			R	18.3	11.3	25.6	12.1	367.9	107.4	260.6			
VA-F204	F	YA	L	21.0	11.3	22.1	9.1	364.5	80.8	283.7	-1.0	-9.5	1.4
			R	19.9	11.0	23.1	8.5	361.0	73.4	287.6			
VA-F205	F	MA	L	-	-	-	-	-	-	-	-	-	-
			R	23.5	13.3	21.9	11.4	404.2	119.1	285.1			

Skeleton Number	Sex	Age	Side	AP	ap	ML	ml	T_A	M_A	C_A	T_A %DA	M_A %DA	C_A %DA
VA-F207	M?	YA	L	24.8	12.1	24.5	8.2	477.2	77.9	399.3	4.3	0.7	5.0
			R	24.4	11.9	26.0	8.4	498.3	78.5	419.7			
VA-F211	F	YA	L	19.9	9.8	19.2	8.1	300.1	62.3	237.7	12.4	-6.3	16.8
			R	18.1	9.2	23.9	8.1	339.8	58.5	281.2			
VA-F213	M	MA	L	20.7	8.2	21.4	6.9	347.9	44.4	303.5	4.4	28.1	0.4
			R	20.3	9.5	22.8	7.9	363.5	58.9	304.6			
VA-F214	M	MA	L	25.4	10.7	24.3	8.4	484.8	70.6	414.2	-4.0	-11.3	-2.8
			R	24.1	11.0	24.6	7.3	465.6	63.1	402.6			
VA-F215	F	YA	L	26.4	13.3	25.8	11.1	535.0	115.9	419.0	-12.4	-10.1	-13.0
			R	22.2	11.4	27.1	11.7	472.5	104.8	367.8			
VA-F216	M	MA	L	25.3	11.7	25.6	9.4	508.7	86.4	422.3	11.6	1.7	13.5
			R	28.2	11.9	25.8	9.4	571.4	87.9	483.6			
VA-F220	M	MA	L	24.7	12.1	28.1	10.4	545.1	98.8	446.3	-9.7	-25.9	-6.4
			R	23.6	10.1	26.7	9.6	494.9	76.2	418.7			
VA-F231	M?	YA	L	20.5	10.7	22.5	8.5	362.3	71.4	290.8	23.2	22.7	23.4
			R	23.3	11.2	25.0	10.2	457.5	89.7	367.8			
VA-F234	M	YA	L	26.5	7.9	29.6	8.5	616.1	52.7	563.3	-10.4	-27.1	-9.0
			R	27.4	7.1	25.8	7.2	555.2	40.1	515.1			
VA-F235	M	OA	L	26.0	10.6	30.4	11.6	620.8	96.6	524.2	19.3	27.9	17.6
			R	28.8	11.8	33.3	13.8	753.2	127.9	625.3			
VA-F249	F?	YA	L	20.4	11.3	24.0	9.2	384.5	81.6	302.9	-13.2	-8.4	-14.5
			R	19.5	10.5	22.0	9.1	336.9	75.0	261.9			
VA-F250	M?	YA	L	23.5	13.5	25.9	12.4	478.0	131.5	346.6	20.2	7.5	24.6
			R	27.2	14.1	27.4	12.8	585.3	141.7	443.6			
VA-F252	F?	ADO	L	22.8	9.7	28.0	11.2	501.4	85.3	416.1	-2.0	-19.8	1.2
			R	22.5	11.0	27.8	8.1	491.3	70.0	421.3			

Skeleton Number	Sex	Age	Side	AP	ap	ML	ml	T_A	M_A	C_A	T_A %DA	M_A %DA	C_A %DA
VA-F284	F	YA	L	22.3	12.2	25.0	12.2	437.9	116.9	321.0	4.1	2.8	4.5
			R	22.0	13.2	26.4	11.6	456.2	120.3	335.9			
VA-F287	M	MA	L	24.8	11.3	27.2	11.8	529.8	104.7	425.1	-13.9	12.4	-21.5
			R	23.3	12.9	25.2	11.7	461.2	118.5	342.6			
VA-F288	M?	YA	L	24.5	11.1	19.8	6.6	381.0	57.5	323.5	2.5	18.8	-0.7
			R	23.8	11.2	20.9	7.9	390.7	69.5	321.2			
VA-F290	M	MA	L	26.8	12.8	26.3	13.1	553.6	131.7	421.9	-31.1	-11.9	-37.8
			R	22.9	12.4	22.5	12.0	404.7	116.9	287.8			
VA-F294	F?	OA	L	25.1	13.0	21.8	13.1	429.8	133.8	296.0	-13.7	-17.9	-11.8
			R	24.1	11.3	19.8	12.6	374.8	111.8	263.0			
VA-F296	F	YA	L	20.8	10.5	21.5	8.3	351.2	68.4	282.8	-1.5	-7.1	-0.2
			R	20.4	9.9	21.6	8.2	346.1	63.8	282.3			
VA-F306	F?	MA	L	-	-	-	-	-	-	-	-	-	-
			R	20.9	13.0	21.8	9.0	357.8	91.9	266.0			
VA-F312	F?	YA	L	21.7	11.6	21.3	9.0	363.0	82.0	281.0	-0.3	-16.7	4.1
			R	19.7	10.9	23.4	8.1	362.1	69.3	292.7			

F=Female; F?=Probable female; U=Unknown sex; M?=Probable male; M=Male; ADO=Adolescent; YA=Young adult; MA=Middle adult; OA=Old adult; L=Left; R=Right; AP=Antero-posterior total width; ap=Antero-posterior medullary width; ML=Medio-lateral total width; ml=Medio-lateral medullary width; T_A=Total area; M_A=Medullary area; C_A=Cortical area; T_A%DA=Total area directional asymmetry; M_A%DA=Medullary area directional asymmetry; C_A%DA=Cortical area directional asymmetry

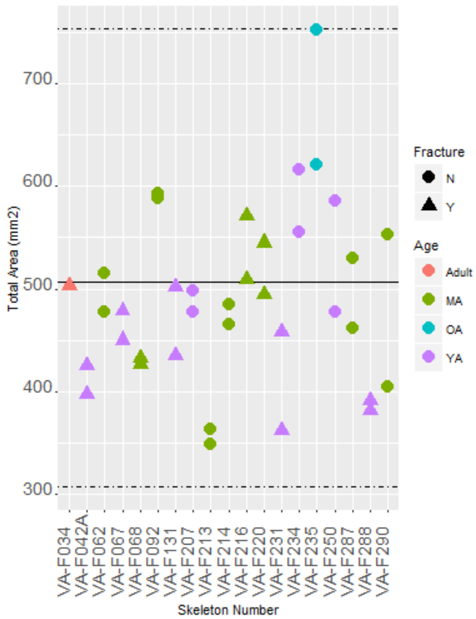

Figure I.68 – Vagnari male tibial total areas (mm^2).

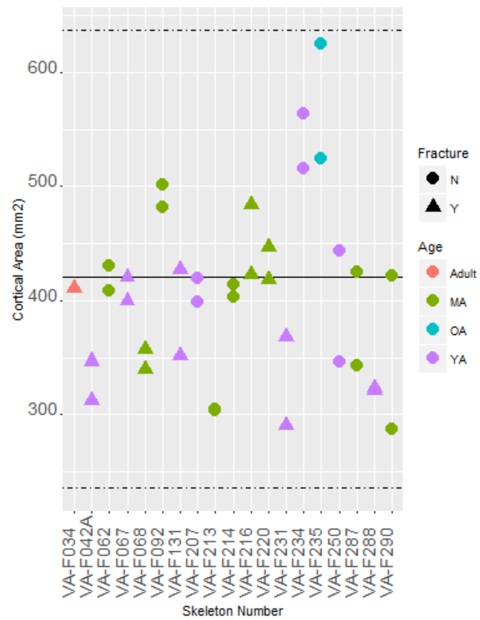

Figure I.69 – Vagnari male tibial cortical areas (mm^2).

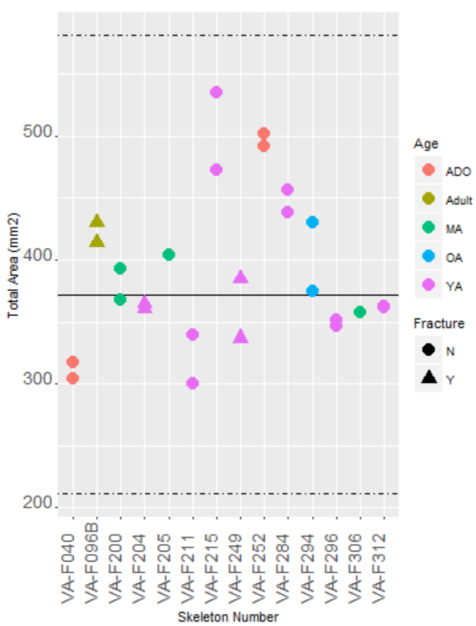

Figure I.70 – Vagnari female tibial total areas (mm^2).

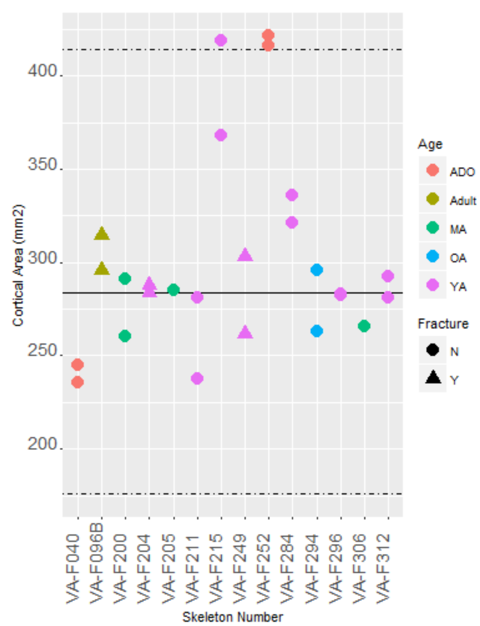

Figure I.71 – Vagnari female tibial cortical areas (mm^2).

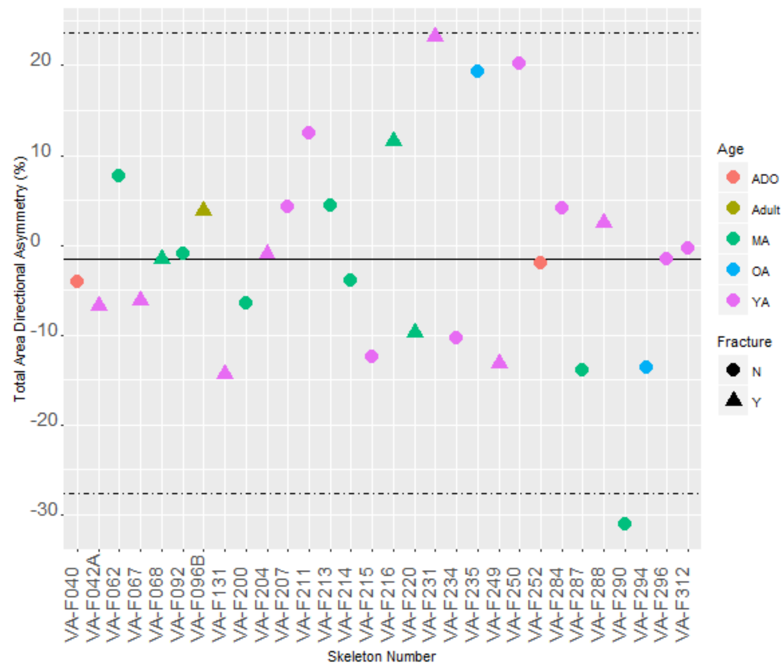

Figure I.72 – Vagnari tibial total area directional asymmetry (%).

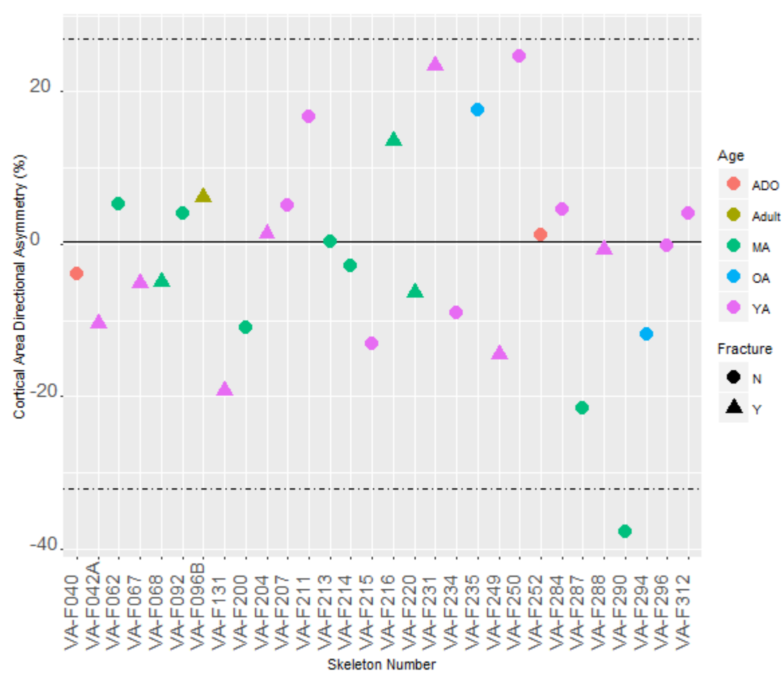

Figure I.73 – Vagnari cortical total area directional asymmetry (%).

I.2.7 – Second Metatarsal Region of Interest

Table I.14 – Radiographically measured bone diameters, and calculated bone areas and asymmetries for second metatarsal region of interest at Vagnari.

Skeleton Number	Sex	Age	L ROI	R ROI	ROI %DA
VA-F040	F	ADO	95.8	100.3	4.6
VA-F062	M?	MA	100.6	89.5	-11.7
VA-F067	M	YA	126.1	-	-
VA-F068	M	MA	132.6	-	-
VA-F096B	F?	Adult	80.8	-	-
VA-F131	M	YA	-	116.4	-
VA-F204	F	YA	121.2	-	-
VA-F214	M	MA	98.4	115.6	16.1
VA-F215	F	YA	-	130.1	-
VA-F220	M	MA	111.0	-	-
VA-F231	M?	YA	-	109.4	-
VA-F234	M	YA	148.8	178.1	17.9
VA-F250	M?	YA	87.0	94.3	8.1
VA-F252	F?	ADO	-	120.8	-
VA-F288	M?	YA	92.7	95.4	2.9
VA-F290	M	MA	118.1	-	-
VA-F294	F?	OA	84.8	-	-
VA-F312	F?	YA	107.7	-	-

F=Female; F?=Probable female; U=Unknown sex; M?=Probable male; M=Male; ADO=Adolescent; YA=Young adult; MA=Middle adult; OA=Old adult; L=Left; R=Right; ROI=Region of interest; directional asymmetry; ROI%DA=Region of interest area directional asymmetry

Figure I.74 – Vagnari male second metatarsal region of interest areas (mm²).

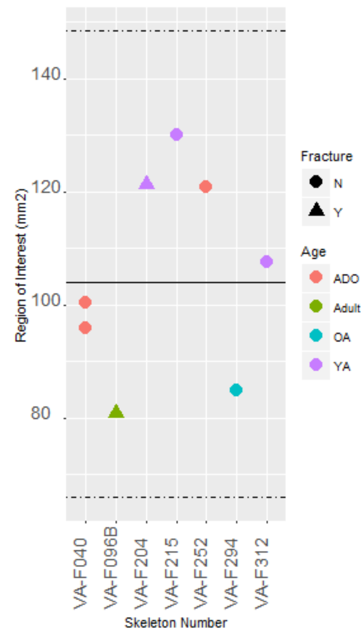

Figure I.75 – Vagnari female second metatarsal region of interest areas (mm²).

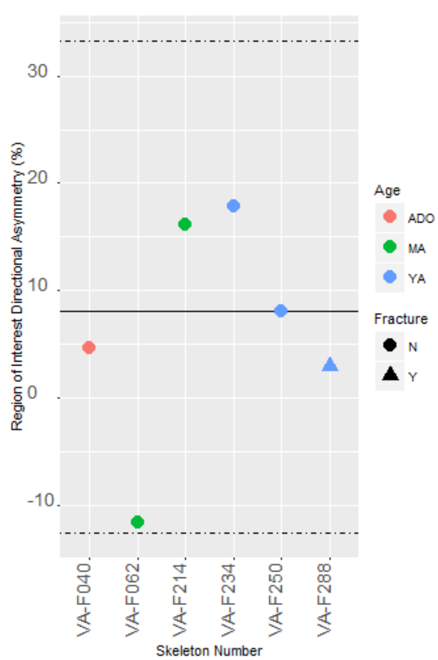

Figure I.76 – Vagnari second metatarsal region of interest area directional asymmetry (%).

Appendix J: Tests of Normality

This appendix reports the results of the Shapiro-Wilks tests for normality and identifies which cross-sectional properties were normally distributed. No individuals with fractures were included in normality tests.

The normality of the distribution for each element and measurement location for total and cortical areas, total and cortical areas corrected by body mass, and total and cortical area asymmetries are reported by sex and site in Table J.1. As some elements and cross-sectional properties had significant age-related differences, the distribution of data within the age categories were also tested, and the results of age-controlled tests for normalcy are reported for females in Table J.2, and males in Table J.3. As no significant sex or age differences in the cross-sectional asymmetry data were identified, it was not necessary to split this data by sex; Table J.4 reports the Shapiro-Wilks tests for normality of asymmetry cross-sectional properties.

Abbreviations used in the charts include:

- – Insufficient measurements to compare
MC2 50% – Measurement taken at the second metacarpal midshaft
ROI – Region of interest
MC2 – Second metacarpal
MT2 – Second metatarsal
T_A/BM – Total area corrected by body mass
T_A – Total area
T_A%DA – Total area directional asymmetry
C_A/BM – Cortical area corrected by body mass
C_A – Cortical area
C_A%DA – Cortical area directional asymmetry

Table J.1 – Shapiro-Wilks tests for normality of cross-sectional properties by sex and site.

Element	Vagnari		Ancaster	
	Female	Male	Female	Male
		T_A/BM		
Humerus	W(20)=.946, *p*=.307	W(18)=.933, *p*=.216	W(56)=.961, *p*=.066	W(62)=.983, *p*=.564
MC2 50%	**W(7)=.664, *p*=.001**	-	W(37)=.982, *p*=.808	W(11)=.917, *p*=.293
Radius	W(17)=.957, *p*=.584	W(12)=.966, *p*=.865	**W(48)=.949, *p*=.037**	W(61)=.980, *p*=.416
Tibia	W(20)=.907, *p*=.057	W(20)=.961, *p*=.566	**W(57)=.946, *p*=.014**	W(62)=.982, *p*=.482
		T_A		
Humerus	W(20)=.969, *p*=.739	W(18)=.936, *p*=.247	**W(56)=.957, *p*=.045**	W(62)=.981, *p*=.467
MC2 50%	W(7)=.847, *p*=.116	-	W(37)=.961, *p*=.216	W(11)=.917, *p*=.293
Radius	W(17)=.936, *p*=.272	W(12)=.967, *p*=.873	W(48)=.959, *p*=.096	W(61)=.972, *p*=.179
Tibia	W(20)=.943, *p*=.267	W(20)=.965, *p*=.649	W(57)=.979, *p*=.428	W(62)=.984, *p*=.594
		T_A%DA		
Humerus	W(10)=.913, *p*=.304	**W(9)=.806, *p*=.024**	W(28)=.977, *p*=.771	W(31)=.997, *p*=.443
MC2 50%	-	-	W(17)=.917, *p*=.133	W(5)=.980, *p*=.933
Radius	W(7)=.945, *p*=.686	W(4)=.986, *p*=.935	W(21)=.966, *p*=.652	W(29)=.948, *p*=.167
Tibia	W(9)=.960, *p*=.793	W(10)=.957, *p*=.749	W(29)=.969, *p*=.545	W(31)=.949, *p*=.143
		C_A/BM		
Humerus	W(20)=.934, *p*=.182	W(18)=.960, *p*=.595	**W(56)=.951, *p*=.023**	W(62)=.984, *p*=.591
Radius	W(17)=.976, *p*=.912	W(12)=.934, *p*=.420	W(48)=.986, *p*=.847	W(61)=.977, *p*=.320
Ulna ROI	W(17)=.975, *p*=.894	W(12)=.937, *p*=.463	W(48)=.959, *p*=.089	W(57)=.976, *p*=.307
MC2 50%	**W(7)=.664, *p*=.001**	-	**W(37)=.935, *p*=.032**	W(11)=.884, *p*=.117
MC2 ROI	W(11)=.901, *p*=.188	W(7)=.915, *p*=.432	**W(40)=.944, *p*=.047**	W(12)=.917, *p*=.264
Tibia	W(20)=.929, *p*=.148	W(20)=.971, *p*=.784	W(57)=.976, *p*=.308	W(62)=.983, *p*=.568
MT2 ROI	**W(6)=.611, *p*=.001**	W(9)=.858, *p*=.090	W(46)=.982, *p*=.676	W(31)=.972, *p*=.579
		C_A		
Humerus	W(20)=.910, *p*=.064	W(18)=.960, *p*=.596	**W(56)=.941, *p*=.009**	W(62)=.979, *p*=.370
Radius	W(17)=.951, *p*=.471	W(12)=.956, *p*=.728	W(48)=.975, *p*=.396	W(61)=.981, *p*=.465
Ulna ROI	W(17)=.982, *p*=.972	W)12)=.927, *p*=.349	W(48)=.953, *p*=.054	W(57)=.977, *p*=.334
MC2 50%	W(7)=.900, *p*=.331	-	**W(37)=.911, *p*=.006**	W(11)=.884, *p*=.117
MC2 ROI	W(11)=.943, *p*=.558	W(7)=.983, *p*=.971	W(40)=.945, *p*=.052	W(12)=.917, *p*=.264
Tibia	**W(20)=.845, *p*=.004**	W(20)=.963, *p*=.597	W(57)=.975, *p*=.297	W(62)=.988, *p*=.804
MT2 ROI	W(6)=.976, *p*=.933	W(9)=.839, *p*=.056	W(46)=.958, *p*=.100	W(31)=.961, *p*=.305
		C_A%DA		
Humerus	W(10)=.889, *p*=.164	**W(9)=.809, *p*=.026**	W(28)=.957, *p*=.302	W(31)=.967, *p*=.438
Radius	W(7)=.904, *p*=.355	**W(4)=.640, *p*=.002**	W(21)=.958, *p*=.469	W(29)=.981, *p*=.859
Ulna ROI	W(8)=.830, *p*=.059	W(4)=.938, *p*=.644	W(23)=.972, *p*=.729	W(27)=.981, *p*=.874
MC2 50%	-	-	W(17)=.947, *p*=.405	W(5)=.962, *p*=.823
MC2 ROI	W(4)=.862, *p*=.266	-	W(20)=.957, *p*=.479	W(6)=.948, *p*=.722
Tibia	W(9)=.928, *p*=.467	W(10)=.948, *p*=.645	W(29)=.962, *p*=.364	W(31)=.970, *p*=.506
MT2 ROI	-	W(4)=.854, *p*=.240	W(23)=.973, *p*=.754	W(15)=.981, *p*=.874

Bold font indicates that the data is not normally distributed. -=Insufficient measurements to compare; MC2 50%=Measurement taken at the second metacarpal midshaft; ROI=Region of interest; MC2=Second metacarpal; MT2=Second metatarsal; T_A/BM=Total area corrected by body mass; T_A=Total area; T_A%DA=Total area directional asymmetry; C_A/BM=Cortical area corrected by body mass; C_A=Cortical area; C_A%DA=Cortical area directional asymmetry

Table J.2 – Shapiro-Wilks tests for normality of female cross-sectional properties by age and site.

Element	Vagnari		Ancaster	
	Young Adult Female	Middle & Old Adult Female	Young Adult Female	Middle & Old Adult Female
	T_A/BM			
Humerus	W(14)=.936, *p*=.375	W(6)=.927, *p*=.559	W(30)=.938, *p*=.079	W(24)=.954, *p*=.333
MC2 50%	**W(4)=.729, *p*=.024**	**W(3)=.750, *p*=.000**	W(16)=.925, *p*=.205	W(21)=.975, *p*=.848
Radius	W(13)=.912, *p*=.194	W(4)=.989, *p*=.952	W(26)=.941, *p*=.145	W(22)=.938, *p*=.183
Tibia	W(14)=.904, *p*=.128	W(6)=.854, *p*=.170	W(26)=.926, *p*=.063	**W(31)=.927, *p*=.037**
	TA			
Humerus	W(14)=.959, *p*=.705	W(6)=.899, *p*=.369	**W(30)=.902, *p*=.010**	W(24)=.968, *p*=.618
MC2 50%	**W(4)=.749, *p*=.038**	W(3)=.977, *p*=.710	**W(16)=.856, *p*=.017**	W(21)=.966, *p*=.642
Radius	W(13)=.932, *p*=.365	W(4)=.939, *p*=.648	W(26)=.961, *p*=.408	W(22)=.944, *p*=.234
Tibia	W(14)=.899, *p*=.110	W(6)=.957, *p*=.799	W(26)=.958, *p*=.352	W(31)=.948, *p*=.140
	C_A/BM			
Humerus	W(14)=.900, *p*=.114	W(6)=.798, *p*=.056	**W(30)=.899, *p*=.008**	**W(24)=.915, *p*=.046**
Radius	W(13)=.912, *p*=.195	W(4)=.895, *p*=.406	W(26)=.983, *p*=.925	W(22)=.984, *p*=.962
Ulna ROI	W(13)=.917, *p*=.229	W(4)=.935, *p*=.625	W(25)=.961, *p*=.429	W(23)=.963, *p*=.522
MC2 50%	**W(4)=.630, *p*=.001**	-	W(16)=.929, *p*=.238	**W(21)=.881, *p*=.001**
MC2 ROI	**W(6)=.755, *p*=.022**	W(5)=.871, *p*=.272	W(16)=.911, *p*=.119	W(24)=.919, *p*=.055
Tibia	W(14)=.948, *p*=.524	W(6)=.973, *p*=.910	W(26)=.972, *p*=.675	W(31)=.962, *p*=.337
MT2 ROI	**W(5)=.552, *p*=.000**	-	W(22)=.965, *p*=.603	W(24)=.965, *p*=.550
	CA			
Humerus	W(14)=.904, *p*=.130	**W(6)=.783, *p*=.041**	**W(30)=.908, *p*=.013**	**W(24)=.883, *p*=.010**
Radius	W(13)=.924, *p*=.283	W(4)=.964, *p*=.804	W(26)=.981, *p*=.889	W(22)=.982, *p*=.949
Ulna ROI	W(13)=.950, *p*=.593	W(4)=.947, *p*=.697	W(25)=.967, *p*=.577	W(23)=.967, *p*=.623
MC2 50%	W(4)=.774, *p*=.063	W(3)=.992, *p*=.828	**W(16)=.850, *p*=.014**	**W(21)=.855, *p*=.005**
MC2 ROI	W(6)=.902, *p*=.389	W(5)=.934, *p*=.624	W(16)=.932, *p*=.259	**W(24)=.902, *p*=.024**
Tibia	W(14)=.880, *p*=.058	W(6)=.864, *p*=.202	W(26)=.954, *p*=.288	W(31)=.961, *p*=.315
MT2 ROI	W(5)=.942, *p*=.680	-	W(22)=.974, *p*=.808	W(24)=.960, *p*=.448

Bold font indicates that the data is not normally distributed. -=Insufficient measurements to compare; MC2 50%=Measurement taken at the second metacarpal midshaft; ROI=Region of interest; MC2=Second metacarpal; MT2=Second metatarsal; T_A/BM=Total area corrected by body mass; T_A=Total area; T_A%DA=Total area directional asymmetry; C_A/BM=Cortical area corrected by body mass; C_A=Cortical area; C_A%DA=Cortical area directional asymmetry

Table J.3 – Shapiro-Wilks tests for normality of male cross-sectional properties by age and site.

Element	Vagnari		Ancaster	
	Young Adult Male	Middle & Old Adult Male	Young Adult Male	Middle & Old Adult Male
		T_A/BM		
Humerus	W(6)=.801, *p*=.061	W(12)=.901, *p*=.166	W(32)=.987, *p*=.956	W(30)=.963, *p*=.372
MC2 50%	-	-	W(4)=.954, *p*=.739	W(7)=.976, *p*=.936
Radius	W(5)=.939, *p*=.656	W(7)=.959, *p*=.814	W(31)=.986, *p*=.944	W(30)=.953, *p*=.202
Tibia	W(6)=.886, *p*=.296	W(14)=.964, *p*=.793	W(28)=.965, *p*=.452	W(34)=.969, *p*=.444
		TA		
Humerus	W(6)=.895, *p*=.343	W(12)=.903, *p*=.174	W(32)=.982, *p*=.844	W(30)=.958, *p*=.275
MC2 50%	-	-	W(4)=.954, *p*=.739	W(7)=.976, *p*=.936
Radius	W(5)=.808, *p*=.095	W(7)=.952, *p*=.747	W(31)=.988, *p*=.972	W(30)=.937, *p*=.075
Tibia	W(6)=.887, *p*=.305	W(14)=.967, *p*=.832	W(28)=.968, *p*=.540	W(34)=.970, *p*=.453
		C_A/BM		
Humerus	W(6)=.938, *p*=.643	W(12)=.913, *p*=.234	W(32)=.955, *p*=.204	W(30)=.965, *p*=.416
Radius	W(5)=.821, *p*=.119	W(7)=.844, *p*=.108	W(31)=.981, *p*=.836	W(30)=.960, *p*=.316
Ulna ROI	W(4)=.927, *p*=.578	W(8)=.898, *p*=.279	W(32)=.943, *p*=.092	W(25)=.976, *p*=.806
MC2 50%	**-**	-	W(4)=.929, *p*=.589	**W(7)=.779, *p*=.025**
MC2 ROI	W(4)=.863, *p*=.272	**W(3)=.750, *p*=.000**	W(4)=.953, *p*=.733	W(8)=.877, *p*=.177
Tibia	W(6)=.933, *p*=.607	W(14)=.946, *p*=.495	W(28)=.964, *p*=.440	W(34)=.966, *p*=.364
MT2 ROI	W(4)=.887, *p*=.371	W(5)=.817, *p*=.111	W(13)=.957, *p*=.710	W(18)=.940, *p*=.293
		CA		
Humerus	W(6)=.938, *p*=.645	W(12)=.910, *p*=.210	W(32)=.959, *p*=.262	W(30)=.956, *p*=.246
Radius	W(5)=.958, *p*=.795	W(7)=.846, *p*=.114	W(31)=.972, *p*=.571	W(30)=.964, *p*=.388
Ulna ROI	W(4)=.896, *p*=.410	W(8)=.923, *p*=.452	W(32)=.966, *p*=.402	W(25)=.988, *p*=.988
MC2 50%	-	-	W(4)=.929, *p*=.589	**W(7)=.779, *p*=.025**
MC2 ROI	W(4)=.911, *p*=.485	W(3)=.872, *p*=.302	W(4)=.953, *p*=.733	W(8)=.877, *p*=.177
Tibia	W(6)=.968, *p*=.876	W(14)=.945, *p*=.481	W(28)=.979, *p*=.821	W(34)=.970, *p*=.457
MT2 ROI	W(4)=.893, *p*=.395	W(5)=.916, *p*=.505	W(13)=.975, *p*=.947	W(18)=.935, *p*=.240

Bold font indicates that the data is not normally distributed. -=Insufficient measurements to compare; MC2 50%=Measurement taken at the second metacarpal midshaft; ROI=Region of interest; MC2=Second metacarpal; MT2=Second metatarsal; T_A/BM=Total area corrected by body mass; T_A=Total area; T_A%DA=Total area directional asymmetry; C_A/BM=Cortical area corrected by body mass; C_A=Cortical area; C_A%DA=Cortical area directional asymmetry

Table J.4 – Shapiro-Wilks tests for normality of cross-sectional asymmetries by site.

Element	Vagnari	Ancaster
	T_A%DA	
Humerus	**W(19)=.745, *p*=.000**	W(59)=.980, *p*=.456
MC2 50%	-	W(22)=.928, *p*=.113
Radius	W(11)=.933, *p*=.441	W(50)=.968, *p*=.199
Tibia	W(19)=.966, *p*=.689	**W(60)=.947, *p*=.011**
	C_A%DA	
Humerus	**W(19)=.827, *p*=.003**	W(59)=.987, *p*=.801
Radius	W(11)=.943, *p*=.559	W(50)=.979, *p*=.492
Ulna ROI	**W(12)=.793, *p*=.008**	W(50)=.987, *p*=.861
MC2 50%	-	W(22)=.973, *p*=.788
MC2 ROI	W(6)=.901, *p*=.377	**W(26)=.824, *p*=.000**
Tibia	W(19)=.954, *p*=.467	W(60)=.972, *p*=.191
MT2 ROI	W(5)=.904, *p*=.432	W(38)=.975, *p*=.535

Bold font indicates that the data is not normally distributed. -=Insufficient measurements to compare; MC2 50%=Measurement taken at the second metacarpal midshaft; ROI=Region of interest; MC2=Second metacarpal; MT2=Second metatarsal; T_A%DA=Total area directional asymmetry; C_A%DA=Cortical area directional asymmetry

Appendix K: Combinations of Sex and Age Groups for Cross-Sectional Area Comparisons

Total and cortical area measurements were split between males and females. Age differences in areas were tested, and age groups were combined when no significant difference in area was identified. Table K.1 reports how sex and age groups were divided for total and cortical area comparisons at Ancaster. Table K.2 reports these combinations for Vagnari.

Abbreviations used in the charts include:

T_A – Total Area
C_A – Cortical Area
ROI – Region of interest
M – Male
F – Female
MC2 – Second metacarpal
MC2 50% - Measurement taken at the second metacarpal midshaft
MT2 – Second metatarsal
YA – Young Adult
MA – Middle Adult
OA – Old Adult

Table K.1 – Combinations of Ancaster age groups based on significant differences in total and cortical areas in the comparative sample.[1]

Element	Sex	T_A		C_A or ROI	
		Group 1	Group 2	Group 1	Group 2
Humerus	M	YA + MA + OA		YA + MA + OA	
	F	YA + MA + OA		YA	MA + OA
Radius	M	YA + MA + OA		YA + MA + OA	
	F	YA + MA + OA		YA	MA + OA
Ulna ROI	M	-		YA	MA + OA
	F	-		YA	MA + OA
MC2 ROI	M	-		YA + MA + OA	
	F	-		YA	MA + OA
MC2 50%	M	YA + MA + OA		YA	MA + OA
	F	YA	MA + OA	YA	MA + OA
Tibia	M	YA + MA + OA		YA + MA + OA	
	F	YA + MA + OA		YA + MA + OA	
MT2 ROI	M	-		YA + MA + OA	
	F	-		YA	MA + OA

[1] T_A=total area; C_A=cortical area; ROI=region of interest; M=male; F=female; YA=young adult; MA=middle adult; OA=old adult.

Table K.2 – Combinations of Vagnari age groups based on significant differences in total and cortical areas in the comparative sample.[1]

Element	Sex	T_A		C_A or ROI	
		Group 1	Group 2*	Group 1	Group 2
Humerus	M	YA + MA + OA		YA + MA + OA	
	F	YA + MA + OA		YA	MA + OA
Radius	M	YA + MA + OA		YA + MA + OA	
	F	YA + MA + OA		YA	MA + OA
Ulna ROI	M	-		YA + MA + OA	
	F	-		YA	MA + OA
MC2 ROI	M	-		YA + MA + OA	
	F	-		YA + MA + OA	
MC2 50%	M	YA + MA + OA		YA + MA + OA	
	F	YA + MA + OA		YA + MA + OA	
Tibia	M	YA + MA + OA**		YA + MA + OA**	
	F	YA + MA + OA		YA + MA + OA	
MT2 ROI	M	-		YA + MA + OA	
	F	-		YA + MA + OA	

[1] * No groups listed in the T_A Group 2 column as no significant differences were identified among the age groups, allowing them to all be grouped together for comparisons. **these categories were pooled due to unreliable results associated with a small, old adult sample size. T_A = total area; C_A = cortical area; ROI = region of interest; MC2 = second metacarpal; MC2 50% = measurements taken at the 2nd metacarpal midshaft; MT2 = second metatarsal; M = male; F = female; YA = young adult; MA = middle adult; OA = old adult.

Appendix L: Age and Sex Differences between Directional Asymmetries

Tables L.1 and L.2 in this appendix report the differences in the amount of asymmetry for total and cortical areas at Ancaster and Vagnari. These differences were compared for each element type separately and divided by age and sex categories. The tables also report the number of samples included in the comparison, along with the degrees of freedom associated with the statistical tests. Mann-Whitney U tests were used to compare the differences in asymmetry between the sexes, and Kruskal-Wallis tests were used to compare asymmetry differences among the age categories. Bolded values indicate the presence of significant differences between compared groups.

Abbreviations used in the table are as follows:

%DA – Directional asymmetry
ROI – region of interest
MC2 – second metacarpal
MC2 50% - second metacarpal measured at the midshaft
MT2 – second metatarsal
N – number of elements compared
df – degrees of freedom associated with the statistical test
T_A%DA – Total area directional asymmetry
C_A%DA – Cortical area directional asymmetry
U – Mann-Whitney U value
χ^2 – Kruskal-Wallis value
p – significant at ≤ 0.05

Table L.1 – Differences in the directional asymmetries at Ancaster between sexes and among age groups.

Element	%DA	Sex Differences	Female Age Differences	Male Age Differences	Both Sexes Age Differences
Humerus	Counts and df	N=59	N=28, df=3	N=31, df=4	N=59, df=4
	T_A%DA	U=421.0, p=0.844	χ^2=4.425, p=0.219	χ^2=0.557, p=0.906	χ^2=3.338, p=0.503
	C_A%DA	U=334.0, p=0.129	χ^2=2.971, p=0.396	χ^2=2.282, p=0.516	χ^2=2.288, p=0.683
Radius	Counts and df	N=50	N=21, df=2	N=29, df=3	N=50, df=3
	T_A%DA	U=261.5, p=0.398	χ^2=0.541, p=0.763	χ^2=1.174, p=0.759	χ^2=1.883, p=0.597
	C_A%DA	U=242.0, p=0.219	χ^2=2.846, p=0.241	χ^2=2.115, p=0.549	χ^2=1.243, p=0.743
Ulna ROI	Counts and df	N=50	N=23, df=2	N=27, df=3	N=50, df=3
	ROI%DA	U=265.0, p=0.376	χ^2=2.843, p=0.241	χ^2=1.841, p=0.606	χ^2=1.887, p=0.596
MC2 50%	Counts and df	N=22	N=17, df=2	N=5, df=2	N=22, df=3
	T_A%DA	U=11.0, p=0.014	χ^2=3.5, p=0.174	χ^2=3.2, p=0.202	χ^2=6.447, p=0.092
	C_A%DA	U=38.0, p=0.724	χ^2=0.436, p=0.804	χ^2=3.2, p=0.202	χ^2=3.281, p=0.350
MC2 ROI	Counts and df	N=26	N=20, df=2	N=6, df=2	N=26, df=3
	ROI%DA	U=49.0, p=0.503	χ^2=2.647, p=0.168	χ^2=3.571, p=0.168	χ^2=4.107, p=0.250
Tibia	Counts and df	N=60	N=29, df=2	N=31, df=3	N=60, df=3
	T_A%DA	U=372.5, p=0.255	χ^2=3.242, p=0.198	χ^2=2.446, p=0.485	χ^2=1.501, p=0.682
	C_A%DA	U =408.0, p=0.539	χ^2=5.894, p=0.052	χ^2=1.835, p=0.607	χ^2=1.519, p=0.678
MT2 ROI	Counts and df	N=38	N=23, df=2	N=15, df=2	N=38, df=3
	ROI%DA	U=314.0, p=0.281	χ^2=1.202 , p=0.548	χ^2=1.367 , p=0.505	χ^2=2.353, p=0.502

Table L.2 – Differences in the directional asymmetries at Vagnari between sexes and among age groups.

Element	%DA	Sex Differences	Female Age Differences	Male Age Differences	Both Sexes Age Differences
Humerus	Counts and df	N=19	N=19, df=2	N=10, df=2	N=9, df=1
	T_A%DA	U=40.0, p=0.720	χ^2=0.135, *p*=0.935	χ^2=3.778, *p*=0.151	χ^2=0.000, *p*=1.000
	C_A%DA	U=42.5, p=0.842	χ^2=3.971, *p*=0.137	**χ^2=6.415, *p*=0.040**	χ^2=0.600, *p*=0.439
Radius	Counts and df	N=10	N=10, df=2	N=6, df=2	N=9, df=1
	T_A%DA	U=10.0, p=0.762	χ^2=0.622, *p*=0.733	χ^2=2.143, *p*=0.343	χ^2=2.40, *p*=0.121
	C_A%DA	U=7.0, p=0.352	χ^2=1.595, *p*=0.450	χ^2=2.381, *p*=0.304	χ^2=0.167, *p*=0.683
Ulna ROI	Counts and df	N=12	N=12, df=3	N=8, df=3	N=4, df=1
	ROI%DA	U=6.0, p=0.109	χ^2=3.022, *p*=0.388	χ^2=2.533, *p*=0.469	χ^2=0.600, *p*=0.439
MC2 ROI	Counts and df	N=6	N=6, df=2	N=4, df=2	-
	ROI%DA	*U*=3.0, *p*=0.800	χ^2=0.000, *p*=1.000	χ^2=0.300, *p*=0.861	
Tibia	Counts and df	N=19	N=19, df=3	N=9, df=3	N=10, df=2
	T_A%DA	*U*=36.0, *p*=0.497	χ^2=1.588, *p*=0.662	χ^2=4.040, *p*=0.257	χ^2=2.218, *p*=0.330
	C_A%DA	*U* =38.0, *p*=0.604	χ^2=2.292, *p*=0.514	χ^2=2.400, *p*=0.494	χ^2=2.673, *p*=0.263
MT2 ROI	Counts and df	N=5	N=5, df=2	-	N=4, df=1
	ROI%DA	*U*=1.00, *p*=0.800	χ^2=1.40, *p*=0.497		χ^2=0.600, *p*=0.439

Appendix M: Individuals and Elements with Outlying Cross-Sectional Properties

The individuals at Ancaster and Vagnari that had outlying cross-sectional properties are presented in Tables M.1 and M.2, respectively. The element that was outlying is noted, and the cross-sectional property or properties are recorded; the bone side that was found to be outlying is indicated, along with if it was larger or smaller than the norm. Individuals with fractures and the fractured element and side are also indicated.

Abbreviations used in this appendix include:

T_A – Total area
T_A%DA – Total area directional asymmetry
C_A – Cortical area
ROI – Region of interest
C_A%DA – Cortical area directional asymmetry
ROI%DA – Region of interest directional asymmetry
> – Larger than normal
< – Smaller than normal
L – Left
R – Right
F – Female
M – Male
YA – Young adult
MA – Middle adult
OA – Old adult
MC2 50% - Second metacarpal midshaft
MT2 – Second metatarsal
- – No outlying property observed

Table M.1 –Ancaster individuals with outlying cross-sectional properties.

Skeleton	Sex	Age	Fracture	Outlying Element	T_A	T_A%DA	C_A/ROI	C_A%DA/ ROI%DA
AN-001	F	YA	R Tibia	Radius	-	-	> R&L	-
AN-005	M	MA		Radius	> L	-	> R	-
AN-006	M	MA		Tibia	-	L>R	-	L>R
AN-011	M	MA		MC2 50%	> R	-	-	-
AN-013	M	YA	L Fibula	MC2 50%	-	L>R	>L	L>R
AN-024	M	MA	L Radius and Ulna	Humerus	-	L>R	-	L>R
AN-026	M	YA		MC2 ROI	-	-	< R	L>R
				MC2 50%	-	-	-	L>R
AN-027	M	MA		Tibia	-	L>R	-	L>R
AN-041	F	YA		Humerus	-	-	-	L>R
AN-045A	F	MA		MC2 ROI	-	-	> L & R	-
				MC2 50%	-	-	> L	-
AN-046	M	YA	L Tibia	Humerus	-	-	-	R>L
AN-052	F	MA		Radius	> R			
AN-061	M	MA	L Clavicle	Humerus	-	-	-	R>L
AN-072	F	YA		Tibia	-	-	-	R>L
AN-093	M	MA		Radius	> R	-	-	-
AN-098	M	OA	R Clavicle & L Tibia	Ulna	-	-	< R	-
AN-102	F	YA		Humerus	> R	-	>L&R	-
				MC2 ROI	-	-	> L	-
				MC2 50%	-	-	> L	-
AN-104	F	MA	R Radius	Humerus	-	-	-	R>L
AN-113	F	MA	L Femur	Humerus	> L	-	-	-
AN-118	M	YA		Radius	> R	-	-	-
AN-142	F	MA		MC2 ROI	-	-	>L&R	-
AN-162	F	YA		MC2 ROI	-	-	< R	-
AN-172	F	MA	L Radius	Tibia	-	R>L	-	R>L
				Radius	-	-	-	L>R
AN-177	M	MA	L Radius	Tibia	-	-	> L	-
AN-178	F	YA		MC2 50%	-	-	> R	-
AN-184	M	MA		Humerus	-	-	-	R>L
AN-185A	M	MA	R Clavicle	MT2 ROI	-	-	-	R>L
AN-191	F	MA	R Radius & Ulna	MC2 50%	-	-	< R	L>R
AN-216	M	YA		Radius	-	L>R	-	-
AN-217	F	MA		MC2 50%				R>L
AN-218	F	YA	L Tibia & Fibula	MT2 ROI	-	-	> R	-
				Radius	-	-	< L	-

Skeleton	Sex	Age	Fracture	Outlying Element	T_A	T_A%DA	C_A/ROI	C_A%DA/ ROI%DA
AN-220	F	OA		Humerus	-	-	< R	-
AN-241	F	OA	L Radius	Tibia	-	R>L	-	-
				Humerus	-	-	< R	L>R
				MT2 ROI	-	-	-	R>L
AN-252	M	MA		Humerus	-	-	-	L>R
AN-252	M	MA		Radius	-	-	-	L>R
AN-263	F	OA		Humerus	> R	-	< L & R	-
				Radius	-	-	-	R>L
				MT2 ROI	-	-	< R	-
				Tibia	-	-	< R	L>R
AN-269	M	MA		Radius	-	L>R	-	-
				Humerus	-	L>R	-	-

T_A=Total area; T_A%DA=Total area directional asymmetry; C_A=Cortical area; ROI=Region of interest; C_A%DA=Cortical area directional asymmetry; ROI%DA=Region of interest directional asymmetry; >=Larger than normal; <=Smaller than normal; L=Left; R=Right; F=Female; M=Male; YA=Young adult; MA=Middle adult; OA=Old adult; MC2 50%=Second metacarpal midshaft; MT2=Second metatarsal; -=No outlying property observed

Table M.2 –Vagnari individuals with outlying cross-sectional properties.

Skeleton	Sex	Age	Fracture	Outlying Element	T_A	T_A%DA	C_A/ROI	C_A%DA/ ROI%DA
VA-F042A	M	YA	L Tibia	MC2 50%	>R	-	-	-
VA-F062	M?	MA		Humerus	< L	R>L	< L	R>L
VA-F204	F	YA	L Humerus	Humerus	< L	-	-	-
VA-F207	M?	YA		Humerus	< L	-	-	-
VA-F213	M	MA		Humerus	> L	-	-	-
VA-F214	M	MA		MC2 50%	>R			
VA-F215	F	YA		Tibia	-	-	> L	-
VA-F216	M	MA	R Fibula	MC2 ROI	-	-	> R	-
VA-F234	M	YA		MT2 ROI	-	-	> R	-
				Ulna	-	-	> L	-
VA-F249	F?	YA	L Clavicle	Humerus	> R	-	-	-
				Ulna	-	-	> L	
VA-F288	M?	YA	L Ulna	Humerus	< R	-	-	-
VA-F290	M	MA		Tibia	-	L>R	-	L>R
VA-F294	F	OA		Ulna	-	-	>R	R>L
VA-F306	F	MA		Humerus	-	-	-	L>R

T_A=Total area; T_A%DA=Total area directional asymmetry; C_A=Cortical area; ROI=Region of interest; C_A%DA=Cortical area directional asymmetry; ROI%DA=Region of interest directional asymmetry; >=Larger than normal; <=Smaller than normal; L=Left; R=Right; F=Female; M=Male; YA=Young adult; MA=Middle adult; OA=Old adult; MC2 50%=Second metacarpal midshaft; MT2=Second metatarsal; -=No outlying property observed

Appendix N: Post-Hoc Age Differences in Cross-Sectional Outlier Prevalence Rates

This appendix reports supplementary age differences in the number of individuals with outlying cross-sectional properties. Age differences in the counts of all outliers, including individuals without fractures, are provided in Section N.1, and reported separately by site. Section N.2 reports post-hoc age differences in the counts of individuals with both fractures and outlying cross-sectional properties.

N.1: All Outliers

N.1.1: Ancaster

Table N.1 – Age differences in the prevalence of male and female outlying total areas at Ancaster.[1]

	Young Adult	Middle Adult	Old Adult
		Male	
Young Adult		OR=2.2, CI 0.2-21.2 p_{FET}=.643	p_{FET}=1.000
Middle Adult	OR=2.2, CI 0.2-25.0 p_{FET}=.605		p_{FET}=1.000
Old Adult	OR=3.7, CI 0.2-60.3 p_{FET}=.389	OR=1.6, CI 0.1-18.7 p_{FET}=.555	
	Female		

[1] Groups compared using odds ratio and Fisher's Exact tests. Bold font indicates that a significant difference is present. In all instances the older age category had greater odds of outlying total areas as the younger age category. OR=odds ratio; CI=confidence interval.

Table N.2 – Differences in the prevalence of individuals with outlying total area directional asymmetries between age categories at Ancaster by sex. [1]

	Young Adult	Middle Adult	Old Adult
		Male	
Young Adult		OR=1.9, CI 0.4-10.1 p_{FET}=0.698	p_{FET}=1.000
Middle Adult	p_{FET}=0.470		*p_{FET}=1.000*
Old Adult	OR=1.9, CI 0.2-22.4 p_{FET}=0.519	OR=3.5, CI 0.2-59.9 p_{FET}=0.407	
	Female		

[1] Groups compared using odds ratio and Fisher's Exact tests. Bold font indicates that a significant difference is present. In most instances the older age category had greater odds of outlying total areas as the younger age category; italic font indicates when greater odds are present in the younger cohort. OR=odds ratio; CI=confidence interval.

Table N.3 – Differences in the prevalence of individuals with outlying cortical areas between age groups at Ancaster by sex. [1]

	Young Adult	Middle Adult	Old Adult
		Male	
Young Adult		OR=1.4, CI 0.3-8.0 p_{FET}=1.000	OR=3.1, CI 0.3-35.8 p_{FET}=0.367
Middle Adult	*OR=1.8, CI 0.6-5.4* *p_{FET}=0.416*		OR=2.2, CI 0.2-20.2 p_{FET}=0.429
Old Adult	OR=1.7, CI .6-4.8 p_{FET}=0.385	OR=2.9, CI 0.9-9.8 p_{FET}=0.095	
	Female		

[1] Groups compared using odds ratio and Fisher's Exact tests. Bold font indicates that a significant difference is present. In most instances the older age category had greater odds of outlying total areas as the younger age category; italic font indicates when greater odds are present in the younger cohort. OR=odds ratio; CI=confidence interval.

N.1.2: Vagnari

Table N.4 – Age differences in the number of outlying total areas at Vagnari by sex. [1]

	Young Adult	Middle Adult	Old Adult
		Male	
Young Adult		OR=1.1, CI 0.2-5.9 p_{FET}=1.000	p_{FET}=1.000
Middle Adult	p_{FET}=1.000		p_{FET}=1.000
Old Adult	p_{FET}=1.000	-	
	Female		

[1] Groups compared using odds ratio and Fisher's Exact tests. Bold font indicates that a significant difference is present. In most instances the older age category had greater odds of outlying total areas as the younger age category; italic font indicates when greater odds are present in the younger cohort. OR=odds ratio; CI=confidence interval.

Table N.5 – Age differences in the prevalence of Vagnari outlying total area directional asymmetries by sex. [1]

	Young Adult	Middle Adult	Old Adult
		Male	
Young Adult		p_{FET}=.491	-
Middle Adult	-		*p_{FET}=1.000*
Old Adult	-	-	
	Female		

[1] Age groups were compared using Fisher's Exact tests. Bold font indicates that a significant difference is present. Italic font is used to indicate instances when greater odds of outlying total areas were present in younger adults, rather than older adults. –=no outliers available to compare.

Table N.6 – Differences in the number of Vagnari elements with outlying cortical areas between the age groups by sex. [1]

	Adolescent	Young Adult	Middle Adult	Old Adult
		Male		
Adolescent		-	-	-
Young Adult	*OR=2.9, CI 0.4-22.0* *p_{FET}=.291*		OR=1.0, CI 0.1-7.3 p_{FET}=1.000	*p_{FET}=1.000*
Middle Adult	*p_{FET}=.490*	*p_{FET}=1.000*		*p_{FET}=1.000*
Old Adult	OR=1.7, CI 0.1-21.7 p_{FET}=1.000	OR=4.8, CI 0.4-61.5 p_{FET}=.286	OR=1.6, CI 0.1-20.7 p_{FET}=1.000	
	Female			

[1] Groups compared using odds ratio and Fisher's Exact tests. Bold font indicates that a significant difference is present. In most instances the older age category had greater odds of outlying total areas as the younger age category; italic font indicates when greater odds are present in the younger cohort. OR=odds ratio; CI=confidence interval.

N.2: Individuals with Fractures and Outliers

Table N.7 – Age differences in the prevalence of individuals with both fractures and outlying cross-sectional properties at Ancaster by age and sex. [1]

	Young Adult	Middle Adult	Old Adult
		Male	
Young Adult		*OR=1.3, CI 0.2-11.5* *p_{FET}=1.000*	*p_{FET}=1.000*
Middle Adult	OR=5.0, CI 0.5-53.0 p_{FET}=0.286		*p_{FET}=.385*
Old Adult	OR=1.3, CI 0.1-22.9 p_{FET}=1.000	*OR=4.0, CI 0.2-75.7* *p_{FET}=0.524*	
	Female		

[1] Groups compared using odds ratio and Fisher's Exact tests. Bold font indicates that a significant difference is present. In most instances the older age category had greater odds of outlying total areas as the younger age category; italic font indicates when greater odds are present in the younger cohort. OR=odds ratio; CI=confidence interval.

Table N.8 – Age differences in the prevalence of Vagnari individuals with both fractures and outlying cross-sectional properties by sex. [1]

	Young Adult	Middle Adult	Old Adult
		Male	
Young Adult		*OR=3.0, CI 0.2-59.9* p_{FET}*=1.000*	-
Middle Adult	p_{FET}*=1.000*		-
Old Adult	p_{FET}*=1.000*	-	
	Female		

[1] Groups compared using odds ratio and Fisher's Exact tests. Bold font indicates that a significant difference is present. In most instances the older age category had greater odds of outlying total areas as the younger age category; italic font indicates when greater odds are present in the younger cohort. OR=odds ratio; CI=confidence interval.

Appendix O: Fractured Elements with Outlying Cross-Sectional Properties & Complications

Attributes of each fractured element that was associated with an outlying cross-sectional property are presented for Ancaster (Table O.1) and Vagnari (Table O.2). The fracture type, location, and any associated complications are noted in relation to the element and specific cross-sectional property or properties that were outlying. The outlying element is indicated by side and if it was larger or smaller than normal.

Abbreviations used in the tables include:

T_A – Total area
M_A – Medullary area
C_A – Cortical area
T_A%DA – Total area directional asymmetry
M_A%DA – Medullary area directional asymmetry
C_A%DA – Cortical area directional asymmetry
ROI%DA – Region of interest area directional asymmetry
M –Male
F – Female
YA – Young adult
MA – Middle adult
OA – Old adult
R – Right
L – Left
INF – Inflammation
APP – Apposition
RO – Rotation
OA_x – Osteoarthritis
OV – Overlap
ANG – Angulation
MC2 50% – second metacarpal midshaft
MT2 – Second metatarsal

Table O.1 – The Ancaster elements belonging to individuals with fractures with outlying cross-sectional properties.

Skeleton Number	Sex	Age	Fracture	Fracture Type	Complications	Outlying Element	T_A	T_A%DA	C_A/ROI	C_A%DA/ ROI%DA
AN-001	F	YA	R Tibia	Crush		Radius	-	-	> R	-
AN-013	M	YA	L Fibula	Avulsion		MC2 50%	-	L>R	-	-
AN-024	M	MA	L Radius and Ulna	Spiral	APP, RO, OA_x	Humerus	-	-	-	L>R
AN-046	M	YA	L Tibia	Avulsion		Humerus	-	-	-	R>L
AN-061	M	MA	L Clavicle	Transverse		Humerus	-	-	-	R>L
AN-098	M	OA	R Clavicle L Tibia	Transverse Avulsion		Ulna	-	-	< R	-
AN-104	F	MA	R Radius	Spiral Butterfly (Comminuted)	RO	Humerus	-	-	-	R>L
AN-113	F	MA	L Femur	Insufficiency		Humerus	> L	-	-	-
AN-172	F	MA	L Radius	Transverse & Crush	OA_x	Radius	-	-	-	L>R
						Tibia	-	R>L	-	R>L
AN-177	M	MA	L Radius	Oblique	OA_x	Tibia	-	-	> L	
AN-185A	M	MA	R Clavicle	Unknown		MT2 ROI	-	-	-	R>L
AN-191	F	MA	R Radius & Ulna	Oblique & Crush	OA_x	MC2 50%	-	-	< R	-
AN-218	F	YA	L Tibia & Fibula	Spiral	APP, RO, OV, OA_x	Radius	-	-	< L	-
						MT2 ROI	-	-	> R	-
AN-241	F	OA	L Radius	Oblique	OA_x	Humerus	-	-	< R	L>R
						Tibia	-	R>L	-	-
						MT2 ROI	-	-	-	R>L

F=Female; M=Male; YA=Young adult; MA=Middle adult; OA=Old adult; T_A=Total area; T_A%DA=Total area directional asymmetry; C_A=Cortical area; ROI=Region of interest; C_A%DA=Cortical area directional asymmetry; ROI%DA=Region of interest directional asymmetry; APP=Poor apposition; RO=Rotation; OA_x=Osteoarthritis; OV=Overlap; MC2 50%=measurement of the second metacarpal taken at the midshaft; MT2=second metatarsal; R=Right; L=Left

Table O.2 – The Vagnari elements belonging to individuals with fractures with outlying cross-sectional properties.

Skeleton	Sex	Age	Fracture	Fracture Type	Complications	Outlying Element	T_A	T_A%DA	C_A/ROI	C_A%DA/ ROI%DA
VA-F042A	M	YA	L Tibia	Spiral		MC2 50%	> R	-	-	-
VA-F204	F	YA	L Humerus	Unknown		Humerus	< L	-	-	-
VA-F216	M	MA	R Fibula	Oblique	OA_x	MC2 ROI	-	-	> R	-
VA-F249	F	YA	L Clavicle	Transverse	ANG	Humerus	> R	-	-	-
						Ulna	-	-	> L	-
VA-F288	M	YA	L Ulna	Unknown		Humerus	< R	-	-	-

F=Female; M=Male; YA=Young adult; MA=Middle adult; OA=Old adult; T_A=Total area; T_A%DA=Total area directional asymmetry; C_A=Cortical area; ROI=Region of interest; C_A%DA=Cortical area directional asymmetry; ROI%DA=Region of interest directional asymmetry; OA_x=Osteoarthritis; ANG=Angulation; MC2 50%=measurement of the second metacarpal taken at the midshaft; R=Right; L=Left